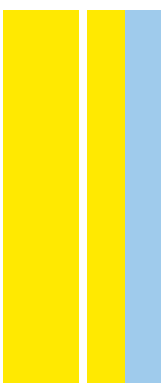


DOUTORAMENTO
PROGRAMA DOUTORAL EM PATOLOGIA E GENÉTICA MOLECULAR

Uncovering the role of epigenetic mechanisms in bladder cancer aggressiveness: from biology to clinical setting

Sara Monteiro Reis

D
2020

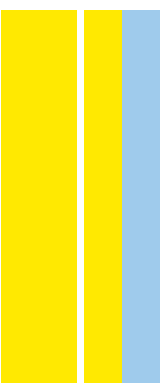


Sara Monteiro Reis. Uncovering the role of epigenetic mechanisms in bladder cancer aggressiveness: from biology to clinical setting



Uncovering the role of epigenetic mechanisms in bladder cancer aggressiveness: from biology to clinical setting

Sara Raquel Monteiro dos Reis



Sara Raquel Monteiro dos Reis

UNCOVERING THE ROLE OF EPIGENETIC MECHANISMS IN BLADDER CANCER AGGRESSIVENESS: FROM BIOLOGY TO CLINICAL SETTING

Tese de Candidatura ao grau de Doutor em Patologia e Genética Molecular submetida ao Instituto de Ciências Biomédicas Abel Salazar e Faculdade de Medicina da Universidade do Porto

Orientador – **Carmen de Lurdes Fonseca Jerónimo**

Professora Catedrática Convidada, Instituto de Ciências Biomédicas Abel Salazar da Universidade do Porto

Investigadora Auxiliar & Coordenadora, Grupo de Epigenética & Biologia do Cancro, Centro de Investigação, Instituto Português de Oncologia do Porto Francisco Gentil, E.P.E

Co-orientador – **Rui Manuel Ferreira Henrique**

Professor Catedrático Convidado, Instituto de Ciências Biomédicas Abel Salazar da Universidade do Porto

Consultor do Serviço de Anatomia Patológica & Investigador Sénior, Grupo de Epigenética & Biologia do Cancro, Centro de Investigação, Instituto Português de Oncologia do Porto Francisco Gentil, E.P.E

UNCOVERING THE ROLE OF EPIGENETIC MECHANISMS IN BLADDER CANCER AGGRESSIVENESS: FROM BIOLOGY TO CLINICAL SETTING

Sara Monteiro-Reis

U. PORTO



INSTITUTO DE CIÊNCIAS BIOMÉDICAS ABEL SALAZAR
UNIVERSIDADE DO PORTO



FACULDADE DE MEDICINA
UNIVERSIDADE DO PORTO

Copyright © 2020 by Sara Raquel Monteiro dos Reis

All rights reserved. No part of this book may be reproduced, stored in a database or retrieval system, or published, in any form or in any way, electronically, mechanically, by print, photo print, microfilm or any other means without prior written permission by the author, or when appropriate, of the publisher of the publications.

The candidate performed the experimental work with the support of a doctoral fellowship (SFRH/BD/112673/2015) supported by the “Fundação para a Ciência e a Tecnologia”.



REPÚBLICA
PORTUGUESA

Ciência, Tecnologia
e Ensino Superior

FCT

Fundação
para a Ciência
e a Tecnologia



PORTUGAL
2020



UNIÃO EUROPEIA
Fundo Social Europeu

The research described in this Thesis was conducted at:

Cancer Biology and Epigenetics Group – Research Centre, Portuguese Oncology Institute of Porto, Porto, Portugal.



Authors Declaration

Under the terms of the “no 2, alínea a, do Art.º 31º do Decreto-lei no 230/2009”, is hereby declared that the author afforded a major contribution to the conceptual design and technical execution of the work, interpretation of the results and manuscript preparation of the published articles included in this doctoral thesis.

Under the terms of the “no 2, alinea a, do Art.º 31º do Decreto-lei no 230/2009” is hereby declared that the following original publications were prepared within the scope of this doctoral thesis.

Scientific Publications

Articles in international peer-reviewed journals

Review articles

Sara Monteiro-Reis*, João Lobo*, Rui Henrique, Carmen Jerónimo: Epigenetic Mechanisms Influencing Epithelial to Mesenchymal Transition in Bladder Cancer. *Int J Mol Sci.* 2019, Jan 13;20(2):297. doi: 10.3390/ijms20020297

Research articles

Nuno André Padrão, **Sara Monteiro-Reis**, Jorge Torres-Ferreira, Luís Antunes, Luís Leça, Diana Montezuma, João Ramalho-Carvalho, Paula C Dias, Paula Monteiro, Jorge Oliveira, Rui Henrique, Carmen Jerónimo: MicroRNA promoter methylation: a new tool for accurate detection of urothelial carcinoma. *Br J Cancer* 2017, Feb 28;116(5):634-639. doi: 10.1038/bjc.2016.454

Sara Monteiro-Reis, Ana Blanca, Joana Tedim-Moreira, Isa Carneiro, Diana Montezuma, Paula Monteiro, Jorge Oliveira, Luís Antunes, Rui Henrique, António Lopez-Beltran, Carmen Jerónimo: A Multiplex Test Assessing MiR663a_{me} and VIM_{me} in Urine Accurately Discriminates Bladder Cancer from Inflammatory Conditions. *J Clin Med.* 2020 Feb 24;9(2):605. doi: 10.3390/jcm9020605

João Lobo*, **Sara Monteiro-Reis***, Catarina Guimarães-Teixeira*, Paula Lopes, Isa Carneiro, Carmen Jerónimo, Rui Henrique: Practicability of clinical application of bladder

cancer molecular classification and additional value of epithelial-to-mesenchymal transition: prognostic value of vimentin expression. *J Transl Med.* 2020, Aug 5;18(1):303. doi: 10.1186/s12967-020-02475-w

Sara Monteiro-Reis*, Ana Lameirinhas*, Vera Miranda-Gonçalves, Diana Felizardo, Paula C Dias, Jorge Oliveira, Inês Graça, Céline S Gonçalves, Bruno M Costa, Rui Henrique, Carmen Jerónimo: Sirtuins' Deregulation in Bladder Cancer: SIRT7 Is Implicated in Tumor Progression through Epithelial to Mesenchymal Transition Promotion. *Cancers (Basel)* 2020, Apr 25;12(5):1066. doi: 10.3390/cancers12051066

Sara Monteiro-Reis, Vera Miranda-Gonçalves, Catarina Guimarães-Teixeira, Cláudia Martins-Lima, João Lobo, Diana Montezuma, Paula Lopes, Paula C. Dias, Isabelle Bernard-Pierrot, Rui Henrique, Carmen Jerónimo: Epigenetic deregulation of Vimentin expression in Bladder Cancer associates with acquisition of invasive and metastatic phenotype through epithelial to mesenchymal transition. (In preparation)

Abstracts published in international periodicals with referees

Sara Monteiro-Reis, Ana Blanca, Joana Tedim-Moreira, Isa Carneiro, Diana Montezuma, Paula Monteiro, Jorge Oliveira, Luís Antunes, Rui Henrique, António Lopez-Beltran, Carmen Jerónimo: MiR663a and VIM promoter methylation: a multiplex test for discriminating bladder cancer from inflammatory disease. *European Urology Supplements* 18(8):e3085. doi: 10.1016/S1569-9056(19)33332-9

*These authors contributed equally to the study.

Agradecimentos

Como tudo na vida, o percurso que culminou nesta Tese não foi feito sozinho. O resultado final desta etapa da minha vida não seria possível sem o contributo de algumas pessoas.

Em primeiro lugar gostaria de agradecer à Professora Carmen Jerónimo, não só na qualidade de Orientadora desta Tese, mas como mentora de todo o meu percurso académico e profissional. Desde a minha chegada ao seu grupo de investigação, há 10 anos atrás, a Professora esteve presente em todas as etapas, desde ir para “a bancada” ensinar-me a fazer extrações de DNA, passando por vários altos e baixos, alegrias e tristezas, a sua presença foi uma verdadeira constante. Por tudo isto serei eternamente grata, e nunca me esquecerei das oportunidades que me proporcionou. Será sempre a minha mentora.

Ao Professor Rui Henrique, na qualidade de co-orientador desta Tese e, mais importante que isto, na qualidade de meu Professor. O meu profundo agradecimento por todos os ensinamentos que me passou, por todas as sugestões e críticas construtivas, e pela boa disposição com que sempre me brindou nas nossas várias conversas, muito obrigada!

Não poderia deixar de agradecer ao IPO do Porto e aos seus vários departamentos, com especial ênfase para o Serviço de Anatomia Patológica, pela sua contribuição significativa para a realização do meu trabalho. Um agradecimento especial ao Centro de Investigação do IPO do Porto, por permitir o usufruto das respectivas instalações.

De igual forma, agradeço ao Instituto de Ciências Biomédicas Abel Salazar, em especial à Professora Fátima Gartner, por me aceitar no Programa Doutoral.

A todos os antigos e atuais membros do Grupo de Epigenética e Biologia do Cancro, o meu profundo e sincero agradecimento. Ao longo de todos estes anos houve um sentimento constante que sempre traduziu o espírito do nosso Grupo: boa disposição e companheirismo. Não seria justo nomear pessoas neste agradecimento, que considero coletivo. Por isso, a todos os “GEBCCianos”, o meu muito obrigada pelo contributo para o meu trabalho, pelas discussões científicas (e não-científicas), pelas horas de almoço, pelas gargalhadas, pelo incentivo quando algo corria mal, pelos festejos quando alcançamos o desejado, pelo espírito de união. Guardo um lugar especial no meu coração para vocês.

Existe uma verdadeira rede de pessoas que, não estando diretamente ligadas a um contexto profissional, foram tão ou mais importantes para o concluir desta etapa. São estes os meus amigos e a minha família.

Aos meus queridos amigos. Cat e Ro, as “minhas” meninas, obrigada pelo carinho e amizade, e por me fazerem alienar do mundo que nos rodeia cada vez que estamos juntas. Ao meu “Gangue das Aves”: Diana, Ana, Tiago e Guilherme. Sem vocês não conseguiria manter a minha sanidade mental. Com vocês posso disparatar, rir e chorar, descarregar as minhas frustrações e celebrar, em grande, as minhas vitórias. O poeta Eugénio de Andrade disse, um dia, que os amigos tornam o mundo mais habitável, e é este, precisamente, o sentimento que surge quando penso em vocês. Diana e Ana, minhas BFFs, vocês são as minhas irmãs do coração. Obrigada por sempre cuidarem de mim. Tiago, nosso preguiça, obrigada por sempre contribuíres para o meu sorriso.

Ao Guilherme, as palavras falham para te agradecer. Tu és o meu ponto de abrigo, a minha constante. Concerteza não seria o que sou hoje se não tivesse tido a felicidade de me cruzar contigo na vida, e construir a relação que temos hoje. Obrigada por me acompanhares, pela tua ajuda no meu trabalho, por estares sempre comigo (nos bons e maus momentos), por me obrigares a olhar para o mundo sob outra perspectiva, por me fazeres rir quando me apetecia chorar, por seres “meu” e por me aceites como “tua”. Há um bocadinho de ti em tudo o que faço. Para sempre, obrigada meu amor.

A toda a minha família, por serem eles os verdadeiros responsáveis por quem eu sou. Aos meus irmãos, Miguel e Amadeu, e as suas famílias, obrigada por sempre me incentivarem e vibrarem com os meus sucessos. Foram vocês os dois que me ensinaram a dar os primeiros passos, e ainda hoje caminham comigo. Um especial agradecimento ao meu querido sobrinho, Tiaguinho, por me fazer lembrar o quão “fixe” é ser cientista, por me acompanhar nas idas ao laboratório aos fins-de-semana para alimentar as células, e se deslumbrar com as pequenas coisas que nós adultos nos esquecemos. Obrigada!

Por fim, aos meus pais, Amadeu e Madalena. Vocês são a minha inspiração. Pelo vosso espírito batalhador, os valores e a moral que me passaram, o vosso incentivo para que eu sempre perseguisse os meus sonhos, pelo esforço que foi feito para que eu chegasse até aqui. Pelo amor e carinho que sempre abundaram na nossa casa. Sem vocês não existiria Sara. Por vocês, esta Tese hoje existe. Obrigada.

Esta Tese é dedicada aos meus Pais, Amadeu e Madalena.

*“There's real poetry in the real world.
Science is the poetry of reality.”*

Richard Dawkins

Abstract

Bladder Cancer (BlCa) is the 10th most common cancer type worldwide, with an estimated 400,000 new cases per year and 160,000 deaths in both genders. In more developed regions, BlCa is the 6th most incident cancer for men, and it constitutes a major health concern. Muscle-invasive bladder cancer (MIBC) represents a more aggressive form, which is more likely to progress and metastasize, whereas non-muscle-invasive bladder cancer (NMIBC) is mostly characterized by multiple local recurrences that eventually progress over time. In an effort to better understand the molecular mechanisms associated with BlCa carcinogenesis and to better stratify and treat these patients a molecular classification of MIBC has been proposed in the last few years.

Aberrations in epigenetic mechanisms, including DNA methylation, histone post-translational modifications (PTMs), chromatin remodelers and non-coding RNAs, have been implicated in cancer, and also suggested to have a value as cancer biomarkers. Specifically, DNA promoter methylation of protein coding genes and non-coding genes, were shown to be useful for non-invasive early detection/diagnosis, as well as for prognosis and response prediction to therapy.

Globally, the main aim of this Thesis was to explore the contribution of epigenetic mechanisms deregulation in BlCa, either at a clinical approach - by proposing new biomarkers for disease detection and management - and at a tumour biology approach - by investigating the mechanisms of action of known epigenetic enzymes, as well as epigenetic regulation of genes implicated in BlCa invasive phenotype.

Regarding the clinical approach, the results obtained in this Thesis allowed for the proposal of two new methylation-based biomarker panels for BlCa management. The first one focused on urothelial cancer (UC) detection by a panel of two methylated microRNAs promoters – *miR129-2* and *miR663a*. Using this panel, we were able to detect UC in voided urines, with a high performance and, discriminated UC from other genitourinary neoplasms. The second proposed panel was a multiplex panel composed by *miR663a* and VIM methylation and was more targeted to BlCa detection within an “at-risk” population, e.g. patients without cancer but showing shared symptoms. With this study we were able to show that *miR663a_{me}*-*VIM_{me}* panel could eventually help in the reduction of unnecessary cystoscopies, by specifically identifying BlCa patients among other urogenital diseases patients. Moreover, we have also showed that *miR663a_{me}* analysis might provide relevant information for patient monitoring, identifying patients at higher risk for cancer progression. The results obtained from this Thesis also allowed for an improvement on the knowledge of BlCa disease biology. Firstly, we have investigated the histones deacetylases class of

enzymes, the Sirtuins. Herein, *SIRT7* was identified as an important molecular player for cells invasive phenotype and the EMT process. *In vitro* studies showed that cells with reduced SIRT7 displayed decreased ECAD, while mesenchymal markers were augmented. Moreover, increased EZH2 acetylation and H3K27^{me3} deposition in *CDH1* promoter was also found in sh-SIRT7 cells, contributing to the ultimate repression of this cadherin expression. Thus, unveiling a new regulation axis in BICa, connecting SIRT7-EZH2-CDH1. Since EMT was implicated in the acquisition of more aggressive BICa phenotype, the usefulness of the current molecular classification was assessed in a BICa cohort of both NMIBC and MIBC disease, and the potential contribution of the EMT marker VIM to the stratification strategy. In here, we showed that the current classification has the potential to be implemented in routine, but further adjustments in practical scoring should be defined, and extended to NMIBC. Moreover, in NMIBC patients, higher vimentin immunoexpression endured poorer disease-free survival, and increased expression was observed from normal bladder-NMIBC-MIBC-metastases. Thus, we propose a focus on finding additional markers, including those related to EMT, which may further refine BICa molecular taxonomy. Finally, and as we had previously found that *VIM* promoter methylation accurately identified UC and that its expression associated with unfavourable prognosis, we sought to investigate *VIM* expression regulation and its role in malignant transformation and progression of BICa. In fact, were able to demonstrate that *VIM* promoter was epigenetically regulated in normal and neoplastic urothelial cells, involving histone PTMs and promoter methylation, which determine a VIM switch associated with EMT and acquisition of invasive and metastatic properties. These findings might allow for the development of new, epigenetic-based, therapeutic strategies for BICa. Overall, the work presented in this Thesis provided both clinical and mechanistic views of how epigenetic mechanisms deregulation can either be used as auxiliary tools for BICa detection and prognostic management, and as direct players in various steps of bladder carcinogenesis processes.

Resumo

O cancro da bexiga (BICa) é o décimo tipo de cancro mais comum em todo o mundo, com uma estimativa de 400.000 novos casos por ano e 160.000 mortes em ambos os sexos. Nas regiões mais desenvolvidas, o BICa é o sexto cancro mais incidente em homens e representa um importante problema de saúde. Os carcinomas da bexiga que invadem a camada muscular (MIBC) representam a forma mais agressiva, com maior probabilidade de progressão e metastização, ao passo que os tumores que não invadem a camada muscular (NMIBC) são caracterizados principalmente por apresentarem múltiplas recorrências locais, que eventualmente poderão progredir para doença avançada ao longo do tempo. Nos últimos anos, num esforço para melhor compreender os mecanismos moleculares associados à carcinogénese do BICa, e para melhor estratificar e tratar estes doentes, foi também proposta uma classificação molecular para os MIBC.

As alterações nos mecanismos epigenéticos, em que se englobam a metilação do DNA, as modificações pós-traducionais de histonas (PTMs), os remodeladores da cromatina e os RNAs não-codificantes implicadas na tumorigénese são também utilizadas como biomarcadores nesta doença. Especificamente, a metilação do promotor do DNA de genes codificantes e genes não-codificantes de proteínas mostrou ser útil para detecção/diagnóstico precoce não invasivo, bem como para o prognóstico e predição de resposta às terapias.

Deste modo, o objetivo principal desta Tese foi explorar a contribuição da desregulação dos mecanismos epigenéticos em BICa, seja numa abordagem clínica - através da proposta de novos biomarcadores para detecção e gestão desta doença - como numa abordagem da biologia do tumor da bexiga - ao investigar os mecanismos de ação das enzimas epigenéticas mais estudadas, assim como a regulação epigenética de genes implicados no fenótipo invasivo dos BICa.

Em relação à abordagem clínica, os resultados obtidos nesta Tese permitiram a proposta de dois novos painéis de biomarcadores, baseados na metilação do DNA, para os BICa. O primeiro estudo foi direcionado para a detecção dos carcinomas uroteliais (UC) por um painel composto pela metilação do promotor de dois microRNAs - *miR129-2* e *miR663a*. Ao aplicar este painel, fomos capazes de detectar UC, com óptima eficiência, em urinas de doentes com BICa, e discriminar estes tumores de outras neoplasias genitourinárias. O segundo painel que propomos é um painel multiplex composto pela metilação do promotor do *miR663a* e da *VIM*, e foi direcionado para a detecção de BICa dentro de uma população "em risco", por exemplo, pacientes sem diagnóstico de neoplasia da bexiga, mas que apresentam sintomas comuns a esta doença. Com este estudo conseguimos demonstrar

que o painel miR663a_{me}-VIM_{me} poderá auxiliar na redução de cistoscopias desnecessárias, e identificar especificamente doentes com BICa entre outros doentes com patologias urogenitais. Além disso, demonstramos também que a análise do miR663a_{me} poderá fornecer informações relevantes para a monitorização do doente, ao identificar os sujeitos com maior risco de progressão da doença.

Os resultados obtidos nesta Tese permitiram, também, um aprimoramento no conhecimento da biologia desta doença. Em primeiro lugar, investigamos uma classe de desacetilases das histonas, as Sirtuínas. Aqui, a SIRT7 foi identificada como uma molécula importante para o fenótipo invasor das células e para o processo da transição epitélio-mesênquima (EMT). Os estudos *in vitro* mostraram que as células com redução da proteína SIRT7 exibiram menos ECAD e um aumento nos marcadores mesenquimais. Além disso, estas mesmas células apresentaram o aumento da acetilação da EZH2 e da deposição da marca H3K27_{me3} no promotor da *CDH1*, o que contribuiu diretamente para a repressão final da expressão desta caderina. Assim, com este estudo, identificamos um novo eixo de regulação em BICa, que envolve as moléculas SIRT7-EZH2-CDH1.

Dado o papel preponderante da EMT na aquisição de um fenótipo mais agressivo em BICa, decidimos avaliar a utilidade da classificação molecular atual numa coorte de casos NMIBC e MIBC, e a potencial contribuição do marcador da EMT VIM para esta estratégia de estratificação. Neste estudo, mostramos que a classificação molecular tem potencial para ser implementada na rotina, embora devam ser realizados ajustes adicionais na sua aplicação prática, e a inclusão de tumores NMIBC. Além disso, e especificamente em doentes com NMIBC, a elevada imunoexpressão da VIM foi correlacionada com pior sobrevida livre de doença. Foi igualmente observado um aumento gradual da expressão de Vimentina desde os tecidos de urotélio normal, NMIBC, MIBC e metástases uroteliais. Assim, com este estudo, sugerimos que novos marcadores deverão ser adicionados à classificação molecular, incluindo marcadores relacionados com a EMT, para melhor refinar a taxonomia molecular destes tumores em contexto clínico.

Por último, e como tínhamos anteriormente observado que a metilação do promotor da *VIM* identificava com precisão casos de UC, e que sua expressão estava associada a um prognóstico desfavorável, procuramos investigar a regulação da expressão da *VIM* e seu papel na transformação maligna e progressão de BICa. De facto, neste último estudo, conseguimos demonstrar que o promotor da *VIM* é regulado epigeneticamente em células uroteliais normais e neoplásicas, e que esta regulação é feita através de PTMs de histonas e da metilação do seu promotor, que juntos determinam o “switch” na expressão da *VIM*. Este denominado “switch” está associado com a EMT e, conseqüentemente, com a aquisição de propriedades invasivas e metastáticas. Estas descobertas poderão permitir o

desenvolvimento de novas estratégias terapêuticas para BICa, baseadas na regulação epigenética desta molécula.

Em conclusão, o trabalho discutido nesta Tese forneceu novos princípios clínicos e mecanicistas de como a desregulação dos mecanismos epigenéticos poderá ser utilizada como ferramenta auxiliar na detecção/prognóstico de BICa, bem como agentes diretos nas várias etapas do processo de carcinogénese destes tumores.

Table of Contents

AUTHORS DECLARATION	V
AGRADECIMENTOS	VII
ABSTRACT	XI
RESUMO	XIII
TABLE OF CONTENTS	XVII
INDEX OF FIGURES	XIX
INDEX OF TABLES	XXIII
LIST OF COMMON ABBREVIATIONS	XXV
CHAPTER I – GENERAL INTRODUCTION	1
BLADDER CANCER	3
<i>The urinary bladder</i>	3
<i>Urothelial Carcinoma of the Bladder</i>	4
Epidemiology and Etiology of Bladder Cancer	5
Symptoms, Diagnosis and Tumour Staging and Grading	5
Approved Biomarkers for Bladder Cancer Detection and Management	8
Therapeutic Challenges and Molecular Classification of Bladder Cancer	10
MOLECULAR BASIS OF BLADDER CANCER	12
<i>Genetic alterations</i>	12
Mutations and Copy Number alterations	12
Models of Bladder Carcinogenesis Based on Genomic Alterations	13
<i>Epigenetic alterations</i>	14
DNA Methylation	15
Histone Post-Translational Modifications	17
Non-Coding RNAs.....	19
Methylation Biomarkers for Bladder Cancer – Current Challenges	19
EPITHELIAL TO MESENCHYMAL TRANSITION IN CANCER	22
<i>EMT Types, Markers and Regulation</i>	22
<i>EMT in Bladder Cancer</i>	24
<i>Review Paper - Epigenetic mechanisms influencing EMT in Bladder Cancer</i>	27
REFERENCES (CHAPTER I)	53
CHAPTER II – RATIONAL AND AIMS	65
CHAPTER III – DIAGNOSTIC/PROGNOSTIC EPIMARKERS IN BLADDER CANCER VOIDED URINES	69
<i>Paper I: MicroRNA promoter methylation: a new tool for accurate detection of urothelial carcinoma</i>	71
<i>Paper II: A Multiplex Test Assessing MiR663a_{me} and VIM_{me} in Urine Accurately Discriminates Bladder Cancer from Inflammatory Conditions</i>	89
CHAPTER IV – BLADDER CANCER MECHANISMS AND BIOLOGY	109
<i>Paper III: Sirtuins’ Deregulation in Bladder Cancer: SIRT7 is Implicated in Tumour Progression through Epithelial to Mesenchymal Transition Promotion</i>	111
<i>Paper IV: Practicability of clinical application of bladder cancer molecular classification and additional value of epithelial-to-mesenchymal transition: prognostic value of vimentin expression</i>	145
<i>Paper V: Epigenetic deregulation of Vimentin expression in Bladder Cancer associates with acquisition of invasive and metastatic phenotype through epithelial to mesenchymal transition</i>	167
CHAPTER V – MAJOR FINDINGS	193

CHAPTER VI – GENERAL DISCUSSION.....	199
REFERENCES (CHAPTER VI)	211
CHAPTER VII – CONCLUSIONS AND FUTURE PERSPECTIVES	215
APPENDIX – ORIGINAL PDF FILES OF THE PUBLISHED PAPERS INCLUDED IN THE THESIS	219

Index of Figures

Chapter I

General Introduction

Figure 1. Illustration of the bladder wall composition and tumour invasion by stage. Created with BioRender.com.....	3
Figure 2. Estimated number of major cancer incident cases and deaths worldwide, both sexes, all ages. Adapted from (2).....	4
Figure 3. Different types of epigenetic information. DNA methylation, histone variants and post-translational modifications, chromatin remodelling complexes and RNA-mediated gene silencing constitute the main distinct mechanisms of epigenetic regulation. Created with BioRender.com...	14
Figure 4. DNA methylation changes in cancer: Tumour-suppressor genes promoter hypermethylation and global genome-wide methylation loss.....	20

Review Paper

Figure 1. In silico analysis of The Cancer Genome Atlas database for bladder cancer (using the online resource cBioPortal for Cancer Genomics).	30
Figure 2. Epigenetic mechanisms' interplay with the epithelial-to-mesenchymal transition process in bladder cancer.	43

Chapter III

Paper I

Figure 1. Distribution of miR-129-2 and miR-663a promoter methylation levels in normal urothelium and urothelial carcinoma tissue samples.	78
Figure 2. ROC curves evaluating the performance of the gene panel promoter methylation (mir-129-2/miR-663a) for the identification of urothelial carcinoma in tissue and for discrimination of UC from other genitourinary malignancies in urine samples.	79
Figure 3. Percentage of urothelial carcinoma cases correctly identified with the gene panel promoter methylation test and a standard cytopathology analysis.	80

Paper II

Figure 1. Distribution of VIM_{me} and $miR663a_{me}$ levels in normal bladder mucosae and bladder carcinoma tissue samples. ROC curve evaluating the performance of the VIM_{me} - $miR663a_{me}$ panel for the identification of BICa in tissue samples.	96
--	----

Figure 2. Distribution of VIM _{me} and miR663a _{me} levels in the Testing Cohort, composed by healthy donors and bladder carcinoma urine samples. ROC curve evaluating the performance of the VIM _{me} -miR663a _{me} panel for the identification of BICa in urine samples of the Testing Cohort.	96
Figure 3. Distribution of VIM _{me} and miR663a _{me} levels in the Validation Cohort #1, composed by healthy donors and bladder carcinoma urine samples. ROC curve evaluating the performance of the VIM _{me} -miR663a _{me} panel for the identification of BICa in urine samples of the Validation Cohort #1. Distribution of VIM _{me} and miR663a _{me} levels in the Validation Cohort #2, composed by inflammatory controls and bladder carcinoma urine samples.	97
Figure 4. Representation of the percentage of BICa cases correctly identified with the VIM _{me} -miR663a _{me} panel and a standard urine cytology analysis.	98
Figure 5. Proposed algorithm for the combination of urine cytology and VIM _{me} -miR663a _{me} panel as a first-line diagnostic tests in patients with common urinary complaints.	103

Chapter IV

Paper III

Figure 1. Sirtuin family transcript levels characterization in bladder urothelial carcinoma.	115
Figure 2. <i>SIRT7</i> expression downregulation in invasive and TCGA “basal-like” urothelial tumors.	116
Figure 3. <i>SIRT7</i> expression in bladder cancer cell lines.	118
Figure 4. <i>SIRT7</i> downregulation promotes invasiveness and EMT in bladder cancer cells.	120
Figure 5. <i>SIRT7</i> downregulation associates with E-Cadherin repression mediated by histone methyltransferase EZH2.	122
Supplementary Figure S1. Characterization of <i>SIRT1</i> , <i>SIRT2</i> , <i>SIRT3</i> , <i>SIRT4</i> and <i>SIRT5</i> , and <i>SIRT6</i> and <i>SIRT7</i> in the TCGA bladder cancer cohort by quantitative RT-PCR.	138
Supplementary Figure S2. Characterization of Sirtuin family (<i>SIRT1</i> to <i>SIRT7</i>) gene expression in bladder cancer tissues and TCGA cohort categorized by clinical grade.	139
Supplementary Figure S3. Immunohistochemistry representative images for <i>SIRT7</i> immunoexpression in normal urothelium and bladder urothelial carcinoma tissue sections.	140
Supplementary Figure S4. Immunofluorescence representative images for <i>SIRT7</i> immunoexpression in MGHU3, 5637 and J82 bladder cancer cell lines.	140
Supplementary Figure S5. Immunofluorescence representative images for E-Cadherin and N-Cadherin immunoexpression in sh-CTRL and sh- <i>SIRT7</i> MGHU3, 5637 and J82 bladder cancer cell lines.	141
Supplementary Figure S6. Characterization of <i>CDH1</i> gene expression in the bladder cancer and normal mucosae tissue samples, and in NMIBC and MIBC, by quantitative RT-PCR. Characterization of <i>CDH2</i> gene expression in the bladder cancer and normal mucosae tissue samples, and in NMIBC and MIBC cases, by quantitative RT-PCR.	142
Supplementary Figure S7. Heat map showing <i>SIRT7</i> and <i>EZH2</i> expression in MIBC cases.	143

Paper IV

Figure 1. Immunoexpression of luminal and basal markers in the bladder cancer cohort.	153
Figure 2. Correlation between mRNA and protein expression of the several luminal and basal markers in the bladder cancer cohort (both MIBC and NMIBC included).	154
Figure 3. <i>Vimentin</i> transcript and protein levels within the bladder cancer cohort.	155
Figure 4. Disease-free survival in NMIBC patients according to vimentin protein expression.	156
Figure 5. Immunoexpression of vimentin in the bladder cancer cohort.	156
Supplementary Figure 1. Immunoexpression of neuroendocrine markers in a bladder cancer specimen negative for CK5/6, FOXA1 and GATA3.	165

Paper V

Figure 1. <i>VIM</i> expression and methylation in normal urothelium and bladder cancer tissues.	178
Figure 2. Cadherins genes expression in bladder cancer tissues.	179
Figure 3. <i>VIM</i> expression in bladder cancer cell lines.	180
Figure 4. <i>VIM</i> methylation modulation in bladder cancer cell lines.	180
Figure 5. ChIP-qPCR results for J82 and TCCSUP cell lines concerning acH3, H3K4me3, H3K36me2 and H4K20me3 histones marks across <i>VIM</i> promoter, after treatment with epigenetic modulating drugs. ChIP-seq representative results for NHU cells across <i>VIM</i> gene promoter and body. ChIP-qPCR results for NHU cells concerning H3K9ac, H3K27ac, H3K4me3, H3K9me3 and H3K27me3 histones marks across <i>VIM</i> promoter.	182
Figure 6. <i>VIM</i> downregulation promotes invasiveness and EMT in bladder cancer cells.	184
Supplementary Figure 1. <i>VIM</i> expression and methylation in normal urothelium, bladder cancer and bladder cancer metastasis.	191
Supplementary Figure 2. Comparison between <i>VIM</i> and Cadherins genes transcript levels.	192
Supplementary Figure 3. ChIP-qPCR for histone PTMs across <i>VIM</i> promoter, in SVHUC1 immortalized urothelial cell line.	192

Chapter VI

Figure 1. Schematic representation of the major outcomes achieved in this doctoral Thesis.	210
--	-----

Index of Tables

Chapter I

General Introduction

Table 1. Tumour, Node, Metastasis (TNM) classification system for bladder cancer. Adapted from (19).....	7
Table 2. List of FDA approved available urinary biomarkers for Bladder Cancer. Adapted from (31).	9

Review Paper

Table 1. Epigenetically modulated protein-coding genes implicated in Bladder Cancer EMT.	32
Table 2. Non-coding RNAs associated with EMT in bladder cancer.	35

Chapter III

Paper I

Table 1. Clinical and histopathological characteristics of patients with urothelial carcinoma and providers of normal urothelium.	75
Table 2. Clinical and histopathological characteristics of patients with urothelial carcinoma and of controls, which provided urine samples for this study.	76
Table 3. Performance of epigenetic biomarkers for the detection of urothelial carcinoma in tissue and urine.	79
Supplementary Table 1. Cox regression models assessing the potential of clinical and epigenetic variables in the prediction of disease-specific survival of BUC and UTUC patients separately and combined as Urothelial carcinoma.	88

Paper II

Table 1. Clinical and histopathological characteristics of patients with bladder carcinoma (BICa), normal bladder mucosae, healthy donors and inflammatory controls.	93
Table 2. Performance of VIM _{me} -miR663a _{me} panel for the detection of bladder cancer in Validation Cohorts #1 and #2.	98
Table 3. Cox regression models assessing the potential of clinical and VIM _{me} and miR663a _{me} levels in the prediction of disease-specific survival for bladder carcinoma patients.	100
Table S1. Sequences of the primers and probes used in the quantitative methylation-specific PCR experiments.	108

Chapter IV

Paper III

Table 1. Clinical and histopathological parameters of Bladder Cancer patients, and gender and age distribution of control set individuals.	126
Table 2. Clinical and histopathological parameters of bladder cancer patients, and gender and age distribution of control set individuals from TCGA cohort.	128
Supplementary Table 1. Reference of TaqMan® gene expression assays for studied genes.	137
Supplementary Table 2. Primer sequences used in RT-PCR for studied genes.	138

Paper IV

Table 1. Clinicopathological features of the study cohort.	149
Table 2. Immunoexpression of luminal and basal markers in the bladder cancer cohort.	152
Supplementary Table 1. Immunohistochemistry methods.	164
Supplementary Table 2. Primers sequences.	164

Paper V

Table 1. Clinical and histopathological parameters of Bladder Cancer patients, and gender and age distribution of control set individuals.	171
Table 2. Pearson correlation between <i>CDH1</i> , <i>CDH2</i> , <i>CDH3</i> and <i>VIM</i> transcript levels in Bladder cancer tissues.	179
Supplementary Table 1. Primer sequences used in qMSP and RT-qPCR for studied genes.	190
Supplementary Table 2. References of antibodies used in ChIP assays for studied histones and histones posttranslational modifications.	191

List of Common Abbreviations

A

ACTB: β -Actin
AUC: Area Under the Curve

B

BCG: Bacillus Calmette-Guerin
BICa: Bladder Cancer
bp: Base Pair
BTA: Bladder Tumour Antigen

C

CDH1: Cadherin 1
CDH2: Cadherin 2
CDH3: Cadherin 3
CDKN2A: Cyclin Dependent Kinase Inhibitor 2A
ChIP: Chromatin Immunoprecipitation
CI: Confidence Interval
Cis: Carcinoma in situ
CK5/6: Cytokeratin 5/6
CSS: Cancer-Specific Survival
CpG: Cytosine-phosphate-Guanine

D

DAC: 5'aza-2'-deoxycytidine
DFS: Disease-Free Survival
DNA: Deoxyribonucleic Acid
DNMT: DNA Methyltransferases
DSS: Disease-Specific Survival

E

ECAD: Epithelial Cadherin
EMT: Epithelial-to-Mesenchymal Transition
EZH2: Enhancer Of Zeste 2 Polycomb Repressive Complex 2 Subunit

F

FAM: 6-carboxy-fluorescein
FBS: Fetal Bovine Serum
FGFR3: Fibroblast growth factor receptor 3
FOXA1: Forkhead Box A1

G

GATA3: GATA Binding Protein 3
GUSB: Beta Glucuronidase

H

H3: Histone H3
H3K4: Lysine 4 of Histone H3
H3K9: Lysine 9 of Histone H3
H3K27: Lysine 27 of Histone H3
H3K36: Lysine 36 of Histone H3
H3K79: Lysine 79 of Histone H3
H4: Histone H4
H4K20: Lysine 20 of Histone H3
HAT: Histone Acetyltransferase
HD: Healthy Donors
HDAC: Histone Deacetylase
HDM: Histone Demethylase
HG: High Grade
HMT: Histone Methyltransferase
HPRT: Hypoxanthine Phosphoribosiltransferase
HR: Hazard Ratio

I

IF: Immunofluorescence
IHC: Immunohistochemistry
IHG: Invasive High-Grade Bladder Cancer
IP: Immunoprecipitation

K

Kb: Kilobase
KRT5: Keratin 5
KRT6: Keratin 6

L

LG: Low Grade
lncRNA: Long non-coding RNA
LOH: Loss of Heterozygosity

M

MBD: Methyl-CpG-Binding Domain

MET: Mesenchymal-to-Epithelial Transition
MIBC: Muscle-Invasive Bladder Cancer
miRNA: microRNA
MMP: Metalloproteinase
mRNA: Messenger RNA
MSP: Methylation-Specific PCR
MTT: 3-(4,5-dimethyl-2-thiazolyl)-2,5
diphenyl-2H-tetrazolium bromide assay
MVAC: Methotrexate, Vinblastine,
Adriamycin and Cisplatin

N

NAC: Neoadjuvant Chemotherapy
NB: Normal Bladder
NCAD: Neural Cadherin
ncRNA: Non-coding RNA
NMIBC: Non-Muscle Invasive Bladder
Cancer
NPV: Negative Predictive Value
NUTU: Normal Upper Tract Urothelium

O

OS: Overall Survival
OR: Odds Ratio

P

PBS: Phosphate-Buffered Saline
PCa: Prostate Cancer
PCAD: Placental Cadherin
PCR: Polymerase Chain Reaction
PHG: Papillary High-Grade Bladder Cancer
PLG: Papillary Low-Grade Bladder Cancer
PPV: Positive Predictive Value
PRC: Polycomb Repressive Complex
pT: Pathological Stage
PTM: Post-Translational Modification
PUNLMP: Papillary Urothelial Neoplasm of
Low Malignant Potential

Q

qMSP: Quantitative Real-Time Methylation-
Specific PCR

R

RB: RB Transcriptional Corepressor 1
RISC: RNA-Induced Silencing Complex
RNA: Ribonucleic Acid
ROC: Receiver Operator Characteristics
RT-qPCR: Reverse Transcription
Quantitative Polymerase Chain Reaction

S

SAM: S-adenosylmethionine
siRNA: Small Interfering RNA
SIRT: Sirtuin
shRNA: Short-Hairpin RNA
SNAIL1: Snail family transcriptional
repressor 1
sncRNA: Small non-coding RNA

T

TAMRA: 6-carboxy-tetramethyl-rhodamine
TCGA: The Cancer Genome Atlas
TERT: Telomerase Reverse Transcriptase
TF: Transcription Factor
TGF- β : Transforming Growth Factor Beta
TNM: Tumor, Node and Metastasis system
TP53: Tumor Protein 53
TSA: Trichostatin A
TSG: Tumor Suppressor Gene
TSS: Transcription Start Site
TURBT: Transurethral Resection of the
Bladder Tumour

U

UC: Urothelial Cancer
UTR: Untranslated Region
UTUC: Upper Tract Urothelial Carcinoma

V

VIM: Vimentin

Z

ZEB1: Zinc Finger e-box binding homeobox

CHAPTER I – General Introduction

Bladder Cancer

The urinary bladder

The urinary bladder is a muscular organ made out of singular tissue layers, and acts as a transient storage compartment for urine, which contains various waste compounds filtered by the kidneys. The urothelium is the innermost stratified epithelium, composed by 5-7 cell layers, which covers most of the urinary tract, including the upper tract renal pelvis and ureters, and lower tract bladder and urethra. This specialized epithelium is composed of basal, intermediate, and luminal cells, and performs as a tight barrier for urine, achieved primarily by the unique specialization of the apical plasma membrane of the superficial luminal cells (also called umbrella cells). This particular layer is mechanically flexible, which takes into account the filling and voiding of the bladder. Underneath the umbrella cells layer we can find the intermediate cells, which may vary in number, followed by a one-cell layer of basal cells directly adjacent to the basement membrane. The basal cells layer is also the site where new urothelial cells arise, with a slow regeneration rate, which increments in response to inflammation or injury conditions. Past the basement membrane, the submucosa, or lamina propria, can be found. This collagen-rich and highly vascularized elastic layer of connective tissue and nerves is, in turn, surrounded by smooth muscle (also known as muscularis propria), that on the outside is covered by a layer of perivesical fat (Figure 1) (1).

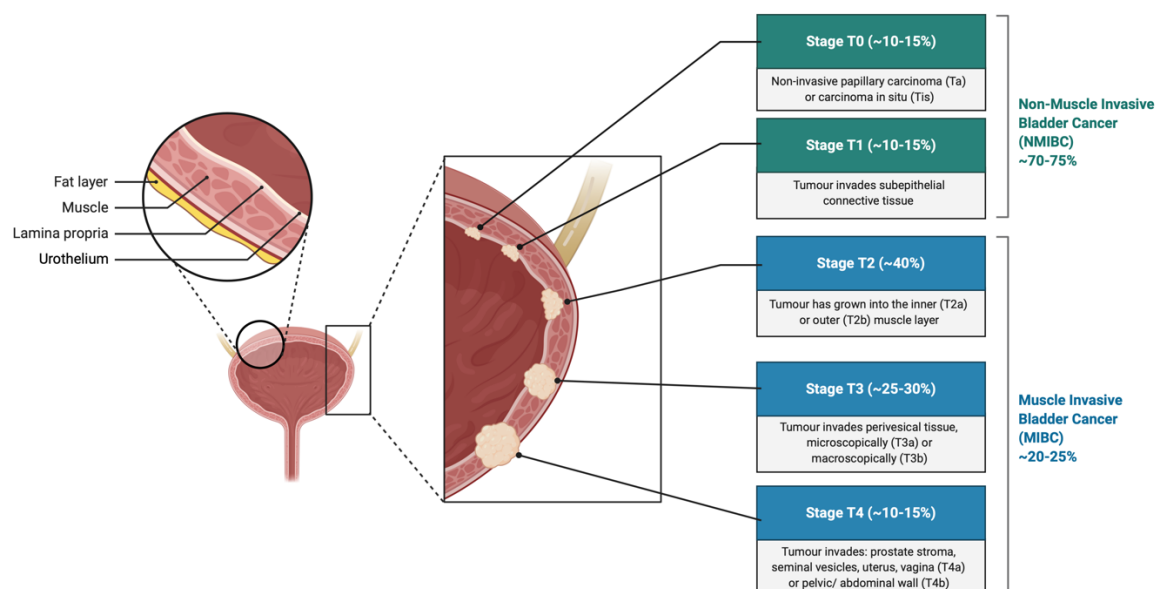


Figure 1. Illustration of the bladder wall composition and tumour invasion by stage. Created with BioRender.com.

Urothelial Carcinoma of the Bladder

Bladder cancer (BICa) is one of the most common malignancies worldwide, ranking tenth in incidence worldwide. It is expected that, by 2040, the number of estimated new cases and cancer-related deaths will almost double the 549,393 newly diagnosed cases and 199,922 deaths recorded in 2018 (Figure 2) (2, 3). In men, where the incidence is roughly 3-4-fold higher when compared to women, BICa represents the second most frequent urological malignancy after prostate cancer. Bladder cancer can occur at any age, but the risk increases with age, with a median age of diagnosis of 70 years old (4). Similar to other urological malignancies, mortality-to-incidence ratios are higher in underdeveloped countries, which probably reflects different environmental exposures and/or inequalities in healthcare accessibility (3). Importantly, due to its high prevalence, mortality and, particularly, the propensity for multiple recurrences and/or disease progression and consequent additional treatments, BICa is the costliest neoplastic disease, constituting an important financial burden (costs about €4.9 billion in the European Union, alone, in 2012) (5). Bladder cancer generally refers to a cancer derived from the urothelium, hence, although other much rarer tumour formations with other cellular origins occur, its major histological subtype is urothelial carcinoma (UC), which is the focus of this work. For this reason, the terms “urothelial carcinoma” and “bladder cancer” will be used somewhat as synonyms through this thesis.

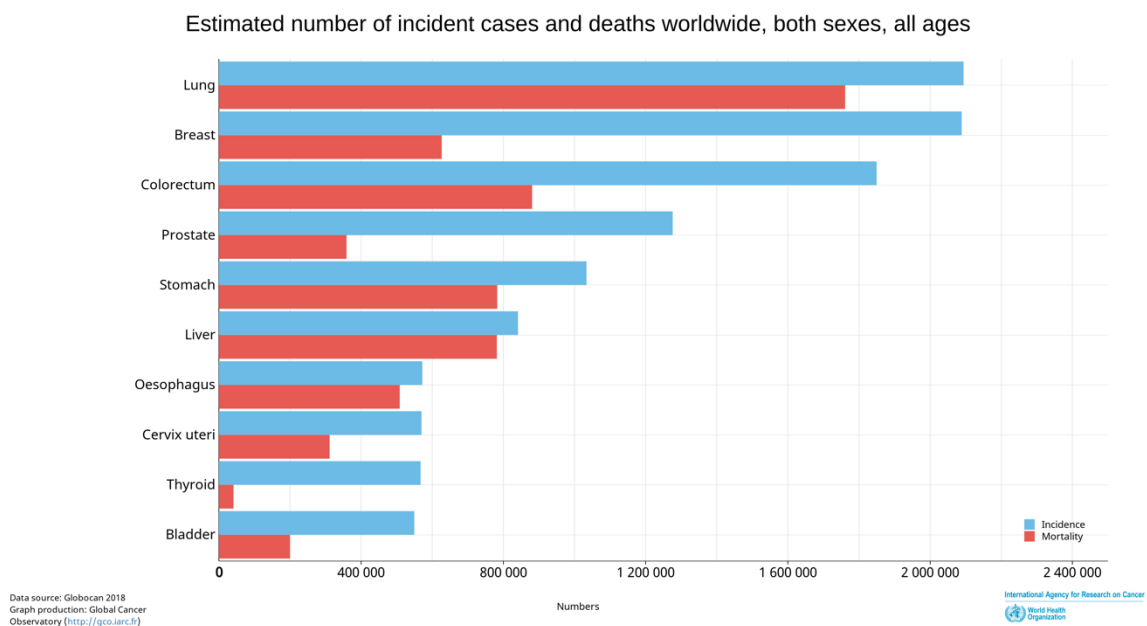


Figure 2. Estimated number of major cancer incident cases and deaths worldwide, both sexes, all ages. Adapted from (2).

Epidemiology and Etiology of Bladder Cancer

The main risk factor for BICa is smoking (6). Compared with non-smokers, the risk of smokers for developing the disease is approximately three times higher (7). It is estimated that about a quarter of bladder cancer in women and about half of bladder cancer in men can be attributed to smoking (7, 8). Although the link between tobacco and bladder cancer may seem hard to acknowledge, it is well explained by the fact that tobacco carcinogens are released and leave the body through the urinary tract. Indeed, when urine is in contact with the bladder for several hours at a time, this organ may be exposed to high levels of toxins produced by cigarette smoke, prolonging the contact of the later with the urothelium, which ultimately may provoke damage to these cells. Although the proportion of smokers in many countries has declined, the inevitable global population growth has translated into an increased total number of daily smokers in the last decades, contributing to the strong effect of smoking for the great majority of newly diagnosed cancers (9).

As stated before, urine is the vehicle for releasing waste compounds from our body, which can include not only carcinogens and toxins produced by smoking, but also from occupational exposure associated to some professions, as dye, rubber, metal, or petroleum workers, and hairdressers, for example. Indeed, occupational exposure to carcinogens such as polycyclic aromatic hydrocarbons, aromatic amines, heavy metals and combustion products, constitutes the second most relevant risk factor for BICa (10). It is estimated that about 8% of all BICa cases can be associated with occupational factors (11, 12). However, these numbers are expected to decrease, due to the evolution in the health authorities' inspections and regulations across the world.

Gender differences in the numbers of newly diagnosed BICa are still a challenge to solve, because gender-specific risk differences prevail even after model-adjusting for major risk factors such as smoking and occupational exposure. This could be due to some biological factors, such as differences in male vs. female anatomy and/or sex hormone composition (13, 14).

Symptoms, Diagnosis and Tumour Staging and Grading

Urothelial BICa mainly manifests either as a papillary growth into the bladder lumen, a flat lesion, or a solid tumour which may grow into the various bladder layers. More than 50% of most BICa cases are diagnosed after macroscopic blood (haematuria) is detected in the patient's urine, constituting the most common isolated symptom associated with the disease (15). Other symptoms include dysuria, frequent and/or sudden urge to urinate, and frequent

urinary tract inflammation or infections with microorganisms (6). The common diagnostic pathway for BICa is the follow: a patient presenting haematuria and/or other mentioned symptoms is proposed to do a cystoscopy - the procedure that allows for endoscopic bladder examination - along with a urine cytology, for morphological evaluation of the exfoliated cells (16). In some cases, imaging techniques, such as computerized tomography (CT), can be used as a complement to help in the differential diagnosis of other urogenital pathological conditions. When a suspected lesion is detected, according to the first clinical assessment of the disease extension providing a clinical tumour stage, a decision is made to either perform a transurethral resection of the bladder tumour (TURBT), where the identified lesion is removed by a tool designated resectoscope, or to perform a biopsy, for cases where the tumour is well spread into the bladder wall (16). For the first group of patients, TURBT is considered not only a diagnostic surgical procedure, but also a therapeutic one. For patients who fall under the second group, all bladder removal, or radical cystectomy, is the following act after TURBT (17).

After TURBT or cystectomy, the pathological evaluation can now be performed to determine not only the pathological stage (pT) using the Tumour, Node, Metastasis (TNM) classification system (Table 1), but also the histopathological designation of the tumour (18, 19). Regarding the TNM classification for BICa, it characterizes the extension of tumour growth into the various bladder tissue layers, and its spreading outside the bladder to other organs. Briefly, pathological stage Ta comprehends superficial malignant papillary lesions confined to the urothelial layer; stage Tis includes flat lesions that also never invade the basal membrane; stage T1 tumours show invasion of the lamina propria; stage T2 tumours extend into to the muscle layer; stage T3 tumours show invasion of the tissues adjacent to the bladder; and stage T4 tumours show an spread to surrounding organs such as the prostate, vagina, or the pelvic wall. Additional sub classification of the T2-T4 stages reflects the extent of invasion. To complete the assessment of the TNM classification, the presence of tumour spreading into lymph nodes (N) and/or distant metastasis (M) also have to be performed (19). Whereas the first can be obtained during the TURBT or cystoscopy procedure, to determine metastasis status other examination, such as CT-based techniques, have to be performed. A complete and thoroughly performed TNM staging is considered essential for BICa management, prognosis and therapeutics decision (Table 1).

Table 1. Tumour, Node, Metastasis (TNM) classification system for bladder cancer. Adapted from (19).

T – Primary Tumour	
Ta	Non-invasive papillary carcinoma
Tis	Carcinoma in situ: 'flat tumour'
T1	Tumour invades subepithelial connective tissue
T2	Tumour invades muscle
T2a	Tumour invades superficial muscle (inner half)
T2b	Tumour invades deep muscle (outer half)
T3	Tumour invades perivesical tissue:
T3a	microscopically
T3b	macroscopically (extravesical mass)
T4	Tumour invades any of the following: prostate stroma, seminal vesicles, uterus, vagina, pelvic wall, abdominal wall
T4a	Tumour invades prostate stroma, seminal vesicles, uterus or vagina
T4b	Tumour invades pelvic wall or abdominal wall
TX	Primary tumour cannot be assessed
T0	No evidence of primary tumour
N – Regional Lymph Nodes	
N0	No regional lymph node metastasis
N1	Metastasis in a single lymph node in the true pelvis (hypogastric, obturator, external iliac, or presacral)
N2	Metastasis in multiple regional lymph nodes in the true pelvis (hypogastric, obturator, external iliac, or presacral)
N3	Metastasis in a common iliac lymph node(s)
NX	Regional lymph nodes cannot be assessed
M – Distant Metastasis	
M0	No distant metastasis
M1a	Non regional lymph nodes
M1b	Other distant metastasis

Following the TNM classification, BICa is nowadays usually divided into non-muscle invasive bladder cancer (NMIBC), which comprehends stages Ta, Tis, and T1, and muscle invasive bladder cancer (MIBC), including stages T2-T4. This division is performed because the two categorized groups of cases usually show very different disease evolution and prognosis. NMIBC account for approximately 70%-75% of newly diagnosed BICa, whereas the remaining 25%-30% are MIBC (6, 20). Regarding NMIBC, although representing more

bladder confined disease with better initial prognosis, usually have a high propensity for tumour recurrence within the first years after treatment. It is estimated that, among all NMIBC patients, approximately 50% will relapse at some point, and 5%-20% will later develop MIBC (21, 22). On the other hand, MIBC cases have a considerable aggressive disease, which accompanies a higher risk of disease spreading and metastization. Due to this fact, if not early diagnosed, MIBC may ultimately lead to morbidity and death.

A grading system is also applied to BICa, with the tumours being graded histologically according to the degree of cell atypia, growth pattern and mitotic activity. This is an important classification due to the heterogeneity of NMIBC, and the difficulties that it entails to clinical management. Although tumour staging is the most important factor for treatment decision, the grade reflects the inherent aggressiveness of the tumour, constituting an important prognostic indicator (23). For this instance, a higher histological grade indicates a higher risk for recurrence or progression to MIBC, which may translate into more aggressive treatment and stricter disease follow-up. The most frequently used grading system is the WHO/ISUP 2004/2016 (International Society of Urological Pathology) grading system, first proposed in 1973, and updated in 1998, and then in 2004 and 2016 (24-27). The WHO/ISUP system classify tumors into two main categories: low-grade (LG) and high-grade (HG). Besides this, a third group designated papillary urothelial neoplasm of low malignant potential (PUNLMP) was created to discriminate low-grade urothelial tumours with a papillary architecture and relative low incidence of recurrence and progression (28).

Approved Biomarkers for Bladder Cancer Detection and Management

As previously mentioned, standard diagnostic tests for BICa include cystoscopy, and imaging-based techniques. However, these tests have limited sensitivity to small neoplastic lesions, which is the main reason many urologists rely on urine cytology as an auxiliary test. Despite its usefulness for accessing the morphology of exfoliated cells in the urine, cytology is also hindered by low sensitivity, sampling errors, deviations in the quality of urine processing, and differences between interpreters of cytopathology (16, 29, 30). Furthermore, there is an urgent demand for urinary biomarkers with improved sensitivity and specificity, so that the clinical management of BICa improves in a cost-effectiveness way.

Table 2. List of FDA approved available urinary biomarkers for Bladder Cancer. Adapted from (31).

Urinary Biomarker	Usage	Assay Principle	Sensitivity (%)	Specificity (%)	Reference
Cytology	Diagnosis & Follow-Up	Haematoxylin eosin staining	34 (20 – 53)	99 (83 – 99.7)	(30)
FISH – UroVysion	Diagnosis & Follow-Up	Gene amplification and aneuploidy detection	69–75	82–85	(32)
NMP 22	Follow-Up	ELISA	40	99	(37)
NMP 22	Diagnosis & Follow-Up	POC	62–74	74–84	(39)
BTA stat	Diagnosis & Follow-Up	Dipstick Immunoassay	70	75	(41)
BTA Trak	Diagnosis & Follow-Up	ELISA	65	65	(41)
ImmunoCyt	Follow-Up	Immunohistochemistry	77 – 90	68 – 83	(39)

Currently, besides urine cytology, there are a few FDA-approved urinary biomarkers for either diagnosis and/or follow-up of BICa patients (Table 2) (31). Among them, UroVysion (Abbott Laboratories, Abbott Park, Illinois, USA) is a test which detects aneuploidy for chromosomes 3, 7, 17, and loss of the 9p21 locus via fluorescence in situ hybridization (FISH) in urine, and was found to have a sensitivity and specificity of 72% and 83%, respectively (32). However, it demonstrates low sensitivity (41%) for the detection of low-grade tumours. Besides the diagnostic application, UroVysion has also been used in the follow-up of BICa patients, either to help predict and monitor disease recurrence, and also for BCG-therapy response monitoring (33-35). Nuclear matrix proteins (NMP22) are highly detected in urines from BICa patients, which led to the development of two NMP22-based assays for BICa surveillance (36). Although the tests sensitivity is higher than cytology, specificity is significantly lesser (37). Furthermore, for surveillance purposes, combining NMP22 tests with cystoscopy significantly increases the detection of recurrent tumours (38, 39). Also, for surveillance purposes, and in combination with cystoscopy, two more tests, one quantitative and another qualitative assay, based on the bladder tumour antigen (BTA) were approved by de FDA. Although receiving the approval, these tests are not widely used

in clinical practice due to their relative low sensitivity and specificity (40, 41). Lastly, the ImmunoCyt (Diagnocure Inc, Quebec, Canada) assay, which is based on the use of three fluorescent monoclonal antibodies to detect M344, LDQ10, and 19A11 antigens in exfoliated cells acquired through urine cytology. Albeit the general improvement that ImmunoCyt assay brings to the conventional urine cytology test results, especially for sensitivity, it does not rule out the need for a cystoscopy (32, 42, 43).

Therapeutic Challenges and Molecular Classification of Bladder Cancer

On the therapeutic front, the clinical management of NMIBC and MIBC cases is very distinct, and it remained almost unchanged until the approval of immune checkpoint inhibitors in first-line or metastatic settings (44-46). While the first line treatment for the majority of BICa cases is the surgical removal of the tumour or the whole bladder, many patients also fulfil a therapeutic drug-based plan as part of their treatment plan, which depends on tumour stage and grade, as well as other factors. For patients with NMIBC disease who have undergone TURBT, intravesical immunotherapy in the form of Bacillus Calmette-Guerin (BCG) instillations or intravesical cytostatic chemotherapy using Mitomycin C, a DNA crosslinking drug, is generally suggested. Intravesical instillations is particularly suitable for NMIBC due to the anatomical characteristics of the bladder, allowing for a prolonged exposure to the therapeutic agent directly to the target-cells, and aiming to reduce the risk of recurrence and progression. For MIBC, before cystectomy, and if the patient is eligible, a systemic neoadjuvant chemotherapy (NAC) to target potential micrometastatic disease may be suggested, and it has been shown to improve overall survival (OS) and cancer specific survival (CSS) in some cases (47-49). Either for neoadjuvant or adjuvant settings, the offered chemotherapy options for MIBC patients mainly consists of cisplatin-based combination, e.g. gemcitabine and cisplatin, or methotrexate, vinblastine, adriamycin, and cisplatin (MVAC) (50). Recently, and especially for patients with advanced and metastatic bladder cancers as well as specific other forms of the disease, immunotherapy (checkpoint-inhibitors) has been used as a treatment option. Immunotherapy drugs approved for treating BICa patients include: Atezolizumab (Tecentriq), Durvalumab (Imfinzi), Nivolumab (Opdivo), Avelumab (Bavencio) and Pembrolizumab (Keytruda) (16).

Nevertheless, a considerable percentage of BICa patients do not benefit from current treatment options. Clinicians still have to deal with a high number of cases with recurrence and progression and, as a result, patients endure a long follow-up, making BICa one of the

costliest malignancies worldwide (5). Hence, there is a need to improve risk stratification of these patients and to uncover biomarkers that may better select patients to the specific therapy that will give the higher benefit with less toxicity. In this line, an effort has been made to improve BICa classification; various research teams have reported the importance of a molecular stratification of BICa, and presented classifications based on different molecular traits, either for all urothelial carcinomas, or focusing on NMIBC and MIBC separately (51-61). This molecular stratification is also useful for predicting responses to current treatment options and provides insights for the development of new therapies (56, 62-65). Although specific differences in classification emerge out of each research group analyses, they all share as an overlapping feature the existence of two major BICa subtypes - basal/squamous and luminal - for MIBC cases (66). Briefly, basal/squamous subtype are commonly advanced stages and metastatic disease, being enriched in inactivating mutations and deletions of TP53 and RB1 genes, whereas the luminal subtype is associated with papillary histopathological features and enriched in fibroblast growth factor receptor 3 (FGFR3) mutations (67, 68). An effort has been made to reach a single consensus classification and to generate a list of specific biomarkers (such as FOXA1, GATA3, KRT5/6 and KRT14) that can be effectively translated from wide screening genomic and transcriptomics analyses into the clinic for any BICa setting (both MIBC or NMIBC) (54, 67). However, to date, this has not been achieved.

Molecular Basis of Bladder Cancer

Due to relatively low sensitivity and/or specificity, the approved biomarker-based methods have not been widely and consistently used in routine. Therefore, not only a reliable, accurate and convenient method for diagnosing and monitoring the recurrence/progression of NMIBC is needed, but also the identification of new therapeutic targets for MIBC patients. Moreover, understanding the molecular basis of BICa is of great significance for guiding clinical decision-making, hence the above-mentioned investment in the molecular classification of this tumours. With the fast improvement of high-throughput DNA sequencing technology, numerous genome and epigenome changes have been discovered, bringing a step forward in uncovering the molecular basis of BICa. A special detailed description on epigenetic alterations will be given, since these will be the focus of this Thesis.

Genetic alterations

Mutations and Copy Number alterations

Bladder cancer exhibits extensive and frequently occurring somatic DNA changes, including mutations and copy number alterations, constituting one of the most mutated cancers, with an average total mutation burden of 7.7 mutations per megabase and 302 exon mutations per tumour (61, 67, 69).

Low-grade tumours are usually near-diploid, with a limited number of mutations in oncogenes that drive hyperproliferation (such as FGFR3, PI3KCA, and HRAS), accompanied by inactivation of CDKN2A, which encodes the cell cycle inhibitor p16INK4A. On the other hand, invasive cancer usually encompasses a high rate of point mutations in various oncogenes and TSGs and has a large number of numerical and structural chromosomal aberrations. Mutations which lead to TP53 inactivation and hTERT (telomerase) promoter activation are the most common, while FGFR3 mutations are rare (61).

Some mutations on genes responsible by cell division and checkpoint proteins may cause chromosomal instability. Invasive tumours are generally rich in CDKN2A homozygous deletions, which is primarily due to the deletion of chromosome 9, which is seen in >50% of BICa cases. Moreover, amplification of CCND1/Cyclin D1 and CCNE1/ Cyclin E1 may also drive cell cycle control loss in these tumours.

Whereas MIBC often show extensive genomic instability, low-grade tumours have relatively few genomic alterations (70). Recent studies showed that, while the overall frequency of individual tumour alterations can be minute, nearly every analysed single tumour show some form of genetic alteration or dysregulation within the major pathways (67).

Models of Bladder Carcinogenesis Based on Genomic Alterations

Various models have been proposed for the development of non-invasive and invasive BICa (71, 72). The loss of heterozygosity (LOH) of chromosome 9 in the normal urothelium is not only related to BICa, but also to the formation of hyperplasia and dysplasia, which may indicate that this change is involved in the earliest stage of these tumours (73). According to the histological and molecular characteristics, the development of BICa can be divided into two models: the papillary and the carcinoma in situ (Cis) pathways (72, 74-76).

The papillary pathway begins with the formation of hyperplasia caused by the deletion of chromosome 9 and FGFR3/RAS mutations, which in turn are mutually exclusive with urothelial hyperplasia (77). FGFR3 mutations are very frequent in NMIBC (80% of cases) and are associated with a higher risk of recurrence (78). Similarly, when PIK3CA/STAG2 mutation occurs, the lesions progress to a low-grade stage Ta tumour, which in turn, may develop into a high-grade non-invasive Ta tumour, although the genomic alterations underlying this progression are still rather unknown (73, 78). On the other hand, invasive tumors are considered to be caused by Cis or urothelial hyperplasia, as a result of RB1 and TP53 mutations and genome instability (73, 78). Mutations in TP53 and additional genomic aberrations are proposed as events almost exclusive of the Cis pathway that promote the progression of NMIBC to MIBC, eventually leading to metastases formation on some cases (70).

Although the model of two BICa pathways corresponds well to the wide variation patterns observed between NMIBC and MIBC, it does not fully describe the complexity of how BICa develops and progresses, nor it explains the multiple subtypes described in light with recent proposed molecular classification.

Epigenetic alterations

The term *Epigenetics* was first used by C. H. Waddington in 1941, when referring to the study of the “causal mechanisms by which the genes of the genotype bring about phenotypic effects. A decade later, DNA was identified as the molecule of inheritance by Watson and Crick, and since then the definition of Epigenetics suffered an evolution. The actual definition of Epigenetics is now less focused on genotype, and more related to mechanisms that control gene expression in a potentially heritable way, with no change in the primary DNA sequence (79, 80). Epigenetic changes are preserved when cells divide and the majority of these only occur within the course of one individual organism's lifetime. However, if epigenetic changes which result in gene deactivation occurs in a sperm or egg cell that will be later fertilized, these can be transferred to the next generation (81, 82).

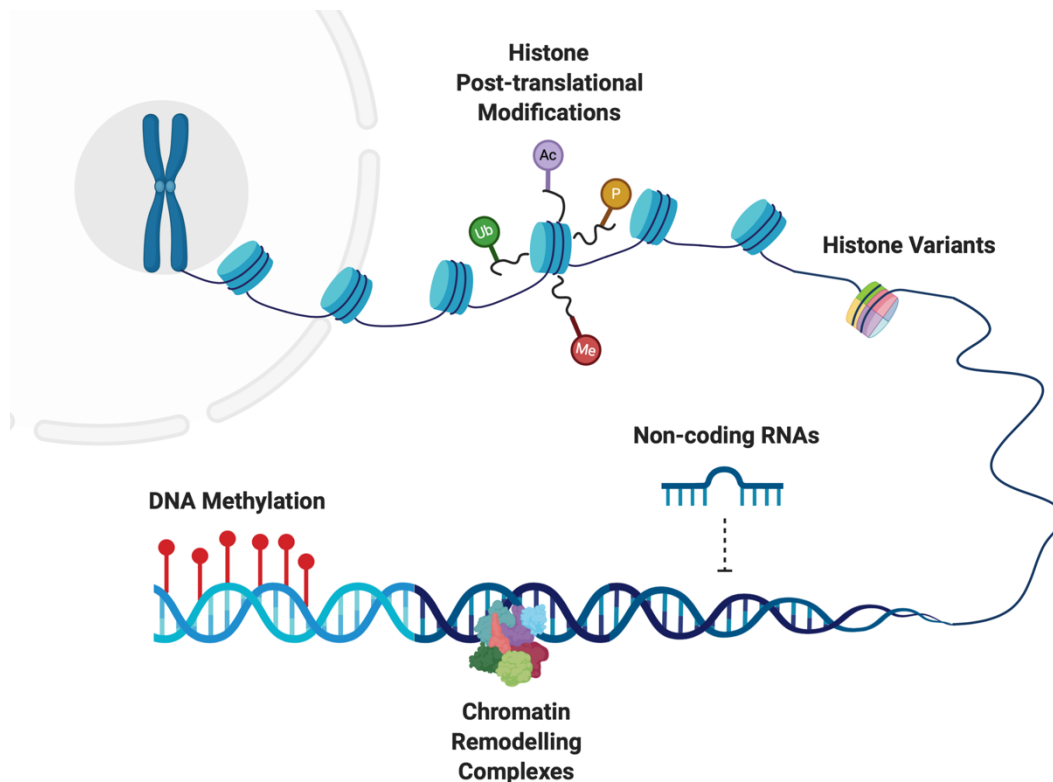


Figure 3. Different types of epigenetic information. DNA methylation, histone variants and post-translational modifications, chromatin remodelling complexes and RNA-mediated gene silencing constitute the main distinct mechanisms of epigenetic regulation. Created with BioRender.com.

The epigenetic molecular mechanisms may be grouped into major categories: DNA methylation, histone variants, chromatin remodelling, and histone post-translation modifications (Figure 3). Although the controversy regarding RNA-associated

transcriptional silencing by non-coding RNAs as an epigenetic mechanism, we will also include these in this category (83-86).

DNA Methylation

Cytosine DNA methylation, the most studied of epigenetic changes, is a covalent modification of DNA, in which a methyl group (CH_3) is transferred from S-adenosylmethionine (SAM) to the fifth carbon (C-5) of cytosine by a family of (DNA-5)-methyltransferases (DNMTs), resulting in a new DNA base - 5-methylcytosine (m^5C). This specific DNA base accounts for ~1% of all bases, varying slightly among different tissue types, and corresponding to 3-6% of all cytosines and 70-80% of all CpG dinucleotides (87, 88). CpG sequences are underrepresented in the genome owing to the evolutionary trend for depletion of such dinucleotides due to spontaneous deamination of m^5C into thymine (T) and the failure of recognition by the mismatch repair mechanism (89-91).

DNA methylation occurs almost exclusively at CpG dinucleotides and has an important role in the gene expression regulation and in the silencing of repeat elements in the genome (92). Across the genome we often find clustered regions of CpG dinucleotides, also known as CpG islands, defined as regions of more than 200 bases with a G+C content of at least 50% and a ratio of observed to statistically expected CpG frequencies of at least 0.6(93). It is estimated that approximately 60% of human gene promoters contain CpG islands (89) and are normally unmethylated in the majority of cells, corresponding to the maintenance of an open chromatin structure and a potentially active state of transcription (94). However, some conditions require a change in the gene-promoter unmethylated to methylated status, such as in some imprinted genes, X-chromosome genes in the female gender and in tissue and germline specific genes (95).

In human cells, three major DNMTs are responsible for DNA methylation. Methylation patterns are maintained by DNMT1, which preferentially methylates hemi-methylated DNA (e.g., duplex DNA in which only one of the strands is methylated) following DNA replication. DNMT3A and DNMT3B are known as the *de novo* methyltransferases. Although DNMT3A and DNMT3B show no preference for unmethylated DNA over hemi-methylated DNA, the low level of the *de novo* methylation carried out by DNMT1 relative to DNMT3A and DNMT3B have led to the latter two enzymes being designated as the *de novo* methyltransferases (96, 97). The DNA methyltransferases family includes another two members: DNMT2 and DNMT3L. DNMT2 is the smallest mammalian DNA methyltransferase and it shows reduced methyltransferase activity (96, 98). DNMT3L is a

DNMT-related protein, which does not have a methyltransferase activity. Instead, it interacts with de novo DNA methyltransferases, and appears to have an important role in imprinting, namely in maternal imprinted genes (96, 99). Changes in the expression of the DNMTs are a contributing factor to changes in methylation patterns.

As previously mentioned, promoter DNA methylation interferes directly with gene expression by obstructing the action of transcription activators on methylated regions in or near the promoter. In addition to this, another mechanism by which DNA methylation can indirectly regulate transcription is through the recruitment of DNA methyl-binding proteins containing methyl-CpG-binding domains (MBD). These regions present in proteins such as MeCP1 and MeCP2 include amino acid residues capable of binding to methylated DNA. Currently there are several proteins that have been identified and that are referred to as MBD proteins (MBPs), which have the capacity to silence transcription by binding to both hemi-methylated and fully methylated DNA (96, 100). They act towards the recruitment of transcriptional co-repressors such as histone deacetylating complexes, Polycomb proteins, and chromatin remodelling complexes, and attract chromodomain-binding proteins.

Herein, two of the most studied examples of the importance of natural CpG island methylation for the normal development of mammalian cells are the inactivation of one of the X chromosomes in females and the imprinted genes. The first is responsible for the maintenance of stable long-term random transcriptional silencing of one of the X chromosomes in the female gender, leading to gene-dosage compensation; whereas the second is a non-Mendelian inheritance phenomenon, by which one of the parental alleles of a gene becomes transcriptionally silenced, in male or female germ lines, leading to monoallelic expression in progeny in a parent-of-origin specific manner (101, 102). The spontaneous and natural occurrence of DNA methylation not only occurs in the course of cell early development, but also is an integral part of aging and cellular senescence. It is known that the overall content of cytosine methylation decreases with age, while other genes acquire methylation at their promoters, a phenomenon which resembles the methylation changes that are found in cancer (103).

DNA methylation plays an important role in the maintenance of genome integrity by transcriptional silencing of repetitive genomic regions, such as those of pericentromeric regions, transposons (DNA sequences that are able to move across the genome) and inserted viral sequences (104). In fact, these regions are naturally densely methylated, which in this case comprises a protective effect against chromosomal instability and potentially deleterious recombination events between non-allelic repeats caused by these

mobile genetic elements (105). In addition, as previously stated, methylation increases the mutation rate of m⁵C to T, leading to a faster divergence of identical sequences and disabling of many retrotransposons (106).

Histone Post-Translational Modifications

Nucleosomes are the basic units that compose the chromatin fiber. In eukaryotes, each of these primary building units consists of four core histones (H3, H4, H2A and H2B), which form a histone octamer, assembled from two heterodimers of H3 and H4 with two heterodimers of H2A and H2B. Wrapped to the histone octamer are 146 base pairs of DNA, thereby forming the complete structure of the nucleosome. Another histone, H1, binds to DNA between nucleosomes, and this structure is twisted and folded in highly ordered and compacted chromatic filaments (107). Not so long ago, histones were thought to be static elements, which only function comprised the DNA packing; however, these proteins are currently considered key players in epigenetics, as explained below.

The histone proteins contain a globular C-terminal domain and an unstructured N-terminal tail, being the last a target to various residue-specific post-translational covalent modifications, such as acetylation, methylation, phosphorylation, ubiquitylation, sumoylation, and ADP ribosylation (108, 109). These histone modifications have important roles in various cellular mechanisms, as in transcriptional regulation, DNA repair, DNA replication, alternative splicing and chromosome condensation, by unwrapping nucleosomal DNA or sliding nucleosomes along it, allowing the protein machinery to access the DNA sequence (110).

The concept of the “histone code” arises by the establishment of different combinatorial patterns of post-translational modifications in different residues of each one of the nucleosome core histones. Once read out by other proteins, this code is responsible by determining the structure and activity of different chromatin regions, being more or less stable accordingly to the cell environment stimuli (111, 112).

The acetylation and methylation status of specific lysine residues contained within the tails of nucleosomal core histones is known to play a critical role in regulating chromatin structure and gene expression. Lysine acetylation is a reaction catalysed by histone acetyltransferases (HATs), and is commonly associated with transcriptional activation, whereas the reverse reaction, performed by histone deacetylases (HDACs), leads to a negative gene expression regulation (109). The above-mentioned transcriptional activation due to acetylation happens because it partially neutralizes the positive charge of histones,

weakening their interaction with the nucleosomal DNA, thereby facilitating the access of transcription factors to their recognition element. Additionally, acetylation helps gene transcription by creating a specific signal for regulatory factors or chromatin-remodelling complexes, contributing to their targeting to a specific region (113, 114). The dynamic equilibrium between HATs and HDACs regulates the overall histone acetylation status.

Between the various HDACs enzymes, sirtuins (SIRT), which are also known as Class III HDACs, is a family of NAD⁺-dependent deacetylases highly conserved among all living organisms, and of particular interest. Seven different SIRTs (SIRT1–7) are described in mammals, which differ among each other in substrate specificity and catalytic activity (115). Within the cell, these enzymes participate in control of important biological processes, including cell division, differentiation, metabolism, genomic stability, survival, senescence and organismal lifespan (116). In addition, SIRT expression is also deregulated in many cancer types, either acting as oncogenes and/or tumour suppressor genes, depending on the disease model context (117-120).

Methylation as a histone post-translational modification is substantially different from acetylation: it may occur at lysines and arginines; histone lysines can become mono-, di-, or trimethylated, whereas arginines may only be mono- or dimethylated (symmetrically or asymmetrically); it does not alter the histone tails charge; and it has been implicated in both transcriptional activation and repression, depending on the altered residue, its position, and its histone code context (114, 121). For example, open chromatin is characterized by trimethylation of lysines 4, 36 and 79 of H3 (H3K4^{me3}, H3K36^{me3} and H3K79^{me3}), while heterochromatin features high monomethylation levels of lysines 9 and 27 of H3 (H3K9^{me} and H3K27^{me}), and lysine 20 of H4 (H4K20^{me}) (122). The effectors of these operations are the histone methyltransferases (HMTs), which catalyse the addition of a methyl group to histone residues using SAM as a cofactor and display higher substrate specificity when comparing with HATs and HDACs. Together with the HMTs, the histone demethylases (HDMs) are the answer of how histone methylation can regulate transcription and enable gene maintenance in an on or off state (114). Overall, these histone modifiers generally act together in complexes, such as the repressive Polycomb (PcG) and activating Trithorax (TrxG) group complexes, which counterbalance each other in gene regulation (123).

In normal mammalian cells, histone hypoacetylation and hypermethylation are characteristic of DNA sequences that are naturally methylated and repressed – such as in the previously mentioned inactive X chromosome in females, and silenced imprinted and tissue-specific genes (124).

Non-Coding RNAs

Increasing evidence from the sequencing and annotation of the human genome shows that only 2-3% of the human genome constitutes protein-coding genes, and most of the genome is transcribed as non-coding RNA (125, 126). A microRNA (miRNA) is a small sequence of 19 to 22 nucleotides of non-coding RNA that binds to the 3'untranslated region (3'-UTR) to inhibit translation or cause the target mRNA to degrade (127). Contrarily, a lncRNA is a transcript with a length greater than 200 nucleotides which are not translated into protein (128, 129). Unlike the above two linear RNAs, a circRNA is a single-stranded RNA that can form a covalently closed continuous loop, which, in turn, is not sensitive to ribonucleases due to the connected 3'and 5'ends (130, 131).

MicroRNAs, particularly, are processed from much longer transcripts, by RNA polymerase III, and arise from hairpin structures after successive enzymatic maturation steps, performed by the sequential action of Drosha and Dicer endonucleases (132). Following incorporation into the ribonucleoprotein complex RISC (RNA-induced silencing complex), the miRNAs bind mRNAs, primarily at their 3'-UTRs, through partial complementarity of their both sequences. Consequently, mRNA suffers decay and the translation is suppressed, leading to a reduction on protein levels. Moreover, recent reports showed that some miRNAs might also bind to the 5' UTR of the target genes, functioning as transcription activators (132-134).

The behaviour of this class of molecules is considered somehow promiscuous, because each miRNA has many targets and the individual mRNAs can be targeted by multiple miRNAs (135). Indeed, nowadays miRNAs are considered one of the most important groups of gene regulatory molecules, by controlling a wide range of biological processes, such as differentiation, proliferation, and apoptosis (135).

A connection between epigenetics, non-coding-RNAs and the field of Epitranscriptomics, which relates to modifications in RNA molecules, has been sustained in the last few years, which can explain how these mechanisms can directly and indirectly modulate the activity of the epigenetic machinery in several biological and pathological processes(136).

Methylation Biomarkers for Bladder Cancer – Current Challenges

Cancer initiation and progression is accompanied by deep variations in DNA methylation landscape. Indeed, a cancer cell is generally characterized by a genome-wide loss of m5C, contrasting with the subsequent hypermethylation of CpG islands, more precisely TSGs

CpG island promoter methylation (137). Defects and perturbations in DNA methylation have been observed in nearly all forms of cancer, and ultimately cause deregulation of multiple cell cycle, DNA repair, and chromosome stability genes, and hence contribute to genomic instability (Figure 4) (83). In BICa, the main research concerning epigenetic changes has majorly focused on DNA methylation, particularly its usefulness in biomarker discovery for disease detection and prognosis.

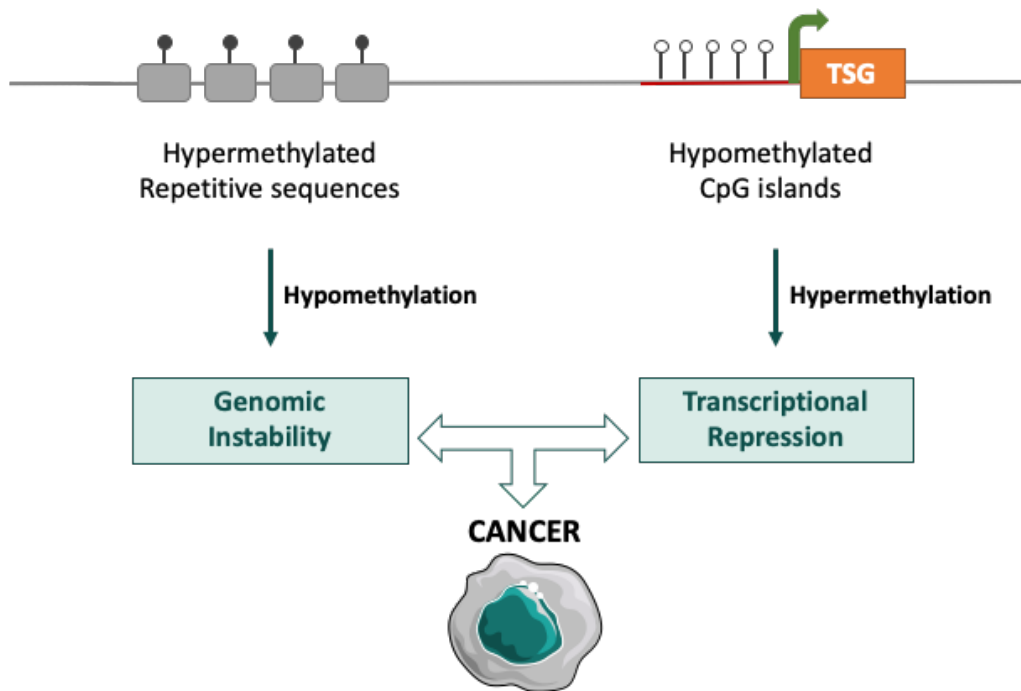


Figure 4. DNA methylation changes in cancer: Tumour-suppressor genes promoter hypermethylation and global genome-wide methylation loss.

Due to the chemical stability of DNA methylation, several research teams have been investigating the use of methylation levels alteration as potential biomarkers for detection and prognostication of urothelial malignancies (138), mainly using methylation-specific PCR (MSP)-based techniques or bisulfite conversion based sequencing methods.

As one of the main concerns regarding BICa management is to find a non-invasive method for disease detection and monitoring, the majority of these studies aim to discover differentially expressed methylation markers in urine of BICa patients. Because tumour-derived DNA in urine is usually accompanied by large quantities of DNA from normal exfoliated cells, an important characteristic of a methylation biomarker is that it's highly specific for urothelial malignancy. Furthermore, and because it is highly unlikely that an epigenetic alteration is present in all urine-exfoliated neoplastic urothelial cells, usually a combination of various methylation markers is investigated as a combination panel. Finally, if the aim of the study is to find a test to be used as a first-step detection method in patients

with unknown disease status, it should be taken into account its sensitivity and negative predictive value (NPV), to assure the lowest number of false-negative results(139).

As an example, in 2010 Costa VL et al identified a three-gene panel comprised GDF15, TMEFF2 and VIM methylation identified BICa with 94% sensitivity and 100% specificity in urine samples from 51 BICa patients (140). Another example is the work done by Roperch and colleagues proposed a three gene multiplex methylation panel (HS3ST2, SEPTIN9 and SLIT2) combined with FGFR3 mutations assessment, age and smoking-status at time of diagnosis in a multivariate model, for diagnosis of NMIBC in urine samples, disclosing 97.6% sensitivity and 84.8% specificity(141). Although the list of publications reporting similar studies greatly increased in the past decade, large multicentre validation studies are needed for the evaluation of the application of these tests in the clinical setting. Moreover, methylation-based biomarkers have been developed for the detection and prognosis management of BICa, discrimination of this neoplasm from other urinary tract malignancies and, more importantly, from benign conditions causing haematuria, including inflammatory diseases, remains a challenge. Indeed, most control samples used in biomarker discovery studies mostly comprise normal/healthy donors, disregarding the fact that a biomarker-based test would be offered to an “at-risk” population, including patients experiencing suspicious symptoms.

Epithelial to Mesenchymal Transition in Cancer

The starting point of a metastasis requires cells to invade and escape from the primary tumour to the vasculature, and then settle in the secondary site. Epithelial-to-mesenchymal transition (EMT), which is a reversible biological process in which polarized epithelial cells undergo a variety of molecular and cellular changes to obtain a more invasive and mesenchymal phenotype, can promote tumour invasion and intravasation (142).

EMT Types, Markers and Regulation

The EMT process is essential during early vertebrates' development. Based on the biological background of their occurrence, three different EMT subtypes are proposed: Type 1 regulates embryogenesis and organ development; Type 2 regulates tissue regeneration and organ fibrosis; and type 3 is related to cancer progression and metastasis (142). Type 1 EMT produces cells with a mesenchymal phenotype, forming new tissues with diverse functions, e.g. during embryonic development when the epithelial cells of the neuroectoderm generate migratory neural crest cells through the EMT program. It also plays an important role in the production of mesenchyme, which then generates secondary epithelium through Mesenchymal-to-Epithelial transition (MET) during development. Type 2 EMT is characterized as an auxiliary repair event in tissue reconstruction after inflammatory injury or trauma. It is related to wound healing, tissue regeneration and organ fibrosis. In addition, sustained inflammatory signals can induce type 2 EMT and ultimately lead to the destruction of affected organs (142). Type 3 EMT occurs in neoplastic cells through genetic and epigenetic changes, which are conducive to their growth and local extravasation from primary tumour location. Indeed, due to these properties, EMT can cause tumour cells to develop distant metastases.

The E-cadherin (ECAD) loss of function alteration is considered to be the key event to obtain the EMT phenotype. ECAD regulates cell adhesion, and its expression decreases during embryonic development, tissue fibrosis and EMT in cancer (143). In addition, the "switch" from ECAD to N-cadherin (NCAD), present in mesenchymal cells, is commonly used as a marker of EMT progression during embryonic development and cancer progression. Vimentin (VIM), an intermediate filament characteristic of cells with mesenchymal phenotype, is also commonly used to identify cells undergoing EMT in cancer, because its

expression is positively correlated with the increase in tumour invasion and metastasis (144). Other epithelial markers may include tight junction proteins, such as occludins or claudins, cytokeratins 5 and 6, and zonula occludens-1 (ZO-1). On the other hand, besides NCAD and Vimentin, the main mesenchymal markers also include fibronectin and various members of the matrix metalloproteinases (MMPs) family (145).

EMT is regulated by a variety of EMT transcription factors (TFs) that directly or indirectly inhibit CDH1 (the gene encoding ECAD). Snail, Slug, Zeb1 and Zeb2 TFs can bind to the CDH1 promoter and inhibit its transcription, while other factors, such as Twist, indirectly inhibit CDH1. Snail is part of the zinc finger transcription factors family that are active during the development of the embryo. Slug is also a member of the Snail family, and its expression is closely related to the loss of ECAD (146-153).

The regulation of EMT through its TFs is also tightly correlated with a variety of molecular networks, including TGF- β and Notch, Wnt, Hedgehog and NF- κ B signalling pathways, all of which play an important role in carcinogenesis, invasiveness and metastasis (154). Wnt signalling can cause EMT by inhibiting β -catenin degradation through GSK-3 β -mediated phosphorylation. The Notch signalling pathway has also been shown to be a modulator of EMT induction, along with TGF- β . These pathways are directly responsible by EMT-TFs upregulation, thereby activating EMT and increasing cell migration and invasion (155-158).

EMT in Bladder Cancer

Generally, low ECAD levels promote changes in cell morphology and increase in migration and invasion capabilities (159-161). In BICa this is no different. Previous studies have shown that normal urothelium exhibits high ECAD expression. Contrarily, in the majority of MIBC cases (80%), the amount of this protein is rather low or absent (162). Consequently, lower ECAD levels are associated with poor survival and high recurrence rates, and the promotion of BICa progression (163, 164).

Evidence of previously mentioned cadherins-switch have been also observed in BICa. Where we usually do not detect NCAD expression on normal urothelium and NMIBC, 60% of advanced MIBCs show a “de-novo” expression of this protein (162, 165-167). Indeed, in BICa, there is correlation with this glycoprotein and lymph node metastasis and lymphovascular invasion, which consequently leads to a worse clinical outcome (165, 168). Still on the topic of cadherins-switch, various authors proposed that for some BICa cases ECAD expression could also be replaced by P-cadherin (PCAD), although this process needs further clarification (162, 167, 169, 170).

The characterization of EMT-TFs in BICa is still also unclear. For instance, in a study by Yu et al. the expression of Slug and Twist was found to be increased in BICa, whereas the expression of Snail appeared to decrease (171). However, in another study by Bruyere et al. high Snail expression was indicated as a strong predictor of tumour recurrence for NMIBC (172).

As previously mentioned, the regulation of EMT through its TFs is tightly correlated with a variety of molecular networks. Within these, epigenetic mechanisms and enzymes play an important role, not only in deciphering and better understanding how EMT occurs in cells, but also its implications for cancer. In the next sub-chapter we provide a review on the epigenetic enzymes, protein-coding and non-coding genes, and mechanisms altered in the EMT process occurring in BICa cells, as well as its implications for the disease.

Review Paper

Epigenetic mechanisms influencing EMT in Bladder Cancer

International Journal of Molecular Sciences 2019, 20(2), 297

DOI: 10.3390/ijms20020297

Sara Monteiro-Reis*, João Lobo*, Rui Henrique, Carmen Jerónimo

Author personal contribution:

Conceptual design, retrieval of records to review, interpretation of the gathered information and manuscript preparation.

Review Paper - Epigenetic mechanisms influencing EMT in Bladder Cancer

Abstract

Bladder cancer is one of the most incident neoplasms worldwide, and its treatment remains a significant challenge, since the mechanisms underlying disease progression are still poorly understood. The epithelial to mesenchymal transition (EMT) has been proven to play an important role in the tumorigenic process, particularly in cancer cell invasiveness and metastatic potential. Several studies have reported the importance of epigenetic mechanisms and enzymes, which orchestrate them in several features of cancer cells and, specifically, in EMT. In this paper, we discuss the epigenetic enzymes, protein-coding and non-coding genes, and mechanisms altered in the EMT process occurring in bladder cancer cells, as well as its implications, which allows for improved understanding of bladder cancer biology and for the development of novel targeted therapies.

Introduction

Bladder Cancer

Bladder cancer (BlCa) is the seventh most prevalent cancer worldwide and the second most frequent urological malignancy after prostate cancer. Incidence has been rising in most countries, with an estimated 549,393 new cases diagnosed in 2018 and 990,724 new cases expected in 2040. Therefore, this almost doubled the number. Moreover, BlCa constitutes an important cause of cancer-related death with 199,922 deaths estimated in 2018 and 387,232 predicted for 2040 [1,2]. There is a strong male predominance, approximating a 3:1 ratio, and epidemiological trends track closely the prevalence of tobacco smoking [3]. Similar to other urological malignancies, mortality-to-incidence ratios are higher in underdeveloped countries, which probably reflects different environmental exposures and/or inequalities in healthcare accessibility [4]. Importantly, due to its high prevalence, mortality and, particularly, the propensity for multiple recurrences and/or disease progression and consequent additional treatments, BlCa is the most costly neoplastic disease constituting an important financial burden (costs about €4.9 billion in the European Union, alone, in 2012) [5].

BlCa generally refers to a cancer derived from epithelial layer, the urothelium, which is shared with other organs of the urinary tract and it extends from the renal pelvis to the urethra. Hence, although other much rarer tumour formations occur, its major histological

subtype is urothelial carcinoma, which will be the focus of this review. Two major forms of BICa are acknowledged, differing clinically, pathologically, and molecularly. Non-muscle invasive BICa (NMIBC, corresponding to 75% to 80% of all cases, disclosing papillary architecture, with the propensity to recur and eventually invade the bladder wall over time) and muscle-invasive BICa (MIBC, 20% to 25% of all cases, mostly derived from urothelial carcinoma in situ, which constitutes an aggressive disease that invades locally and metastasizes systemically) [6,7].

Epigenetics

During many years, scientists believed that living organisms' identity was defined by the genetic component of its cells, but, rapidly, it became clear that this could not explain how cells with the same genomic composition could disclose different phenotypes depending on different conditions. Now it is known that the identity of a cell is defined by both genetic and epigenetic patterns with the latter being crucial for fetal development in mammals, as well as cell and tissue differentiation [8-11]. Epigenetics is defined as the study of heritable modifications of DNA or associated proteins, which carry information related to gene expression during cell division, and currently encompasses all potentially reversible mechanisms that lead to changes in expression regulation without affecting the DNA sequence [12]. The most well-known epigenetic mechanisms comprise four major groups: DNA methylation, histone post-translational modifications or chromatin remodelling, histone variants, and non-coding RNAs' regulation [11]. These modifications are tightly regulated by several enzymes, which may act isolated or in chromatin remodelling complexes, and grouped according to function. These epigenetic enzymes include: DNA methyltransferases (DNMTs) and demethylases (TETs), histone methyltransferases (HTMs) and demethylases (HDMs), histone acetyltransferases (HATs) and deacetylases (HDACs), and histone ubiquitin ligases (Ubls) and deubiquitinases (dUbs) [12].

Cancer cells exhibit a distinct epigenetic landscape and they take advantage of all of the previously mentioned mechanisms to acquire the characteristic malignant features, from transformation to progression [13]. BICa is no exception. Several studies have associated epigenetic machinery deregulation and this cancer type. Moreover, the potential of epigenetic biomarkers to assist in clinical management of BICa patients, not only for detection, but also for follow-up, treatment monitoring and prediction of recurrence/progression has been intensively investigated [14,15]. In parallel, efforts have been made to understand how epigenetic mechanisms are involved in the various steps of urothelial carcinogenesis [16,17]. One question remains mostly unanswered. What mechanisms distinguish neoplastic cells with the ability to invade the muscle layer of the

bladder, and eventually metastasize, from those that do not have this ability? In fact, epigenetics may help answer this question.

Epithelial to Mesenchymal Transition

The epithelial to mesenchymal transition (EMT) is a multistep process in which epithelial cells acquire a range of mesenchymal characteristics, which enables cell motility and invasiveness [18]. Importantly, these mesenchymal characteristics are reversible, with cells resuming their epithelial phenotype, through a process named mesenchymal to epithelial transition (MET). Recently, the classic concept of EMT, which strictly pointed out to mutually exclusive epithelial or mesenchymal phenotypes, has been challenged by “partial EMT” in which cells may transiently display both epithelial and mesenchymal features, corresponding to an intermediate state of EMT [19,20]. The concept of a partial EMT may be explained by implicating epigenetic regulation of EMT/MET reversibility and cell plasticity. Various factors and cellular environmental conditions are known to induce EMT, by triggering a cascade of signalling pathways that lead to post-transcriptional modification of the most well-known EMT transcription factors (EMT-TFs): Snail, Slug, ZEB1, ZEB2, and TWIST [21,22]. The interplay between the EMT-TFs and various key regulatory proteins and epigenetic enzymes that regulate EMT-TFs themselves, results in overexpression or repression of well-described EMT effectors, such as the cadherin family (CDH1, CDH2, and CDH3) and vimentin [23,24,25,26].

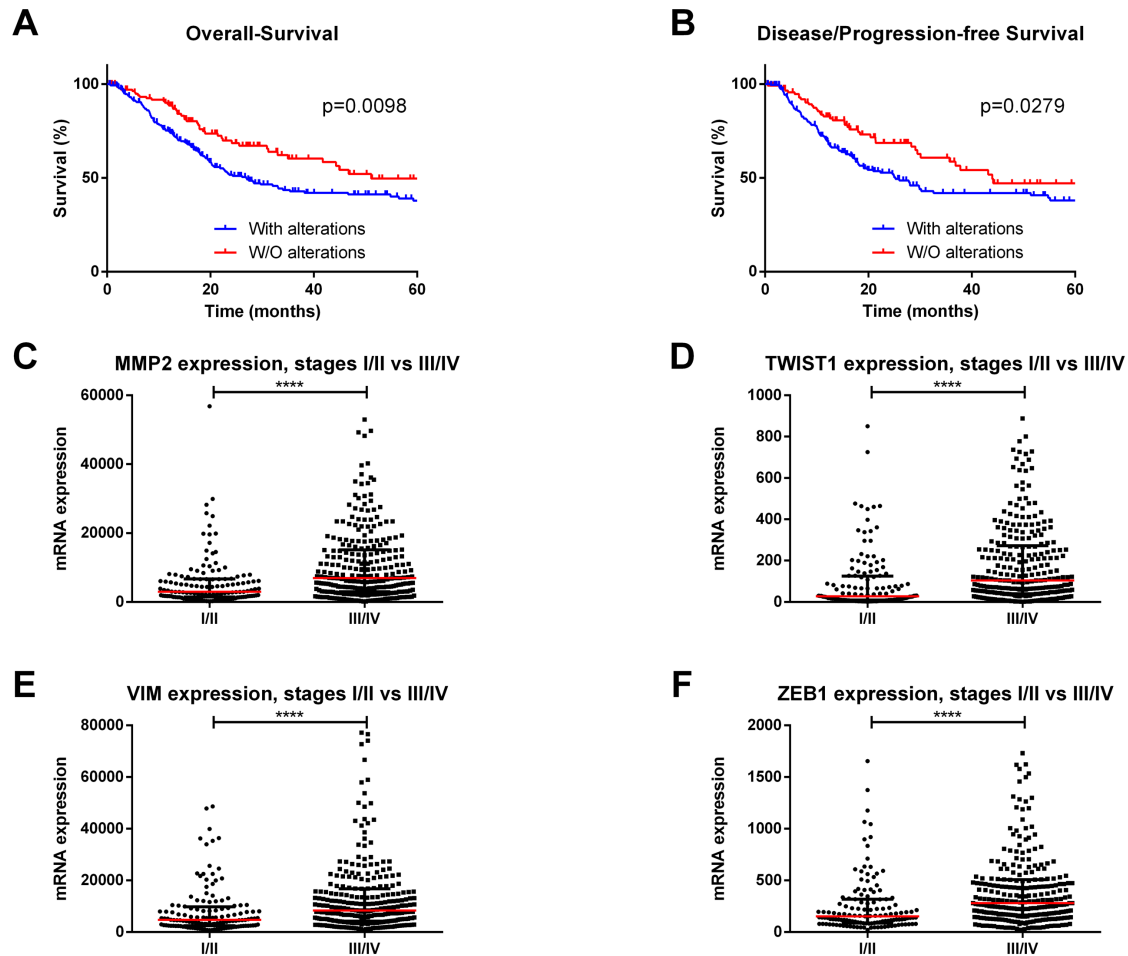


Figure 1. In silico analysis of The Cancer Genome Atlas database for bladder cancer (using the online resource cBioPortal for Cancer Genomics). (A) Overall and (B) Disease/Progression-free survival curves according to major EMT players' alterations. (C) MMP2, (D) TWIST1, (E) VIM, and (F) ZEB1 transcript levels in stages I/II vs. III/IV bladder cancer cases. **** $p < 0.0001$.

Influence of EMT Major Players in Bladder Cancer

EMT is essential for various physiological processes, including early embryogenesis as well as in cancer. Accordingly, in vitro and in vivo studies implicated EMT in cell invasion and metastatic potential in several cancer types [19]. Intense research efforts uncovered the major EMT players in epithelial cancers, including BICa. We performed an in silico analysis of The Cancer Genome Atlas (TCGA) database for BICa (using the online resource cBioPortal for Cancer Genomics [27]), with a user-defined entry set of major EMT players (CDH1, CDH2, CDH3, CTNNB1, GSK3B, MMP2, MUC1, SNAI2, SNAI1, TWIST1, VIM, ZEB1, and ZEB2), and we found that these genes are deregulated in 272/413 (66%) tumors being significantly associated with reduced overall survival ($p = 0.0098$) and disease/progression-free survival ($p = 0.0279$) (Figure 1A,B). Furthermore, the expression

levels of mesenchymal markers, like MMP2, VIM, TWIST1, ZEB1, and ZEB2, were significantly higher in stages III/IV when compared to stages I/II ($p < 0.0001$) (Figure 1C–F).

Epigenetic Enzymes and Mechanisms Altering EMT in Bladder Cancer

Protein-Coding Genes

DNA methylation and chromatin remodelling deregulation in cancer result from aberrant epigenetic enzymes' activity that ultimately lead to abnormal gene expression, which empowers tumors to quickly evolve. It facilitates invasion and metastasis. Overall, while the importance of these epigenetic enzymes in promoting bladder cancer transformation has been already acknowledged, only a limited number of studies have characterized its role in the context of EMT process in this tumor model.

One of the epigenetic enzymes involved in EMT is the enhancer of zeste homolog 2 (EZH2), which is a core subunit of the polycomb repressive complex 2 (PRC2) that acts as a chromatin modifier by adding two or three methyl groups at H3K27 residues [28]. In several cancer models, EZH2 was proven to be associated with CDH1 transcriptional silencing and the mesenchymal phenotype [29,30,31]. Using chromatin immunoprecipitation (ChIP), Luo M. et al. demonstrated EZH2 and H3K23me3 enrichment within CDH1 promoter in BICa cells even though no clues were yet provided on how PRC2 is specifically recruited to CDH1 [32]. Nonetheless, Kottakis et al. suggested that EZH2 might be regulated by FGF-2 upregulation in BICa cells, which, in turn, upregulates the lysine demethylase 2B (KDM2B) and triggers EZH2 recruitment. The upregulation of these two enzymes is associated with miR-101 transcription repression, due to H3K36 demethylation by KDM2B, and H3K27 trimethylation by EZH2. As a result, and because EZH2 is also post-transcriptionally regulated by miR-101, these events ultimately contribute to EZH2 overexpression in a loop [33,34,35]. Moreover, several EMT-TFs were also found to be overexpressed in these cells, which further supports EZH2 implication in EMT [33,36]. The E2F1 transcription factor and the epigenetic reader BRD4 were also suggested as possible EZH2 regulators in BICa, but its direct link with EMT and respective TFs is still elusive [37,38]. Importantly, because EZH2 overexpression is common to several tumors, inhibitors for this histone methyltransferase are under evaluation as potential anticancer drugs in phase one and two clinical trials [39]. Nevertheless, just one of the undergoing studies targets BICa patients, and only those that have unresectable or metastatic disease [40]. The development of new therapies for BICa is still an unmet need since these tumors have limited treatment options. Specifically, EZH2 inhibition might restrain the progression of non-muscle to muscle invasive disease.

DNA methylation—a covalent modification of DNA, in which a methyl group is transferred from S-adenosylmethionine (SAM) to the fifth carbon of a cytosine—constitutes a stable and heritable mark frequently associated with the maintenance of a closed chromatin structure, which results in the silencing of repeat elements in the genome and genes’ transcriptional repression [41]. Across the genome, clustered regions of CpG dinucleotides, also known as CpG islands, are often found in genes’ promoter regions. Several cancer-related genes were reported to be regulated by promoter methylation, some of which were implicated in BICa EMT (Table 1). Among these, serine protease PRSS8 was found to be downregulated by promoter methylation in high-grade BICa tissues, and its overexpression in cell lines was associated with E-Cadherin upregulation, which suggests an interplay between these two proteins during epithelial differentiation [42,43].

Table 1. Epigenetically modulated protein-coding genes implicated in Bladder Cancer EMT.

Gene	Expression in BICa	Effect on EMT	Epigenetic Regulation	Sample type and size	Author
MAEL	Upregulated	↑EMT (↓ECAD, ↓β-catenin, ↑Fibronectin, ↑VIM) Recruitment of DNMT3B and HDAC1/2 to MTSS1 promoter)	Downregulated by miR186	184 primary tumors, <i>in vitro</i> and <i>in vivo</i> assays	Li XD, 2016 (173)
GDF15	Downregulated	↓EMT (knockdown cells with ↓ECAD, ↑NCAD, ↑Snail, ↑Slug)	Upregulated by demethylation	<i>In vivo</i> assays	Tsui KH and Hsu SY, 2015 (174)
KLF4	Downregulated	↓EMT (↑ECAD, ↓NCAD, ↓β-catenin, ↓VIM, ↓Snail, ↓Slug)	Promoter methylation; Upregulated by 5AZA treatment	139 non-muscle invasive primary tumors, <i>in vitro</i> and <i>in vivo</i> assays	Li H and Wang J, 2013 (175)

		↓EMT (Upregulation)	Promoter methylation confirmed by BSP	<i>In vitro</i> assays	Xu X, 2017 (176)
PRSS8	Downregulated	↓EMT (↑ECAD in cells with forced PRSS8 expression)	Promoter methylation; Upregulated by 5AZA and TSA treatment	40 primary tumors and <i>in vivo</i> assays	Chen LM, 2009 (177)
ELF5	Downregulated	↓EMT (↑ECAD, ↓NCAD, ↓VIM, ↓Snail, ↓ZEB1)	Promoter methylation; Upregulated by 5AZA treatment	182 FFPE + 50 FF primary tumors and <i>in vivo</i> assays	Wu B, 2015 (178)

Abbreviations: 5AZA – 5-Azacytidine; BICa – bladder cancer; BSP – Bisulfite sequencing; EMT – epithelial to mesenchymal transition; FF – Fresh-frozen; FFPE – Formalin-fixed paraffin-embedded; miR – microRNA; TSA – Trichostatin A.

Similarly, the Elf5 transcription factor, which is also regulated by methylation in several cellular developmental processes, was associated with EMT in primary BICa and *in vitro* studies [44,45,46]. Elf5 reduced expression, both at mRNA and protein levels, is associated with disease progression, and, in BICa cell lines, its downregulation is associated with increased mesenchymal markers, such as Snail, ZEB1, and vimentin. Furthermore, ELF5-silenced BICa cells exhibited an invasive phenotype, and exposure to the demethylating agent 5-AZA restored ELF5 expression in the same cells, which attenuated its invasion capacity [46].

Furthermore, hypermethylation of the growth differentiation factor-15 (GDF15), which is a member of the TGF- β superfamily reported as an urothelial cancer biomarker [51,52], was found to be lower in BICa cell lines derived from MIBC tumors. Moreover, GDF15-knockdown cells displayed E-Cadherin downregulation while several EMT-TFs were upregulated [48]. Thus, the discovery of epigenetically downregulated genes in MIBC provides new insights about BICa progression and metastasis.

KLF4, which is a zinc finger transcription factor, is commonly downregulated in several cancers [53,54,55,56] including BICa [49,50]. Specifically, KLF4 was found to be repressed by promoter methylation [49,50]. Furthermore, (CRISPR)-ON upregulation reduced BICa cells' migration, invasion and EMT abilities, which is paralleled by the growth inhibition of tumor xenografts and lung metastasis formation in mice. However, epigenetic editing (e.g., residue specific methylation or demethylation) would be more suitable for assessing the

specific role of KLF4 promoter methylation in gene expression regulation [57,58]. The new epigenetic tools available would allow for the clarification of promoter methylation's regulation of all the previously mentioned genes implicated in BICa EMT and metastasis. Several epigenetic mechanisms act synergistically to maintain the epigenetic landscape through a regulation loop in which they simultaneously control protein-coding genes' expression and other epigenetic players at different regulation levels. Specifically, for BICa, the oncogene maelstrom (MAEL), frequently upregulated in this malignancy, downregulates the metastasis suppressor MTSS1 gene by recruiting DNMT3B and HDAC1/2 to its promoter. Moreover, MAEL is also targeted by miR-186 and, possibly, by loss of promoter methylation, which constitutes an example of a gene that recruits epigenetic enzymes and is, in turn, regulated by epigenetic mechanisms [47].

Non-Coding RNAs

Non-coding RNAs (ncRNAs) are also involved in the dynamic regulation of EMT-related genes' expression. There are several ncRNA categories, commonly classified according to their size, including the long ncRNAs (lncRNAs) with more than 200 nt and the small ncRNAs (sncRNAs), which present less than 200 nt [59,60]. ncRNAs, not only directly hinder messenger RNA (mRNA), but also interact (directly or indirectly) with DNMTs, various histone modifying enzymes, and remodelling complexes, which establishes important links between all epigenetic players that modulate gene expression. Therefore, ncRNAs have been implicated in a broad range of biological processes, including proliferation, adhesion, invasion, migration, metastasis, stemness, apoptosis, genomic instability, and, also, EMT, by mediating cell-cell communication (via ncRNA-containing extracellular vesicles), which binds to transcription factors and proteins, DNA methylation regulation, splicing, and scaffolding [61,62].

Among ncRNAs, sncRNAs have been considered the most biologically relevant in the context of EMT. They are involved in post-transcriptional regulation of target RNAs (by forming complexes with proteins of the Argonaute family) with microRNAs being the most intensively studied within this class. Their mature forms are single-stranded and have 20–25 nt in length, which constitutes the final product of a processing pathway involving DROSHA, DICER, and RISC [63]. In fact, *in silico* analysis has shown several up-regulated and downregulated microRNAs that target the most important EMT players associated with aggressive disease [64].

Our literature review disclosed 31 different microRNAs, which participate in BICa EMT regulation [(Table 2), [65-92]]. Most studies were performed in patients' samples (n = 25) and/or in cell lines (n = 31), but some have also tested animal models (n = 9). For most microRNAs, the net effect was to counteract an EMT phenomenon (n = 25), while only

miR92 family/miR92b, miR135a, miR221, miR224, and miR301b were reported to promote EMT. In addition, to a putative value as diagnostic markers, 13 microRNAs were shown to have prognostic and/or predictive value as well, associated with clinicopathological variables such as tumor grade, stage, occurrence of metastases, and patients' survival.

Table 2. Non-coding RNAs associated with EMT in bladder cancer.

Non-coding RNA	Effect on EMT (and others)	Main regulators	Main targets / pathways	Sample type and size	Author
Small non-coding RNAs					
miR22	↓EMT; diagnostic value (↓ in tumor, vs. normal)		Snail and MAPK/ Slug/ VIM	13 primary tumors, <i>in vitro</i> and <i>in vivo</i> assays	Xu M, 2018 (179)
miR23b	↓EMT; diagnostic (↓ in tumor, vs. normal) and prognostic (↑OS) value		ZEB1	20 primary tumors and <i>in vivo</i> assays	Majid S, 2013 (180)
miR24	↓EMT; diagnostic value (↓ in tumor, vs. normal)		CARMA3	<i>In vitro</i> assays	Zhang S, 2015 (181)
miR34a	↓EMT; diagnostic value (↓ in tumor, vs. normal)		CD44	8 primary tumors, <i>in vitro</i> and <i>in vivo</i> assays	Yu G, 2014 (182)
miR92 (family)	↑EMT; diagnostic (↑ in tumor, vs. normal) value; induces cisplatin resistance		GSK-3β/ Wnt/ c-myc/ MMP7	20 primary tumors and <i>In vitro</i> assays	Wang H, 2016 (183)
miR92b	↑EMT		DAB2IP	<i>In vitro</i> assays	Huang J, 2016 (184)
miR-124-3p	↓EMT; diagnostic value (↓ in tumor, vs. normal)		ROCK1, MMP2, MMP9	13 primary tumors and <i>in vitro</i> assays	Xu X, 2013 (185)

miR135a	↑EMT		GSK-3β	165 primary tumors and <i>in vitro</i> assays	Mao XW, 2018 (186)
miR141	↓EMT; prognostic value (LN metastases)		MMP2 and 9, Vimentin, N-Cadherin; E-Cadherin	30 primary tumors, 78 urine samples and <i>in vitro</i> assays	Liu W and Qi L, 2015 (187)
miR-148a-3p	↓EMT; diagnostic value (↓ in tumor, vs. normal)	↓expression mediated by DNA methylation (DNMT1) – ↑expression with 5AZA	ERBB3-AKT2-c-myc/ SNAIL axis	59 primary tumors, <i>in vitro</i> and <i>in vivo</i> assays	Wang X, 2016 (188)
miR186	↓EMT; diagnostic value (↓ in tumor, vs. normal)		NSBP1	20 primary tumors and <i>in vitro</i> assays	Yao K, 2015 (189)
miR-199a-5p	↓EMT; diagnostic (↓ in tumor, vs. normal) and prognostic (stage, grade) value		CCR7, MMP9	40 primary tumors and <i>in vitro</i> assays	Zhou M, 2016 (190)
miR200 (family)	↓EMT; prognostic value (↑ survival)	↓expression mediated by EZH2 and BMI-1	BMI-1, ZEB1, ZEB2	87 primary tumors and <i>in vitro</i> assays	Martínez-Fernández M and Duenas M, 2015 (191)
	↓EMT and proliferation; diagnostic (↓ in tumor, vs. normal) and prognostic (↑ survival) value		BMI-1 and E2F3	15 primary tumors and <i>in vitro</i> assays	Liu L, 2014 (192)
miR200b	↓EMT; prognostic value (LN metastases)		MMP2 and 9, Vimentin, N-Cadherin, E-Cadherin	30 primary tumors, 78 urine samples	Liu W and Qi L, 2015 (187)

					<i>and in vitro</i> assays	
	↓EMT		↓expression mediated by TGF-β1	MMP16	<i>In vitro</i> assays	Chen MF and Zeng F, 2014 (193)
miR200c	↓EMT; restores sensitivity to EGFR inhibitors			ZEB1, ZEB2 and ERRFI-1	<i>In vitro</i> assays	Adam L, 2009 (194)
miR203	↓EMT; diagnostic value (↓ in tumor, vs. normal)			Twist1	24 primary tumors <i>and in vitro</i> assays	Shen J, 2017 (195)
miR205	↓EMT; poor prognosis	poor	↑expression mediated by p63 isoform ΔNp63α	ZEB1, ZEB2	98 primary tumors and <i>in vitro</i> assays	Tran MN, 2013 (196)
miR221	↑EMT		↑expression mediated by TGF-β1	STMN1	<i>In vitro</i> assays	Liu J, 2015 (197)
miR224	↑EMT; diagnostic (↑ in tumor, vs. normal) and prognostic (stage, metastases, ↓survival) value			SUFU/ Hedgehog pathway	97 primary tumors, <i>in vitro</i> and <i>in vivo</i> assays	Miao X, Gao H and Liu S, 2018 (198)
miR301b	↑EMT; diagnostic value (↑ in tumor, vs. normal)			EGR1	<i>In vitro</i> assays	Yan L, 2017 (199)
miR-323a-3p	↓EMT; diagnostic (↓ in tumor, vs. normal) and prognostic (↑OS) value		↓expression mediated by methylation of IG-DMR	Met/ SMAD3/ Snail	9 primary tumors and <i>in vivo</i> assays	Li J, 2017 (200)
miR-370-3p	↓EMT			Wnt7a	41 primary tumors <i>in vitro</i> and <i>in vivo</i> assays	Huang X and Zhu H, 2018 (201)

miR-370-5p	↓EMT		p21	<i>In vitro</i> assays	Wang C, 2016 (202)
miR424	↓EMT; diagnostic (↓ in tumor, vs. normal) and prognostic (stage, ↑OS and DFS) value	↓expression mediated by DNMT1	EGFR pathway	124 primary tumors, <i>in vitro</i> and <i>in vivo</i> assays	Wu CT, 2015 (203)
miR429	↓EMT		ZEB1/ βcatenin axis	<i>In vitro</i> assays	Wu CL, 2016 (204)
miR433	↓EMT; diagnostic value (↓ in tumor, vs. normal)		c-Met/ CREB1- Akt/ GSK-3β/ Snail	13 primary tumors and <i>in vitro</i> assays	Xu X, 2016 (205)
miR451	↓EMT; diagnostic (↓ in tumor, vs. normal) and prognostic (grade and stage) value		E-Cadherin, N-Cadherin	40 primary tumors and <i>in vitro</i> assays	Zeng T and Peng L, 2014 (206)
miR-485-5p	↓EMT; diagnostic value (↓ in tumor, vs. normal)		HMG2	15 primary tumors and <i>in vitro</i> assays	Chen Z, 2015 (207)
miR497	↓EMT; diagnostic (↓ in tumor, vs. normal) and prognostic (stage, metastases) value		E-Cadherin, Vimentin	50 primary tumors and <i>in vitro</i> assays	Wei Z, 2017 (208)
miR612	↓EMT; diagnostic (↓ in tumor, vs. normal) and prognostic (stage, metastases) value		ME1	46 primary tumors and <i>in vitro</i> assays	Liu M and Chen Y, 2018 (209)
miR613	↓EMT; diagnostic value (↓ in tumor, vs. normal)		SphK1	35 primary tumors and <i>in vitro</i> assays	Yu H, 2017 (210)

Long non-coding RNAs

circRNA MYLK	↑EMT; prognostic value (stage, grade)			miR29a/ VEGFA/ VEGFR2 axis	32 primary tumors, <i>in vitro</i> and <i>in vivo</i> assays	Zhong Z, 2017 (211)
lncRNA GHET1	↑EMT; diagnostic (↑ in tumor, vs. normal) and prognostic (grade, stage, metastases, ↓OS) value			E-Cadherin, Vimentin, Fibronectin, Slug, Twist, Snail, ZEB1	80 primary tumors and <i>in vitro</i> assays	Li LJ, 2014 (212)
lncRNA HOTAIR	↑EMT			Various players	10 primary tumors and <i>in vitro</i> assays	Berrondo C, 2016 (213)
lncRNA H19	↑EMT; diagnostic value (↑ in tumor, vs. normal)			miR-29b-3p/ DNMT3B axis	35 primary tumors; <i>in vitro</i> and <i>in vivo</i> assays	Lv M, 2017 (214)
lncRNA Malat1	↑EMT; poor prognosis	↑expression mediated by TGF-β		suz12	95 primary tumors; <i>in vitro</i> and <i>in vivo</i> assays	Fan Y, 2014 (215)
lncRNA ROR	↑EMT; diagnostic value (↑ in tumor, vs. normal)			ZEB1	36 primary tumors and <i>in vitro</i> assays	Chen Y, 2017 (216)
lncRNA TP73-AS1	↓EMT; diagnostic (↓ in tumor, vs. normal) and prognostic (↑OS and PFS) value			Various players	128 primary tumors and <i>in vitro</i> assays	Tuo Z, 2018 (217)
lncRNA TUG1	↑EMT; diagnostic (↑ in tumor, vs. normal) and prognostic (stage, ↓OS) value; promotes radioresistance			miR145/ ZEB2 axis	54 primary tumors; <i>in vitro</i> and <i>in vivo</i> assays	Tan J, 2015 (218)

lncRNA UCA1	↑EMT		miR145-ZEB1/ 2-FSCN1 axis	<i>In vitro</i> assays	Xue M, 2016 (219)
			miR143/ HMGB1	52 primary tumors and <i>in vitro</i> assays	Luo J, 2017 (220)
lncRNA XIST	↑EMT		miR200c	<i>In vitro</i> and <i>in vivo</i> assays	Xu R, 2018 (221)
lncRNA ZEB2NAT	↑EMT; diagnostic value (↑ in tumor, vs. normal)	↑expression mediated by TGF-β1	ZEB2	30 primary tumors and <i>in vitro</i> assays	Zhuang J and Lu Q, 2015 (222)

Abbreviations: DFS – disease-free survival; EMT – epithelial to mesenchymal transition; lncRNA – long non-coding RNA; miR – microRNA; OS – overall survival.

Some of the most well-studied microRNAs belong to the miR200 family. Their expression has been found to hamper EMT in different tumor models such as breast, prostate, ovarian, and endometrial carcinomas, in part by affecting different EMT players like ZEB1, ZEB2, and E-Cadherin [109,110,111,112,113]. Martínez-Fernández et al. [74] showed that PRC members EZH2 and BMI1 repress miR200 family, which results in EMT activation and aggressive disease, which is in accordance with the association of EZH2 overexpression with high risk for recurrence in NMIBC [114]. These findings support the dynamic regulation and cooperation between protein coding and non-coding RNAs in EMT. Since EZH2 pharmacological inhibition is already available and efficiently increases miR200 in BICa cell lines, this might constitute a therapeutic opportunity for hindering cancer progression. It has also been reported that epidermal growth factor receptor (EGFR) inhibition may lead to therapeutic resistance due to mesenchymal features. Additionally, miR200c induction (which targets the ERBB receptor feedback inhibitor 1–ERRFI-1) is effective in restoring sensitivity to EGFR inhibitors, which constitutes another example of pharmacological modulation of EMT that could be translated into clinical practice [65]. Lastly, another member of the miR200 family, miR200b, was demonstrated to target matrix metalloproteinase-16 (MMP16) in BICa cell lines, which is downregulated by transforming growth factor beta 1 (TGF-β1), previously associated with metastatic potential acquisition. This leads to miR downregulation having a net effect of promoting EMT [75]. In fact, TGF-β1 also cooperates with several other miRs, including miR221. Liu et al. showed that, by targeting STMN1, miR221 facilitates TGF-β1-induced EMT, and that its inhibition resulted

in increased levels of epithelial marker E-cadherin and reduction of mesenchymal markers such as vimentin, fibroactin, and N-cadherin [76].

A connection between microRNAs and methylation was also reported, which disclosed a feedback loop between DNMT1 and miR-148a-3p [79]. miR-148a-3p, a BICa tumor suppressor, and an EMT inhibitor, by targeting the ERBB3/AKT2/c-MYC axis, was shown to be downregulated by DNMT1-induced methylation. Moreover, re-expression was observed after treatment with 5-Aza-2'-deoxycytidine (5AZA) [79]. Wu et al. obtained similar findings for miR424 in BICa cell lines, in vivo models, and patient-derived specimens. DNMT1 inhibition resulted in substantial miR424 upregulation, which, in turn, promoted epithelial characteristics of BICa cells (changing the relative expression levels of E-cadherin and Twist) and resulted in reduced invasion ability. Additionally, the same authors identified the EGFR-PI3K-AKT axis as the target of miR424, explaining its effect on EMT [77]. Lastly, miR-323a-3p was also implicated in EMT of BICa cells by targeting MET and SMAD3, which interfered with their regulation of Snail and resulted in the net effect of repressing EMT. On the other hand, miR-323a-3p is downregulated by aberrant methylation of the intergenic differential methylated region (IG-DMR) [87]. In addition, miRs might also be regulated by methylation and this feature might be used for urothelial carcinoma detection in bodily fluids, such as urine [115].

EMT-related miRs have also been demonstrated to impact the resistance to cytotoxic drugs. Furthermore, miR-92 was found to promote EMT (changing the relative expression levels of two of its major players, E-cadherin, and vimentin) by activating glycogen synthase kinase 3 beta (GSK3B) and the Wnt signalling pathway, inducing resistance to cisplatin (increasing BICa cells viability and decreasing apoptosis upon treatment with cisplatin) [79]. Most of the human genome is transcribed into structural ncRNAs. LncRNAs, which include both linear and circular forms (the latter being referred to as circRNAs), display different regulatory functions, according to their cellular location. Whereas nuclear lncRNAs can either sequester transcription factors and recruit chromatin-remodelling complexes to a cell-site (hence impeding transcription), or trigger chromatin-modifying complexes (thus, activating transcription), cytoplasmic lncRNAs modulate RNAs stability and translation, competing with endogenous RNAs (ceRNAs) for microRNA binding. Additionally, having a longer half-life than their linear counterparts, circRNAs may also act as microRNA "sponges" [116,117].

Eleven lncRNAs (ten linear and one circRNA) [97-108] have been reported to modulate EMT in BICa. Contrary to microRNAs, only one lncRNA (TP73-AS1) was implicated in negative regulation of EMT, whereas all the remainder substances promoted its activation. Five of the lncRNAs (including circRNA MYLK and lncRNAs GHET1, Malat1, TP73-AS1, and TUG1) were explored as potential diagnostic and prognostic biomarkers.

CircRNA MYLK was found to function as ceRNA for miR-29a, which, in result, promotes EMT and activates the vascular endothelial growth factor receptor (VEGFR) pathway, which is associated with BICa progression [97]. Thus, circRNA MYLK modulation might constitute a therapeutic target in combination with anti-VEGF drugs such as bevacizumab. Moreover, Lv et al. [100] have shown that lncRNA H19 also functions as a ceRNA for miR-29b-3p, which is another member of the miR29 family. Therefore, this allows for the expression of target DNMT3B, reprograms DNA methylation patterns, and promotes EMT (through Twist, vimentin, and MMP9 upregulation and E-cadherin downregulation) and metastasis.

Non-coding RNAs may modulate not only the response to systemic treatments, but also to local therapies such as radiotherapy. Tan et al. [104] showed that miR145's downmodulation by lncRNA TUG1 associated with EMT and radio-resistance due to its action on the ZEB2 axis. Targeting this lncRNA might re-sensitize BICa to radiotherapy, which results in a better patient response and outcome.

Furthermore, TGF- β 1 leads to overexpression of lncRNA malat1, which is associated with suppressor of zeste 12 (suz12), decreases E-cadherin, and increases N-cadherin and fibronectin expression levels [101]. Moreover, another lncRNA-ZEB2NAT—was shown to be essential for the role of TGF- β 1-secreting cancer associated fibroblasts (CAFs) in promoting EMT in BICa cells. Zhuang et al. elegantly showed that CAFs induce EMT by activating the TGF- β 1/ZEB2NAT/ZEB2 axis, whereas ZEB2NAT inhibition reduced ZEB2 expression levels and inhibited BICa cells invasion capacity [108].

Several lncRNAs might target the same microRNA and the same lncRNA may influence more than one microRNA simultaneously. Such is the case of lncRNA UCA1, which induces EMT either by targeting miR145 or miR143 [105,106]. These studies suggest that lncRNAs might be implicated in EMT by interfering with several pathways through various regulatory functions, due to their redundancy.

Conclusions

As discussed in this review, epigenetic mechanisms and connected enzymes are intrinsically involved in the various steps of EMT in BICa cells, which acts in concert and controlling EMT-TFs as well as several upstream targets (Figure 2). All the studies published to the date illuminate the way for the development of specific anti-cancer drugs, which could abrogate EMT by targeting epigenetic enzymes and genes regulated by these reversible modifications.

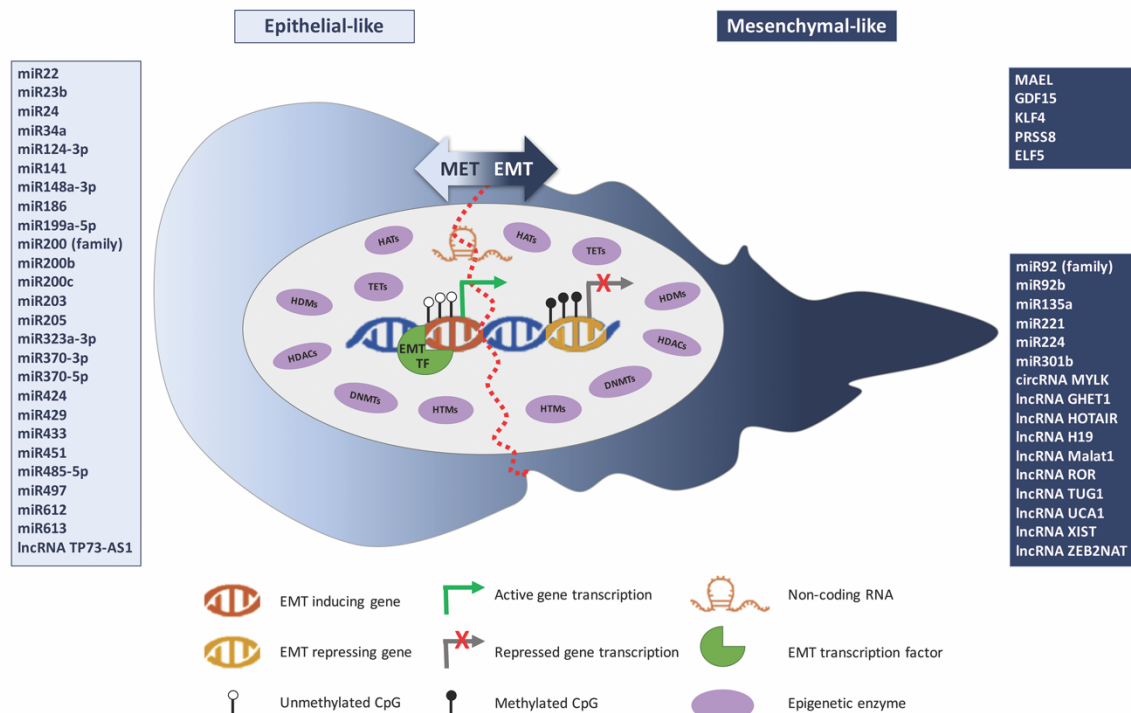


Figure 2. Epigenetic mechanisms' interplay with the epithelial-to-mesenchymal transition process in bladder cancer.

Nevertheless, the epigenetic regulation of EMT requires further investigation to provide clinically useful information for BICa patient management.

References

1. Wong, M. C. S.; Fung, F. D. H.; Leung, C.; Cheung, W. W. L.; Goggins, W. B.; Ng, C. F., The global epidemiology of bladder cancer: a joinpoint regression analysis of its incidence and mortality trends and projection. *Sci Rep* 2018, 8, (1), 1129.
2. Ferlay, J.; Ervik, M.; Lam, F.; Colombet, M.; Mery, L.; Piñeros, M.; Znaor, A.; Soerjomataram, I.; Bray, F. Global Cancer Observatory: Cancer Tomorrow. (03 December 2018),
3. Antoni, S.; Ferlay, J.; Soerjomataram, I.; Znaor, A.; Jemal, A.; Bray, F., Bladder Cancer Incidence and Mortality: A Global Overview and Recent Trends. *Eur Urol* 2017, 71, (1), 96-108.
4. Greiman, A. K.; Rosoff, J. S.; Prasad, S. M., Association of Human Development Index with global bladder, kidney, prostate and testis cancer incidence and mortality. *BJU Int* 2017, 120, (6), 799-807.
5. Leal, J.; Luengo-Fernandez, R.; Sullivan, R.; Witjes, J. A., Economic Burden of Bladder Cancer Across the European Union. *Eur Urol* 2016, 69, (3), 438-47.
6. Sanli, O.; Dobruch, J.; Knowles, M. A.; Burger, M.; Alemozaffar, M.; Nielsen, M. E.; Lotan, Y., Bladder cancer. *Nat Rev Dis Primers* 2017, 3, 17022.

7. Moch, H.; Ulbright, T.; Humphrey, P.; Reuter, V., WHO Classification of Tumours of the Urinary System and Male Genital Organs (4th Edition). IARC: Lyon 2016.
8. Meissner, A., Epigenetic modifications in pluripotent and differentiated cells. *Nat Biotechnol* 2010, 28, (10), 1079-88.
9. Skinner, M. K., Role of epigenetics in developmental biology and transgenerational inheritance. *Birth Defects Res C Embryo Today* 2011, 93, (1), 51-5.
10. Saitou, M.; Kagiwada, S.; Kurimoto, K., Epigenetic reprogramming in mouse pre-implantation development and primordial germ cells. *Development* 2012, 139, (1), 15-31.
11. Kelly, A. D.; Issa, J. J., The promise of epigenetic therapy: reprogramming the cancer epigenome. *Curr Opin Genet Dev* 2017, 42, 68-77.
12. Baylin, S. B.; Jones, P. A., Epigenetic Determinants of Cancer. *Cold Spring Harb Perspect Biol* 2016, 8, (9).
13. Esteller, M., Epigenetics in cancer. *N Engl J Med* 2008, 358, (11), 1148-59.
14. Mossanen, M.; Gore, J. L., The burden of bladder cancer care: direct and indirect costs. *Curr Opin Urol* 2014, 24, (5), 487-91.
15. Kojima, T.; Kawai, K.; Miyazaki, J.; Nishiyama, H., Biomarkers for precision medicine in bladder cancer. *Int J Clin Oncol* 2017, 22, (2), 207-213.
16. Dudzic, E.; Goepel, J. R.; Catto, J. W., Global epigenetic profiling in bladder cancer. *Epigenomics* 2011, 3, (1), 35-45.
17. Schulz, W. A.; Koutsogiannouli, E. A.; Niegisch, G.; Hoffmann, M. J., Epigenetics of urothelial carcinoma. *Methods Mol Biol* 2015, 1238, 183-215.
18. Kalluri, R.; Weinberg, R. A., The basics of epithelial-mesenchymal transition. *J Clin Invest* 2009, 119, (6), 1420-8.
19. Nieto, M. A.; Huang, R. Y.; Jackson, R. A.; Thiery, J. P., EMT: 2016. *Cell* 2016, 166, (1), 21-45.
20. Tam, W. L.; Weinberg, R. A., The epigenetics of epithelial-mesenchymal plasticity in cancer. *Nat Med* 2013, 19, (11), 1438-49.
21. Thiery, J. P.; Sleeman, J. P., Complex networks orchestrate epithelial-mesenchymal transitions. *Nat Rev Mol Cell Biol* 2006, 7, (2), 131-42.
22. De Craene, B.; Berx, G., Regulatory networks defining EMT during cancer initiation and progression. *Nat Rev Cancer* 2013, 13, (2), 97-110.
23. van Roy, F.; Berx, G., The cell-cell adhesion molecule E-cadherin. *Cell Mol Life Sci* 2008, 65, (23), 3756-88.
24. Bracken, C. P.; Gregory, P. A.; Kolesnikoff, N.; Bert, A. G.; Wang, J.; Shannon, M. F.; Goodall, G. J., A double-negative feedback loop between ZEB1-SIP1 and the microRNA-200 family regulates epithelial-mesenchymal transition. *Cancer Res* 2008, 68, (19), 7846-54.
25. Chaffer, C. L.; Brennan, J. P.; Slavin, J. L.; Blick, T.; Thompson, E. W.; Williams, E. D., Mesenchymal-to-epithelial transition facilitates bladder cancer metastasis: role of fibroblast growth factor receptor-2. *Cancer Res* 2006, 66, (23), 11271-8.

26. Choi, J.; Park, S. Y.; Joo, C. K., Transforming growth factor-beta1 represses E-cadherin production via slug expression in lens epithelial cells. *Invest Ophthalmol Vis Sci* 2007, 48, (6), 2708-18.
27. Cerami, E.; Gao, J.; Dogrusoz, U.; Gross, B. E.; Sumer, S. O.; Aksoy, B. A.; Jacobsen, A.; Byrne, C. J.; Heuer, M. L.; Larsson, E.; Antipin, Y.; Reva, B.; Goldberg, A. P.; Sander, C.; Schultz, N., The cBio cancer genomics portal: an open platform for exploring multidimensional cancer genomics data. *Cancer Discov* 2012, 2, (5), 401-4.
28. Cao, Q.; Yu, J.; Dhanasekaran, S. M.; Kim, J. H.; Mani, R. S.; Tomlins, S. A.; Mehra, R.; Laxman, B.; Cao, X.; Yu, J.; Kleer, C. G.; Varambally, S.; Chinnaiyan, A. M., Repression of E-cadherin by the polycomb group protein EZH2 in cancer. *Oncogene* 2008, 27, (58), 7274-84.
29. Tiwari, N.; Tiwari, V. K.; Waldmeier, L.; Balwierz, P. J.; Arnold, P.; Pachkov, M.; Meyer-Schaller, N.; Schubeler, D.; van Nimwegen, E.; Christofori, G., Sox4 is a master regulator of epithelial-mesenchymal transition by controlling Ezh2 expression and epigenetic reprogramming. *Cancer Cell* 2013, 23, (6), 768-83.
30. Liu, L.; Xu, Z.; Zhong, L.; Wang, H.; Jiang, S.; Long, Q.; Xu, J.; Guo, J., Enhancer of zeste homolog 2 (EZH2) promotes tumour cell migration and invasion via epigenetic repression of E-cadherin in renal cell carcinoma. *BJU Int* 2016, 117, (2), 351-62.
31. Liu, X.; Wang, C.; Chen, Z.; Jin, Y.; Wang, Y.; Kolokythas, A.; Dai, Y.; Zhou, X., MicroRNA-138 suppresses epithelial-mesenchymal transition in squamous cell carcinoma cell lines. *Biochem J* 2011, 440, (1), 23-31.
32. Luo, M.; Li, Z.; Wang, W.; Zeng, Y.; Liu, Z.; Qiu, J., Long non-coding RNA H19 increases bladder cancer metastasis by associating with EZH2 and inhibiting E-cadherin expression. *Cancer Lett* 2013, 333, (2), 213-21.
33. Kottakis, F.; Polytaichou, C.; Foltopoulou, P.; Sanidas, I.; Kampranis, S. C.; Tsiichlis, P. N., FGF-2 regulates cell proliferation, migration, and angiogenesis through an NDY1/KDM2B-miR-101-EZH2 pathway. *Mol Cell* 2011, 43, (2), 285-98.
34. Friedman, J. M.; Liang, G.; Liu, C. C.; Wolff, E. M.; Tsai, Y. C.; Ye, W.; Zhou, X.; Jones, P. A., The putative tumor suppressor microRNA-101 modulates the cancer epigenome by repressing the polycomb group protein EZH2. *Cancer Res* 2009, 69, (6), 2623-9.
35. Varambally, S.; Cao, Q.; Mani, R. S.; Shankar, S.; Wang, X.; Ateeq, B.; Laxman, B.; Cao, X.; Jing, X.; Ramnarayanan, K.; Brenner, J. C.; Yu, J.; Kim, J. H.; Han, B.; Tan, P.; Kumar-Sinha, C.; Lonigro, R. J.; Palanisamy, N.; Maher, C. A.; Chinnaiyan, A. M., Genomic loss of microRNA-101 leads to overexpression of histone methyltransferase EZH2 in cancer. *Science* 2008, 322, (5908), 1695-9.
36. McNiel, E. A.; Tsiichlis, P. N., Analyses of publicly available genomics resources define FGF-2-expressing bladder carcinomas as EMT-prone, proliferative tumors with low mutation rates and high expression of CTLA-4, PD-1 and PD-L1. *Signal Transduct Target Ther* 2017, 2.
37. Lee, S. R.; Roh, Y. G.; Kim, S. K.; Lee, J. S.; Seol, S. Y.; Lee, H. H.; Kim, W. T.; Kim, W. J.; Heo, J.; Cha, H. J.; Kang, T. H.; Chung, J. W.; Chu, I. S.; Leem, S. H., Activation of EZH2 and SUZ12

Regulated by E2F1 Predicts the Disease Progression and Aggressive Characteristics of Bladder Cancer. *Clin Cancer Res* 2015, 21, (23), 5391-403.

38. Wu, X.; Liu, D.; Tao, D.; Xiang, W.; Xiao, X.; Wang, M.; Wang, L.; Luo, G.; Li, Y.; Zeng, F.; Jiang, G., BRD4 Regulates EZH2 Transcription through Upregulation of C-MYC and Represents a Novel Therapeutic Target in Bladder Cancer. *Mol Cancer Ther* 2016, 15, (5), 1029-42.

39. Jones, B. A.; Varambally, S.; Arend, R. C., Histone Methyltransferase EZH2: A Therapeutic Target for Ovarian Cancer. *Mol Cancer Ther* 2018, 17, (3), 591-602.

40. ORION-E: A Study Evaluating CPI-1205 in Patients With Advanced Solid Tumors. In <https://clinicaltrials.gov/show/NCT03525795>.

41. Bird, A., DNA methylation patterns and epigenetic memory. *Genes Dev* 2002, 16, (1), 6-21.

42. Leyvraz, C.; Charles, R. P.; Rubera, I.; Guitard, M.; Rotman, S.; Breiden, B.; Sandhoff, K.; Hummler, E., The epidermal barrier function is dependent on the serine protease CAP1/Prss8. *J Cell Biol* 2005, 170, (3), 487-96.

43. Chen, L. M.; Verity, N. J.; Chai, K. X., Loss of prostaticin (PRSS8) in human bladder transitional cell carcinoma cell lines is associated with epithelial-mesenchymal transition (EMT). *BMC Cancer* 2009, 9, 377.

44. Hemberger, M.; Udayashankar, R.; Tesar, P.; Moore, H.; Burton, G. J., ELF5-enforced transcriptional networks define an epigenetically regulated trophoblast stem cell compartment in the human placenta. *Hum Mol Genet* 2010, 19, (12), 2456-67.

45. Ng, R. K.; Dean, W.; Dawson, C.; Lucifero, D.; Madeja, Z.; Reik, W.; Hemberger, M., Epigenetic restriction of embryonic cell lineage fate by methylation of Elf5. *Nat Cell Biol* 2008, 10, (11), 1280-90.

46. Wu, B.; Cao, X.; Liang, X.; Zhang, X.; Zhang, W.; Sun, G.; Wang, D., Epigenetic regulation of Elf5 is associated with epithelial-mesenchymal transition in urothelial cancer. *PLoS One* 2015, 10, (1), e0117510.

47. Li, X. D.; Zhang, J. X.; Jiang, L. J.; Wang, F. W.; Liu, L. L.; Liao, Y. J.; Jin, X. H.; Chen, W. H.; Chen, X.; Guo, S. J.; Zhou, F. J.; Zeng, Y. X.; Guan, X. Y.; Liu, Z. W.; Xie, D., Overexpression of maelstrom promotes bladder urothelial carcinoma cell aggressiveness by epigenetically downregulating MTSS1 through DNMT3B. *Oncogene* 2016, 35, (49), 6281-6292.

48. Tsui, K. H.; Hsu, S. Y.; Chung, L. C.; Lin, Y. H.; Feng, T. H.; Lee, T. Y.; Chang, P. L.; Juang, H. H., Growth differentiation factor-15: a p53- and demethylation-upregulating gene represses cell proliferation, invasion, and tumorigenesis in bladder carcinoma cells. *Sci Rep* 2015, 5, 12870.

49. Li, H.; Wang, J.; Xiao, W.; Xia, D.; Lang, B.; Wang, T.; Guo, X.; Hu, Z.; Ye, Z.; Xu, H., Epigenetic inactivation of KLF4 is associated with urothelial cancer progression and early recurrence. *J Urol* 2014, 191, (2), 493-501.

50. Xu, X.; Li, J.; Zhu, Y.; Xie, B.; Wang, X.; Wang, S.; Xie, H.; Yan, H.; Ying, Y.; Lin, Y.; Liu, B.; Wang, W.; Zheng, X., CRISPR-ON-Mediated KLF4 overexpression inhibits the proliferation, migration and invasion of urothelial bladder cancer in vitro and in vivo. *Oncotarget* 2017, 8, (60), 102078-102087.

51. Costa, V. L.; Henrique, R.; Danielsen, S. A.; Duarte-Pereira, S.; Eknaes, M.; Skotheim, R. I.; Rodrigues, A.; Magalhaes, J. S.; Oliveira, J.; Lothe, R. A.; Teixeira, M. R.; Jeronimo, C.; Lind, G. E., Three epigenetic biomarkers, GDF15, TMEFF2, and VIM, accurately predict bladder cancer from DNA-based analyses of urine samples. *Clin Cancer Res* 2010, 16, (23), 5842-51.
52. Monteiro-Reis, S.; Leca, L.; Almeida, M.; Antunes, L.; Monteiro, P.; Dias, P. C.; Morais, A.; Oliveira, J.; Henrique, R.; Jeronimo, C., Accurate detection of upper tract urothelial carcinoma in tissue and urine by means of quantitative GDF15, TMEFF2 and VIM promoter methylation. *Eur J Cancer* 2014, 50, (1), 226-33.
53. Wei, D.; Gong, W.; Kanai, M.; Schlunk, C.; Wang, L.; Yao, J. C.; Wu, T. T.; Huang, S.; Xie, K., Drastic down-regulation of Kruppel-like factor 4 expression is critical in human gastric cancer development and progression. *Cancer Res* 2005, 65, (7), 2746-54.
54. Yang, Y.; Goldstein, B. G.; Chao, H. H.; Katz, J. P., KLF4 and KLF5 regulate proliferation, apoptosis and invasion in esophageal cancer cells. *Cancer Biol Ther* 2005, 4, (11), 1216-21.
55. Wang, J.; Place, R. F.; Huang, V.; Wang, X.; Noonan, E. J.; Magyar, C. E.; Huang, J.; Li, L. C., Prognostic value and function of KLF4 in prostate cancer: RNAi and vector-mediated overexpression identify KLF4 as an inhibitor of tumor cell growth and migration. *Cancer Res* 2010, 70, (24), 10182-91.
56. Hu, W.; Hofstetter, W. L.; Li, H.; Zhou, Y.; He, Y.; Pataer, A.; Wang, L.; Xie, K.; Swisher, S. G.; Fang, B., Putative tumor-suppressive function of Kruppel-like factor 4 in primary lung carcinoma. *Clin Cancer Res* 2009, 15, (18), 5688-95.
57. Xu, X.; Tao, Y.; Gao, X.; Zhang, L.; Li, X.; Zou, W.; Ruan, K.; Wang, F.; Xu, G. L.; Hu, R., A CRISPR-based approach for targeted DNA demethylation. *Cell Discov* 2016, 2, 16009.
58. Chen, H.; Kazemier, H. G.; de Groote, M. L.; Ruiters, M. H.; Xu, G. L.; Rots, M. G., Induced DNA demethylation by targeting Ten-Eleven Translocation 2 to the human ICAM-1 promoter. *Nucleic Acids Res* 2014, 42, (3), 1563-74.
59. Mattick, J. S.; Rinn, J. L., Discovery and annotation of long noncoding RNAs. *Nat Struct Mol Biol* 2015, 22, (1), 5-7.
60. Ramalho-Carvalho, J.; Fromm, B.; Henrique, R.; Jeronimo, C., Deciphering the function of non-coding RNAs in prostate cancer. *Cancer Metastasis Rev* 2016, 35, (2), 235-62.
61. Peschansky, V. J.; Wahlestedt, C., Non-coding RNAs as direct and indirect modulators of epigenetic regulation. *Epigenetics* 2014, 9, (1), 3-12.
62. Anfossi, S.; Babayan, A.; Pantel, K.; Calin, G. A., Clinical utility of circulating non-coding RNAs - an update. *Nat Rev Clin Oncol* 2018.
63. Ghildiyal, M.; Zamore, P. D., Small silencing RNAs: an expanding universe. *Nat Rev Genet* 2009, 10, (2), 94-108.
64. Falzone, L.; Candido, S.; Salemi, R.; Basile, M. S.; Scalisi, A.; McCubrey, J. A.; Torino, F.; Signorelli, S. S.; Montella, M.; Libra, M., Computational identification of microRNAs associated to both epithelial to mesenchymal transition and NGAL/MMP-9 pathways in bladder cancer. *Oncotarget* 2016, 7, (45), 72758-72766.

65. Adam, L.; Zhong, M.; Choi, W.; Qi, W.; Nicoloso, M.; Arora, A.; Calin, G.; Wang, H.; Siefker-Radtke, A.; McConkey, D.; Bar-Eli, M.; Dinney, C., miR-200 expression regulates epithelial-to-mesenchymal transition in bladder cancer cells and reverses resistance to epidermal growth factor receptor therapy. *Clin Cancer Res* 2009, 15, (16), 5060-72.
66. Xu, X.; Li, S.; Lin, Y.; Chen, H.; Hu, Z.; Mao, Y.; Xu, X.; Wu, J.; Zhu, Y.; Zheng, X.; Luo, J.; Xie, L., MicroRNA-124-3p inhibits cell migration and invasion in bladder cancer cells by targeting ROCK1. *J Transl Med* 2013, 11, 276.
67. Tran, M. N.; Choi, W.; Wszolek, M. F.; Navai, N.; Lee, I. L.; Nitti, G.; Wen, S.; Flores, E. R.; Siefker-Radtke, A.; Czerniak, B.; Dinney, C.; Barton, M.; McConkey, D. J., The p63 protein isoform DeltaNp63alpha inhibits epithelial-mesenchymal transition in human bladder cancer cells: role of MIR-205. *J Biol Chem* 2013, 288, (5), 3275-88.
68. Majid, S.; Dar, A. A.; Saini, S.; Deng, G.; Chang, I.; Greene, K.; Tanaka, Y.; Dahiya, R.; Yamamura, S., MicroRNA-23b functions as a tumor suppressor by regulating Zeb1 in bladder cancer. *PLoS One* 2013, 8, (7), e67686.
69. Liu, L.; Qiu, M.; Tan, G.; Liang, Z.; Qin, Y.; Chen, L.; Chen, H.; Liu, J., miR-200c inhibits invasion, migration and proliferation of bladder cancer cells through down-regulation of BMI-1 and E2F3. *J Transl Med* 2014, 12, 305.
70. Zeng, T.; Peng, L.; Chao, C.; Fu, B.; Wang, G.; Wang, Y.; Zhu, X., miR-451 inhibits invasion and proliferation of bladder cancer by regulating EMT. *Int J Clin Exp Pathol* 2014, 7, (11), 7653-62.
71. Zhang, S.; Zhang, C.; Liu, W.; Zheng, W.; Zhang, Y.; Wang, S.; Huang, D.; Liu, X.; Bai, Z., MicroRNA-24 upregulation inhibits proliferation, metastasis and induces apoptosis in bladder cancer cells by targeting CARMA3. *Int J Oncol* 2015, 47, (4), 1351-60.
72. Yu, G.; Xu, K.; Xu, S.; Zhang, X.; Huang, Q.; Lang, B., [MicroRNA-34a regulates cell cycle by targeting CD44 in human bladder carcinoma cells]. *Nan Fang Yi Ke Da Xue Xue Bao* 2015, 35, (7), 935-40.
73. Yao, K.; He, L.; Gan, Y.; Zeng, Q.; Dai, Y.; Tan, J., MiR-186 suppresses the growth and metastasis of bladder cancer by targeting NSBP1. *Diagn Pathol* 2015, 10, 146.
74. Martinez-Fernandez, M.; Duenas, M.; Feber, A.; Segovia, C.; Garcia-Escudero, R.; Rubio, C.; Lopez-Calderon, F. F.; Diaz-Garcia, C.; Villacampa, F.; Duarte, J.; Gomez-Rodriguez, M. J.; Castellano, D.; Rodriguez-Peralto, J. L.; de la Rosa, F.; Beck, S.; Paramio, J. M., A Polycomb-mir200 loop regulates clinical outcome in bladder cancer. *Oncotarget* 2015, 6, (39), 42258-75.
75. Chen, M. F.; Zeng, F.; Qi, L.; Zu, X. B.; Wang, J.; Liu, L. F.; Li, Y., Transforming growth factorbeta1 induces epithelialmesenchymal transition and increased expression of matrix metalloproteinase16 via miR200b downregulation in bladder cancer cells. *Mol Med Rep* 2014, 10, (3), 1549-54.
76. Liu, J.; Cao, J.; Zhao, X., miR-221 facilitates the TGFbeta1-induced epithelial-mesenchymal transition in human bladder cancer cells by targeting STMN1. *BMC Urol* 2015, 15, 36.
77. Wu, C. T.; Lin, W. Y.; Chang, Y. H.; Lin, P. Y.; Chen, W. C.; Chen, M. F., DNMT1-dependent suppression of microRNA424 regulates tumor progression in human bladder cancer. *Oncotarget* 2015, 6, (27), 24119-31.

78. Chen, Z.; Li, Q.; Wang, S.; Zhang, J., miR4855p inhibits bladder cancer metastasis by targeting HMGA2. *Int J Mol Med* 2015, 36, (4), 1136-42.
79. Wang, H.; Ke, C.; Ma, X.; Zhao, Q.; Yang, M.; Zhang, W.; Wang, J., MicroRNA-92 promotes invasion and chemoresistance by targeting GSK3beta and activating Wnt signaling in bladder cancer cells. *Tumour Biol* 2016.
80. Huang, J.; Wang, B.; Hui, K.; Zeng, J.; Fan, J.; Wang, X.; Hsieh, J. T.; He, D.; Wu, K., miR-92b targets DAB2IP to promote EMT in bladder cancer migration and invasion. *Oncol Rep* 2016, 36, (3), 1693-701.
81. Zhou, M.; Wang, S.; Hu, L.; Liu, F.; Zhang, Q.; Zhang, D., miR-199a-5p suppresses human bladder cancer cell metastasis by targeting CCR7. *BMC Urol* 2016, 16, (1), 64.
82. Wang, X.; Liang, Z.; Xu, X.; Li, J.; Zhu, Y.; Meng, S.; Li, S.; Wang, S.; Xie, B.; Ji, A.; Liu, B.; Zheng, X.; Xie, L., miR-148a-3p represses proliferation and EMT by establishing regulatory circuits between ERBB3/AKT2/c-myc and DNMT1 in bladder cancer. *Cell Death Dis* 2016, 7, (12), e2503.
83. Wu, C. L.; Ho, J. Y.; Chou, S. C.; Yu, D. S., MiR-429 reverses epithelial-mesenchymal transition by restoring E-cadherin expression in bladder cancer. *Oncotarget* 2016, 7, (18), 26593-603.
84. Xu, X.; Zhu, Y.; Liang, Z.; Li, S.; Xu, X.; Wang, X.; Wu, J.; Hu, Z.; Meng, S.; Liu, B.; Qin, J.; Xie, L.; Zheng, X., c-Met and CREB1 are involved in miR-433-mediated inhibition of the epithelial-mesenchymal transition in bladder cancer by regulating Akt/GSK-3beta/Snail signaling. *Cell Death Dis* 2016, 7, e2088.
85. Shen, J.; Zhang, J.; Xiao, M.; Yang, J.; Zhang, N., MiR-203 Suppresses Bladder Cancer Cell Growth and Targets the Twist1. *Oncol Res* 2017.
86. Miao, X.; Gao, H.; Liu, S.; Chen, M.; Xu, W.; Ling, X.; Deng, X.; Rao, C., Down-regulation of microRNA-224 -inhibites growth and epithelial-to-mesenchymal transition phenotype -via modulating SUFU expression in bladder cancer cells. *Int J Biol Macromol* 2018, 106, 234-240.
87. Li, J.; Xu, X.; Meng, S.; Liang, Z.; Wang, X.; Xu, M.; Wang, S.; Li, S.; Zhu, Y.; Xie, B.; Lin, Y.; Zheng, X.; Liu, B.; Xie, L., MET/SMAD3/SNAIL circuit mediated by miR-323a-3p is involved in regulating epithelial-mesenchymal transition progression in bladder cancer. *Cell Death Dis* 2017, 8, (8), e3010.
88. Wei, Z.; Hu, X.; Liu, J.; Zhu, W.; Zhan, X.; Sun, S., MicroRNA-497 upregulation inhibits cell invasion and metastasis in T24 and BIU-87 bladder cancer cells. *Mol Med Rep* 2017, 16, (2), 2055-2060.
89. Yu, H.; Duan, P.; Zhu, H.; Rao, D., miR-613 inhibits bladder cancer proliferation and migration through targeting SphK1. *Am J Transl Res* 2017, 9, (3), 1213-1221.
90. Xu, M.; Li, J.; Wang, X.; Meng, S.; Shen, J.; Wang, S.; Xu, X.; Xie, B.; Liu, B.; Xie, L., MiR-22 suppresses epithelial-mesenchymal transition in bladder cancer by inhibiting Snail and MAPK1/Slug/vimentin feedback loop. *Cell Death Dis* 2018, 9, (2), 209.
91. Mao, X. W.; Xiao, J. Q.; Li, Z. Y.; Zheng, Y. C.; Zhang, N., Effects of microRNA-135a on the epithelial-mesenchymal transition, migration and invasion of bladder cancer cells by targeting GSK3beta through the Wnt/beta-catenin signaling pathway. *Exp Mol Med* 2018, 50, (1), e429.

92. Huang, X.; Zhu, H.; Gao, Z.; Li, J.; Zhuang, J.; Dong, Y.; Shen, B.; Li, M.; Zhou, H.; Guo, H.; Huang, R.; Yan, J., Wnt7a activates canonical Wnt signaling, promotes bladder cancer cell invasion, and is suppressed by miR-370-3p. *J Biol Chem* 2018.
93. Liu, W.; Qi, L.; Lv, H.; Zu, X.; Chen, M.; Wang, J.; Liu, L.; Zeng, F.; Li, Y., MiRNA-141 and miRNA-200b are closely related to invasive ability and considered as decision-making biomarkers for the extent of PLND during cystectomy. *BMC Cancer* 2015, 15, 92.
94. Yan, L.; Wang, Y.; Liang, J.; Liu, Z.; Sun, X.; Cai, K., MiR-301b promotes the proliferation, mobility, and epithelial-to-mesenchymal transition of bladder cancer cells by targeting EGR1. *Biochem Cell Biol* 2017, 95, (5), 571-577.
95. Wang, C.; Ge, Q.; Chen, Z.; Hu, J.; Li, F.; Ye, Z., Promoter-associated endogenous and exogenous small RNAs suppress human bladder cancer cell metastasis by activating p21 (CIP1/WAF1) expression. *Tumour Biol* 2016, 37, (5), 6589-98.
96. Liu, M.; Chen, Y.; Huang, B.; Mao, S.; Cai, K.; Wang, L.; Yao, X., Tumor-suppressing effects of microRNA-612 in bladder cancer cells by targeting malic enzyme 1 expression. *Int J Oncol* 2018.
97. Zhong, Z.; Huang, M.; Lv, M.; He, Y.; Duan, C.; Zhang, L.; Chen, J., Circular RNA MYLK as a competing endogenous RNA promotes bladder cancer progression through modulating VEGFA/VEGFR2 signaling pathway. *Cancer Lett* 2017, 403, 305-317.
98. Li, L. J.; Zhu, J. L.; Bao, W. S.; Chen, D. K.; Huang, W. W.; Weng, Z. L., Long noncoding RNA GHET1 promotes the development of bladder cancer. *Int J Clin Exp Pathol* 2014, 7, (10), 7196-205.
99. Berrondo, C.; Flax, J.; Kucherov, V.; Siebert, A.; Osinski, T.; Rosenberg, A.; Fucile, C.; Richeimer, S.; Beckham, C. J., Expression of the Long Non-Coding RNA HOTAIR Correlates with Disease Progression in Bladder Cancer and Is Contained in Bladder Cancer Patient Urinary Exosomes. *PLoS One* 2016, 11, (1), e0147236.
100. Lv, M.; Zhong, Z.; Huang, M.; Tian, Q.; Jiang, R.; Chen, J., lncRNA H19 regulates epithelial-mesenchymal transition and metastasis of bladder cancer by miR-29b-3p as competing endogenous RNA. *Biochim Biophys Acta* 2017, 1864, (10), 1887-1899.
101. Fan, Y.; Shen, B.; Tan, M.; Mu, X.; Qin, Y.; Zhang, F.; Liu, Y., TGF-beta-induced upregulation of malat1 promotes bladder cancer metastasis by associating with suz12. *Clin Cancer Res* 2014, 20, (6), 1531-41.
102. Chen, Y.; Peng, Y.; Xu, Z.; Ge, B.; Xiang, X.; Zhang, T.; Gao, L.; Shi, H.; Wang, C.; Huang, J., lncROR Promotes Bladder Cancer Cell Proliferation, Migration, and Epithelial-Mesenchymal Transition. *Cell Physiol Biochem* 2017, 41, (6), 2399-2410.
103. Tuo, Z.; Zhang, J.; Xue, W., lncRNA TP73-AS1 predicts the prognosis of bladder cancer patients and functions as a suppressor for bladder cancer by EMT pathway. *Biochem Biophys Res Commun* 2018.
104. Tan, J.; Qiu, K.; Li, M.; Liang, Y., Double-negative feedback loop between long non-coding RNA TUG1 and miR-145 promotes epithelial to mesenchymal transition and radioresistance in human bladder cancer cells. *FEBS Lett* 2015, 589, (20 Pt B), 3175-81.

105. Xue, M.; Pang, H.; Li, X.; Li, H.; Pan, J.; Chen, W., Long non-coding RNA urothelial cancer-associated 1 promotes bladder cancer cell migration and invasion by way of the hsa-miR-145-ZEB1/2-FSCN1 pathway. *Cancer Sci* 2016, 107, (1), 18-27.
106. Luo, J.; Chen, J.; Li, H.; Yang, Y.; Yun, H.; Yang, S.; Mao, X., LncRNA UCA1 promotes the invasion and EMT of bladder cancer cells by regulating the miR-143/HMGB1 pathway. *Oncol Lett* 2017, 14, (5), 5556-5562.
107. Xu, R.; Zhu, X.; Chen, F.; Huang, C.; Ai, K.; Wu, H.; Zhang, L.; Zhao, X., LncRNA XIST/miR-200c regulates the stemness properties and tumorigenicity of human bladder cancer stem cell-like cells. *Cancer Cell Int* 2018, 18, 41.
108. Zhuang, J.; Lu, Q.; Shen, B.; Huang, X.; Shen, L.; Zheng, X.; Huang, R.; Yan, J.; Guo, H., TGFbeta1 secreted by cancer-associated fibroblasts induces epithelial-mesenchymal transition of bladder cancer cells through lncRNA-ZEB2NAT. *Sci Rep* 2015, 5, 11924.
109. Gregory, P. A.; Bert, A. G.; Paterson, E. L.; Barry, S. C.; Tsykin, A.; Farshid, G.; Vadas, M. A.; Khew-Goodall, Y.; Goodall, G. J., The miR-200 family and miR-205 regulate epithelial to mesenchymal transition by targeting ZEB1 and SIP1. *Nat Cell Biol* 2008, 10, (5), 593-601.
110. Shimono, Y.; Zabala, M.; Cho, R. W.; Lobo, N.; Dalerba, P.; Qian, D.; Diehn, M.; Liu, H.; Panula, S. P.; Chiao, E.; Dirbas, F. M.; Somlo, G.; Pera, R. A.; Lao, K.; Clarke, M. F., Downregulation of miRNA-200c links breast cancer stem cells with normal stem cells. *Cell* 2009, 138, (3), 592-603.
111. Leskela, S.; Leandro-Garcia, L. J.; Mendiola, M.; Barriuso, J.; Inglada-Perez, L.; Munoz, I.; Martinez-Delgado, B.; Redondo, A.; de Santiago, J.; Robledo, M.; Hardisson, D.; Rodriguez-Antona, C., The miR-200 family controls beta-tubulin III expression and is associated with paclitaxel-based treatment response and progression-free survival in ovarian cancer patients. *Endocr Relat Cancer* 2011, 18, (1), 85-95.
112. Vallejo, D. M.; Caparros, E.; Dominguez, M., Targeting Notch signalling by the conserved miR-8/200 microRNA family in development and cancer cells. *EMBO J* 2011, 30, (4), 756-69.
113. Lee, J. W.; Park, Y. A.; Choi, J. J.; Lee, Y. Y.; Kim, C. J.; Choi, C.; Kim, T. J.; Lee, N. W.; Kim, B. G.; Bae, D. S., The expression of the miRNA-200 family in endometrial endometrioid carcinoma. *Gynecol Oncol* 2011, 120, (1), 56-62.
114. Santos, M.; Martinez-Fernandez, M.; Duenas, M.; Garcia-Escudero, R.; Alfaya, B.; Villacampa, F.; Saiz-Ladera, C.; Costa, C.; Oteo, M.; Duarte, J.; Martinez, V.; Gomez-Rodriguez, M. J.; Martin, M. L.; Fernandez, M.; Viatour, P.; Morcillo, M. A.; Sage, J.; Castellano, D.; Rodriguez-Peralto, J. L.; de la Rosa, F.; Paramio, J. M., In vivo disruption of an Rb-E2F-Ezh2 signaling loop causes bladder cancer. *Cancer Res* 2014, 74, (22), 6565-6577.
115. Padrao, N. A.; Monteiro-Reis, S.; Torres-Ferreira, J.; Antunes, L.; Leca, L.; Montezuma, D.; Ramalho-Carvalho, J.; Dias, P. C.; Monteiro, P.; Oliveira, J.; Henrique, R.; Jeronimo, C., MicroRNA promoter methylation: a new tool for accurate detection of urothelial carcinoma. *Br J Cancer* 2017, 116, (5), 634-639.
116. Hansen, T. B.; Jensen, T. I.; Clausen, B. H.; Bramsen, J. B.; Finsen, B.; Damgaard, C. K.; Kjems, J., Natural RNA circles function as efficient microRNA sponges. *Nature* 2013, 495, (7441), 384-8.

117. Morris, K. V.; Mattick, J. S., The rise of regulatory RNA. *Nat Rev Genet* 2014, 15, (6), 423-37.

References (Chapter I)

1. Khandelwal P, Abraham SN, Apodaca G. Cell biology and physiology of the uroepithelium. *Am J Physiol Renal Physiol*. 2009;297(6):F1477-501.
2. Ferlay J, Ervik M, Lam F, Colombet M, Mery L, Piñeros M, et al. Global Cancer Observatory: Cancer Tomorrow Available from: <https://gco.iarc.fr/tomorrow2018> [
3. Antoni S, Ferlay J, Soerjomataram I, Znaor A, Jemal A, Bray F. Bladder Cancer Incidence and Mortality: A Global Overview and Recent Trends. *Eur Urol*. 2017;71(1):96-108.
4. Saginala K, Barsouk A, Aluru JS, Rawla P, Padala SA, Barsouk A. Epidemiology of Bladder Cancer. *Med Sci (Basel)*. 2020;8(1).
5. Leal J, Luengo-Fernandez R, Sullivan R, Witjies JA. Economic Burden of Bladder Cancer Across the European Union. *Eur Urol*. 2016;69(3):438-47.
6. Sanli O, Dobruch J, Knowles MA, Burger M, Alemozaffar M, Nielsen ME, et al. Bladder cancer. *Nat Rev Dis Primers*. 2017;3:17022.
7. van Osch FH, Jochems SH, van Schooten FJ, Bryan RT, Zeegers MP. Quantified relations between exposure to tobacco smoking and bladder cancer risk: a meta-analysis of 89 observational studies. *Int J Epidemiol*. 2016;45(3):857-70.
8. Letasiova S, Medve'ova A, Sovcikova A, Dusinska M, Volkovova K, Mosoiu C, et al. Bladder cancer, a review of the environmental risk factors. *Environ Health*. 2012;11 Suppl 1:S11.
9. Ng M, Freeman MK, Fleming TD, Robinson M, Dwyer-Lindgren L, Thomson B, et al. Smoking prevalence and cigarette consumption in 187 countries, 1980-2012. *JAMA*. 2014;311(2):183-92.
10. Burger M, Catto JW, Dalbagni G, Grossman HB, Herr H, Karakiewicz P, et al. Epidemiology and risk factors of urothelial bladder cancer. *Eur Urol*. 2013;63(2):234-41.
11. Cumberbatch MG, Cox A, Teare D, Catto JW. Contemporary Occupational Carcinogen Exposure and Bladder Cancer: A Systematic Review and Meta-analysis. *JAMA Oncol*. 2015;1(9):1282-90.
12. Purdue MP, Hutchings SJ, Rushton L, Silverman DT. The proportion of cancer attributable to occupational exposures. *Ann Epidemiol*. 2015;25(3):188-92.
13. Zhang Y. Understanding the gender disparity in bladder cancer risk: the impact of sex hormones and liver on bladder susceptibility to carcinogens. *J Environ Sci Health C Environ Carcinog Ecotoxicol Rev*. 2013;31(4):287-304.
14. Freedman ND, Silverman DT, Hollenbeck AR, Schatzkin A, Abnet CC. Association between smoking and risk of bladder cancer among men and women. *JAMA*. 2011;306(7):737-45.

15. Schmidt-Hansen M, Berendse S, Hamilton W. The association between symptoms and bladder or renal tract cancer in primary care: a systematic review. *Br J Gen Pract.* 2015;65(640):e769-75.
16. Babjuk M, Burger M, Comperat EM, Gontero P, Mostafid AH, Palou J, et al. European Association of Urology Guidelines on Non-muscle-invasive Bladder Cancer (TaT1 and Carcinoma In Situ) - 2019 Update. *Eur Urol.* 2019;76(5):639-57.
17. Alfred Witjes J, Le Bret T, Comperat EM, Cowan NC, De Santis M, Bruins HM, et al. Updated 2016 EAU Guidelines on Muscle-invasive and Metastatic Bladder Cancer. *Eur Urol.* 2017;71(3):462-75.
18. Brierley J, Gospodarowicz MK, Wittekind C. TNM classification of malignant tumours. Eighth edition. ed. Chichester, West Sussex, UK ; Hoboken, NJ: John Wiley & Sons, Inc.; 2017. p. p.
19. Amin MB, American Joint Committee on Cancer., American Cancer Society. AJCC cancer staging manual. Eight edition / editor-in-chief, Mahul B. Amin, MD, FACS ; editors, Stephen B. Edge, MD, FACS and 16 others ; Donna M. Gress, RHIT, CTR - Technical editor ; Laura R. Meyer, CAPM - Managing editor. ed. Chicago IL: American Joint Committee on Cancer, Springer; 2017. xvii, 1024 pages p.
20. Humphrey PA, Moch H, Cubilla AL, Ulbright TM, Reuter VE. The 2016 WHO Classification of Tumours of the Urinary System and Male Genital Organs-Part B: Prostate and Bladder Tumours. *Eur Urol.* 2016;70(1):106-19.
21. Sylvester RJ, van der Meijden AP, Oosterlinck W, Witjes JA, Bouffieux C, Denis L, et al. Predicting recurrence and progression in individual patients with stage Ta T1 bladder cancer using EORTC risk tables: a combined analysis of 2596 patients from seven EORTC trials. *Eur Urol.* 2006;49(3):466-5; discussion 75-7.
22. Ravnaz K, Walz ME, Weissert JA, Downs TM. Predicting Nonmuscle Invasive Bladder Cancer Recurrence and Progression in a United States Population. *J Urol.* 2017;198(4):824-31.
23. Comperat EM, Burger M, Gontero P, Mostafid AH, Palou J, Roupret M, et al. Grading of Urothelial Carcinoma and The New "World Health Organisation Classification of Tumours of the Urinary System and Male Genital Organs 2016". *Eur Urol Focus.* 2019;5(3):457-66.
24. F.K.S.L. M, H. T. Histologic typing of urinary bladder tumors: international histological classification of tumors. Geneva, Switzerland: World Health Organization; 1973.
25. Epstein JI, Amin MB, Reuter VR, Mostofi FK. The World Health Organization/International Society of Urological Pathology consensus classification of urothelial (transitional cell) neoplasms of the urinary bladder. Bladder Consensus Conference Committee. *Am J Surg Pathol.* 1998;22(12):1435-48.

26. Eble J.N. SG, Epstein J.I., Sesterhenn I.A. World Health Organization classification of tumours. Pathology and genetics of tumours of the urinary system and male genital organs. Lyon, France: International Agency for Research on Cancer; 2004.
27. Moch H, Ulbright T, Humphrey P, Reuter V. WHO Classification of Tumours of the Urinary System and Male Genital Organs (4th Edition). IARC: Lyon 2016.
28. Pan CC, Chang YH, Chen KK, Yu HJ, Sun CH, Ho DM. Prognostic significance of the 2004 WHO/ISUP classification for prediction of recurrence, progression, and cancer-specific mortality of non-muscle-invasive urothelial tumors of the urinary bladder: a clinicopathologic study of 1,515 cases. *Am J Clin Pathol.* 2010;133(5):788-95.
29. Brimo F, Vollmer RT, Case B, Aprikian A, Kassouf W, Auger M. Accuracy of urine cytology and the significance of an atypical category. *Am J Clin Pathol.* 2009;132(5):785-93.
30. Lotan Y, Roehrborn CG. Sensitivity and specificity of commonly available bladder tumor markers versus cytology: results of a comprehensive literature review and meta-analyses. *Urology.* 2003;61(1):109-18; discussion 18.
31. Bhat A, Ritch CR. Urinary biomarkers in bladder cancer: where do we stand? *Curr Opin Urol.* 2019;29(3):203-9.
32. Hajdinjak T. UroVysion FISH test for detecting urothelial cancers: meta-analysis of diagnostic accuracy and comparison with urinary cytology testing. *Urol Oncol.* 2008;26(6):646-51.
33. Seideman C, Canter D, Kim P, Cordon B, Weizer A, Oliva I, et al. Multicenter evaluation of the role of UroVysion FISH assay in surveillance of patients with bladder cancer: does FISH positivity anticipate recurrence? *World J Urol.* 2015;33(9):1309-13.
34. Kim PH, Sukhu R, Cordon BH, Sfakianos JP, Sjoberg DD, Hakimi AA, et al. Reflex fluorescence in situ hybridization assay for suspicious urinary cytology in patients with bladder cancer with negative surveillance cystoscopy. *BJU Int.* 2014;114(3):354-9.
35. Savic S, Zlobec I, Thalmann GN, Engeler D, Schmauss M, Lehmann K, et al. The prognostic value of cytology and fluorescence in situ hybridization in the follow-up of nonmuscle-invasive bladder cancer after intravesical Bacillus Calmette-Guerin therapy. *Int J Cancer.* 2009;124(12):2899-904.
36. Jamshidian H, Kor K, Djalali M. Urine concentration of nuclear matrix protein 22 for diagnosis of transitional cell carcinoma of bladder. *Urol J.* 2008;5(4):243-7.
37. Shariat SF, Karam JA, Raman JD. Urine cytology and urine-based markers for bladder urothelial carcinoma detection and monitoring: developments and future prospects. *Biomark Med.* 2008;2(2):165-80.

38. Grossman HB, Soloway M, Messing E, Katz G, Stein B, Kassabian V, et al. Surveillance for recurrent bladder cancer using a point-of-care proteomic assay. *JAMA*. 2006;295(3):299-305.
39. Mowatt G, Zhu S, Kilonzo M, Boachie C, Fraser C, Griffiths TR, et al. Systematic review of the clinical effectiveness and cost-effectiveness of photodynamic diagnosis and urine biomarkers (FISH, ImmunoCyt, NMP22) and cytology for the detection and follow-up of bladder cancer. *Health Technol Assess*. 2010;14(4):1-331, iii-iv.
40. Miyake M, Goodison S, Rizwani W, Ross S, Bart Grossman H, Rosser CJ. Urinary BTA: indicator of bladder cancer or of hematuria. *World J Urol*. 2012;30(6):869-73.
41. Glas AS, Roos D, Deutekom M, Zwinderman AH, Bossuyt PM, Kurth KH. Tumor markers in the diagnosis of primary bladder cancer. A systematic review. *J Urol*. 2003;169(6):1975-82.
42. He H, Han C, Hao L, Zang G. ImmunoCyt test compared to cytology in the diagnosis of bladder cancer: A meta-analysis. *Oncol Lett*. 2016;12(1):83-8.
43. Todenhofer T, Hennenlotter J, Tews V, Gakis G, Aufderklamm S, Kuehs U, et al. Impact of different grades of microscopic hematuria on the performance of urine-based markers for the detection of urothelial carcinoma. *Urol Oncol*. 2013;31(7):1148-54.
44. Rouanne M, Lorient Y, Leuret T, Soria JC. Novel therapeutic targets in advanced urothelial carcinoma. *Crit Rev Oncol Hematol*. 2016;98:106-15.
45. Powles T, Eder JP, Fine GD, Braithwaite FS, Lorient Y, Cruz C, et al. MPDL3280A (anti-PD-L1) treatment leads to clinical activity in metastatic bladder cancer. *Nature*. 2014;515(7528):558-62.
46. Davarpanah NN, Yuno A, Trepel JB, Apolo AB. Immunotherapy: a new treatment paradigm in bladder cancer. *Curr Opin Oncol*. 2017.
47. Advanced Bladder Cancer Meta-analysis C. Neoadjuvant chemotherapy in invasive bladder cancer: update of a systematic review and meta-analysis of individual patient data advanced bladder cancer (ABC) meta-analysis collaboration. *Eur Urol*. 2005;48(2):202-5; discussion 5-6.
48. Grossman HB, Natale RB, Tangen CM, Speights VO, Vogelzang NJ, Trump DL, et al. Neoadjuvant chemotherapy plus cystectomy compared with cystectomy alone for locally advanced bladder cancer. *N Engl J Med*. 2003;349(9):859-66.
49. Yin M, Joshi M, Meijer RP, Glantz M, Holder S, Harvey HA, et al. Neoadjuvant Chemotherapy for Muscle-Invasive Bladder Cancer: A Systematic Review and Two-Step Meta-Analysis. *Oncologist*. 2016;21(6):708-15.
50. Zargar H, Shah JB, van Rhijn BW, Daneshmand S, Bivalacqua TJ, Spiess PE, et al. Neoadjuvant Dose Dense MVAC versus Gemcitabine and Cisplatin in Patients with cT3-4aN0M0 Bladder Cancer Treated with Radical Cystectomy. *J Urol*. 2018;199(6):1452-8.

51. Kamoun A, de Reynies A, Allory Y, Sjobahl G, Robertson AG, Seiler R, et al. A Consensus Molecular Classification of Muscle-invasive Bladder Cancer. *Eur Urol.* 2020;77(4):420-33.
52. Tan TZ, Rouanne M, Tan KT, Huang RY, Thiery JP. Molecular Subtypes of Urothelial Bladder Cancer: Results from a Meta-cohort Analysis of 2411 Tumors. *Eur Urol.* 2019;75(3):423-32.
53. Dyrskjot L, Thykjaer T, Kruhoffer M, Jensen JL, Marcussen N, Hamilton-Dutoit S, et al. Identifying distinct classes of bladder carcinoma using microarrays. *Nat Genet.* 2003;33(1):90-6.
54. Lerner SP, McConkey DJ, Hoadley KA, Chan KS, Kim WY, Radvanyi F, et al. Bladder Cancer Molecular Taxonomy: Summary from a Consensus Meeting. *Bladder Cancer.* 2016;2(1):37-47.
55. Dyrskjot L. Molecular Subtypes of Bladder Cancer: Academic Exercise or Clinical Relevance? *Eur Urol.* 2019;75(3):433-4.
56. Blinova E, Roshchin D, Kogan E, Samishina E, Demura T, Deryabina O, et al. Patient-Derived Non-Muscular Invasive Bladder Cancer Xenografts of Main Molecular Subtypes of the Tumor for Anti-Pd-11 Treatment Assessment. *Cells.* 2019;8(6).
57. Blaveri E, Simko JP, Korkola JE, Brewer JL, Baehner F, Mehta K, et al. Bladder cancer outcome and subtype classification by gene expression. *Clin Cancer Res.* 2005;11(11):4044-55.
58. Lindgren D, Frigyesi A, Gudjonsson S, Sjobahl G, Hallden C, Chebil G, et al. Combined gene expression and genomic profiling define two intrinsic molecular subtypes of urothelial carcinoma and gene signatures for molecular grading and outcome. *Cancer Res.* 2010;70(9):3463-72.
59. Sjobahl G, Lauss M, Lovgren K, Chebil G, Gudjonsson S, Veerla S, et al. A molecular taxonomy for urothelial carcinoma. *Clin Cancer Res.* 2012;18(12):3377-86.
60. Marzouka NA, Eriksson P, Rovira C, Liedberg F, Sjobahl G, Hoglund M. A validation and extended description of the Lund taxonomy for urothelial carcinoma using the TCGA cohort. *Sci Rep.* 2018;8(1):3737.
61. Cancer Genome Atlas Research N. Comprehensive molecular characterization of urothelial bladder carcinoma. *Nature.* 2014;507(7492):315-22.
62. Todenhofer T, Seiler R. Molecular subtypes and response to immunotherapy in bladder cancer patients. *Transl Androl Urol.* 2019;8(Suppl 3):S293-S5.
63. Choi W, Porten S, Kim S, Willis D, Plimack ER, Hoffman-Censits J, et al. Identification of distinct basal and luminal subtypes of muscle-invasive bladder cancer with different sensitivities to frontline chemotherapy. *Cancer Cell.* 2014;25(2):152-65.

64. Rosenberg JE, Hoffman-Censits J, Powles T, van der Heijden MS, Balar AV, Necchi A, et al. Atezolizumab in patients with locally advanced and metastatic urothelial carcinoma who have progressed following treatment with platinum-based chemotherapy: a single-arm, multicentre, phase 2 trial. *Lancet*. 2016;387(10031):1909-20.
65. Seiler R, Ashab HAD, Erho N, van Rhijn BWG, Winters B, Douglas J, et al. Impact of Molecular Subtypes in Muscle-invasive Bladder Cancer on Predicting Response and Survival after Neoadjuvant Chemotherapy. *Eur Urol*. 2017;72(4):544-54.
66. Stone L. Bladder cancer: Two molecular subtypes identified. *Nat Rev Urol*. 2016;13(10):566.
67. Robertson AG, Kim J, Al-Ahmadie H, Bellmunt J, Guo G, Cherniack AD, et al. Comprehensive Molecular Characterization of Muscle-Invasive Bladder Cancer. *Cell*. 2018;174(4):1033.
68. McConkey DJ, Choi W. Molecular Subtypes of Bladder Cancer. *Curr Oncol Rep*. 2018;20(10):77.
69. Alexandrov LB, Nik-Zainal S, Wedge DC, Aparicio SA, Behjati S, Biankin AV, et al. Signatures of mutational processes in human cancer. *Nature*. 2013;500(7463):415-21.
70. Lindgren D, Sjobahl G, Lauss M, Staaf J, Chebil G, Lovgren K, et al. Integrated genomic and gene expression profiling identifies two major genomic circuits in urothelial carcinoma. *PLoS One*. 2012;7(6):e38863.
71. Knowles MA, Hurst CD. Molecular biology of bladder cancer: new insights into pathogenesis and clinical diversity. *Nat Rev Cancer*. 2015;15(1):25-41.
72. Wu XR. Urothelial tumorigenesis: a tale of divergent pathways. *Nat Rev Cancer*. 2005;5(9):713-25.
73. Inamura K. Bladder Cancer: New Insights into Its Molecular Pathology. *Cancers (Basel)*. 2018;10(4).
74. Knowles MA. Molecular genetics of bladder cancer: pathways of development and progression. *Cancer Surv*. 1998;31:49-76.
75. Spruck CH, 3rd, Ohneseit PF, Gonzalez-Zulueta M, Esrig D, Miyao N, Tsai YC, et al. Two molecular pathways to transitional cell carcinoma of the bladder. *Cancer Res*. 1994;54(3):784-8.
76. Chandrasekar T, Erlich A, Zlotta AR. Molecular Characterization of Bladder Cancer. *Curr Urol Rep*. 2018;19(12):107.
77. Li HT, Duymich CE, Weisenberger DJ, Liang G. Genetic and Epigenetic Alterations in Bladder Cancer. *Int Neurourol J*. 2016;20(Suppl 2):S84-94.
78. Mitra AP. Molecular substratification of bladder cancer: moving towards individualized patient management. *Ther Adv Urol*. 2016;8(3):215-33.

79. Feinberg AP, Tycko B. The history of cancer epigenetics. *Nat Rev Cancer*. 2004;4(2):143-53.
80. Holliday R. Epigenetics: a historical overview. *Epigenetics*. 2006;1(2):76-80.
81. Feinberg AP. Genome-scale approaches to the epigenetics of common human disease. *Virchows Arch*. 2010;456(1):13-21.
82. Meissner A. Epigenetic modifications in pluripotent and differentiated cells. *Nat Biotechnol*. 2010;28(10):1079-88.
83. Esteller M. Epigenetics in cancer. *N Engl J Med*. 2008;358(11):1148-59.
84. Costa-Pinheiro P, Montezuma D, Henrique R, Jeronimo C. Diagnostic and prognostic epigenetic biomarkers in cancer. *Epigenomics*. 2015;7(6):1003-15.
85. Sawan C, Vaissiere T, Murr R, Herceg Z. Epigenetic drivers and genetic passengers on the road to cancer. *Mutat Res*. 2008;642(1-2):1-13.
86. Yang X, Liu M, Li M, Zhang S, Hiju H, Sun J, et al. Epigenetic modulations of noncoding RNA: a novel dimension of Cancer biology. *Mol Cancer*. 2020;19(1):64.
87. Ehrlich M, Gama-Sosa MA, Huang LH, Midgett RM, Kuo KC, McCune RA, et al. Amount and distribution of 5-methylcytosine in human DNA from different types of tissues of cells. *Nucleic Acids Res*. 1982;10(8):2709-21.
88. Illingworth RS, Bird AP. CpG islands--'a rough guide'. *FEBS Lett*. 2009;583(11):1713-20.
89. Herman JG, Baylin SB. Gene silencing in cancer in association with promoter hypermethylation. *N Engl J Med*. 2003;349(21):2042-54.
90. Bernstein BE, Meissner A, Lander ES. The mammalian epigenome. *Cell*. 2007;128(4):669-81.
91. Esteller M. Aberrant DNA methylation as a cancer-inducing mechanism. *Annu Rev Pharmacol Toxicol*. 2005;45:629-56.
92. Jones PA, Baylin SB. The epigenomics of cancer. *Cell*. 2007;128(4):683-92.
93. Takai D, Jones PA. Comprehensive analysis of CpG islands in human chromosomes 21 and 22. *Proc Natl Acad Sci U S A*. 2002;99(6):3740-5.
94. Antequera F, Bird A. CpG islands. *EXS*. 1993;64:169-85.
95. Vaissiere T, Sawan C, Herceg Z. Epigenetic interplay between histone modifications and DNA methylation in gene silencing. *Mutat Res*. 2008;659(1-2):40-8.
96. Klose RJ, Bird AP. Genomic DNA methylation: the mark and its mediators. *Trends Biochem Sci*. 2006;31(2):89-97.
97. Cheng X, Blumenthal RM. Mammalian DNA methyltransferases: a structural perspective. *Structure*. 2008;16(3):341-50.
98. Turek-Plewa J, Jagodzinski PP. The role of mammalian DNA methyltransferases in the regulation of gene expression. *Cell Mol Biol Lett*. 2005;10(4):631-47.

99. Mulero-Navarro S, Esteller M. Epigenetic biomarkers for human cancer: the time is now. *Crit Rev Oncol Hematol*. 2008;68(1):1-11.
100. Sasai N, Defossez PA. Many paths to one goal? The proteins that recognize methylated DNA in eukaryotes. *Int J Dev Biol*. 2009;53(2-3):323-34.
101. Bird A. DNA methylation patterns and epigenetic memory. *Genes Dev*. 2002;16(1):6-21.
102. Gartler SM, Dyer KA, Goldman MA. Mammalian X chromosome inactivation. *Mol Genet Med*. 1992;2:121-60.
103. Klutstein M, Nejman D, Greenfield R, Cedar H. DNA Methylation in Cancer and Aging. *Cancer Res*. 2016;76(12):3446-50.
104. Miranda TB, Jones PA. DNA methylation: the nuts and bolts of repression. *J Cell Physiol*. 2007;213(2):384-90.
105. Esteller M. Cancer epigenomics: DNA methylomes and histone-modification maps. *Nat Rev Genet*. 2007;8(4):286-98.
106. Tost J. DNA methylation: an introduction to the biology and the disease-associated changes of a promising biomarker. *Mol Biotechnol*. 2010;44(1):71-81.
107. Kornberg RD, Lorch Y. Twenty-five years of the nucleosome, fundamental particle of the eukaryote chromosome. *Cell*. 1999;98(3):285-94.
108. Luger K, Mader AW, Richmond RK, Sargent DF, Richmond TJ. Crystal structure of the nucleosome core particle at 2.8 Å resolution. *Nature*. 1997;389(6648):251-60.
109. Kouzarides T. Chromatin modifications and their function. *Cell*. 2007;128(4):693-705.
110. Tessarz P, Kouzarides T. Histone core modifications regulating nucleosome structure and dynamics. *Nat Rev Mol Cell Biol*. 2014;15(11):703-8.
111. Jenuwein T, Allis CD. Translating the histone code. *Science*. 2001;293(5532):1074-80.
112. Lennartsson A, Ekwall K. Histone modification patterns and epigenetic codes. *Biochim Biophys Acta*. 2009;1790(9):863-8.
113. Grunstein M. Histone acetylation in chromatin structure and transcription. *Nature*. 1997;389(6649):349-52.
114. Bhaumik SR, Smith E, Shilatifard A. Covalent modifications of histones during development and disease pathogenesis. *Nat Struct Mol Biol*. 2007;14(11):1008-16.
115. Carafa V, Rotili D, Forgione M, Cuomo F, Serretiello E, Hailu GS, et al. Sirtuin functions and modulation: from chemistry to the clinic. *Clin Epigenetics*. 2016;8:61.
116. Vaquero A. The conserved role of sirtuins in chromatin regulation. *Int J Dev Biol*. 2009;53(2-3):303-22.

117. Bosch-Presegue L, Vaquero A. The dual role of sirtuins in cancer. *Genes Cancer*. 2011;2(6):648-62.
118. Martinez-Pastor B, Mostoslavsky R. Sirtuins, metabolism, and cancer. *Front Pharmacol*. 2012;3:22.
119. Chalkiadaki A, Guarente L. The multifaceted functions of sirtuins in cancer. *Nat Rev Cancer*. 2015;15(10):608-24.
120. Montezuma D, Henrique RM, Jeronimo C. Altered expression of histone deacetylases in cancer. *Crit Rev Oncog*. 2015;20(1-2):19-34.
121. Santos-Rosa H, Caldas C. Chromatin modifier enzymes, the histone code and cancer. *Eur J Cancer*. 2005;41(16):2381-402.
122. Li B, Carey M, Workman JL. The role of chromatin during transcription. *Cell*. 2007;128(4):707-19.
123. Mills AA. Throwing the cancer switch: reciprocal roles of polycomb and trithorax proteins. *Nat Rev Cancer*. 2010;10(10):669-82.
124. Lopez J, Percharde M, Coley HM, Webb A, Crook T. The context and potential of epigenetics in oncology. *Br J Cancer*. 2009;100(4):571-7.
125. Guttman M, Amit I, Garber M, French C, Lin MF, Feldser D, et al. Chromatin signature reveals over a thousand highly conserved large non-coding RNAs in mammals. *Nature*. 2009;458(7235):223-7.
126. Carninci P, Kasukawa T, Katayama S, Gough J, Frith MC, Maeda N, et al. The transcriptional landscape of the mammalian genome. *Science*. 2005;309(5740):1559-63.
127. Schickel R, Boyerinas B, Park SM, Peter ME. MicroRNAs: key players in the immune system, differentiation, tumorigenesis and cell death. *Oncogene*. 2008;27(45):5959-74.
128. Ponting CP, Oliver PL, Reik W. Evolution and functions of long noncoding RNAs. *Cell*. 2009;136(4):629-41.
129. Clark MB, Mattick JS. Long noncoding RNAs in cell biology. *Semin Cell Dev Biol*. 2011;22(4):366-76.
130. Ashwal-Fluss R, Meyer M, Pamudurti NR, Ivanov A, Bartok O, Hanan M, et al. circRNA biogenesis competes with pre-mRNA splicing. *Mol Cell*. 2014;56(1):55-66.
131. Li Z, Huang C, Bao C, Chen L, Lin M, Wang X, et al. Exon-intron circular RNAs regulate transcription in the nucleus. *Nat Struct Mol Biol*. 2015;22(3):256-64.
132. Bartel DP. MicroRNAs: target recognition and regulatory functions. *Cell*. 2009;136(2):215-33.
133. Filipowicz W, Bhattacharyya SN, Sonenberg N. Mechanisms of post-transcriptional regulation by microRNAs: are the answers in sight? *Nat Rev Genet*. 2008;9(2):102-14.
134. Ambros V. The functions of animal microRNAs. *Nature*. 2004;431(7006):350-5.

135. Bartel DP. MicroRNAs: genomics, biogenesis, mechanism, and function. *Cell*. 2004;116(2):281-97.
136. Lobo J, Barros-Silva D, Henrique R, Jeronimo C. The Emerging Role of Epitranscriptomics in Cancer: Focus on Urological Tumors. *Genes (Basel)*. 2018;9(11).
137. Baylin SB, Jones PA. A decade of exploring the cancer epigenome - biological and translational implications. *Nat Rev Cancer*. 2011;11(10):726-34.
138. Schulz WA, Goering W. DNA methylation in urothelial carcinoma. *Epigenomics*. 2016;8(10):1415-28.
139. Trevethan R. Sensitivity, Specificity, and Predictive Values: Foundations, Pliabilities, and Pitfalls in Research and Practice. *Front Public Health*. 2017;5:307.
140. Costa VL, Henrique R, Danielsen SA, Duarte-Pereira S, Eknaes M, Skotheim RI, et al. Three epigenetic biomarkers, GDF15, TMEFF2, and VIM, accurately predict bladder cancer from DNA-based analyses of urine samples. *Clin Cancer Res*. 2010;16(23):5842-51.
141. Roperch JP, Grandchamp B, Desgrandchamps F, Mongiat-Artus P, Ravery V, Ouzaid I, et al. Promoter hypermethylation of HS3ST2, SEPTIN9 and SLIT2 combined with FGFR3 mutations as a sensitive/specific urinary assay for diagnosis and surveillance in patients with low or high-risk non-muscle-invasive bladder cancer. *BMC Cancer*. 2016;16:704.
142. Kalluri R, Weinberg RA. The basics of epithelial-mesenchymal transition. *J Clin Invest*. 2009;119(6):1420-8.
143. Hay ED. An overview of epithelio-mesenchymal transformation. *Acta Anat (Basel)*. 1995;154(1):8-20.
144. Satelli A, Li S. Vimentin in cancer and its potential as a molecular target for cancer therapy. *Cell Mol Life Sci*. 2011;68(18):3033-46.
145. Lu W, Kang Y. Epithelial-Mesenchymal Plasticity in Cancer Progression and Metastasis. *Dev Cell*. 2019;49(3):361-74.
146. Battle E, Sancho E, Franci C, Dominguez D, Monfar M, Baulida J, et al. The transcription factor snail is a repressor of E-cadherin gene expression in epithelial tumour cells. *Nat Cell Biol*. 2000;2(2):84-9.
147. Cano A, Perez-Moreno MA, Rodrigo I, Locascio A, Blanco MJ, del Barrio MG, et al. The transcription factor snail controls epithelial-mesenchymal transitions by repressing E-cadherin expression. *Nat Cell Biol*. 2000;2(2):76-83.
148. Bolos V, Peinado H, Perez-Moreno MA, Fraga MF, Esteller M, Cano A. The transcription factor Slug represses E-cadherin expression and induces epithelial to mesenchymal transitions: a comparison with Snail and E47 repressors. *J Cell Sci*. 2003;116(Pt 3):499-511.

149. Comijn J, Berx G, Vermassen P, Verschueren K, van Grunsven L, Bruyneel E, et al. The two-handed E box binding zinc finger protein SIP1 downregulates E-cadherin and induces invasion. *Mol Cell*. 2001;7(6):1267-78.
150. Yang J, Mani SA, Donaher JL, Ramaswamy S, Itzykson RA, Come C, et al. Twist, a master regulator of morphogenesis, plays an essential role in tumor metastasis. *Cell*. 2004;117(7):927-39.
151. Nieto MA. The snail superfamily of zinc-finger transcription factors. *Nat Rev Mol Cell Biol*. 2002;3(3):155-66.
152. Boulay JL, Dennefeld C, Alberga A. The *Drosophila* developmental gene snail encodes a protein with nucleic acid binding fingers. *Nature*. 1987;330(6146):395-8.
153. Hajra KM, Chen DY, Fearon ER. The SLUG zinc-finger protein represses E-cadherin in breast cancer. *Cancer Res*. 2002;62(6):1613-8.
154. Huber MA, Kraut N, Beug H. Molecular requirements for epithelial-mesenchymal transition during tumor progression. *Curr Opin Cell Biol*. 2005;17(5):548-58.
155. Niessen K, Fu Y, Chang L, Hoodless PA, McFadden D, Karsan A. Slug is a direct Notch target required for initiation of cardiac cushion cellularization. *J Cell Biol*. 2008;182(2):315-25.
156. Sahlgren C, Gustafsson MV, Jin S, Poellinger L, Lendahl U. Notch signaling mediates hypoxia-induced tumor cell migration and invasion. *Proc Natl Acad Sci U S A*. 2008;105(17):6392-7.
157. Micalizzi DS, Farabaugh SM, Ford HL. Epithelial-mesenchymal transition in cancer: parallels between normal development and tumor progression. *J Mammary Gland Biol Neoplasia*. 2010;15(2):117-34.
158. Zavadil J, Cermak L, Soto-Nieves N, Bottinger EP. Integration of TGF-beta/Smad and Jagged1/Notch signalling in epithelial-to-mesenchymal transition. *EMBO J*. 2004;23(5):1155-65.
159. Tanaka T, Miyazawa K, Tsukamoto T, Kuno T, Suzuki K. Pathobiology and chemoprevention of bladder cancer. *J Oncol*. 2011;2011:528353.
160. Mandeville JA, Silva Neto B, Vanni AJ, Smith GL, Rieger-Christ KM, Zeheb R, et al. P-cadherin as a prognostic indicator and a modulator of migratory behaviour in bladder carcinoma cells. *BJU Int*. 2008;102(11):1707-14.
161. Popov Z, Gil-Diez de Medina S, Lefrere-Belda MA, Hoznek A, Bastuji-Garin S, Abbou CC, et al. Low E-cadherin expression in bladder cancer at the transcriptional and protein level provides prognostic information. *Br J Cancer*. 2000;83(2):209-14.
162. Yun SJ, Kim WJ. Role of the epithelial-mesenchymal transition in bladder cancer: from prognosis to therapeutic target. *Korean J Urol*. 2013;54(10):645-50.

163. Khorrami MH, Hadi M, Gharaati MR, Izadpanahi MH, Javid A, Zargham M. E-cadherin expression as a prognostic factor in transitional cell carcinoma of the bladder after transurethral resection. *Urol J.* 2012;9(3):581-5.
164. Imao T, Koshida K, Endo Y, Uchibayashi T, Sasaki T, Namiki M. Dominant role of E-cadherin in the progression of bladder cancer. *J Urol.* 1999;161(2):692-8.
165. Abufaraj M, Haitel A, Moschini M, Gust K, Foerster B, Ozsoy M, et al. Prognostic Role of N-cadherin Expression in Patients With Invasive Bladder Cancer. *Clin Genitourin Cancer.* 2017.
166. Rieger-Christ KM, Cain JW, Braasch JW, Dugan JM, Silverman ML, Bouyounes B, et al. Expression of classic cadherins type I in urothelial neoplastic progression. *Hum Pathol.* 2001;32(1):18-23.
167. Bryan RT, Tselepis C. Cadherin switching and bladder cancer. *J Urol.* 2010;184(2):423-31.
168. Mrozik KM, Blaschuk OW, Cheong CM, Zannettino ACW, Vandyke K. N-cadherin in cancer metastasis, its emerging role in haematological malignancies and potential as a therapeutic target in cancer. *BMC Cancer.* 2018;18(1):939.
169. Bryan RT, Atherfold PA, Yeo Y, Jones LJ, Harrison RF, Wallace DM, et al. Cadherin switching dictates the biology of transitional cell carcinoma of the bladder: ex vivo and in vitro studies. *J Pathol.* 2008;215(2):184-94.
170. van Roy F. Beyond E-cadherin: roles of other cadherin superfamily members in cancer. *Nat Rev Cancer.* 2014;14(2):121-34.
171. Yu Q, Zhang K, Wang X, Liu X, Zhang Z. Expression of transcription factors snail, slug, and twist in human bladder carcinoma. *J Exp Clin Cancer Res.* 2010;29:119.
172. Bruyere F, Namdarian B, Corcoran NM, Pedersen J, Ockrim J, Voelzke BB, et al. Snail expression is an independent predictor of tumor recurrence in superficial bladder cancers. *Urol Oncol.* 2010;28(6):591-6.

CHAPTER II – Rational and Aims

Rational and Aims

The main goal of this Doctoral Thesis was to unveil the value of novel epigenetic alterations in Bladder Cancer clinical management and also to tackle specific biological and molecular mechanisms implicated in the disease development, progression and aggressiveness.

With this in mind, this Thesis encompasses two major chapters, specifically Chapter III - Diagnostic/Prognostic Epimarkers in Bladder Cancer Voided Urines, and Chapter IV - Bladder Cancer Mechanisms and Biology. The specific aims of each Chapter were the following:

Chapter III - Diagnostic/Prognostic Epimarkers in Bladder Cancer Voided Urines

- Investigate specific biomarkers for early BICa diagnosis by testing the feasibility of using a panel of miRNAs quantitative promoter methylation as a tool for accurate non-invasive detection of urothelial cancer in voided urine, emphasizing its specificity for UC among other genitourinary malignancies;
- Assess whether a panel of two methylation markers might accurately discriminate BICa from inflammatory conditions in voided urine, allowing for the development of a multiplex test that could be used for early detection in clinical practice;

Chapter IV - Bladder Cancer Mechanisms and Biology

- Illuminate the role of sirtuins' family in BICa and evaluate their implication in disease progression and aggressiveness;
- Characterize the expression of a set of markers for defining the most common BICa biological/phenotypic subtypes: luminal and basal/squamous;
- Assess the relevance of epigenetic mechanisms for the vimentin "switch" in normal to malignant urothelial cells;
- Unveil the implication of VIM deregulation in BICa progression.

**CHAPTER III –
Diagnostic/Prognostic
Epimarkers in Bladder Cancer
Voided Urines**

Research Paper I

Paper I: MicroRNA promoter methylation: a new tool for accurate detection of urothelial carcinoma

British Journal of Cancer 2017, 116, 634–639

DOI: 10.1038/bjc.2016.454

Nuno André Padrão, **Sara Monteiro-Reis**, Jorge Torres-Ferreira, Luís Antunes, Luís Leça, Diana Montezuma, João Ramalho-Carvalho, Paula C Dias, Paula Monteiro, Jorge Oliveira, Rui Henrique, Carmen Jerónimo

Author personal contribution:

Technical execution of the work and interpretation of the results.

Abstract

Background: Urothelial carcinoma (UC) is the most common cancer affecting the urinary system, worldwide. Lack of accurate early detection tools entails delayed diagnosis, precluding more efficient and timely treatment. In a previous study, we found that miR-129-2 and miR-663a were differentially methylated in UC compared with other genitourinary tract malignancies. Here, we evaluated the diagnostic performance of those microRNAs in urine.

Methods: Promoter methylation levels of miR-129-2 and miR-663a were assessed, using real-time quantitative methylation-specific PCR, in UC tissue samples (using normal urothelium as control) and, subsequently, in urine samples from UC and other genitourinary malignancies. Diagnostic and prognostic performances were evaluated by receiver operator characteristics curve and survival analyses, respectively.

Results: Promoter methylation levels of both microRNAs were significantly higher in UC tissue samples compared with normal urothelium. In urine, the assay was able to distinguish UC from other genitourinary tract carcinomas with 87.7% sensitivity and 84% specificity, resulting in 85.85% overall accuracy.

Conclusions: This panel of miRNAs promoter methylation accurately detects UC in urine, comparing well with other promising epigenetic-based biomarkers. This may constitute the basis for a non-invasive assay to detect UC.

Main

Urothelial carcinoma (UC), which affects the upper (renal pelvis and ureters) and lower (bladder, urethra) urinary tract, is the fourth most common cancer type in worldwide males, with 330 380 new cases diagnosed in 2012, mostly afflicting elderly individuals (Torre et al, 2015). Haematuria is the most common clinical sign of UC, particularly of those arising in the lower urinary tract, but several prevalent benign conditions, such as urinary tract infection and/or lithiasis, are also associated with haematuria, thus limiting its cancer specificity. Moreover, upper tract UC (UTUC), although much less common (5–10% of all cases), is mostly clinically asymptomatic. Consequently, although upper and lower tract UC display clinical and genomic similarities (Zhang et al, 2010), 60% of UTUC are diagnosed at invasive stage, contrasting with 10% of bladder UC (BUC; Margulis et al, 2009). Thus, early detection is decisive to improve patient's survival.

Currently, BUC diagnosis usually consists on non-invasive (voided) urine cytology (which displays modest accuracy), followed by cystoscopic examination (Kaufman et al, 2009), whereas suspected cases of UTUC are investigated with computer tomographic urography or urinary cytology followed by ureteroscopy, but these methods have low sensitivity, especially for low-grade tumours, and are often associated with patient discomfort

(Kaufman et al, 2009; Remzi et al, 2011; Rouprêt et al, 2011). Follow-up of patients with UC is also based on periodic cystoscopy, an invasive, uncomfortable and expensive procedure, making UC one of the heaviest economical burdens in health systems (Lokeshwar et al, 2005). Thus, early, accurate and non-invasive diagnostic tools are critical to improve patient outcome and increase the cost-effectiveness of follow-up procedures. MicroRNAs (miRNAs) are small (~22 nucleotides in length), non-coding RNA molecules involved in many important regulatory pathways including cell growth, proliferation, differentiation and cell death (Bartel, 2009; Silahtaroglu and Stenvang, 2010). In animals, they regulate the expression of complementary mRNA, thus inhibiting protein expression (Ambros, 2004). Recently, the role of deregulated miRNAs in oncogenesis has been emphasised and depending on its function and type of abnormal expression, they might act as oncogenes or tumour suppressor genes, in many types of cancer (Volinia et al, 2006). Expression of miRNAs might be epigenetically regulated, namely through methylation of CpG islands located at promoter regions, as well as histone post-translational modifications. Alterations in those mechanisms might deregulate miRNAs expression in cancer cells and might, thus, be used advantageously as specific cancer biomarkers early detection, diagnosis, prognostication, prediction of response to treatment and monitoring (Silahtaroglu and Stenvang, 2010).

In search for epigenetic biomarkers in genitourinary cancer, we identified two miRNAs – miR-129-2 and miR-663a – that displayed significantly higher promoter methylation levels in a small series of BUC tissues. Thus, we aimed at validating that finding in larger series of UC, encompassing BUC and UTUC tissues, and test the feasibility of using miR-129-2 and miR-663a quantitative promoter methylation as a tool for accurate non-invasive detection of UC in voided urine, emphasising its specificity for UC among genitourinary malignancies.

Material and Methods

Patients and tumour sample collection

One hundred and fourteen BUC tissue samples were obtained from a consecutive series of patients diagnosed and treated with transurethral resection or radical cystectomy, with no previous history of UTUC, between 2005 and 2014, and 55 UTUC samples were obtained from another consecutive series of patients diagnosed and treated with radical nephroureterectomy or ureterectomy, with no previous history of BUC, between 2000 and 2011. Both the groups of patients were followed-up at the Portuguese Oncology Institute of Porto, Portugal. For the BUC samples, a small tumour sample was immediately snap-

frozen, stored at -80°C and subsequently cut in cryostat for DNA extraction. Routine collection and processing of tissue sample allowed for pathological examination, classification, grading and staging (Eble et al, 2004; Edge et al, 2010). UTUC samples were obtained from routinely fixed and paraffin-embedded tissue used for pathological assessment (Eble et al, 2004; Edge et al, 2010). Controls for BUC consisted on an independent set of 19 normal bladder mucosae collected from BICa-free individuals (prostate cancer patients submitted to radical prostatectomy), and 31 paraffin-embedded normal upper tract urothelium (NUTU) set of samples obtained from renal cell carcinoma patients were used as UTUC controls. Relevant clinical data were collected from clinical charts and is depicted in Table 1.

Table 1. Clinical and histopathological characteristics of patients with urothelial carcinoma and providers of normal urothelium.

Clinicopathological features	UC	Normal urothelium	P -value
Patients, <i>n</i>	169	50	
Gender, <i>n</i> (%)			
Male	130 (77%)	38 (76%)	
Female	39 (23%)	12 (24%)	
Median age, years (range)	73 (42–93)	62.5 (48–82)	<i>P</i> <0.001
Pathological stage, <i>n</i> (%)			
pTa	43 (26%)	NA	
pT1	63 (37%)	NA	
pT2	31 (18%)	NA	
pT3	25 (15%)	NA	
pT4	7 (4%)	NA	
Grade, <i>n</i> (%)			
Papillary, low grade	59 (35%)	NA	
Papillary, high grade	62 (37%)	NA	
Invasive, high grade	48 (28%)	NA	

Urine sample collection and processing

Voided urine (one sample per patient) was collected from 49 patients with BUC and UTUC, diagnosed and treated between 2006 and 2012 at the Portuguese Oncology Institute – Porto, Portugal. A set of 75 voided urine samples from patients with prostate cancer (n=25), renal cancer (n=25) and healthy blood donors with no personal or familial history of cancer (n=25) were also collected and used as controls (Table 2). Informed consents were obtained from patients and controls and used in this study after approval from the ethics committee (Comissão de Ética para a Saúde) of the Portuguese Oncology Institute of Porto (CES-IPO 019/08). All urine samples were processed by immediate centrifugation at 4000 r.p.m. for 10 min, the respective pellet was washed twice with phosphate-buffered saline and stored at -80°C .

Table 2. Clinical and histopathological characteristics of patients with urothelial carcinoma and of controls (healthy donors (n=25), prostate cancer (n=25) and renal cancer (n=25) patients), which provided urine samples for this study. UC – urothelial carcinoma; NA – non-applicable.

Clinicopathological features	UC	Control Set	P -value
Patients, <i>n</i>	49	75	NA
Gender, <i>n</i> (%)			
Male	29 (60%)	53 (71%)	NA
Female	20 (40%)	22 (29%)	NA
Median age, years (range)	70 (53–83)	63 (51–88)	<i>P</i> =0.066
Grade, <i>n</i> (%)			
Papillary, low grade	17 (35%)	NA	NA
Papillary, high grade	18 (37%)	NA	NA
Invasive, high grade	14 (28%)	NA	NA

Nucleic acids isolation, bisulphite modification and qMSP analysis

DNA was extracted from frozen BUC tissue samples using AllPrep DNA/RNA Mini Kit (Qiagen Inc., Germatown, MD, USA). For UTUC and NUTU tissue samples, a representative paraffin block was selected and the tumour area was delimited, allowing for macrodissection of tumour from 10 to 20 serial 7- μm thick sections, followed by digestion with proteinase K (20 mg ml⁻¹, 50 μl). DNA from all samples was extracted using a standard

phenol-chloroform protocol (Pearson and Stirling, 2003), and its concentration determined using ND-1000 NanoDrop (NanoDrop Technologies, Wilmington, DE, USA). Bisulphite modification was performed using sodium bisulphite with EZ DNA Methylation-Gold Kit (Zymo Research, Irvine, CA, USA) according to manufacturer's protocol. Quantitative methylation levels were performed using KAPA SYBR FAST qPCR Kit (Kapa Biosystems, Wilmington, MA, USA) and all reactions were run in triplicates in 384-well plates using Roche LightCycler 480 II, with Beta-Actin (ACTB) as internal reference gene for normalisation. Primer sequences were designed using Methyl Primer Express 1.0 (Methyl Primer Express 1.0, ThermoFisher Scientific, Waltham, MA, USA) and purchased from Sigma-Aldrich (St Louis, MO, USA): miR-129-2 F3'-CGGCGAATCGAAGAAGTC-5' and R3'-TACGCCCTCCGCAAATAC-5', miR-663a F3'-GGGATAGCGAGGTTAGGTC-5' and R3'-CATTCGTAAACGAATAAAACCC-5'.

Statistical analysis

Median, frequency and interquartile range of miR-129-2 and miR-663a promoter methylation levels of normal, BUC and UTUC tissue samples as well as UC, prostate, kidney and healthy blood donor urine samples were determined. Receiver operator characteristics (ROC) curves were constructed by plotting the true-positive (sensitivity) against false-positive (1-specificity) rate, and the area under the curve (AUC) was calculated. The higher value obtained from the sum of sensitivity and 1-specificity in each ROC curve was used for cut off to categorise samples as methylated or non-methylated. Sensitivity, specificity, negative predictive value, positive predictive value and accuracy of the test were also determined. Differences in quantitative methylation values were assessed with the non-parametric Mann–Whitney U-test. Associations between age, gender, grade, pathological stage and miRNAs methylation levels were carried out using Spearman's method, Mann–Whitney or Kruskal–Wallis tests, as appropriate. DeLong's test for ROC curves comparison was performed to assess differences in performance of the miRNAs promoter methylation test between upper and lower urinary tract cancers, and between the age groups (lower than 65 years vs higher than 65 years). McNemar proportion test was used to compare the diagnostic performance of methylation analysis with urine cytology.

Disease-specific survival curves, (Kaplan–Meier with log rank test) were computed for standard variables (tumour stage and grade) and for categorised miRNA promoter methylation status. A Cox regression model comprising all significant variables (univariable and multivariable model) was computed to assess the relative contribution of each variable to the follow-up status.

All two-tailed P-values were derived from statistical tests, using a computer-assisted program (SPSS Version 23.0, IBM, Armonk, NY, USA) and the results were considered statistically significant at $P < 0.05$. Bonferroni correction for multiple comparisons was used when applicable.

Results

Methylation analysis in UC tissues and performance of methylation panel in urine

The promoters of both miR-129-2 and miR-663a were found to be methylated in most UC tissue samples, and methylation levels were significantly higher compared with the control group ($P < 0.001$ and $P < 0.001$, respectively; Figure 1). Moreover, in tissue samples, the panel discriminated UC from normal mucosa with 94.7% sensitivity and 84.0% specificity (Table 3), corresponding to an AUC of 0.941 (95% confidence interval (CI): 0.911–0.972, $P < 0.001$) in ROC curve analysis (Figure 2A).

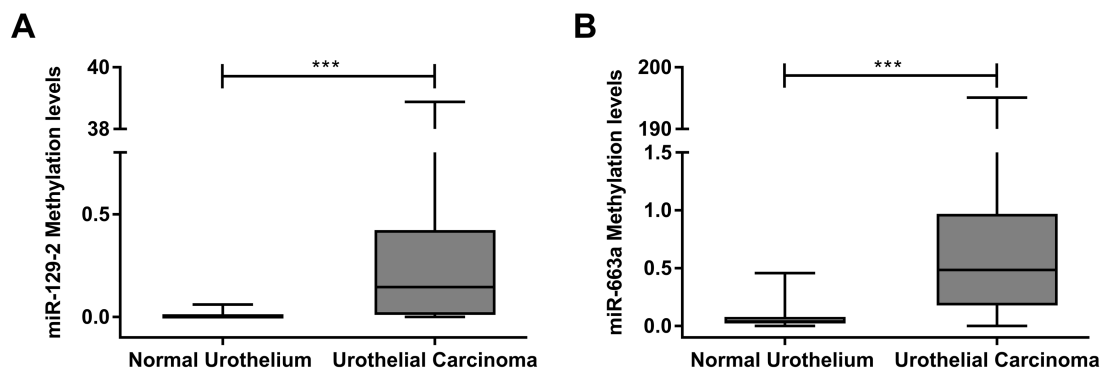


Figure 1. Distribution of (A) miR-129-2 and (B) miR-663a promoter methylation levels in normal urothelium (n=50) and urothelial carcinoma (UC) tissue samples (n=169). Mann-Whitney U test. *** $P < 0.001$.

Table 3. Performance of epigenetic biomarkers for the detection of urothelial carcinoma in tissue and urine. UC – urothelial carcinoma; HD – healthy donors; PCa – prostate cancer; RC – renal cancer; PPV – positive predictive value; NPV – negative predictive value.

	Sensitivity % (n positive/ n total)	Specificity % (n negative/ n total)	PPV (%)	NPV (%)	Accuracy (%)
Tissue samples					
miR-129-2	72.8 (123/169)	96.0 (48/50)	98.4	51.1	78.1
mirR-663a	87.0 (147/169)	86.0 (43/50)	95.5	66.2	86.8
miR-129-2/miR-663a	94.7 (160/169)	84.0 (42/50)	95.2	82.4	92.2
Urine samples (UC patients vs HD)					
miR-129-2/miR-663a	83.7 (41/49)	88.0 (22/25)	93.2	73.3	85.1
Urine samples (UC patients vs PCa and RC patients)					
miR-129-2/miR-663a	87.8 (43/49)	84 (42/50)	84.3	87.5	85.9
Urine samples (UC patients vs all controls)					
miR-129-2	75.5 (37/49)	85.3 (64/75)	77.1	84.2	81.5
mirR-663a	71.4 (35/49)	94.7 (71/75)	89.7	83.5	85.5
miR-129-2/miR-663a	87.8 (43/49)	82.7 (62/75)	76.8	91.2	84.7

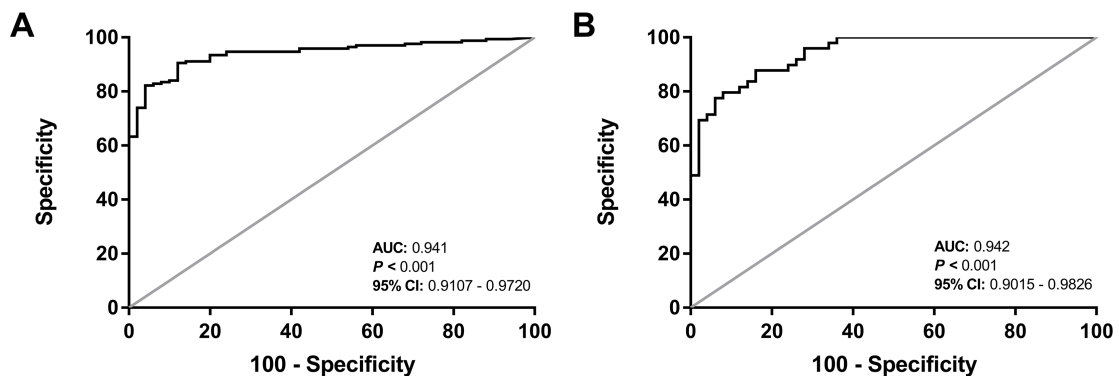


Figure 2. Receiver operator characteristic (ROC) curves evaluating the performance of the gene panel promoter methylation (mir-129-2/miR-663a);(A) for the identification of urothelial carcinoma (UC) in tissue; and (B) for discrimination of UC from other genitourinary malignancies in urine samples.

The same panel was then tested in a set of 49 urine sediments from UC patients and in a control group of 75 urines from subjects not carrying UC. Remarkably, methylation levels of both miRNAs in UC urine samples were significantly higher than those of controls ($P < 0.001$ and $P < 0.001$, respectively). In urine samples, the methylation test was able to detect UC with 87.8% sensitivity and 84.0% specificity (Table 3), corresponding to an AUC of 0.942 (95% CI: 0.9015–0.9826, $P < 0.001$; Figure 2B). Moreover, the methylation test was able to discriminate UC patients both from other genitourinary malignancies and from healthy donors (Table 3).

Because urine cytology is frequently the first test to be performed in UC suspects, we compared the performance of the methylation panel with cytopathological examination by an experienced cytopathologist. Interestingly, the proportion of true-positive cases detected by the methylation test was significantly higher than that of cytology ($P < 0.001$). Of 47 UC cases analysed, cytopathology detected only 17 as positive, 15 as negative and 15 as 'inconclusive/suspicious', corresponding to 34.7% sensitivity. Conversely, the miRNAs promoter methylation panel identified 41 cases as true positive, corresponding to an overall sensitivity of 87.2%, although 1 of the 6 cases negative in the methylation test was correctly diagnosed as UC by cytopathology (Figure 3).

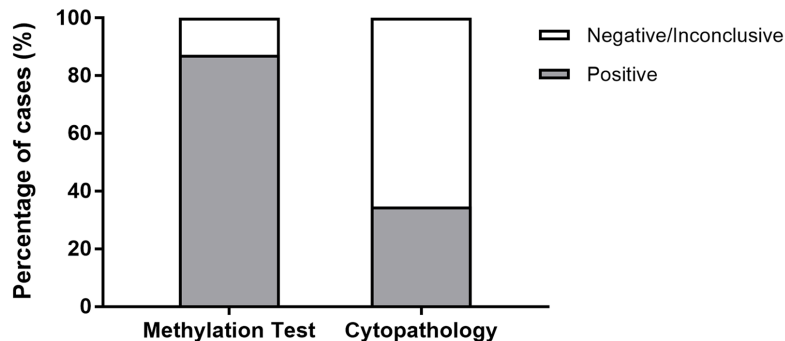


Figure 3. Percentage of urothelial carcinoma (UC) cases correctly identified with the gene panel promoter methylation test and a standard cytopathology analysis.

Clinicopathological correlates and survival analyses

Significantly higher miR-129-2 methylation levels were found in high-grade papillary UC compared with low-grade papillary UC ($P = 0.048$), whereas for miR-663a, high-grade papillary UC displayed significantly higher methylation levels than invasive UC ($P = 0.003$). In addition, miR-663a methylation levels differed significantly between non-muscle invasive and muscle invasive UC (stages pTa-1 vs pT2-4; $P = 0.016$), as well as between papillary and invasive UC ($P = 0.012$).

A significant association was found between promoter methylation levels and patients' age at diagnosis for both miR-129-2 and miR-663a ($P=0.023$; $P=0.016$, respectively). After normalisation of the ROC curve for this variable, no significant difference in the panel's performance was found between younger and older patients and an AUC of 94.3% was obtained. Furthermore, no association was disclosed between miRNAs promoter methylation and patients' gender.

Of the 114 patients enrolled, 3 BUC and 1 UTUC patients were lost to follow-up. The median follow-up time of BUC patients was 66 months (range: 1–323 months). At the last follow-up time point, 58 patients were alive with no evidence of cancer, 10 patients were alive with disease, 11 died from other causes and 32 had deceased due to UC. Considering UTUC patients, the follow-up time was of 55 months (range: 1–186 months). At the last follow-up, 16 patients were alive without disease, 6 were alive with disease progression, whereas 32 patients had perished, 23 due to UTUC. Overall, for UC, the median follow-up time was 62 months. A poor outcome was depicted for UC patients with higher grade, pathological stage and age at diagnosis (Log rank test; $P<0.001$, for all variables). Univariable and multivariable Cox regression analysis were performed separately for BUC, UTUC and UC patients, including the three above mentioned variables (Supplementary Table 1). As expected, a poor outcome was depicted for UC patients with higher pathological stage, grade and age in a multivariable model (Supplementary Table 1; $P=0.03$, $P=0.002$ and $P<0.001$, respectively). However, considering the two patients' subsets separately, only grade (for BUC) and age (for UTUC) were selected in the final model as independent predictors of outcome (Supplementary Table 1; $P=0.009$ and $P=0.017$). No prognostic value was depicted for miR-129-2 or miR-663a promoter methylation levels in UC or in BUC or UTUC, when analysed separately (Supplementary Table 1).

Discussion

Upper and lower UC are among the most common neoplasms worldwide and although several risk factors have been clearly identified (e.g., smoking habits, chemical exposure to aromatic amines like benzidine or β -naphthalene, Schistosoma infection (Babjuk et al, 2013; Torre et al, 2015)), early detection is critical for adequate therapeutic management towards reducing disease-specific mortality (Hall et al, 1998; Margulis et al, 2009). Moreover, it is important to discriminate UC from other genitourinary cancers, especially those originating in the prostate and kidney. Although several biomarkers have been previously reported, including miRNAs promoter methylation (Phé et al, 2009; van der Kwast and Bapat, 2009; Shimizu et al, 2013), they have been mostly focused on BUC, disregarding upper urothelial tract UC, and its performance might be perfected by the addition of more sensitive and specific biomarkers. Within a project aimed at characterising miRNAs deregulated through

aberrant promoter methylation in genitourinary neoplasms, we identified miR-129-2 and miR-663a promoters as potential UC biomarkers (submitted). We, thus, tested the biomarker performance of quantitative miR-129-2 and miR-663a promoter methylation both in upper and lower urinary tract UC.

Because miR-129-2 and miR-663a promoter methylation was initially identified in BUC, we first assessed methylation levels in tissue samples of upper and lower urinary tract UC. Owing to biological and genomic similarity between the urothelium from upper and lower urinary tract (Zhang et al, 2010), we hypothesised that this panel would perform well in both the settings. Indeed, the methylation panel discriminated UC from normal urothelial mucosa with high sensitivity and specificity, which did not differ between upper and lower urinary tract UC. This result enabled us to proceed with urine testing, as the ultimate goal of the study would be the identification of a non-invasive test, intended for early detection and disease monitoring. In urine samples, sensitivity and specificity were lower than those found in tissues, but it should be recalled that the accuracy of the panel was tested not only against healthy volunteers, but also prostate and kidney cancer patients.

Recently, several studies attempted to identify novel epigenetic biomarkers for UC detection, some of them with an apparent superior performance to the panel reported herein. TWIST1 and NID2 promoter methylation were previously reported to detect BUC in urine samples with 94% sensitivity and 91% specificity (Renard et al, 2010). However, specificity was only tested against urinary infections or other benign conditions and its ability to discriminate UC from prostate and kidney cancer was not evaluated. BCL2, CDKN2A and NID2 promoter methylation have also been proposed as epigenetic biomarkers for bladder cancer (Scher et al, 2012). Although the number of genes is higher than that of our panel, sensitivity and specificity were lower (80.9% and 86.4%, respectively) and this was accomplished through nested PCR, which may compromise the speed and cost of the assay. Moreover, the number of samples from prostate and kidney cancer tested was lower than those included in our study. We have also previously reported a gene promoter methylation panel (GDF15, TMEFF2 and VIM) that accurately identified BUC in urine samples (Costa et al, 2010) which we, subsequently, demonstrated to have similar performance in upper urinary tract UC (Monteiro-Reis et al, 2014). Both studies, however, used specific TaqMan probes, contrarily to the present study, where a SYBR Green-based protocol was used, thus, also, improving cost-effectiveness.

Some previous studies have also focused on miRNAs promoter methylation as UC biomarkers. Whereas, Vogt et al (2011) reported 57% sensitivity (n=7) for miR-34a promoter methylation in bladder tissues and Shimizu et al (2013) achieved 81% specificity and 89% sensitivity in urine sediments from BUC (n=47) using a panel of several miRNAs. Our results compare well with those reports and provide some significant advantages, as

only two miRNA promoters are tested, and its specificity was evaluated against other genitourinary malignancies.

Although urinary cytology is frequently used as an initial diagnostic approach in UC suspects, its diagnostic yield is rather limited, especially for upper urinary tract UC (Rouprêt et al, 2013). Moreover, imaging techniques might have difficulty in discriminating upper urinary tract UC from renal cell carcinoma, a quite relevant differential diagnosis setting owing to marked differences in therapy and prognosis (Browne et al, 2005), thus emphasising the need for biomarkers that may accurately discriminate among those tumour types. In the present study, the sensitivity of urinary cytology was only ~35%, which was easily surpassed by the miRNA methylation panel, with the additional gain of discriminating UC from renal cell carcinoma.

Whereas no biological role has been previously ascribed to miR-129-2 and miR-663a promoter methylation in urothelial carcinogenesis, several studies in other tumour models have unveiled the pathological significance of those epigenetic aberrations. Transcriptional silencing of miR-129-2 due to promoter methylation was found in gastric (Pan et al, 2010; Shen et al, 2010), endometrial (Huang et al, 2009) and hepatocellular (Lu et al, 2013) carcinomas, as well as in acute myeloid leukaemia (Yan-Fang et al, 2013), and it has been implicated in overexpression of two oncogenic proteins, SOX4 (Huang et al, 2009; Shen et al, 2010) and Cdk6 (Wu et al, 2010). On the other hand, miR-663a promoter methylation and downregulation was associated with JunD overexpression in small-cell lung carcinoma (Zhang et al, 2016) and HMGA2 overexpression in hepatocellular carcinoma (Huang et al, 2016), fostering cell proliferation. Owing to the prevalence of miR-129-2 and miR-663a promoter methylation in UC, across primary localisations, histological subtype, grade and stage, it is tempting to speculate whether it may also play a key role in urothelial carcinogenesis.

In summary, we demonstrated that aberrant miR-129-2 and miR-663a promoter methylation accurately discriminate UC from normal urothelial mucosa and allow for sensitive and specific identification of upper and lower urinary tract UC in urine samples, discriminating also from other common genitourinary tract carcinomas (kidney and prostate). Thus, this panel might be useful for complementing other epigenetic biomarkers for non-invasive detection and/or monitoring of UC patients.

References

Ambros V (2004) The functions of animal microRNAs. *Nature* 431(7006): 350-355

Babjuk M, Burger M, Zigeuner R, Shariat SF, van Rhijn BW, Comperat E, Sylvester RJ, Kaasinen E, Böhle A, Redorta JP (2013) EAU guidelines on non-muscle-invasive urothelial carcinoma of the bladder: update 2013. *European urology* 64(4): 639-653

Bartel DP (2009) MicroRNAs: target recognition and regulatory functions. *Cell* 136(2): 215-233

Browne RF, Meehan CP, Colville J, Power R, Torreggiani WC (2005) Transitional Cell Carcinoma of the Upper Urinary Tract: Spectrum of Imaging Findings 1. *Radiographics* 25(6): 1609-1627

Costa VL, Henrique R, Danielsen SA, Duarte-Pereira S, Eknaes M, Skotheim RI, Rodrigues Â, Magalhães JS, Oliveira J, Lothe RA (2010) Three epigenetic biomarkers, GDF15, TMEFF2, and VIM, accurately predict bladder cancer from DNA-based analyses of urine samples. *Clinical Cancer Research* 16(23): 5842-5851

Eble J, Sauter G, Epstein J, Sesterhenn I (2004) Tumours of the urinary system and male genital organs: pathology and genetics. *World Health Organization Classification of Tumours Lyon*

Edge SB BD, Compton CC, Fritz AG, Greene FL, Trotti A (2010) American Joint Committee on Cancer: cancer staging manual. , 7th ed. edn. Philadelphia: Lippincott-Raven Publishers

Hall MC, Womack S, Sagalowsky AI, Carmody T, Erickstad MD, Roehrborn CG (1998) Prognostic factors, recurrence, and survival in transitional cell carcinoma of the upper urinary tract: a 30-year experience in 252 patients. *Urology* 52(4): 594-601

Huang W, Li J, Guo X, Zhao Y, Yuan X (2016) miR-663a inhibits hepatocellular carcinoma cell proliferation and invasion by targeting HMGA2. *Biomedicine & Pharmacotherapy* 81: 431-438

Huang Y-W, Liu JC, Deatherage DE, Luo J, Mutch DG, Goodfellow PJ, Miller DS, Huang TH (2009) Epigenetic repression of microRNA-129-2 leads to overexpression of SOX4 oncogene in endometrial cancer. *Cancer research* 69(23): 9038-9046

Kaufman DS, Shipley WU, Feldman AS (2009) Bladder cancer. *Lancet (London, England)* 374(9685): 239-49

Lokeshwar VB, Habuchi T, Grossman HB, Murphy WM, Hautmann SH, Hemstreet GP, Bono AV, Getzenberg RH, Goebell P, Schmitz-Dräger BJ (2005) Bladder tumor markers beyond cytology: International Consensus Panel on bladder tumor markers. *Urology* 66(6): 35-63

Lu CY, Lin KY, Tien MT, Wu CT, Uen YH, Tseng TL (2013) Frequent DNA methylation of MiR-129-2 and its potential clinical implication in hepatocellular carcinoma. *Genes, Chromosomes and Cancer* 52(7): 636-643

Margulis V, Shariat SF, Matin SF, Kamat AM, Zigeuner R, Kikuchi E, Lotan Y, Weizer A, Raman JD, Wood CG (2009) Outcomes of radical nephroureterectomy: a series from the Upper Tract Urothelial Carcinoma Collaboration. *Cancer* 115(6): 1224-1233

Monteiro-Reis S, Leça L, Almeida M, Antunes L, Monteiro P, Dias PC, Morais A, Oliveira J, Henrique R, Jerónimo C (2014) Accurate detection of upper tract urothelial carcinoma in tissue and urine by means of quantitative GDF15, TMEFF2 and VIM promoter methylation. *European Journal of Cancer* 50(1): 226-233

Pan J, Hu H, Zhou Z, Sun L, Peng L, Yu L, Sun L, Liu J, Yang Z, Ran Y (2010) Tumor-suppressive mir-663 gene induces mitotic catastrophe growth arrest in human gastric cancer cells. *Oncology reports* 24(1): 105-112

Pearson H, Stirling D (2003) DNA extraction from tissue. *Methods in molecular biology* (Clifton, NJ) 226: 33-4

Phé V, Cussenot O, Rouprêt M (2009) Interest of methylated genes as biomarkers in urothelial cell carcinomas of the urinary tract. *BJU international* 104(7): 896-901

Remzi M, Shariat S, Huebner W, Fajkovic H, Seitz C (2011) Upper urinary tract urothelial carcinoma: what have we learned in the last 4 years? *Therapeutic advances in urology* 3(2): 69-80

Renard I, Joniau S, Van Cleynenbreugel B, Collette C, Naômé C, Vlassenbroeck I, Nicolas H, de Leval J, Straub J, Van Criekinge W (2010) Identification and validation of the methylated TWIST1 and NID2 genes through real-time methylation-specific polymerase chain reaction assays for the noninvasive detection of primary bladder cancer in urine samples. *European urology* 58(1): 96-104

Rouprêt M, Babjuk M, Compérat E, Zigeuner R, Sylvester R, Burger M, Cowan N, Böhle A, Van Rhijn BW, Kaasinen E (2013) European guidelines on upper tract urothelial carcinomas: 2013 update. *European urology* 63(6): 1059-1071

Rouprêt M, Zigeuner R, Palou J, Boehle A, Kaasinen E, Sylvester R, Babjuk M, Oosterlinck W (2011) European guidelines for the diagnosis and management of upper urinary tract urothelial cell carcinomas: 2011 update. *European urology* 59(4): 584-594

Scher MB, Elbaum MB, Mogilevkin Y, Hilbert DW, Mydlo JH, Sidi AA, Adelson ME, Mordechai E, Trama JP (2012) Detecting DNA methylation of the BCL2, CDKN2A and NID2 genes in urine using a nested methylation specific polymerase chain reaction assay to predict bladder cancer. *The Journal of urology* 188(6): 2101-2107

Shen R, Pan S, Qi S, Lin X, Cheng S (2010) Epigenetic repression of microRNA-129-2 leads to overexpression of SOX4 in gastric cancer. *Biochemical and biophysical research communications* 394(4): 1047-1052

Shimizu T, Suzuki H, Nojima M, Kitamura H, Yamamoto E, Maruyama R, Ashida M, Hatahira T, Kai M, Masumori N (2013) Methylation of a panel of microRNA genes is a novel biomarker for detection of bladder cancer. *European urology* 63(6): 1091-1100

Silahtaroglu A, Stenvang J (2010) MicroRNAs, epigenetics and disease. *Essays in biochemistry* 48: 165-185

Torre LA, Bray F, Siegel RL, Ferlay J, Lortet-Tieulent J, Jemal A (2015) Global cancer statistics, 2012. *CA: a cancer journal for clinicians* 65(2): 87-108

van der Kwast TH, Bapat B (2009) Predicting favourable prognosis of urothelial carcinoma: gene expression and genome profiling. *Current opinion in urology* 19(5): 516-521

Vogt M, Munding J, Grüner M, Liffers S-T, Verdoodt B, Hauk J, Steinstraesser L, Tannapfel A, Hermeking H (2011) Frequent concomitant inactivation of miR-34a and miR-34b/c by CpG methylation in colorectal, pancreatic, mammary, ovarian, urothelial, and renal cell carcinomas and soft tissue sarcomas. *Virchows Archiv* 458(3): 313-322

Volinia S, Calin GA, Liu C-G, Ambs S, Cimmino A, Petrocca F, Visone R, Iorio M, Roldo C, Ferracin M (2006) A microRNA expression signature of human solid tumors defines cancer gene targets. *Proceedings of the National academy of Sciences of the United States of America* 103(7): 2257-2261

Wu J, Qian J, Li C, Kwok L, Cheng F, Liu P, Perdomo C, Kotton D, Vaziri C, Anderlind C (2010) miR-129 regulates cell proliferation by downregulating Cdk6 expression. *Cell cycle* 9(9): 1809-1818

Yan-Fang T, Jian N, Jun L, Na W, Pei-Fang X, Wen-Li Z, Dong W, Li P, Jian W, Xing F (2013) The promoter of miR-663 is hypermethylated in Chinese pediatric acute myeloid leukemia (AML). *BMC medical genetics* 14(1): 74

Zhang Y, Xu X, Zhang M, Wang X, Bai X, Li H, Kan L, Zhou Y, Niu H, He P (2016) MicroRNA-663a is downregulated in non-small cell lung cancer and inhibits proliferation and invasion by targeting JunD. *BMC cancer* 16(1): 1

Zhang Z, Furge KA, Yang XJ, Teh BT, Hansel DE (2010) Comparative gene expression profiling analysis of urothelial carcinoma of the renal pelvis and bladder. *BMC medical genomics* 3(1): 58

Supplementary Data (Paper I)

Supplementary Table 1: Cox regression models assessing the potential of clinical and epigenetic variables in the prediction of disease-specific survival of BUC and UTUC patients separately and combined as Urothelial carcinoma (UC).

Disease-specific survival	BUC			UTUC			UC			
	Univariable	HR	95% CI for HR	P	HR	95% CI for HR	P	HR	95% CI for HR	P
pTNM		5.24	(2.55 - 10.74)	0.001	2.12	(0.90 - 4.97)	0.084	4.07	(2.35 - 7.05)	0.001
Grade										
PLG vs. PHG		20.96	(2.76 - 159.18)	0.003	2.36	(0.65 - 8.60)	0.194	7.44	(2.58 - 21.49)	0.001
PLG vs. IHG		37.00	(4.90 - 279.37)	0.001	4.78	(1.28 - 17.82)	0.020	13.34	(4.65 - 38.27)	0.001
Age		2.14	(1.00 - 4.60)	0.050	2.78	(1.14 - 6.81)	0.025	2.75	(1.61 - 4.72)	0.001
miR-129-2 methylation > P50		1.40	(0.69 - 2.86)	0.352	0.68	(0.29 - 1.56)	0.360	0.84	(0.49 - 1.42)	0.520
miR-663a methylation > P50		0.56	(0.27 - 1.14)	0.108	1.06	(0.47 - 2.38)	0.890	1.27	(0.75 - 2.16)	0.370
Multivariable										
pTNM		0.35	(0.11- 1.08)	0.067	1.73	(0.70 - 4.27)	0.230	2.10	(1.06 - 4.16)	0.030
Grade										
PLG vs. PHG		12.21	(1.19 - 125.41)	0.035	1.84	(0.49 - 6.83)	0.370	5.45	(1.85 - 16.07)	0.002
PLG vs. IHG		16.09	(2.06 - 125.52)	0.008	3.76	(0.97 - 14.58)	0.056	6.75	(2.05 - 22.21)	0.002
Age		1.97	(0.90 - 4.31)	0.089	3.05	(1.22 - 7.59)	0.017	2.45	(1.43 - 4.19)	0.001

Significance for bold values: Results were considered statistically significant at $P < 0.005$.

Abbreviations: UC - urothelial carcinoma; BUC - Bladder urothelial carcinoma; UTUC - upper tract urothelial carcinoma; HR - Hazard Ratio; CI - confidence interval; PLG - Papillary low-grade; PHG - Papillary high-grade; IHG - Invasive high-grade.

Research Paper II

Paper II: A Multiplex Test Assessing MiR663a_{me} and VIM_{me} in Urine Accurately Discriminates Bladder Cancer from Inflammatory Conditions

Journal of Clinical Medicine 2020, 9(2), 605

DOI: 10.3390/jcm9020605

Sara Monteiro-Reis, Ana Blanca, Joana Tedim-Moreira, Isa Carneiro, Diana Montezuma, Paula Monteiro, Jorge Oliveira, Luís Antunes, Rui Henrique, António Lopez-Beltran, Carmen Jerónimo

Author personal contribution:

Conceptual design and technical execution of the work, interpretation of the results and manuscript preparation.

Abstract

Bladder cancer (BICa) is a common malignancy with significant morbidity and mortality. Current diagnostic methods are invasive and costly, showing the need for newer biomarkers. Although several epigenetic-based biomarkers have been proposed, their ability to discriminate BICa from common benign conditions of the urinary tract, especially inflammatory diseases, has not been adequately explored. Herein, we sought to determine whether VIM_{me} and $miR663a_{me}$ might accurately discriminate those two conditions, using a multiplex test. Performance of VIM_{me} and $miR663a_{me}$ in tissue samples and urines in testing set confirmed previous results (96.3% sensitivity, 88.2% specificity, area under de curve (AUC) 0.98 and 92.6% sensitivity, 75% specificity, AUC 0.83, respectively). In the validation sets, VIM_{me} - $miR663a_{me}$ multiplex test in urine discriminated BICa patients from healthy donors or patients with inflammatory conditions, with 87% sensitivity, 86% specificity and 80% sensitivity, 75% specificity, respectively. Furthermore, positive likelihood ratio (LR) of 2.41 and negative LR of 0.21 were also disclosed. Compared to urinary cytology, VIM_{me} - $miR663a_{me}$ multiplex panel correctly detected 87% of the analysed cases, whereas cytology only forecasted 41%. Furthermore, high $miR663a_{me}$ independently predicted worse clinical outcome, especially in patients with invasive BICa. We concluded that the implementation of this panel might better stratify patients for confirmatory, invasive examinations, ultimately improving the cost-effectiveness of BICa diagnosis and management. Moreover, $miR663a_{me}$ analysis might provide relevant information for patient monitoring, identifying patients at higher risk for cancer progression.

Introduction

Bladder cancer (BICa) is one of the most incident cancers, ranking ninth in prevalence worldwide [1,2]. In men, which are more prone to develop BICa, it represents the second most frequent urological malignancy after prostate cancer [1,2]. Moreover, it is expected that, by 2040, the number of estimated new cases and cancer-related deaths will almost double the 549,393 newly diagnosed cases and 199,922 deaths recorded in 2018 [1,2]. Most BICa cases correspond to urothelial carcinoma, generally presenting as non-muscle invasive BICa (NMIBC), accounting for 75–80% of all new cases, characterized by frequent recurrences and eventual progression to more aggressive, deeply invasive and metastatic disease, or muscle-invasive BICa (MIBC), an aggressive, locally invading carcinoma, corresponding to 20–25% of all cases, with propensity for metastization [3,4]. Haematuria is the most common clinical sign of BICa, although it also occurs in several common benign disease such as urinary tract infections and non-infectious inflammatory conditions. Presently, BICa diagnosis generally involves cystoscopic examination, an expensive and invasive procedure, complemented by urine cytology [5,6,7]. However, the latter has limited

accuracy, particularly for identification of low-grade papillary tumours, and the invasive nature of cystoscopic examination entails patient discomfort and, in some cases, infection [5]. Moreover, because of the high incidence, recurrence and progression rate, active long follow-up is required, making BICa the costliest malignancy [8]. Thus, early, accurate and non-invasive BICa detection is the determinant to improve both patients and healthcare financial management.

Epigenetic changes, including DNA methylation, have been largely investigated for cancer detection [9]. Owing to chemical and biological stability, DNA methylation-based biomarkers have potential clinical applications in early cancer detection, diagnosis, follow-up and targeted therapies [10]. Previously, two independent DNA methylation-based biomarker panels have been reported as promising tests for accurate early detection of BICa [11,12]. In 2010, a three-gene panel comprised GDF15, TMEFF2 and VIM methylation identified BICa with 94% sensitivity and 100% specificity in urine samples from 51 BICa patients [11]. More recently, a panel testing the promoter methylation of two microRNAs—miR129-2 and miR663a—identified urothelial carcinoma (from upper and lower urinary tracts) with a sensitivity of 87.8% and specificity of 82.7% in 49 urine samples from patients with urothelial carcinoma [12]. Furthermore, the same panels could discriminate BICa from other common genitourinary cancers (i.e., from kidney and prostate). Nonetheless, both studies used a singleplex approach, and the ability of these tests to discriminate BICa from common benign conditions of the urinary tract with overlapping manifestations, especially inflammatory diseases, has not been adequately explored, thus far. Indeed, inflammatory conditions of the urinary tract may negatively impact the specificity of urinary-based biomarkers for BICa detection, increasing false positive results and entailing unnecessary complementary invasive tests [6,13,14].

Thus, we sought to assess whether the most promising markers in each published panel—miR-663a (miR663a_{me}) and Vimentin (VIM_{me})—might accurately discriminate BICa from inflammatory conditions in voided urine, allowing for the development of a multiplex test that could be used for early detection in clinical practice.

Experimental Section

Patients and Tumour Sample Collection

Ninety-four primary BICa tissue samples were obtained from a consecutive series of patients diagnosed, treated with transurethral resection (TUR) or radical cystectomy, between 1994 and 2011, and followed at Portuguese Oncology Institute of Porto (IPO Porto), Portugal (Table 1). Briefly, tumour samples were obtained during surgery and immediately snap-frozen, stored at $-80\text{ }^{\circ}\text{C}$ and subsequently macrodissected for tumours'

cells enrichment and cut in cryostat for DNA extraction. Routine collection and processing of tissue samples allowed for pathological examination, classification, grading and staging [15]. For control purposes, an independent set of 19 normal bladder mucosae (NB) samples were also collected from BICa-free individuals (prostate cancer patients submitted to radical prostatectomy) (Table 1).

Table 1. Clinical and histopathological characteristics of patients with bladder carcinoma (BICa), normal bladder mucosae (NB), healthy donors (HD) and inflammatory controls (IC).

Clinicopathological features	Tissues		Urines				
			Testing Set		Validation Sets		
	Bladder UC	Normal Bladder Mucosae	Bladder UC	Healthy Donors	Bladder UC	Healthy Donors (#1)	Inflammatory Controls (#2)
Patients, <i>n</i>	94	19	27	24	100	57	174
Gender, <i>n</i>							
Males	78	19	20	13	79	16	132
Females	16	0	7	12	21	41	42
Median age, yrs (range)	69 (45 - 91)	63 (48 - 75)	69 (47 - 88)	45 (39 - 61)	68 (38 - 91)	49 (41 - 64)	64 (18- 92)
Grade, <i>n</i>							
Papillary, low-grade	34	n.a.	13	n.a.	51	n.a.	n.a.
Papillary, high-grade	33	n.a.	8	n.a.	26	n.a.	n.a.
Invasive, high-grade	27	n.a.	6	n.a.	23	n.a.	n.a.
Invasion of Muscular Layer, <i>n</i>							
NMIBC	67	n.a.	19	n.a.	77	n.a.	n.a.
MIBC	27	n.a.	8	n.a.	23	n.a.	n.a.

(#1 – Validation Set #1; #2 – Validation Set #2; yrs – years; n.a.—non applicable; NMIBC—Non-Muscle Invasive Bladder Cancer; MIBC—Muscle Invasive Bladder Cancer, UC – Urothelial Carcinoma).

Urine Sample Collection and Processing

For the “Testing sets”, 27 voided urine samples (one per patient) were collected from BICa patients, diagnosed and treated between 2006 and 2016 at IPO Porto, as well as a set of 24 voided urine samples from healthy donors (HD), also from IPO Porto, with no personal or familial history of cancer, used as controls (Table 1). The “Validation sets” comprised: (1) 100 urine samples from BICa patients, diagnosed and treated between 2002 and 2016 at IPO Porto, and 57 urine samples from HD collected at IPO Porto, and (2) an independent set of control urine sediments ($n = 174$) from patients diagnosed with urinary tract inflammatory conditions (IC), diagnosed between 2008 and 2014 at the University Hospital of Cordoba (UHC). All BICa patients’ urines were obtained before treatment. Moreover, all sets of samples were collected from different cohorts of patients. Informed consent was obtained from patients and controls after approval from the ethics committees of IPO Porto and UHC (CES-IPO 019/08, approval date: 16th January 2008). All urine samples were processed by immediate centrifugation at 4000 rpm for 10 min; the respective pellet was washed twice with phosphate-buffered saline (PBS) and stored at $-80\text{ }^{\circ}\text{C}$.

Nucleic Acids Isolation, Bisulfite Modification and Multiplex qMSP Analysis

DNA was extracted from frozen BICa and NB tissues, and all urine sample sets, using a standard phenol-chloroform protocol [16], and its concentration determined using a Qubit 3 Fluorometer (Thermo Fisher Scientific, Waltham, MA, USA). Bisulfite modification was performed through sodium bisulfite, using the EZ DNA Methylation-Gold™ Kit (Zymo Research, Irvine, CA, USA), according to manufacturer’s protocol. For this, 1000 ng and 50 ng of DNA were converted for tissues and urine sediments, respectively. Quantitative methylation levels were performed using Xpert Fast Probe Master Mix (GRiSP, Porto, Portugal), and multiplex reactions were run in triplicates in 96-well plates using an Applied Biosystems 7500 Sequence Detector (Perkin Elmer, Waltham, CA, USA), with Beta-Actin (ACTB) as internal reference gene for normalization. Primer and probe sequences were designed using Methyl Primer Express 1.0 and purchased from Sigma-Aldrich (St. Louis, MO, USA) (Supplementary Table S1). Additionally, six serial dilutions (dilution factor of $5\times$) of a fully methylated bisulphite modified universal DNA control were included in each plate to generate a standard curve. In each sample and for each gene, the relative DNA methylation levels were determined using the following formula: $((\text{target gene}/\text{ACTB}) \times 1000)$. A run was considered valid when previously reported criteria were met [11].

Statistical Analysis

Differences in quantitative methylation values were assessed with the non-parametric Mann-Whitney U (MW) and Kruskal-Wallis (KW) tests. Associations between age, gender,

grade, invasion of muscular layer and methylation levels were carried out using Spearman's correlation, MW or KW tests, as appropriate. For multiple comparisons, Bonferroni's correction was applied in pairwise comparisons.

Biomarker performance parameters, including sensitivity, specificity, positive predictive value (PPV), negative predictive value (NPV), accuracy and positive and negative likelihood ratios (LR), were estimated [17]. Receiver operator characteristics (ROC) curves were constructed by plotting the true positive (sensitivity) against false positive (1-specificity) rate, and the area under the curve (AUC) was calculated. The higher value obtained from the sum of sensitivity and 1-specificity in each ROC-curve was used as cut-off to categorise samples as methylated or non-methylated. ROC curves were constructed using logistic regression model for DNA methylation panel. Disease-specific and disease-free survival curves (Kaplan-Meier with log rank test) were computed for standard variables and for categorised genes' promoter methylation status. A Cox-regression model comprising all significant variables (univariable and multivariable model) was computed to assess the relative contribution of each variable to the follow-up status. All two-tailed p values were derived from statistical tests, using a computer-assisted program (SPSS Version 26.0, IBM, Armonk, NY, EUA) and the results were considered statistically significant at $p < 0.05$. Bonferroni's correction for multiple comparisons was used when applicable.

Results

Methylation Analysis and Performance of the Multiplex Panel in BICa Tissue Series

To confirm the previously published performance of miR663a and VIM promoter methylation as BICa biomarkers, tissue samples were tested. As expected, both miR663a and VIM were found hypermethylated (76.6% and 94.4%, respectively) in most BICa tissue samples, and methylation levels were significantly higher compared to NB ($p < 0.0001$ and $p < 0.0001$, respectively) (Figure 1A). The two genes independently performed well as BICa detection biomarkers in tissues, with an AUC of 0.979 for VIMme (95% confidence interval (CI): 0.956–1.002, $p < 0.0001$), and of 0.897 for miR663ame (95% CI: 0.836–0.959, $p < 0.0001$). Moreover, in combination as multiplex panel, it accurately discriminated BICa from NB with 96.3% sensitivity and 88.2% specificity, corresponding to an AUC of 0.982 (Figure 1B; Supplementary Table S2).

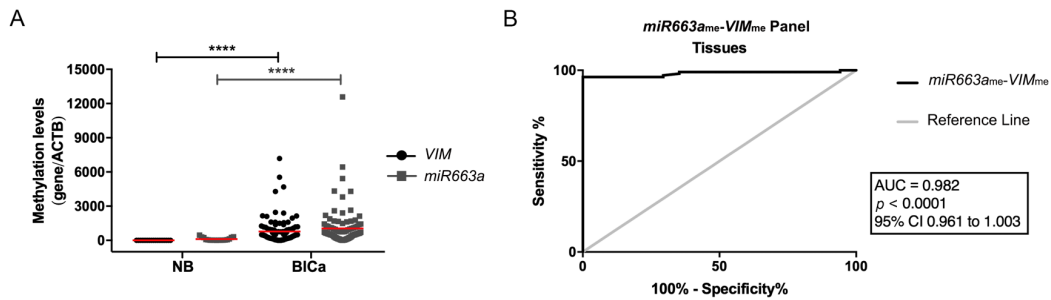


Figure 1. (A) Distribution of VIM_{me} and miR663a_{me} levels in normal bladder mucosae (NB; n = 19) and bladder carcinoma (BICa; n = 94) tissue samples. Mann-Whitney U test, **** p < 0.0001. Median is represented by the red line. (B) Receiver operator characteristic (ROC) curve evaluating the performance of the VIM_{me}-miR663a_{me} panel for the identification of BICa in tissue samples. (AUC—Area under the curve; CI—Confidence interval; ACTB—Beta-Actin; VIM—Vimentin).

Methylation Analysis and Performance of Multiplex Panel in BICa Testing Set

Paralleling the previous observations in tissues, miR663a_{me} and VIM_{me} levels were significantly higher in BICa urine samples than in those of controls (p < 0.0001 and p < 0.0001, Figure 2A), and the multiplex panel discriminated BICa from HD with 92.6% sensitivity and 90% NPV (Supplementary Table S2), corresponding to an AUC of 0.83 (Figure 2B).

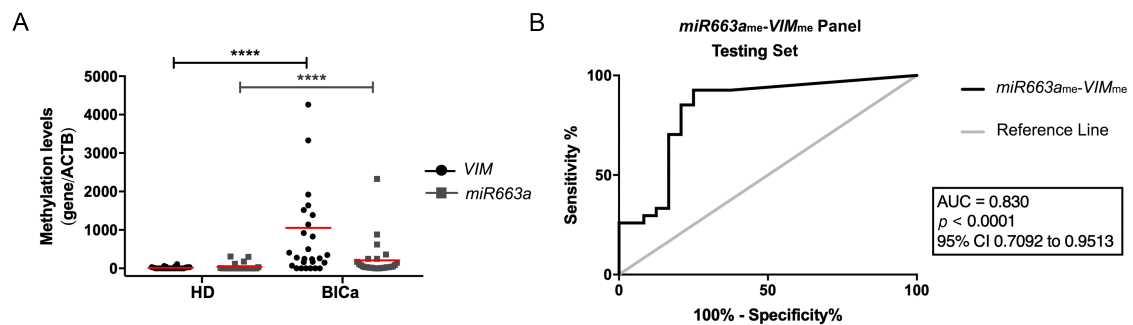


Figure 2. (A) Distribution of VIM_{me} and miR663a_{me} levels in the Testing Cohort, composed by healthy donors (HD; n = 24) and bladder carcinoma (BICa; n = 27) urine samples. Mann-Whitney U test, **** p < 0.0001. Median is represented by the red line. (B) Receiver operator characteristic (ROC) curve evaluating the performance of the VIM_{me}-miR663a_{me} panel for the identification of BICa in urine samples of the Testing Cohort. (AUC—Area under the curve; CI—Confidence interval; ACTB—Beta-Actin; VIM—Vimentin).

Methylation Analysis and Performance of VIM_{me} and miR663a_{me} Multiplex Panel for BICa vs. HD

In line with the testing set results, a higher number of malignant samples disclosed significantly higher miR663a_{me} and VIM_{me} levels than HDs ($p < 0.0001$ and $p < 0.0001$, respectively) in the validation sets (Figure 3A). ROC curve analysis confirmed a high discriminative ability of VIM_{me}-miR663a_{me} panel, with an AUC of 0.91 (Figure 3B). Indeed, the multiplex panel discriminated BICa from HD subjects with 87% sensitivity and 86% specificity (Table 2).

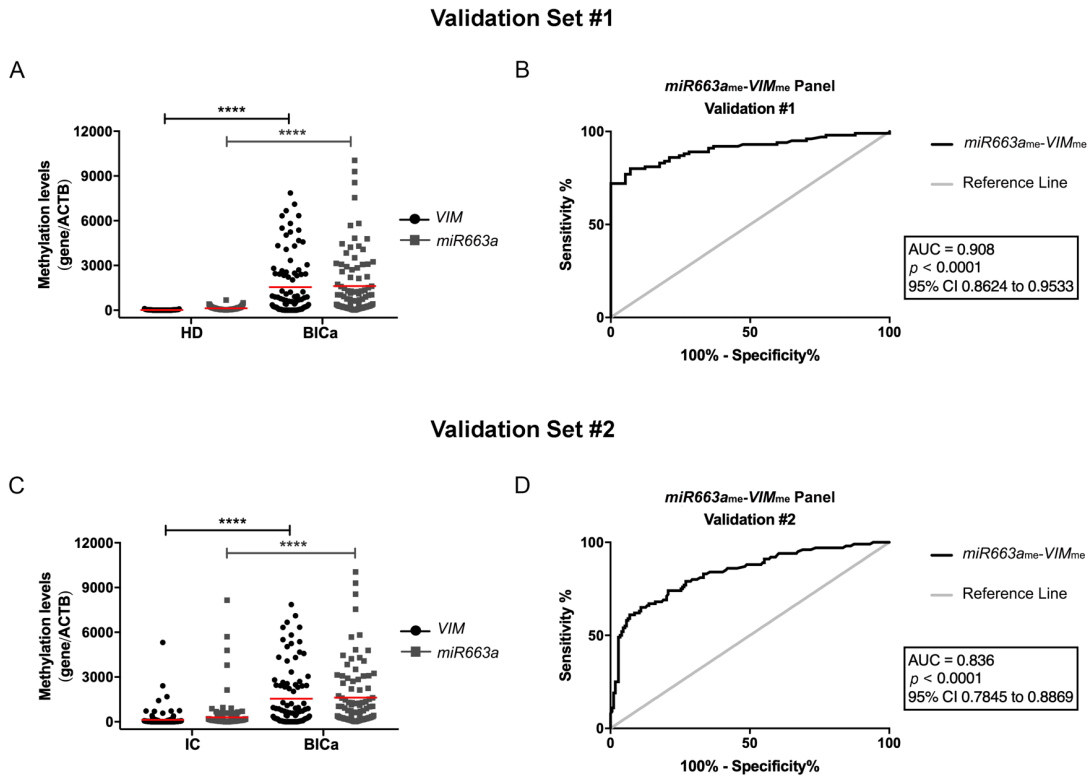


Figure 3. Distribution of VIM_{me} and miR663a_{me} levels in the Validation Cohort #1, composed by healthy donors (HD; $n = 57$) and bladder carcinoma (BICa; $n = 100$) urine samples. Mann-Whitney U (MW) test, **** $p < 0.0001$. Median is represented by the red line. (B) Receiver operator characteristic (ROC) curve evaluating the performance of the VIM_{me}-miR663a_{me} panel for the identification of BICa in urine samples of the Validation Cohort #1. (C) Distribution of VIM_{me} and miR663a_{me} levels in the Validation Cohort #2, composed by inflammatory controls (IC; $n = 174$) and bladder carcinoma (BICa; $n = 100$) urine samples. MW test, **** $p < 0.0001$. (D) ROC curve evaluating the performance of the VIM_{me}-miR663a_{me} panel for the identification of BICa in urine samples of the Validation Cohort #2. (AUC—Area under the curve; CI—Confidence interval; ACTB—Beta-Actin; VIM—Vimentin).

Table 2. Performance of VIM_{me}-miR663a_{me} panel for the detection of bladder cancer in Validation Cohorts #1 and #2. (PPV—positive predictive value; NPV—negative predictive value).

Samples	Biomarker Performance	miR663a _{me} -VIM _{me} (%)
Validation #1	Sensitivity	87.0
	Specificity	86.0
	PPV	91.6
	NPV	79.0
	Accuracy	86.6
Validation #2	Sensitivity	80.0
	Specificity	75.3
	PPV	65.0
	NPV	86.8
	Accuracy	77.0

Remarkably, the proportion of true positive cases detected by the VIM_{me}-miR663_{me} multiplex panel was significantly higher than that of urine cytology ($p < 0.001$). Indeed, of 46 BlCa cases with valid urine cytology results, only 19 were classified as positive, 17 as negative and 10 as “inconclusive/suspicious”, corresponding to 41% sensitivity (Figure 4). Contrarily, the VIM_{me}-miR663_{me} multiplex panel correctly identified 40/46 cases as BlCa, corresponding to an overall sensitivity of 87% (Figure 4). Importantly, 12 of 14 low-grade papillary carcinomas were accurately identified by VIM_{me}-miR663_{me} multiplex panel, whereas cytology merely identified four cases.

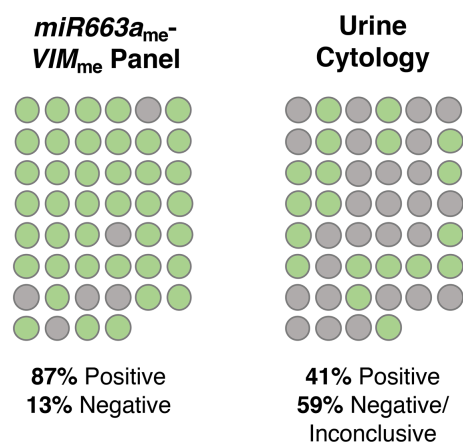


Figure 4. Representation of the percentage of bladder cancer (BlCa) cases correctly identified with the VIM_{me}-miR663a_{me} panel and a standard urine cytology analysis. Green circles represent positive cases, grey circles represent negative/inconclusive cases.

Methylation Analysis and Performance of VIM_{me} and miR663_{me} Multiplex Panel for BICa vs. IC

In urine samples, VIM_{me}-miR663_{me} levels discriminated BICa from IC patients (Figure 3C), with 80% sensitivity, 75.3% specificity and, importantly, 86.8% NPV (Table 2), corresponding to an AUC of 0.836 (Figure 3D). Remarkably, a 2.86 Positive LR and a Negative LR of 0.21 were also disclosed by VIM_{me}-miR663_{me} multiplex panel in this setting.

Clinicopathologic Correlations and Survival Analyses

High-grade papillary BICa showed significantly higher miR663_{me} levels than low-grade papillary BICa ($p = 0.007$), in tissue samples. The same was observed in urine samples from the validation set ($p = 0.0072$), a result which was extensive to VIM_{me} ($p = 0.0052$) (Supplementary Figure S1). No additional associations were disclosed between VIM_{me} and miR663_{me} levels and other standard clinical variables, including patients' age and gender. Follow-up data was available for 91 (out of 94) IPO Porto's BICa patients that provided tissue samples. The median follow-up time was 66 months (range: 1–203 months). At the last follow-up timepoint, 30 patients were alive with no evidence of cancer, 12 patients were alive with disease, 29 had deceased due to BICa and 23 died from other causes. Univariable and multivariable Cox regression analysis were performed, including the variables grade, invasion of muscular layer, gender and age. As expected, a poor outcome was depicted for patients with higher grade and muscle invasive BICa ($p = 0.001$ and $p < 0.0001$, respectively) (Table 3). In the multivariate model for disease-specific survival, miR663_{me} levels, higher grade and muscle invasion were independent predictors of outcome ($p = 0.04$, $p = 0.035$ and $p = 0.031$, respectively; Table 3). Moreover, after categorization into NMIBC vs. MIBC, tumours with higher miR663_{me} levels implied a 3.7-fold increased risk of cancer-related death among patients with MIBC (95% CI: 1.32–10.25, $p = 0.013$; Supplementary Figure S2). Contrarily, no associations were found for miR663_{me} or VIM_{me} levels concerning disease-free survival.

Table 3. Cox regression models assessing the potential of clinical and VIM_{me} and miR663a_{me} levels in the prediction of disease-specific survival for bladder carcinoma (BlCa) patients. (PLG - papillary low-grade; PHG - papillary high-grade; IHG – invasive high-grade; HR – hazard ratio; OR – odds ratio; CI – confidence interval).

Disease-specific Survival	Variables	Hazard Ratio (HR)	95% CI* for OR	p
Univariate	Invasion of muscular layer	6.15	2.76 - 13.72	0.0001
	Grade			
	PLG vs. PHG	15.59	2.03 - 119.94	0.008
	PLG vs. IHG	32.83	4.31 - 250.06	0.001
	Age	2.34	0.98 - 5.59	0.060
	Gender	1.02	0.39 - 2.70	0.970
	miR663a methylation ≤ median	1.61	0.75 - 3.48	0.225
	VIM methylation ≤ median	1.07	0.50 - 2.28	0.861
Multivariate	Invasion of muscular layer	3.54	1.12 - 11.19	0.031
	Grade			
	PLG vs. PHG	8.03	0.97- 66.32	0.053
	PLG vs. IHG	11.89	1.18 - 119.37	0.035
	miR663a methylation ≤ median	2.67	1.05 - 6.81	0.040
	VIM methylation ≤ median	1.12	0.51 - 2.42	0.783

Discussion

Bladder cancer is a major health concern worldwide, with an expected significant increase in incidence and mortality within the next two decades [1,2]. Early detection is critical for adequate management, aiming to reduce disease-specific mortality, as well as the economic burden imposed by BlCa treatment and follow-up. Because currently available diagnostic tools require invasive examination [13,14], development of non-invasive and less costly tests for early detection and monitoring are likely to have a significant impact in clinical practice. Although several molecular biomarkers, including epigenetic-based, have been developed for that end, discrimination of BlCa from other urinary tract malignancies and, more importantly, from benign conditions causing haematuria, including inflammatory diseases, remains a challenge. Indeed, most control samples used in biomarker discovery studies, including our own, mostly comprise normal/healthy donors, disregarding the fact that a biomarker-based test would be offered to an “at-risk” population, including patients experiencing suspicious symptoms. Therefore, based on two previously published studies

by our research team [11,12], we tested whether a VIM_{me} and miR663a_{me} multiplex panel could accurately discriminate BICa from normal individuals and those afflicted with inflammatory conditions of the genitourinary tract.

Because both VIM_{me} and miR663a_{me} were previously assessed using two different “simplex” multi-gene biomarker panels, we firstly tested miR663a_{me} and VIM_{me} in multiplex in a consecutive series of primary BICa tissue samples and normal urothelial mucosae to confirm those previous results. Indeed, employing a multiplex reaction allows for downscaling the initial tissue/body fluid sample requirements, but also the quantity of DNA required for each test [18]. Remarkably, as expected, the VIM_{me}-miR663a_{me} multiplex panel discriminated BICa from NB tissues with high sensitivity and specificity (96.3% and 88.2%, respectively), confirming the previous observations for the two markers separately [11,12]. In urine samples from the testing set, although the performance of the multiplex panel was slightly inferior to that of tissues, 92.6% sensitivity and 90% NPV was reached. Indeed, it should be recalled that a relatively small number of cancer cells are exfoliated into urine, which are subsequently “diluted” among a larger population of normal-looking urothelial cells. Thus, the tumour DNA content in urine is actually minute [19] and sensitivity over 90% should be regarded as a very encouraging result. Furthermore, in the validation set, comprising a larger independent cohort, specificity of the VIM_{me}-miR663a_{me} multiplex panel increased to 86%, further increasing the potential usefulness of the test.

It should be emphasised, however, that the foremost aim of this study was to assess the multiplex panel ability to discriminate BICa from IC, since this panel is envisaged to be tested in an “at-risk” population, including individuals complaining of haematuria, many of which will be found to harbour urinary tract inflammatory conditions. Although, in this setting, sensitivity and specificity were slightly reduced, NPV increased (86.8%), which is an important finding [20]. Indeed, it is expected that among tested individuals, most will not have a neoplastic condition and, thus, the higher the NPV, the larger the proportion of those subjects that will not be submitted to confirmatory, invasive, procedures, supporting the good performance of the test in discriminating patients negative for malignant condition. Importantly, an LR (+) of 2.86 and an LR (-) of 0.21 values were observed, indicating that a negative result decreases by 30% the probability of misdiagnosis [17].

Despite the fact that several studies suggest various genomic mutations and/or proteins' expression deregulation as biomarkers for BICa detection and prognostication [21], the search for novel epigenetic biomarkers, mostly DNA methylation-based, for BICa detection has been attempted by several research teams, probably due to the stability of the markers and the possibility of high-throughput tests. Although some of those previous studies report an apparently superior performance to the panel reported herein, it should be recalled that in most cases the patients' series were smaller, only healthy donors were included as

controls or these were comprised of a mixed group of healthy donors and patients with diverse urological diseases, and/or did not use a multiplex approach, which might impact in sample availability, testing time length and cost [22-28]. Roperch et al. proposed a three gene multiplex methylation panel (HS3ST2, SEPTIN9 and SLIT2) combined with FGFR3 mutations assessment, age and smoking-status at time of diagnosis in a multivariate model, for diagnosis of NMIBC in urine samples, disclosing 97.6% sensitivity and 84.8% specificity, in a smaller control cohort [29]. Nonetheless, this strategy might be more difficult to implement in clinical practice, since it requires both mutation and methylation analyses, in which the multiplex is performed in two distinct gene duplex reactions. Similarly, Dahmcke et al. proposed a six gene methylation panel (SALL3, ONECUT2, CCNA1, BCL2, EOMES and VIM) combined with the mutational analysis of TERT and FGFR3, for early detection of BICa, in urine samples, comparing BICa patients and patients with gross haematuria [30]. Although this panel disclosed higher sensitivity (97%), specificity was similar (76.9%) [30], and, once again, our test uses a single technique in a single reaction, requiring less amount of sample, enabling shorter response time, reduced technical skills and lower cost.

Although urine cytology and UroVysion™ fluorescence in situ hybridization (FISH) assay are the two most commonly used urine-based tests in daily practice, they present important limitations. On one hand, UroVysion™ presents a not-negligible rate of false positive results; on the other hand, urine cytology has limited accuracy, especially in low grade tumours detection [6,31,32]. Although no direct comparison can be done with UroVysion™, the 91.6% PPV obtained for the multiplex panel clearly demonstrates higher accuracy in identifying true positive BICa cases. In the present study, urine cytology reached 41% sensitivity, which was easily surpassed by the 86% displayed by VIM_{me}-miR663a_{me} multiplex panel. Notwithstanding, urine cytology remains an easy-to-perform and informative test, as it allows pathologists to have the first look at exfoliated neoplastic cells in urine. Having that in mind, we propose an algorithm where a urine cytology and the VIM_{me}-miR663a_{me} multiplex panel could be combined as first-line diagnostic tests in patients with common urinary complaints, with the ultimate goal of reducing the number of unnecessary cystoscopies, which are invasive, uncomfortable and costly procedures (Figure 5).

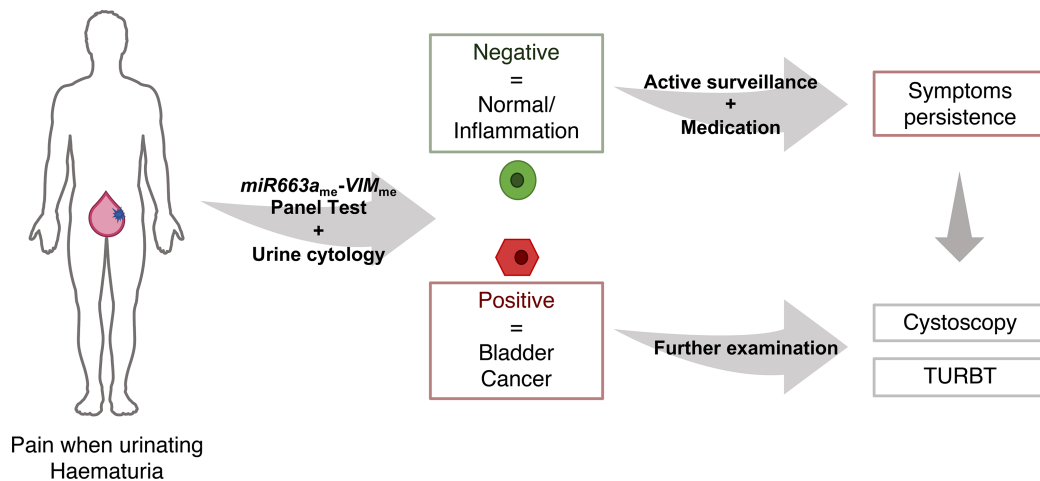


Figure 5. Proposed algorithm for the combination of urine cytology and VIM_{me}-miR663a_{me} panel as a first-line diagnostic tests in patients with common urinary complaints. (TURBT—Transurethral Resection of Bladder Tumour).

In this work, we further explored the prognostic ability of the gene methylation markers, aiming to strengthen its clinical potential. Interestingly, survival analysis revealed that high miR663a_{me} levels independently predicted poor disease-specific survival in Bladder Cancer patients, especially those with Muscle Invasive Bladder Cancer. Thus, the VIM_{me}-miR663a_{me} multiplex panel not only conveys diagnostic, but also prognostic information.

Taking into account the promising results obtained, unveiling the putative biological relevance of miR663a and VIM promoter methylation in bladder carcinogenesis may provide new important insights. VIM encodes for vimentin, an intermediate filament characteristic of cells with mesenchymal phenotype, not expressed in most normal epithelia (including urothelium), nor in most carcinomas [33]. VIM de-novo expression or overexpression has been reported in various epithelial cancers, including those of prostate [34], breast [35] and lung [36], associating with increased tumour growth and invasion. In these instances, vimentin expression has been associated with epithelial to mesenchymal transition (EMT), a biological process associated with tumour invasiveness [33]. Although VIM promoter methylation has been proposed as a detection and/or prognostic marker for other malignancies, biological functions are yet to be truly explored. Moreover, microRNAs have been extensively implicated in urological malignancies [37]. Interestingly, a dual role has already been described for miR663a, having a tumour suppressive activity in thyroid carcinoma [38] and glioblastoma [39], whereas an oncogenic function was reported in prostate cancer [40] and osteosarcoma [41]. Additionally, miR663a's downregulation fostered cell proliferation by JunD overexpression in small-cell lung carcinoma [42], and HMGA2 in hepatocellular carcinoma [43], while Transforming Growth Factor-1 (TGF-β1)

[44] overexpression was linked with invasion in the tumour type. Nevertheless, it should be recalled that not all biomarkers require to have a relevant biological role in tumorigenesis. Importantly, to assure accuracy and validity of the proposed methylation multiplex test, additional validation by others, with larger sets of samples from prospectively collected data (from both BICa and inflammatory conditions) is warrant.

Conclusions

In summary, we demonstrated that a VIM_{me}-miR663a_{me} multiplex panel accurately identifies BICa, allowing for precise identification of this common neoplasm in urine samples. Importantly, it also discriminates BICa patients from those with urinary tract inflammatory conditions, although with inferior performance comparatively to healthy subjects. Thus, the implementation of this panel might assist clinicians in better stratifying patients for confirmatory, invasive examinations, ultimately improving the cost-effectiveness of BICa diagnosis and management. Moreover, in the same analysis, miR663a_{me} analysis would identify patients at higher risk for cancer progression, further highlighting the promise of this panel for patient monitoring.

References

1. Ferlay, J.; Ervik, M.; Lam, F.; Colombet, M.; Mery, L.; Piñeros, M.; Znaor, A.; Soerjomataram, I.; Bray, F. Global Cancer Observatory: Cancer Tomorrow. Available online: <http://gco.iarc.fr/tomorrow2018> (accessed on 26 October 2019).
2. Antoni, S.; Ferlay, J.; Soerjomataram, I.; Znaor, A.; Jemal, A.; Bray, F. Bladder Cancer Incidence and Mortality: A Global Overview and Recent Trends. *Eur. Urol.* 2017, 71, 96–108, doi:10.1016/j.eururo.2016.06.010.
3. Sanli, O.; Dobruch, J.; Knowles, M.A.; Burger, M.; Alemozaffar, M.; Nielsen, M.E.; Lotan, Y. Bladder cancer. *Nat. Rev. Dis. Primers* 2017, 3, 17022, doi:10.1038/nrdp.2017.22.
4. International Agency for Cancer Research. WHO Classification of Tumours of the Urinary System and Male Genital Organs, 4th Edition; Moch, H.; Ulbright, T.; Humphrey, P.; Reuter, V., Eds.; IARC: Lyon, France, 2016.
5. Kaufman, D.S.; Shipley, W.U.; Feldman, A.S. Bladder cancer. *Lancet (London, England)* 2009, 374, 239–249, doi:10.1016/s0140-6736(09)60491-8.
6. Babjuk, M.; Burger, M.; Comperat, E.M.; Gontero, P.; Mostafid, A.H.; Palou, J.; van Rhijn, B.W.G.; Roupert, M.; Shariat, S.F.; Sylvester, R., et al. European Association of Urology Guidelines on Non-muscle-invasive Bladder Cancer (TaT1 and Carcinoma In Situ) - 2019 Update. *Eur. Urol.* 2019, 76, 639–657, doi:10.1016/j.eururo.2019.08.016.
7. Alfred Witjes, J.; Lebet, T.; Comperat, E.M.; Cowan, N.C.; De Santis, M.; Bruins, H.M.; Hernandez, V.; Espinos, E.L.; Dunn, J.; Rouanne, M., et al. Updated 2016 EAU Guidelines on Muscle-invasive and Metastatic Bladder Cancer. *Eur. Urol.* 2017, 71, 462–475, doi:10.1016/j.eururo.2016.06.020.

8. Leal, J.; Luengo-Fernandez, R.; Sullivan, R.; Witjes, J.A. Economic Burden of Bladder Cancer Across the European Union. *Eur. Urol.* 2016, 69, 438–447, doi:10.1016/j.eururo.2015.10.024.
9. Esteller, M. Epigenetics in cancer. *N. Engl. J. Med.* 2008, 358, 1148–1159, doi:10.1056/NEJMra072067.
10. Costa-Pinheiro, P.; Montezuma, D.; Henrique, R.; Jeronimo, C. Diagnostic and prognostic epigenetic biomarkers in cancer. *Epigenomics* 2015, 7, 1003–1015, doi:10.2217/epi.15.56.
11. Costa, V.L.; Henrique, R.; Danielsen, S.A.; Duarte-Pereira, S.; Eknaes, M.; Skotheim, R.I.; Rodrigues, A.; Magalhaes, J.S.; Oliveira, J.; Lothe, R.A., et al. Three epigenetic biomarkers, GDF15, TMEFF2, and VIM, accurately predict bladder cancer from DNA-based analyses of urine samples. *Clin. Cancer Res.* 2010, 16, 5842–5851, doi:10.1158/1078-0432.CCR-10-1312.
12. Padrao, N.A.; Monteiro-Reis, S.; Torres-Ferreira, J.; Antunes, L.; Leca, L.; Montezuma, D.; Ramalho-Carvalho, J.; Dias, P.C.; Monteiro, P.; Oliveira, J., et al. MicroRNA promoter methylation: a new tool for accurate detection of urothelial carcinoma. *Br. J. Cancer* 2017, 116, 634–639, doi:10.1038/bjc.2016.454.
13. Heller, M.T.; Tublin, M.E. In search of a consensus: evaluation of the patient with hematuria in an era of cost containment. *AJR Am. J. Roentgenol.* 2014, 202, 1179–1186, doi:10.2214/AJR.13.12266.
14. Grover, S.; Srivastava, A.; Lee, R.; Tewari, A.K.; Te, A.E. Role of inflammation in bladder function and interstitial cystitis. *Ther. Adv. Urol.* 2011, 3, 19–33, doi:10.1177/1756287211398255.
15. Humphrey, P.A.; Moch, H.; Cubilla, A.L.; Ulbright, T.M.; Reuter, V.E. The 2016 WHO Classification of Tumours of the Urinary System and Male Genital Organs-Part B: Prostate and Bladder Tumours. *Eur. Urol.* 2016, 70, 106–119, doi:10.1016/j.eururo.2016.02.028.
16. Pearson, H.; Stirling, D. DNA extraction from tissue. In *PCR Protocols*, 2nd Edition. Bartlett, J.M.S; Stirling, D., Eds. Humana Press: Totowa, USA, 2003.
17. McGee, S. Simplifying likelihood ratios. *J. Gen. Intern. Med.* 2002, 17, 646–649, doi:10.1046/j.1525-1497.2002.10750.x.
18. Guest, P.C. Multiplex Biomarker Approaches to Enable Point-of-Care Testing and Personalized Medicine. *Methods Mol. Biol.* 2017, 1546, 311–315, doi:10.1007/978-1-4939-6730-8_28.
19. Larsen, L.K.; Lind, G.E.; Guldborg, P.; Dahl, C. DNA-Methylation-Based Detection of Urological Cancer in Urine: Overview of Biomarkers and Considerations on Biomarker Design, Source of DNA, and Detection Technologies. *Int. J. Mol. Sci.* 2019, 20, 2657, doi:10.3390/ijms20112657.
20. Anna K Füzéry, D.W.C. Cancer Biomarker Assays: Performance Standards. In *Biomarkers in Cancer Screening and Early Detection*, First Edition; Srivastava, S.; John Wiley & Sons: Hoboken, EUA, 2017.
21. Tan, W.S.; Tan, W.P.; Tan, M.Y.; Khetrapal, P.; Dong, L.; deWinter, P.; Feber, A.; Kelly, J.D. Novel urinary biomarkers for the detection of bladder cancer: A systematic review. *Cancer Treat Rev.* 2018, 69, 39–52, doi:10.1016/j.ctrv.2018.05.012.

22. Chihara, Y.; Kanai, Y.; Fujimoto, H.; Sugano, K.; Kawashima, K.; Liang, G.; Jones, P.A.; Fujimoto, K.; Kuniyasu, H.; Hirao, Y. Diagnostic markers of urothelial cancer based on DNA methylation analysis. *BMC Cancer* 2013, 13, 275, doi:10.1186/1471-2407-13-275.
23. Wang, Y.; Yu, Y.; Ye, R.; Zhang, D.; Li, Q.; An, D.; Fang, L.; Lin, Y.; Hou, Y.; Xu, A., et al. An epigenetic biomarker combination of PCDH17 and POU4F2 detects bladder cancer accurately by methylation analyses of urine sediment DNA in Han Chinese. *Oncotarget* 2016, 7, 2754–2764, doi:10.18632/oncotarget.6666.
24. Yegin, Z.; Gunes, S.; Buyukalpelli, R. Hypermethylation of TWIST1 and NID2 in tumor tissues and voided urine in urinary bladder cancer patients. *DNA Cell Biol.* 2013, 32, 386–392, doi:10.1089/dna.2013.2030.
25. Renard, I.; Joniau, S.; van Cleynenbreugel, B.; Collette, C.; Naome, C.; Vlassenbroeck, I.; Nicolas, H.; de Leval, J.; Straub, J.; Van Criekinge, W., et al. Identification and validation of the methylated TWIST1 and NID2 genes through real-time methylation-specific polymerase chain reaction assays for the noninvasive detection of primary bladder cancer in urine samples. *Eur. Urol.* 2010, 58, 96–104, doi:10.1016/j.eururo.2009.07.041.
26. Yu, J.; Zhu, T.; Wang, Z.; Zhang, H.; Qian, Z.; Xu, H.; Gao, B.; Wang, W.; Gu, L.; Meng, J., et al. A novel set of DNA methylation markers in urine sediments for sensitive/specific detection of bladder cancer. *Clin. Cancer Res.* 2007, 13, 7296–7304, doi:10.1158/1078-0432.CCR-07-0861.
27. Sun, J.; Chen, Z.; Zhu, T.; Yu, J.; Ma, K.; Zhang, H.; He, Y.; Luo, X.; Zhu, J. Hypermethylated SFRP1, but none of other nine genes "informative" for western countries, is valuable for bladder cancer detection in Mainland China. *J. Cancer Res. Clin. Oncol.* 2009, 135, 1717–1727, doi:10.1007/s00432-009-0619-z.
28. Chan, M.W.; Chan, L.W.; Tang, N.L.; Tong, J.H.; Lo, K.W.; Lee, T.L.; Cheung, H.Y.; Wong, W.S.; Chan, P.S.; Lai, F.M., et al. Hypermethylation of multiple genes in tumor tissues and voided urine in urinary bladder cancer patients. *Clin Cancer Res.* 2002, 8, 464–470.
29. Roperch, J.P.; Grandchamp, B.; Desgrandchamps, F.; Mongiat-Artus, P.; Ravery, V.; Ouzaid, I.; Roupret, M.; Phe, V.; Ciofu, C.; Tubach, F., et al. Promoter hypermethylation of HS3ST2, SEPTIN9 and SLIT2 combined with FGFR3 mutations as a sensitive/specific urinary assay for diagnosis and surveillance in patients with low or high-risk non-muscle-invasive bladder cancer. *BMC cancer* 2016, 16, 704, doi:10.1186/s12885-016-2748-5.
30. Dahmcke, C.M.; Steven, K.E.; Larsen, L.K.; Poulsen, A.L.; Abdul-AI, A.; Dahl, C.; Guldborg, P. A Prospective Blinded Evaluation of Urine-DNA Testing for Detection of Urothelial Bladder Carcinoma in Patients with Gross Hematuria. *Eur. Urol.* 2016, 70, 916–919, doi:10.1016/j.eururo.2016.06.035.
31. Brimo, F.; Vollmer, R.T.; Case, B.; Aprikian, A.; Kassouf, W.; Auger, M. Accuracy of urine cytology and the significance of an atypical category. *Am. J. Clin. Pathol.* 2009, 132, 785–793, doi:10.1309/AJCPPRZLG9KT9AXL.
32. Lavery, H.J.; Zaharieva, B.; McFaddin, A.; Heerema, N.; Pohar, K.S. A prospective comparison of UroVysion FISH and urine cytology in bladder cancer detection. *BMC Cancer* 2017, 17, 247. doi:10.1186/s12885-017-3227-3.

33. Satelli, A.; Li, S. Vimentin in cancer and its potential as a molecular target for cancer therapy. *Cell Mol. Life Sci.* 2011, 68, 3033. doi:10.1007/s00018-011-0735-1.
34. Singh, S.; Sadacharan, S.; Su, S.; Beldegrun, A.; Persad, S.; Singh, G. Overexpression of vimentin: role in the invasive phenotype in an androgen-independent model of prostate cancer. *Cancer Res.* 2003, 63, 2306–11.
35. Kokkinos, M.I.; Wafai, R.; Wong, M.K.; Newgreen, D.F.; Thompson, E.W.; Waltham, M. Vimentin and Epithelial-Mesenchymal Transition in Human Breast Cancer – Observations in vitro and in vivo. *Cells Tissues Organs* 2007, 185, 191–203. doi:10.1159/000101320.
36. Al-Saad, S.; Al-Shibli, K.; Donnem, T.; Persson, M.; Bremnes, R.M.; Busund, L.T. The prognostic impact of NF-kappaB p105, vimentin, E-cadherin and Par6 expression in epithelial and stromal compartment in non-small-cell lung cancer. *Br. J. Cancer* 2008, 99, 1476–1483.
37. Jerónimo, C.; Henrique, R. Epigenetic biomarkers in urological tumors: A systematic review. *Cancer Lett.* 2014, 342, 264–274. doi:10.1016/j.canlet.2011.12.026.
38. Wang, Z.; Zhang, H.; Zhang, P.; Dong, W.; He, L. MicroRNA-663 suppresses cell invasion and migration by targeting transforming growth factor beta 1 in papillary thyroid carcinoma. *Tumour Biol.* 2015, 37, 7633–7644. doi:10.1007/s13277-015-4653-y.
39. Shi, Y.; Chen, C.; Yu, S.; Liu, Q.; Rao, J.; Zhang, H.R.; Xiao, H.L.; Fu, T.W.; Long, H.; He, Z., et al. MiR-663 suppresses oncogenic function of CXCR4 in glioblastoma. *Clin Cancer Res.* 2015, 21, 4004–4013. doi:10.1158/1078-0432.CCR-14-2807.
40. Jiao, L.; Deng, Z.; Xu, C.; Yu, Y.; Li, Y.; Yang, C.; Chen, J.; Liu, Z.; Huang, G.; Li, L.C.; et al. MiR-663 induces castration-resistant prostate cancer transformation and predicts clinical recurrence. *J. Cell Physiol.* 2014, 229, 834–844. doi:10.1002/jcp.24510.
41. Huang, C.; Sun, Y.; Ma, S.; Vadamotoo, A.S.; Wang, L.; Jin, C. Identification of circulating miR-663a as a potential biomarker for diagnosing osteosarcoma. *Pathol. Res. Pract.* 2019, 215, 152411. doi:10.1016/j.prp.2019.04.003.
42. Zhang, Y.; Xu, X.; Zhang, M.; Wang, X.; Bai, X.; Li, H.; Kan, L.; Zhou, Y.; Niu, H.; He, P. MicroRNA-663a is downregulated in non-small cell lung cancer and inhibits proliferation and invasion by targeting JunD. *BMC Cancer* 2016, 16, 315. doi: 10.1186/s12885-016-2350-x.
43. Huang, W.; Li, J.; Guo, X.; Zhao, Y.; Yuan, X. MiR-663a inhibits hepatocellular carcinoma cell proliferation and invasion by targeting HMGA2. *Biomed. Pharmacother.* 2016, 81, 431–438. doi: 10.1016/j.biopha.2016.04.034.
44. Zhang, C.; Chen, B.; Jiao, A.; Li, F.; Sun, N.; Zhang, G.; Zhang, J. MiR-663a inhibits tumor growth and invasion by regulating TGF- β 1 in hepatocellular carcinoma. *BMC Cancer* 2018, 18, 1179. doi:10.1186/s12885-018-5016-z.

Supplementary Data (Paper II)

Table S1: Sequences of the primers and probes used in the quantitative methylation-specific PCR experiments.

Primer Set		Sequence (5' – 3')	Product size, bp	T _{Annealing} °C
ACTB	F Primer	TGGTGATGGAGGAGGTTTAGTAAGT	133	60
	R Primer	AACCAATAAACCTACTCCTCCCTTAA		
	Probe	CY5 - ACCACCACCCAACACACAATAACAAACACA - MGB		
miR663a	F Primer	GGGATAGCGAGGTTAGGTC	101	60
	R Primer	CATTCGTAACGAATAAAACCC		
	Probe	VIC - CTCTCCTCGCCTACG - MGB		
VIM	F Primer	TTCGGGAGTTAGTTCGCGTT	108	60
	R Primer	ACCGCCGAACATCCTACGA		
	Probe	FAM - TCGTCGTTTAGGTTATCGT - MGB		

CHAPTER IV – Bladder Cancer

Mechanisms and Biology

Research Paper III

Paper III: Sirtuins' Deregulation in Bladder Cancer: SIRT7 is Implicated in Tumour Progression through Epithelial to Mesenchymal Transition Promotion

Cancers 2020, 12(5), 1066

DOI: 10.3390/cancers12051066

Sara Monteiro-Reis*, Ana Lameirinhas*, Vera Miranda-Gonçalves, Diana Felizardo, Paula C Dias, Jorge Oliveira, Inês Graça, Céline S Gonçalves, Bruno M Costa, Rui Henrique, Carmen Jerónimo

Author personal contribution:

Conceptual design and technical execution of the work, interpretation of the results and manuscript preparation.

Abstract

Sirtuins are emerging players in cancer biology and other age-related disorders, and their putative role in bladder cancer (BlCa) remains elusive. Further understanding of disease biology may allow for generation of more effective pathway-based biomarkers and targeted therapies. Herein, we aimed to illuminate the role of sirtuins' family in BlCa and evaluate their potential as disease biomarkers and therapeutic targets. *SIRT1-7* transcripts and protein levels were evaluated in a series of primary BlCa and normal bladder mucosa tissues. *SIRT7* knockdown was performed through lentiviral transduction in MGHU3, 5637 and J82 cells and its functional role was assessed. *SIRT1, 2, 4* and *5* expression levels were significantly lower in BlCa, whereas *SIRT6* and *7* were overexpressed, and these results were corroborated by TCGA cohort analysis. *SIRT7* transcript levels were significantly decreased in muscle-invasive vs. papillary BlCa. In vitro studies showed that *SIRT7* downregulation promoted cells migration and invasion. Accordingly, increased EMT markers expression and decreased E-Cadherin (*CDH1*) was observed in those BlCa cells. Moreover, increased EZH2 expression and H3K27^{me3} deposition in *CDH1* promoter was found in sh-*SIRT7* cells. We demonstrated that sirtuins are globally deregulated in BlCa, and specifically *SIRT7* downregulation is implicated in EMT, fostering BlCa invasiveness through *SIRT7*-EZH2-*CDH1* axis.

Introduction

Bladder cancer (BlCa) is the 9th most common cancer type worldwide, with an estimated 400,000 new cases and 160,000 deaths per year, in both genders [1]. Men are more susceptible and in more developed regions, BlCa represents has the 6th highest incidence among different cancers. BlCa may be categorized according to clinical, pathological, or molecular characteristics. Muscle-invasive bladder cancer (MIBC) which accounts for about 20% of all cases, represents the more aggressive form, being more likely to progress and metastasize, whereas non-muscle-invasive bladder cancer (NMIBC) is mostly characterized by multiple local recurrences, which, over time, also entail increased risk of invasion. Indeed, although most newly diagnosed patients present NMIBC (approximately 80%), there is variable risk of progression, with increased morbidity [2,3,4].

Sirtuins (SIRT) are a family of NAD⁺-dependent deacetylases highly conserved among all living organisms. Seven different SIRTs (SIRT1–7) are described in mammals, also known as Class III histone deacetylases (HDACs), which differing among each other in substrate specificity and catalytic activity [5]. Within the cell, these enzymes participate in control of important biological processes, including cell division, differentiation, metabolism, genomic stability, survival, senescence and organismal lifespan [6]. In addition, SIRT expression is deregulated in many cancer types [7,8,9]. *SIRT1* and *SIRT3* may be up- or downregulated

depending on the cancer type, acting either as oncogenes (e.g., colorectal or oral cancer) [10,11], or tumour suppressors (e.g., SIRT1 in BICa, SIRT1 and SIRT3 in breast and prostate cancer) [12,13]. *SIRT2* and *SIRT4*, on the other hand, are considered tumor suppressor, downregulated in glioma and hepatocellular carcinoma (*SIRT2*) [14,15], and bladder, gastric and lung cancer (*SIRT4*) [16], among others. Although little is known about the role of SIRT5 in neoplastic transformation, it is overexpressed in non-small-cell lung cancer (NSCLC) [17]. Concerning *SIRT6*, it is downregulated in several cancers, including hepatocellular carcinoma [18,19], but it is overexpressed in breast cancer and NSCLC [20,21]. Finally, an oncogenic function has been proposed for *SIRT7* as it was found overexpressed in several epithelial cancers [22,23]. Moreover, SIRT7 is mostly localized in the nucleus and its deacetylase function needs to be disclosed, with only a few well characterized substrates reported [24,25]. SIRT7 deacetylase activity is related with histones, disclosing highly selective activity for lysine 18 of histone H3 (H3K18Ac), notwithstanding other protein targets involved in cell homeostasis and stress response [24]. SIRT7 is also involved in ribosomes biogenesis and other mechanisms of cell proliferation [26,27].

Although sirtuins have been characterized in various neoplasms, their putative role in BICa development and progression remains elusive with only a few published studies to date [12,16,28]. Thus, we sought to comprehensively characterize SIRTs expression in BICa tissues, comparing with normal bladder mucosa, assessing their potential as prognostic biomarkers. Furthermore, the phenotypic impact of SIRT7 deregulation in BICa cells was also evaluated.

Results

Sirtuins Transcript Levels Characterization in Bladder Urothelial Carcinoma

Transcript levels of all sirtuins (*SIRT1-7*) were evaluated in 94 BICa samples (UCC) by RT-qPCR and compared with normal mucosa (controls). Statistically significant differences were disclosed for all sirtuins, except for SIRT3 (MW $p = 0.0612$; Figure 1A). Reduced *SIRT1*, 2, 4 and 5 expression levels were depicted in BICa (MW $p < 0.0001$ for all; Figure 1A), whereas *SIRT6* and *SIRT7* were overexpressed (MW $p < 0.0001$ for both; Figure 1B). In TCGA dataset, SIRTs expression in BICa compared to paired NB samples disclosed similar results, with a significant decrease of *SIRT1* and *SIRT3* expression (MW $p < 0.0001$ and $p = 0.0422$, respectively; Figure S1A), and significant increase in *SIRT6* and *SIRT7* expression in BICa tissues (MW $p < 0.0001$ for both; Figure S1B).

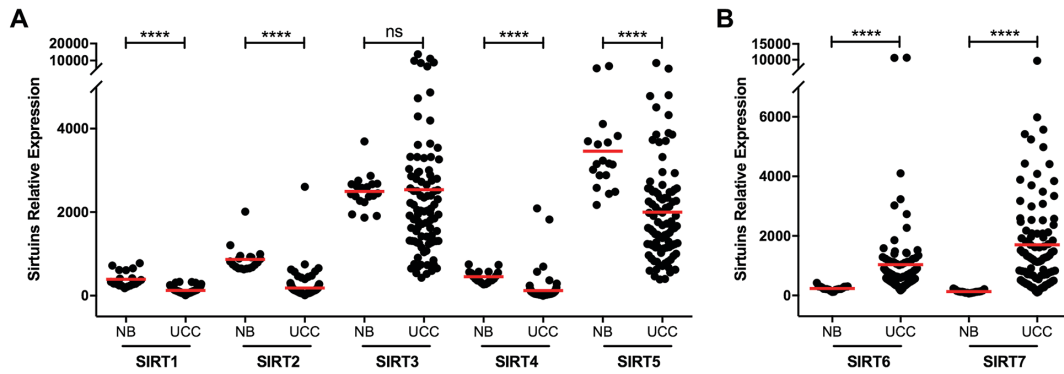


Figure 1. Sirtuin family transcript levels characterization in bladder urothelial carcinoma. Characterization of *SIRT1*, *SIRT2*, *SIRT3*, *SIRT4* and *SIRT5* (A), and *SIRT6* and *SIRT7* (B) in the bladder cancer and normal mucosae cohorts, by quantitative RT-PCR. **** $p < 0.0001$, ns - nonsignificant. UCC - urothelial cell carcinoma, NB - normal bladder mucosae.

SIRT7 Expression Is Decreased in Invasive and TCGA “Basal-Like” Urothelial Carcinoma

Characterization of SIRTs expression was then evaluated according to tumor subtype. Overall, lower transcript levels were observed in invasive high-grade carcinomas (IHG) comparing with papillary low-grade carcinomas (PLG) (Figure S2A), although statistical significance was only reached for *SIRT7* (KW $p < 0.0001$; Figure 2A). Additionally, significantly decreased *SIRT7* expression was also observed in IHG compared to papillary high-grade carcinomas (PHG) (Figure 2A). Contrarily, *SIRT4* expression levels were significantly higher in IHG compared to PLG (KW $p = 0.0012$; Figure S2A). The same analysis was also performed in a TCGA bladder urothelial cancer cohort and a similar SIRTs expression profile was found, with IHG showing significantly increased *SIRT4* expression levels comparing to PLG, whereas *SIRT5* and *SIRT6* expression levels were decreased (Figure S2B). Furthermore, in TCGA dataset, *SIRT7* expression was significantly lower in IHG compared to PHG and PLG (KW $p < 0.0001$ for both; Figure 2B), although no significant differences were disclosed between PLG and PHG.

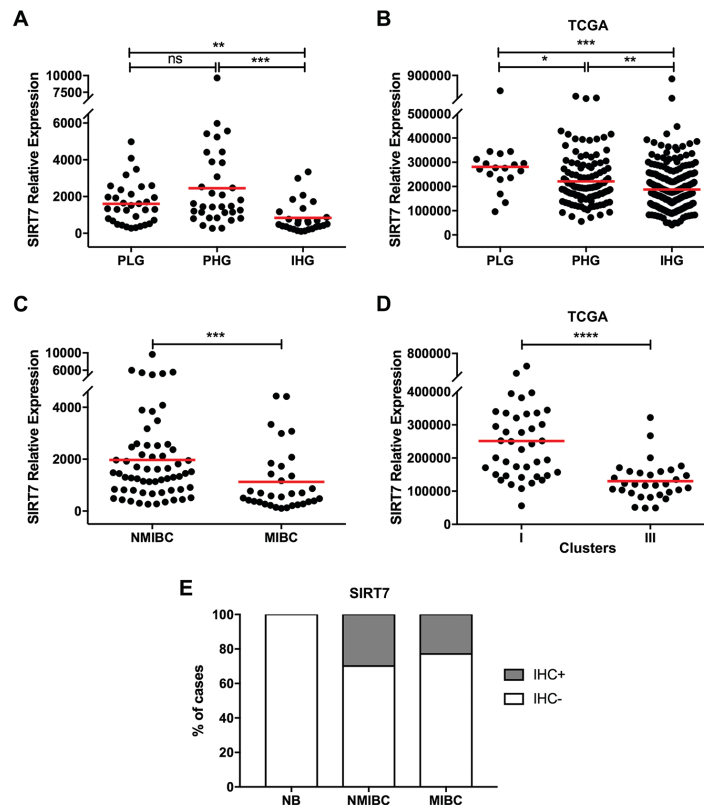


Figure 2. *SIRT7* expression downregulation in invasive and TCGA “basal-like” urothelial tumors. Characterization of *SIRT7* gene expression in the bladder cancer cohort (A) and TCGA cohort (B) categorized by clinical grade. Characterization of *SIRT7* gene expression in the bladder cancer cohort categorized by non-muscle invasive and muscle invasive bladder cancer (C). *SIRT7* gene expression according to TCGA molecular clusters analysis in the TCGA cohort (D). *SIRT7* immunohistochemistry results for the normal and tumour tissue samples cohort, categorized by non-muscle invasive and muscle invasive bladder cancer, regarding the calculated immunoscore (E). * p < 0.05, ** p < 0.01, *** p < 0.001 and **** p < 0.0001. PLG—papillary low-grade, PHG—papillary high-grade, IHG—invasive high-grade, NMIBC—non-muscle invasive bladder cancer, MIBC—muscle invasive bladder cancer.

Concerning pathological stage, two categories were considered: pTa-1/NMIBC (tumors confined to the bladder mucosa), and pT2-4/MIBC (tumors that invade the bladder muscular layer or beyond). In MIBC, *SIRT4* expression levels were significantly higher (MW p = 0.0009 s) and *SIRT7* levels were significantly lower (MW p = 0.0006; Figure 2C) comparing with NMIBC. In TCGA cohort, no statistically significant differences were disclosed, since only two cases are classified as NMIBC. Furthermore, in both IPO Porto’s and TGCA cohorts, no association was found between SIRTs expression levels and patients’ gender or age at diagnosis.

Since alterations in *SIRT7* altered expression were concordant in both cohorts, we further assessed the prognostic value of *SIRT7* expression. Of the 94 patients enrolled, four were

lost to follow-up. The median follow-up time of BICa patients was 72 months (range: 1–248 months). At the last follow-up time point, 44 patients were alive with no evidence of cancer, eight patients were alive with disease, 10 had died from other causes and 28 had deceased due to BICa. In IPO Porto's cohort, high tumour grade and pathological stage, as well as more advanced age at diagnosis, were significantly associated with shorter overall survival in multivariable Cox-regression model ($p = 0.031$, $p = 0.037$ and $p = 0.030$, respectively). Although *SIRT7* expression levels did not associate with patients' prognosis in IPO Porto's cohort, in TCGA dataset, cases with lower *SIRT7* expression (percentile 25) disclosed shorter overall survival, although only in univariable analysis ($p = 0.028$). Moreover, sirtuins' expression did not associate with disease-free survival, both considering the total cohort of patients and in patients without (NMIBC) or with (MIBC) invasive disease, separately. Furthermore, TCGA clusters for molecular markers signatures in BICa were also carried out. These clusters categorize samples using various known molecular characteristics. Cluster I subset consists of tumors with "papillary-like" morphology and higher expression of epithelial markers like E-cadherin (ECAD), whereas cluster III is characterized by low ECAD expression and high cytokeratins expression, consistent with a "basal-like" phenotype [29]. *SIRT7* expression was significantly lower in "basal-like" phenotype (cluster III) than in "papillary-like" phenotype (cluster I) (MW $p < 0.0001$, Figure 2D). Immunoexpression analysis showed that both normal urothelial and BICa cells expressed nuclear *SIRT7* (Figure S3). Although no significant correlation was found between *SIRT7* mRNA and protein levels, higher staining intensity and/or percentage of positive cells was observed in BICa compared to normal urothelium (Figure 2E). Furthermore, a slight reduction of *SIRT7* expression in MIBC was depicted (Figure 2E), paralleling *SIRT7* transcript level results.

SIRT7 Expression in Bladder Cancer Cell Lines

SIRT7 nuclear protein levels were evaluated in five BICa cell lines and one immortalized normal urothelial cell line (SV-HUC1), where MGHU3, J82 and 5637 cells displayed the highest *SIRT7* protein levels (Figure 3A). The lowest levels were found in the more aggressive cell line, namely TCCSUP cell line derived from a Grade IV carcinoma, whereas MGHU3 derived from a Grade I carcinoma, 5637 from a Grade II carcinoma, and J82 cell line originated from a Grade III carcinoma.

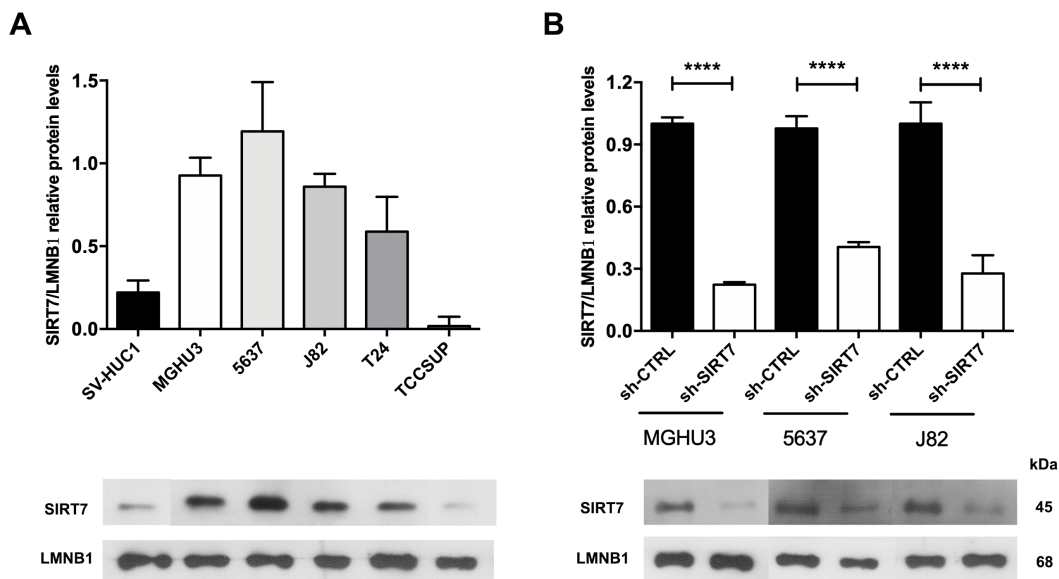


Figure 3. SIRT7 expression in bladder cancer cell lines. Expression of SIRT7 nuclear protein (**A**) in bladder cancer cell lines by Western blot; results are representative of three independent experiments with mean \pm SD. Confirmation of SIRT7 knockdown in MGHU3, 5637 and J82 cell lines at nuclear protein level (**B**) by Western blot; **** $p < 0.0001$, results are representative of three independent experiments with mean \pm SD.

Because these three cell lines disclosed the highest SIRT7 nuclear protein expression, they were chosen for lentiviral downregulation experiments. Before transfection, SIRT7 nuclear localization was confirmed by immunofluorescence for the three selected cell lines (Figure S4). Furthermore, after lentiviral transfection, a significant reduction was achieved for the three cell lines (MW $p < 0.0001$; Figure 3B), and reduced SIRT7 nuclear expression was confirmed by immunofluorescence in sh-SIRT7 cells compared to sh-scramble/CTRL cells.

SIRT7 Downregulation Promotes Invasiveness and EMT in Bladder Cancer Cells

Although no significant alterations in cell proliferation (Figure 4A) and apoptosis (Figure 4B) were found in sh-SIRT7 vs. sh-scramble/CTRL MGHU3 and J82 cells, 5637 sh-SIRT7 displayed a higher proliferation rate (especially at the 48 h time-point), and reduced apoptosis levels ($p < 0.001$ and $p < 0.01$, respectively). Moreover, a significant increase in cell migration was observed at all time points in MGHU3, 5637 and J82 sh-SIRT7 cells (Figure 4C), and the same was depicted for cell invasion (Figure 4D).

Moreover, sh-SIRT7 cells disclosed E-cadherin (or ECAD, an epithelial marker) decreased expression compared to wild type cell lines that expressed this protein (MGHU3 and 5637), whereas significantly increased N-cadherin (or NCAD, mesenchymal marker) protein levels

were found in all tested cell lines. Moreover, these results were corroborated by immunofluorescence analysis for the same markers in the same cell lines (Figure S5). Furthermore, EMT transcription factors, SLUG and SNAIL, paralleled the same expression pattern as ECAD in the same cell lines (Figure 4E).

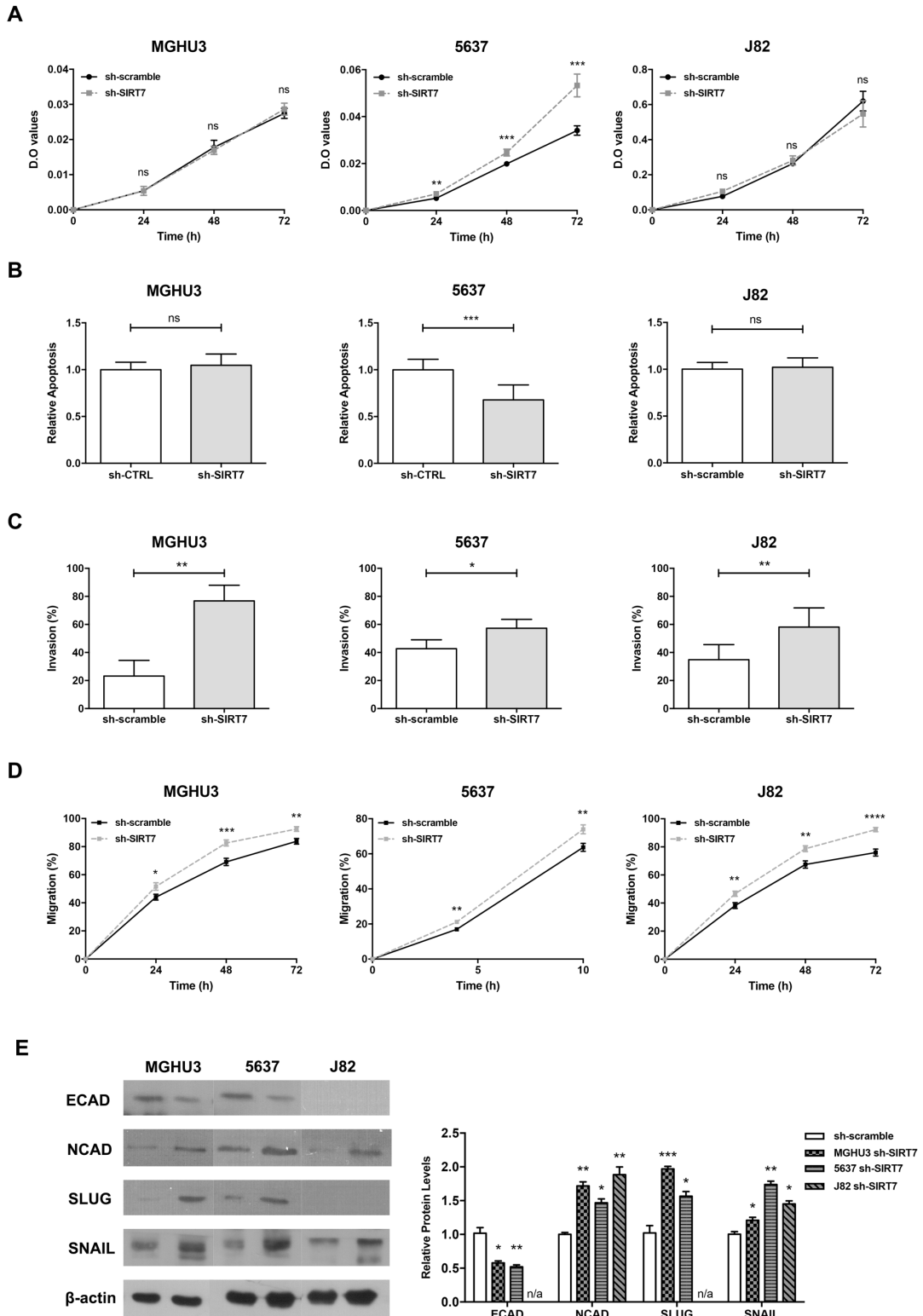


Figure 4. SIRT7 downregulation promotes invasiveness and EMT in bladder cancer cells. Effect of SIRT7 knockdown for MGHU3, 5637 and J82 cell lines at **(A)** cell viability by MTT assay, **(B)** apoptosis- cell death by APOPercentage assay, **(C)** cell invasion by BD Biocoat Matrigel Invasion Chambers and **(D)** cell migration by wound-healing assay; * $p < 0.05$, ** $p < 0.01$, *** $p < 0.001$ and **** $p < 0.0001$; results are representative of three independent experiments with mean \pm SD, each of

them in triplicates. Expression of epithelial and mesenchymal markers and EMT transcription factors (E) in MGHU3, 5637 and J82 SIRT7 knockdown by western blot; results are representative of three independent experiments with mean \pm SD.

SIRT7 Downregulation Associates with E-Cadherin Repression Mediated by Histone Methyltransferase EZH2

Because a global increase in both invasion and migration were found in sh-SIRT7 cell lines, with a concomitant decrease of the epithelial marker and key EMT player ECAD (*CDH1* gene), we further investigated the expression of *CDH1* in tissue samples from IPO Porto's cohort. Indeed, MIBC showed decreased *CDH1* transcript levels and *CDH2* upregulation (MW $p < 0.0001$ and $p = 0.0011$, respectively; Figure S6). Moreover, *SIRT7* and *CDH1* transcript levels positively correlated ($r = 0.58$, 95% CI 0.422 to 0.704, $p < 0.0001$) whereas *SIRT7* and *CDH2* transcript levels negatively correlated ($r = -0.22$, 95% CI -0.403 to -0.00187 , $p < 0.05$) in MIBC patients.

As *CDH1*, which is transcriptionally regulated by EZH2 [a SIRT7 substrate [30]], was found decreased in MIBC cases, and taking into account the previous results in SIRT7 modulated cell lines (Figure 4), we decided to explore the interplay between SIRT7, EZH2 and *CDH1*/ECAD. Indeed, *EZH2* transcript levels were significantly higher in BICa tissues compared to NB samples (MW $p < 0.0001$, Figure 5A). Furthermore, MIBC depicted the highest *EZH2* transcript levels (MW $p = 0.0444$, Figure 5B), and an inverse expression pattern was depicted for *SIRT7* and *EZH2* transcripts in MIBC (Figure S7). Moreover, EZH2 protein levels were significantly increased in sh-SIRT7 5637 cells (chosen because it showed differences in all phenotypic assays), compared to sh-CTRL cells (MW $p < 0.01$, Figure 5C).

Additionally, since EZH2 represses several genes, including *CDH1*, through its histone methyltransferase activity, especially by histone 3 lysine 27 tri-methylation ($H3K27^{me3}$) deposition within the respective promoters, PLA, co-immunoprecipitation (co-IP) and ChIP assays were performed. Firstly, PLA assay showed that EZH2 and SIRT7 physically interact in sh-CTRL 5637 cells ($p < 0.0001$; Figure 5D), and that sh-SIRT7 cells showed more $H3K27^{me3}$ mark ($p < 0.001$; Figure 5D). Next, a co-IP with an acetylated-lysine antibody disclosed higher acetylated EZH2 in sh-SIRT7 cells, comparatively to sh-CTRL cells (Figure 5E). Lastly, a ChIP assay was performed to assess the deposition of $H3K27^{me3}$ mark at *CDH1* promoter region in all transfected cell lines. As expected, increased $H3K27^{me3}$ was observed across the *CDH1* promoter in sh-SIRT7 cells, with a significant increase in both MGHU3 and J82 cells (2-way ANOVA $p = 0.01$; Figure 5F), suggesting that *CDH1* repression associated with SIRT7 downregulation occurs through EZH2 overexpression.

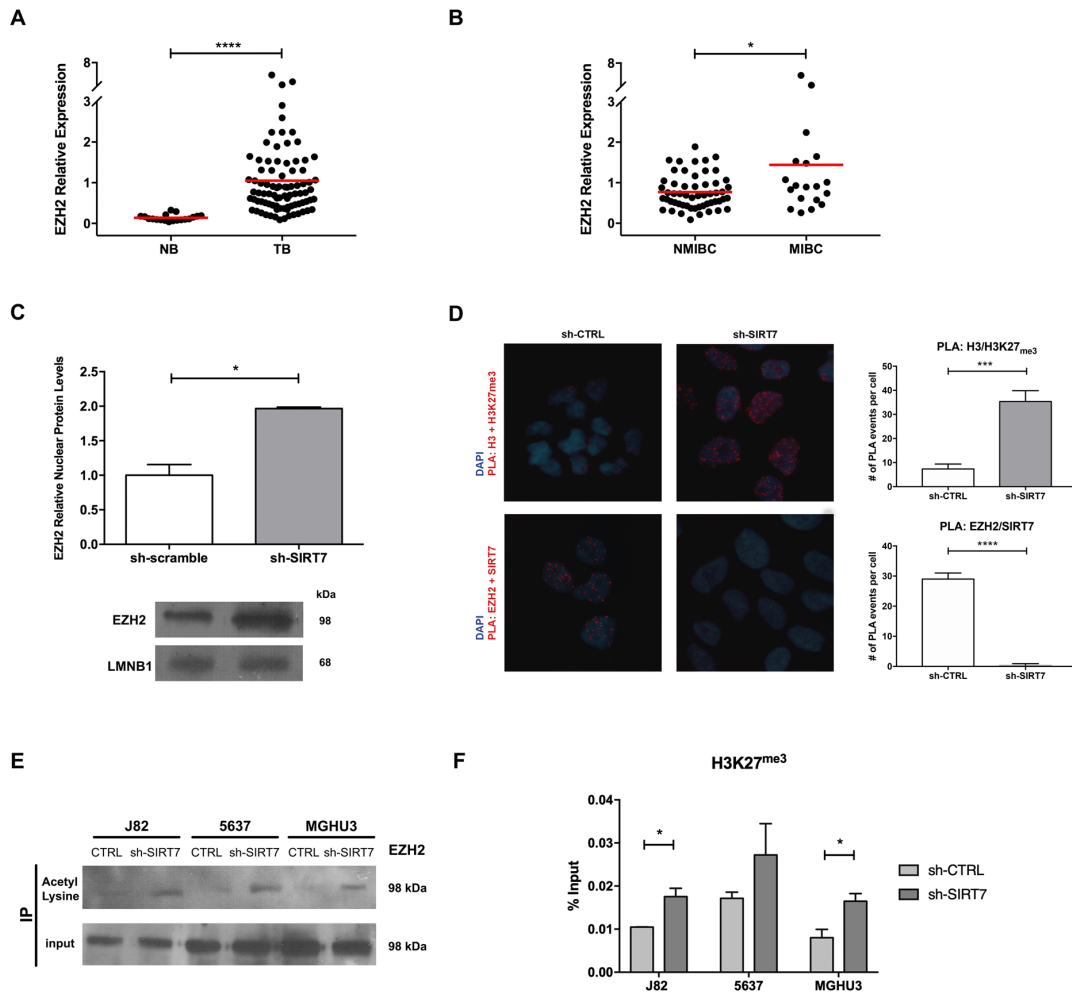


Figure 5. SIRT7 downregulation associates with E-Cadherin repression mediated by histone methyltransferase EZH2. Characterization of *EZH2* gene expression in the bladder cancer and normal mucosae cohort (**A**), and in non-muscle invasive and muscle-invasive bladder cancer cases (**B**), by quantitative RT-qPCR. Characterization of EZH2 protein expression (**C**) in 5637 sh-CTRL and sh-SIRT7 cells, by western blot analysis. Proximity Ligation Assay for assessment of interaction of Histone 3 with Histone 3 lysine 27 tri-methylation (H3K27^{me3}) and EZH2 with SIRT7, in 5637 sh-scramble and sh-SIRT7 cells (100× magnification) (**D**). Western blot analysis for EZH2 protein, after co-immunoprecipitation assay with acetyl-lysine antibody in J82, 5637 and MGHU3 sh-scramble/CTRL and sh-SIRT7 cells (**E**). Chromatin immunoprecipitation results for H3K27^{me3} deposition across the *CDH1* gene promoter, in MGHU3, 5637 and J82 sh-scramble/CTRL and sh-SIRT7 cells (**F**). * $p < 0.05$, *** $p < 0.001$ and **** $p < 0.0001$.

Discussion

Sirtuins, also known as Class III HDACs, are involved in many biological processes, including cell division, differentiation, metabolism, genomic stability, survival, senescence and organismal lifespan [6], and variable SIRT deregulated expression has been reported in many cancer types [7-9]. Remarkably, sirtuins may act either as oncogenes or tumour suppressor genes in different tumour models [12-16]. Thus, better understanding of the biological role of these unique enzymes in tumorigenesis might provide novel biomarkers for disease management as well as putative therapeutic targets.

Herein, we report, for the first time, a comprehensive evaluation of sirtuins (*SIRT1-7*) mRNA expression in a series of 94 BICa cases from a single institution and respective validation in TCGA dataset, comparing with normal bladder mucosa. Significant differences were depicted for all sirtuins, except for *SIRT3*, with *SIRT1*, *2*, *4* and *5* downregulation and *SIRT6* and *7* overexpression. These findings were mostly validated in TCGA dataset, especially for *SIRT6* and *SIRT7*. Previous studies on BICa have mainly focused on *SIRT1* and *SIRT4* and were mostly based in publicly available datasets only [12,16], not providing a global picture of sirtuin deregulation in BICa. Interestingly, besides significant differences between BICa and urothelium, differential expression of some sirtuins was also disclosed between tumors with dissimilar clinical and biological behaviour. Interestingly, although *SIRT7* was overexpressed in BICa, the more aggressive tumors (IHG) disclosed significantly lower expression levels compared to PLG and PHG, both in IPO Porto's and TCGA cohorts. Furthermore, in MIBC both *SIRT7* transcript and protein disclosed a significant reduction compared to NMIBC. Remarkably, previous reports on *SIRT7* in uterus, colon, kidney, ovary and prostate cancers revealed increased expression levels [22,24]. Nevertheless, in all those models, a strict oncogenic role was proposed for *SIRT7*, whereas our findings suggest that, at the least in bladder carcinogenesis, *SIRT7* may play a dual role, eventually context-dependent. Furthermore, although we did not find significant differences in *SIRT6* transcript levels between PHG and IHG tumors (either in our and TCGA cohort), nor between different stages of MIBC, Wu et al. reported that *SIRT6* protein levels declined significantly from T2 to T4 MIBC, which also suggests that the functional importance of sirtuins may change along cancer progression [28]. The observed decreased overall survival in BICa patients with lower *SIRT7* expression in TCGA cohort (eventually associated with higher grade and stage, as well as molecular BICa subtype) further suggests that decreased *SIRT7* impacts on neoplastic cell biology, promoting a more aggressive phenotype.

Taking in consideration *SIRT7* expression patterns in normal and neoplastic urothelium, we sought to characterize the effects of its deregulated expression at molecular level. Thus, after characterization of *SIRT7* transcript and protein expression levels in neoplastic and

benign urothelial cell lines, three cell lines were chosen for further experiments as their profile more closely replicated that of a spectrum of BICa tissues. Interestingly, in vitro phenotypic assays demonstrated that although SIRT7 downregulation did not affect cell proliferation or apoptosis, with the exception of 5637 cell line, rather impairing cell motility, decreasing both cell migration and cell invasion capabilities in all modulated cell lines. These effects immediately suggested a putative association between SIRT7 and EMT, a process that is key for tumour invasion and metastization [31,32]. This hypothesis was confirmed as *SIRT7* knockdown significantly associated with decreased E-Cadherin expression and augmented expression of a mesenchymal marker (N-Cadherin), and EMT-inducing transcription factors (SLUG and SNAIL), in the modulated BICa cells. Although only a few studies investigated the relationship between sirtuins and EMT [33], SIRT7 depletion in PC3 prostate cancer cell line was shown to impair migration and invasiveness, reprogramming neoplastic cells towards epithelial gene expression [22]. Our results indicate the opposite trend in BICa cells, which might be due to the pleiotropic effects of sirtuins and/or the dissimilar molecular profile of prostate and urothelial cancer cells [34].

Remarkably, we found that the mechanism by which SIRT7 affects *CDH1* expression, and thus EMT, is probably linked to EZH2. EZH2 is a well-known member of the Polycomb repressive complex 2 (PRC2), described as being involved in the transcription repression by catalysing the repressive H3K27^{me3} mark at several gene promoters, including *CDH1* [35,36,37]. Previously, proteomic analyses demonstrated that among 250 candidate substrates, EZH2 was a SIRT7 substrate [30,38]. In our study, sh-SIRT7 cells showed increased total and acetylated EZH2 expression, followed by decreased ECAD protein. Concurrently, increased H3K27^{me3} deposition at *CDH1* promoter was also observed in the same cells. Thus, when SIRT7 is downregulated, EZH2 activity might be enhanced by acetylation, contributing to *CDH1* transcription repression through H3K27^{me3} deposition in its promoter, as previously reported [30]. *CDH1* repression and concomitant EMT transcription factors' upregulation (e.g., SNAIL and SLUG), might then lead to a shift from epithelial to mesenchymal phenotype, allowing for increased cancer cell motility. Indeed, upregulation of these specific EMT transcription factors, due to diverse upstream signals and post-transcriptional mechanisms, also corroborates our hypothetical mechanism. Indeed, both SNAIL and SLUG were shown to cooperate with PRC2, and specifically with EZH2, towards controlling the expression of several genes, relevant for neural crest development, including *CDH1* [39,40]. Moreover, during EMT, Snail was proven to recruit EZH2 to specific genomic sites by the enrolment of the long non-coding RNA HOTAIR [41]. Thus, our results suggest that EMT transcription factors' upregulation in sh-SIRT7 BICa cells might be due to the phenotypic shift in invasion and migration and, at the molecular level, by recruitment of EZH2 to specific targets.

Thus far, only a limited number of upstream *SIRT7* transcription regulators, such as histone deacetylase 3 (HDAC3) and the X-box binding protein 1 (XBP1) molecules have been identified [42,43]. At post-transcriptional level, *SIRT7* was shown to be negatively regulated by microRNAs, such as those from microRNA-125 family [44]. However, few reports deal with *SIRT7* regulation by post-translational modifications [45,46,47]. Hence, it would be important to further explore how regulation of *SIRT7* occurs in BICa, and unveil how *SIRT7* expression shift occurs from non-invasive to invasive BICa.

Moreover, although discovery of new prognostic biomarkers for BICa is imperative for more effective disease management, the aim of our study was mostly to uncover how expression of all sirtuins was altered in BICa, and to investigate whether they might be implicated in bladder carcinogenesis and/or disease progression and invasiveness. Indeed, we were able to demonstrate that for *SIRT7*. Nonetheless, the analysed cohort was composed by patients diagnosed over a large time span (1991–2011) and the small number of events occurring in this cohort precluded a more robust and detailed statistical analysis.

Overall, our results suggest that increased *SIRT7* expression occurs during urothelium neoplastic transformation, which usually results in the formation of non-invasive, papillary neoplasms or flat lesions like urothelial carcinoma in situ [48]. At this stage, it is likely that *SIRT7* is involved in promoting cell growth and survival, which are key to neoplastic development, eventually through deacetylation of H3K18 [24]. Then, transition to an invasive phenotype might require *SIRT7* downregulation, involving EZH2 upregulation and acetylation, among other mechanisms, which promote EMT. Although the mechanism of *SIRT7* deregulation in BICa remains elusive, it is tempting to speculate whether it might be due to epigenetic mechanisms, which allow for the suggested plasticity of *SIRT7* gene expression during carcinogenesis and tumour progression.

Materials and Methods

Patients and Samples

Patients with primary bladder urothelial carcinoma (UCC), treated with transurethral resection (TUR) or radical cystectomy, between 1991 and 2011 at Portuguese Oncology Institute of Porto (IPO Porto), Portugal (n = 94). A set of 19 morphologically normal bladder mucosa (NB) tissue samples was obtained from BICa-free individuals (prostate cancer patients submitted to radical prostatectomy) and served as controls. All specimens were fresh-frozen at –80 °C and subsequently cut in a cryostat for confirmation of representativity and nucleic acid extraction. From each specimen, fragments were collected, formalin-fixed, and paraffin embedded for routine histopathological examination, including grading and pathological staging, by a dedicated uropathologist [49]. Relevant clinical data was

collected from clinical charts (Table 1). Patients and controls were enrolled after informed consent. This study was approved by the institutional review board (Comissão de Ética para a Saúde) of IPO Porto (CES103-14).

Table 1. Clinical and histopathological parameters of Bladder Cancer patients, and gender and age distribution of control set individuals.

Clinicopathological features	Bladder UCC	Normal Bladder Mucosae
Patients, n	94	19
Gender, n (%)		
Males	78 (83)	19 (100)
Females	16 (17)	0
Median age, yrs (range)	69 (45-91)	63 (48-75)
Grade, n (%)		
Papillary, low-grade	33 (35)	n.a.
Papillary, high-grade	33 (35)	n.a.
Invasive, high-grade	28 (30)	n.a.
Pathological Stage, n (%)		
pTa/pT1 (NMIBC)	61 (65)	n.a.
pT2-4 (MIBC)	33 (35)	n.a.

(UCC – Urothelial Cell Carcinoma; yrs – years; NMIBC – non-muscle invasive bladder cancer; MIBC - muscle invasive bladder cancer)

Real-Time Quantitative PCR (RT-qPCR)

RNA was extracted from tissues and from MGHU3, 5637 and J82 sh-scramble and sh-SIRT7 cells using TRIzol® (Invitrogen, Carlsbad, CA, USA), according to manufacturer's instructions. For tissue RNA, cDNA synthesis was performed using the High Capacity cDNA Reverse Transcription Kit (Applied Biosystems®, Foster City, CA, USA), according to manufacturer's instructions. Sirtuins transcript levels were quantified by RT-qPCR. Expression levels were evaluated using 4.5µL of diluted cDNA, 5µL of TaqMan® Universal PCR Master Mix No AmpErase® UNG (Applied Biosystems®) and 0.5µL of TaqMan® Gene Expression Assay, specific for each sirtuin and reference genes, as described in Table S1 (Applied Biosystems®). Each sample was run in triplicate and the RT-qPCR conditions were: 2min at 50°C, followed by enzyme activation for 10min at 95°C, and 45 cycles which included a denaturation stage at 95°C for 15s and an extending stage at 60°C for 60s. *HPRT* and *SDHA* were both used as reference genes for normalization. Relative expression of target genes tested in each sample was determined as: [Gene Expression Level = (*Gene* Mean Quantity)/(*HPRT1* & *SDHA*) Mean Quantity) × 1000].

Concerning cell lines, 1000ng of RNA were reverse transcribed using RevertAid RT kit (Thermo Fisher Scientific Inc., Waltham, MA, USA), according to manufacturer's instructions. For 100ng of cDNA, *SIRT7* and *CDH2* transcript levels were quantified using

TaqMan® Gene Expression Assay, as described above, in 396 well plates LightCycler480II (Roche, Basel, Switzerland). For *CDH1* and *EZH2* genes, transcription levels were also evaluated in J82 sh-scramble and sh-SIRT7 cells in 396 well plates LightCycler480II (Roche) using Xpert Fast SYBER Mastermix Blue (GRiSP Research Solutions, Porto, Portugal) with specific primers (S2). Transcript levels for studied genes were then evaluated using $\Delta\Delta C_t$ method, with *HPRT* and *BGUS* housekeeping genes as reference genes.

Immunohistochemistry

Immunohistochemistry was performed using the Novolink™ Max Polymer Detection System (Leica Biosystems, Wetzlar, Germany]. Three- μ m thick tissues sections from formalin-fixed and paraffin-embedded BICa (corresponding to 88 of the 94 cases, for which there was archived tissue available) and controls (n = 25, consisting of normal urothelial mucosa collected from the urether of nephrectomy specimens with renal cell tumors) were cut, deparaffinized and rehydrated. Antigen retrieval was accomplished by microwaving the specimens at 800W for 20min in 10mM sodium citrate buffer, pH=6. Endogenous peroxidase activity was blocked by incubating the sections in 0.6% hydrogen peroxide solution for 20min. Primary monoclonal antibody for SIRT7 (HPA053669, Sigma-Aldrich™, St. Louis, MO, USA) was used in 1:500 dilution, and incubated at room-temperature (RT) for one hour. Then, 3,3'-diaminobenzidine (Sigma-Aldrich™) was used as chromogen for visualization and slides were mounted with Entellan® (Merck-Millipore, Burlington, MA, USA). Normal testicular tissue, showing intense SIRT7 immunoreactivity was used as positive control. SIRT7 immunoexpression was evaluated by a dedicated uropathologist and cases were classified using a semi-quantitative scale for both staining intensity (0—no staining; 1—intensity lower than normal urothelium; 2—intensity equal to normal urothelium; 3—intensity higher than normal urothelium) and percentage of positive cells (0—< 10%; 1—10–33%; 2—33–67%; 3— > 67%), in each tumour. Staining intensity and percentage of positive cell results were then combined in a single score (Score S = staining intensity x percentage of positive cells) assigned to each tumour, and further stratified into low expression (S<4 = IHC-) and high expression (S \geq 4 = IHC+) groups, which correspond to cases with less than 33% stained cells or staining intensity lower than normal urothelium, and cases with at least 33% stained cells with an intensity equal to or higher than normal urothelium.

TCGA Dataset Analysis in Bladder Urothelial Carcinoma Patients

The Cancer Genome Atlas (TCGA) dataset was interrogated for data on *SIRT1-7* expression and clinical information, when available, of 408 BICa patients and 19 matched controls. All expression data from samples hybridized at the University of North Carolina,

Lineberger Comprehensive Cancer Center, using Illumina HiSeq 2000 RNA Sequencing version 2 analysis, were downloaded from the GDC data portal (<https://portal.gdc.cancer.gov/>). Biospecimen Core Resources (BCRs) provided the clinical data of each patient. This data is available for download through the GDC data portal (<https://portal.gdc.cancer.gov/>) (Table 2).

Table 2. Clinical and histopathological parameters of bladder cancer patients, and gender and age distribution of control set individuals from TCGA cohort.

Clinicopathological features	Bladder UCC	Matched Normal Bladder Mucosae
Patients, n	408	19
Gender, n (%)		
Males	301 (83)	10 (53)
Females	107 (17)	9 (47)
Median age, yrs (range)	69 (34-90)	71 (48-90)
Grade, n (%)		
Papillary, low-grade	18 (4)	n.a.
Papillary, high-grade	112 (28)	n.a.
Invasive, high-grade	278 (68)	n.a.
Pathological stage, n (%)		
pTa/pT1 (NMIBC)	2 (1)	n.a.
pT2-4 (MIBC)	406 (99)	n.a.

(UCC – Urothelial Cell Carcinoma; yrs – years; NMIBC – non-muscle invasive bladder cancer; MIBC - muscle invasive bladder cancer)

Cell Lines Culture

5637, J82, T24 and TCCSUP BICa cell lines and normal bladder cell line SV-HUC1 were selected for this study. All cell lines were purchased from ATCC and grown using recommended medium (Biochrom-Merck, Berlin, Germany) supplemented with 10% fetal bovine serum (FBS, Biochrom) and 1% penicillin/streptomycin (GIBCO, Invitrogen) at 37°C and 5% CO₂. Mycoplasma test was regularly performed for all cell lines using TaKaRa PCR Mycoplasma Detection Set (Clontech Laboratories, Mountain View, CA, USA).

Lentiviral Transduction

SIRT7 knockdown was performed through lentiviral transduction in J82 cell line using GIPZ™ Lentiviral shRNA particles (Dharmacon™, Lafayette, CO, USA), and in MGHU3 and 5637 cell lines using SMARTvector™ Inducible Lentiviral shRNA particles (target sequence: 5'-CCCTGCGTGCTGGTGAAGA-3'). All sh-SIRT7 vectors included the green fluorescent protein (GFP). Briefly, cells were seeded in 12 well/plate at density of 4×10⁴ cells/well and incubated during 24h in humidified chamber at 37°C and 5% CO₂. Then,

culture medium was removed and 500 μ L of completed medium with 8 μ g/mL polybrene and lentiviral sh-SIRT7 particles with MOI 10 concentration were added. After 48h, 1 μ g/mL of puromycin dihydrochloride (Clontech Laboratories) was added to select stably transfected cells. For MGHU3 and 5637 cells, after puromycin selection, a treatment was performed with 100 ng/mL doxycycline in order to induce the Tet-On 3 G bipartite induction system. Additionally, J82, MGHU3 and 5637 control cells were generated using a non-target scramble shRNA under the same previously described conditions.

For clone selection, 10, 20 and 50 cells/well were seeded in 96 well plate after stable selection, and the isolated clones were grown until confluence for protein extraction, and subsequent western blot analysis for SIRT7 expression. Moreover, sh-SIRT7 cells were observed under the fluorescence microscope for GFP expression.

Protein Extraction

BICa cell lines, sh-scramble/CTRL and sh-SIRT7 cells were grown until 80% confluence and homogenized in Kinexus lysis buffer supplemented with proteases inhibitors cocktail. Then, cells were sonicated for 5 cycles of 30s ON and 30s OFF (Bioruptor®, Diagenode, Liège, Belgium). After centrifugation, the supernatant was collected, and total protein was quantified according the Pierce BCA Protein Assay Kit (Thermo Fisher Scientific Inc.), according to the manufacture procedure.

For subcellular fractionation, Nuclear Extract kit (Active Motif, Carlsbad, CA, USA) was used. Briefly, bladder cancer cell lines, sh-scramble/CTRL and sh-SIRT7 cells were washed in 1 X PBS with phosphate inhibitors and scrapped. Subsequently, cells were suspended in hypotonic buffer and incubated on ice during 15min. Additionally, a detergent was added, and samples were centrifuged at 14,000rpm during 30s at 4°C. Supernatant (cytoplasmic fraction) was collected and stored at -80°C until use. Then, cell pellets were resuspended and incubated in a complete lysis buffer solution (lysis buffer with proteases inhibitor cocktail and 10mM DTT), following centrifugation and supernatant (nuclear fraction) collection and storage at -80°C. Nuclear and cytoplasmic proteins were then quantified using the Pierce BCA Protein Assay Kit (Thermo Fisher Scientific Inc.), according to manufacture procedure.

Western Blot and Co-Immunoprecipitation

Aliquots of 30 μ g total protein was separated in 10% polyacrylamide gel by SDS-PAGE and transferred onto an immunoblot PVDF membrane (Bio-Rad Laboratories, Hercules, CA, USA) in a 25mM Tris-base/glycine buffer using a Trans-Blot Turbo Transfer system (Bio-Rad Laboratories). Membranes were blocked with 5% milk in TBS/0.1% Tween (TBS/T pH=7.6) for 1 hour at RT. After incubation with primary antibodies for SIRT7 (1:350, HPA053669, Sigma-Aldrich) or EZH2 (1:500, NCL-L-EZH2, Leica Biosystems) for 1h30min

at RT, the membranes were washed in TBS/T and incubated with secondary antibody coupled with horseradish peroxidase for 1h at RT. The bound was visualized by chemiluminescence (Clarity WB ECL substrate, Bio-Rad) and quantification was performed using band densitometry analysis from the ImageJ software (version 1.6.1, National Institutes of Health). β -Actin (1:10,000, A1978, Sigma-Aldrich) for total protein and cytoplasmic protein analysis, and Laminin B1 (1:1000, D4Q42, Cell Signaling Technologies, Danvers, MA, USA) for nuclear protein, were used as loading controls. For co-immunoprecipitation assays, 200 μ g of total protein from cell lysates were incubated with anti-acetylated-lysine antibody (#9441, Cell Signaling Technology) and immunoprecipitated with Protein A/G magnetic beads (#16-663, Sigma-Aldrich) overnight at 4°C. The final eluates were blotted with EZH2 primary antibody, as detailed above. Detailed information about western blot can be found at Figure S8.

Immunofluorescence (IF)

Wild-type MGHU3, 5637 and J82, sh-scramble/CTRL and/or sh-SIRT7 cells were seeded on cover slips at 20,000 cells/well, overnight. Briefly, cells were fixed in methanol during 10min and then blocked with 5% bovine serum albumin (BSA) during 30min. After overnight SIRT7 (1:500, HPA053669, Sigma-Aldrich), ECAD (1:150, #3195, Cell Signaling Technology) and/or NCAD (1:50, #13116, Cell Signaling Technology) incubation at RT, cells were incubated with secondary antibody anti-rabbit IgG-TRITC (1:500, T6778, Sigma-Aldrich) during 1h at RT. Finally, after 1 \times PBS wash, cells were stained with 4',6-diamidino-2-phenylindole (DAPI) (AR1176, BOSTER Biological Technologies (Pleasanton, CA, USA) in mounting medium. Pictures were taken on a IX51 fluorescence microscope (Olympus, Tokyo, Japan) equipped with an Olympus XM10digital camera using CellSens software.

Chromatin Immunoprecipitation (ChIP)

Chromatin immunoprecipitation (ChIP) analysis was performed in sh-scramble/CTRL and sh-SIRT7 cells. For the crosslink step, formaldehyde solution (Sigma) was added to adherent cells ($\sim 1 \times 10^7$) media at 1% final concentration, and after an 8 minutes' incubation at RT, reaction was immediately stopped by adding 1.5mL of 2.5M glycine and incubating for 5min. Cells were then washed twice with ice-cold 1 \times PBS, scraped, harvested and centrifuged at 4°C.

Cell pellets were homogenized with cell lysis buffer (10 mM Tris-HCL pH7.5, 10 mM NaCl, 0.5% NP-40) and left on ice for 1h30, with intermittent vortexing, and then centrifuged at 4°C. At this point, pellets were re-suspended in nuclei lysis buffer (50 mM Tris-HCL pH=7.5, 10mM EDTA pH=8, 1% SDS) and incubated for 15 min on ice, followed by adding of 2 \times volumes of IP dilution buffer (16.7mM Tris-HCL pH7.5, 167 mM NaCl, 1.2 mM EDTA pH=8,

0.01% SDS). Chromatin was solubilized and sheared to 200–400 bp fragments using an ultra-sonicator (Bioruptor®, Diagenode) for 15 cycles of 30s ON and 30s OFF. Soluble chromatin was then centrifuged and stored at –80°C until further use.

Before immunoprecipitation (IP), each 50µL of chromatin was 1:10 diluted in dilution buffer (1.2 mM EDTA pH=8, 16.7 mM Tris pH=8, 167mM NaCl, 1.1% Triton X-100, 0.01% SDS), and 5 µL of this solution was reserved in a new tube for the input control. After this, 20µL of protein A+G magnetic beads (Millipore) were added to each IP sample, as well as ChIP-grade antibodies for Histone H3 (ab1791, Abcam, Cambridge, UK), tri-methylation of lysine 27 of histone H3 (H3K27^{me3}, 07-449, Millipore), positive control (RNA polymerase II) and negative control (mouse IgG), at assay dependent concentration. IPs were incubated overnight at 4°C with rotation. After incubation, magnetic beads were precipitated using 1.5mL tubes magnet rack and washed with four different salt concentration buffers. At this point, elution buffer (50mM Tris-HCL pH=7.5, 10mM EDTA pH=8, 1% SDS) was added to all samples and input control, as well as 200 µg/mL of RNase A, following an incubation of 30min at 37°C. After this, samples were incubated with proteinase K for 2h at 62°C, followed by an incubation of 10min at 95°C, for cross-link reversion.

DNA was extracted from samples using the Qiaquick gel extraction kit (Qiagen, Hilden, Germany), according to manufacture procedures, and stored at –20°C until further use. For qPCR, two pairs of primers for *CDH1* promoter were designed, both for ~325 bp before TSS (F—5'-TAACCCACCTAGACCCTAGCAA-3', R–5'-GCTGATTGGCTGAGGGTTCA-3') and for ~600 bp before TSS (F-5'-ACCTGTACTCCCAGCTACTAGA-3', R-5'-GATGGGGTCTCACTCTTTCACC-3'). RT-qPCR was performed as mentioned above, and the relative amount of promoter DNA was normalized using Input Percent method.

Proximity Ligation Assay (PLA)

Sh-scramble/CTRL and sh-SIRT7 cells, were seeded in 1 cm² coverslips and allowed to grow overnight. Then, cells were fixed in 4% formaldehyde (Sigma) for 10min and permeabilized in 0.5% Triton X-100 (Sigma), for 5min, at RT and gently stirred. PLA assay was performed using the commercial kit Duolink In Situ (OLINK Bioscience, Uppsala, Sweden), according to manufacturer's instructions. The antibodies used were Histone H3 (ab1791, Abcam, Cambridge, UK), tri-methylation of Lysine 27 of Histone H3 (H3K27^{me3}, 07-449, Millipore), SIRT7 (HPA053669, Sigma-Aldrich) and EZH2 (NCL-L-EZH2, Leica Biosystems). After the procedure, cells were stained with 4',6-diamidino-2-phenylindole (DAPI) (AR1176, BOSTER Biological Technology, Pleasanton, CA, USA) in mounting medium. Pictures were taken on an Olympus IX51 fluorescence microscope equipped with an Olympus XM10 digital camera using CellSens software.

Cell Viability Assay

To assess the role of SIRT7 in cell growth, 3-(4,5-dimethylthiazol-2-yl)-2,5-diphenyltetrazolium (MTT) assay (Sigma-Aldrich) was performed. Briefly, sh-scramble/CTRL and sh-SIRT7 cells were seeded at 3000 cell/well density, overnight, in 96 well plate. Then, 5 µg/mL MTT solution in completed MEM medium was incubated during 1h at 37°C for 0h, 24h, 48h and 72h. Then, formazan crystals formed were dissolved in dimethyl sulfoxide (DMSO) and spectrophotometric measurement was done at 540nm, using 655nm as a reference absorbance (Fluostar Omega, BMG Labtech, Offenburg, Germany). The optical density (OD) obtained for 24h, 48h and 72h was normalized for the 0h time point. At least three independent experiments were performed.

Apoptosis Assay

Apoptosis was assessed using the APOPercentage™ kit (Biocolor Ltd., Belfast, Northern Ireland, UK). This assay uses a dye that is integrated by cells undergoing at early stage of apoptosis due to phosphatidylserine transmembrane movements, which results in APOPercentage dye incorporation by cells. Briefly, sh-scramble/CTRL and sh-SIRT7 cells were seeded in 24 well plate at density of 25,000 cell/well and incubated during 72h in a humidified chamber at 37°C and 5% CO₂. At this time point, cells were incubated with 300 µL/well of APOPercentage dye solution at ratio 1:20 respectively, during 20min at 37°C. Then, cells were washed with PBS1 X and detached from well plate with Tryple™ Express (GBICO) during 10min at 37°C. After that, APOPercentage Dye Release reagent was added and plate were vigorously agitated during 15 min, following colorimetric measurement at 550nm with 620nm reference filter (Fluostar Omega). The H₂O₂ was used as a positive control. The OD obtained for apoptosis assay was normalized for the OD obtained by viability assay at the same time point. At least three independent experiments were performed.

Wound Healing Assay

Cells were seeded in 6 well plate at a density of 7.5×10^5 cell/well and allowed reach confluence at 37°C, 5% CO₂. Then, a “wound” was made by manual scratching with a 200 µL pipette tip and cells were gently washed with 1× PBS. The “wounded” areas were photographed in specific wound sites (two sites for each wound) at 40× magnification using an Olympus IX51 inverted microscope equipped with an Olympus XM10 Digital Camera System every 24h until wound closure. The relative migration distance (5 measures by wound) was calculated with the following formula: relative migration distance (%) = $(A-B)/C \times 100$, where A is the width of cell wound at 0 h incubation, B is the width of cell wound after specific h of incubation, and C is the width mean of cell wound for 0h of incubation. For

relative migration distance, the results were analysed using the beWound-Cell Migration Tool (Version 1.5) [50]. At least three independent experiments were performed.

Invasion Assay

Invasion capacity of sh-scramble/CTRL and sh-SIRT7 cells was evaluated using a 24 well BD Biocoat Matrigel Invasion Chambers (BD Biosciences, San Jose, CA, USA). After rehydration of BD Matrigel Chambers during 2h with MEM medium at 37°C, cells at a density of 25,000 cells/ insert were seeded and incubated during 24 h at 37°C in 5% CO₂. Then, the non-invading cells were removed by with swab and invaded cells were fixed with methanol and staining with DAPI. Invaded cells were counted on an Olympus IX51 fluorescence microscope equipped with an Olympus XM10 digital camera using CellSens software. The % invasion normalized for total of amount cell seeded in BD Matrigel Chamber.

Statistical Analysis

All statistical analyses were performed using IBM® SPSS® Statistic software version 23 (IBM-SPSS Inc., Chicago, IL, USA) and graphs were built using GraphPad Prim 7.0 (GraphPad Software Inc., La Jolla, CA, USA). Significance level was set at $p < 0.05$, and Bonferroni's correction was used when appropriate.

For both BICa cohorts (IPO's and TCGA), when applicable, Mann-Whitney U test (MW) was used to test for differences in sirtuins expression levels between NB and UCC tissue samples, pathological stages of cases divided in Ta-1 (NMIBC) and T2-4 (MIBC), and patients' gender, and to assess differences in sh-scramble versus sh-SIRT7 conditions. Kruskal-Wallis test (KW) was performed to test for differences among UCC subtypes (papillary-low grade, papillary-high grade and invasive-high grade). Spearman's rho was used to assess the correlation between SIRTs expression levels and age of the patients at diagnosis, and between *SIRT7* and *CDH1* or *CDH2* expression levels. Associations between clinical grade or pathological stage and immunoexpression results were assessed by chi-square or Fisher's exact test, and Somers'd directional measure was also computed. Disease-specific and disease-free survival curves (Kaplan-Meier with log rank test) were computed for standard variables (tumour stage and grade) and for categorized SIRTs transcript levels. Moreover, the same analyses were also performed separately for NMIBC and MIBC cases. A Cox-regression model comprising all significant variables (univariable and multivariable model) was computed to assess the relative contribution of each variable to the follow-up status.

Conclusions

In conclusion, this study provides a global view on sirtuin family expression deregulation in BICa. Specifically, *SIRT7* overexpression seems to play an important role in the first steps of urothelial carcinogenesis, whereas subsequent downregulation is associated with acquisition of an invasive and aggressive phenotype, through stimulation of EMT phenotype involving the *SIRT7*-*EZH2*-*CDH1* axis. Although further studies are required to clarify the mechanism underlying *SIRT7* deregulation in BICa, it might constitute an attractive target for innovative therapeutic strategies.

References

1. Torre, L.A.; Bray, F.; Siegel, R.L.; Ferlay, J.; Lortet-Tieulent, J.; Jemal, A. Global cancer statistics, 2012. *CA Cancer J. Clin.* 2015, 65, 87–108.
2. Sanli, O.; Dobruch, J.; Knowles, M.A.; Burger, M.; Alemozaffar, M.; Nielsen, M.E.; Lotan, Y. Bladder cancer. *Nat. Rev. Dis. Primers* 2017, 3, 17022.
3. Babjuk, M.; Bohle, A.; Burger, M.; Capoun, O.; Cohen, D.; Comperat, E.M.; Hernandez, V.; Kaasinen, E.; Palou, J.; Roupret, M.; et al. EAU Guidelines on Non-Muscle-invasive Urothelial Carcinoma of the Bladder: Update 2016. *Eur. Urol.* 2017, 71, 447–461.
4. Alfred Witjes, J.; Lebre, T.; Comperat, E.M.; Cowan, N.C.; De Santis, M.; Bruins, H.M.; Hernandez, V.; Espinos, E.L.; Dunn, J.; Rouanne, M.; et al. Updated 2016 EAU Guidelines on Muscle-invasive and Metastatic Bladder Cancer. *Eur. Urol.* 2017, 71, 462–475.
5. Carafa, V.; Rotili, D.; Forgione, M.; Cuomo, F.; Serretiello, E.; Hailu, G.S.; Jarho, E.; Lahtela-Kakkonen, M.; Mai, A.; Altucci, L. Sirtuin functions and modulation: From chemistry to the clinic. *Clin. Epigenetics* 2016, 8, 61
6. Vaquero, A. The conserved role of sirtuins in chromatin regulation. *Int. J. Dev. Biol.* 2009, 53, 303–322.
7. Bosch-Presegue, L.; Vaquero, A. The dual role of sirtuins in cancer. *Genes Cancer* 2011, 2, 648–662.
8. Martinez-Pastor, B.; Mostoslavsky, R. Sirtuins, metabolism, and cancer. *Front. Pharmacol.* 2012, 3, 22.
9. Chalkiadaki, A.; Guarente, L. The multifaceted functions of sirtuins in cancer. *Nat. Rev. Cancer* 2015, 15, 608–624.
10. Chen, X.; Sun, K.; Jiao, S.; Cai, N.; Zhao, X.; Zou, H.; Xie, Y.; Wang, Z.; Zhong, M.; Wei, L. High levels of *SIRT1* expression enhance tumorigenesis and associate with a poor prognosis of colorectal carcinoma patients. *Sci. Rep.* 2014, 4, 7481.
11. Alhazzazi, T.Y.; Kamarajan, P.; Joo, N.; Huang, J.Y.; Verdin, E.; D’Silva, N.J.; Kapila, Y.L. Sirtuin-3 (*SIRT3*), a novel potential therapeutic target for oral cancer. *Cancer* 2011, 117, 1670–1678.

12. Wang, R.H.; Sengupta, K.; Li, C.; Kim, H.S.; Cao, L.; Xiao, C.; Kim, S.; Xu, X.; Zheng, Y.; Chilton, B.; et al. Impaired DNA damage response, genome instability, and tumorigenesis in SIRT1 mutant mice. *Cancer Cell* 2008, 14, 312–323
13. Kim, H.S.; Patel, K.; Muldoon-Jacobs, K.; Bisht, K.S.; Aykin-Burns, N.; Pennington, J.D.; van der Meer, R.; Nguyen, P.; Savage, J.; Owens, K.M.; et al. SIRT3 is a mitochondria-localized tumor suppressor required for maintenance of mitochondrial integrity and metabolism during stress. *Cancer Cell* 2010, 17, 41–52.
14. Hiratsuka, M.; Inoue, T.; Toda, T.; Kimura, N.; Shirayoshi, Y.; Kamitani, H.; Watanabe, T.; Ohama, E.; Tahimic, C.G.; Kurimasa, A.; et al. Proteomics-based identification of differentially expressed genes in human gliomas: Down-regulation of SIRT2 gene. *Biochem. Biophys. Res. Commun.* 2003, 309, 558–566.
15. Kim, H.S.; Vassilopoulos, A.; Wang, R.H.; Lahusen, T.; Xiao, Z.; Xu, X.; Li, C.; Veenstra, T.D.; Li, B.; Yu, H.; et al. SIRT2 maintains genome integrity and suppresses tumorigenesis through regulating APC/C activity. *Cancer Cell* 2011, 20, 487–499.
16. Jeong, S.M.; Xiao, C.; Finley, L.W.; Lahusen, T.; Souza, A.L.; Pierce, K.; Li, Y.H.; Wang, X.; Laurent, G.; German, N.J.; et al. SIRT4 has tumor-suppressive activity and regulates the cellular metabolic response to DNA damage by inhibiting mitochondrial glutamine metabolism. *Cancer Cell* 2013, 23, 450–463.
17. Lu, W.; Zuo, Y.; Feng, Y.; Zhang, M. SIRT5 facilitates cancer cell growth and drug resistance in non-small cell lung cancer. *Tumour Biol.* 2014, 35, 10699–10705.
18. Sebastian, C.; Mostoslavsky, R. The role of mammalian sirtuins in cancer metabolism. *Semin. Cell Dev. Biol.* 2015, 43, 33–42.
19. Marquardt, J.U.; Fischer, K.; Baus, K.; Kashyap, A.; Ma, S.; Krupp, M.; Linke, M.; Teufel, A.; Zechner, U.; Strand, D.; et al. Sirtuin-6-dependent genetic and epigenetic alterations are associated with poor clinical outcome in hepatocellular carcinoma patients. *Hepatology* 2013, 58, 1054–1064.
20. Khongkow, M.; Olmos, Y.; Gong, C.; Gomes, A.R.; Monteiro, L.J.; Yague, E.; Cavaco, T.B.; Khongkow, P.; Man, E.P.; Laohasinnarong, S.; et al. SIRT6 modulates paclitaxel and epirubicin resistance and survival in breast cancer. *Carcinogenesis* 2013, 34, 1476–1486.
21. Bai, L.; Lin, G.; Sun, L.; Liu, Y.; Huang, X.; Cao, C.; Guo, Y.; Xie, C. Upregulation of SIRT6 predicts poor prognosis and promotes metastasis of non-small cell lung cancer via the ERK1/2/MMP9 pathway. *Oncotarget* 2016, 7, 40377–40386.
22. Malik, S.; Villanova, L.; Tanaka, S.; Aonuma, M.; Roy, N.; Berber, E.; Pollack, J.R.; Michishita-Kioi, E.; Chua, K.F. SIRT7 inactivation reverses metastatic phenotypes in epithelial and mesenchymal tumors. *Sci. Rep.* 2015, 5, 9841.
23. Bartosch, C.; Monteiro-Reis, S.; Almeida-Rios, D.; Vieira, R.; Castro, A.; Moutinho, M.; Rodrigues, M.; Graca, I.; Lopes, J.M.; Jeronimo, C. Assessing sirtuin expression in endometrial carcinoma and non-neoplastic endometrium. *Oncotarget* 2016, 7, 1144–1154.
24. Barber, M.F.; Michishita-Kioi, E.; Xi, Y.; Tasselli, L.; Kioi, M.; Moqtaderi, Z.; Tennen, R.I.; Paredes, S.; Young, N.L.; Chen, K.; et al. SIRT7 links H3K18 deacetylation to maintenance of oncogenic transformation. *Nature* 2012, 487, 114–118.

25. Paredes, S.; Villanova, L.; Chua, K.F. Molecular pathways: Emerging roles of mammalian Sirtuin SIRT7 in cancer. *Clin. Cancer Res.* 2014, 20, 1741–1746.
26. Ford, E.; Voit, R.; Liszt, G.; Magin, C.; Grummt, I.; Guarente, L. Mammalian Sir2 homolog SIRT7 is an activator of RNA polymerase I transcription. *Genes Dev.* 2006, 20, 1075–1080.
27. Chen, S.; Seiler, J.; Santiago-Reichert, M.; Felbel, K.; Grummt, I.; Voit, R. Repression of RNA polymerase I upon stress is caused by inhibition of RNA-dependent deacetylation of PAF53 by SIRT7. *Mol. Cell* 2013, 52, 303–313.
28. Wu, M.; Dickinson, S.I.; Wang, X.; Zhang, J. Expression and function of SIRT6 in muscle invasive urothelial carcinoma of the bladder. *Int. J. Clin. Exp. Pathol.* 2014, 7, 6504–6513.
29. Cancer Genome Atlas Research Network. Comprehensive molecular characterization of urothelial bladder carcinoma. *Nature* 2014, 507, 315–322.
30. Zhang, C.; Zhai, Z.; Tang, M.; Cheng, Z.; Li, T.; Wang, H.; Zhu, W.G. Quantitative proteome-based systematic identification of SIRT7 substrates. *Proteomics* 2017, 17.
31. Kalluri, R.; Weinberg, R.A. The basics of epithelial-mesenchymal transition. *J. Clin. Investig.* 2009, 119, 1420–1428.
32. Nieto, M.A.; Huang, R.Y.; Jackson, R.A.; Thiery, J.P. EMT: 2016. *Cell* 2016, 166, 21–45.
33. Palmirotta, R.; Cives, M.; Della-Morte, D.; Capuani, B.; Lauro, D.; Guadagni, F.; Silvestris, F. Sirtuins and Cancer: Role in the Epithelial-Mesenchymal Transition. *Oxidative Med. Cell. Longev.* 2016, 2016, 3031459.
34. Robertson, A.G.; Kim, J.; Al-Ahmadie, H.; Bellmunt, J.; Guo, G.; Cherniack, A.D.; Hinoue, T.; Laird, P.W.; Hoadley, K.A.; Akbani, R.; et al. Comprehensive Molecular Characterization of Muscle-Invasive Bladder Cancer. *Cell* 2017.
35. Nichol, J.N.; Dupere-Richer, D.; Ezponda, T.; Licht, J.D.; Miller, W.H., Jr. H3K27 Methylation: A Focal Point of Epigenetic Dereglulation in Cancer. *Adv. Cancer Res.* 2016, 131, 59–95.
36. Herranz, N.; Pasini, D.; Diaz, V.M.; Franci, C.; Gutierrez, A.; Dave, N.; Escriva, M.; Hernandez-Munoz, I.; Di Croce, L.; Helin, K.; et al. Polycomb complex 2 is required for E-cadherin repression by the Snail1 transcription factor. *Mol. Cell. Biol.* 2008, 28, 4772–4781.
37. Cho, H.M.; Jeon, H.S.; Lee, S.Y.; Jeong, K.J.; Park, S.Y.; Lee, H.Y.; Lee, J.U.; Kim, J.H.; Kwon, S.J.; Choi, E.; et al. microRNA-101 inhibits lung cancer invasion through the regulation of enhancer of zeste homolog 2. *Exp. Ther. Med.* 2011, 2, 963–967.
38. Gall Troselj, K.; Novak Kujundzic, R.; Ugarkovic, D. Polycomb repressive complex's evolutionary conserved function: The role of EZH2 status and cellular background. *Clin. Epigenetics* 2016, 8, 55.
39. Stemmler, M.P.; Eccles, R.L.; Brabletz, S.; Brabletz, T. Non-redundant functions of EMT transcription factors. *Nat. Cell Biol.* 2019, 21, 102–112.
40. Tien, C.L.; Jones, A.; Wang, H.; Gerigk, M.; Nozell, S.; Chang, C. Snail2/Slug cooperates with Polycomb repressive complex 2 (PRC2) to regulate neural crest development. *Development* 2015, 142, 722–731.
41. Battistelli, C.; Cicchini, C.; Santangelo, L.; Tramontano, A.; Grassi, L.; Gonzalez, F.J.; de Nonno, V.; Grassi, G.; Amicone, L.; Tripodi, M. The Snail repressor recruits EZH2 to specific genomic sites

through the enrolment of the lncRNA HOTAIR in epithelial-to-mesenchymal transition. *Oncogene* 2017, 36, 942–955.

42. Liu, G.F.; Lu, J.Y.; Zhang, Y.J.; Zhang, L.X.; Lu, G.D.; Xie, Z.J.; Cheng, M.; Shen, Y.; Zhang, Y. C/EBPalpha negatively regulates SIRT7 expression via recruiting HDAC3 to the upstream-promoter of hepatocellular carcinoma cells. *Biochim. Biophys. Acta* 2016, 1859, 348–354.

43. Shin, J.; He, M.; Liu, Y.; Paredes, S.; Villanova, L.; Brown, K.; Qiu, X.; Nabavi, N.; Mohrin, M.; Wojnoonski, K.; et al. SIRT7 represses Myc activity to suppress ER stress and prevent fatty liver disease. *Cell Rep.* 2013, 5, 654–665.

44. Kim, J.K.; Noh, J.H.; Jung, K.H.; Eun, J.W.; Bae, H.J.; Kim, M.G.; Chang, Y.G.; Shen, Q.; Park, W.S.; Lee, J.Y.; et al. Sirtuin7 oncogenic potential in human hepatocellular carcinoma and its regulation by the tumor suppressors MiR-125a-5p and MiR-125b. *Hepatology* 2013, 57, 1055–1067.

45. Grob, A.; Roussel, P.; Wright, J.E.; McStay, B.; Hernandez-Verdun, D.; Sirri, V. Involvement of SIRT7 in resumption of rDNA transcription at the exit from mitosis. *J. Cell Sci.* 2009, 122, 489–498.

46. Sun, L.; Fan, G.; Shan, P.; Qiu, X.; Dong, S.; Liao, L.; Yu, C.; Wang, T.; Gu, X.; Li, Q.; et al. Regulation of energy homeostasis by the ubiquitin-independent REGy proteasome. *Nat. Commun.* 2016, 7, 12497.

47. Jiang, L.; Xiong, J.; Zhan, J.; Yuan, F.; Tang, M.; Zhang, C.; Cao, J.; Chen, Y.; Lu, X.; Li, Y.; et al. Ubiquitin-specific peptidase 7 (USP7)-mediated deubiquitination of the histone deacetylase SIRT7 regulates gluconeogenesis. *J. Biol. Chem.* 2017, 292, 13296–13311.

48. Solomon, J.P.; Hansel, D.E. The Emerging Molecular Landscape of Urothelial Carcinoma. *Surg. Pathol. Clin.* 2016, 9, 391–404.

49. Edge, S.B.; Compton, C.C. The American Joint Committee on Cancer: The 7th edition of the AJCC cancer staging manual and the future of TNM. *Ann. Surg. Oncol.* 2010, 17, 1471–1474.

50. Moreira, A.H.J.; Queirós, S.; Vilaça, J.L. Biomedical Engineering Solutions Research Group, Life and Health Sciences Research Institute, University of Minho. Available online: <http://www.besurg.com/sites/default/files/beWoundApp.zip> (accessed on 21 April 2020).

Supplementary Data (Paper III)

Supplementary Tables

Supplementary Table 1. Reference of TaqMan® gene expression assays for studied genes.

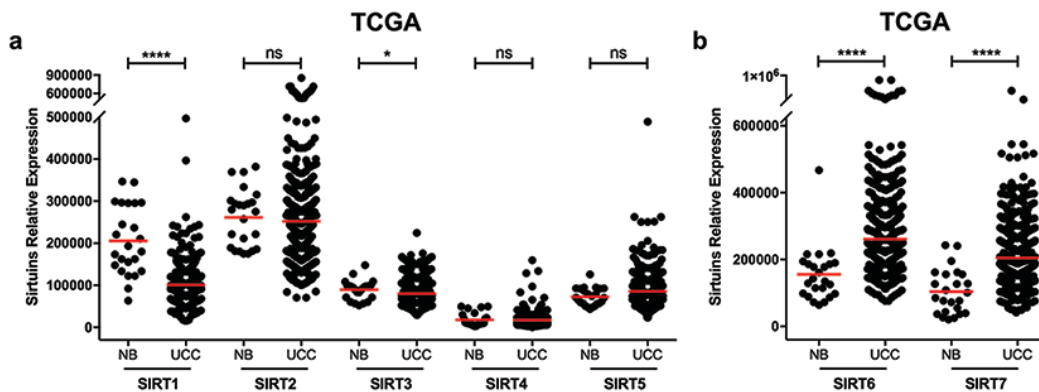
Gene	Reference ID
<i>HPRT1</i>	Hs01003267_m1
<i>CDH2</i>	Hs00354986_m1
<i>SDHA</i>	Hs00417200_m1
<i>SIRT1</i>	Hs01009005_m1

<i>SIRT2</i>	Hs00247263_m1
<i>SIRT3</i>	Hs00202030_m1
<i>SIRT4</i>	Hs00202033_m1
<i>SIRT5</i>	Hs00978335_m1
<i>SIRT6</i>	Hs00213036_m1
<i>SIRT7</i>	Hs01034735_m1

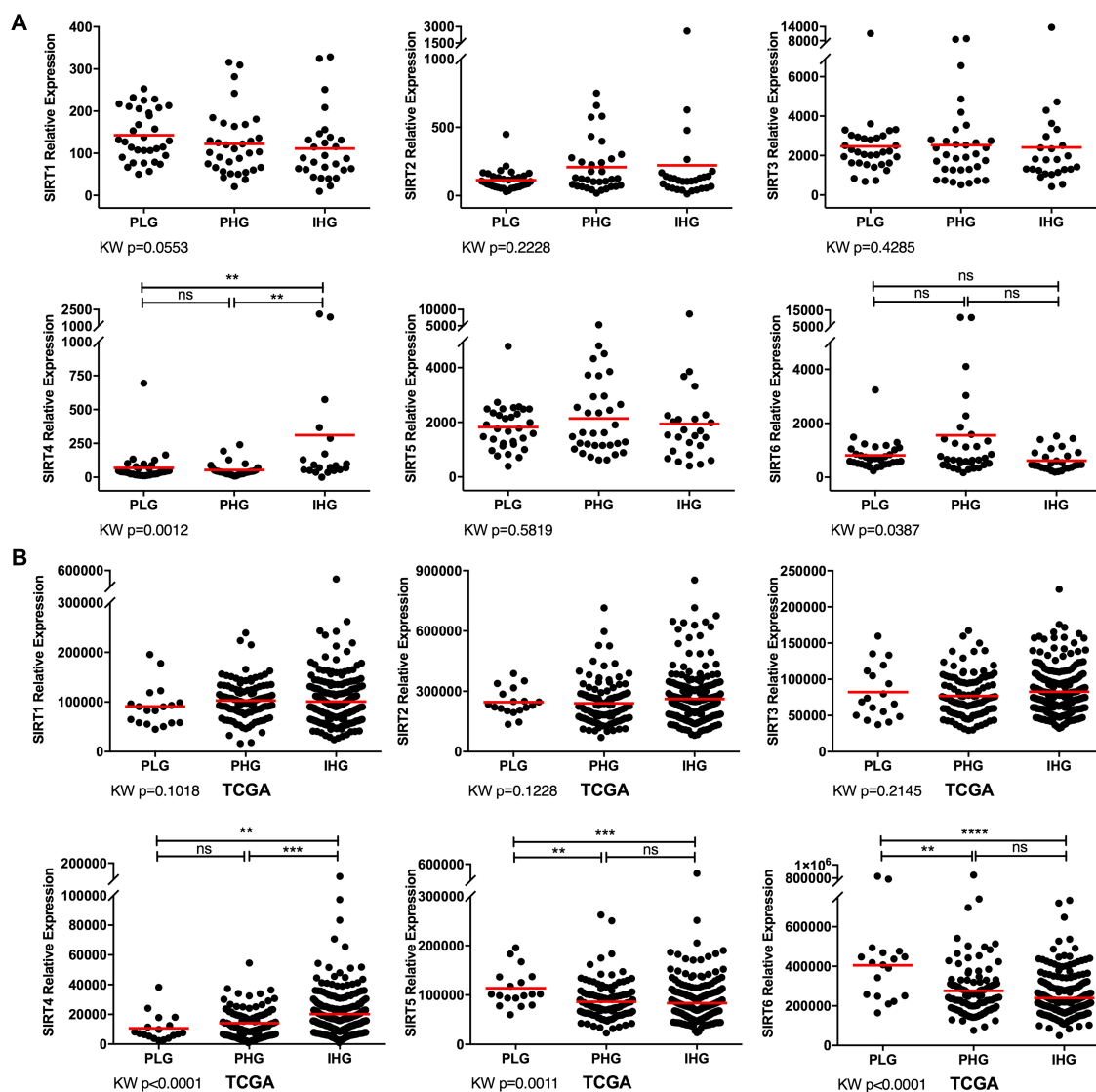
Supplementary Table 2. Primer sequences used in RT-PCR for studied genes.

Gene	Forward sequence (5'- 3')	Reverse sequence (5'- 3')	Annealing T. (°C)
<i>BGUS</i>	CTCATTGGGAATTTTGCCGATT	CCGAGTGAAGATCCCCTTTTTA	60
<i>CDH1</i>	CTTTGACGCCGAGAGCTACA	AAATTCACCTCTGCCAGGACG	64
<i>EZH2</i>	CCCTGACCTCTGTCTTACTTGTGGA	ACGTCAGATGGTGCCAGCAATA	60

Supplementary Figures

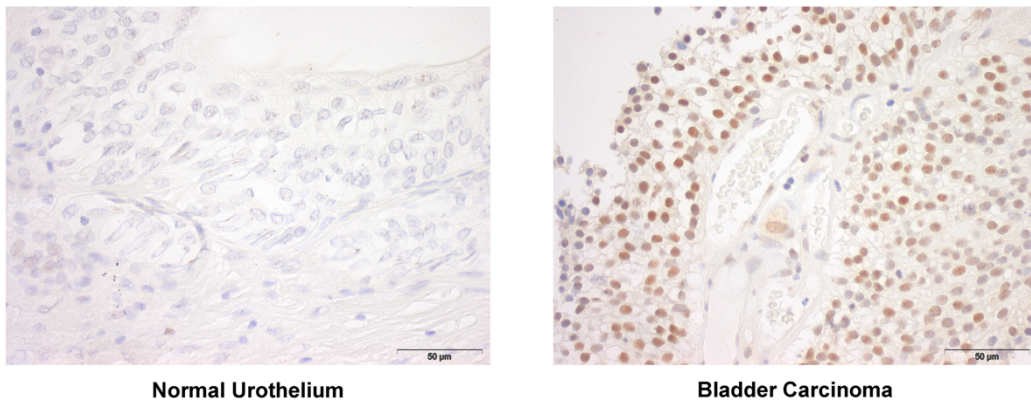


Supplementary Figure S1: Characterization of *SIRT1*, *SIRT2*, *SIRT3*, *SIRT4* and *SIRT5* (a), and *SIRT6* and *SIRT7* (b) in the TCGA bladder cancer cohort by quantitative RT-PCR. * $p < 0.05$, **** $p < 0.0001$ and ns – non-significant. UCC – urothelial cell carcinoma, NB – normal bladder mucosae.

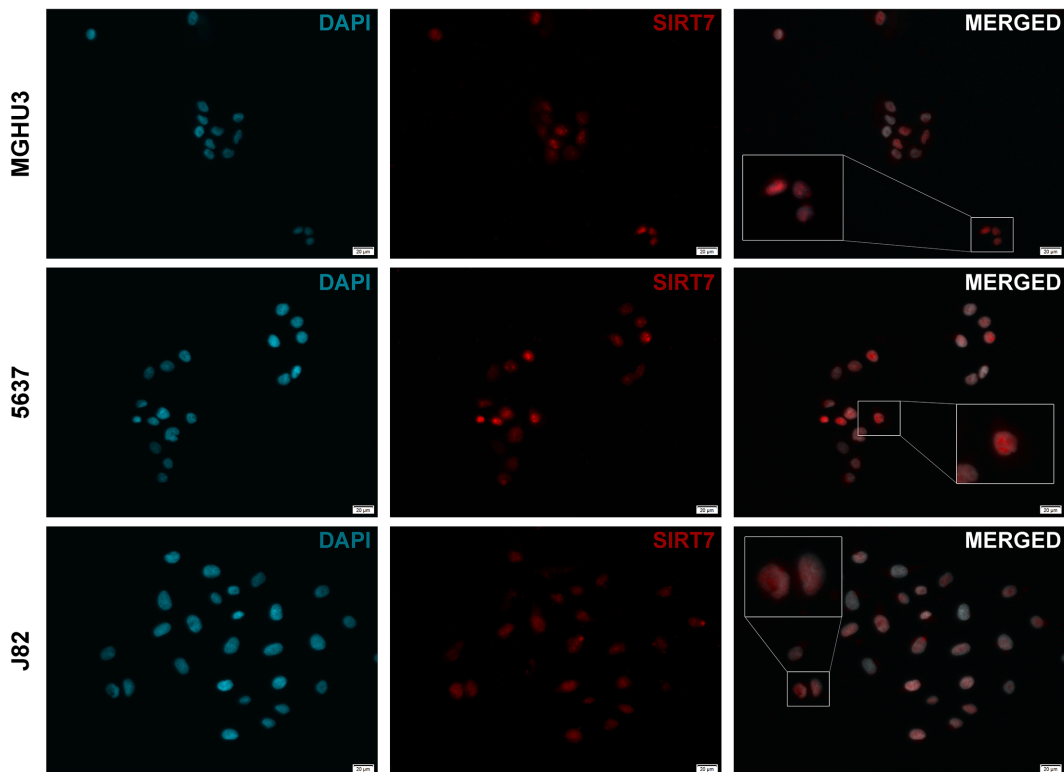


Supplementary Figure S2: Characterization of Sirtuin family (*SIRT1* to *SIRT7*) gene expression in bladder cancer tissues (a) and TCGA cohort (b) categorized by clinical grade. ** $p<0.01$, *** $p<0.001$, **** $p<0.0001$ and ns – non-significant. PLG – papillary low-grade, PHG – papillary high-grade, IHG – invasive high-grade.

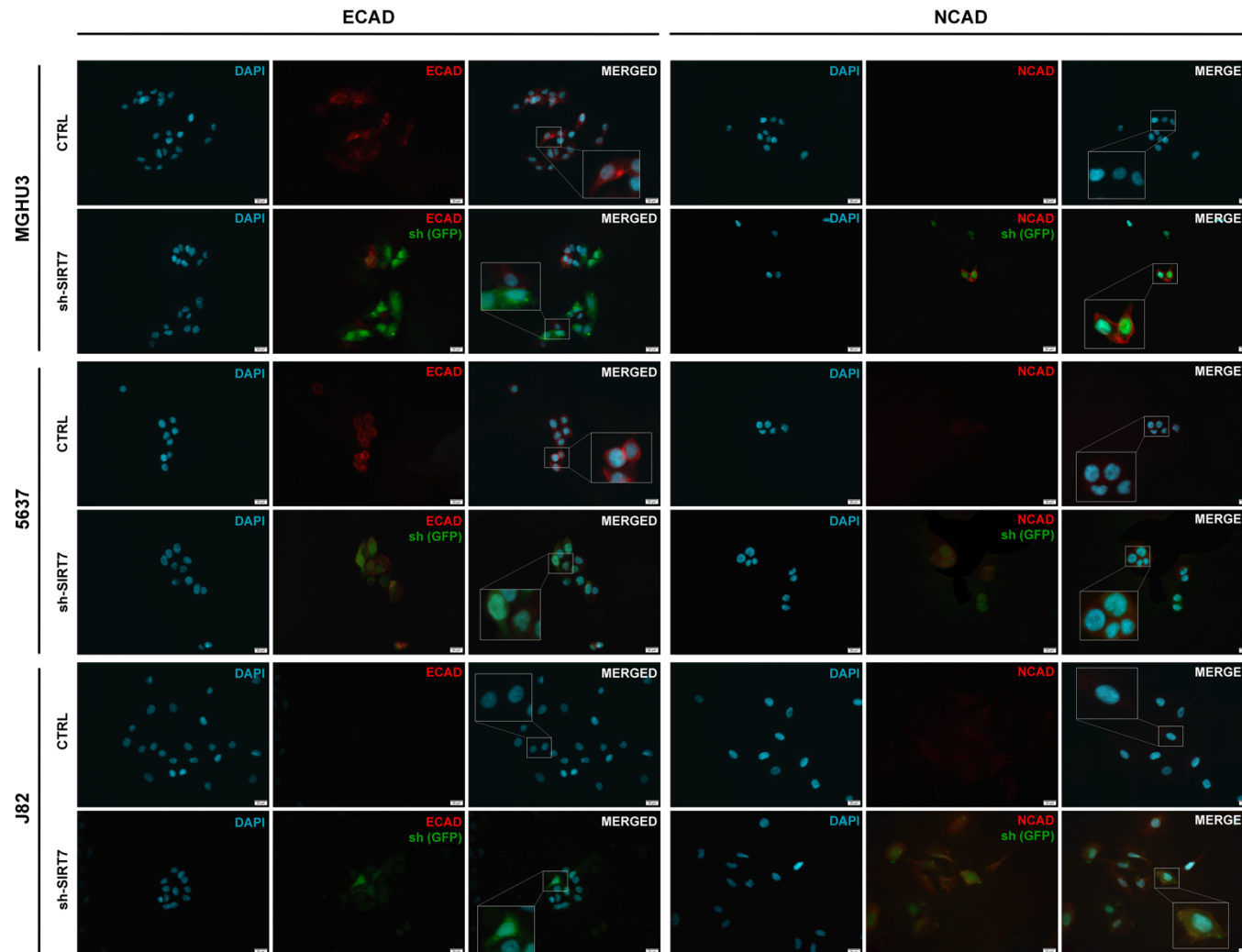
SIRT7 Immunohistochemistry



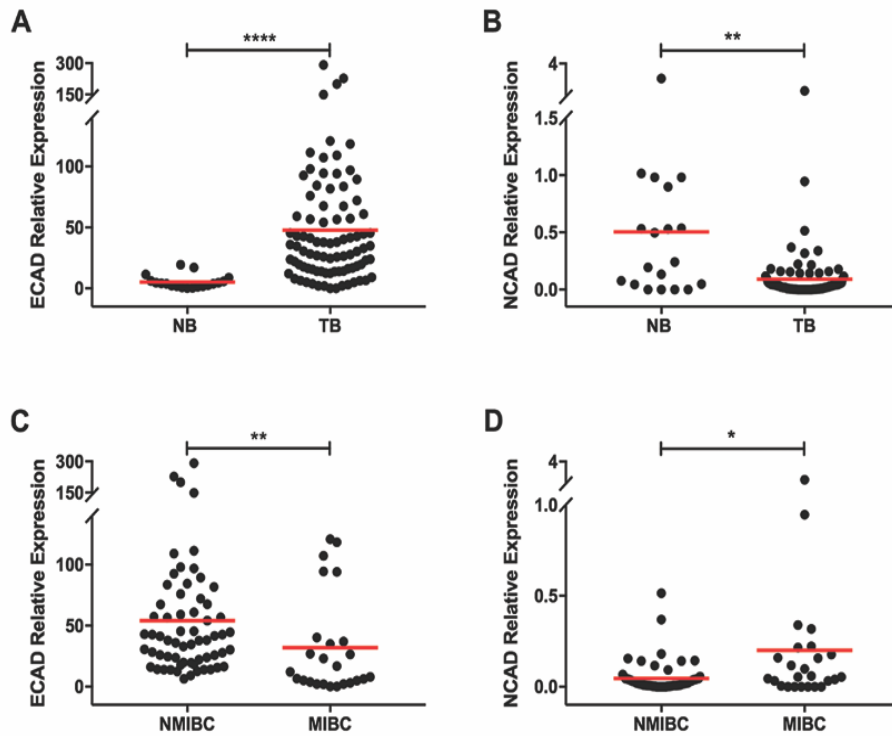
Supplementary Figure S3: Immunohistochemistry representative images for SIRT7 immunoexpression in normal urothelium and bladder urothelial carcinoma tissue sections.



Supplementary Figure S4: Immunofluorescence representative images for SIRT7 immunoexpression in MGHU3, 5637 and J82 bladder cancer cell lines (100X magnification).

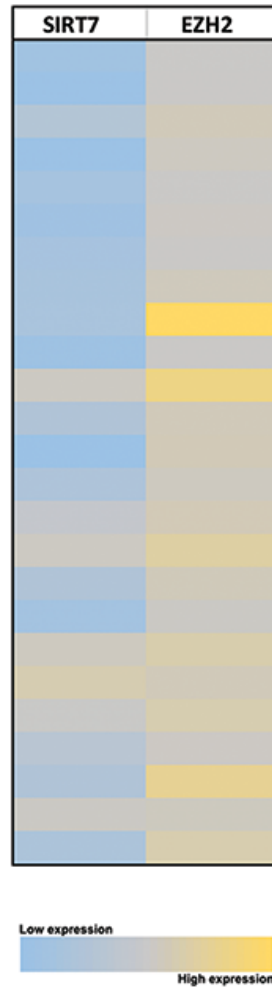


Supplementary Figure S5: Immunofluorescence representative images for E-Cadherin and N-Cadherin immunoexpression in sh-CTRL and sh-SIRT7 MGHU3, 5637 and J82 bladder cancer cell lines (100X magnification).



Supplementary Figure S6: Characterization of *CDH1* gene expression in the bladder cancer and normal mucosae tissue samples (a), and in non-muscle invasive bladder cancer cases (b), by quantitative RT-PCR. Characterization of *CDH2* gene expression in the bladder cancer and normal mucosae tissue samples (c), and in non-muscle invasive (NMIBC) and muscle-invasive bladder cancer (MIBC) cases (d), by quantitative RT-PCR. *p<0.05, **p<0.01 and ****p<0.0001.

MIBC



Supplementary Figure S7: Heat map showing *SIRT7* and *EZH2* expression in muscle invasive bladder cancer (MIBC) cases (n= 26). Relative expression levels are depicted in colours from dark blue (lower expression), to dark yellow (higher expression) as shown in the colour bar below the graphic.

Research Paper IV

Paper IV: Practicability of clinical application of bladder cancer molecular classification and additional value of epithelial-to-mesenchymal transition: prognostic value of vimentin expression

Journal of Translational Medicine 2020, 18(1): 303

DOI: 10.1186/s12967-020-02475-w

João Lobo*, **Sara Monteiro-Reis***, Catarina Guimarães-Teixeira*, Paula Lopes, Isa Carneiro, Carmen Jerónimo, Rui Henrique

Author personal contribution:

Conceptual design, technical execution of the work and interpretation of the results.

Abstract

Background: Bladder cancer (BlCa) taxonomy has proved its impact in patient outcome and selection for targeted therapies, but such transcriptomic-based classification has not yet translated to routine practice. Moreover, epithelial-to-mesenchymal transition (EMT) has shown relevance in acquisition of more aggressive BlCa phenotype. We aimed to test the usefulness of the molecular classification, as defined by immunohistochemistry (a routinely performed and easy-to-implement technique), in a well-defined BlCa cohort of both non-muscle invasive (NMIBC) and muscle invasive (MIBC) disease. Also, we aimed to assess the additional prognostic value of the mesenchymal marker vimentin to the stratification strategy.

Methods: A total of 186 samples were available. Immunohistochemistry/RT-qPCR for luminal markers GATA3/FOXA1, basal markers KRT5/KRT6A and vimentin were performed.

Results: mRNA expression levels of the markers positively correlated with immunoexpression scores. We found substantial overlapping in immunoexpression of luminal and basal markers, evidencing tumour heterogeneity. In MIBC, basal tumors developed recurrence more frequently. NMIBC patients with higher vimentin immunoexpression endured poorer disease-free survival, and increased expression was observed from normal bladder-NMIBC-MIBC-metastases.

Conclusions: The classification has the potential to be implemented in routine, but further adjustments in practical scoring should be defined; focusing on additional markers, including those related to EMT, may further refine BlCa molecular taxonomy.

Background

Bladder cancer (BlCa) is one of the most incident cancers worldwide. It ranks ninth in prevalence, with a number of estimated new cases and cancer-related deaths of 549,393 and 199,922, respectively [1-3]. These figures are estimated to almost double by 2040 [1], representing an important toll on health services [4]. Most BlCa cases correspond to urothelial carcinoma, which is often divided into two major forms: 75–80% of all patients are diagnosed with non-muscle invasive BlCa (NMIBC), characterized by frequent recurrences and eventual progression to invasion; and the remaining 20–25% patients present with muscle-invasive BlCa (MIBC), which constitutes an aggressive, locally invading carcinoma, with propensity for metastization [5, 6]. On the therapeutic front, the clinical management of NMIBC and MIBC cases is very distinct, and it remained almost unchanged until the approval of immune checkpoint inhibitors in first-line or metastatic settings [7-9]. Nevertheless, a considerable percentage of BlCa patients do not benefit from current treatment options. Clinicians still have to deal with a high number of cases

with recurrence and progression and, as a result, patients endure a long follow-up, making BICa one of the costliest malignancies worldwide [4]. Hence, there is a need to improve risk stratification of these patients and to uncover biomarkers that may better select patients to the specific therapy that will give the higher benefit with less toxicity. In this line, an effort has been made to improve BICa classification; various research teams have reported the importance of a molecular stratification of BICa, and presented classifications based on different molecular traits, either for all urothelial carcinomas, or focusing on NMIBC and MIBC separately [10-20]. This molecular stratification is also useful for predicting responses to current treatment options, and provides insights for the development of new therapies [14, 21-24]. Although specific differences in classification emerge out of each research group analyses, they all share as an overlapping feature the existence of two major BICa subtypes—basal/squamous and luminal—for MIBC cases [25]. Briefly, basal/squamous subtype is mainly composed of advanced stage tumors and metastatic disease, being enriched in inactivating mutations and deletions of TP53 and RB1, whereas the luminal subtype is associated with papillary histopathological features, and enriched in fibroblast growth factor receptor 3 (FGFR3) mutations [26, 27]. An effort has been made to reach a single consensus classification and to generate a list of specific biomarkers (such as FOXA1, GATA3, KRT5/6 and KRT14) that can be effectively translated from wide screening genomic and transcriptomics analyses into the clinic for any BICa setting (both MIBC or NMIBC) [13, 26]. However, to date, this has not been achieved. On the other hand, the role of epithelial-to-mesenchymal transition (EMT) in BICa prognosis has been widely discussed [28]. It has been shown to be highly related to an aggressive tumor biology, culminating in poor clinical outcome both in NMIBC and MIBC, namely poorer survival, increased recurrences, propensity to metastasize, and inferior response to treatment [29-33].

Herein, we aimed to characterize the expression of a set of markers for defining both luminal and basal/squamous subtypes in a well characterized patient cohort of BICa, looking for clinicopathological correlates and testing their potential for clinical application, both within MIBC and NMIBC cases. Moreover, we explored the value of adding the expression of a classic EMT marker, vimentin (VIM), to the risk stratification strategy. We have chosen VIM because among the EMT markers it is routinely performed in all Pathology departments and it has been consistently associated with BICa prognosis, including in our previous *in silico* analysis [28].

Methods

Patients and samples

126 patients with primary BICa (urothelial carcinoma) treated with transurethral resection (TUR) or radical cystectomy/cystoprostatectomy between 1991 and 2011 at the Portuguese Oncology Institute of Porto (IPO Porto) were retrospectively selected for the study. A set of 25 morphologically normal bladder mucosa tissue samples was obtained from BICa-free individuals (prostate cancer patients submitted to radical prostatectomy with no bladder lesions) and served as controls. Additionally, a total of 35 metastases from BICa were also included in the study. All specimens were formalin-fixed and paraffin-embedded for routine pathological examination by a dedicated uropathologist and used for immunohistochemistry studies. For some patients (see detailed numbers below) freshly collected tissue could be additionally obtained (a section matching the one embedded in paraffin). These were stored immediately at -80°C after surgical intervention and subsequently cut in a cryostat for confirmation of representativity. These freshly collected samples were specifically used for nucleic acid extraction (for mRNA expression analyses). Staging was performed using the American Joint Committee on Cancer (AJCC) 8th Edition manual [34]. Relevant clinical data was collected from clinical charts, by an investigator blinded to other study findings. A summary of the study cohort is presented in Table 1.

Table 1. Clinicopathological features of the study cohort.

Clinicopathological features of the immunohistochemistry cohort	Primary Bladder Cancer
Individuals, n	126
Gender, n (%)	
Male	101 (80.2)
Female	25 (19.8)
Median age, years (range)	71 (61–77)
Grade, n (%)	
Papillary, low-grade	28/126 (22.2)
Papillary, high-grade	20/126 (15.9)
Invasive, high-grade	78/126 (61.9)
Pathological Stage, n (%) ^a	
pTa/pT1 (NMIBC)	51/123 (41.5)
pT2-4 (MIBC)	72/123 (58.5)

(NMIBC - non-muscle invasive bladder cancer; MIBC - muscle invasive bladder cancer)

^aFor 3 patients stage could not be ascertained as clinical data was missing/not available to the investigators

Immunohistochemistry

In total, 186 samples were available for immunohistochemistry studies: the 126 primary BICa specimens, plus the 25 normal bladder mucosae and 35 BICa metastases. Immunohistochemistry methods are described in detail in Additional file 1: Table S1. Briefly, three micrometer-thick tissue sections from the formalin-fixed and paraffin-embedded samples were ordered, antigen retrieval was performed, and slides were incubated with the primary antibodies for FOXA1, GATA3, CK5/6 and VIM. Then, 3,3'-diaminobenzidine (Sigma-Aldrich™) was used as chromogen for visualization and slides were counterstained with hematoxylin. Appropriate tissue controls were used per run. Immunoexpression patterns were evaluated by a dedicated uropathologist. Cases were classified using a semi-quantitative scale for both staining intensity (0—no staining; 1—low intensity, only barely discernible at 400 × magnification; 2—moderate intensity, well appreciated at 400× magnification but faint at 100× magnification; 3—high intensity, strong and well appreciated at 40× magnification) and percentage of positive cells (0—< 10%; 1—10–33%; 2—33–67%; 3—> 67%), in each case. Results were then combined in a single continuous score (Score S = staining intensity × percentage of positive cells) assigned to each tumor.

BICa specimens were considered “basal-like” when at least focal positivity for CK5/6 was detected (independently of positivity for FOXA1 or GATA3), with the remaining samples (with complete absence of expression of CK5/6) being considered “luminal-like”, following the classification of Choi et al., centered on basal keratin expression for defining subtypes [22].

Real-time quantitative PCR (RT-qPCR)

As mentioned, mRNA expression analyses were performed on fresh frozen tissues, available for 108 of the patients included in the study (all were run for *VIM* expression, and 83 for *FOXA1*, *GATA3*, *KRT5* and *KRT6A*, due to sample limitation issues). RNA was extracted from tissues using TRIzol® (Invitrogen, Carlsbad, CA, USA), according to manufacturer’s instructions. RNA quantification and purity were assessed in NanoDrop™ Lite Spectrophotometer (Cat. ND-LITE, Thermo Scientific™). cDNA synthesis was performed using the RevertAid™ RT Reverse Transcription Kit (Cat. K1691, Thermo Scientific™). The reaction was performed in MyCycler™ Thermal Cycler System (Cat. 1709703, Bio-Rad) using the following conditions: 5min at 25°C, 60min at 42°C and 5min at 70°C. *VIM* mRNA expression levels were evaluated using 4.5µL of

diluted cDNA, 5µL of TaqMan® Universal PCR Master Mix No AmpErase® UNG (Applied Biosystems®) and 0.5µL of TaqMan® Gene Expression Assay, specific for VIM gene - assay ID Hs00185584. For normalization purposes, two TaqMan® Gene Expression assays were used as internal controls: beta-glucuronidase—GUSB—assay ID Hs99999908, Applied biosystems®; and Hypoxanthine—guanine phosphoribosyltransferase—HPRT1—assay ID Hs01003267. RT-qPCR was run in 96-well plates, in an ABI 7500 Real Time PCR System (Thermo Fisher) in the following conditions: 2min at 50°C, followed by enzyme activation for 10min at 95°C, and 45 cycles which included a denaturation stage at 95°C for 15s and an extending stage at 60°C for 60s. Serial dilutions of cDNA obtained from Human Reference Total RNA (Cat. 750500, Agilent Technologies®) were used to compute standard curves for each plate. All experiments were run in triplicate and two negative controls were included in each plate. Relative expression of target genes tested in each sample was determined as: [Gene Expression Level = (*Gene* Mean Quantity)/(*HPRT1* & *GUSB*) Mean Quantity) × 1000]. For *GATA3*, *FOXA1*, *KRT5* and *KRT6A* genes, transcript levels were also assessed using 2.5µL of diluted cDNA, 0.25µL of forward and reverse primers (Additional file 2: Table S2), 5µL of Xpert Fast SYBER Mastermix Blue (GRiSP Research Solutions, Porto, Portugal) and 2µL of bidistilled water. GUSB was used for normalization and plates were set as described above. The run followed the following conditions: 2min at 95°C, followed by 45 cycles of 5s at 95°C and 30s at 60°C, followed by the melt curve stage.

Statistical analysis

Data was tabulated using Microsoft Excel 2016 and analyzed and plotted using GraphPad Prism 6 and IBM Statistical Package for Social Sciences (SPSS v24). Percentages were calculated based on the number of cases with available data. Individual data points are plotted, together with median and interquartile range. Mann–Whitney and Kruskal–Wallis tests were used for comparing expression levels among samples, as necessary. p-values were adjusted for multiple comparisons using Dunn’s test. Chi square and Fisher exact test were used as necessary for establishing associations between categorical variables. Spearman correlation test was used to correlate continuous variables. Disease-specific survival (DSS) and disease-free survival (DFS) curves were plotted using Kaplan–Meier statistics, and Cox regression models with respective hazard ratios (HR) were computed, including multivariable analysis. Statistical significance was set at $p < 0.05$.

Results

Clinical outcome of “luminal-like” and “basal-like” BICa patients as determined by immunohistochemistry

There were no significant differences between the age distribution of patients with NMIBC and MIBC ($p = 0.951$). A total of 56/126 (44.4%) BICa specimens showed “basal-like” features (following the Choi et al. stratification strategy, based on CK5/6 expression [22]). This occurred more frequently in MIBC (34/72, 47.2%) compared to NMIBC (20/51, 39.2%). However, 51/56 (91.1%) of the cases showing CK5/6 immunoreexpression also exhibited immunoreexpression of at least one of the markers GATA3/FOXA1, evidencing that most tumors show evidence of staining for both kinds of markers, in scattered cells. Four tumors showed no immunoreexpression of either CK5/6, FOXA1 or GATA3 (three of those being MIBC) (Table 2). For the latter, we performed additional immunohistochemistry for neuroendocrine markers to look for the presence of the neuroendocrine-like molecular type of BICa [10]. Indeed, one of the cases showed clear-cut strong immunoreexpression of neuroendocrine markers synaptophysin, chromogranin and CD56 (Additional file 3: Fig. S1).

Table 2. Immunoreexpression of luminal and basal markers in the bladder cancer cohort.

	GATA3 and FOXA1 -	GATA3 and/or FOXA1 +
WHOLE COHORT		
CK5/6 -	4 (3.1%)	66 (52.4%)
CK5/6 +	5 (4.0%)	51 (40.5%)
NMIBC		
CK5/6 -	1 (2.0%)	30 (58.8%)
CK5/6 +	1 (2.0%)	19 (37.2%)
MIBC		
CK5/6 -	3 (4.2%)	35 (48.6%)
CK5/6 +	4 (5.5%)	30 (41.7%)

(NMIBC - non-muscle invasive bladder cancer; MIBC - muscle invasive bladder cancer)

For MIBC, there was no significant association between the luminal/basal-like subtype (as defined by immunohistochemistry, described above) and the event of metastization ($p = 0.933$). Within NMIBC, the “basal-like” cases disclosed disease recurrence in 8/20 cases (40.0%) and the “luminal-like” in a similar proportion of cases (13/31, 41.9%). However, considering MIBC, “basal-like” cancer developed recurrence in 11/34 cases

(32.4%), whereas in “luminal-like” this occurred in a lower proportion of patients [only 5/38 cases (13.2%)].

Concerning survival analyses, the luminal/basal-like classification did not show significant impact on DSS or DFS, both for NMIBC or MIBC (NMIBC: $p = 0.762$ and $p = 0.625$; MIBC: $p = 0.346$, $p = 0.185$, respectively). Illustrative examples of immunoexpression patterns for the several markers are depicted in Fig. 1.

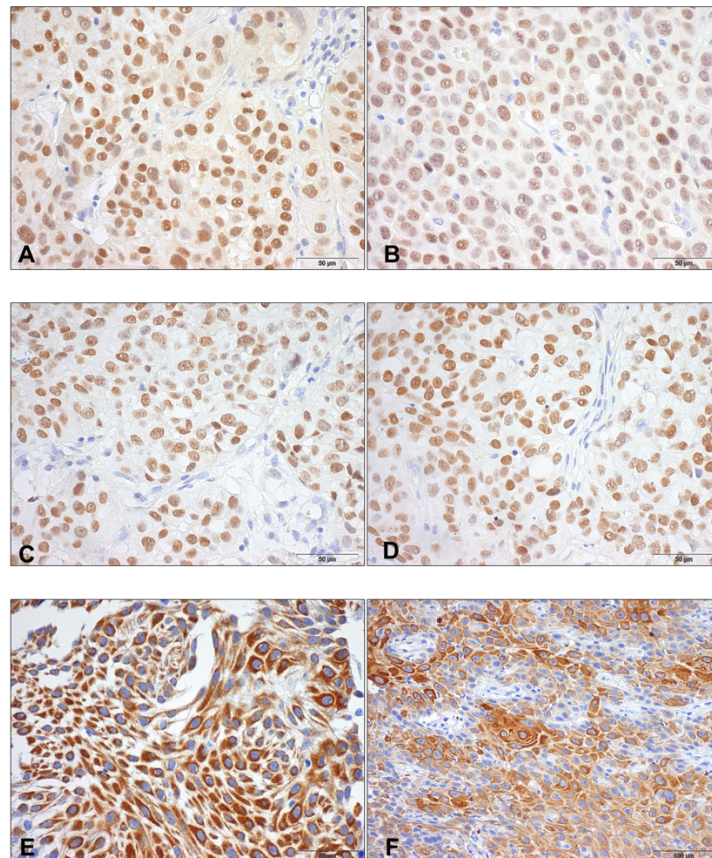


Figure 1. Immunoexpression of luminal and basal markers in the bladder cancer cohort. **a, b** FOXA1 strong and diffuse immunoexpression in two bladder cancer specimens, one NMIBC (a) and one MIBC (b); **c, d**: GATA3 strong and diffuse immunoexpression in two bladder cancer specimens, one NMIBC (c) and one MIBC (d); **e, f**: CK5/6 strong multifocal immunoexpression in two bladder cancer specimens, one NMIBC (e) and one MIBC (f)

Correlation between luminal/basal markers mRNA expression and protein expression

We then checked for reproducibility between protein and transcript levels of the markers under study. Importantly, we found a significant, positive (albeit moderate), correlation between transcript levels of *GATA3* and its protein expression as assessed by immunoexpression score ($r = 0.36$, $p = 0.010$). However, the same was not found for

FOXA1 ($r = 0.10$, $p = 0.3460$). For basal markers *KRT5* and *KRT6A*, mRNA expression showed a significant positive, also moderate, correlation with the immunoprotein score ($r = 0.49$, $p < 0.0001$; and $r = 0.68$, $p < 0.0001$). Tumour samples with absent immunoprotein expression of GATA3, FOXA1 and CK5/6 showed significantly lower transcript levels of *GATA3*, *FOXA1* and *KRT5/KRT6A*, respectively ($p < 0.001$, $p = 0.0130$, $p < 0.0001$ and $p = 0.0278$) (Fig. 2).

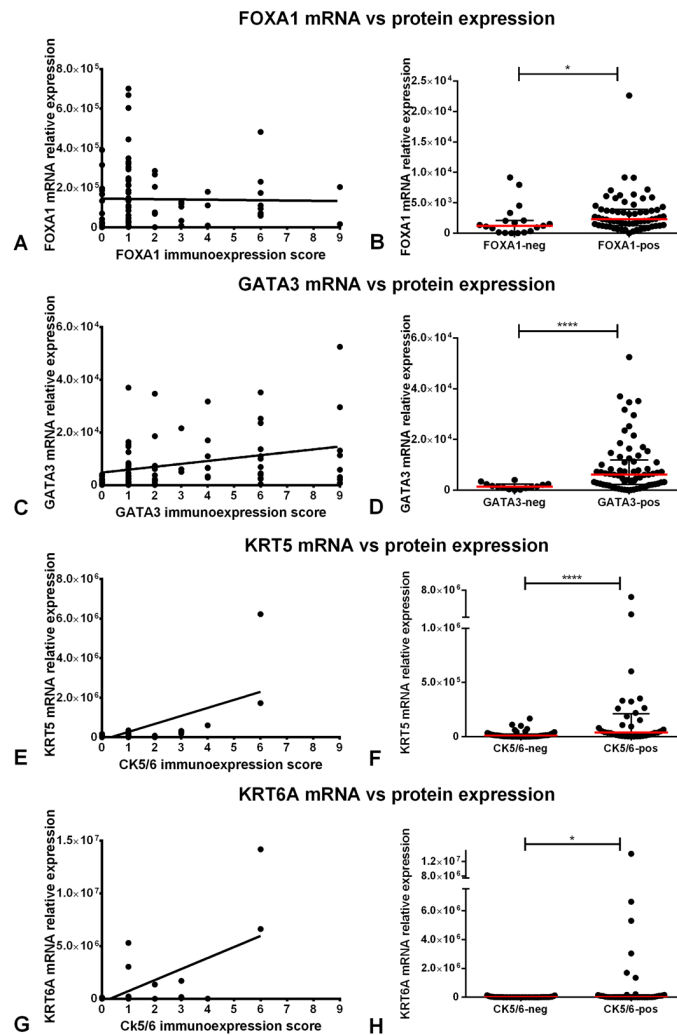


Figure 2. Correlation between mRNA and protein expression of the several luminal and basal markers in the bladder cancer cohort (both MIBC and NMIBC included). *FOXA1* (a and b), *GATA3* (c and d), *KRT5* (e and f) and *KRT6A* (g and h) analyses. mRNA expression levels are plotted as relative expression levels, normalized to *GUSB*. Red dash and bars represent median and interquartile range. The immunoprotein score (intensity \times percentage) is plotted in the xx-axis. The graphs include $n = 83$ matched samples (* $p < 0.05$; **** $p < 0.0001$)

Additional value of VIM expression in predicting clinical outcome

VIM transcript levels were significantly higher in MIBC compared to NMIBC ($p = 0.0001$, Fig. 3a). This was additionally validated at protein level by immunohistochemistry ($p = 0.0013$, Fig. 3b). Moreover, there was an overall progressive increase in immunoexpression scores for VIM, which were lower in normal urothelium and NMIBC, followed by MIBC, and attained the highest levels in BICa metastases ($p < 0.0001$, Fig. 3c). Specifically, VIM immunoexpression scores were significantly higher in MIBC and metastases compared to normal urothelium and to NMIBC (after correction for multiple comparisons), however, differences between normal urothelium and NMIBC categories did not reach statistical significance (Fig. 3c).

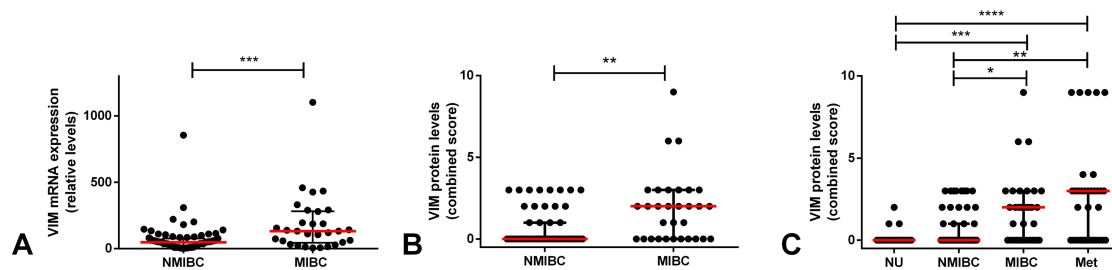


Figure 3. *Vimentin* transcript and protein levels within the bladder cancer cohort. **a** differential mRNA expression of vimentin between non-muscle (NMIBC) and muscle-invasive (MIBC) bladder cancer. mRNA expression levels are plotted as relative expression levels, normalized to *GUSB* and *HPRT1*; **b** differential protein (immuno)expression of vimentin between NMIBC and MIBC. The immunoexpression score (intensity \times percentage) is plotted; **c** immunoexpression of vimentin among normal bladder, NMIBC, MIBC and bladder cancer metastases. The immunoexpression score (intensity \times percentage) is plotted. Red dash and bars represent median and interquartile range. Correction for multiple comparisons was employed and adjusted p-values are represented (* $p < 0.05$; ** $p < 0.01$; *** $p < 0.001$; **** $p < 0.0001$)

VIM immunoexpression score did not have a significant impact on DSS and DFS for MIBC patients ($p = 0.141$ and $p = 0.512$, respectively). It also did not significantly influence DSS of NMIBC patients ($p = 0.296$). Importantly, however, NMIBC patients with VIM immunoexpression in tumor cells endured significantly worse DFS ($p = 0.005$, Fig. 4). DFS of NMIBC patients with VIM immunoexpression was significantly poorer (HR = 3.541, 95% confidence interval 1.402–8.943), and this was maintained after adjusting for patients' age (HR = 3.678, 95% confidence interval 1.435–9.423) and tumor grade (HR = 3.223, 95% confidence interval 1.104–9.408). Illustrative examples of VIM immunoexpression patterns are depicted in Fig. 5.

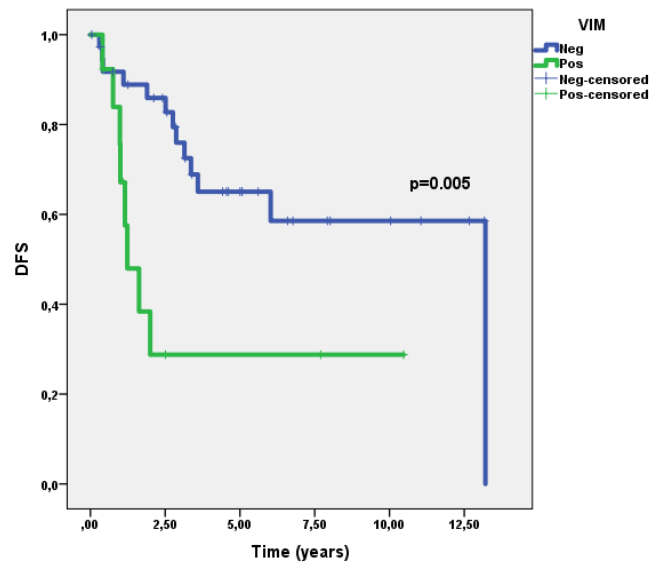


Figure 4. Disease-free survival in non-muscle invasive bladder cancer (NMIBC) patients according to vimentin protein expression.

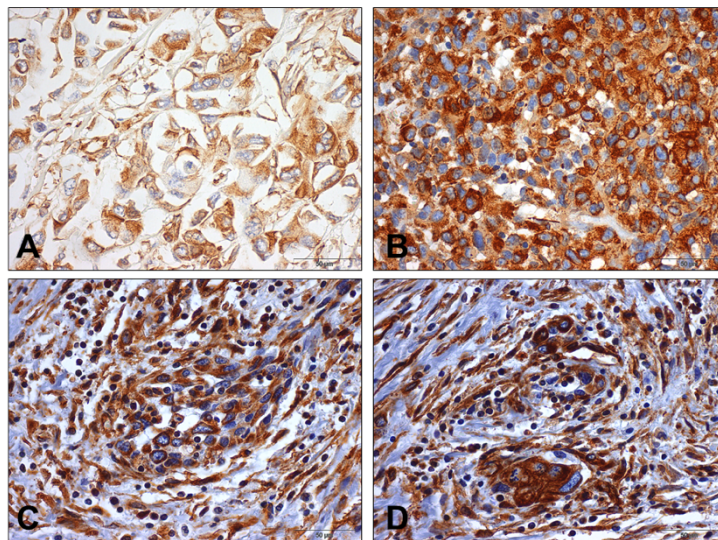


Figure 5. Immunoeexpression of vimentin in the bladder cancer cohort. **a, b:** immunoeexpression of vimentin in primary bladder cancer specimens, one NMIBC (a) and one MIBC (b); **c** and **d:** immunoeexpression of vimentin in bladder cancer metastases.

Discussion

BICa remains a clinically challenging disease, owing to heterogeneity in presentation, progression and distinct treatment strategies. On the one hand, NMIBC is the most frequent BICa phenotype [35], and disease recurrence is very frequent. Substantial research efforts have been put towards uncovering non-invasive, liquid biopsy-based biomarkers for accurately diagnosing and following-up these patients [36, 37]. One major

gap in NMIBC relates to patient prognostication and risk stratification after resection, fundamental for establishing the most appropriate follow-up strategy. In this context, tissue biomarkers that predict relapse may be clinically useful, especially if easily and reproducibly assessed, by cost-effective methodologies [38]. On the other end of the spectrum, around 20–25% of patients present already with MIBC. This subtype has dismal prognosis and survival has remained overall unchanged in the last couple of decades. Recently, immunotherapy has proved useful in the metastatic setting, with several agents being approved and shown to be effective [39, 40]. However, again, there is a need for better biomarkers predictive of response to specific agents [41, 42], that can be determined in tissue samples upon radical cystectomy and also non-invasively, in liquid biopsy context.

Being such a heterogeneous disease, molecular classification of BICa was introduced and gained popularity in the past years [10-20]. It is intended to meet these current needs, improving risk stratification of BICa, and also aiding in identifying specific targets that can be druggable with specific agents. The several analyses concur in the fact that two major types of BICa are molecularly defined, with important prognostication value: the “luminal” and the “basal” cancers. Such classification is achieved based on genomic and transcriptomic analyses, which point to differential expression of specific markers among tumors: the basal cytokeratins KRT5/KRT6A and KRT14, as hallmarks of basal BICa, and the luminal markers FOXA1 and GATA3, as hallmarks of luminal cancer. The value of the classification seems undoubtful; however, and despite multiple confirmations of this, such classification is still not being used in routine clinical practice. There is a lack of works attempting to validate it in the diagnostic setting using immunohistochemistry, with the ones available also finding difficulties in purely classifying the tumors into subtypes or retrieving the same prognostic value [18, 22]. The main aim of our work was to assess the protein expression of these markers and attempt to classify these tumors in a well-defined cohort of BICa, representative of the diagnostic routine of a tertiary cancer center.

We have witnessed substantial overlapping in protein expression of luminal and basal markers within BICa specimens, with 40.5% of our cohort showing protein expression of both types of markers. Such overlapping was maintained across both MIBC and NMIBC. We believe that this may be explained by intratumor heterogeneity and specific tumour cell clones within the tumour mass (also acknowledged by Kamoun et al. [10]), which are captured by immunohistochemistry technique, but may go unnoticed in wide transcriptomic analyses. Moreover, we provide data not only on expression patterns in

MIBC, but also in NMIBC. The former depicted higher proportion of CK5/6 positive cases (47.2% versus 39.2%), but basal features could be already pinpointed in NMIBC, as well. Although in NMIBC this did not dictate differences in recurrence, it might be due to small size of our cohort; on the same line, the proportion of recurrences in MIBC was higher in cases with CK5/6 expression (32.4% versus 13.2%), again with the lack of significant impact on DFS likely due to small number of cases tested (or simply because of other cohort selection issues, like for Choi et al. [22]). Additionally, the neuroendocrine-like subtype was recently added to the classification [10], and we identified one such case within the four tumors negative for both luminal and basal markers. We hypothesize that the remaining cases might also belong in this category, but they are still changing their program and progressing towards a more pronounced neuroendocrine phenotype. Overall, the classification proposed based on expression of these markers remains informative and has potential to be translated to practice if appropriate definitions and methodologies are set (i.e. accurate definitions of “luminal” and “basal” tumors at the protein level, as determined by immunohistochemistry should be established and validated, in order to maintain the clinical value). Prospective, multicenter studies with systematic evaluation of these markers by the same methodology and reporting system should be instrumental for achieving a consensus. We found significant positive correlations between mRNA expression levels of *GATA3*, *KRT5* and *KRT6A* and the matched immunoexpression scoring for the same markers on the same samples (like in the work of Choi et al. [22]). This also substantiates the applicability of the classification. We hypothesize that the classification could also be extended to upper urothelial tract carcinomas, a work ongoing in our Group, with 15/57 tumors (26.3%) showing CK5/6 immunoexpression (data not shown).

In another setting, the EMT signalling pathway and its players have been implicated in acquisition of a more aggressive cancer phenotype among various tumour models, demonstrated both in vitro, in vivo and validated in clinical studies with human specimens [43, 44]. The role of expression of epithelial markers such as E-cadherin, the phenomenon of cadherin switch and overexpression of mesenchymal markers (like Snail, Twist, ZEB1/2, Slug and VIM) has been shown across tumour models [45-48]. BICa is no exception, with studies evidencing that mesenchymal features significantly associate with higher propensity for disease recurrence, metastatic spread, tumour progression and worse prognosis, including poorer survival and treatment resistance [31, 33, 49-52]. In this work, we have assessed the role of the intermediate filament VIM, characteristic of cells with mesenchymal phenotype, not expressed in most normal epithelia (including urothelium), in predicting prognosis of BICa patients. In accordance,

we have shown that *VIM* mRNA and protein expression levels were significantly higher in MIBC compared to NMIBC, illustrating association with increased stage (Fig. 3a, b). The increase in *VIM* protein expression within increasingly aggressive samples (Fig. 3c) reflects the influence of EMT in acquisition of a more aggressive phenotype. Finally, translating this to patient outcome, patients with NMIBC disclosing higher *VIM* expression were shown to have shorter DFS (Fig. 4), even when adjusting (in multivariable analysis) for patient age and grade. Indeed, *VIM* de-novo expression or overexpression has been consistently reported in various epithelial cancers, including those of prostate, breast and lung, associating with increased tumor growth, invasion, poor prognosis, and ultimately, with EMT [53-55]. In BICa, several reports suggest that *VIM* associates with higher grade and stage [32, 56, 57], and with propensity for recurrence and metastasis; however, vimentin immunohistochemistry is not routinely performed when assessing BICa specimens. Also, *VIM* was shown to be expressed in 100% of the cases of sarcomatoid urothelial carcinoma (along with positivity for other mesenchymal markers such as Snail in a high proportion of cases), a particularly aggressive form of the disease, with dismal prognosis [58]. Our work goes further and indicates the clinical potential of *VIM* as a prognostic marker within luminal vs. basal-like BICa cases, although larger studies, including both NMIBC and MIBC, are needed to confirm this hypothesis.

Limitations of this work include its retrospective nature, and the relatively low number of samples with complete clinical information available. Also, not all samples in which immunohistochemistry was performed had fresh-frozen material available for performing transcript analyses. Moreover, although immunohistochemistry may be subjected to inter-observer variability, it is a widespread technique, used in routine histopathology, allowing for evaluating morphology simultaneously and perceiving details related to tumor heterogeneity. Importantly, this work also extends the molecular classification to NMIBC, which should be further explored in the future.

Conclusions

In conclusion, we show that BICa molecular classification has the potential to be effectively translated to the diagnostic routine, but effort must be made to consistently define the tumour categories acknowledged by transcriptomic studies using routine techniques, with the ultimate goal of maintaining the same clinically meaningful input. On the other hand, expression of EMT markers may be useful for predicting relapse and adjusting therapeutic strategy, like *VIM* in our work, in which it provided useful prognostic

information and dictated survival outcome. Adjunctive markers to the molecular classification merit attention as they might further improve BICa molecular taxonomy.

References

1. Bray F, Ferlay J, Soerjomataram I, Siegel RL, Torre LA, Jemal A: Global cancer statistics 2018: GLOBOCAN estimates of incidence and mortality worldwide for 36 cancers in 185 countries. *CA Cancer J Clin* 2018, 68:394-424.
2. Saginala K, Barsouk A, Aluru JS, Rawla P, Padala SA, Barsouk A: Epidemiology of Bladder Cancer. *Med Sci (Basel)* 2020, 8.
3. Antoni S, Ferlay J, Soerjomataram I, Znaor A, Jemal A, Bray F: Bladder Cancer Incidence and Mortality: A Global Overview and Recent Trends. *Eur Urol* 2017, 71:96-108.
4. Leal J, Luengo-Fernandez R, Sullivan R, Witjes JA: Economic Burden of Bladder Cancer Across the European Union. *Eur Urol* 2016, 69:438-447.
5. Sanli O, Dobruch J, Knowles MA, Burger M, Alemozaffar M, Nielsen ME, Lotan Y: Bladder cancer. *Nat Rev Dis Primers* 2017, 3:17022.
6. Moch H, Ulbright T, Humphrey P, Reuter V: WHO Classification of Tumours of the Urinary System and Male Genital Organs (4th Edition). IARC: Lyon 2016.
7. Rouanne M, Loriot Y, Lebreton T, Soria JC: Novel therapeutic targets in advanced urothelial carcinoma. *Crit Rev Oncol Hematol* 2016, 98:106-115.
8. Powles T, Eder JP, Fine GD, Braiteh FS, Loriot Y, Cruz C, Bellmunt J, Burris HA, Petrylak DP, Teng SL, et al: MPDL3280A (anti-PD-L1) treatment leads to clinical activity in metastatic bladder cancer. *Nature* 2014, 515:558-562.
9. Davarpanah NN, Yuno A, Trepel JB, Apolo AB: Immunotherapy: a new treatment paradigm in bladder cancer. *Curr Opin Oncol* 2017.
10. Kamoun A, de Reynies A, Allory Y, Sjudahl G, Robertson AG, Seiler R, Hoadley KA, Groeneveld CS, Al-Ahmadie H, Choi W, et al: A Consensus Molecular Classification of Muscle-invasive Bladder Cancer. *Eur Urol* 2020, 77:420-433.
11. Tan TZ, Rouanne M, Tan KT, Huang RY, Thiery JP: Molecular Subtypes of Urothelial Bladder Cancer: Results from a Meta-cohort Analysis of 2411 Tumors. *Eur Urol* 2019, 75:423-432.
12. Dyrskjot L: Molecular Subtypes of Bladder Cancer: Academic Exercise or Clinical Relevance? *Eur Urol* 2019, 75:433-434.
13. Lerner SP, Robertson AG: Molecular Subtypes of Non-muscle Invasive Bladder Cancer. *Cancer Cell* 2016, 30:1-3.
14. Blinova E, Roshchin D, Kogan E, Samishina E, Demura T, Deryabina O, Suslova I, Blinov D, Zhdanov P, Osmanov U, et al: Patient-Derived Non-Muscular Invasive Bladder Cancer Xenografts of Main Molecular Subtypes of the Tumor for Anti-Pd-I1 Treatment Assessment. *Cells* 2019, 8.

15. Dyrskjot L, Thykjaer T, Kruhoffer M, Jensen JL, Marcussen N, Hamilton-Dutoit S, Wolf H, Orntoft TF: Identifying distinct classes of bladder carcinoma using microarrays. *Nat Genet* 2003, 33:90-96.
16. Blaveri E, Simko JP, Korkola JE, Brewer JL, Baehner F, Mehta K, Devries S, Koppie T, Pejavar S, Carroll P, Waldman FM: Bladder cancer outcome and subtype classification by gene expression. *Clin Cancer Res* 2005, 11:4044-4055.
17. Lindgren D, Frigyesi A, Gudjonsson S, Sjobahl G, Hallden C, Chebil G, Veerla S, Ryden T, Mansson W, Liedberg F, Hoglund M: Combined gene expression and genomic profiling define two intrinsic molecular subtypes of urothelial carcinoma and gene signatures for molecular grading and outcome. *Cancer Res* 2010, 70:3463-3472.
18. Sjobahl G, Lauss M, Lovgren K, Chebil G, Gudjonsson S, Veerla S, Patschan O, Aine M, Ferno M, Ringner M, et al: A molecular taxonomy for urothelial carcinoma. *Clin Cancer Res* 2012, 18:3377-3386.
19. Marzouka NA, Eriksson P, Rovira C, Liedberg F, Sjobahl G, Hoglund M: A validation and extended description of the Lund taxonomy for urothelial carcinoma using the TCGA cohort. *Sci Rep* 2018, 8:3737.
20. Cancer Genome Atlas Research N: Comprehensive molecular characterization of urothelial bladder carcinoma. *Nature* 2014, 507:315-322.
21. Todenhofer T, Seiler R: Molecular subtypes and response to immunotherapy in bladder cancer patients. *Transl Androl Urol* 2019, 8:S293-S295.
22. Choi W, Porten S, Kim S, Willis D, Plimack ER, Hoffman-Censits J, Roth B, Cheng T, Tran M, Lee IL, et al: Identification of distinct basal and luminal subtypes of muscle-invasive bladder cancer with different sensitivities to frontline chemotherapy. *Cancer Cell* 2014, 25:152-165.
23. Rosenberg JE, Hoffman-Censits J, Powles T, van der Heijden MS, Balar AV, Necchi A, Dawson N, O'Donnell PH, Balmanoukian A, Loriot Y, et al: Atezolizumab in patients with locally advanced and metastatic urothelial carcinoma who have progressed following treatment with platinum-based chemotherapy: a single-arm, multicentre, phase 2 trial. *Lancet* 2016, 387:1909-1920.
24. Seiler R, Ashab HAD, Erho N, van Rhijn BWG, Winters B, Douglas J, Van Kessel KE, Fransen van de Putte EE, Sommerlad M, Wang NQ, et al: Impact of Molecular Subtypes in Muscle-invasive Bladder Cancer on Predicting Response and Survival after Neoadjuvant Chemotherapy. *Eur Urol* 2017, 72:544-554.
25. Stone L: Bladder cancer: Two molecular subtypes identified. *Nat Rev Urol* 2016, 13:566.
26. Robertson AG, Kim J, Al-Ahmadie H, Bellmunt J, Guo G, Cherniack AD, Hinoue T, Laird PW, Hoadley KA, Akbani R, et al: Comprehensive Molecular Characterization of Muscle-Invasive Bladder Cancer. *Cell* 2018, 174:1033.
27. McConkey DJ, Choi W: Molecular Subtypes of Bladder Cancer. *Curr Oncol Rep* 2018, 20:77.

28. Monteiro-Reis S, Lobo J, Henrique R, Jeronimo C: Epigenetic Mechanisms Influencing Epithelial to Mesenchymal Transition in Bladder Cancer. *Int J Mol Sci* 2019, 20.
29. Garg M, Singh R: Epithelial-to-mesenchymal transition: Event and core associates in bladder cancer. *Front Biosci (Elite Ed)* 2019, 11:150-165.
30. Moussa RA, Khalil EZI, Ali AI: Prognostic Role of Epithelial-Mesenchymal Transition Markers "E-Cadherin, beta-Catenin, ZEB1, ZEB2 and p63" in Bladder Carcinoma. *World J Oncol* 2019, 10:199-217.
31. McConkey DJ, Choi W, Marquis L, Martin F, Williams MB, Shah J, Svatek R, Das A, Adam L, Kamat A, et al: Role of epithelial-to-mesenchymal transition (EMT) in drug sensitivity and metastasis in bladder cancer. *Cancer Metastasis Rev* 2009, 28:335-344.
32. Singh R, Ansari JA, Maurya N, Mandhani A, Agrawal V, Garg M: Epithelial-To-Mesenchymal Transition and Its Correlation With Clinicopathologic Features in Patients With Urothelial Carcinoma of the Bladder. *Clin Genitourin Cancer* 2017, 15:e187-e197.
33. Liu B, Miyake H, Nishikawa M, Fujisawa M: Expression profile of epithelial-mesenchymal transition markers in non-muscle-invasive urothelial carcinoma of the bladder: correlation with intravesical recurrence following transurethral resection. *Urol Oncol* 2015, 33:110 e111-118.
34. Amin MB: *AJCC Cancer Staging Manual*, 8th Edition. 2017.
35. Aldousari S, Kassouf W: Update on the management of non-muscle invasive bladder cancer. *Can Urol Assoc J* 2010, 4:56-64.
36. Monteiro-Reis S, Blanca A, Tedim-Moreira J, Carneiro I, Montezuma D, Monteiro P, Oliveira J, Antunes L, Henrique R, Lopez-Beltran A, Jeronimo C: A Multiplex Test Assessing MiR663ame and VIMme in Urine Accurately Discriminates Bladder Cancer from Inflammatory Conditions. *J Clin Med* 2020, 9.
37. Avogbe PH, Manel A, Vian E, Durand G, Forey N, Voegele C, Zvereva M, Hosen MI, Meziani S, De Tilly B, et al: Urinary TERT promoter mutations as non-invasive biomarkers for the comprehensive detection of urothelial cancer. *EBioMedicine* 2019, 44:431-438.
38. Babjuk M, Bohle A, Burger M, Capoun O, Cohen D, Comperat EM, Hernandez V, Kaasinen E, Palou J, Roupret M, et al: EAU Guidelines on Non-Muscle-invasive Urothelial Carcinoma of the Bladder: Update 2016. *Eur Urol* 2017, 71:447-461.
39. Farina MS, Lundgren KT, Bellmunt J: Immunotherapy in Urothelial Cancer: Recent Results and Future Perspectives. *Drugs* 2017, 77:1077-1089.
40. Lobo J, Jeronimo C, Henrique R: Targeting the Immune system and Epigenetic Landscape of Urological Tumors. *Int J Mol Sci* 2020, 21.
41. Lodewijk I, Duenas M, Rubio C, Munera-Maravilla E, Segovia C, Bernardini A, Teixeira A, Paramio JM, Suarez-Cabrera C: Liquid Biopsy Biomarkers in Bladder Cancer: A Current Need for Patient Diagnosis and Monitoring. *Int J Mol Sci* 2018, 19.
42. Yang Y, Miller CR, Lopez-Beltran A, Montironi R, Cheng M, Zhang S, Koch MO, Kaimakliotis HZ, Cheng L: Liquid Biopsies in the Management of Bladder Cancer: Next-Generation Biomarkers for Diagnosis, Surveillance, and Treatment-Response Prediction. *Crit Rev Oncog* 2017, 22:389-401.

43. Dongre A, Weinberg RA: New insights into the mechanisms of epithelial-mesenchymal transition and implications for cancer. *Nat Rev Mol Cell Biol* 2019, 20:69-84.
44. Kang Y, Massague J: Epithelial-mesenchymal transitions: twist in development and metastasis. *Cell* 2004, 118:277-279.
45. Ferreira C, Lobo J, Antunes L, Lopes P, Jeronimo C, Henrique R: Differential expression of E-cadherin and P-cadherin in pT3 prostate cancer: correlation with clinical and pathological features. *Virchows Arch* 2018, 473:443-452.
46. Lobo J, Petronilho S, Newell AH, Coach J, Harlow G, Cruz A, Lopes P, Antunes L, Bai I, Walker E, Henrique R: E-cadherin clone 36 nuclear staining dictates adverse disease outcome in lobular breast cancer patients. *Mod Pathol* 2019, 32:1574-1586.
47. Piva F, Giulietti M, Santoni M, Occhipinti G, Scarpelli M, Lopez-Beltran A, Cheng L, Principato G, Montironi R: Epithelial to Mesenchymal Transition in Renal Cell Carcinoma: Implications for Cancer Therapy. *Mol Diagn Ther* 2016, 20:111-117.
48. Huang L, Wu RL, Xu AM: Epithelial-mesenchymal transition in gastric cancer. *Am J Transl Res* 2015, 7:2141-2158.
49. Guo CC, Majewski T, Zhang L, Yao H, Bondaruk J, Wang Y, Zhang S, Wang Z, Lee JG, Lee S, et al: Dysregulation of EMT Drives the Progression to Clinically Aggressive Sarcomatoid Bladder Cancer. *Cell Rep* 2019, 27:1781-1793 e1784.
50. Luo Y, Zhu YT, Ma LL, Pang SY, Wei LJ, Lei CY, He CW, Tan WL: Characteristics of bladder transitional cell carcinoma with E-cadherin and N-cadherin double-negative expression. *Oncol Lett* 2016, 12:530-536.
51. Bryan RT: Cell adhesion and urothelial bladder cancer: the role of cadherin switching and related phenomena. *Philos Trans R Soc Lond B Biol Sci* 2015, 370:20140042.
52. Zhao J, Dong D, Sun L, Zhang G, Sun L: Prognostic significance of the epithelial-to-mesenchymal transition markers e-cadherin, vimentin and twist in bladder cancer. *Int Braz J Urol* 2014, 40:179-189.
53. Singh S, Sadacharan S, Su S, Beldegrun A, Persad S, Singh G: Overexpression of vimentin: role in the invasive phenotype in an androgen-independent model of prostate cancer. *Cancer Res* 2003, 63:2306-2311.
54. Kokkinos MI, Wafai R, Wong MK, Newgreen DF, Thompson EW, Waltham M: Vimentin and epithelial-mesenchymal transition in human breast cancer--observations in vitro and in vivo. *Cells Tissues Organs* 2007, 185:191-203.
55. Al-Saad S, Al-Shibli K, Donnem T, Persson M, Bremnes RM, Busund LT: The prognostic impact of NF-kappaB p105, vimentin, E-cadherin and Par6 expression in epithelial and stromal compartment in non-small-cell lung cancer. *Br J Cancer* 2008, 99:1476-1483.
56. Baumgart E, Cohen MS, Silva Neto B, Jacobs MA, Wotkowicz C, Rieger-Christ KM, Biolo A, Zeheb R, Loda M, Libertino JA, Summerhayes IC: Identification and prognostic significance of an epithelial-mesenchymal transition expression profile in human bladder tumors. *Clin Cancer Res* 2007, 13:1685-1694.

57. Paliwal P, Arora D, Mishra AK: Epithelial mesenchymal transition in urothelial carcinoma: twist in the tale. Indian J Pathol Microbiol 2012, 55:443-449.

58. Sanfrancesco J, McKenney JK, Leivo MZ, Gupta S, Elson P, Hansel DE: Sarcomatoid Urothelial Carcinoma of the Bladder: Analysis of 28 Cases With Emphasis on Clinicopathologic Features and Markers of Epithelial-to-Mesenchymal Transition. Arch Pathol Lab Med 2016, 140:543-551.

Supplementary Data (Paper IV)

Supplementary Tables

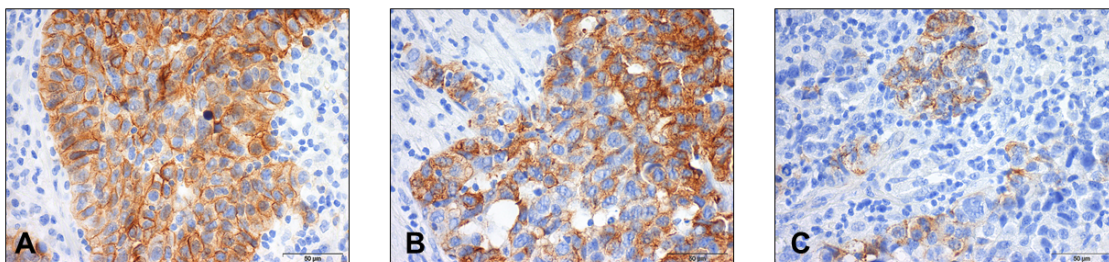
Supplementary Table 1. Immunohistochemistry methods.

Antibody	Clone/Ref	Vendor	Antigenic recovery	Dilution	Detection system	Incubation/Platform	Positive control
GATA3	Polyclonal/HPA029731	Sigma	Citrate, 20 min	1:350	Novolink Max Polymer DS	1h	Breast cancer
FOXA1	Polyclonal/HPA050505	Sigma	Citrate, 20 min	1:300	Novolink Max Polymer DS	1h	Breast cancer
CK5/6	Monoclonal (D5/16B4)/355M-18	Cell Marque	ER2, 20 min	1:200	Bond Polymer Refine DK	Leica Bond III	Squamous cell carcinoma
VIM	Monoclonal (V9)/NCL-L-VIM-V9	Leica	ER1, 10min	1:100	Bond Polymer Refine DK	Leica Bond III	Tonsil
Synaptophysin	Monoclonal (DAK-SYNAP)	Dako	ER2, 10 min	1:100	Bond Polymer Refine DK	Leica Bond III	Pancreas
Chromogranin	Monoclonal (DAK-A3)	Dako	ER1, 10 min	1:1000	Bond Polymer Refine DK	Leica Bond III	Pancreas
CD56	Monoclonal (CD564)	Leica	ER2, 10 min	1:100	Bond Polymer Refine DK	Leica Bond III	Pancreas

Supplementary Table 2. Primers sequences.

Gene	Forward (5'-3')	Reverse (5'-3')
GATA3	CAGACCACCACAACCACACTCT	GGATGCCTCCTTCTTCATAGTCA
FOXA1	GGGTGGCTCCAGGATGTTAGG	GGGTCATGTTGCCGCTCGTAG
KRT5	ATCGCCACTTACCGCAAGCTGCTGGAGGG	AAACACTGCTTGTGACAACAGAG
KRT6A	AGAGAATGAATTTGTGACTCTGAAGAAG	TACAAGGCTCTCAGGAAGTTGATCT
GUSB	CACTGAAGAGTACCAGAAAAGTC	TCTCTGCCGAGTGAAGATCC

Supplementary Figures



Supplementary Figure 1: Immunoeexpression of neuroendocrine markers in a bladder cancer specimen negative for CK5/6, FOXA1 and GATA3. **A:** CD56; **B:** Synaptophysin; **C:** Chromogranin.

Research Paper V

Paper V: Epigenetic deregulation of Vimentin expression in Bladder Cancer associates with acquisition of invasive and metastatic phenotype through epithelial to mesenchymal transition

In preparation

Sara Monteiro-Reis, Vera Miranda-Gonçalves, Catarina Guimarães-Teixeira, Cláudia Martins-Lima, João Lobo, Diana Montezuma, Paula C. Dias, Isabelle Bernard-Pierrot, Rui Henrique and Carmen Jerónimo

Author personal contribution:

Participation in the conceptual design and technical execution of the work, interpretation of the results and manuscript preparation.

Abstract

Bladder cancer (BICa) is the tenth most common cancer worldwide, associated with significant morbidity and mortality. Thus, understand the biological mechanisms underlying tumour progression to identify tumour subsets with distinctive potential of aggressiveness is of great clinical significance. Vimentin (VIM), an intermediate filament characteristic of mesenchymal cells, is (over)expressed in several carcinomas, putatively in association with epithelial to mesenchymal transition (EMT). We have previously found that VIM promoter methylation accurately identified urothelial carcinoma and VIM expression associated with unfavourable prognosis. Thus, we sought to investigate VIM expression regulation and its role in malignant transformation and progression of BICa. Analysis of tissue samples disclosed higher VIM transcript, protein and methylation levels in BICa compared with normal urothelium. Moreover, VIM protein and transcript levels significantly increased from non-muscle invasive BICa (NMIBC), to muscle-invasive BICa (MIBC) and to BICa metastases. Decreased *CDH1* (E-Cadherin) and increased *CDH2* (N-Cadherin) transcript levels were observed in MIBC, with inverse correlations between *CDH1* & *CDH2* and *CDH1* & *VIM*, and positive correlation between *CDH2* & *VIM*. In J82 and TCCSUP BICa cell lines, exposure to a demethylating agent increased VIM protein levels, with a concomitant decrease in *VIM* methylation. In TCCSUP cells, exposure to histone deacetylases pan-inhibitor significantly increased the deposit of active post-translational marks (PTMs) across VIM promoter. In primary normal urothelium cells, lower levels of active PTMs with concomitant higher levels of repressive marks deposit was observed. Finally, CRISPR-Cas9 mediated VIM knockdown in UMUC3 BICa cell line resulted in epithelial-like features and decreased migration and invasion.

We demonstrated that *VIM* promoter is epigenetically regulated in normal and neoplastic urothelial cells, involving histone PTM and promoter methylation, which determine a VIM switch associated with EMT and acquisition of invasive and metastatic properties. These findings might allow for development of new, epigenetic-based, therapeutic strategies for BICa.

Introduction

Bladder cancer (BICa) is a leading cause of cancer-related morbidity and mortality, being the 10th most incident tumour worldwide (1, 2). Urothelial cell carcinomas (UCCs) are the most common form of BICa, arising along the urinary tract, mostly in the lower tract (bladder and urethra), but also in the upper tract (renal pelvis and ureters) (3-7). The gold-standard diagnostic techniques are mostly invasive and uncomfortable, which led us and others to develop non-invasive tests (8-13). We have previously shown that a

biomarker panel (*VIM*, *GDF15* and *TMEFF2* promoter methylation) accurately detected both lower and upper tract UCC in urine, and, more recently, that a multiplex panel (*VIM* and miR663a promoter methylation) accurately discriminated BICa from inflammatory bladder conditions (8, 9, 11). From these studies, Vimentin (*VIM*) promoter methylation surfaced as the most promising biomarker, detecting alone the majority of samples, as reported for other malignancies (14-19). Additionally, survival analysis showed that lower *VIM* promoter methylation levels independently predicted for poor disease-specific survival in upper tract urothelial carcinoma (UTUC) patients (9). Similar findings have been previously reported in cell lines of other epithelial tumours in which *VIM* expression/overexpression was associated with increased tumour growth, invasion and poor prognosis (20, 21). Indeed, *VIM* is an intermediate filament characteristic of mesenchymal cells, usually not expressed in most normal epithelia (including urothelium) and epithelial tumours (22).

EMT is a multistep process through which epithelial cells develop mesenchymal characteristics, such as motility and invasive properties (23, 24). *In vitro* and *in vivo* studies indicate that EMT is associated with cancer cell invasion and metastasis in various malignancies (25-28). Remarkably, EMT is a reversible phenomenon, as cells may return to their epithelial phenotype in a process known as mesenchymal-epithelial transition (MET). Changes in expression of various molecular markers have been associated with EMT, including cadherin family and transcriptional repressors Zeb-1 and Zeb-2, Twist, Snail, Slug (29, 30). *VIM* is usually upregulated in cells undergoing EMT, a feature that has been implicated both normal in development and neoplastic progression (31). Nonetheless, the role of vimentin in EMT needs further clarification, and it is not clear how *VIM* expression is fine-tuned from its absence in normal cells to its (over)expression in invasive carcinoma cells. Moreover, the discovery of the molecular mechanisms that lead to this "switch" of *VIM* expression might identify novel therapeutic agents aiming to prevent cancer progression and metastization.

Epigenetic mechanisms, including DNA methylation and histone post-translational modifications (PTMs) dictate gene expression regulation, are reversible and its deregulation is common in cancer, (32, 33). Considering our previous observations on *VIM* promoter methylation in BICa and its association with disease aggressiveness, we sought to characterize in depth the epigenetic mechanisms putatively responsible for *VIM* switch in this tumour model, and ascertain the relevance of *VIM* expression deregulation for BICa progression.

Materials and Methods

Patients and Samples

Patients (n=108) with primary BICa, treated with transurethral resection (TUR) or radical cystectomy between 1991 and 2011 at Portuguese Oncology Institute of Porto (IPO Porto), with available frozen and formalin-fixed paraffin-embedded (FFPE) tissue at the Department of Pathology, were included in this study. A set of 36 morphologically normal bladder mucosa (NB) tissue samples was obtained from BICa-free individuals (prostate cancer patients submitted to radical prostatectomy) and served as controls. Additionally, a set of FFPE tissue samples from 28 metastasis (Met) of BICa patients were also collected. All primary specimens were fresh-frozen at -80°C and subsequently cut in a cryostat for confirmation of representativity and nucleic acid extraction. From each specimen, fragments were collected, formalin-fixed, and paraffin embedded for routine histopathological examination, including grading and pathological staging, by a dedicated uropathologist (34). Relevant clinical data was collected from clinical charts (Table 1). Patients and controls were enrolled after informed consent. This study was approved by the institutional review board (Comissão de Ética para a Saúde) of IPO Porto (CES015-2016).

Table 1. Clinical and histopathological parameters of Bladder Cancer patients, and gender and age distribution of control set individuals.

Clinicopathological features	Bladder Cancer	Normal Urothelium
Patients, n	108	36
Gender, n (%)		
Males	78 (72)	23 (64)
Females	30 (28)	13 (36)
Median age, yrs (range)	69 (45-91)	63 (48-75)
Grade, n (%)		
Papillary, low-grade	37 (34)	n.a.
Papillary, high-grade	31 (29)	n.a.
Invasive, high-grade	40 (37)	n.a.
Pathological Stage, n (%)		
pTa/pT1 (NMIBC)	68 (63)	n.a.
pT2-4 (MIBC)	40 (37)	n.a.

(NMIBC – non-muscle invasive bladder cancer; MIBC - muscle invasive bladder cancer)

Cell lines

BICa cell lines (RT112, MGHU2, 5637, J82, T24, UMUC3 and TCCSUP) and normal bladder cell line SV-HUC1, available at our lab, were selected for this study. All cell lines were purchased from ATCC and grown using recommended medium (Biochrom-Merck, Berlin, Germany) supplemented with 10% fetal bovine serum (FBS, Biochrom) and 1% penicillin/streptomycin (GBICO, Invitrogen) at 37°C and 5% CO₂. Additionally, a primary cell line culture from normal human urothelium (NHU), kindly provided by Dr. Isabelle Pierrot (Institut Curie, Paris, France) was also cultured for ChIP-qPCR assays.

Mycoplasma test was regularly performed (every two weeks) in all cell lines, using TaKaRa PCR Mycoplasma Detection Set (Clontech Laboratories, Mountain View, CA, EUA).

RNA isolation and Real-Time Quantitative PCR (RT-qPCR)

RNA was extracted from tissues using TRIzol® (Invitrogen, Carlsbad, CA, USA), according to manufacturer's instructions. cDNA synthesis was performed using the High Capacity cDNA Reverse Transcription Kit (Applied Biosystems®, Foster City, CA, USA), according to manufacturer's instructions. Target genes transcript levels were quantified by RT-qPCR. Expression levels were evaluated using either 4.5µL of diluted cDNA, 5µL of TaqMan® Universal PCR Master Mix No AmpErase® UNG (Applied Biosystems®) and 0.5µL of specific TaqMan® Gene Expression Assay (HPRT1 – Ref. ID Hs01003267_m1, VIM – Ref. ID Hs00185584_m1), or using Xpert Fast SYBER Mastermix Blue (GRiSP Research Solutions, Porto, Portugal) with specific primers for each target and reference genes, as described in Supplementary Table S1. Each sample was run in triplicate under the following RT-qPCR conditions: 2 minutes at 50°C, followed by enzyme activation for 10 minutes at 95°C, and 45 cycles which included a denaturation stage at 95°C for 15 seconds and an extending stage at 60°C for 60 seconds. HPRT was used as reference gene for normalization. Relative expression of target genes tested in each sample was determined as: [Gene Expression Level = (Gene Mean Quantity / Reference Gene Mean Quantity) x 1000].

DNA isolation, Bisulfite Modification and Quantitative Methylation Specific PCR (qMSP) Analysis

DNA was extracted from frozen BICa and NB tissues using a standard phenol-chloroform protocol (35), and its concentration determined using a Qubit 3 Fluorometer (Thermo Fisher Scientific, Waltham, MA, USA). Bisulfite modification was performed through sodium bisulfite, using the EZ DNA Methylation-Gold™ Kit (Zymo Research, Irvine, CA, USA), according to manufacturer's protocol. For this, 1000ng of DNA were converted.

Quantitative methylation levels were performed using Xpert Fast Probe Master Mix (GRiSP, Porto, Portugal), in 96-well plates using an Applied Biosystems 7500 Sequence Detector (Perkin Elmer, Waltham, CA, USA), with Beta-Actin (ACTB) as internal reference gene for normalization. Primer and probe sequences were designed using Methyl Primer Express 1.0 and purchased from Sigma-Aldrich (St. Louis, MO, USA) (Supplementary Table S1). Additionally, six serial dilutions (dilution factor of 5×) of a fully methylated bisulphite modified universal DNA control were included in each plate to generate a standard curve. In each sample and for each gene, the relative DNA methylation levels were determined using the following formula: ((target gene/ACTB) ×1000). A run was considered valid when previously reported criteria were met (8).

Immunohistochemistry

Immunohistochemistry was performed using the Novolink™ Max Polymer Detection System (Leica Biosystems, Wetzlar, Germany]. Three-µm thick tissues sections from formalin-fixed and paraffin-embedded BICa, NU and Met samples were cut, deparaffinized and rehydrated. Antigen retrieval was accomplished by microwaving the specimens at 800W for 10 minutes in 10mM sodium citrate buffer, pH=6. After, endogenous peroxidase activity was blocked, primary monoclonal antibody for VIM (NCL-L-VIM-V9, Leica) was used in 1:100 dilution, and incubated at room-temperature (RT) for one hour. Then, 3, 3'-diaminobenzidine (Sigma-Aldrich™) was used as chromogen for visualization and slides were mounted with Entellan® (Merck-Millipore, Burlington, MA, EUA). Normal tonsil tissue, showing intense VIM immunoreactivity was used as positive control. VIM immunoexpression was evaluated by a dedicated uropathologist and cases were classified using a semi-quantitative scale for both staining intensity (0—no staining; 1—intensity lower than normal urothelium; 2—intensity equal to normal urothelium; 3—intensity higher than normal urothelium) and percentage of positive cells (0—< 10%; 1—10-33%; 2—33-67%; 3—>67%), in each tumor. Staining intensity and percentage of positive cell results were then combined into a single score (Score S = staining intensity x percentage of positive cells) assigned to each tumor.

Cell lines treatment with epigenetic drugs

Cell lines TCCSUP and J82 were grown, until 20 to 30% confluence was reached, in 75cm³ cell culture flasks. Then, media containing the corresponding drug(s) - a pharmacologic inhibitor of DNMTs, 5-aza-2-deoxycytidine (DAC) (Sigma-Aldrich®, Germany) and/or a pan-inhibitor of HDAC, Trichostatin A (TSA) (Sigma-Aldrich®, Germany) - were added at 1µM and 0.5µM concentrations, respectively. Culture medium and appropriate drug(s) were renewed every 24h, on a total of 72h. Mock cells served

as controls as they were submitted to the medium change procedure but were only exposed to drug(s) vehicle(s). All treatment experiments were done in triplicate. On the fourth day of the treatment schedule, cells were harvested by trypsinization and centrifuged. Then, either pellets were washed in PBS 1x and stored at -80°C for DNA extraction or were immediately processed for protein extraction or ChIP analysis.

VIM gene knockdown

VIM knockdown was performed through CRISPR/Cas9 system, delivered to cells through a plasmid including a specific guide RNA (gRNA) sequence targeting *VIM*, and puromycin-resistance gene (GenScript, Piscataway, NJ, EUA). Briefly, UMUC3 cells were seeded in 24 well/plates and let to grow until approximately 85% confluency. Then, transfection was performed using Lipofectamine 3000 reagent (Invitrogen, USA), and cells were incubated with the plasmid for 48h. Subsequently, 1µg/mL of puromycin dihydrochloride (Clontech Laboratories) was added to select stably transfected cells (UMUC3^{KD}). Control cells were generated using only Lipofectamine incubation without targeting gene-plasmid (UMUC3^{CTRL}). Cells were then grown until confluence, and passed at least two times, until protein extraction and subsequent western blot analysis for *VIM* expression.

Protein extraction and Western Blot (WB) analysis

SVHUC1, UMUC3^{KD} and UMUC3^{CTRL} cell lines were grown until 80% confluence and homogenized in Kinexus lysis buffer supplemented with proteases inhibitors cocktail. Then, cells were sonicated for 5 cycles of 30 seconds ON and 30 seconds OFF (Bioruptor®, Diagenode, Liège, Belgium). After centrifugation, the supernatant was collected, and total protein was quantified according the Pierce BCA Protein Assay Kit (Thermo Fisher Scientific Inc.), according to the manufacture procedure.

Thirty µg total protein were separated in 10% polyacrylamide gel by SDS-PAGE and transferred onto an immunoblot PVDF membrane (Bio-Rad Laboratories, Hercules, CA, USA) in a 25mM Tris-base/ glycine buffer using a Trans-Blot Turbo Transfer system (Bio-Rad Laboratories). Membranes were blocked with 5% bovine serum albumin (BSA) in TBS/0.1% Tween (TBS/T pH=7.6) for 2h at RT. After incubation with *VIM* primary antibody (NCL-L-VIM-V9, Leica), membranes were washed in TBS/T and incubated with secondary antibody coupled with horseradish peroxidase, for 1h at RT. Binding was visualized by chemiluminescence (Clarity WB ECL substrate, Bio-Rad) and quantification was performed using band densitometry analysis from the ImageJ software (version 1.6.1, National Institutes of Health). β-Actin (1:10,000, A1978, Sigma-Aldrich) was used as loading control.

Immunofluorescence (IF) and morphometric analysis

SVHUC1, UMUC3^{KD} and UMUC3^{CTRL} cell lines were seeded on cover slips at 20,000 cells/well, overnight. Briefly, cells were fixed in methanol during 10min and then blocked with 5% bovine serum albumin (BSA) during 30min. After overnight VIM (1:150, #3195, Cell Signaling Technology) incubation at room temperature, cells were incubated with secondary antibody anti-rabbit IgG-TRITC (1:500, T6778, Sigma-Aldrich) during 1h at RT. Finally, after washing in 1X PBS, cells were stained with 4',6-diamidino-2-phenylindole (DAPI) (AR1176, BOSTER Biological Technologies) in mounting medium. Pictures were taken in a fluorescence microscope Olympus IX51 with a digital camera Olympus XM10 using CellSens software (Olympus Corporation, Shinjuku, Japan). Cell morphometric parameters – roundness and aspect ratio (cell length/ cell width) - were calculated for UMUC3^{KD} and UMUC3^{CTRL} cells using the ImageJ software, in three independent experiments.

Chromatin Immunoprecipitation (ChIP)

Chromatin Immunoprecipitation (ChIP) analysis was performed in J82, TCCSUP, SVHUC1 and NHU cells, following a previously published protocol (36). ChIP-grade antibodies for specific PTMs (Supplementary Table 2), positive control (RNA polymerase II) and negative control (mouse IgG), were used at assay dependent concentration. For qPCR, two pairs of primers for *VIM* promoter were designed, both for ~325bp (VIM A) before TSS (F—5'- TAGTGAGCAGGAGAAAGCACAG-3', R—5'- AAAGACAGGACATGGAGGATGT-3') and for ~600bp (VIM B) before TSS (F—5'- CTGAACTGATACAGTGGCAAGTGA-3', R—5'-TCAGGATATGCATGCCAAAG-3'). RT-qPCR was performed as mentioned above, and the relative amount of promoter DNA was normalized using Input Percent method.

Cell viability assay

To assess the role of VIM in cell growth, 3-(4,5-dimethylthiazol-2-yl)-2,5-diphenyltetrazolium (MTT) assay (Sigma-Aldrich) was performed. Briefly, UMUC3^{KD} and UMUC3^{CTRL} cells were seeded at 3000 cell/well density, overnight, in 96 well plate. Then, 5µg/mL MTT solution in completed DMEM medium was incubated during 1h at 37°C for 0h, 24h, 48h and 72h. Then, formazan crystals formed were dissolved in dimethyl sulfoxide (DMSO) and spectrophotometric measurement was done at 540nm, using 655nm as a reference absorbance (Fluostar Omega, BMG Labtech, Offenburg, Germany). The optical density (OD) obtained for 24h, 48h and 72h was normalized for the 0h time point. At least three independent experiments were performed.

Apoptosis assay

Apoptosis was assessed using the APOPercentage™ kit (Biocolor Ltd., Belfast, Northern Ireland, UK). This assay uses a dye that is integrated by cells undergoing at early stage of apoptosis due to phosphatidylserine transmembrane movements, which results in APOPercentage dye incorporation by cells. Briefly, UMUC3^{KD} and UMUC3^{CTRL} cells were seeded in 24 well plate at density of 25,000 cell/well and incubated during 72hours in a humidified chamber at 37°C and 5% CO₂. At this time point, cells were incubated with 300µl/well of APOPercentage dye solution at ratio 1:20 respectively, during 20min at 37°C. Then, cells were washed with PBS1X and detached from well plate with Tryple™ Express (GBICO) during 10min at 37°C. After that, APOPercentage Dye Release reagent was added and plate were vigorously agitated during 15min, following colorimetric measurement at 550nm with 620nm reference filter (Fluostar Omega). The H₂O₂ was used as a positive control. The OD obtained for apoptosis assay was normalized for the OD obtained by viability assay at the same time point. At least three independent experiments were performed.

Wound healing assay

UMUC3^{KD} and UMUC3^{CTRL} cells were seeded in 6-well plate at a density of 7.5x10⁵ cell/well and allowed reach confluence at 37°C, 5% CO₂. Then, a “wound” was made by manual scratching with a 200 µL pipette tip and cells were gently washed with 1X PBS. The “wounded” areas were photographed in specific wound sites (two sites for each wound) at 40x magnification using an Olympus IX51 inverted microscope equipped with an Olympus XM10 Digital Camera System every 24h until wound closure. The relative migration distance (5 measures by wound) was calculated with the following formula: relative migration distance (%) = (A–B)/C x100, where A is the width of cell wound at 0h incubation, B is the width of cell wound after specific hours of incubation, and C is the width mean of cell wound for 0h of incubation. For relative migration distance, the results were analyzed using the beWound-Cell Migration Tool (Version 1.5) (developed by A.H.J. Moreira, S. Queirós and J.L. Vilaça, Biomedical Engineering Solutions Research Group, Life and Health Sciences Research Institute- University of Minho; available at <http://www.besurg.com/sites/default/files/beWoundApp.zip>). At least three independent experiments were performed.

Invasion assay

Invasion capacity of UMUC3^{KD} and UMUC3^{CTRL} cells was evaluated using a 24-well BD Biocoat Matrigel Invasion Chambers (BD Biosciences). After rehydration of BD Matrigel Chambers during 2h with DMEM medium at 37°C, 25,000 cells/insert were seeded and

incubated during 24h at 37°C in 5% CO₂. Then, the non-invading cells were removed by with swab and invaded cells were fixed with methanol and staining with DAPI. Invaded cells were counted in a fluorescence microscope Olympus IX51 with a digital camera Olympus XM10 using CellSens software. The % invasion was normalized for total amount of cells seeded in BD Matrigel Chamber.

Statistical analysis

All statistical analyses were performed using IBM® SPSS® Statistic software version 23 (IBM-SPSS Inc., Chicago, IL, USA) and graphs were built using GraphPad Prim 7.0 (GraphPad Software Inc., La Jolla, CA, USA). Significance level was set at $p < 0.05$, and Bonferroni's correction was used when appropriate.

Mann-Whitney U test (MW) was used to test for differences in VIM expression or methylation levels between NB and BICa, pathological stages of cases divided into Ta-1 (non-muscle invasive BICa, NMIBC) and T2-4 (muscle invasive BICa, MIBC), and patients' gender, and to assess differences in UMUC3^{KD} and UMUC3^{CTRL} conditions. Kruskal-Wallis test (KW) was performed to test for differences among more than two groups of samples then followed by MW test when appropriate. Spearman's rho was used to assess the correlation between VIM expression or methylation levels and age of the patients at diagnosis, and between *VIM* and *CDH1*, *CDH2* or *CDH3* expression levels. Associations between clinical grade or pathological stage and immunoexpression results were assessed by chi-square or Fisher's exact test, and Somers' D directional measure was also computed.

Disease-specific and disease-free survival curves (Kaplan-Meier with log rank test) were computed for standard variables (tumor stage and grade) and for categorized *VIM* transcript and methylation levels. Moreover, the same analyses were also performed separately for NMIBC and MIBC cases. A Cox-regression model comprising all significant variables (univariable and multivariable model) was computed to assess the relative contribution of each variable to the follow-up status.

Results

Protein, transcript and methylation analysis of Vimentin in Bladder cancer tissues

Immunohistochemistry and RT-qPCR analysis of VIM in NB tissue samples demonstrated that protein and transcript levels were low or undetectable (Figure 1A and 1B). Moreover, in the same samples, no methylation levels were detected at the *VIM* promoter (Figure 1C). BICa cases disclosed higher VIM transcript, protein and methylation levels, compared with NB (Figure 1). Importantly, VIM protein and transcript

levels were significantly increased in MIBC compared to NMIBC, although no significant difference was apparent concerning *VIM* promoter methylation levels (Figure 1). Comparatively to primary BICa tissue samples, metastatic BICa tissues disclosed a significant increase in *VIM* protein levels and a concomitant decrease in *VIM* promoter methylation (Supplementary Figure 1).

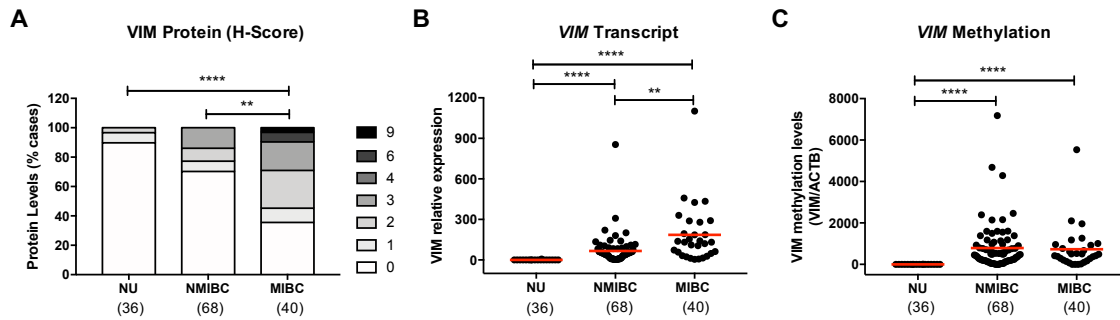


Figure 1. VIM expression and methylation in normal urothelium and bladder cancer tissues. (A) VIM immunohistochemistry results for normal urothelium (NU), non-muscle-invasive bladder cancer (NMIBC) tissues and muscle-invasive bladder cancer (MIBC) tissues, regarding the calculated immunoscore. (B) *VIM* transcript levels for NU, NMIBC and MIBC tissue samples by RT-qPCR. (C) *VIM* promoter methylation levels for NU, NMIBC and MIBC tissue samples by qMSP. * $p < 0.05$, ** $p < 0.01$, *** $p < 0.001$ and **** $p < 0.0001$.

Association between Cadherins and Vimentin in Bladder cancer tissues

To ascertain whether the increase of *VIM* expression in more invasive cases was related with EMT, *CDH1*, *CDH2* and *CDH3* (which correspond to ECAD, NCAD and PCAD, respectively) transcript levels were first assessed in the same BICa tissue samples. As expected, a significant decrease in *CDH1* (the epithelial cadherin) and a concomitant increase in *CDH2* (the mesenchymal cadherin) transcript levels were observed in MIBC, compared with NMIBC (Figure 2A and B). Moreover, no significant differences were observed for *CDH3* (Figure 2C). Importantly, significant inverse correlations between *CDH1* and *CDH2*, and *CDH1* and *VIM* expression levels were found, whereas a positive significant correlation was depicted between *CDH1* and *CDH3* and *CDH2* and *VIM* transcript levels (Table 2; Supplementary Figure 2).

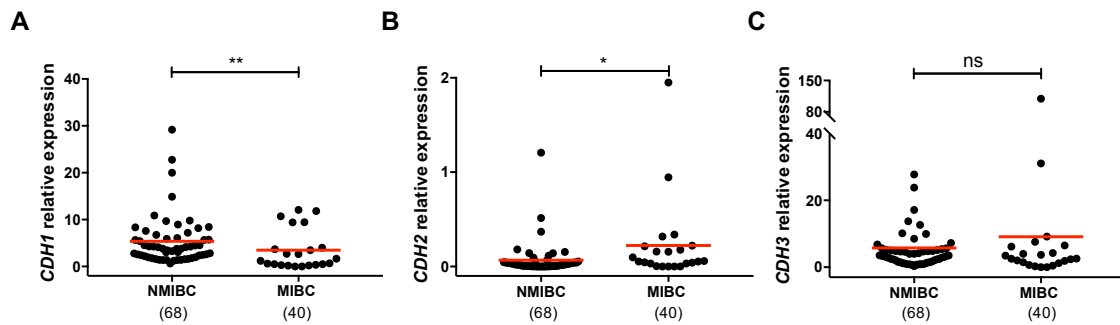


Figure 2. Cadherins genes expression in bladder cancer tissues. Transcript levels of (A) *CDH1*, (B) *CDH2* and (C) *CDH3* in non-muscle-invasive bladder cancer (NMIBC) tissues and muscle-invasive bladder cancer (MIBC) tissues by RT-qPCR.

Table 2. Pearson correlation between *CDH1*, *CDH2*, *CDH3* and *VIM* transcript levels in Bladder cancer tissues. (grey results are non-significant).

Pearson R ²	<i>CDH1</i>	<i>CDH2</i>	<i>CDH3</i>	<i>VIM</i>
<i>CDH1</i>		-0.268	0.330	-0.405
<i>CDH2</i>	-0.268		0.193	0.419
<i>CDH3</i>	0.330	0.193		-0.127
<i>VIM</i>	-0.405	0.419	-0.127	

Modulation of Vimentin methylation in BICa cell lines and its impact in expression

Considering the previous results in tissue samples, we investigated whether promoter methylation might regulate *VIM* expression in BICa, using in vitro models. First, *VIM* protein levels were assessed by WB and IF in the available BICa and normal bladder immortalized cell lines, to determine which cells disclosed the lowest *VIM* expression levels (Figure 3). Then, using the same cell lines, *VIM* promoter methylation was assessed, and J82 and TCCSUP were chosen to perform subsequent treatment with epigenetic drugs DAC and TSA, as these two cell lines disclosed low *VIM* expression with concomitant high *VIM* promoter methylation levels (Figure 3A and 4A).

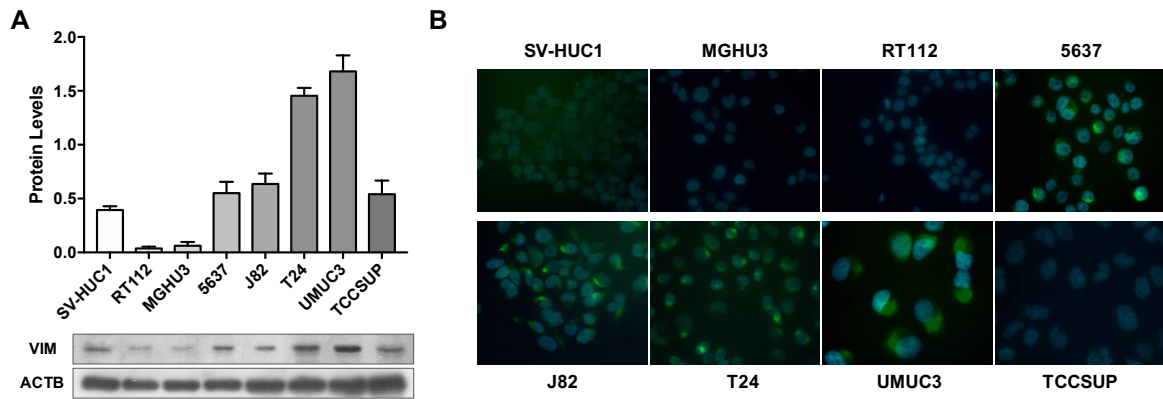


Figure 3. VIM expression in bladder cancer cell lines. (A) Expression of VIM protein in bladder cancer cell lines by Western blot; results are representative of three independent experiments with mean \pm SD. **(B)** Representative images of VIM protein localization in bladder cancer cell lines by immunofluorescence.

In J82 and TCCSUP cells, 1 μ M DAC exposure significantly increased VIM protein levels ($p < 0.01$ and $p < 0.0001$, respectively; Figure 4B), and the same was observed in TCCSUP cells treated with both drugs ($p < 0.001$), compared to mock cells. Cell lines treated with TSA only did not disclose variation of VIM expression levels. When *VIM* methylation levels were assessed in the same treated cell lines, for the same conditions, lower methylation levels were observed in cells treated with DAC and/or DAC+TSA (Figure 4C), supporting a role for promoter methylation in *VIM* expression regulation in BICa cells.

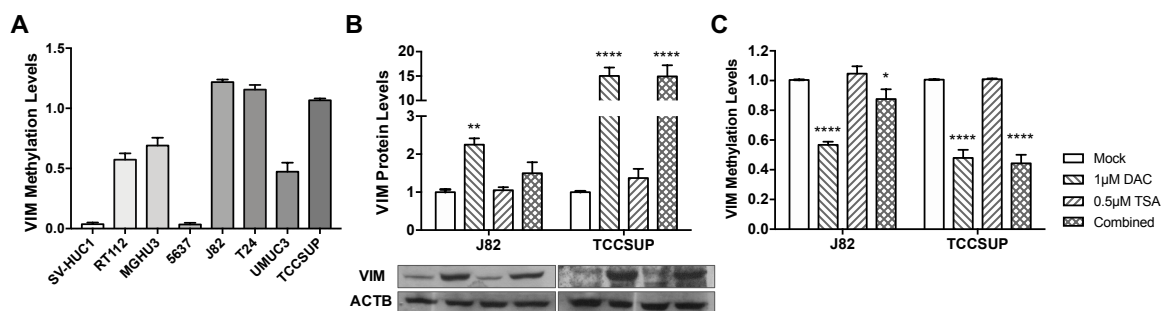


Figure 4. VIM methylation modulation in bladder cancer cell lines. (A) *VIM* promoter methylation levels in bladder cancer cell lines by qMSP. **(B)** Expression of VIM protein in J82 and TCCSUP bladder cancer cell lines by Western blot, after treatment with epigenetic modulating drugs. **(C)** *VIM* promoter methylation levels in J82 and TCCSUP bladder cancer cell lines by qMSP, after treatment with epigenetic modulating drugs.

Regulation of VIM by histone posttranslational modifications

To determine whether histones PTMs might also contribute to VIM expression regulation, ChIP-qPCR analysis for known repressive and activating PTMs was performed in the same cell lines exposed to epigenetic drugs. For TCCSUP cell line, treatment with TSA (alone or in combination) significantly increased the deposit of AcH3, H3K4me3 and H3K36me2 active marks across VIM promoter (Figure 5B), corroborating the previously observed increase in protein levels for the same conditions (Figure 4B). Although no significant increment in VIM protein levels was previously observed in J82 cells exposed to TSA or DAC+TSA, similar deposit of active marks across VIM promoter was depicted by ChIP (Figure 5A). For both cell lines, a decrease in H4K20me3 repressive mark was also observed in all treatment conditions (Figure 5A and B).

Because the previous results suggested that PTMs might play a role in *VIM* regulation and considering that *VIM* methylation was not detected in normal urothelial cells, we hypothesized whether PTMs might be involved in *VIM* downregulation in normal urothelium. Thus, ChIP-qPCR for known repressive and activating PTMs was performed in SVHUC1 immortalized urothelial cell line. Interestingly, high levels of two active marks – H3K27ac and H3K36^{me2} – and lower levels of two repressive marks - H3K9^{me3} and H3K27^{me3} – were detected across *VIM* promoter in this cell line (Supplementary Figure 3), which may explain the low/moderate VIM protein levels previously detected in these cells (Figure 3). Subsequently, ChIP-seq was performed in a primary normal human urothelial cell line, followed by validation with ChIP-qPCR for the most relevant PTMs. Remarkably, lower levels of active PTMs – H3K9ac and H3K27ac – with concomitant higher levels of repressive marks deposit - H3K4^{me3}, H3K9^{me3} and H3K27^{me3} – was observed, suggesting that histones PTMs are indeed important for the repression of *VIM* expression in normal urothelium (Figure 5C and D).

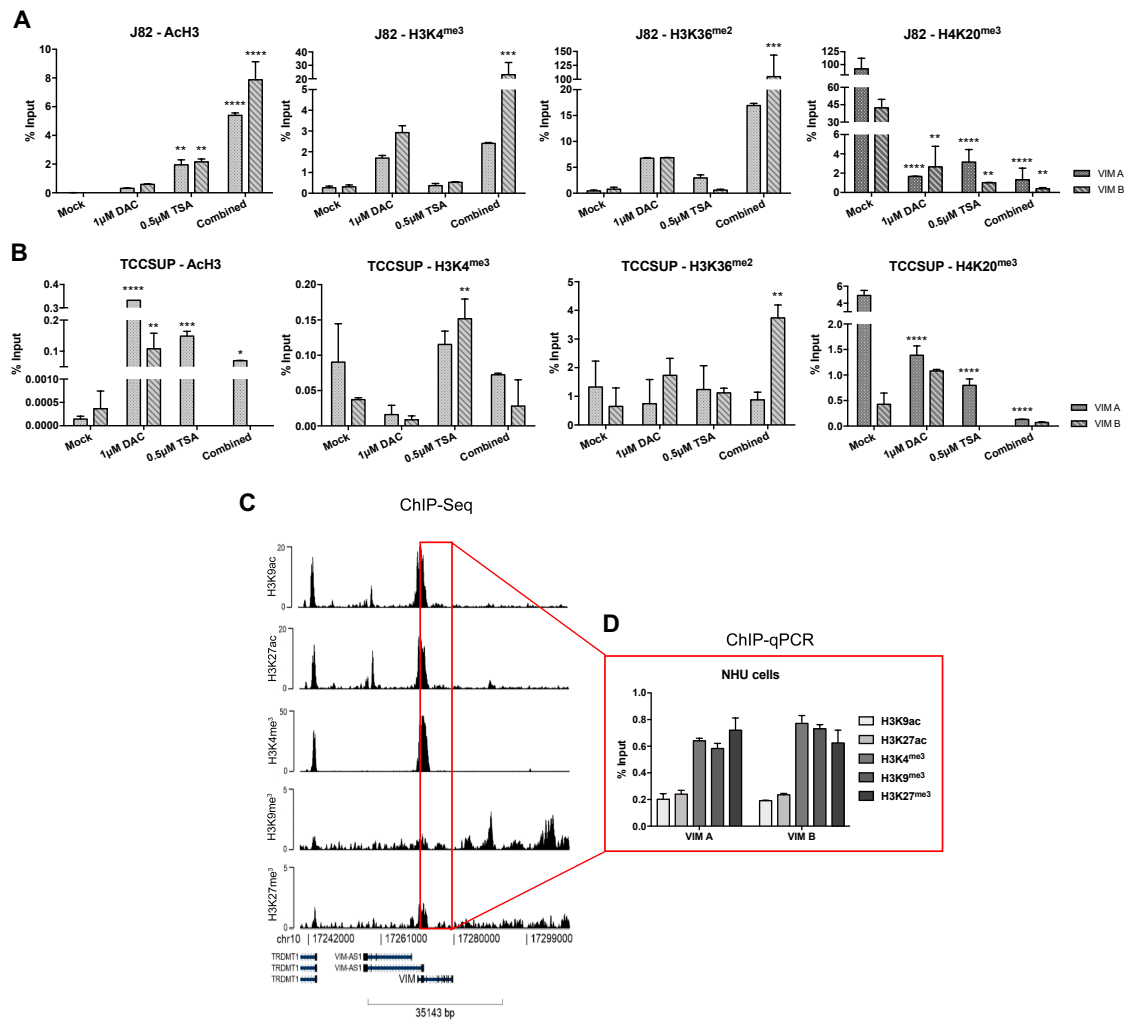


Figure 5. ChIP-qPCR results for **(A)** J82 and **(B)** TCCSUP cell line concerning acH3, H3K4^{me3}, H3K36^{me2} and H4K20^{me3} histones marks across VIM promoter, after treatment with epigenetic modulating drugs. **(C)** ChIP-seq representative results for NHU cells across VIM gene promoter and body. **(D)** ChIP-qPCR results for NHU cells concerning H3K9ac, H3K27ac, H3K4^{me3}, H3K9^{me3} and H3K27^{me3} histones marks across VIM promoter. Results are normalized with the input of total sonicated chromatin.

Phenotypic impact of VIM modulation in BICa

To assess the phenotypic impact of VIM deregulation in BICa, UMUC3 cell line was selected to perform VIM forced knockdown, as this cell line disclosed the highest protein expression (Figure 3). After CRISPR/Cas9 mediated gene knockdown, a significant reduction in VIM protein levels (approximately 70%) was achieved in UMUC3^{KD} cells ($p < 0.0001$; Figure 6A).

Morphological alterations were observed in UMUC3^{KD} cells, displaying more cobblestone (i.e., epithelial-like) features and increased cell-cell contacts, whereas UMUC3^{CTRL} cells

adopted a more elongated (mesenchymal-like) shape (Figure 6B). The observed morphological differences were corroborated by morphometric analysis: UMUC3^{KD} cells presented significantly higher roundness and decreased aspect ratio parameter (Figure 6C). Moreover, UMUC3^{KD} cells disclosed increased ECAD (epithelial marker) expression, compared to control cells, whereas a significant decrease in NCAD (mesenchymal marker) protein levels was found in the same VIM-knockdown cells (Figure 6D).

Although no significant alterations in cell proliferation (Figure 6E) and apoptosis (Figure 6F) were depicted in UMUC3^{KD} vs. UMUC3^{CTRL}, a significant decrease in cell invasion and migration was observed at all time points in cells harboring VIM knockdown (Figure 6G and H).

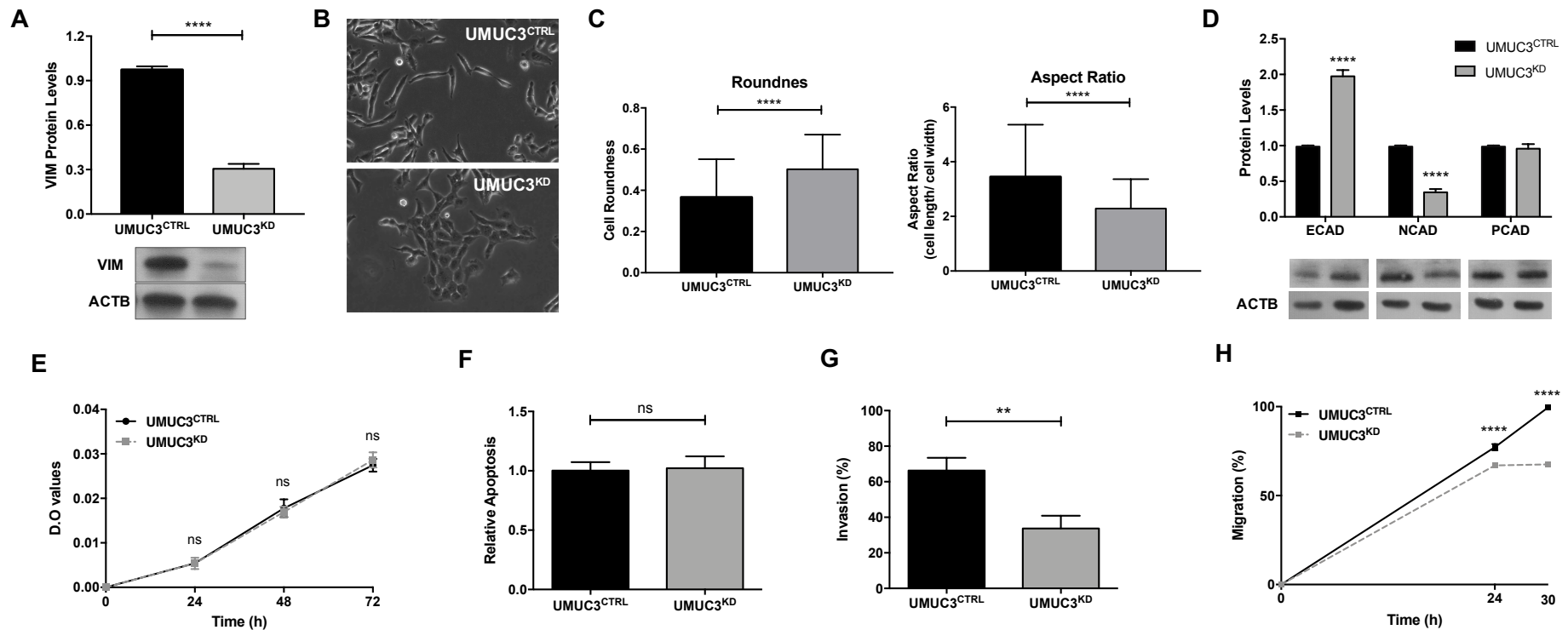


Figure 6. VIM downregulation promotes invasiveness and EMT in bladder cancer cells. (A) Confirmation of VIM knockdown in UMUC3 cell line by Western blot. (B) Representative phase-contrast images of UMUC3^{CTRL} and UMUC3^{KD} cells. (C) Cell morphometric parameters – roundness and aspect ratio (cell length/cell width) – analysis in UMUC3^{CTRL} and UMUC3^{KD} cells. (D) Protein expression of epithelial and mesenchymal markers in UMUC3^{CTRL} and UMUC3^{KD} cells by Western Blot; results are representative of three independent experiments with mean±SD; ****p<0.0001. Effect of VIM knockdown in UMUC3^{CTRL} and UMUC3^{KD} cells at (E) cell viability by MTT assay, (F) apoptosis- cell death by APOPercentage assay, (G) cell invasion by BD Biocoat Matrigel Invasion Chambers and (H) cell migration by wound-healing assay; *p<0.05, **p<0.01, ***p<0.001 and ****p<0.0001; results are representative of three independent experiments with mean±SD, each of them in triplicates.

Discussion

Although clinical management and molecular characterization of BICa have progressed considerably over the past few years, it remains a foremost health concern, due to high incidence and recurrence rates, entailing significant patient morbidity and economic burden. Thus, identification of more accurate biomarkers which might perfect disease monitoring and prognostication will have significant clinical and societal impact. In our previous studies, *VIM* surfaced as potentially useful BICa biomarker, especially quantitative promoter methylation, which disclosed diagnostic and prognostic value (8, 9, 11). Herein, we sought to extend those findings, looking for a putative epigenetic regulation of *VIM* expression, impacting on BICa aggressiveness.

VIM expression and methylation analysis of normal and cancerous (both primary and metastatic) urothelial tissues, confirmed our previous results concerning the specificity of *VIM* promoter methylation in BICa vs. normal urothelium (8, 9, 11). Nonetheless, normal urothelium disclosed very low or even absent levels of *VIM* expression, whereas BICa tissues showed increased expression. Moreover, metastatic lesions disclosed higher *VIM* expression and lower methylation levels, compared to primary BICa. *VIM* is an intermediate filament, characteristic of cells with mesenchymal phenotype, not expressed in most normal epithelia (including urothelium) nor carcinomas (37). However, *VIM* de-novo expression or overexpression has been reported in various epithelial cancers, including those of prostate, breast and lung, associating with increased tumor growth, invasion and poor prognosis (20, 21, 38). Those findings have been related with EMT, a biological process underlying invasive and metastatic properties of malignant epithelial cells. Thus, *VIM* expression pattern in NB, primary and metastatic BICa is consistent with the acquisition of EMT traits by invasive and metastatic neoplastic urothelial cells. As to *VIM* promoter methylation, our findings suggest that it develops during neoplastic transformation, eventually as a bystander alteration in primary tumors, but modulated in secondary lesions to accomplish more effective EMT in metastatic cells.

Although *VIM* promoter methylation and expression patterns in tissues were not fully consistent with a regulatory role, exposure of BICa cell lines to demethylating agent DAC resulted in increased *VIM* expression, confirming that, indeed, *VIM* promoter methylation is involved in gene expression regulation. Nonetheless, additional regulatory mechanisms are required and characterization of histone PTMs across *VIM* promoter in those cell lines uncovered the importance of that epigenetic regulatory mechanisms in the same gene. Remarkably, in a primary normal urothelial cell line, ChIP experiments disclosed deposit of repressive marks at the expense of active PTMs, suggesting that

this mechanism (but not promoter methylation) is determinant for maintaining low *VIM* levels in those normal cells. Thus, we may conclude that both promoter methylation and histone PTMs have important regulatory functions in *VIM* expression in urothelial cells, with histone PMTs playing the foremost role in *VIM* silencing in normal cells, whereas it acts in concert with promoter methylation in cancerous cells to modulate *VIM* expression according to the intensity of invasive and metastatic behavior, orchestrated through EMT.

This hypothesis is further supported by the results of *CDH1* and *CDH2* expression in BICa tissues and its correlation with *VIM* transcript levels, which disclosed *CDH1* downregulation and *CDH2* and *VIM* upregulation in MIBC compared to NMIBC, a pattern which is consistent with ongoing EMT in invasive urothelial cells. The impact of *VIM* expression in cell phenotype was further demonstrated, as malignant urothelial cells in which *VIM* expression was downregulated (re)acquired a more epithelial-like morphology (denoting reversion of EMT) and *in vitro* phenotypic assays disclosed that *VIM* downregulation impaired cell motility, decreasing both cell migration and cell invasion capabilities, although it did not affect cell proliferation or apoptosis. Thus, to the best of our knowledge, this is the first study characterizing the “Vimentin switch” occurring in urothelial carcinogenesis, also demonstrating its biological relevance concerning migratory capabilities of neoplastic cells. Interestingly, we had previously shown that patients with NMIBC disclosing higher *VIM* expression endured poorer disease-free survival, with increased expression depicted along the sequence NB-NMIBC-MIBC-Metastases (39). Furthermore, *VIM* expression has been also associated with BICa grade and stage. Indeed, Baumgart et al. found that *VIM* expression was mainly detected in invasive BICa (31% in MIBC vs. 7% in NMIBC) and positively associated with tumor grade and stage, whereas Paliwal et al. found that *VIM* immunoexpression correlates with BICa stage and grade (40, 41). Thus, *VIM* expression is closely associated with invasive and metastatic properties of malignant urothelial cells and may serve as a marker of disease aggressiveness.

A major limitation of our study is the limited number of cases analyzed. Thus, a larger and, ideally, multicenter study, is required to validate our findings. Furthermore, *in vitro* results should be validated using *in vivo* models [e.g., chick chorioallantoic membrane (CAM) assay] to better support the biological impact of *VIM* expression modulation. Nonetheless, it should be emphasized that our findings are coherent, confirming and extending previous observations from our research team and others, concerning the role of *VIM* in BICa progression.

In conclusion, our findings, based on the analysis of urothelial tissue samples and modulated cell lines, suggest that *VIM* expression is associated with the malignant

urothelial phenotype. We propose a model in which VIM expression is repressed in normal urothelium through histone PTMs and VIM promoter methylation is acquired during neoplastic transformation, most likely as a passenger alteration. Then, as invasive and metastatic phenotypes develop, with some neoplastic cells undergoing EMT, increased VIM expression is achieved through decreased promoter methylation in concert with acquisition of active histone PTMs, enabling migratory capabilities, favoring local invasion and systemic dissemination, fostering disease progression.

References

1. Ferlay J, Ervik M, Lam F, Colombet M, Mery L, Piñeros M, et al. Global Cancer Observatory: Cancer Tomorrow Available from: <https://gco.iarc.fr/tomorrow2018> [
2. Antoni S, Ferlay J, Soerjomataram I, Znaor A, Jemal A, Bray F. Bladder Cancer Incidence and Mortality: A Global Overview and Recent Trends. *Eur Urol.* 2017;71(1):96-108.
3. Sanli O, Dobruch J, Knowles MA, Burger M, Alemozaffar M, Nielsen ME, et al. Bladder cancer. *Nat Rev Dis Primers.* 2017;3:17022.
4. Moch H, Ulbright T, Humphrey P, Reuter V. WHO Classification of Tumours of the Urinary System and Male Genital Organs (4th Edition). IARC: Lyon 2016.
5. Kaufman DS, Shipley WU, Feldman AS. Bladder cancer. *Lancet.* 2009;374(9685):239-49.
6. Babjuk M, Burger M, Comperat EM, Gontero P, Mostafid AH, Palou J, et al. European Association of Urology Guidelines on Non-muscle-invasive Bladder Cancer (TaT1 and Carcinoma In Situ) - 2019 Update. *Eur Urol.* 2019;76(5):639-57.
7. Alfred Witjes J, Le Bret T, Comperat EM, Cowan NC, De Santis M, Bruins HM, et al. Updated 2016 EAU Guidelines on Muscle-invasive and Metastatic Bladder Cancer. *Eur Urol.* 2017;71(3):462-75.
8. Costa VL, Henrique R, Danielsen SA, Duarte-Pereira S, Eknaes M, Skotheim RI, et al. Three epigenetic biomarkers, GDF15, TMEFF2, and VIM, accurately predict bladder cancer from DNA-based analyses of urine samples. *Clin Cancer Res.* 2010;16(23):5842-51.
9. Monteiro-Reis S, Leca L, Almeida M, Antunes L, Monteiro P, Dias PC, et al. Accurate detection of upper tract urothelial carcinoma in tissue and urine by means of quantitative GDF15, TMEFF2 and VIM promoter methylation. *Eur J Cancer.* 2014;50(1):226-33.
10. Padrao NA, Monteiro-Reis S, Torres-Ferreira J, Antunes L, Leca L, Montezuma D, et al. MicroRNA promoter methylation: a new tool for accurate detection of urothelial carcinoma. *Br J Cancer.* 2017;116(5):634-9.
11. Monteiro-Reis S, Blanca A, Tedim-Moreira J, Carneiro I, Montezuma D, Monteiro P, et al. A Multiplex Test Assessing MiR663ame and VIMme in Urine Accurately Discriminates Bladder Cancer from Inflammatory Conditions. *J Clin Med.* 2020;9(2).
12. Chen LM, Chang M, Dai Y, Chai KX, Dyrskjot L, Sanchez-Carbayo M, et al. External validation of a multiplex urinary protein panel for the detection of bladder cancer in a multicenter cohort. *Cancer Epidemiol Biomarkers Prev.* 2014;23(9):1804-12.

13. Avogbe PH, Manel A, Vian E, Durand G, Forey N, Voegelé C, et al. Urinary TERT promoter mutations as non-invasive biomarkers for the comprehensive detection of urothelial cancer. *EBioMedicine*. 2019;44:431-8.
14. Shirahata A, Sakata M, Sakuraba K, Goto T, Mizukami H, Saito M, et al. Vimentin methylation as a marker for advanced colorectal carcinoma. *Anticancer Res*. 2009;29(1):279-81.
15. Jung S, Yi L, Kim J, Jeong D, Oh T, Kim CH, et al. The role of vimentin as a methylation biomarker for early diagnosis of cervical cancer. *Mol Cells*. 2011;31(5):405-11.
16. Ulirsch J, Fan C, Knafl G, Wu MJ, Coleman B, Perou CM, et al. Vimentin DNA methylation predicts survival in breast cancer. *Breast Cancer Res Treat*. 2013;137(2):383-96.
17. Zhou YF, Xu W, Wang X, Sun JS, Xiang JJ, Li ZS, et al. Negative methylation status of vimentin predicts improved prognosis in pancreatic carcinoma. *World J Gastroenterol*. 2014;20(36):13172-7.
18. Cong H, Yao RY, Sun ZQ, Qiu WS, Yao YS, Feng TT, et al. DNA hypermethylation of the vimentin gene inversely correlates with vimentin expression in intestinal- and diffuse-type gastric cancer. *Oncol Lett*. 2016;11(1):842-8.
19. Liu XY, Fan YC, Gao S, Zhao J, Chen LY, Li F, et al. Methylation of SOX1 and VIM promoters in serum as potential biomarkers for hepatocellular carcinoma. *Neoplasma*. 2017;64(5):745-53.
20. Singh S, Sadacharan S, Su S, Belledegrun A, Persad S, Singh G. Overexpression of vimentin: role in the invasive phenotype in an androgen-independent model of prostate cancer. *Cancer Res*. 2003;63(9):2306-11.
21. Kokkinos MI, Wafai R, Wong MK, Newgreen DF, Thompson EW, Waltham M. Vimentin and epithelial-mesenchymal transition in human breast cancer--observations in vitro and in vivo. *Cells Tissues Organs*. 2007;185(1-3):191-203.
22. Chung BM, Rotty JD, Coulombe PA. Networking galore: intermediate filaments and cell migration. *Curr Opin Cell Biol*. 2013;25(5):600-12.
23. Kalluri R, Weinberg RA. The basics of epithelial-mesenchymal transition. *J Clin Invest*. 2009;119(6):1420-8.
24. Nieto MA, Huang RY, Jackson RA, Thiery JP. EMT: 2016. *Cell*. 2016;166(1):21-45.
25. Tran HD, Luitel K, Kim M, Zhang K, Longmore GD, Tran DD. Transient SNAIL1 expression is necessary for metastatic competence in breast cancer. *Cancer Res*. 2014;74(21):6330-40.
26. Krebs AM, Mitschke J, Lasierra Losada M, Schmalhofer O, Boerries M, Busch H, et al. The EMT-activator Zeb1 is a key factor for cell plasticity and promotes metastasis in pancreatic cancer. *Nat Cell Biol*. 2017;19(5):518-29.
27. Denecker G, Vandamme N, Akay O, Koludrovic D, Taminiau J, Lemeire K, et al. Identification of a ZEB2-MITF-ZEB1 transcriptional network that controls melanogenesis and melanoma progression. *Cell Death Differ*. 2014;21(8):1250-61.

28. Kahlert UD, Joseph JV, Kruyt FAE. EMT- and MET-related processes in nonepithelial tumors: importance for disease progression, prognosis, and therapeutic opportunities. *Mol Oncol*. 2017;11(7):860-77.
29. Stemmler MP, Eccles RL, Brabletz S, Brabletz T. Non-redundant functions of EMT transcription factors. *Nat Cell Biol*. 2019;21(1):102-12.
30. Loh CY, Chai JY, Tang TF, Wong WF, Sethi G, Shanmugam MK, et al. The E-Cadherin and N-Cadherin Switch in Epithelial-to-Mesenchymal Transition: Signaling, Therapeutic Implications, and Challenges. *Cells*. 2019;8(10).
31. Mendez MG, Kojima S, Goldman RD. Vimentin induces changes in cell shape, motility, and adhesion during the epithelial to mesenchymal transition. *FASEB J*. 2010;24(6):1838-51.
32. Esteller M. Epigenetics in cancer. *N Engl J Med*. 2008;358(11):1148-59.
33. Costa-Pinheiro P, Montezuma D, Henrique R, Jeronimo C. Diagnostic and prognostic epigenetic biomarkers in cancer. *Epigenomics*. 2015;7(6):1003-15.
34. Edge SB, Compton CC. The American Joint Committee on Cancer: the 7th edition of the AJCC cancer staging manual and the future of TNM. *Ann Surg Oncol*. 2010;17(6):1471-4.
35. Pearson H, Stirling D. DNA extraction from tissue. *Methods Mol Biol*. 2003;226:33-4.
36. Monteiro-Reis S, Lameirinhas A, Miranda-Goncalves V, Felizardo D, Dias PC, Oliveira J, et al. Sirtuins' Deregulation in Bladder Cancer: SIRT7 Is Implicated in Tumor Progression through Epithelial to Mesenchymal Transition Promotion. *Cancers (Basel)*. 2020;12(5).
37. Satelli A, Li S. Vimentin in cancer and its potential as a molecular target for cancer therapy. *Cell Mol Life Sci*. 2011;68(18):3033-46.
38. Al-Saad S, Al-Shibli K, Donnem T, Persson M, Bremnes RM, Busund LT. The prognostic impact of NF-kappaB p105, vimentin, E-cadherin and Par6 expression in epithelial and stromal compartment in non-small-cell lung cancer. *Br J Cancer*. 2008;99(9):1476-83.
39. Lobo J, Monteiro-Reis S, Guimaraes-Teixeira C, Lopes P, Carneiro I, Jeronimo C, et al. Practicability of clinical application of bladder cancer molecular classification and additional value of epithelial-to-mesenchymal transition: prognostic value of vimentin expression. *J Transl Med*. 2020;18(1):303.
40. Baumgart E, Cohen MS, Silva Neto B, Jacobs MA, Wotkowicz C, Rieger-Christ KM, et al. Identification and prognostic significance of an epithelial-mesenchymal transition expression profile in human bladder tumors. *Clin Cancer Res*. 2007;13(6):1685-94.
41. Paliwal P, Arora D, Mishra AK. Epithelial mesenchymal transition in urothelial carcinoma: twist in the tale. *Indian J Pathol Microbiol*. 2012;55(4):443-9.

Supplementary Data (Paper V)

Supplementary Tables

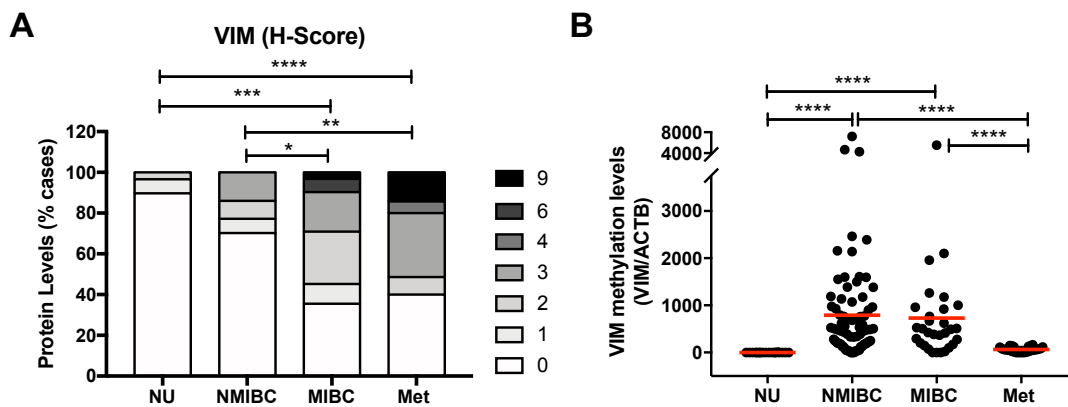
Supplementary Table 1. Primer sequences used in qMSP and RT-qPCR for studied genes.

Target Gene		Sequence (5' - 3')	T _{Annealing} °C
Quantitative Methylation Specific PCR			
ACTB	Forward Primer	TGGTGATGGAGGAGGTTTAGTAAGT	60
	Reverse Primer	AACCAATAAAACCTACTCCTCCCTTAA	
	Probe	FAM - ACCACCACCCAACACACAATAACAAACACA - MGB	
VIM	Forward Primer	TTCGGGAGTTAGTTCGCGTT	60
	Reverse Primer	ACCGCCGAACATCCTACGA	
	Probe	FAM - TCGTCGTTTAGGTTATCGT - MGB	
Real-Time Quantitative PCR			
CDH1	Forward Primer	CTTTGACGCCGAGAGCTACA	64
	Reverse Primer	AAATTCAGTCTGCCAGGACG	
CDH2	Forward Primer	TGTATGTTTTCTTTTCAGTGAATCTT	60
	Reverse Primer	TGGAAAGCTTCTCACGGCAT	
CDH3	Forward Primer	ACGAAGACACAAGAGAGATTGG	60
	Reverse Primer	CGATGATGGAGATGTTTCATGG	
HPRT1	Forward Primer	TGACACTGGCAAACAATGCAGACTT	60
	Reverse Primer	TTCGTGGGGTCCCTTTTCACCAGCAA	

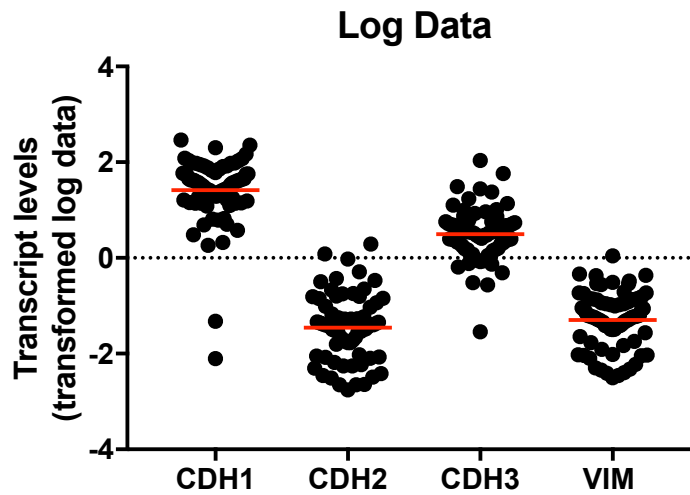
Supplementary Table 2. References of antibodies used in ChIP assays for studied histones and histones posttranslational modifications.

Histone/ Histone PTM	Antibody Reference
H3	ab1791 (Abcam)
AcH3	06-599 (Millipore)
H3K4 ^{me3}	ab8580 (Abcam)
H3K9Ac	17-658 (Millipore)
H3K9 ^{me3}	07-442 (Millipore)
H3K27 ^{me3}	07-499 (Millipore)
H3K27Ac	ab4729 (Abcam)
H3K36 ^{me2}	ab9049 (Abcam)
H4	ab70701 (Abcam)
H4K20 ^{me3}	ab9053 (Abcam)

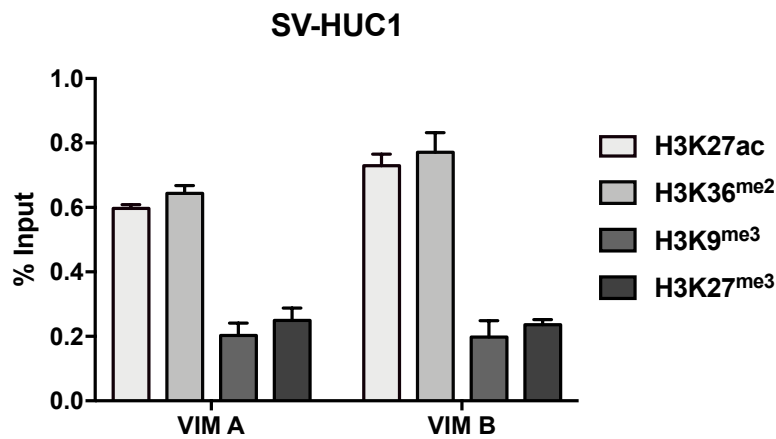
Supplementary Figures



Supplementary Figure 1: *VIM* expression and methylation in normal urothelium, bladder cancer and bladder cancer metastasis. (A) *VIM* immunohistochemistry results for normal urothelium (NU), non-muscle-invasive bladder cancer (NMIBC), muscle-invasive bladder cancer (MIBC) and metastasis (Met) tissues regarding the calculated immunoscore. **(B)** Methylation levels for NU, NMIBC, MIBC and Metastasis tissue samples by qMSP. * $p < 0.05$, ** $p < 0.01$, *** $p < 0.001$ and **** $p < 0.0001$.



Supplementary Figure 2: Comparison between *VIM* and Cadherins genes transcript levels. Graphical representation of transformed log data comparison of *VIM*, *CDH1*, *CDH2* and *CDH3* transcript levels in bladder cancer tissue samples. Transcript levels were obtained by RT-qPCR.



Supplementary Figure 3: ChIP-qPCR for histone PTMs across *VIM* promoter, in SVHUC1 immortalized urothelial cell line. ChIP-qPCR results for H3K27Ac, H3K36^{me2}, H3K9^{me3} and H3K27^{me3} across *VIM* promoter region. VIM A represents a region ~325bp before TSS, and VIM B a region ~600bp before TSS. Results are normalized with the input of total sonicated chrom

CHAPTER V – Major Findings

Chapter III - Diagnostic/Prognostic Epimarkers in Bladder Cancer Voided Urines

Paper I

- The promoters of both miR129-2 and miR663a were found to be methylated in most UC tissue samples, and methylation levels were significantly higher compared with the control group;
- In tissue samples, the panel discriminated UC from normal mucosa with 94.7% sensitivity and 84.0% specificity, corresponding to an AUC of 0.94;
- In urine samples, the methylation test was able to detect UC with 87.8% sensitivity and 84.0% specificity, corresponding to an AUC of 0.942;
- The panel was able to discriminate UC patients both from other genitourinary malignancies and from healthy donors;
- The proportion of true-positive cases detected by the methylation test was significantly higher than that of cytology;
- MiR-663a_{me} differed significantly between non-muscle invasive and muscle invasive UC, as well as between papillary and invasive UC.

Paper II

- Both miR663a and VIM were found hypermethylated (76.6% and 94.4%, respectively) in most BICa tissue samples, and methylation levels were significantly higher compared to normal mucosa;
- The multiplex panel accurately discriminated BICa from NB with 96.3% sensitivity and 88.2% specificity, corresponding to an AUC of 0.982;
- In line with the testing set results, a higher number of malignant samples disclosed significantly higher VIM_{me} and miR663_{me} levels than healthy donors in the urine validation sets;
- The multiplex panel discriminated BICa from HD subjects with 87% sensitivity and 86% specificity, and an AUC of 0.91;

- The proportion of true positive cases detected by the VIMme-miR663me multiplex panel was significantly higher than that of urine cytology;
- VIMme-miR663me levels discriminated BICa from IC patients with 80% sensitivity, 75.3% specificity and, importantly, 86.8% NPV, corresponding to an AUC of 0.836.

Chapter IV – Bladder Cancer Mechanisms and Biology

Paper III

- SIRT1, 2, 4 and 5 expression levels were significantly lower in BICa, whereas SIRT6 and 7 were overexpressed (corroborated by TCGA analysis);
- SIRT7 transcript levels were significantly decreased in MIBC vs. NMIBC;
- In vitro studies showed that SIRT7 downregulation promoted cells migration and invasion;
- Increased EMT markers expression and decreased E-Cadherin were also observed in sh-SIRT7 cells;
- Downregulation of SIRT7 promoted an increase in EZH2 acetylated protein, which resulted in higher deposition of H3K27me3 in E-Cadherin promoter, and its ultimate repression.

Paper IV

- A total of 56/126 (44.4%) BICa specimens showed “basal-like” features (following the Choi et al stratification strategy, based on CK5/6 expression);
- MIBC showed a higher percentage (34/72, 47.2%) of basal-like cases when compared to NMIBC (20/51, 39.2%);
- Fifty one out of fifty six (91.1%) of the cases showing CK5/6 immunoexpression also exhibited immunoexpression of at least one of the markers GATA3/FOXA1;
- For MIBC, “basal-like” cancer developed recurrence in 11/34 cases (32.4%), whereas in “luminal-like” this occurred in a lower proportion of patients [only 5/38 cases (13.2%)];

- A positive correlation was found between transcript levels of GATA3, KRT5 and KRT6A and its protein expression as assessed by immunoeexpression score;
- VIM transcript and protein levels were significantly higher in MIBC compared to NMIBC;
- NMIBC patients with VIM immunoeexpression in tumour cells endured significantly worse DFS.

Paper V

- BICa presented higher VIM transcript, protein and methylation levels, when compared with normal mucosa;
- VIM protein and transcript levels were significantly higher in Metastasis < MIBC < NMIBC groups;
- A significant decrease in ECAD and increase in NCAD transcript levels were observed in MIBC;
- An inverse correlation was found between CDH1 & CDH2 and CDH1 & VIM, whereas a positive correlation was found between CDH1 & CDH3 and CDH2 & VIM;
- DAC exposure significantly increased VIM protein levels in the J82 and TCCSUP cell lines, with a concomitant decrease in methylation levels;
- For TCCSUP cell line, treatment with TSA significantly increased the deposition of active PTMs across VIM promoter;
- For primary NHU cells, lower levels of active PTMs with concomitant higher levels of repressive marks deposition was observed;
- VIM downregulated cells associated with more epithelial features and showed a decrease in migration and invasion capacities.

CHAPTER VI – General Discussion

General Discussion

Bladder carcinomas are leading causes of cancer-related morbidity and mortality worldwide (1). Of those, urothelial cell carcinomas, which might arise in both upper and lower urinary tract, are the most common (2). Regarding the clinical management of these neoplasms, there is an urgent need for urine-based testing implementation. Since there are currently no routine screening tests for BICa, the majority of cases are only discovered after patients report the occurring of blood in their urine. Despite this, and although haematuria is one of the most common symptoms of BICa, it is estimated to happen on only 10% of all BICa cases and it is a shared symptom for other common disorders, such as urinary-tract infections and inflammation. Furthermore, the other frequently reported symptoms are also commonly shared by these bladder conditions, such as the increased urge and frequency of urination, which in many cases can also be accompanied by pain. The current gold standard for tracking these symptoms is the cystoscopy, but this invasive procedure is both uncomfortable for patients and expensive for health care systems. Moreover, in some cases, cystoscopy is also unable to detect some initial forms of BICa, such as carcinoma in situ, which may evolve to invasive BICa in a short period of time. Furthermore, another current problem regarding BICa is the high recurrence rate among NMIBC cases, which not only may occur several times for the same patient, but also may come back as more aggressive and invasive disease (3, 4). Taking all this into account, the search for non-invasive, sensitive and highly specific urine-based biomarkers for early detection and monitoring of BICa is a hot topic among clinicians and researchers who work with this model. Indeed, in **Chapter III** of this Thesis, our focus was to aid solving this need by exploring the value of methylation-based biomarkers in BICa diagnostic and prognostic management.

Where in Chapter III we focused on current issues in BICa clinical management, a panorama where the disease already exists, in **Chapter IV** we aimed at looking at the molecular mechanisms, especially epigenetic-related, inherent to the disease arising and progression. Thus, the results obtained from the studies composing Chapters III and IV provide new insights and concepts within BICa model, namely:

- Two new methylation-based biomarker panels for BICa management. The first one focusing on urothelial cancer detection (Paper I), and the second focusing on BICa discrimination within an “at-risk” population (Paper II);
- The novel function of the HDAC SIRT7 in BICa invasive phenotype (Paper III);
- The unexplored contribution of the new molecular classification of BICa in NMIBC cases (Paper IV);

- The newly described epigenetic regulation of Vimentin expression in normal and neoplastic urothelial cells, and its contribution to acquisition of invasive and metastatic phenotypes (Paper V).

Thereunder, the most relevant results of the manuscripts previously presented are discussed.

Two new methylation-based biomarker panels for BICa management

It is well established that DNA methylation plays a key role in the repression of several cancer-related genes, which explains the deregulation of methylation levels through cells neoplastic transformation. Also widely altered in cancer is the expression of miRNAs, which are important regulators of gene expression. Moreover, these miRNAs can also be targets of deregulation in cancer, mainly through their promoter methylation. Indeed, many authors have been exploring the use of miRNAs promoter methylation as biomarkers for cancer detection. With that in mind, in our first study – **Paper I** – we explored the usefulness of a panel of two previously identified (5) miRNAs promoter methylation – miR-129-2 and miR-663a – in the detection of urothelial carcinomas (BICa and UTUC). Indeed, there is a current need for urinary biomarkers able to discriminate UCs, which gather biological and genomic similarities, from the most common genitourinary malignancies – prostate and renal carcinomas (6). The studied methylation panel was able to discriminate UC, not only from normal urothelial mucosa in a tissue set of samples, but also against healthy volunteers and, more importantly, prostate and kidney cancer patients in a urine-testing set, with high sensitivity and specificity. These results are particularly important because they allowed for the discrimination of UTUC from renal cell carcinoma, which are frequently difficult to discern in gold standard examination due to their anatomical proximity. Moreover, the studied methylation panel sensitivity was also much superior to the respective results of urine cytology for the same cases. Despite cytology providing important information about exfoliated cells in urine, many researchers and clinicians have expressed their concerns regarding its use as an auxiliary test for UC detection, due to low sensitivity in detecting non-invasive urothelial neoplasms (7, 8). The main novelty of our proposed panel is the ability to detect all UCs, whereas the majority of other comparable studies focused on only BICa or UTUC separately, and not all compared their results with samples from other genitourinary neoplasms, which we found important to assess (9). Indeed, since our results were published, and to the best of our knowledge, no new studies within these specificities were divulged. Despite this, it is important to mention that our panel is a laboratory-

developed test, and larger multicentre prospective studies are required to better assess its for in vitro diagnostic (IVD) settings.

Another important issue regarding biomarker research in BICa is the need for a highly specific test which may be offered to an “at-risk” population, whom share the same common previously mentioned BICa symptoms, such as haematuria. Taking into consideration this demand, we designed the study which originated **Paper II**. Herein, we used the most promising methylation biomarkers explored in two previously published panels - miR-663a (miR663a_{me}) from Paper I, and Vimentin (VIM_{me}) from a previous work from our research team (10) – and we sought to use these markers in voided urines as a multiplex panel for accurate discrimination of BICa from patients afflicted with inflammatory conditions of the genitourinary tract. The most important result obtained in this study was the ability of VIM_{me}-miR663a_{me} multiplex test to discriminate BICa cases from patients with inflammatory conditions with 80% sensitivity and 87% NPV, which are very promising results taking into account that the main goal is to offer this test to an “at-risk” population. In these cases, a test with high NPV is crucial because it could avoid unnecessary cystoscopies. Indeed, and despite the need for further validation in larger multicentre studies, the ultimate implementation of this panel on clinical practice might help better stratify patients for confirmatory, invasive examinations, ultimately improving the cost-effectiveness of BICa diagnosis and management by reducing the number of unnecessary cystoscopies (11).

Currently, only three methylation-based tests are approved for IVD use in the context of BICa management: AssureMDx and Bladder CARETM tests for diagnostic use, and EpiCheck[®] test for post-treatment monitoring (12). Whereas Bladder CARETM test performed its validation using only healthy donor’s as control samples, AssureMDx took a more similar approach to ours (13). AssureMDx combines the evaluation of OTX1, ONECUT2 and TWIST genes promoter methylation and the mutational load of FGFR3, TERT and HRAS, and intends to assess the risk of developing BICa in urine samples of patients with haematuria. This test was validated in a prospective, multicentre study, with a cohort similar to ours, comprised by 97 BICa patients and 103 non-malignant haematuria patients (13). The reported sensitivity and specificity for BICa detection was 93% and 86%, respectively. Although our VIM_{me}-miR663a_{me} test reached a lower sensitivity and specificity, it should be mentioned that we have performed our validation in a bigger group of non-malignant haematuria patients (N= 174). Moreover, when using an approach similar to those used in the AssureMDx validation paper, where NPV was calculated taking into account the predicted percentage of BICa cases in a population of haematuria patients (5%), our NPV increased to 99% (data not published) (13,14). This result reinforces the value of the VIM_{me}-miR663a_{me} panel as an auxiliary test which might

be offered to patients with haematuria. Moreover, our test uses a single detection technique (qMSP) to provide a result, whereas the aforementioned AssureMDx relies on both methylation and mutation analysis, which difficulties its implementation in clinical practice workflow. Indeed, although the usage of a single biomarker may be inadequate and a combination of several biomarkers better informs clinical decision, it is known that the greater the number of genes to be analysed, the higher cost associated. Therefore, panels should be constituted by a minimum number of biomarkers in order to enhance their applicability in clinical settings. Indeed, this may be the main obstacle in the implementation of EpiCheck test into the clinical practice, which is based in the analysis of 15 genes promoter methylation in urines of patients previously diagnosed with BICa, in order to detect possible recurrences and to reduce the number of follow-up cystoscopies (15). This methylation-based test is, currently, one of the IVD tests with most advanced clinical validation for post-treatment monitoring/surveillance purposes, and it developed to be used in combination with cytology to reduce the invasiveness in the follow-up of NMIBC patients. We propose a similar algorithm for the VIM_{me}-miR663a_{me}, to be applied in an early stage of primary disease detection. Finally, we have also found that high miR663a_{me} independently predicted worse clinical outcome, especially for patients with invasive BICa. This is an important result, considering the aforementioned difficulty in stratifying patients which would benefit on a stricter and more personalized treatment options and follow-up (2). Hence, miR663a_{me} analysis might also provide relevant information for patient monitoring.

The quest for biomarkers in BICa, especially epigenetic/methylation-based, is not new, and it is the research focus of various teams (16, 17). As the number of proposed detection and prognostic markers in these studies increases, in Chapter III we have proposed answers to current demands: to find highly specific markers, either to be used among other genitourinary malignancies (Paper I), or among benign urogenital tract conditions (Paper II), which could ultimately help in better manage this disease.

The novel function of the HDAC SIRT7 in BICa invasive phenotype

As a long-term interest of our research team, we have started by looking at the role of HDACs family of Sirtuins in BICa. Sirtuins are a class of epigenetic regulators that modulate the activity of their targets by removing covalently attached acetyl groups (18). These proteins have been clearly shown as key factors in regulating important cellular processes, with functions described in the central/peripheral nervous system, cardiovascular and immune systems, as well as tissue regeneration. Because of their biological function in cells, sirtuins are also deregulated in most age-related diseases, especially metabolic disorders and cancer (19). Thus, better understanding of the

biological role of these unique enzymes in tumorigenesis might provide novel putative therapeutic targets. Although sirtuins have been characterized in various neoplasms, their putative role in BICa remained elusive. Thus, in **Paper III** we sought to comprehensively characterize all sirtuins expression in BICa tissues and provide insights about a majorly deregulated sirtuin – SIRT7 – and the molecular mechanisms underlying BICa cells invasive phenotype. Herein, we have started by showing that all sirtuins, except for SIRT3, were deregulated in BICa tissues when compared with normal mucosa, providing a global analysis of all members of the family in the same samples' cohorts (both ours and TCGA) and bringing together the previous fragmented knowledge about the expression of these molecules in BICa. This analysis allowed for the observation that a particular sirtuin – SIRT7 – which was globally overexpressed in BICa, had its expression reduced in more aggressive tumours, suggesting a possible dual role in BICa carcinogenesis. This hypothesis was enhanced by the observed decrease in overall survival in BICa patients with lower SIRT7 expression for the TCGA cohort. Taking this into consideration, we then sought to characterize the effects of its deregulated expression at the molecular level and observed a decrease in both cell migration and invasion capabilities in SIRT7 *in vitro* downregulated cell lines, which suggested a putative association between SIRT7 and EMT, a process that is key for tumour invasion and metastization. This hypothesis was then confirmed as SIRT7 knockdown significantly associated with decreased E-Cadherin expression and augmented expression of the mesenchymal N-Cadherin and EMT-inducing transcription factors (SLUG and SNAIL). Moreover, we have also found that the mechanism by which SIRT7 affects CDH1 expression, and thus EMT, is probably linked to EZH2 acetylation in the absence of this HDAC protein, contributing to the H3K27^{me3} mark deposition at CDH1 promoter, and leading to its ultimate transcription repression. This mechanism, in synergy with EMT transcription factors' upregulation (SNAIL and SLUG), might then lead to a shift from epithelial to mesenchymal phenotype, allowing for increased cancer cell motility. The major novelty of this work is the newly proposed SIRT7-EZH2-CDH1 regulation axis, fostering BICa invasiveness.

The role of SIRT7 in cancer has been highly debated. SIRT7 is abnormally increased in several epithelial cancers, associating with tumour promotion and cell growth (20). Paradoxically, SIRT7 also inhibits breast cancer metastasis and oral squamous cell carcinoma by antagonizing TGF- β signalling (21,22). Indeed, Tang et al. has recently demonstrated that SIRT7 was transcriptionally downregulated through TGF- β , which in turn has also a dual role in cancer (23,24). Generally, TGF- β has a tumour suppressor effect by inducing cell cycle arrest and apoptosis. However, malignant tumors usually bypass this adverse effect by acquiring mutations on TGF- β receptors or SMADs, for

example, which provide them with a growth advantage (24). This concept is in-line with the oncogenic properties of SIRT7 in the majority of epithelial cancers. On the contrary, for tumours where TGF- β signalling is intact and involved in promoting EMT, SIRT7 is usually downregulated (22). Some studies in BICa reported that TGF- β overexpression was significantly associated with high tumour grade and advanced pathologic stage (25, 26). Gathering these results, we may speculate that the mechanism by which SIRT7 deregulation occurs along BICa carcinogenesis was by TGF- β interference.

Although additional studies to prove on exactly how SIRT7 deregulated expression occurs along BICa carcinogenesis are needed, we have provided insights on a new pathway implicated in aggressive phenotype, and which may lead to new putative therapeutic targets. Indeed, there is a fresh demand for new BICa therapeutic options, as a considerable percentage of BICa patients do not benefit from current treatment options, which, apart for new immunotherapy-based drugs, did not overly changed in the last decades (27, 28). Indeed, nowadays, clinicians still have to deal with a high number of patients with disease recurrence and progression and, as a result, patients endure a long follow-up (29).

The contribution of the new molecular classification of BICa in NMIBC cases

Since BICa therapeutic landscape did not suffer major improvements in the recent years, excluding the approval of immune checkpoint inhibitors for metastatic cases, scientists became more interested in exploring the molecular basis of this neoplasms, which have resulted in an effort to reach a molecular classification based on different molecular traits, either for all urothelial carcinomas, or focusing on NMIBC and MIBC separately. Although specific differences in classification emerge out of different research teams' analyses, they all share as an overlapping feature the existence of two major BICa subtypes—basal/squamous and luminal—for MIBC cases (30). Briefly, basal/squamous subtype is mainly composed of advanced stage tumours and metastatic disease, being enriched in inactivating mutations and deletions of *TP53* and *RB1*, whereas the luminal subtype is associated with papillary histopathological features and enriched in *FGFR3* mutations (31). To simplify this stratification, an effort has been made to reach a single list of specific biomarkers (such as *FOXA1*, *GATA3*, *KRT5/6* and *KRT14*) that can be effectively translated from wide screening genomic and transcriptomics analyses into the clinic for any BICa setting (both MIBC or NMIBC), but this has not been achieved yet. Moreover, and as previously mentioned, the role of EMT in BICa progression and prognosis is of major interest and could provide answers on how to translate this newly found molecular traits into BICa clinical outcomes. Herein, in **Paper IV**, we aimed to characterize the expression of a set of immunohistochemistry markers for defining both

luminal and basal/squamous subtypes in a well characterized patient cohort of BICa, looking for clinicopathological correlates and testing their potential for clinical application, both within MIBC and, especially, NMIBC cases. Moreover, we have also explored the value of adding the expression of VIM, as a classic EMT marker, to the risk stratification strategy. In this regard, we have chosen VIM because among the EMT markers it is routinely performed in all Pathology departments and it has been consistently associated with BICa detection (Paper II) and prognosis, including in our previous *in silico* analysis (**Review Paper I**). One of our main conclusions from this work is that there was a substantial overlapping in protein expression of luminal and basal markers within BICa specimens, which maintained across both MIBC and NMIBC. Although we believe that this may be explained by intratumor heterogeneity and specific tumour cell clones within the tumour mass, this result also points out to a major issue, which is finding specific tissue markers for each molecular subtype group (30). One of our goals was to perform the analysis in both MIBC and NMIBC cases, as the majority of studies focus on the former, which are the focus of the transcriptomic-based classifications. In here, some NMIBC also depicted basal features, and although this did not dictate differences in recurrence, we hypothesize that it might be due to small size of our cohort, and it should definitely be a target of further analysis in larger cohorts. Despite the need for more specific tissue markers to provide a clear stratification of cases, in general, we conclude that the proposed classification remains informative and should be pursued for validation in clinical practice by prospective, multicentre studies. The heterogeneity of data and methods hinders the prognostic and predictive value of BICa molecular classification to some extent. Indeed, a recent systematic review by Parizi et al. evaluated, in 66 published studies, the predictive value of molecular subtypes on oncological outcomes and response to cancer treatment in patients with BICa (32). The authors concluded that, although current BICa molecular classification is indeed an important predictor of tumour prognosis and can identify patients who would be most likely to benefit from different treatment schemes, fine-tuned prospective studies are still necessary to verify the best consensus on molecular classification for accurate prognosis and predictive value evaluation.

Moreover, and because EMT is a major important process for the acquisition of an aggressive phenotype by cancer cells, we decided to also investigate, for the same set of samples, the contribution of VIM, as a mesenchymal marker, in predicting prognosis of BICa patients (33). Indeed, and after the observation of an increase in VIM protein expression within increasingly aggressive samples, we have showed that NMIBC patients disclosing higher VIM expression had shorter disease-free survival. As vimentin immunohistochemistry is not routinely performed when assessing BICa specimens, we

propose that, after luminal vs. basal-like BICa cases stratification, this protein could have clinical potential as a prognostic marker within these groups, although larger studies are needed to confirm this hypothesis.

The newly described epigenetic regulation of Vimentin expression in normal and neoplastic urothelial cells

One of the most well-performing markers proposed in Papers II and IV, either for detection or prognosis of BICa, respectively, was VIM. Vimentin is an intermediate filament, characteristic of cells with mesenchymal phenotype, not expressed in most normal epithelia (including urothelium) neither in most carcinomas (34). However, VIM de-novo expression or overexpression has been reported in various epithelial cancers, associating with increased tumour growth, invasion and poor prognosis (35). Indeed, and as previously mentioned, VIM expression has been associated with EMT, constituting a well-known mesenchymal marker. Nonetheless, the role of vimentin in EMT development needs further clarification, and it is not established how VIM expression is fine-tuned from its absence in normal urothelial cells to its overexpression in invasive carcinoma cells. Indeed, a deeper understanding of the EMT molecular events would allow the identification of the subset of patients that harbour aggressive tumours, which require a different treatment approach and managing procedures. Moreover, the discovery of the molecular mechanisms, which lead to this "switch" of expression of vimentin, may also point to new therapeutic agents to prevent BICa progression and metastization. Thus, in our final work - **Paper V** - we aimed to investigate VIM expression and regulation in normal urothelium and BICa, and if VIM deregulation is implicated in the disease progression and aggressiveness. As we had previously observed in our previous papers, we began by confirming that BICa tissue samples disclosed higher VIM methylation levels than normal urothelium samples, and that these levels decreased in metastases tissues. Regarding normal urothelium samples, and because one of the major goals of this work was to pinpoint if VIM expression is epigenetically regulated in these cells, we have first focused our attention in the methylation analysis for this group of samples, where we found that VIM methylation was null/undetected. We then hypothesised if histone PTMs could be influencing gene repression and performed, for that purpose, ChIP-seq and ChIP-qPCR experiments in normal urothelium primary cells, where we detected a high deposition of repressive marks at the expense of active PTMs through VIM promoter region, suggesting that this mechanism has a role in maintaining low VIM expression levels in normal urothelium. This finding was very important to consolidate the putative role of epigenetic mechanisms in VIM regulation in urothelial cells. Indeed, when we exposed immortalized BICa cells to epigenetic modulating drugs,

we observed not only a deregulation in VIM methylation levels, but also a differential deposition of histone PTMs across its promoter, reinforcing the importance of different layers of epigenetic regulatory mechanisms for this gene. Thus, and to the best of our knowledge, this is the first study which thoroughly attempts to describe how the Vimentin “switch” occurs in normal to cancer urothelial cells and the importance of regulatory epigenetic mechanisms for this feature, which could open new pathways for epigenetic-based therapies with this specific molecular target (36).

Moreover, the second major goal of this work was to unveil the phenotypic impact of VIM deregulation in BICa cells. For that purpose, and after *in vitro* CRISPR-Cas9 forced knockdown of VIM gene, phenotypic assays demonstrated that, although VIM downregulation did not affect cell proliferation or apoptosis, it impaired cell motility, decreasing both cell migration and cell invasion capabilities. These effects, combined with the negative correlation between VIM and ECAD and positive association between VIM and NCAD, either in tissue or VIM modulated cells, immediately consolidated its putative association with EMT. Moreover, the morphological changes in VIM knockdown cells towards epithelial-like features also corroborated the previous observations. Some authors have proposed that neoplastic cells present Vimentin at its surface, and this finding has led to efforts to target it as a potential therapy. For example, Noh et al. found that glioblastoma multiforme stem cells expressing surface vimentin had higher spheroid formation capabilities, and that treatment of these cells with an anti-VIM antibody lead to internalization of surface vimentin, which in turn associated with lower cell viability due to apoptosis and diminished tumour growth in a mouse model (37, 38). With these concepts, along with our new results regarding VIM regulation in BICa, we propose that future efforts should be made to study VIM as a biological target and modulator of BICa cells migratory capabilities.

Bringing together the major outcomes of this Thesis, we can clearly separate them into the two above mentioned Chapters III and IV. Where in the former we suggested new epigenetic markers for possible future implementation into the clinical management of BICa, in the latter we focused on highlighting new mechanisms which could help in a better understanding on how the disease occurs and the suggestion of new possible therapy targets (Figure X).

Uncovering the role of epigenetic mechanisms in Bladder Cancer aggressiveness: from Biology to Clinical setting

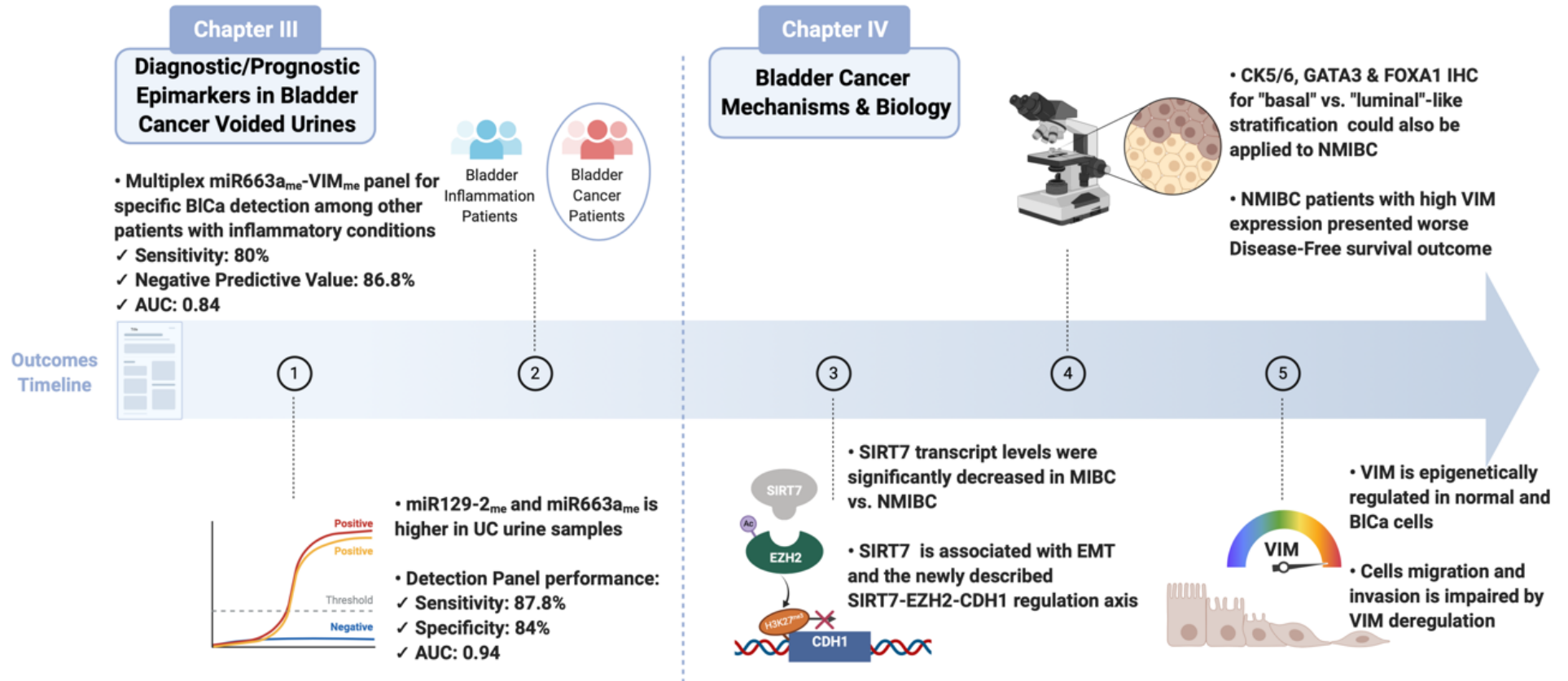


Figure 1. Schematic representation of the major outcomes achieved in this doctoral Thesis. Created with BioRender.com.

References (Chapter VI)

1. Antoni S, Ferlay J, Soerjomataram I, Znaor A, Jemal A, Bray F. Bladder Cancer Incidence and Mortality: A Global Overview and Recent Trends. *Eur Urol.* 2017;71(1):96-108.
2. Sanli O, Dobruch J, Knowles MA, Burger M, Alemozaffar M, Nielsen ME, et al. Bladder cancer. *Nat Rev Dis Primers.* 2017;3:17022.
3. Babjuk M, Burger M, Comperat EM, Gontero P, Mostafid AH, Palou J, et al. European Association of Urology Guidelines on Non-muscle-invasive Bladder Cancer (TaT1 and Carcinoma In Situ) - 2019 Update. *Eur Urol.* 2019;76(5):639-57.
4. Alfred Witjes J, Lebrecht T, Comperat EM, Cowan NC, De Santis M, Bruins HM, et al. Updated 2016 EAU Guidelines on Muscle-invasive and Metastatic Bladder Cancer. *Eur Urol.* 2017;71(3):462-75.
5. Torres-Ferreira J, Ramalho-Carvalho J, Gomez A, Menezes FD, Freitas R, Oliveira J, et al. MiR-193b promoter methylation accurately detects prostate cancer in urine sediments and miR-34b/c or miR-129-2 promoter methylation define subsets of clinically aggressive tumors. *Mol Cancer.* 2017;16(1):26.
6. Zhang Z, Furge KA, Yang XJ, Teh BT, Hansel DE. Comparative gene expression profiling analysis of urothelial carcinoma of the renal pelvis and bladder. *BMC Med Genomics.* 2010;3:58.
7. Shariat SF, Karam JA, Raman JD. Urine cytology and urine-based markers for bladder urothelial carcinoma detection and monitoring: developments and future prospects. *Biomark Med.* 2008;2(2):165-80.
8. Comploj E, Trenti E, Palermo S, Pycha A, Mian C. Urinary cytology in bladder cancer: why is it still relevant? *Urologia.* 2015;82(4):203-5.
9. Bhat A, Ritch CR. Urinary biomarkers in bladder cancer: where do we stand? *Curr Opin Urol.* 2019;29(3):203-9.
10. Costa VL, Henrique R, Danielsen SA, Duarte-Pereira S, Eknaes M, Skotheim RI, et al. Three epigenetic biomarkers, GDF15, TMEFF2, and VIM, accurately predict bladder cancer from DNA-based analyses of urine samples. *Clin Cancer Res.* 2010;16(23):5842-51.
11. Leal J, Luengo-Fernandez R, Sullivan R, Witjes JA. Economic Burden of Bladder Cancer Across the European Union. *Eur Urol.* 2016;69(3):438-47.
12. Taryma-Lesniak O, Sokolowska KE, Wojdacz TK. Current status of development of methylation biomarkers for in vitro diagnostic IVD applications. *Clin Epigenetics.* 2020;12(1):100.

13. van Kessel KE, Beukers W, Lurkin I, Ziel-van der Made A, van der Keur KA, Boormans JL, et al. Validation of a DNA Methylation-Mutation Urine Assay to Select Patients with Hematuria for Cystoscopy. *J Urol*. 2017;197(3 Pt 1):590-5.
14. Gonzalez AN, Lipsky MJ, Li G, Rutman MP, Cooper KL, Weiner DM, et al. The Prevalence of Bladder Cancer During Cystoscopy for Asymptomatic Microscopic Hematuria. *Urology*. 2019;126:34-8.
15. Mancini M, Righetto M, Zumerle S, Montopoli M, Zattoni F. The Bladder EpiCheck Test as a Non-Invasive Tool Based on the Identification of DNA Methylation in Bladder Cancer Cells in the Urine: A Review of Published Evidence. *Int J Mol Sci*. 2020;21(18).
16. Jeronimo C, Henrique R. Epigenetic biomarkers in urological tumors: A systematic review. *Cancer Lett*. 2014;342(2):264-74.
17. Larsen LK, Lind GE, Guldborg P, Dahl C. DNA-Methylation-Based Detection of Urological Cancer in Urine: Overview of Biomarkers and Considerations on Biomarker Design, Source of DNA, and Detection Technologies. *Int J Mol Sci*. 2019;20(11).
18. Vaquero A. The conserved role of sirtuins in chromatin regulation. *Int J Dev Biol*. 2009;53(2-3):303-22.
19. Mei Z, Zhang X, Yi J, Huang J, He J, Tao Y. Sirtuins in metabolism, DNA repair and cancer. *J Exp Clin Cancer Res*. 2016;35(1):182.
20. Wu D, Li Y, Zhu KS, Wang H, Zhu WG. Advances in Cellular Characterization of the Sirtuin Isoform, SIRT7. *Front Endocrinol (Lausanne)*. 2018;9:652.
21. Li W, Zhu D, Qin S. SIRT7 suppresses the epithelial-to-mesenchymal transition in oral squamous cell carcinoma metastasis by promoting SMAD4 deacetylation. *J Exp Clin Cancer Res*. 2018;37(1):148.
22. Tang X, Shi L, Xie N, Liu Z, Qian M, Meng F, et al. SIRT7 antagonizes TGF-beta signaling and inhibits breast cancer metastasis. *Nat Commun*. 2017;8(1):318.
23. Tang X, Li G, Su F, Cai Y, Shi L, Meng Y, et al. HDAC8 cooperates with SMAD3/4 complex to suppress SIRT7 and promote cell survival and migration. *Nucleic Acids Res*. 2020;48(6):2912-23.
24. Akhurst RJ, Derynck R. TGF-beta signaling in cancer--a double-edged sword. *Trends Cell Biol*. 2001;11(11):S44-51.
25. Stojnev S, Krstic M, Cukuranovic Kokoris J, Conic I, Petkovic I, Ilic S, et al. Prognostic Impact of Canonical TGF-beta Signaling in Urothelial Bladder Cancer. *Medicina (Kaunas)*. 2019;55(6).
26. Gupta S, Hau AM, Al-Ahmadie HA, Harwalkar J, Shoskes AC, Elson P, et al. Transforming Growth Factor-beta Is an Upstream Regulator of Mammalian Target of Rapamycin Complex 2-Dependent Bladder Cancer Cell Migration and Invasion. *Am J Pathol*. 2016;186(5):1351-60.

27. Davarpanah NN, Yuno A, Trepel JB, Apolo AB. Immunotherapy: a new treatment paradigm in bladder cancer. *Curr Opin Oncol*. 2017.
28. Song YP, McWilliam A, Hoskin PJ, Choudhury A. Organ preservation in bladder cancer: an opportunity for truly personalized treatment. *Nat Rev Urol*. 2019;16(9):511-22.
29. Soukup V, Babjuk M, Bellmunt J, Dalbagni G, Giannarini G, Hakenberg OW, et al. Follow-up after surgical treatment of bladder cancer: a critical analysis of the literature. *Eur Urol*. 2012;62(2):290-302.
30. Kamoun A, de Reynies A, Allory Y, Sjudahl G, Robertson AG, Seiler R, et al. A Consensus Molecular Classification of Muscle-invasive Bladder Cancer. *Eur Urol*. 2020;77(4):420-33.
31. McConkey DJ, Choi W. Molecular Subtypes of Bladder Cancer. *Curr Oncol Rep*. 2018;20(10):77.
32. Kardoust Parizi M, Margulis V, Compe Rat E, Shariat SF. The value and limitations of urothelial bladder carcinoma molecular classifications to predict oncological outcomes and cancer treatment response: A systematic review and meta-analysis. *Urol Oncol*. 2020.
33. Nieto MA, Huang RY, Jackson RA, Thiery JP. EMT: 2016. *Cell*. 2016;166(1):21-45.
34. Chung BM, Rotty JD, Coulombe PA. Networking galore: intermediate filaments and cell migration. *Curr Opin Cell Biol*. 2013;25(5):600-12.
35. Satelli A, Li S. Vimentin in cancer and its potential as a molecular target for cancer therapy. *Cell Mol Life Sci*. 2011;68(18):3033-46.
36. Strouhalova K, Prechova M, Gandalovicova A, Brabek J, Gregor M, Rosel D. Vimentin Intermediate Filaments as Potential Target for Cancer Treatment. *Cancers (Basel)*. 2020;12(1).
37. Noh H, Yan J, Hong S, Kong LY, Gabrusiewicz K, Xia X, et al. Discovery of cell surface vimentin targeting mAb for direct disruption of GBM tumor initiating cells. *Oncotarget*. 2016;7(44):72021-32.
38. Noh H, Zhao Q, Yan J, Kong LY, Gabrusiewicz K, Hong S, et al. Cell surface vimentin-targeted monoclonal antibody 86C increases sensitivity to temozolomide in glioma stem cells. *Cancer Lett*. 2018;433:176-85.

CHAPTER VII – Conclusions and Future Perspectives

Conclusions and Future Perspectives

Albeit this Thesis provides both clinical and mechanistic views of how epigenetic mechanisms deregulation can either be used as auxiliary tools for BICa detection and prognostic management and as direct players in various steps of bladder carcinogenesis processes, there are some interesting questions and hypothesis that either derived from these results or are emergent topics in current BICa research landscape.

1) Validate proposed epigenetic markers for BICa detection and prognostic.

In this Thesis we propose two panels of methylation markers which could be potentially used in clinical practice to improve BICa detection, and which could also carry prognostic value for some patients. Although these results are promising, a proper multicentre validation, with larger cohorts of patients, should be carried to confirm its application and test-offering to a target population. Thus, an investment by governments and hospitals should be done, to apply the results of translational research into clinical practice.

2) Investigate the use of new epigenetic markers for BICa therapeutic surveillance.

Current therapeutic options for BICa are somehow limited. While the first line treatment for the majority of BICa cases is the surgical removal of the tumour or the whole bladder, many patients also fulfil a therapeutic drug-based plan as part of their treatment plan, which depends on tumour stage and grade, as well as other factors. These include BCG or Mitomycin C bladder instillations for patients with NMIBC disease or systemic NAC therapies for MIBC cases. However, the high recurrence rate or the inability to fulfil therapeutic treatment plans due to associated comorbidities is still a problem. Thus, there is an urgent need to find specific biomarkers which could help better predict treatment response and whose patients would benefit from a specific therapy. The advantage of studying epigenetic-based biomarkers is the fact that the majority of main epigenetic mechanisms, such as methylation, is highly susceptible of changes in cell's microenvironment, which is highly shuffled through a drug-based treatment.

3) Explore new therapeutic options, especially as a result of immuno-oncology and checkpoint inhibitors.

In the last decade, immunotherapy has changed the landscape of cancer treatment. Although some drugs have been used in a specific group of BICa, with the stratification

of patients based on their tumour specific molecular traits, the future aims at finding personalized treatment options according to these features. In this regard, combining epigenetic drugs with standard chemotherapy or immunotherapy has gained increased interest. The notion that epigenetic drugs may help reverse drug resistance or induce immune responses has fueled this hypothesis. Thus, exploring new potential epigenetic targets with therapeutic purpose is of great interest for current BICa research. In this Thesis we have explored some new biological mechanisms in Paper III and V, which could be pursued for this purpose.

4) Better stratify BICa tumours by seeking the molecular classification and its application into clinical practice.

One of the main conclusions of Paper IV is that the application of BICa molecular groups into clinical practice is not yet fine-tuned. Although the current proposed markers for basal/squamous vs. luminal-like stratification are a good starting point for the translation of this classification into routine, new highly specific tissue markers should be investigated and added to a panel, easily assessed by immunohistochemistry. Moreover, an effort should be made in order to apply the current molecular classification to non-invasive BICa cases, which still represent a major problem regarding recurrence rates and unpredictable prognosis.

5) Explore the role of non-coding RNAs and Epitranscriptomics regulation in BICa.

Throughout this Thesis we substantiate the notion that BICa is driven by epigenetic mechanisms, such as DNA hypermethylation-associated gene silencing and aberrant histone modifications. More recently, a third component has surfaced: the field of Epitranscriptomics, which refers to RNA chemical modifications, being implicated in post-transcriptional regulation. Indeed, research on the genetic and epigenetic factors that affect RNA might greatly improved our understanding of cancer biology and mechanisms. In addition, the development of anticancer drugs based on these alterations may also bring new promising therapeutic strategies for cancers, especially BICa.

Appendix – Original PDF Files of the published papers included in the Thesis



Review

Epigenetic Mechanisms Influencing Epithelial to Mesenchymal Transition in Bladder Cancer

Sara Monteiro-Reis ^{1,†}, João Lobo ^{1,2,3,†} , Rui Henrique ^{1,2,3} and Carmen Jerónimo ^{1,3,*}

¹ Cancer Biology and Epigenetics Group, Research Center, Portuguese Oncology Institute of Porto (CI-IPOP), R. Dr. António Bernardino de Almeida, 4200-072 Porto, Portugal; sara.raquel.reis@ipopoporto.min-saude.pt (S.M.-R.); jpedro.lobo@ipopoporto.min-saude.pt (J.L.); rmhenrique@icbas.up.pt (R.H.)

² Department of Pathology, Portuguese Oncology Institute of Porto (IPOP), R. Dr. António Bernardino de Almeida, 4200-072 Porto, Portugal

³ Department of Pathology and Molecular Immunology, Institute of Biomedical Sciences Abel Salazar, University of Porto (ICBAS-UP), Rua Jorge Viterbo Ferreira 228, 4050-513 Porto, Portugal

* Correspondence: carmenjeronimo@ipopoporto.min-saude.pt; Tel.: +351-22-508-4000

† These authors contributed equally to the paper.

Received: 12 December 2018; Accepted: 9 January 2019; Published: 13 January 2019



Abstract: Bladder cancer is one of the most incident neoplasms worldwide, and its treatment remains a significant challenge, since the mechanisms underlying disease progression are still poorly understood. The epithelial to mesenchymal transition (EMT) has been proven to play an important role in the tumorigenic process, particularly in cancer cell invasiveness and metastatic potential. Several studies have reported the importance of epigenetic mechanisms and enzymes, which orchestrate them in several features of cancer cells and, specifically, in EMT. In this paper, we discuss the epigenetic enzymes, protein-coding and non-coding genes, and mechanisms altered in the EMT process occurring in bladder cancer cells, as well as its implications, which allows for improved understanding of bladder cancer biology and for the development of novel targeted therapies.

Keywords: bladder cancer; EMT; miRNA; lncRNA; epigenetics

1. Introduction

1.1. Bladder Cancer

Bladder cancer (BlCa) is the seventh most prevalent cancer worldwide and the second most frequent urological malignancy after prostate cancer. Incidence has been rising in most countries, with an estimated 549,393 new cases diagnosed in 2018 and 990,724 new cases expected in 2040. Therefore, this almost doubled the number. Moreover, BlCa constitutes an important cause of cancer-related death with 199,922 deaths estimated in 2018 and 387,232 predicted for 2040 [1,2]. There is a strong male predominance, approximating a 3:1 ratio, and epidemiological trends track closely the prevalence of tobacco smoking [3]. Similar to other urological malignancies, mortality-to-incidence ratios are higher in underdeveloped countries, which probably reflects different environmental exposures and/or inequalities in healthcare accessibility [4]. Importantly, due to its high prevalence, mortality and, particularly, the propensity for multiple recurrences and/or disease progression and consequent additional treatments, BlCa is the most costly neoplastic disease constituting an important financial burden (costs about €4.9 billion in the European Union, alone, in 2012) [5].

BlCa generally refers to a cancer derived from epithelial layer, the urothelium, which is shared with other organs of the urinary tract and it extends from the renal pelvis to the urethra. Hence, although other much rarer tumor formations occur, its major histological subtype is urothelial carcinoma, which

will be the focus of this review. Two major forms of BlCa are acknowledged, differing clinically, pathologically, and molecularly. Non-muscle invasive BlCa (NMIBC, corresponding to 75% to 80% of all cases, disclosing papillary architecture, with the propensity to recur and eventually invade the bladder wall over time) and muscle-invasive BlCa (MIBC, 20% to 25% of all cases, mostly derived from urothelial carcinoma in situ, which constitutes an aggressive disease that invades locally and metastasizes systemically) [6,7].

1.2. Epigenetics

During many years, scientists believed that living organisms' identity was defined by the genetic component of its cells, but, rapidly, it became clear that this could not explain how cells with the same genomic composition could disclose different phenotypes depending on different conditions. Now it is known that the identity of a cell is defined by both genetic and epigenetic patterns with the latter being crucial for fetal development in mammals, as well as cell and tissue differentiation [8–11]. Epigenetics is defined as the study of heritable modifications of DNA or associated proteins, which carry information related to gene expression during cell division, and currently encompasses all potentially reversible mechanisms that lead to changes in expression regulation without affecting the DNA sequence [12]. The most well-known epigenetic mechanisms comprise four major groups: DNA methylation, histone post-translational modifications or chromatin remodeling, histone variants, and non-coding RNAs' regulation [11]. These modifications are tightly regulated by several enzymes, which may act isolated or in chromatin remodeling complexes, and grouped according to function. These epigenetic enzymes include: DNA methyltransferases (DNMTs) and demethylases (TETs), histone methyltransferases (HTMs) and demethylases (HDMs), histone acetyltransferases (HATs) and deacetylases (HDACs), and histone ubiquitin ligases (UbLs) and deubiquitinases (dUbs) [12].

Cancer cells exhibit a distinct epigenetic landscape and they take advantage of all of the previously mentioned mechanisms to acquire the characteristic malignant features, from transformation to progression [13]. BlCa is no exception. Several studies have associated epigenetic machinery deregulation and this cancer type. Moreover, the potential of epigenetic biomarkers to assist in clinical management of BlCa patients, not only for detection, but also for follow-up, treatment monitoring and prediction of recurrence/progression has been intensively investigated [14,15]. In parallel, efforts have been made to understand how epigenetic mechanisms are involved in the various steps of urothelial carcinogenesis [16,17]. One question remains mostly unanswered. What mechanisms distinguish neoplastic cells with the ability to invade the muscle layer of the bladder, and eventually metastasize, from those that do not have this ability? In fact, epigenetics may help answer this question.

1.3. Epithelial to Mesenchymal Transition

The epithelial to mesenchymal transition (EMT) is a multistep process in which epithelial cells acquire a range of mesenchymal characteristics, which enables cell motility and invasiveness [18]. Importantly, these mesenchymal characteristics are reversible, with cells resuming their epithelial phenotype, through a process named mesenchymal to epithelial transition (MET). Recently, the classic concept of EMT, which strictly pointed out to mutually exclusive epithelial or mesenchymal phenotypes, has been challenged by "partial EMT" in which cells may transiently display both epithelial and mesenchymal features, corresponding to an intermediate state of EMT [19,20]. The concept of a partial EMT may be explained by implicating epigenetic regulation of EMT/MET reversibility and cell plasticity. Various factors and cellular environmental conditions are known to induce EMT, by triggering a cascade of signalling pathways that lead to post-transcriptional modification of the most well-known EMT transcription factors (EMT-TFs): Snail, Slug, ZEB1, ZEB2, and TWIST [21,22]. The interplay between the EMT-TFs and various key regulatory proteins and epigenetic enzymes that regulate EMT-TFs themselves, results in overexpression or repression of well-described EMT effectors, such as the cadherin family (CDH1, CDH2, and CDH3) and vimentin [23–26].

1.4. Influence of EMT Major Players in Bladder Cancer

EMT is essential for various physiological processes, including early embryogenesis as well as in cancer. Accordingly, *in vitro* and *in vivo* studies implicated EMT in cell invasion and metastatic potential in several cancer types [19]. Intense research efforts uncovered the major EMT players in epithelial cancers, including BlCa. We performed an *in silico* analysis of The Cancer Genome Atlas (TCGA) database for BlCa (using the online resource cBioPortal for Cancer Genomics [27]), with a user-defined entry set of major EMT players (CDH1, CDH2, CDH3, CTNNB1, GSK3B, MMP2, MUC1, SNAI2, SNAI1, TWIST1, VIM, ZEB1, and ZEB2), and we found that these genes are deregulated in 272/413 (66%) tumors being significantly associated with reduced overall survival ($p = 0.0098$) and disease/progression-free survival ($p = 0.0279$) (Figure 1A,B). Furthermore, the expression levels of mesenchymal markers, like MMP2, VIM, TWIST1, ZEB1, and ZEB2, were significantly higher in stages III/IV when compared to stages I/II ($p < 0.0001$) (Figure 1C–F).

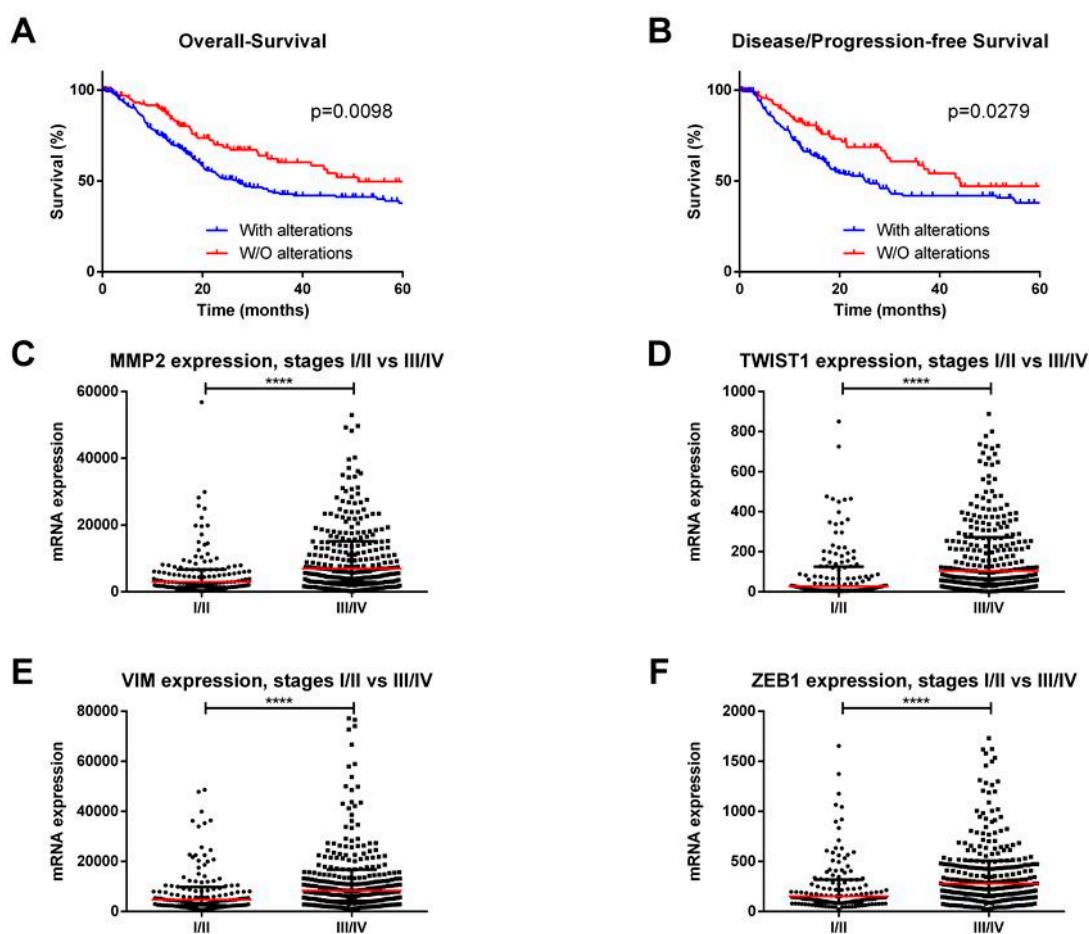


Figure 1. *In silico* analysis of The Cancer Genome Atlas database for bladder cancer (using the online resource cBioPortal for Cancer Genomics). (A) Overall and (B) Disease/Progression-free survival curves according to major EMT players' alterations. (C) MMP2, (D) TWIST1, (E) VIM, and (F) ZEB1 transcript levels in stages I/II vs. III/IV bladder cancer cases. **** $p < 0.0001$.

2. Epigenetic Enzymes and Mechanisms Altering EMT in Bladder Cancer

2.1. Protein-Coding Genes

DNA methylation and chromatin remodelling deregulation in cancer result from aberrant epigenetic enzymes' activity that ultimately lead to abnormal gene expression, which empowers tumors to quickly evolve. It facilitates invasion and metastasis. Overall, while the importance of these epigenetic

enzymes in promoting bladder cancer transformation has been already acknowledged, only a limited number of studies have characterized its role in the context of EMT process in this tumor model.

One of the epigenetic enzymes involved in EMT is the enhancer of zeste homolog 2 (EZH2), which is a core subunit of the polycomb repressive complex 2 (PRC2) that acts as a chromatin modifier by adding two or three methyl groups at H3K27 residues [28]. In several cancer models, EZH2 was proven to be associated with CDH1 transcriptional silencing and the mesenchymal phenotype [29–31]. Using chromatin immunoprecipitation (ChIP), Luo M. et al. demonstrated EZH2 and H3K23me3 enrichment within CDH1 promoter in BlCa cells even though no clues were yet provided on how PRC2 is specifically recruited to CDH1 [32]. Nonetheless, Kottakis et al. suggested that EZH2 might be regulated by FGF-2 upregulation in BlCa cells, which, in turn, upregulates the lysine demethylase 2B (KDM2B) and triggers EZH2 recruitment. The upregulation of these two enzymes is associated with miR-101 transcription repression, due to H3K36 demethylation by KDM2B, and H3K27 trimethylation by EZH2. As a result, and because EZH2 is also post-transcriptionally regulated by miR-101, these events ultimately contribute to EZH2 overexpression in a loop [33–35]. Moreover, several EMT-TFs were also found to be overexpressed in these cells, which further supports EZH2 implication in EMT [33,36]. The E2F1 transcription factor and the epigenetic reader BRD4 were also suggested as possible EZH2 regulators in BlCa, but its direct link with EMT and respective TFs is still elusive [37,38]. Importantly, because EZH2 overexpression is common to several tumors, inhibitors for this histone methyltransferase are under evaluation as potential anticancer drugs in phase one and two clinical trials [39]. Nevertheless, just one of the undergoing studies targets BlCa patients, and only those that have unresectable or metastatic disease [40]. The development of new therapies for BlCa is still an unmet need since these tumors have limited treatment options. Specifically, EZH2 inhibition might restrain the progression of non-muscle to muscle invasive disease.

DNA methylation—a covalent modification of DNA, in which a methyl group is transferred from S-adenosylmethionine (SAM) to the fifth carbon of a cytosine—constitutes a stable and heritable mark frequently associated with the maintenance of a closed chromatin structure, which results in the silencing of repeat elements in the genome and genes' transcriptional repression [41]. Across the genome, clustered regions of CpG dinucleotides, also known as CpG islands, are often found in genes' promoter regions. Several cancer-related genes were reported to be regulated by promoter methylation, some of which were implicated in BlCa EMT (Table 1). Among these, serine protease PRSS8 was found to be downregulated by promoter methylation in high-grade BlCa tissues, and its overexpression in cell lines was associated with E-Cadherin upregulation, which suggests an interplay between these two proteins during epithelial differentiation [42,43].

Similarly, the Elf5 transcription factor, which is also regulated by methylation in several cellular developmental processes, was associated with EMT in primary BlCa and *in vitro* studies [44–46]. Elf5 reduced expression, both at mRNA and protein levels, is associated with disease progression, and, in BlCa cell lines, its downregulation is associated with increased mesenchymal markers, such as Snail, ZEB1, and vimentin. Furthermore, ELF5-silenced BlCa cells exhibited an invasive phenotype, and exposure to the demethylating agent 5-AZA restored ELF5 expression in the same cells, which attenuated its invasion capacity [46].

Table 1. Epigenetically modulated protein-coding genes implicated in Bladder Cancer EMT.

Gene	Expression in BICa	Effect on EMT	Epigenetic Regulation	Sample Type and Size	Author
<i>MAEL</i>	Upregulated	↑EMT (↓ECAD, ↓β-catenin, ↑Fibronectin, ↑VIM) Recruitment of DNMT3B and HDAC1/2 to MTSS1 promoter)	Downregulated by miR186	184 primary tumors, <i>in vitro</i> and <i>in vivo</i> assays	Li, X.D., 2016 [47]
<i>GDF15</i>	Downregulated	↓EMT (knockdown cells with ↓ECAD, ↑NCAD, ↑Snail, ↑Slug)	Upregulated by demethylation	<i>In vivo</i> assays	Tsui, K.H. and Hsu, S.Y., 2015 [48]
<i>KLF4</i>	Downregulated	↓EMT (↑ECAD, ↓NCAD, ↓β-catenin, ↓VIM, ↓Snail, ↓Slug)	Promoter methylation; Upregulated by 5AZA treatment	139 non-muscle invasive primary tumors, <i>in vitro</i> and <i>in vivo</i> assays	Li, H. and Wang, J., 2013 [49]
		↓EMT (Upregulation)	Promoter methylation confirmed by BSP	<i>In vitro</i> assays	Xu, X., 2017 [50]
<i>PRSS8</i>	Downregulated	↓EMT (↑ECAD in cells with forced PRSS8 expression)	Promoter methylation. Upregulated by 5AZA and TSA treatment	40 primary tumors and <i>in vivo</i> assays	Chen, L.M., 2009 [43]
<i>ELF5</i>	Downregulated	↓EMT (↑ECAD, ↓NCAD, ↓VIM, ↓Snail, ↓ZEB1)	Promoter methylation. Upregulated by 5AZA treatment	182 FFPE + 50 FF primary tumors and <i>in vivo</i> assays	Wu, B., 2015 [46]

Abbreviations: 5AZA—5-Azacytidine. BICa—bladder cancer. BSP—Bisulfite sequencing. EMT—epithelial to mesenchymal transition. FF—Fresh-frozen. FFPE—Formalin-fixed paraffin-embedded. miR—microRNA. TSA—Trichostatin A.

Furthermore, hypermethylation of the growth differentiation factor-15 (GDF15), which is a member of the TGF- β superfamily reported as an urothelial cancer biomarker [51,52], was found to be lower in BlCa cell lines derived from MIBC tumors. Moreover, GDF15-knockdown cells displayed E-Cadherin downregulation while several EMT-TFs were upregulated [48]. Thus, the discovery of epigenetically downregulated genes in MIBC provides new insights about BlCa progression and metastasis.

KLF4, which is a zinc finger transcription factor, is commonly downregulated in several cancers [53–56] including BlCa [49,50]. Specifically, KLF4 was found to be repressed by promoter methylation [49,50]. Furthermore, (CRISPR)-ON upregulation reduced BlCa cells' migration, invasion and EMT abilities, which is paralleled by the growth inhibition of tumor xenografts and lung metastasis formation in mice. However, epigenetic editing (e.g., residue specific methylation or demethylation) would be more suitable for assessing the specific role of KLF4 promoter methylation in gene expression regulation [57,58]. The new epigenetic tools available would allow for the clarification of promoter methylation's regulation of all the previously mentioned genes implicated in BlCa EMT and metastasis.

Several epigenetic mechanisms act synergistically to maintain the epigenetic landscape through a regulation loop in which they simultaneously control protein-coding genes' expression and other epigenetic players at different regulation levels. Specifically, for BlCa, the oncogene maelstrom (MAEL), frequently upregulated in this malignancy, downregulates the metastasis suppressor MTSS1 gene by recruiting DNMT3B and HDAC1/2 to its promoter. Moreover, MAEL is also targeted by miR-186 and, possibly, by loss of promoter methylation, which constitutes an example of a gene that recruits epigenetic enzymes and is, in turn, regulated by epigenetic mechanisms [47].

2.2. Non-Coding RNAs

Non-coding RNAs (ncRNAs) are also involved in the dynamic regulation of EMT-related genes' expression. There are several ncRNA categories, commonly classified according to their size, including the long ncRNAs (lncRNAs) with more than 200 nt and the small ncRNAs (sncRNAs), which present less than 200 nt [59,60]. ncRNAs, not only directly hinder messenger RNA (mRNA), but also interact (directly or indirectly) with DNMTs, various histone modifying enzymes, and remodelling complexes, which establishes important links between all epigenetic players that modulate gene expression. Therefore, ncRNAs have been implicated in a broad range of biological processes, including proliferation, adhesion, invasion, migration, metastasis, stemness, apoptosis, genomic instability, and, also, EMT, by mediating cell-cell communication (via ncRNA-containing extracellular vesicles), which binds to transcription factors and proteins, DNA methylation regulation, splicing, and scaffolding [61,62].

Among ncRNAs, sncRNAs have been considered the most biologically relevant in the context of EMT. They are involved in post-transcriptional regulation of target RNAs (by forming complexes with proteins of the Argonaute family) with microRNAs being the most intensively studied within this class. Their mature forms are single-stranded and have 20–25 nt in length, which constitutes the final product of a processing pathway involving DROSHA, DICER, and RISC [63]. In fact, *in silico* analysis has shown several up-regulated and downregulated microRNAs that target the most important EMT players associated with aggressive disease [64].

Our literature review disclosed 31 different microRNAs, which participate in BlCa EMT regulation [(Table 2), [65–92]]. Most studies were performed in patients' samples ($n = 25$) and/or in cell lines ($n = 31$), but some have also tested animal models ($n = 9$). For most microRNAs, the net effect was to counteract an EMT phenomenon ($n = 25$), while only miR92 family/miR92b, miR135a, miR221, miR224, and miR301b were reported to promote EMT. In addition, to a putative value as diagnostic markers, 13 microRNAs were shown to have prognostic and/or predictive value as well, associated with clinicopathological variables such as tumor grade, stage, occurrence of metastases, and patients' survival.

Table 2. Non-coding RNAs associated with EMT in bladder cancer.

Non-Coding RNA	Effect on EMT (and Others)	Main Regulators	Main Targets/Pathways	Sample Type and Size	Author
<i>Small Non-Coding RNAs</i>					
miR22	↓EMT, diagnostic value (↓ in tumor, vs. normal)		Snail and MAPK/Slug/VIM	13 primary tumors, <i>in vitro</i> and <i>in vivo</i> assays	Xu, M., 2018 [90]
miR23b	↓EMT, diagnostic (↓ in tumor vs. normal) and prognostic (↑OS) value		ZEB1	20 primary tumors and <i>in vivo</i> assays	Majid, S., 2013 [68]
miR24	↓EMT, diagnostic value (↓ in tumor, vs. normal)		CARMA3	<i>In vitro</i> assays	Zhang, S., 2015 [71]
miR34a	↓EMT, diagnostic value (↓ in tumor, vs. normal)		CD44	8 primary tumors, <i>in vitro</i> and <i>in vivo</i> assays	Yu, G., 2014 [72]
miR92 (family)	↑EMT, diagnostic (↑ in tumor vs. normal) value, induces cisplatin resistance		GSK-3β/Wnt/c-myc/MMP7	20 primary tumors and <i>In vitro</i> assays	Wang, H., 2016 [79]
miR92b	↑EMT		DAB2IP	<i>In vitro</i> assays	Huang, J., 2016 [80]
miR-124-3p	↓EMT, diagnostic value (↓ in tumor, vs. normal)		ROCK1, MMP2, MMP9	13 primary tumors and <i>in vitro</i> assays	Xu, X., 2013 [66]
miR135a	↑EMT		GSK-3β	165 primary tumors and <i>in vitro</i> assays	Mao, X.W., 2018 [91]
miR141	↓EMT, prognostic value (LN metastases)		MMP2 and 9, Vimentin, N-Cadherin, E-Cadherin	30 primary tumors, 78 urine samples and <i>in vitro</i> assays	Liu, W. and Qi, L., 2015 [93]
miR-148a-3p	↓EMT, diagnostic value (↓ in tumor, vs. normal)	↓expression mediated by DNA methylation (DNMT1) – ↑expression with 5AZA	ERBB3-AKT2-c-myc/SNAIL axis	59 primary tumors, <i>in vitro</i> and <i>in vivo</i> assays	Wang, X., 2016 [82]
miR186	↓EMT, diagnostic value (↓ in tumor, vs. normal)		NSBP1	20 primary tumors and <i>in vitro</i> assays	Yao, K., 2015 [73]
miR-199a-5p	↓EMT, diagnostic (↓ in tumor vs. normal) and prognostic (stage, grade) value		CCR7, MMP9	40 primary tumors and <i>in vitro</i> assays	Zhou, M., 2016 [81]
miR200 (family)	↓EMT, prognostic value (↑ survival)	↓expression mediated by EZH2 and BMI-1	BMI-1, ZEB1, ZEB2	87 primary tumors and <i>in vitro</i> assays	Martínez-Fernández, M. and Duenas, M., 2015 [74]
	↓EMT and proliferation, diagnostic (↓ in tumor vs. normal) and prognostic (↑ survival) value		BMI-1 and E2F3	15 primary tumors and <i>in vitro</i> assays	Liu, L., 2014 [69]

Table 2. Cont.

Non-Coding RNA	Effect on EMT (and Others)	Main Regulators	Main Targets/Pathways	Sample Type and Size	Author
miR200b	↓EMT, prognostic value (LN metastases)		MMP2 and 9, Vimentin, N-Cadherin, E-Cadherin	30 primary tumors, 78 urine samples and <i>in vitro</i> assays	Liu, W. and Qi, L., 2015 [93]
	↓EMT	↓expression mediated by TGF-β1	MMP16	<i>In vitro</i> assays	Chen, M.F. and Zeng, F., 2014 [75]
miR200c	↓EMT, restores sensitivity to EGFR inhibitors		ZEB1, ZEB2 and ERFFI-1	<i>In vitro</i> assays	Adam, L., 2009 [65]
miR203	↓EMT, diagnostic value (↓ in tumor, vs. normal)		Twist1	24 primary tumors and <i>in vitro</i> assays	Shen, J., 2017 [85]
miR205	↓EMT, poor prognosis	↑expression mediated by p63 isoform ΔNp63α	ZEB1, ZEB2	98 primary tumors and <i>in vitro</i> assays	Tran, M.N., 2013 [67]
miR221	↑EMT	↑expression mediated by TGF-β1	STMN1	<i>In vitro</i> assays	Liu, J., 2015 [76]
miR224	↑EMT, diagnostic (↑ in tumor vs. normal) and prognostic (stage, metastases, ↓survival) value		SUFU/Hedgehog pathway	97 primary tumors, <i>in vitro</i> and <i>in vivo</i> assays	Miao, X., Gao, H. and Liu, S., 2018 [86]
miR301b	↑EMT, diagnostic value (↑ in tumor, vs. normal)		EGR1	<i>In vitro</i> assays	Yan, L., 2017 [94]
miR-323a-3p	↓EMT, diagnostic (↓ in tumor vs. normal) and prognostic (↑OS) value	↓expression mediated by methylation of IG-DMR	Met/SMAD3/Snail	9 primary tumors and <i>in vivo</i> assays	Li, J., 2017 [87]
miR-370-3p	↓EMT		Wnt7a	41 primary tumors <i>in vitro</i> and <i>in vivo</i> assays	Huang, X. and Zhu, H., 2018 [92]
miR-370-5p	↓EMT		p21	<i>In vitro</i> assays	Wang, C., 2016 [95]
miR424	↓EMT, diagnostic (↓ in tumor vs. normal) and prognostic (stage, ↑OS and DFS) value	↓expression mediated by DNMT1	EGFR pathway	124 primary tumors, <i>in vitro</i> and <i>in vivo</i> assays	Wu, C.T., 2015 [77]
miR429	↓EMT		ZEB1/βcatenin axis	<i>In vitro</i> assays	Wu, C.L., 2016 [83]
miR433	↓EMT, diagnostic value (↓ in tumor, vs. normal)		c-Met/CREB1-Akt/GSK-3β/Snail	13 primary tumors and <i>in vitro</i> assays	Xu, X., 2016 [84]
miR451	↓EMT, diagnostic (↓ in tumor vs. normal) and prognostic (grade and stage) value		E-Cadherin, N-Cadherin	40 primary tumors and <i>in vitro</i> assays	Zeng, T. and Peng, L., 2014 [70]
miR-485-5p	↓EMT, diagnostic value (↓ in tumor vs. normal)		HMGA2	15 primary tumors and <i>in vitro</i> assays	Chen, Z., 2015 [78]

Table 2. Cont.

Non-Coding RNA	Effect on EMT (and Others)	Main Regulators	Main Targets/Pathways	Sample Type and Size	Author
miR497	↓EMT, diagnostic (↓ in tumor vs. normal) and prognostic (stage, metastases) value		E-Cadherin, Vimentin	50 primary tumors and <i>in vitro</i> assays	Wei, Z., 2017 [88]
miR612	↓EMT, diagnostic (↓ in tumor vs. normal) and prognostic (stage, metastases) value		ME1	46 primary tumors and <i>in vitro</i> assays	Liu, M. and Chen, Y., 2018 [96]
miR613	↓EMT, diagnostic value (↓ in tumor vs. normal)		SphK1	35 primary tumors and <i>in vitro</i> assays	Yu, H., 2017 [89]
<i>Long non-coding RNAs</i>					
circRNA MYLK	↑EMT, prognostic value (stage, grade)		miR29a/VEGFA/VEGFR2 axis	32 primary tumors, <i>in vitro</i> and <i>in vivo</i> assays	Zhong, Z., 2017 [97]
lncRNA GHET1	↑EMT, diagnostic (↑ in tumor vs. normal) and prognostic (grade, stage, metastases, ↓OS) value		E-Cadherin, Vimentin, Fibronectin, Slug, Twist, Snail, ZEB1	80 primary tumors and <i>in vitro</i> assays	Li, L.J., 2014 [98]
lncRNA HOTAIR	↑EMT		Various EMT players	10 primary tumors and <i>in vitro</i> assays	Berrondo, C., 2016 [99]
lncRNA H19	↑EMT, diagnostic value (↑ in tumor vs. normal)		miR-29b-3p/DNMT3B axis	35 primary tumors, <i>in vitro</i> and <i>in vivo</i> assays	Lv, M., 2017 [100]
lncRNA Malat1	↑EMT, poor prognosis	↑expression mediated by TGF-β	suz12	95 primary tumors, <i>in vitro</i> and <i>in vivo</i> assays	Fan, Y., 2014 [101]
lncRNA ROR	↑EMT, diagnostic value (↑ in tumor vs. normal)		ZEB1	36 primary tumors and <i>in vitro</i> assays	Chen, Y., 2017 [102]
lncRNA TP73-AS1	↓EMT, diagnostic (↓ in tumor vs. normal) and prognostic (↑OS and PFS) value		Various EMT players	128 primary tumors and <i>in vitro</i> assays	Tuo, Z., 2018 [103]
lncRNA TUG1	↑EMT, diagnostic (↑ in tumor vs. normal) and prognostic (stage, ↓OS) value, promotes radio-resistance		miR145/ ZEB2 axis	54 primary tumors, <i>in vitro</i> and <i>in vivo</i> assays	Tan, J., 2015 [104]
lncRNA UCA1	↑EMT		miR145-ZEB1/2-FSCN1 axis	<i>In vitro</i> assays	Xue, M., 2016 [105]
lncRNA XIST	↑EMT		miR143/HMGB1	52 primary tumors and <i>in vitro</i> assays	Luo, J., 2017 [106]
lncRNA XIST	↑EMT		miR200c	<i>In vitro</i> and <i>in vivo</i> assays	Xu, R., 2018 [107]
lncRNA ZEB2NAT	↑EMT, diagnostic value (↑ in tumor vs. normal)	↑expression mediated by TGF-β1	ZEB2	30 primary tumors and <i>in vitro</i> assays	Zhuang, J. and Lu, Q., 2015 [108]

Abbreviations: DFS—disease-free survival. EMT—epithelial to mesenchymal transition. lncRNA—long non-coding RNA. miR—microRNA. OS—overall survival.

Some of the most well-studied microRNAs belong to the miR200 family. Their expression has been found to hamper EMT in different tumor models such as breast, prostate, ovarian, and endometrial carcinomas, in part by affecting different EMT players like ZEB1, ZEB2, and E-Cadherin [109–113]. Martínez-Fernández et al. [74] showed that PRC members EZH2 and BMI1 repress miR200 family, which results in EMT activation and aggressive disease, which is in accordance with the association of EZH2 overexpression with high risk for recurrence in NMIBC [114]. These findings support the dynamic regulation and cooperation between protein coding and non-coding RNAs in EMT. Since EZH2 pharmacological inhibition is already available and efficiently increases miR200 in BICa cell lines, this might constitute a therapeutic opportunity for hindering cancer progression. It has also been reported that epidermal growth factor receptor (EGFR) inhibition may lead to therapeutic resistance due to mesenchymal features. Additionally, miR200c induction (which targets the ERBB receptor feedback inhibitor 1-ERRFI-1) is effective in restoring sensitivity to EGFR inhibitors, which constitutes another example of pharmacological modulation of EMT that could be translated into clinical practice [65]. Lastly, another member of the miR200 family, miR200b, was demonstrated to target matrix metalloproteinase-16 (MMP16) in BICa cell lines, which is downregulated by transforming growth factor beta 1 (TGF- β 1), previously associated with metastatic potential acquisition. This leads to miR downregulation having a net effect of promoting EMT [75]. In fact, TGF- β 1 also cooperates with several other miRs, including miR221. Liu et al. showed that, by targeting STMN1, miR221 facilitates TGF- β 1-induced EMT, and that its inhibition resulted in increased levels of epithelial marker E-cadherin and reduction of mesenchymal markers such as vimentin, fibroactin, and N-cadherin [76].

A connection between microRNAs and methylation was also reported, which disclosed a feedback loop between DNMT1 and miR-148a-3p [79]. miR-148a-3p, a BICa tumor suppressor, and an EMT inhibitor, by targeting the ERBB3/AKT2/c-MYC axis, was shown to be downregulated by DNMT1-induced methylation. Moreover, re-expression was observed after treatment with 5-Aza-2'-deoxycytidine (5AZA) [79]. Wu et al. obtained similar findings for miR424 in BICa cell lines, in vivo models, and patient-derived specimens. DNMT1 inhibition resulted in substantial miR424 upregulation, which, in turn, promoted epithelial characteristics of BICa cells (changing the relative expression levels of E-cadherin and Twist) and resulted in reduced invasion ability. Additionally, the same authors identified the EGFR-PI3K-AKT axis as the target of miR424, explaining its effect on EMT [77]. Lastly, miR-323a-3p was also implicated in EMT of BICa cells by targeting MET and SMAD3, which interfered with their regulation of Snail and resulted in the net effect of repressing EMT. On the other hand, miR-323a-3p is downregulated by aberrant methylation of the intergenic differential methylated region (IG-DMR) [87]. In addition, miRs might also be regulated by methylation and this feature might be used for urothelial carcinoma detection in bodily fluids, such as urine [115].

EMT-related miRs have also been demonstrated to impact the resistance to cytotoxic drugs. Furthermore, miR-92 was found to promote EMT (changing the relative expression levels of two of its major players, E-cadherin, and vimentin) by activating glycogen synthase kinase 3 beta (GSK3B) and the Wnt signalling pathway, inducing resistance to cisplatin (increasing BICa cells viability and decreasing apoptosis upon treatment with cisplatin) [79].

Most of the human genome is transcribed into structural ncRNAs. LncRNAs, which include both linear and circular forms (the latter being referred to as circRNAs), display different regulatory functions, according to their cellular location. Whereas nuclear lncRNAs can either sequester transcription factors and recruit chromatin-remodelling complexes to a cell-site (hence impeding transcription), or trigger chromatin-modifying complexes (thus, activating transcription), cytoplasmic lncRNAs modulate RNAs stability and translation, competing with endogenous RNAs (ceRNAs) for microRNA binding. Additionally, having a longer half-life than their linear counterparts, circRNAs may also act as microRNA “sponges” [116,117].

Eleven lncRNAs (ten linear and one circRNA) [97–108] have been reported to modulate EMT in BICa. Contrary to microRNAs, only one lncRNA (TP73-AS1) was implicated in negative regulation of EMT, whereas all the remainder substances promoted its activation. Five of the lncRNAs (including

circRNA MYLK and lncRNAs GHET1, Malat1, TP73-AS1, and TUG1) were explored as potential diagnostic and prognostic biomarkers.

CircRNA MYLK was found to function as ceRNA for miR-29a, which, in result, promotes EMT and activates the vascular endothelial growth factor receptor (VEGFR) pathway, which is associated with BICa progression [97]. Thus, circRNA MYLK modulation might constitute a therapeutic target in combination with anti-VEGF drugs such as bevacizumab. Moreover, Lv et al. [100] have shown that lncRNA H19 also functions as a ceRNA for miR-29b-3p, which is another member of the miR29 family. Therefore, this allows for the expression of target DNMT3B, reprograms DNA methylation patterns, and promotes EMT (through Twist, vimentin, and MMP9 upregulation and E-cadherin downregulation) and metastasis.

Non-coding RNAs may modulate not only the response to systemic treatments, but also to local therapies such as radiotherapy. Tan et al. [104] showed that miR145's downmodulation by lncRNA TUG1 associated with EMT and radio-resistance due to its action on the ZEB2 axis. Targeting this lncRNA might re-sensitize BICa to radiotherapy, which results in a better patient response and outcome.

Furthermore, TGF- β 1 leads to overexpression of lncRNA malat1, which is associated with suppressor of zeste 12 (suz12), decreases E-cadherin, and increases N-cadherin and fibronectin expression levels [101]. Moreover, another lncRNA-ZEB2NAT—was shown to be essential for the role of TGF- β 1-secreting cancer associated fibroblasts (CAFs) in promoting EMT in BICa cells. Zhuang et al. elegantly showed that CAFs induce EMT by activating the TGF- β 1/ZEB2NAT/ZEB2 axis, whereas ZEB2NAT inhibition reduced ZEB2 expression levels and inhibited BICa cells invasion capacity [108].

Several lncRNAs might target the same microRNA and the same lncRNA may influence more than one microRNA simultaneously. Such is the case of lncRNA UCA1, which induces EMT either by targeting miR145 or miR143 [105,106]. These studies suggest that lncRNAs might be implicated in EMT by interfering with several pathways through various regulatory functions, due to their redundancy.

3. Conclusions

As discussed in this review, epigenetic mechanisms and connected enzymes are intrinsically involved in the various steps of EMT in BICa cells, which acts in concert and controlling EMT-TFs as well as several upstream targets (Figure 2). All the studies published to the date illuminate the way for the development of specific anti-cancer drugs, which could abrogate EMT by targeting epigenetic enzymes and genes regulated by these reversible modifications.

Nevertheless, the epigenetic regulation of EMT requires further investigation to provide clinically useful information for BICa patient management.

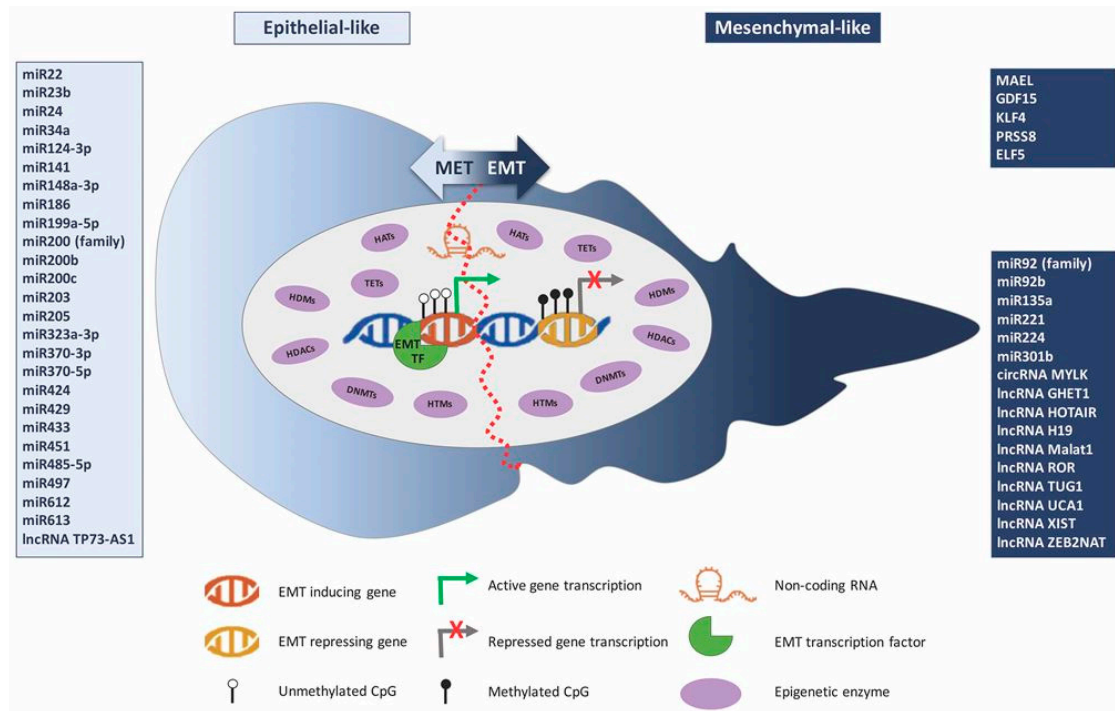


Figure 2. Epigenetic mechanisms' interplay with the epithelial-to-mesenchymal transition process in bladder cancer.

Funding: This research was funded by research grants from the Research Center of Portuguese Oncology Institute of Porto (CI-IPOP-FBGEBC-27) and (PI 74-CI-IPOP-19-2016). SR-M and JL are supported by FCT – Fundação para a Ciência e Tecnologia PhD fellowships (SFRH/BD/112673/2015 and SFRH/BD/132751/2017).

Conflicts of Interest: The authors declare no conflict of interest.

Abbreviations

5AZA	5-Aza-2'-deoxycytidine
BICa	Bladder cancer
CAF	Cancer associated fibroblast
ceRNA	Competing endogenous RNA
circRNA	Circular RNA
DNMT	DNA methyltransferase
dUb	Histone deubiquitinase
ECAD	Cadherin 1, E-Cadherin
ELF5	E74 Like ETS Transcription Factor 5
EMT	Epithelial to mesenchymal transition
EMT-TF	EMT transcription factor
GDF15	Growth Differentiation Factor 15
HAT	Histone acetyltransferase
HDAC	Histone deacetylase
HDM	Histone demethylase
HTM	Histone methyltransferase
KLF4	Kruppel Like Factor 4
lncRNA	Long non-coding RNA
MAEL	Maelstrom Spermatogenic Transposon Silencer
MET	Mesenchymal to epithelial transition
MIBC	Muscle invasive bladder cancer
miR	Micro RNA
MTSS1	Metastasis Suppressor Protein 1

NCAD	Cadherin 2, N-Cadherin
ncRNA	Non-coding RNA
NMIBC	Non-muscle invasive bladder cancer
PRC	Polycomb repressive complex
PRSS8	Serine Protease 8
Snail	Snail Family Transcriptional Repressor 1
Slug	Snail Family Transcriptional Repressor 2
sncRNA	Small non-coding RNA
TET	DNA demethylase
UbL	Histone ubiquitin ligase
VIM	Vimentin
ZEB1	Zinc Finger E-Box Binding Homeobox 1
ZEB2	Zinc Finger E-Box Binding Homeobox 2

References

- Wong, M.C.S.; Fung, F.D.H.; Leung, C.; Cheung, W.W.L.; Goggins, W.B.; Ng, C.F. The global epidemiology of bladder cancer: A joinpoint regression analysis of its incidence and mortality trends and projection. *Sci. Rep.* **2018**, *8*, 1129. [[CrossRef](#)] [[PubMed](#)]
- Ferlay, J.; Ervik, M.; Lam, F.; Colombet, M.; Mery, L.; Piñeros, M.; Znaor, A.; Soerjomataram, I.; Bray, F. *Global Cancer Observatory: Cancer Tomorrow*; WHO: Geneva, Switzerland, 2018.
- Antoni, S.; Ferlay, J.; Soerjomataram, I.; Znaor, A.; Jemal, A.; Bray, F. Bladder Cancer Incidence and Mortality: A Global Overview and Recent Trends. *Eur. Urol.* **2017**, *71*, 96–108. [[CrossRef](#)] [[PubMed](#)]
- Greiman, A.K.; Rosoff, J.S.; Prasad, S.M. Association of Human Development Index with global bladder, kidney, prostate and testis cancer incidence and mortality. *BJU Int.* **2017**, *120*, 799–807. [[CrossRef](#)] [[PubMed](#)]
- Leal, J.; Luengo-Fernandez, R.; Sullivan, R.; Witjes, J.A. Economic Burden of Bladder Cancer Across the European Union. *Eur. Urol.* **2016**, *69*, 438–447. [[CrossRef](#)] [[PubMed](#)]
- Sanli, O.; Dobruch, J.; Knowles, M.A.; Burger, M.; Alemozaffar, M.; Nielsen, M.E.; Lotan, Y. Bladder cancer. *Nat. Rev. Dis. Primers* **2017**, *3*, 17022. [[CrossRef](#)]
- Moch, H.; Ulbright, T.; Humphrey, P.; Reuter, V. *WHO Classification of Tumours of the Urinary System and Male Genital Organs*, 4th ed.; IARC: Lyon, France, 2016.
- Meissner, A. Epigenetic modifications in pluripotent and differentiated cells. *Nat. Biotechnol.* **2010**, *28*, 1079–1088. [[CrossRef](#)]
- Skinner, M.K. Role of epigenetics in developmental biology and transgenerational inheritance. *Birth Defects Res. C Embryo Today* **2011**, *93*, 51–55. [[CrossRef](#)]
- Saitou, M.; Kagiwada, S.; Kurimoto, K. Epigenetic reprogramming in mouse pre-implantation development and primordial germ cells. *Development* **2012**, *139*, 15–31. [[CrossRef](#)]
- Kelly, A.D.; Issa, J.J. The promise of epigenetic therapy: Reprogramming the cancer epigenome. *Curr. Opin. Genet. Dev.* **2017**, *42*, 68–77. [[CrossRef](#)]
- Baylin, S.B.; Jones, P.A. Epigenetic Determinants of Cancer. *Cold Spring Harb. Perspect. Biol.* **2016**, *8*. [[CrossRef](#)]
- Esteller, M. Epigenetics in cancer. *N. Engl. J. Med.* **2008**, *358*, 1148–1159. [[CrossRef](#)] [[PubMed](#)]
- Mossanen, M.; Gore, J.L. The burden of bladder cancer care: Direct and indirect costs. *Curr. Opin. Urol.* **2014**, *24*, 487–491. [[CrossRef](#)] [[PubMed](#)]
- Kojima, T.; Kawai, K.; Miyazaki, J.; Nishiyama, H. Biomarkers for precision medicine in bladder cancer. *Int. J. Clin. Oncol.* **2017**, *22*, 207–213. [[CrossRef](#)] [[PubMed](#)]
- Dudziec, E.; Goepel, J.R.; Catto, J.W. Global epigenetic profiling in bladder cancer. *Epigenomics* **2011**, *3*, 35–45. [[CrossRef](#)] [[PubMed](#)]
- Schulz, W.A.; Koutsogiannouli, E.A.; Niegisch, G.; Hoffmann, M.J. Epigenetics of urothelial carcinoma. *Methods Mol. Biol.* **2015**, *1238*, 183–215. [[PubMed](#)]
- Kalluri, R.; Weinberg, R.A. The basics of epithelial-mesenchymal transition. *J. Clin. Investig.* **2009**, *119*, 1420–1428. [[CrossRef](#)] [[PubMed](#)]
- Nieto, M.A.; Huang, R.Y.; Jackson, R.A.; Thiery, J.P. EMT: 2016. *Cell* **2016**, *166*, 21–45. [[CrossRef](#)] [[PubMed](#)]

20. Tam, W.L.; Weinberg, R.A. The epigenetics of epithelial-mesenchymal plasticity in cancer. *Nat. Med.* **2013**, *19*, 1438–1449. [[CrossRef](#)]
21. Thiery, J.P.; Sleeman, J.P. Complex networks orchestrate epithelial-mesenchymal transitions. *Nat. Rev. Mol. Cell Biol.* **2006**, *7*, 131–142. [[CrossRef](#)]
22. De Craene, B.; Berx, G. Regulatory networks defining EMT during cancer initiation and progression. *Nat. Rev. Cancer* **2013**, *13*, 97–110. [[CrossRef](#)]
23. Van Roy, F.; Berx, G. The cell-cell adhesion molecule E-cadherin. *Cell. Mol. Life Sci.* **2008**, *65*, 3756–3788. [[CrossRef](#)] [[PubMed](#)]
24. Bracken, C.P.; Gregory, P.A.; Kolesnikoff, N.; Bert, A.G.; Wang, J.; Shannon, M.F.; Goodall, G.J. A double-negative feedback loop between ZEB1-SIP1 and the microRNA-200 family regulates epithelial-mesenchymal transition. *Cancer Res.* **2008**, *68*, 7846–7854. [[CrossRef](#)] [[PubMed](#)]
25. Chaffer, C.L.; Brennan, J.P.; Slavin, J.L.; Blick, T.; Thompson, E.W.; Williams, E.D. Mesenchymal-to-epithelial transition facilitates bladder cancer metastasis: Role of fibroblast growth factor receptor-2. *Cancer Res.* **2006**, *66*, 11271–11278. [[CrossRef](#)]
26. Choi, J.; Park, S.Y.; Joo, C.K. Transforming growth factor-beta1 represses E-cadherin production via slug expression in lens epithelial cells. *Investig. Ophthalmol. Vis. Sci.* **2007**, *48*, 2708–2718. [[CrossRef](#)] [[PubMed](#)]
27. Cerami, E.; Gao, J.; Dogrusoz, U.; Gross, B.E.; Sumer, S.O.; Aksoy, B.A.; Jacobsen, A.; Byrne, C.J.; Heuer, M.L.; Larsson, E.; et al. The cBio cancer genomics portal: An open platform for exploring multidimensional cancer genomics data. *Cancer Discov.* **2012**, *2*, 401–404. [[CrossRef](#)] [[PubMed](#)]
28. Cao, Q.; Yu, J.; Dhanasekaran, S.M.; Kim, J.H.; Mani, R.S.; Tomlins, S.A.; Mehra, R.; Laxman, B.; Cao, X.; Yu, J.; et al. Repression of E-cadherin by the polycomb group protein EZH2 in cancer. *Oncogene* **2008**, *27*, 7274–7284. [[CrossRef](#)] [[PubMed](#)]
29. Tiwari, N.; Tiwari, V.K.; Waldmeier, L.; Balwierz, P.J.; Arnold, P.; Pachkov, M.; Meyer-Schaller, N.; Schubeler, D.; van Nimwegen, E.; Christofori, G. Sox4 is a master regulator of epithelial-mesenchymal transition by controlling Ezh2 expression and epigenetic reprogramming. *Cancer Cell* **2013**, *23*, 768–783. [[CrossRef](#)] [[PubMed](#)]
30. Liu, L.; Xu, Z.; Zhong, L.; Wang, H.; Jiang, S.; Long, Q.; Xu, J.; Guo, J. Enhancer of zeste homolog 2 (EZH2) promotes tumour cell migration and invasion via epigenetic repression of E-cadherin in renal cell carcinoma. *BJU Int.* **2016**, *117*, 351–362. [[CrossRef](#)]
31. Liu, X.; Wang, C.; Chen, Z.; Jin, Y.; Wang, Y.; Kolokythas, A.; Dai, Y.; Zhou, X. MicroRNA-138 suppresses epithelial-mesenchymal transition in squamous cell carcinoma cell lines. *Biochem. J.* **2011**, *440*, 23–31. [[CrossRef](#)]
32. Luo, M.; Li, Z.; Wang, W.; Zeng, Y.; Liu, Z.; Qiu, J. Long non-coding RNA H19 increases bladder cancer metastasis by associating with EZH2 and inhibiting E-cadherin expression. *Cancer Lett.* **2013**, *333*, 213–221. [[CrossRef](#)]
33. Kottakis, F.; Polytarchou, C.; Foltopoulou, P.; Sanidas, I.; Kampranis, S.C.; Tschlis, P.N. FGF-2 regulates cell proliferation, migration, and angiogenesis through an NDY1/KDM2B-miR-101-EZH2 pathway. *Mol. Cell* **2011**, *43*, 285–298. [[CrossRef](#)] [[PubMed](#)]
34. Friedman, J.M.; Liang, G.; Liu, C.C.; Wolff, E.M.; Tsai, Y.C.; Ye, W.; Zhou, X.; Jones, P.A. The putative tumor suppressor microRNA-101 modulates the cancer epigenome by repressing the polycomb group protein EZH2. *Cancer Res.* **2009**, *69*, 2623–2629. [[CrossRef](#)] [[PubMed](#)]
35. Varambally, S.; Cao, Q.; Mani, R.S.; Shankar, S.; Wang, X.; Ateeq, B.; Laxman, B.; Cao, X.; Jing, X.; Ramnarayanan, K.; et al. Genomic loss of microRNA-101 leads to overexpression of histone methyltransferase EZH2 in cancer. *Science* **2008**, *322*, 1695–1699. [[CrossRef](#)] [[PubMed](#)]
36. McNiel, E.A.; Tschlis, P.N. Analyses of publicly available genomics resources define FGF-2-expressing bladder carcinomas as EMT-prone, proliferative tumors with low mutation rates and high expression of CTLA-4, PD-1 and PD-L1. *Signal Transduct. Target. Ther.* **2017**, *2*. [[CrossRef](#)]
37. Lee, S.R.; Roh, Y.G.; Kim, S.K.; Lee, J.S.; Seol, S.Y.; Lee, H.H.; Kim, W.T.; Kim, W.J.; Heo, J.; Cha, H.J.; et al. Activation of EZH2 and SUZ12 Regulated by E2F1 Predicts the Disease Progression and Aggressive Characteristics of Bladder Cancer. *Clin. Cancer Res.* **2015**, *21*, 5391–5403. [[CrossRef](#)] [[PubMed](#)]
38. Wu, X.; Liu, D.; Tao, D.; Xiang, W.; Xiao, X.; Wang, M.; Wang, L.; Luo, G.; Li, Y.; Zeng, F.; et al. BRD4 Regulates EZH2 Transcription through Upregulation of C-MYC and Represents a Novel Therapeutic Target in Bladder Cancer. *Mol. Cancer Ther.* **2016**, *15*, 1029–1042. [[CrossRef](#)] [[PubMed](#)]

39. Jones, B.A.; Varambally, S.; Arend, R.C. Histone Methyltransferase EZH2: A Therapeutic Target for Ovarian Cancer. *Mol. Cancer Ther.* **2018**, *17*, 591–602. [[CrossRef](#)]
40. ORION-E: A Study Evaluating CPI-1205 in Patients with Advanced Solid Tumors. Available online: <https://clinicaltrials.gov/show/NCT03525795> (accessed on 03 December 2018).
41. Bird, A. DNA methylation patterns and epigenetic memory. *Genes Dev.* **2002**, *16*, 6–21. [[CrossRef](#)]
42. Leyvraz, C.; Charles, R.P.; Rubera, I.; Guitard, M.; Rotman, S.; Breiden, B.; Sandhoff, K.; Hummler, E. The epidermal barrier function is dependent on the serine protease CAP1/Prss8. *J. Cell Biol.* **2005**, *170*, 487–496. [[CrossRef](#)]
43. Chen, L.M.; Verity, N.J.; Chai, K.X. Loss of prostaticin (PRSS8) in human bladder transitional cell carcinoma cell lines is associated with epithelial-mesenchymal transition (EMT). *BMC Cancer* **2009**, *9*, 377. [[CrossRef](#)]
44. Hemberger, M.; Udayashankar, R.; Tesar, P.; Moore, H.; Burton, G.J. ELF5-enforced transcriptional networks define an epigenetically regulated trophoblast stem cell compartment in the human placenta. *Hum. Mol. Genet.* **2010**, *19*, 2456–2467. [[CrossRef](#)]
45. Ng, R.K.; Dean, W.; Dawson, C.; Lucifero, D.; Madeja, Z.; Reik, W.; Hemberger, M. Epigenetic restriction of embryonic cell lineage fate by methylation of Elf5. *Nat. Cell Biol.* **2008**, *10*, 1280–1290. [[CrossRef](#)] [[PubMed](#)]
46. Wu, B.; Cao, X.; Liang, X.; Zhang, X.; Zhang, W.; Sun, G.; Wang, D. Epigenetic regulation of Elf5 is associated with epithelial-mesenchymal transition in urothelial cancer. *PLoS ONE* **2015**, *10*, e0117510. [[CrossRef](#)] [[PubMed](#)]
47. Li, X.D.; Zhang, J.X.; Jiang, L.J.; Wang, F.W.; Liu, L.L.; Liao, Y.J.; Jin, X.H.; Chen, W.H.; Chen, X.; Guo, S.J.; et al. Overexpression of maelstrom promotes bladder urothelial carcinoma cell aggressiveness by epigenetically downregulating MTSS1 through DNMT3B. *Oncogene* **2016**, *35*, 6281–6292. [[CrossRef](#)] [[PubMed](#)]
48. Tsui, K.H.; Hsu, S.Y.; Chung, L.C.; Lin, Y.H.; Feng, T.H.; Lee, T.Y.; Chang, P.L.; Juang, H.H. Growth differentiation factor-15: A p53- and demethylation-upregulating gene represses cell proliferation, invasion, and tumorigenesis in bladder carcinoma cells. *Sci. Rep.* **2015**, *5*, 12870. [[CrossRef](#)] [[PubMed](#)]
49. Li, H.; Wang, J.; Xiao, W.; Xia, D.; Lang, B.; Wang, T.; Guo, X.; Hu, Z.; Ye, Z.; Xu, H. Epigenetic inactivation of KLF4 is associated with urothelial cancer progression and early recurrence. *J. Urol.* **2014**, *191*, 493–501. [[CrossRef](#)] [[PubMed](#)]
50. Xu, X.; Li, J.; Zhu, Y.; Xie, B.; Wang, X.; Wang, S.; Xie, H.; Yan, H.; Ying, Y.; Lin, Y.; et al. CRISPR-ON-Mediated KLF4 overexpression inhibits the proliferation, migration and invasion of urothelial bladder cancer in vitro and in vivo. *Oncotarget* **2017**, *8*, 102078–102087. [[CrossRef](#)]
51. Costa, V.L.; Henrique, R.; Danielsen, S.A.; Duarte-Pereira, S.; Eknaes, M.; Skotheim, R.I.; Rodrigues, A.; Magalhaes, J.S.; Oliveira, J.; Lothe, R.A.; et al. Three epigenetic biomarkers, GDF15, TMEFF2, and VIM, accurately predict bladder cancer from DNA-based analyses of urine samples. *Clin. Cancer Res.* **2010**, *16*, 5842–5851. [[CrossRef](#)]
52. Monteiro-Reis, S.; Leca, L.; Almeida, M.; Antunes, L.; Monteiro, P.; Dias, P.C.; Morais, A.; Oliveira, J.; Henrique, R.; Jeronimo, C. Accurate detection of upper tract urothelial carcinoma in tissue and urine by means of quantitative GDF15, TMEFF2 and VIM promoter methylation. *Eur. J. Cancer* **2014**, *50*, 226–233. [[CrossRef](#)]
53. Wei, D.; Gong, W.; Kanai, M.; Schlunk, C.; Wang, L.; Yao, J.C.; Wu, T.T.; Huang, S.; Xie, K. Drastic down-regulation of Kruppel-like factor 4 expression is critical in human gastric cancer development and progression. *Cancer Res.* **2005**, *65*, 2746–2754. [[CrossRef](#)]
54. Yang, Y.; Goldstein, B.G.; Chao, H.H.; Katz, J.P. KLF4 and KLF5 regulate proliferation, apoptosis and invasion in esophageal cancer cells. *Cancer Biol. Ther.* **2005**, *4*, 1216–1221. [[CrossRef](#)] [[PubMed](#)]
55. Wang, J.; Place, R.F.; Huang, V.; Wang, X.; Noonan, E.J.; Magyar, C.E.; Huang, J.; Li, L.C. Prognostic value and function of KLF4 in prostate cancer: RNAi and vector-mediated overexpression identify KLF4 as an inhibitor of tumor cell growth and migration. *Cancer Res.* **2010**, *70*, 10182–10191. [[CrossRef](#)] [[PubMed](#)]
56. Hu, W.; Hofstetter, W.L.; Li, H.; Zhou, Y.; He, Y.; Pataer, A.; Wang, L.; Xie, K.; Swisher, S.G.; Fang, B. Putative tumor-suppressive function of Kruppel-like factor 4 in primary lung carcinoma. *Clin. Cancer Res.* **2009**, *15*, 5688–5695. [[CrossRef](#)] [[PubMed](#)]
57. Xu, X.; Tao, Y.; Gao, X.; Zhang, L.; Li, X.; Zou, W.; Ruan, K.; Wang, F.; Xu, G.L.; Hu, R. A CRISPR-based approach for targeted DNA demethylation. *Cell Discov.* **2016**, *2*, 16009. [[CrossRef](#)] [[PubMed](#)]

58. Chen, H.; Kazemier, H.G.; de Groote, M.L.; Ruiters, M.H.; Xu, G.L.; Rots, M.G. Induced DNA demethylation by targeting Ten-Eleven Translocation 2 to the human ICAM-1 promoter. *Nucleic Acids Res.* **2014**, *42*, 1563–1574. [[CrossRef](#)] [[PubMed](#)]
59. Mattick, J.S.; Rinn, J.L. Discovery and annotation of long noncoding RNAs. *Nat. Struct. Mol. Biol.* **2015**, *22*, 5–7. [[CrossRef](#)] [[PubMed](#)]
60. Ramalho-Carvalho, J.; Fromm, B.; Henrique, R.; Jeronimo, C. Deciphering the function of non-coding RNAs in prostate cancer. *Cancer Metastasis Rev.* **2016**, *35*, 235–262. [[CrossRef](#)] [[PubMed](#)]
61. Peschansky, V.J.; Wahlestedt, C. Non-coding RNAs as direct and indirect modulators of epigenetic regulation. *Epigenetics* **2014**, *9*, 3–12. [[CrossRef](#)]
62. Anfosso, S.; Babayan, A.; Pantel, K.; Calin, G.A. Clinical utility of circulating non-coding RNAs—An update. *Nat. Rev. Clin. Oncol.* **2018**, *15*, 541–563. [[CrossRef](#)]
63. Ghildiyal, M.; Zamore, P.D. Small silencing RNAs: An expanding universe. *Nat. Rev. Genet.* **2009**, *10*, 94–108. [[CrossRef](#)]
64. Falzone, L.; Candido, S.; Salemi, R.; Basile, M.S.; Scalisi, A.; McCubrey, J.A.; Torino, F.; Signorelli, S.S.; Montella, M.; Libra, M. Computational identification of microRNAs associated to both epithelial to mesenchymal transition and NGAL/MMP-9 pathways in bladder cancer. *Oncotarget* **2016**, *7*, 72758–72766. [[CrossRef](#)] [[PubMed](#)]
65. Adam, L.; Zhong, M.; Choi, W.; Qi, W.; Nicoloso, M.; Arora, A.; Calin, G.; Wang, H.; Siefker-Radtke, A.; McConkey, D.; et al. miR-200 expression regulates epithelial-to-mesenchymal transition in bladder cancer cells and reverses resistance to epidermal growth factor receptor therapy. *Clin. Cancer Res.* **2009**, *15*, 5060–5072. [[CrossRef](#)] [[PubMed](#)]
66. Xu, X.; Li, S.; Lin, Y.; Chen, H.; Hu, Z.; Mao, Y.; Xu, X.; Wu, J.; Zhu, Y.; Zheng, X.; et al. MicroRNA-124-3p inhibits cell migration and invasion in bladder cancer cells by targeting ROCK1. *J. Transl. Med.* **2013**, *11*, 276. [[CrossRef](#)] [[PubMed](#)]
67. Tran, M.N.; Choi, W.; Wszolek, M.F.; Navai, N.; Lee, I.L.; Nitti, G.; Wen, S.; Flores, E.R.; Siefker-Radtke, A.; Czerniak, B.; et al. The p63 protein isoform DeltaNp63alpha inhibits epithelial-mesenchymal transition in human bladder cancer cells: Role of MIR-205. *J. Biol. Chem.* **2013**, *288*, 3275–3288. [[CrossRef](#)] [[PubMed](#)]
68. Majid, S.; Dar, A.A.; Saini, S.; Deng, G.; Chang, I.; Greene, K.; Tanaka, Y.; Dahiya, R.; Yamamura, S. MicroRNA-23b functions as a tumor suppressor by regulating Zeb1 in bladder cancer. *PLoS ONE* **2013**, *8*, e67686. [[CrossRef](#)] [[PubMed](#)]
69. Liu, L.; Qiu, M.; Tan, G.; Liang, Z.; Qin, Y.; Chen, L.; Chen, H.; Liu, J. miR-200c inhibits invasion, migration and proliferation of bladder cancer cells through down-regulation of BMI-1 and E2F3. *J. Transl. Med.* **2014**, *12*, 305. [[CrossRef](#)] [[PubMed](#)]
70. Zeng, T.; Peng, L.; Chao, C.; Fu, B.; Wang, G.; Wang, Y.; Zhu, X. miR-451 inhibits invasion and proliferation of bladder cancer by regulating EMT. *Int. J. Clin. Exp. Pathol.* **2014**, *7*, 7653–7662.
71. Zhang, S.; Zhang, C.; Liu, W.; Zheng, W.; Zhang, Y.; Wang, S.; Huang, D.; Liu, X.; Bai, Z. MicroRNA-24 upregulation inhibits proliferation, metastasis and induces apoptosis in bladder cancer cells by targeting CARMA3. *Int. J. Oncol.* **2015**, *47*, 1351–1360. [[CrossRef](#)]
72. Yu, G.; Xu, K.; Xu, S.; Zhang, X.; Huang, Q.; Lang, B. MicroRNA-34a regulates cell cycle by targeting CD44 in human bladder carcinoma cells. *Nan Fang Yi Ke Da Xue Xue Bao* **2015**, *35*, 935–940.
73. Yao, K.; He, L.; Gan, Y.; Zeng, Q.; Dai, Y.; Tan, J. MiR-186 suppresses the growth and metastasis of bladder cancer by targeting NSBP1. *Diagn. Pathol.* **2015**, *10*, 146. [[CrossRef](#)]
74. Martinez-Fernandez, M.; Duenas, M.; Feber, A.; Segovia, C.; Garcia-Escudero, R.; Rubio, C.; Lopez-Calderon, F.F.; Diaz-Garcia, C.; Villacampa, F.; Duarte, J.; et al. A Polycomb-mir200 loop regulates clinical outcome in bladder cancer. *Oncotarget* **2015**, *6*, 42258–42275. [[CrossRef](#)] [[PubMed](#)]
75. Chen, M.F.; Zeng, F.; Qi, L.; Zu, X.B.; Wang, J.; Liu, L.F.; Li, Y. Transforming growth factor β 1 induces epithelial-mesenchymal transition and increased expression of matrix metalloproteinase16 via miR200b downregulation in bladder cancer cells. *Mol. Med. Rep.* **2014**, *10*, 1549–1554. [[CrossRef](#)] [[PubMed](#)]
76. Liu, J.; Cao, J.; Zhao, X. miR-221 facilitates the TGFbeta1-induced epithelial-mesenchymal transition in human bladder cancer cells by targeting STMN1. *BMC Urol.* **2015**, *15*, 36. [[CrossRef](#)] [[PubMed](#)]
77. Wu, C.T.; Lin, W.Y.; Chang, Y.H.; Lin, P.Y.; Chen, W.C.; Chen, M.F. DNMT1-dependent suppression of microRNA424 regulates tumor progression in human bladder cancer. *Oncotarget* **2015**, *6*, 24119–24131. [[CrossRef](#)] [[PubMed](#)]

78. Chen, Z.; Li, Q.; Wang, S.; Zhang, J. miR4855p inhibits bladder cancer metastasis by targeting HMG2A. *Int. J. Mol. Med.* **2015**, *36*, 1136–1142. [[CrossRef](#)] [[PubMed](#)]
79. Wang, H.; Ke, C.; Ma, X.; Zhao, Q.; Yang, M.; Zhang, W.; Wang, J. MicroRNA-92 promotes invasion and chemoresistance by targeting GSK3 β and activating Wnt signaling in bladder cancer cells. *Tumour Biol.* **2016**. [[CrossRef](#)]
80. Huang, J.; Wang, B.; Hui, K.; Zeng, J.; Fan, J.; Wang, X.; Hsieh, J.T.; He, D.; Wu, K. miR-92b targets DAB2IP to promote EMT in bladder cancer migration and invasion. *Oncol. Rep.* **2016**, *36*, 1693–1701. [[CrossRef](#)] [[PubMed](#)]
81. Zhou, M.; Wang, S.; Hu, L.; Liu, F.; Zhang, Q.; Zhang, D. miR-199a-5p suppresses human bladder cancer cell metastasis by targeting CCR7. *BMC Urol.* **2016**, *16*, 64. [[CrossRef](#)]
82. Wang, X.; Liang, Z.; Xu, X.; Li, J.; Zhu, Y.; Meng, S.; Li, S.; Wang, S.; Xie, B.; Ji, A.; et al. miR-148a-3p represses proliferation and EMT by establishing regulatory circuits between ERBB3/AKT2/c-myc and DNMT1 in bladder cancer. *Cell Death Dis.* **2016**, *7*, e2503. [[CrossRef](#)]
83. Wu, C.L.; Ho, J.Y.; Chou, S.C.; Yu, D.S. MiR-429 reverses epithelial-mesenchymal transition by restoring E-cadherin expression in bladder cancer. *Oncotarget* **2016**, *7*, 26593–26603. [[CrossRef](#)]
84. Xu, X.; Zhu, Y.; Liang, Z.; Li, S.; Xu, X.; Wang, X.; Wu, J.; Hu, Z.; Meng, S.; Liu, B.; et al. c-Met and CREB1 are involved in miR-433-mediated inhibition of the epithelial-mesenchymal transition in bladder cancer by regulating Akt/GSK-3 β /Snail signaling. *Cell Death Dis.* **2016**, *7*, e2088. [[CrossRef](#)]
85. Shen, J.; Zhang, J.; Xiao, M.; Yang, J.; Zhang, N. MiR-203 Suppresses Bladder Cancer Cell Growth and Targets the Twist1. *Oncol. Res.* **2017**, *26*, 1155–1165. [[CrossRef](#)] [[PubMed](#)]
86. Miao, X.; Gao, H.; Liu, S.; Chen, M.; Xu, W.; Ling, X.; Deng, X.; Rao, C. Down-regulation of microRNA-224-inhibites growth and epithelial-to-mesenchymal transition phenotype -via modulating SUFU expression in bladder cancer cells. *Int. J. Biol. Macromol.* **2018**, *106*, 234–240. [[CrossRef](#)] [[PubMed](#)]
87. Li, J.; Xu, X.; Meng, S.; Liang, Z.; Wang, X.; Xu, M.; Wang, S.; Li, S.; Zhu, Y.; Xie, B.; et al. MET/SMAD3/SNAIL circuit mediated by miR-323a-3p is involved in regulating epithelial-mesenchymal transition progression in bladder cancer. *Cell Death Dis.* **2017**, *8*, e3010. [[CrossRef](#)] [[PubMed](#)]
88. Wei, Z.; Hu, X.; Liu, J.; Zhu, W.; Zhan, X.; Sun, S. MicroRNA-497 upregulation inhibits cell invasion and metastasis in T24 and BIU-87 bladder cancer cells. *Mol. Med. Rep.* **2017**, *16*, 2055–2060. [[CrossRef](#)] [[PubMed](#)]
89. Yu, H.; Duan, P.; Zhu, H.; Rao, D. miR-613 inhibits bladder cancer proliferation and migration through targeting SphK1. *Am. J. Transl. Res.* **2017**, *9*, 1213–1221. [[PubMed](#)]
90. Xu, M.; Li, J.; Wang, X.; Meng, S.; Shen, J.; Wang, S.; Xu, X.; Xie, B.; Liu, B.; Xie, L. MiR-22 suppresses epithelial-mesenchymal transition in bladder cancer by inhibiting Snail and MAPK1/Slug/vimentin feedback loop. *Cell Death Dis.* **2018**, *9*, 209. [[CrossRef](#)]
91. Mao, X.W.; Xiao, J.Q.; Li, Z.Y.; Zheng, Y.C.; Zhang, N. Effects of microRNA-135a on the epithelial-mesenchymal transition, migration and invasion of bladder cancer cells by targeting GSK3 β through the Wnt/ β -catenin signaling pathway. *Exp. Mol. Med.* **2018**, *50*, e429. [[CrossRef](#)]
92. Huang, X.; Zhu, H.; Gao, Z.; Li, J.; Zhuang, J.; Dong, Y.; Shen, B.; Li, M.; Zhou, H.; Guo, H.; et al. Wnt7a activates canonical Wnt signaling, promotes bladder cancer cell invasion, and is suppressed by miR-370-3p. *J. Biol. Chem.* **2018**. [[CrossRef](#)]
93. Liu, W.; Qi, L.; Lv, H.; Zu, X.; Chen, M.; Wang, J.; Liu, L.; Zeng, F.; Li, Y. MiRNA-141 and miRNA-200b are closely related to invasive ability and considered as decision-making biomarkers for the extent of PLND during cystectomy. *BMC Cancer* **2015**, *15*, 92. [[CrossRef](#)]
94. Yan, L.; Wang, Y.; Liang, J.; Liu, Z.; Sun, X.; Cai, K. MiR-301b promotes the proliferation, mobility, and epithelial-to-mesenchymal transition of bladder cancer cells by targeting EGR1. *Biochem. Cell Biol.* **2017**, *95*, 571–577. [[CrossRef](#)] [[PubMed](#)]
95. Wang, C.; Ge, Q.; Chen, Z.; Hu, J.; Li, F.; Ye, Z. Promoter-associated endogenous and exogenous small RNAs suppress human bladder cancer cell metastasis by activating p21 (CIP1/WAF1) expression. *Tumour Biol.* **2016**, *37*, 6589–6598. [[CrossRef](#)] [[PubMed](#)]
96. Liu, M.; Chen, Y.; Huang, B.; Mao, S.; Cai, K.; Wang, L.; Yao, X. Tumor-suppressing effects of microRNA-612 in bladder cancer cells by targeting malic enzyme 1 expression. *Int. J. Oncol.* **2018**, *52*, 1923–1933. [[CrossRef](#)] [[PubMed](#)]

97. Zhong, Z.; Huang, M.; Lv, M.; He, Y.; Duan, C.; Zhang, L.; Chen, J. Circular RNA MYLK as a competing endogenous RNA promotes bladder cancer progression through modulating VEGFA/VEGFR2 signaling pathway. *Cancer Lett.* **2017**, *403*, 305–317. [[CrossRef](#)] [[PubMed](#)]
98. Li, L.J.; Zhu, J.L.; Bao, W.S.; Chen, D.K.; Huang, W.W.; Weng, Z.L. Long noncoding RNA GHET1 promotes the development of bladder cancer. *Int. J. Clin. Exp. Pathol.* **2014**, *7*, 7196–7205.
99. Berrondo, C.; Flax, J.; Kucherov, V.; Siebert, A.; Osinski, T.; Rosenberg, A.; Fucile, C.; Richheimer, S.; Beckham, C.J. Expression of the Long Non-Coding RNA HOTAIR Correlates with Disease Progression in Bladder Cancer and Is Contained in Bladder Cancer Patient Urinary Exosomes. *PLoS ONE* **2016**, *11*, e0147236. [[CrossRef](#)]
100. Lv, M.; Zhong, Z.; Huang, M.; Tian, Q.; Jiang, R.; Chen, J. lncRNA H19 regulates epithelial-mesenchymal transition and metastasis of bladder cancer by miR-29b-3p as competing endogenous RNA. *Biochim. Biophys. Acta* **2017**, *1864*, 1887–1899. [[CrossRef](#)]
101. Fan, Y.; Shen, B.; Tan, M.; Mu, X.; Qin, Y.; Zhang, F.; Liu, Y. TGF-beta-induced upregulation of malat1 promotes bladder cancer metastasis by associating with suz12. *Clin. Cancer Res.* **2014**, *20*, 1531–1541. [[CrossRef](#)]
102. Chen, Y.; Peng, Y.; Xu, Z.; Ge, B.; Xiang, X.; Zhang, T.; Gao, L.; Shi, H.; Wang, C.; Huang, J. LncROR Promotes Bladder Cancer Cell Proliferation, Migration, and Epithelial-Mesenchymal Transition. *Cell. Physiol. Biochem.* **2017**, *41*, 2399–2410. [[CrossRef](#)]
103. Tuo, Z.; Zhang, J.; Xue, W. LncRNA TP73-AS1 predicts the prognosis of bladder cancer patients and functions as a suppressor for bladder cancer by EMT pathway. *Biochem. Biophys. Res. Commun.* **2018**, *499*, 875–881. [[CrossRef](#)]
104. Tan, J.; Qiu, K.; Li, M.; Liang, Y. Double-negative feedback loop between long non-coding RNA TUG1 and miR-145 promotes epithelial to mesenchymal transition and radioresistance in human bladder cancer cells. *FEBS Lett.* **2015**, *589*, 3175–3181. [[CrossRef](#)] [[PubMed](#)]
105. Xue, M.; Pang, H.; Li, X.; Li, H.; Pan, J.; Chen, W. Long non-coding RNA urothelial cancer-associated 1 promotes bladder cancer cell migration and invasion by way of the hsa-miR-145-ZEB1/2-FSCN1 pathway. *Cancer Sci.* **2016**, *107*, 18–27. [[CrossRef](#)] [[PubMed](#)]
106. Luo, J.; Chen, J.; Li, H.; Yang, Y.; Yun, H.; Yang, S.; Mao, X. LncRNA UCA1 promotes the invasion and EMT of bladder cancer cells by regulating the miR-143/HMGB1 pathway. *Oncol. Lett.* **2017**, *14*, 5556–5562. [[CrossRef](#)] [[PubMed](#)]
107. Xu, R.; Zhu, X.; Chen, F.; Huang, C.; Ai, K.; Wu, H.; Zhang, L.; Zhao, X. LncRNA XIST/miR-200c regulates the stemness properties and tumorigenicity of human bladder cancer stem cell-like cells. *Cancer Cell Int.* **2018**, *18*, 41. [[CrossRef](#)]
108. Zhuang, J.; Lu, Q.; Shen, B.; Huang, X.; Shen, L.; Zheng, X.; Huang, R.; Yan, J.; Guo, H. TGFβ1 secreted by cancer-associated fibroblasts induces epithelial-mesenchymal transition of bladder cancer cells through lncRNA-ZEB2NAT. *Sci. Rep.* **2015**, *5*, 11924. [[CrossRef](#)]
109. Gregory, P.A.; Bert, A.G.; Paterson, E.L.; Barry, S.C.; Tsykin, A.; Farshid, G.; Vadas, M.A.; Khew-Goodall, Y.; Goodall, G.J. The miR-200 family and miR-205 regulate epithelial to mesenchymal transition by targeting ZEB1 and SIP1. *Nat. Cell Biol.* **2008**, *10*, 593–601. [[CrossRef](#)] [[PubMed](#)]
110. Shimono, Y.; Zabala, M.; Cho, R.W.; Lobo, N.; Dalerba, P.; Qian, D.; Diehn, M.; Liu, H.; Panula, S.P.; Chiao, E.; et al. Downregulation of miRNA-200c links breast cancer stem cells with normal stem cells. *Cell* **2009**, *138*, 592–603. [[CrossRef](#)]
111. Leskela, S.; Leandro-Garcia, L.J.; Mendiola, M.; Barriuso, J.; Inglada-Perez, L.; Munoz, I.; Martinez-Delgado, B.; Redondo, A.; de Santiago, J.; Robledo, M.; et al. The miR-200 family controls beta-tubulin III expression and is associated with paclitaxel-based treatment response and progression-free survival in ovarian cancer patients. *Endocr. Relat. Cancer* **2011**, *18*, 85–95. [[CrossRef](#)]
112. Vallejo, D.M.; Caparros, E.; Dominguez, M. Targeting Notch signalling by the conserved miR-8/200 microRNA family in development and cancer cells. *EMBO J.* **2011**, *30*, 756–769. [[CrossRef](#)]
113. Lee, J.W.; Park, Y.A.; Choi, J.J.; Lee, Y.Y.; Kim, C.J.; Choi, C.; Kim, T.J.; Lee, N.W.; Kim, B.G.; Bae, D.S. The expression of the miRNA-200 family in endometrial endometrioid carcinoma. *Gynecol. Oncol.* **2011**, *120*, 56–62. [[CrossRef](#)]

114. Santos, M.; Martinez-Fernandez, M.; Duenas, M.; Garcia-Escudero, R.; Alfaya, B.; Villacampa, F.; Saiz-Ladera, C.; Costa, C.; Oteo, M.; Duarte, J.; et al. In vivo disruption of an Rb-E2F-Ezh2 signaling loop causes bladder cancer. *Cancer Res.* **2014**, *74*, 6565–6577. [[CrossRef](#)] [[PubMed](#)]
115. Padrao, N.A.; Monteiro-Reis, S.; Torres-Ferreira, J.; Antunes, L.; Leca, L.; Montezuma, D.; Ramalho-Carvalho, J.; Dias, P.C.; Monteiro, P.; Oliveira, J.; et al. MicroRNA promoter methylation: A new tool for accurate detection of urothelial carcinoma. *Br. J. Cancer* **2017**, *116*, 634–639. [[CrossRef](#)] [[PubMed](#)]
116. Hansen, T.B.; Jensen, T.I.; Clausen, B.H.; Bramsen, J.B.; Finsen, B.; Damgaard, C.K.; Kjems, J. Natural RNA circles function as efficient microRNA sponges. *Nature* **2013**, *495*, 384–388. [[CrossRef](#)] [[PubMed](#)]
117. Morris, K.V.; Mattick, J.S. The rise of regulatory RNA. *Nat. Rev. Genet.* **2014**, *15*, 423–437. [[CrossRef](#)] [[PubMed](#)]



© 2019 by the authors. Licensee MDPI, Basel, Switzerland. This article is an open access article distributed under the terms and conditions of the Creative Commons Attribution (CC BY) license (<http://creativecommons.org/licenses/by/4.0/>).

Keywords: promoter methylation; microRNA; miR-129-2; miR-663a; biomarker urothelial carcinoma; urine; detection

MicroRNA promoter methylation: a new tool for accurate detection of urothelial carcinoma

Nuno André Padrão¹, Sara Monteiro-Reis¹, Jorge Torres-Ferreira^{1,2}, Luís Antunes³, Luís Leça², Diana Montezuma^{1,2}, João Ramalho-Carvalho¹, Paula C Dias^{1,2}, Paula Monteiro^{1,2}, Jorge Oliveira⁴, Rui Henrique^{1,2,5} and Carmen Jerónimo^{*1,5}

¹Cancer Biology and Epigenetics Group – Research Center (CI-IPOP), Portuguese Oncology Institute of Porto (IPO Porto), Rua Dr António Bernardino de Almeida, Porto 4200-072, Portugal; ²Department of Pathology, Portuguese Oncology Institute of Porto (IPO Porto), Rua Dr António Bernardino de Almeida, Porto 4200-072, Portugal; ³Department of Epidemiology, Portuguese Oncology Institute of Porto (IPO Porto), Rua Dr António Bernardino de Almeida, Porto 4200-072, Portugal; ⁴Department of Urology, Portuguese Oncology Institute of Porto (IPO Porto), Rua Dr António Bernardino de Almeida, Porto 4200-072, Portugal and ⁵Department of Pathology and Molecular Immunology, Institute of Biomedical Sciences Abel Salazar (ICBAS) – University of Porto, Rua de Jorge Viterbo Ferreira n.º 228, Porto 4050-313, Portugal

Background: Urothelial carcinoma (UC) is the most common cancer affecting the urinary system, worldwide. Lack of accurate early detection tools entails delayed diagnosis, precluding more efficient and timely treatment. In a previous study, we found that miR-129-2 and miR-663a were differentially methylated in UC compared with other genitourinary tract malignancies. Here, we evaluated the diagnostic performance of those microRNAs in urine.

Methods: Promoter methylation levels of miR-129-2 and miR-663a were assessed, using real-time quantitative methylation-specific PCR, in UC tissue samples (using normal urothelium as control) and, subsequently, in urine samples from UC and other genitourinary malignancies. Diagnostic and prognostic performances were evaluated by receiver operator characteristics curve and survival analyses, respectively.

Results: Promoter methylation levels of both microRNAs were significantly higher in UC tissue samples compared with normal urothelium. In urine, the assay was able to distinguish UC from other genitourinary tract carcinomas with 87.7% sensitivity and 84% specificity, resulting in 85.85% overall accuracy.

Conclusions: This panel of miRNAs promoter methylation accurately detects UC in urine, comparing well with other promising epigenetic-based biomarkers. This may constitute the basis for a non-invasive assay to detect UC.

Urothelial carcinoma (UC), which affects the upper (renal pelvis and ureters) and lower (bladder, urethra) urinary tract, is the fourth most common cancer type in worldwide males, with 330 380 new cases diagnosed in 2012, mostly afflicting elderly individuals (Torre *et al*, 2015). Haematuria is the most common clinical sign of UC, particularly of those arising in the lower urinary tract, but several prevalent benign conditions, such as urinary tract infection and/or lithiasis, are also associated with haematuria, thus limiting its cancer specificity. Moreover, upper tract UC (UTUC), although

much less common (5–10% of all cases), is mostly clinically asymptomatic. Consequently, although upper and lower tract UC display clinical and genomic similarities (Zhang *et al*, 2010), 60% of UTUC are diagnosed at invasive stage, contrasting with 10% of bladder UC (BUC; Margulis *et al*, 2009). Thus, early detection is decisive to improve patient's survival.

Currently, BUC diagnosis usually consists on non-invasive (voided) urine cytology (which displays modest accuracy), followed by cytoscopic examination (Kaufman *et al*, 2009), whereas

*Correspondence: Dr C Jerónimo; E-mail: carmenjeronimo@ipoporto.min-saude.pt

Received 12 August 2016; revised 14 November 2016; accepted 20 December 2016; published online 12 January 2017

© 2017 Cancer Research UK. All rights reserved 0007–0920/17

suspected cases of UTUC are investigated with computer tomographic urography or urinary cytology followed by ureteroscopy, but these methods have low sensitivity, especially for low-grade tumours, and are often associated with patient discomfort (Kaufman *et al*, 2009; Remzi *et al*, 2011; Rouprêt *et al*, 2011). Follow-up of patients with UC is also based on periodic cystoscopy, an invasive, uncomfortable and expensive procedure, making UC one of the heaviest economical burdens in health systems (Lokeshwar *et al*, 2005). Thus, early, accurate and non-invasive diagnostic tools are critical to improve patient outcome and increase the cost-effectiveness of follow-up procedures.

MicroRNAs (miRNAs) are small (~22 nucleotides in length), non-coding RNA molecules involved in many important regulatory pathways including cell growth, proliferation, differentiation and cell death (Bartel, 2009; Silahtaroglu and Stenvang, 2010). In animals, they regulate the expression of complementary mRNA, thus inhibiting protein expression (Ambros, 2004). Recently, the role of deregulated miRNAs in oncogenesis has been emphasised and depending on its function and type of abnormal expression, they might act as oncogenes or tumour suppressor genes, in many types of cancer (Volinia *et al*, 2006). Expression of miRNAs might be epigenetically regulated, namely through methylation of CpG islands located at promoter regions, as well as histone post-translational modifications. Alterations in those mechanisms might deregulate miRNAs expression in cancer cells and might, thus, be used advantageously as specific cancer biomarkers early detection, diagnosis, prognostication, prediction of response to treatment and monitoring (Silahtaroglu and Stenvang, 2010).

In search for epigenetic biomarkers in genitourinary cancer, we identified two miRNAs – miR-129-2 and miR-663a – that displayed significantly higher promoter methylation levels in a small series of BUC tissues. Thus, we aimed at validating that finding in larger series of UC, encompassing BUC and UTUC tissues, and test the feasibility of using miR-129-2 and miR-663a quantitative promoter methylation as a tool for accurate non-invasive detection of UC in voided urine, emphasising its specificity for UC among genitourinary malignancies.

MATERIALS AND METHODS

Patients and tumour sample collection. One hundred and fourteen BUC tissue samples were obtained from a consecutive series of patients diagnosed and treated with transurethral resection or radical cystectomy, with no previous history of UTUC, between 2005 and 2014, and 55 UTUC samples were obtained from another consecutive series of patients diagnosed and treated with radical nephroureterectomy or ureterectomy, with no previous history of BUC, between 2000 and 2011. Both the groups of patients were followed-up at the Portuguese Oncology Institute of Porto, Portugal. For the BUC samples, a small tumour sample was immediately snap-frozen, stored at -80°C and subsequently cut in cryostat for DNA extraction. Routine collection and processing of tissue sample allowed for pathological examination, classification, grading and staging (Eble *et al*, 2004; Edge *et al*, 2010). UTUC samples were obtained from routinely-fixed and paraffin-embedded tissue used for pathological assessment (Eble *et al*, 2004; Edge *et al*, 2010). Controls for BUC consisted on an independent set of 19 normal bladder mucosae collected from BICa-free individuals (prostate cancer patients submitted to radical prostatectomy), and 31 paraffin-embedded normal upper tract urothelium (NUTU) set of samples obtained from renal cell carcinoma patients were used as UTUC controls. Relevant clinical data were collected from clinical charts and is depicted in Table 1.

Urine sample collection and processing. Voided urine (one sample per patient) was collected from 49 patients with BUC and

Table 1. Clinical and histopathological characteristics of patients with urothelial carcinoma and providers of normal urothelium

Clinicopathological features	UC	Normal urothelium	P-value
Patients, n	169	50	
Gender, n (%)			
Male	130 (77%)	38 (76%)	
Female	39 (23%)	12 (24%)	
Median age, years (range)	73 (42–93)	62.5 (48–82)	$P < 0.001$
Pathological stage, n (%)			
pTa	43 (26%)	NA	
pT1	63 (37%)	NA	
pT2	31 (18%)	NA	
pT3	25 (15%)	NA	
pT4	7 (4%)	NA	
Grade, n (%)			
Papillary, low grade	59 (35%)	NA	
Papillary, high grade	62 (37%)	NA	
Invasive, high grade	48 (28%)	NA	

Abbreviations: NA = not applicable; UC = urothelial carcinoma.

Table 2. Clinical and histopathological characteristics of patients with urothelial carcinoma and of controls (healthy donors (n = 25), prostate cancer (n = 25) and renal cancer (n = 25) patients), which provided urine samples for this study

Clinicopathological features	UC	Control set	P-value
Patients, n	49	75	
Gender, n (%)			
Male	29 (60%)	53 (71%)	
Female	20 (40%)	22 (29%)	
Median age, years (range)	70 (53–83)	63 (51–88)	$P < 0.066$
Grade, n (%)			
Papillary, low grade	17 (35%)	NA	
Papillary, high grade	18 (37%)	NA	
Invasive, high grade	14 (28%)	NA	

Abbreviations: NA = not applicable; UC = urothelial carcinoma.

UTUC, diagnosed and treated between 2006 and 2012 at the Portuguese Oncology Institute – Porto, Portugal. A set of 75 voided urine samples from patients with prostate cancer ($n = 25$), renal cancer ($n = 25$) and healthy blood donors with no personal or familial history of cancer ($n = 25$) were also collected and used as controls (Table 2). Informed consents were obtained from patients and controls and used in this study after approval from the ethics committee (Comissão de Ética para a Saúde) of the Portuguese Oncology Institute of Porto (CES-IPO 019/08). All urine samples were processed by immediate centrifugation at 4000 r.p.m. for 10 min, the respective pellet was washed twice with phosphate-buffered saline and stored at -80°C .

Nucleic acids isolation, bisulphite modification and qMSP analysis. DNA was extracted from frozen BUC tissue samples using AllPrep DNA/RNA Mini Kit (Qiagen Inc., Germantown, MD, USA). For UTUC NUTU tissue samples, a representative paraffin block was selected and the tumour area was delimited, allowing for macrodissection of tumour from 10 to 20 serial 7- μm thick sections, followed by digestion with proteinase K (20 mg ml $^{-1}$, 50 μl). DNA from all samples was extracted using a standard phenol-chloroform protocol (Pearson and Stirling, 2003), and its concentration determined using ND-1000 NanoDrop (NanoDrop Technologies, Wilmington, DE, USA). Bisulphite modification was performed using sodium bisulphite with EZ DNA Methylation-Gold Kit (Zymo Research, Irvine, CA, USA) according to manufacturer's protocol. Quantitative methylation levels were

performed using KAPA SYBR FAST qPCR Kit (Kapa Biosystems, Wilmington, MA, USA) and all reactions were run in triplicates in 384-well plates using Roche LightCycler 480 II, with Beta-Actin (*ACTB*) as internal reference gene for normalisation. Primer sequences were designed using Methyl Primer Express 1.0 (Methyl Primer Express 1.0, ThermoFisher Scientific, Waltham, MA, USA) and purchased from Sigma-Aldrich (St Louis, MO, USA): miR-129-2 F3'-CGGCGAATCGAAGAAGTC-5' and R3'-TACGCCCTCCGCAAATAC-5', miR-663a F3'-GGGATAGCGA GGTTAGGTC-5' and R3'-CATTTCGTAACGAATAAAACCC-5'.

Statistical analysis. Median, frequency and interquartile range of miR-129-2 and miR-663a promoter methylation levels of normal, BUC and UTUC tissue samples as well as UC, prostate, kidney and healthy blood donor urine samples were determined. Receiver operator characteristics (ROC) curves were constructed by plotting the true-positive (sensitivity) against false-positive (1-specificity) rate, and the area under the curve (AUC) was calculated. The higher value obtained from the sum of sensitivity and 1-specificity in each ROC curve was used for cut off to categorise samples as methylated or non-methylated. Sensitivity, specificity, negative predictive value, positive predictive value and accuracy of the test were also determined. Differences in quantitative methylation values were assessed with the non-parametric Mann-Whitney *U*-test. Associations between age, gender, grade, pathological stage and miRNAs methylation levels were carried out using Spearman's method, Mann-Whitney or Kruskal-Wallis tests, as appropriate. DeLong's test for ROC curves comparison was performed to assess differences in performance of the miRNAs promoter methylation test between upper and lower urinary tract cancers, and between

the age groups (lower than 65 years vs higher than 65 years). McNemar proportion test was used to compare the diagnostic performance of methylation analysis with urine cytology.

Disease-specific survival curves, (Kaplan-Meier with log rank test) were computed for standard variables (tumour stage and grade) and for categorised miRNA promoter methylation status. A Cox regression model comprising all significant variables (univariable and multivariable model) was computed to assess the relative contribution of each variable to the follow-up status.

All two-tailed *P*-values were derived from statistical tests, using a computer-assisted program (SPSS Version 23.0, IBM, Armonk, NY, USA) and the results were considered statistically significant at $P < 0.05$. Bonferroni correction for multiple comparisons was used when applicable.

RESULTS

Methylation analysis in UC tissues and performance of methylation panel in urine. The promoters of both miR-129-2 and miR-663a were found to be methylated in most UC tissue samples, and methylation levels were significantly higher compared with the control group ($P < 0.001$ and $P < 0.001$, respectively; Figure 1). Moreover, in tissue samples, the panel discriminated UC from normal mucosa with 94.7% sensitivity and 84.0% specificity (Table 3), corresponding to an AUC of 0.941 (95% confidence interval (CI): 0.911–0.972, $P < 0.001$) in ROC curve analysis (Figure 2A).

The same panel was then tested in a set of 49 urine sediments from UC patients and in a control group of 75 urines from subjects

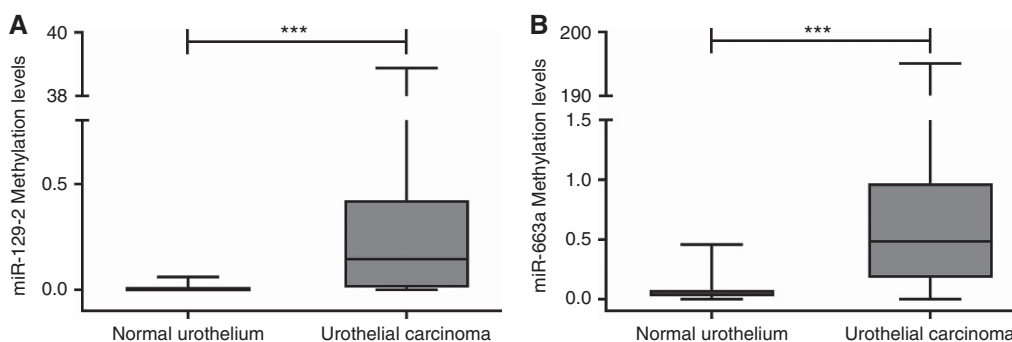


Figure 1. Distribution of (A) miR-129-2 and (B) miR-663a promoter methylation levels in normal urothelium ($n = 50$) and urothelial carcinoma (UC) tissue samples ($n = 169$). Mann-Whitney *U* test. *** $P < 0.001$.

Table 3. Performance of epigenetic biomarkers for the detection of urothelial carcinoma in tissue and urine

	Sensitivity % (n positive/n total)	Specificity % (n negative/n total)	PPV (%)	NPV (%)	Accuracy (%)
Tissue samples					
miR-129-2	72.8 (123/169)	96.0 (48/50)	98.4	51.1	78.1
miR-663a	87.0 (147/169)	86.0 (43/50)	95.5	66.2	86.8
miR-129-2/miR-663a	94.7 (160/169)	84.0 (42/50)	95.2	82.4	92.2
Urine samples (UC patients vs HD)					
miR-129-2/miR-663a	83.7 (41/49)	88.0 (22/25)	93.2	73.3	85.1
Urine samples (UC patients vs PCa and RC patients)					
miR-129-2/miR-663a	87.8 (43/49)	84 (42/50)	84.3	87.5	85.9
Urine samples (UC patients vs all controls)					
miR-129-2	75.5 (37/49)	85.3 (64/75)	77.1	84.2	81.5
miR-663a	71.4 (35/49)	94.7 (71/75)	89.7	83.5	85.5
miR-129-2/miR-663a	87.8 (43/49)	82.7 (62/75)	76.8	91.2	84.7

Abbreviations: HD = healthy donors; NPV = negative predictive value; PCa = prostate cancer; PPV = positive predictive value; RC = renal cancer; UC = urothelial carcinoma.

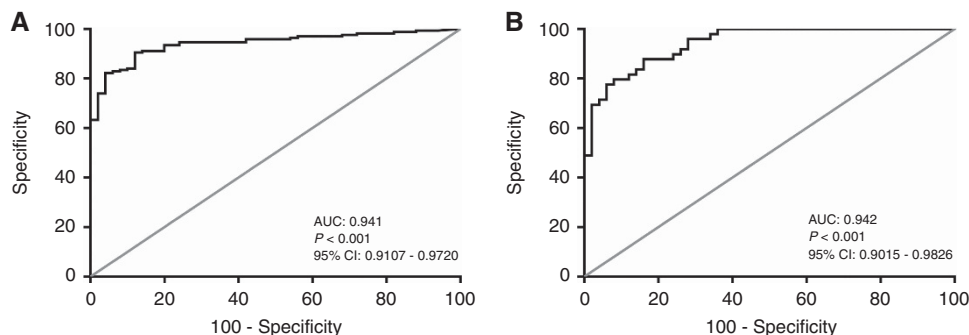


Figure 2. Receiver operator characteristic (ROC) curves evaluating the performance of the gene panel promoter methylation (miR-129-2/miR-663a); (A) for the identification of urothelial carcinoma (UC) in tissue; and (B) for discrimination of UC from other genitourinary malignancies in urine samples.

not carrying UC. Remarkably, methylation levels of both miRNAs in UC urine samples were significantly higher than those of controls ($P < 0.001$ and $P < 0.001$, respectively). In urine samples, the methylation test was able to detect UC with 87.8% sensitivity and 84.0% specificity (Table 3), corresponding to an AUC of 0.942 (95% CI: 0.9015–0.9826, $P < 0.001$; Figure 2B). Moreover, the methylation test was able to discriminate UC patients both from other genitourinary malignancies and from healthy donors (Table 3).

Because urine cytology is frequently the first test to be performed in UC suspects, we compared the performance of the methylation panel with cytopathological examination by an experienced cytopathologist. Interestingly, the proportion of true-positive cases detected by the methylation test was significantly higher than that of cytology ($P < 0.001$). Of 47 UC cases analysed, cytopathology detected only 17 as positive, 15 as negative and 15 as ‘inconclusive/suspicious’, corresponding to 34.7% sensitivity. Conversely, the miRNAs promoter methylation panel identified 41 cases as true positive, corresponding to an overall sensitivity of 87.2%, although 1 of the 6 cases negative in the methylation test was correctly diagnosed as UC by cytopathology (Figure 3).

Clinicopathological correlates and survival analyses. Significantly higher miR-129-2 methylation levels were found in high-grade papillary UC compared with low-grade papillary UC ($P = 0.048$), whereas for miR-663a, high-grade papillary UC displayed significantly higher methylation levels than invasive UC ($P = 0.003$). In addition, miR-663a methylation levels differed significantly between non-muscle invasive and muscle invasive UC (stages pTa-1 vs pT2-4; $P = 0.016$), as well as between papillary and invasive UC ($P = 0.012$).

A significant association was found between promoter methylation levels and patients’ age at diagnosis for both miR-129-2 and miR-663a ($P = 0.023$; $P = 0.016$, respectively). After normalisation of the ROC curve for this variable, no significant difference in the panel’s performance was found between younger and older patients and an AUC of 94.3% was obtained. Furthermore, no association was disclosed between miRNAs promoter methylation and patients’ gender.

Of the 114 patients enrolled, 3 BUC and 1 UTUC patients were lost to follow-up. The median follow-up time of BUC patients was 66 months (range: 1–323 months). At the last follow-up time point, 58 patients were alive with no evidence of cancer, 10 patients were alive with disease, 11 died from other causes and 32 had deceased due to UC. Considering UTUC patients, the follow-up time was 55 months (range: 1–186 months). At the last follow-up, 16 patients were alive without disease, 6 were alive with disease progression, whereas 32 patients had perished, 23 due to UTUC. Overall, for UC, the median follow-up time was 62 months. A poor

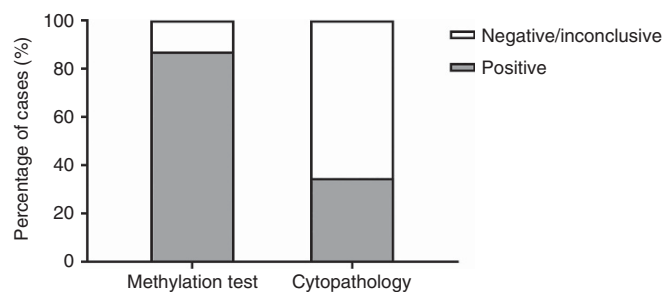


Figure 3. Percentage of urothelial carcinoma (UC) cases correctly identified with the gene panel promoter methylation test and a standard cytopathology analysis.

outcome was depicted for UC patients with higher grade, pathological stage and age at diagnosis (Log rank test; $P < 0.001$, for all variables). Univariable and multivariable Cox regression analysis were performed separately for BUC, UTUC and UC patients, including the three above mentioned variables (Supplementary Table 1). As expected, a poor outcome was depicted for UC patients with higher pathological stage, grade and age in a multivariable model (Supplementary Table 1; $P = 0.03$, $P = 0.002$ and $P < 0.001$, respectively). However, considering the two patients’ subsets separately, only grade (for BUC) and age (for UTUC) were selected in the final model as independent predictors of outcome (Supplementary Table 1; $P = 0.009$ and $P = 0.017$). No prognostic value was depicted for miR-129-2 or miR-663a promoter methylation levels in UC or in BUC or UTUC, when analysed separately (Supplementary Table 1).

DISCUSSION

Upper and lower UC are among the most common neoplasms worldwide and although several risk factors have been clearly identified (e.g., smoking habits, chemical exposure to aromatic amines like benzidine or β -naphthalene, Schistosoma infection (Babjuk *et al*, 2013; Torre *et al*, 2015)), early detection is critical for adequate therapeutic management towards reducing disease-specific mortality (Hall *et al*, 1998; Margulis *et al*, 2009). Moreover, it is important to discriminate UC from other genitourinary cancers, especially those originating in the prostate and kidney. Although several biomarkers have been previously reported, including miRNAs promoter methylation (Phé *et al*, 2009; van der Kwast and Bapat, 2009; Shimizu *et al*, 2013), they have been mostly focused on BUC, disregarding upper urothelial tract UC, and its performance might be perfected by the addition of more

sensitive and specific biomarkers. Within a project aimed at characterising miRNAs deregulated through aberrant promoter methylation in genitourinary neoplasms, we identified miR-129-2 and miR-663a promoters as potential UC biomarkers (submitted). We, thus, tested the biomarker performance of quantitative miR-129-2 and miR-663a promoter methylation both in upper and lower urinary tract UC.

Because miR-129-2 and miR-663a promoter methylation was initially identified in BUC, we first assessed methylation levels in tissue samples of upper and lower urinary tract UC. Owing to biological and genomic similarity between the urothelium from upper and lower urinary tract (Zhang *et al*, 2010), we hypothesised that this panel would perform well in both the settings. Indeed, the methylation panel discriminated UC from normal urothelial mucosa with high sensitivity and specificity, which did not differ between upper and lower urinary tract UC. This result enabled us to proceed with urine testing, as the ultimate goal of the study would be the identification of a non-invasive test, intended for early detection and disease monitoring. In urine samples, sensitivity and specificity were lower than those found in tissues, but it should be recalled that the accuracy of the panel was tested not only against healthy volunteers, but also prostate and kidney cancer patients.

Recently, several studies attempted to identify novel epigenetic biomarkers for UC detection, some of them with an apparent superior performance to the panel reported herein. *TWIST1* and *NID2* promoter methylation were previously reported to detect BUC in urine samples with 94% sensitivity and 91% specificity (Renard *et al*, 2010). However, specificity was only tested against urinary infections or other benign conditions and its ability to discriminate UC from prostate and kidney cancer was not evaluated. *BCL2*, *CDKN2A* and *NID2* promoter methylation have also been proposed as epigenetic biomarkers for bladder cancer (Scher *et al*, 2012). Although the number of genes is higher than that of our panel, sensitivity and specificity were lower (80.9% and 86.4%, respectively) and this was accomplished through nested PCR, which may compromise the speed and cost of the assay. Moreover, the number of samples from prostate and kidney cancer tested was lower than those included in our study. We have also previously reported a gene promoter methylation panel (*GDF15*, *TMEFF2* and *VIM*) that accurately identified BUC in urine samples (Costa *et al*, 2010) which we, subsequently, demonstrated to have similar performance in upper urinary tract UC (Monteiro-Reis *et al*, 2014). Both studies, however, used specific TaqMan probes, contrarily to the present study, where a SYBR Green-based protocol was used, thus, also, improving cost-effectiveness.

Some previous studies have also focused on miRNAs promoter methylation as UC biomarkers. Whereas, Vogt *et al* (2011) reported 57% sensitivity ($n = 7$) for miR-34a promoter methylation in bladder tissues and Shimizu *et al* (2013) achieved 81% specificity and 89% sensitivity in urine sediments from BUC ($n = 47$) using a panel of several miRNAs. Our results compare well with those reports and provide some significant advantages, as only two miRNA promoters are tested and its specificity was evaluated against other genitourinary malignancies.

Although urinary cytology is frequently used as an initial diagnostic approach in UC suspects, its diagnostic yield is rather limited, especially for upper urinary tract UC (Rouprêt *et al*, 2013). Moreover, imaging techniques might have difficulty in discriminating upper urinary tract UC from renal cell carcinoma, a quite relevant differential diagnosis setting owing to marked differences in therapy and prognosis (Browne *et al*, 2005), thus emphasising the need for biomarkers that may accurately discriminate among those tumour types. In the present study, the sensitivity of urinary cytology was only ~35%, which was easily surpassed by the miRNA methylation panel, with the additional gain of discriminating UC from renal cell carcinoma.

Whereas no biological role has been previously ascribed to miR-129-2 and miR-663a promoter methylation in urothelial carcinogenesis, several studies in other tumour models have unveiled the pathological significance of those epigenetic aberrations. Transcriptional silencing of miR-129-2 due to promoter methylation was found in gastric (Pan *et al*, 2010; Shen *et al*, 2010), endometrial (Huang *et al*, 2009) and hepatocellular (Lu *et al*, 2013) carcinomas, as well as in acute myeloid leukaemia (Yan-Fang *et al*, 2013), and it has been implicated in overexpression of two oncogenic proteins, SOX4 (Huang *et al*, 2009; Shen *et al*, 2010) and Cdk6 (Wu *et al*, 2010). On the other hand, miR-663a promoter methylation and downregulation was associated with JunD overexpression in small-cell lung carcinoma (Zhang *et al*, 2016) and HMGA2 overexpression in hepatocellular carcinoma (Huang *et al*, 2016), fostering cell proliferation. Owing to the prevalence of miR-129-2 and miR-663a promoter methylation in UC, across primary localisations, histological subtype, grade and stage, it is tempting to speculate whether it may also play a key role in urothelial carcinogenesis.

In summary, we demonstrated that aberrant miR-129-2 and miR-663a promoter methylation accurately discriminate UC from normal urothelial mucosa and allow for sensitive and specific identification of upper and lower urinary tract UC in urine samples, discriminating also from other common genitourinary tract carcinomas (kidney and prostate). Thus, this panel might be useful for complementing other epigenetic biomarkers for non-invasive detection and/or monitoring of UC patients.

ACKNOWLEDGEMENTS

We are grateful to M^a Conceição Martins, BSc for the skilful technical support and would like to acknowledge the nursing staff of the Departments of Urology and Laboratory Medicine of the Portuguese Oncology Institute of Porto for their collaboration in urine collection. This study was supported by research grants from Research Center of Portuguese Oncology Institute of Porto (CI-IPOP-FBGEB-27) and by Federal funds through Programa Operacional Temático Factores de Competitividade (COMPETE) with co-participation from the European Community Fund (FEDER) and by national funds through Fundação para a Ciência e Tecnologia (FCT) under the projects EXPL/BIM-ONC/0556/2012. SM-R and JR-C are PhD students funded by FCT-Fundação para a Ciência e a Tecnologia fellowship (SFRH/BD/112673/2015 and SFRH/BD/71293/2010, respectively).

CONFLICT OF INTEREST

The authors declare no conflict of interest.

AUTHOR CONTRIBUTIONS

Conceived and designed the experiments: RH, CJ. Performed the experiments: NAP, SM-R, JT-F, LL, DM, JR-C, PCD, PM and JO. Data analysis and interpretation: NAP, SM-R, LA, RH and CJ. Contributed reagents/material/analysis: JT-F, PM, JO, RH and CJ; Manuscript preparation: NAP, SM-R, RH and CJ.

REFERENCES

- Ambros V (2004) The functions of animal microRNAs. *Nature* **431**(7006): 350–355.
- Babjuk M, Burger M, Zigeuner R, Shariat SF, van Rhijn BW, Comperat E, Sylvester RJ, Kaasinen E, Böhle A, Redorta JP (2013) EAU guidelines on

- non-muscle-invasive urothelial carcinoma of the bladder: update 2013. *Eur Urol* **64**(4): 639–653.
- Bartel DP (2009) MicroRNAs: target recognition and regulatory functions. *Cell* **136**(2): 215–233.
- Browne RF, Meehan CP, Colville J, Power R, Torreggiani WC (2005) Transitional cell carcinoma of the upper urinary tract: spectrum of imaging findings 1. *Radiographics* **25**(6): 1609–1627.
- Costa VL, Henrique R, Danielsen SA, Duarte-Pereira S, Eknaes M, Skotheim RI, Rodrigues Á, Magalhães JS, Oliveira J, Lothe RA (2010) Three epigenetic biomarkers, GDF15, TMEFF2, and VIM, accurately predict bladder cancer from DNA-based analyses of urine samples. *Clin Cancer Res* **16**(23): 5842–5851.
- Eble J, Sauter G, Epstein J, Sesterhenn I (2004) Tumours of the urinary system and male genital organs: pathology and genetics. *World Health Organization Classification of Tumours*. IARC Press: Lyon.
- Edge SB, Compton CC, Fritz AG, Greene FL, Trotti A (2010) *American Joint Committee on Cancer: Cancer Staging Manual*. 7th edn. Lippincott-Raven Publishers: Philadelphia.
- Hall MC, Womack S, Sagalowsky AI, Carmody T, Erickstad MD, Roehrborn CG (1998) Prognostic factors, recurrence, and survival in transitional cell carcinoma of the upper urinary tract: a 30-year experience in 252 patients. *Urology* **52**(4): 594–601.
- Huang W, Li J, Guo X, Zhao Y, Yuan X (2016) miR-663a inhibits hepatocellular carcinoma cell proliferation and invasion by targeting HMGA2. *Biomed Pharmacother* **81**: 431–438.
- Huang Y-W, Liu JC, Deatherage DE, Luo J, Mutch DG, Goodfellow PJ, Miller DS, Huang TH (2009) Epigenetic repression of microRNA-129-2 leads to overexpression of SOX4 oncogene in endometrial cancer. *Cancer Res* **69**(23): 9038–9046.
- Kaufman DS, Shipley WU, Feldman AS (2009) Bladder cancer. *Lancet* **374**(9685): 239–249.
- Lokeshwar VB, Habuchi T, Grossman HB, Murphy WM, Hautmann SH, Hemstreet GP, Bono AV, Getzenberg RH, Goebell P, Schmitz-Dräger BJ (2005) Bladder tumor markers beyond cytology: international Consensus Panel on bladder tumor markers. *Urology* **66**(6): 35–63.
- Lu CY, Lin KY, Tien MT, Wu CT, Uen YH, Tseng TL (2013) Frequent DNA methylation of miR-129-2 and its potential clinical implication in hepatocellular carcinoma. *Genes Chromosomes Cancer* **52**(7): 636–643.
- Margulis V, Shariat SF, Matin SF, Kamat AM, Zigeuner R, Kikuchi E, Lotan Y, Weizer A, Raman JD, Wood CG (2009) Outcomes of radical nephroureterectomy: a series from the Upper Tract Urothelial Carcinoma Collaboration. *Cancer* **115**(6): 1224–1233.
- Monteiro-Reis S, Leça L, Almeida M, Antunes L, Monteiro P, Dias PC, Morais A, Oliveira J, Henrique R, Jerónimo C (2014) Accurate detection of upper tract urothelial carcinoma in tissue and urine by means of quantitative GDF15, TMEFF2 and VIM promoter methylation. *Eur J Cancer* **50**(1): 226–233.
- Pan J, Hu H, Zhou Z, Sun L, Peng L, Yu L, Sun L, Liu J, Yang Z, Ran Y (2010) Tumor-suppressive mir-663 gene induces mitotic catastrophe growth arrest in human gastric cancer cells. *Oncol Rep* **24**(1): 105–112.
- Pearson H, Stirling D (2003) DNA extraction from tissue. *Methods Mol Biol* **226**: 33–34.
- Phé V, Cussenot O, Rouprêt M (2009) Interest of methylated genes as biomarkers in urothelial cell carcinomas of the urinary tract. *BJU Int* **104**(7): 896–901.
- Remzi M, Shariat S, Huebner W, Fajkovic H, Seitz C (2011) Upper urinary tract urothelial carcinoma: what have we learned in the last 4 years? *Ther Adv Urol* **3**(2): 69–80.
- Renard I, Joniau S, Van Cleynenbreugel B, Collette C, Naomé C, Vlassenbroeck I, Nicolas H, de Leval J, Straub J, Van Criekinge W (2010) Identification and validation of the methylated TWIST1 and NID2 genes through real-time methylation-specific polymerase chain reaction assays for the noninvasive detection of primary bladder cancer in urine samples. *Eur Urol* **58**(1): 96–104.
- Rouprêt M, Babjuk M, Compérat E, Zigeuner R, Sylvester R, Burger M, Cowan N, Böhle A, Van Rhijn BW, Kaasinen E (2013) European guidelines on upper tract urothelial carcinomas: 2013 update. *Eur Urol* **63**(6): 1059–1071.
- Rouprêt M, Zigeuner R, Palou J, Boehle A, Kaasinen E, Sylvester R, Babjuk M, Oosterlinck W (2011) European guidelines for the diagnosis and management of upper urinary tract urothelial cell carcinomas: 2011 update. *Eur Urol* **59**(4): 584–594.
- Scher MB, Elbaum MB, Mogilevkin Y, Hilbert DW, Mydlo JH, Sidi AA, Adelson ME, Mordechai E, Trama JP (2012) Detecting DNA methylation of the BCL2, CDKN2A and NID2 genes in urine using a nested methylation specific polymerase chain reaction assay to predict bladder cancer. *J Urol* **188**(6): 2101–2107.
- Shen R, Pan S, Qi S, Lin X, Cheng S (2010) Epigenetic repression of microRNA-129-2 leads to overexpression of SOX4 in gastric cancer. *Biochem Biophys Res Commun* **394**(4): 1047–1052.
- Shimizu T, Suzuki H, Nojima M, Kitamura H, Yamamoto E, Maruyama R, Ashida M, Hatahira T, Kai M, Masumori N (2013) Methylation of a panel of microRNA genes is a novel biomarker for detection of bladder cancer. *Eur Urol* **63**(6): 1091–1100.
- Silahtaroglu A, Stenvang J (2010) MicroRNAs, epigenetics and disease. *Essays Biochem* **48**: 165–185.
- Torre LA, Bray F, Siegel RL, Ferlay J, Lortet-Tieulent J, Jemal A (2015) Global cancer statistics, 2012. *CA Cancer J Clin* **65**(2): 87–108.
- van der Kwast TH, Bapat B (2009) Predicting favourable prognosis of urothelial carcinoma: gene expression and genome profiling. *Curr Opin Urol* **19**(5): 516–521.
- Vogt M, Munding J, Grüner M, Liffers S-T, Verdoodt B, Hauk J, Steinstraesser L, Tannapfel A, Hermeking H (2011) Frequent concomitant inactivation of miR-34a and miR-34b/c by CpG methylation in colorectal, pancreatic, mammary, ovarian, urothelial, and renal cell carcinomas and soft tissue sarcomas. *Virchows Arch* **458**(3): 313–322.
- Volinia S, Calin GA, Liu C-G, Ambs S, Cimmino A, Petrocca F, Visone R, Iorio M, Roldo C, Ferracin M (2006) A microRNA expression signature of human solid tumors defines cancer gene targets. *Proc Natl Acad Sci USA* **103**(7): 2257–2261.
- Wu J, Qian J, Li C, Kwok L, Cheng F, Liu P, Perdomo C, Kotton D, Vaziri C, Anderlind C (2010) miR-129 regulates cell proliferation by downregulating Cdk6 expression. *Cell Cycle* **9**(9): 1809–1818.
- Yan-Fang T, Jian N, Jun L, Na W, Pei-Fang X, Wen-Li Z, Dong W, Li P, Jian W, Xing F (2013) The promoter of miR-663 is hypermethylated in Chinese pediatric acute myeloid leukemia (AML). *BMC Med Genet* **14**(1): 74.
- Zhang Y, Xu X, Zhang M, Wang X, Bai X, Li H, Kan L, Zhou Y, Niu H, He P (2016) MicroRNA-663a is downregulated in non-small cell lung cancer and inhibits proliferation and invasion by targeting JunD. *BMC Cancer* **16**(1): 1.
- Zhang Z, Furge KA, Yang XJ, Teh BT, Hansel DE (2010) Comparative gene expression profiling analysis of urothelial carcinoma of the renal pelvis and bladder. *BMC Med Genomics* **3**(1): 58.

This work is published under the standard license to publish agreement. After 12 months the work will become freely available and the license terms will switch to a Creative Commons Attribution-NonCommercial-Share Alike 4.0 Unported License.

Supplementary Information accompanies this paper on British Journal of Cancer website (<http://www.nature.com/bjc>)



Article

A Multiplex Test Assessing *MiR663a_{me}* and *VIM_{me}* in Urine Accurately Discriminates Bladder Cancer from Inflammatory Conditions

Sara Monteiro-Reis ¹, Ana Blanca ², Joana Tedim-Moreira ¹, Isa Carneiro ^{1,3},
Diana Montezuma ^{1,3}, Paula Monteiro ^{1,3}, Jorge Oliveira ⁴, Luís Antunes ⁵ , Rui Henrique ^{1,2,6} ,
António Lopez-Beltran ^{7,8} and Carmen Jerónimo ^{1,6,*}

¹ Cancer Biology and Epigenetics Group—Research Center (CI-IPOP), Portuguese Oncology Institute of Porto (IPO Porto), and Porto Comprehensive Cancer Center (P.CCC), Maimonides Biomedical Research Institute of Cordoba, 14004 Cordoba, Spain; sara.raquel.reis@ipoporto.min-saude.pt (S.M.-R.); joana.matos@ua.pt (J.T.-M.); isa.carneiro@ipoporto.min-saude.pt (I.C.); dianafelizardo@gmail.com (D.M.); paula.monteiro@ipoporto.min-saude.pt (P.M.); henrique@ipoporto.min-saude.pt (R.H.)

² Department of Urology, University Hospital of Reina Sofia, Maimonides Biomedical Research Institute of Cordoba, 14004 Cordoba, Spain; anblape78@hotmail.com

³ Department of Pathology, Portuguese Oncology Institute of Porto (IPO Porto), 4200-072 Porto, Portugal

⁴ Department of Urology, Portuguese Oncology Institute of Porto (IPO-Porto), 4200-072 Porto, Portugal; jorge.oliveira@ipoporto.min-saude.pt

⁵ Department of Epidemiology, Portuguese Oncology Institute of Porto (IPO Porto) & Cancer Epidemiology Group—Research Center (CI-IPOP), 4200-072 Porto, Portugal; luis.antunes@ipoporto.min-saude.pt

⁶ Department of Pathology and Molecular Immunology, Institute of Biomedical Sciences Abel Salazar (ICBAS)—University of Porto, 4050-313 Porto, Portugal

⁷ Department of Surgery and Pathology, Faculty of Medicine, University of Cordoba, 14071 Cordoba, Spain; emllobea@uco.es

⁸ Champalimaud Clinical Center, 1400-038 Lisbon, Portugal

* Correspondence: carmenjeronimo@ipoporto.min-saude.pt; Tel.: +35-122-508-4000

Received: 28 January 2020; Accepted: 18 February 2020; Published: 24 February 2020



Abstract: Bladder cancer (BlCa) is a common malignancy with significant morbidity and mortality. Current diagnostic methods are invasive and costly, showing the need for newer biomarkers. Although several epigenetic-based biomarkers have been proposed, their ability to discriminate BlCa from common benign conditions of the urinary tract, especially inflammatory diseases, has not been adequately explored. Herein, we sought to determine whether *VIM_{me}* and *miR663a_{me}* might accurately discriminate those two conditions, using a multiplex test. Performance of *VIM_{me}* and *miR663a_{me}* in tissue samples and urines in testing set confirmed previous results (96.3% sensitivity, 88.2% specificity, area under de curve (AUC) 0.98 and 92.6% sensitivity, 75% specificity, AUC 0.83, respectively). In the validation sets, *VIM_{me}*-*miR663a_{me}* multiplex test in urine discriminated BlCa patients from healthy donors or patients with inflammatory conditions, with 87% sensitivity, 86% specificity and 80% sensitivity, 75% specificity, respectively. Furthermore, positive likelihood ratio (LR) of 2.41 and negative LR of 0.21 were also disclosed. Compared to urinary cytology, *VIM_{me}*-*miR663a_{me}* multiplex panel correctly detected 87% of the analysed cases, whereas cytology only forecasted 41%. Furthermore, high *miR663a_{me}* independently predicted worse clinical outcome, especially in patients with invasive BlCa. We concluded that the implementation of this panel might better stratify patients for confirmatory, invasive examinations, ultimately improving the cost-effectiveness of BlCa diagnosis and management. Moreover, *miR663a_{me}* analysis might provide relevant information for patient monitoring, identifying patients at higher risk for cancer progression.

Keywords: bladder cancer; methylation; biomarkers

1. Introduction

Bladder cancer (BlCa) is one of the most incident cancers, ranking ninth in prevalence worldwide [1,2]. In men, which are more prone to develop BlCa, it represents the second most frequent urological malignancy after prostate cancer [1,2]. Moreover, it is expected that, by 2040, the number of estimated new cases and cancer-related deaths will almost double the 549,393 newly diagnosed cases and 199,922 deaths recorded in 2018 [1,2]. Most BlCa cases correspond to urothelial carcinoma, generally presenting as non-muscle invasive BlCa (NMIBC), accounting for 75–80% of all new cases, characterised by frequent recurrences and eventual progression to more aggressive, deeply invasive and metastatic disease, or muscle-invasive BlCa (MIBC), an aggressive, locally invading carcinoma, corresponding to 20–25% of all cases, with propensity for metastatisation [3,4]. Haematuria is the most common clinical sign of BlCa, although it also occurs in several common benign disease such as urinary tract infections and non-infectious inflammatory conditions. Presently, BlCa diagnosis generally involves cystoscopic examination, an expensive and invasive procedure, complemented by urine cytology [5–7]. However, the latter has limited accuracy, particularly for identification of low-grade papillary tumours, and the invasive nature of cystoscopic examination entails patient discomfort and, in some cases, infection [5]. Moreover, because of the high incidence, recurrence and progression rate, active long follow-up is required, making BlCa the costliest malignancy [8]. Thus, early, accurate and non-invasive BlCa detection is the determinant to improve both patients and healthcare financial management.

Epigenetic changes, including DNA methylation, have been largely investigated for cancer detection [9]. Owing to chemical and biological stability, DNA methylation-based biomarkers have potential clinical applications in early cancer detection, diagnosis, follow-up and targeted therapies [10]. Previously, two independent DNA methylation-based biomarker panels have been reported as promising tests for accurate early detection of BlCa [11,12]. In 2010, a three-gene panel comprised *GDF15*, *TMEFF2* and *VIM* methylation identified BlCa with 94% sensitivity and 100% specificity in urine samples from 51 BlCa patients [11]. More recently, a panel testing the promoter methylation of two microRNAs—*miR129-2* and *miR663a*—identified urothelial carcinoma (from upper and lower urinary tracts) with a sensitivity of 87.8% and specificity of 82.7% in 49 urine samples from patients with urothelial carcinoma [12]. Furthermore, the same panels could discriminate BlCa from other common genitourinary cancers (i.e., from kidney and prostate). Nonetheless, both studies used a singleplex approach, and the ability of these tests to discriminate BlCa from common benign conditions of the urinary tract with overlapping manifestations, especially inflammatory diseases, has not been adequately explored, thus far. Indeed, inflammatory conditions of the urinary tract may negatively impact the specificity of urinary-based biomarkers for BlCa detection, increasing false positive results and entailing unnecessary complementary invasive tests [6,13,14].

Thus, we sought to assess whether the most promising markers in each published panel—*miR-663a* (*miR663a_{me}*) and *Vimentin* (*VIM_{me}*)—might accurately discriminate BlCa from inflammatory conditions in voided urine, allowing for the development of a multiplex test that could be used for early detection in clinical practice.

2. Experimental Section

2.1. Patients and Tumour Sample Collection

Ninety-four primary BlCa tissue samples were obtained from a consecutive series of patients diagnosed, treated with transurethral resection (TUR) or radical cystectomy, between 1994 and 2011, and followed at Portuguese Oncology Institute of Porto (IPO Porto), Portugal (Table 1). Briefly, tumour samples were obtained during surgery and immediately snap-frozen, stored at -80°C and subsequently macrodissected for tumours' cells enrichment and cut in cryostat for DNA extraction. Routine collection and processing of tissue samples allowed for pathological examination, classification, grading and staging [15]. For control purposes, an independent set of 19 normal bladder mucosae

(NB) samples were also collected from BICa-free individuals (prostate cancer patients submitted to radical prostatectomy) (Table 1).

Table 1. Clinical and histopathological characteristics of patients with bladder carcinoma (BICa), normal bladder mucosae (NB), healthy donors (HD) and inflammatory controls (IC).

Clinicopathological Features	Tissues		Urines				
	Bladder UC	Normal Bladder Mucosae	Testing Set		Validation Sets		
			Bladder UC	Healthy Donors	Bladder UC	Healthy Donors (#1)	Inflammatory Controls (#2)
Patients, <i>n</i>	94	19	27	24	100	57	174
Gender, <i>n</i>							
Males	78	19	20	13	79	16	132
Females	16	0	7	12	21	41	42
Median age, yrs (range)	69 (45–91)	63 (48–75)	69 (47–88)	45 (39–61)	68 (38–91)	49 (41–64)	64 (18–92)
Grade, <i>n</i>							
Papillary, low-grade	34	n.a.	13	n.a.	51	n.a.	n.a.
Papillary, high-grade	33	n.a.	8	n.a.	26	n.a.	n.a.
Invasive, high-grade	27	n.a.	6	n.a.	23	n.a.	n.a.
Invasion of Muscular Layer, <i>n</i>							
NMIBC	67	n.a.	19	n.a.	77	n.a.	n.a.
MIBC	27	n.a.	8	n.a.	23	n.a.	n.a.

#1—Validation Set #1; #2—Validation Set #2; yrs—years; n.a.—non applicable; NMIBC—Non-Muscle Invasive Bladder Cancer; MIBC—Muscle Invasive Bladder Cancer, UC—Urothelial Carcinoma.

2.2. Urine Sample Collection and Processing

For the “Testing sets”, 27 voided urine samples (one per patient) were collected from BICa patients, diagnosed and treated between 2006 and 2016 at IPO Porto, as well as a set of 24 voided urine samples from healthy donors (HD), also from IPO Porto, with no personal or familial history of cancer, used as controls (Table 1). The “Validation sets” comprised: (1) 100 urine samples from BICa patients, diagnosed and treated between 2002 and 2016 at IPO Porto, and 57 urine samples from HD collected at IPO Porto, and (2) an independent set of control urine sediments ($n = 174$) from patients diagnosed with urinary tract inflammatory conditions (IC), diagnosed between 2008 and 2014 at the University Hospital of Cordoba (UHC). All BICa patients’ urines were obtained before treatment. Moreover, all sets of samples were collected from different cohorts of patients. Informed consent was obtained from patients and controls after approval from the ethics committees of IPO Porto and UHC (CES-IPO 019/08, approval date: 16th January 2008). All urine samples were processed by immediate centrifugation at 4000 rpm for 10 min; the respective pellet was washed twice with phosphate-buffered saline (PBS) and stored at $-80\text{ }^{\circ}\text{C}$.

2.3. Nucleic Acids Isolation, Bisulfite Modification and Multiplex qMSP Analysis

DNA was extracted from frozen BICa and NB tissues, and all urine sample sets, using a standard phenol-chloroform protocol [16], and its concentration determined using a Qubit 3 Fluorometer (Thermo Fisher Scientific, Waltham, MA, USA). Bisulfite modification was performed through sodium bisulfite, using the EZ DNA Methylation-Gold™ Kit (Zymo Research, Irvine, CA, USA), according to manufacturer’s protocol. For this, 1000 ng and 50 ng of DNA were converted for tissues and urine sediments, respectively. Quantitative methylation levels were performed using Xpert Fast Probe Master Mix (GRiSP, Porto, Portugal), and multiplex reactions were run in triplicates in 96-well plates using an Applied Biosystems 7500 Sequence Detector (Perkin Elmer, Waltham, CA, USA), with Beta-Actin (ACTB) as internal reference gene for normalization. Primer and probe sequences were designed using Methyl Primer Express 1.0 and purchased from Sigma-Aldrich (St. Louis, MO, USA) (Supplementary Table S1). Additionally, six serial dilutions (dilution factor of 5×) of a fully methylated bisulphite modified universal DNA control were included in each plate to generate a standard curve. In each

sample and for each gene, the relative DNA methylation levels were determined using the following formula: ((target gene/ACTB) × 1000). A run was considered valid when previously reported criteria were met [11].

2.4. Statistical Analysis

Differences in quantitative methylation values were assessed with the non-parametric Mann-Whitney *U* (MW) and Kruskal-Wallis (KW) tests. Associations between age, gender, grade, invasion of muscular layer and methylation levels were carried out using Spearman's correlation, MW or KW tests, as appropriate. For multiple comparisons, Bonferroni's correction was applied in pairwise comparisons.

Biomarker performance parameters, including sensitivity, specificity, positive predictive value (PPV), negative predictive value (NPV), accuracy and positive and negative likelihood ratios (LR), were estimated [17]. Receiver operator characteristics (ROC) curves were constructed by plotting the true positive (sensitivity) against false positive (1-specificity) rate, and the area under the curve (AUC) was calculated. The higher value obtained from the sum of sensitivity and 1-specificity in each ROC-curve was used as cut-off to categorise samples as methylated or non-methylated. ROC curves were constructed using logistic regression model for DNA methylation panel. Disease-specific and disease-free survival curves (Kaplan-Meier with log rank test) were computed for standard variables and for categorised genes' promoter methylation status. A Cox-regression model comprising all significant variables (univariable and multivariable model) was computed to assess the relative contribution of each variable to the follow-up status. All two-tailed *p* values were derived from statistical tests, using a computer-assisted program (SPSS Version 26.0, IBM, Armonk, NY, EUA) and the results were considered statistically significant at *p* < 0.05. Bonferroni's correction for multiple comparisons was used when applicable.

3. Results

3.1. Methylation Analysis and Performance of the Multiplex Panel in BlCa Tissue Series

To confirm the previously published performance of *miR663a* and *VIM* promoter methylation as BlCa biomarkers, tissue samples were tested. As expected, both *miR663a* and *VIM* were found hypermethylated (76.6% and 94.4%, respectively) in most BlCa tissue samples, and methylation levels were significantly higher compared to NB (*p* < 0.0001 and *p* < 0.0001, respectively) (Figure 1A). The two genes independently performed well as BlCa detection biomarkers in tissues, with an AUC of 0.979 for *VIM*_{me} (95% confidence interval (CI): 0.956–1.002, *p* < 0.0001), and of 0.897 for *miR663a*_{me} (95% CI: 0.836–0.959, *p* < 0.0001). Moreover, in combination as multiplex panel, it accurately discriminated BlCa from NB with 96.3% sensitivity and 88.2% specificity, corresponding to an AUC of 0.982 (Figure 1B; Supplementary Table S2).

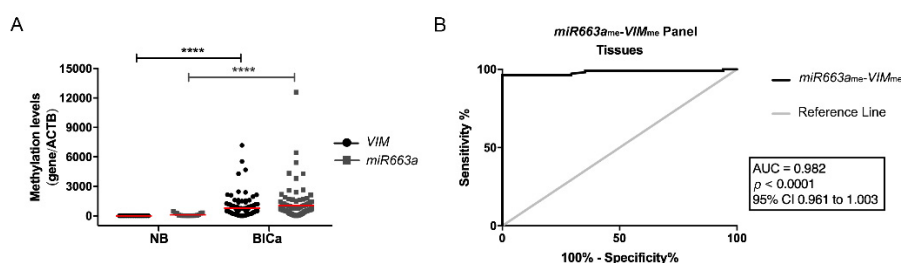


Figure 1. (A) Distribution of *VIM*_{me} and *miR663a*_{me} levels in normal bladder mucosae (NB; *n* = 19) and bladder carcinoma (BlCa; *n* = 94) tissue samples. Mann-Whitney *U* test, **** *p* < 0.0001. Median is represented by the red line. (B) Receiver operator characteristic (ROC) curve evaluating the performance of the *VIM*_{me}-*miR663a*_{me} panel for the identification of BlCa in tissue samples. (AUC—Area under the curve; CI—Confidence interval; ACTB—Beta-Actin; VIM—Vimentin).

3.2. Methylation Analysis and Performance of Multiplex Panel in BlCa Testing Set

Paralleling the previous observations in tissues, *miR663a_{me}* and *VIM_{me}* levels were significantly higher in BlCa urine samples than in those of controls ($p < 0.0001$ and $p < 0.0001$, Figure 2A), and the multiplex panel discriminated BlCa from HD with 92.6% sensitivity and 90% NPV (Supplementary Table S2), corresponding to an AUC of 0.83 (Figure 2B).

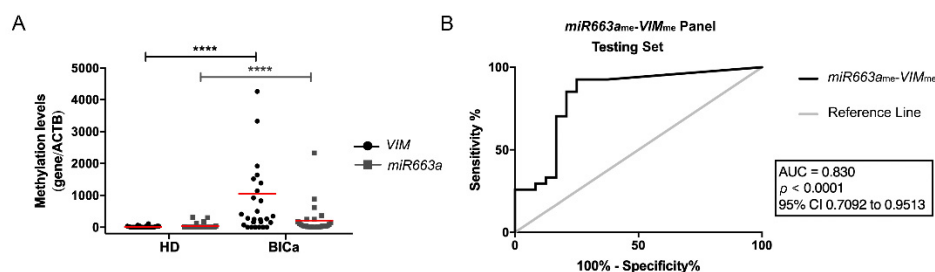


Figure 2. (A) Distribution of *VIM_{me}* and *miR663a_{me}* levels in the Testing Cohort, composed by healthy donors (HD; $n = 24$) and bladder carcinoma (BlCa; $n = 27$) urine samples. Mann-Whitney U test, **** $p < 0.0001$. Median is represented by the red line. (B) Receiver operator characteristic (ROC) curve evaluating the performance of the *VIM_{me}-miR663a_{me}* panel for the identification of BlCa in urine samples of the Testing Cohort. (AUC—Area under the curve; CI—Confidence interval; ACTB—Beta-Actin; VIM—Vimentin).

3.3. Methylation Analysis and Performance of *VIM_{me}* and *miR663_{me}* Multiplex Panel for BlCa vs. HD

In line with the testing set results, a higher number of malignant samples disclosed significantly higher *VIM_{me}* and *miR663_{me}* levels than HDs ($p < 0.0001$ and $p < 0.0001$, respectively) in the validation sets (Figure 3A). ROC curve analysis confirmed a high discriminative ability of *VIM_{me}-miR663_{me}* panel, with an AUC of 0.91 (Figure 3B). Indeed, the multiplex panel discriminated BlCa from HD subjects with 87% sensitivity and 86% specificity (Table 2).

Table 2. Performance of *VIM_{me}-miR663a_{me}* panel for the detection of bladder cancer in Validation Cohorts #1 and #2. (PPV—positive predictive value; NPV—negative predictive value).

Samples	Biomarker Performance	<i>miR663a_{me}-VIM_{me}</i> (%)
Validation #1	Sensitivity	87.0
	Specificity	86.0
	PPV	91.6
	NPV	79.0
	Accuracy	86.6
Validation #2	Sensitivity	80.0
	Specificity	75.3
	PPV	65.0
	NPV	86.8
	Accuracy	77.0

PPV—Positive Predictive Value; NPV—Negative Predictive Value.

Remarkably, the proportion of true positive cases detected by the *VIM_{me}-miR663_{me}* multiplex panel was significantly higher than that of urine cytology ($p < 0.001$). Indeed, of 46 BlCa cases with valid urine cytology results, only 19 were classified as positive, 17 as negative and 10 as “inconclusive/suspicious”, corresponding to 41% sensitivity (Figure 4). Contrarily, the *VIM_{me}-miR663_{me}* multiplex panel correctly identified 40/46 cases as BlCa, corresponding to an overall sensitivity of 87% (Figure 4). Importantly, 12 of 14 low-grade papillary carcinomas were accurately identified by *VIM_{me}-miR663_{me}* multiplex panel, whereas cytology merely identified four cases.

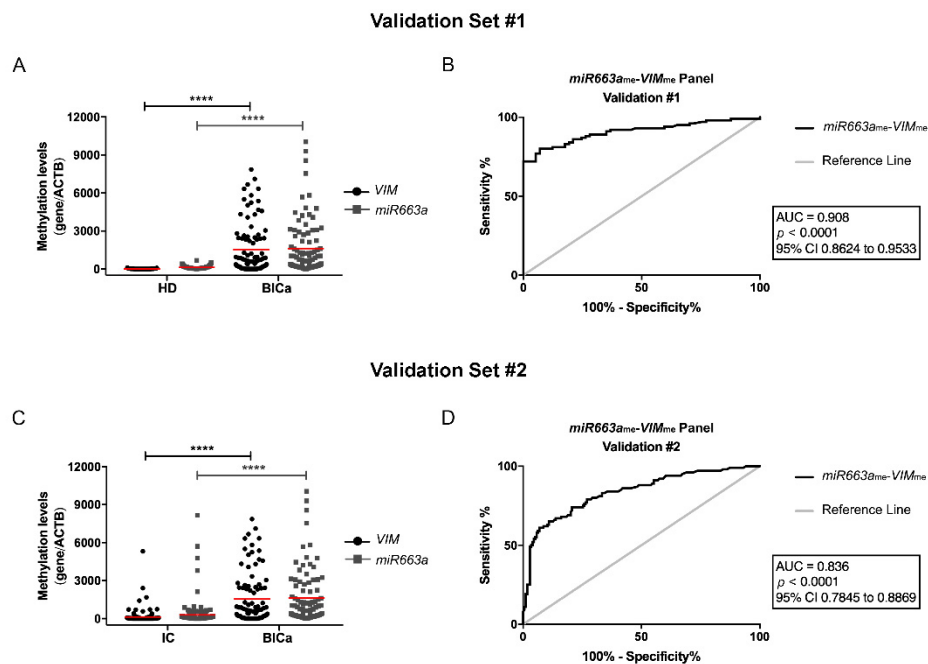


Figure 3. (A) Distribution of VIM_{me} and $miR663a_{me}$ levels in the Validation Cohort #1, composed by healthy donors (HD; $n = 57$) and bladder carcinoma (BICa; $n = 100$) urine samples. Mann-Whitney U (MW) test, **** $p < 0.0001$. Median is represented by the red line. (B) Receiver operator characteristic (ROC) curve evaluating the performance of the VIM_{me} - $miR663a_{me}$ panel for the identification of BICa in urine samples of the Validation Cohort #1. (C) Distribution of VIM_{me} and $miR663a_{me}$ levels in the Validation Cohort #2, composed by inflammatory controls (IC; $n = 174$) and bladder carcinoma (BICa; $n = 100$) urine samples. MW test, **** $p < 0.0001$. (D) ROC curve evaluating the performance of the VIM_{me} - $miR663a_{me}$ panel for the identification of BICa in urine samples of the Validation Cohort #2. (AUC—Area under the curve; CI—Confidence interval; ACTB—Beta-Actin; VIM—Vimentin).

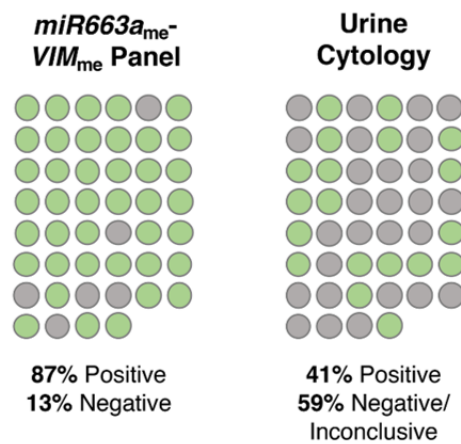


Figure 4. Representation of the percentage of bladder cancer (BICa) cases correctly identified with the VIM_{me} - $miR663a_{me}$ panel and a standard urine cytology analysis. Green circles represent positive cases, grey circles represent negative/inconclusive cases.

3.4. Methylation Analysis and Performance of VIM_{me} and $miR663_{me}$ Multiplex Panel for BICa vs. IC

In urine samples, VIM_{me} - $miR663_{me}$ levels discriminated BICa from IC patients (Figure 3C), with 80% sensitivity, 75.3% specificity and, importantly, 86.8% NPV (Table 2), corresponding to an AUC of 0.836 (Figure 3D). Remarkably, a 2.86 Positive LR and a Negative LR of 0.21 were also disclosed by VIM_{me} - $miR663_{me}$ multiplex panel in this setting.

3.5. Clinicopathologic Correlations and Survival Analyses

High-grade papillary BlCa showed significantly higher *miR663a_{me}* levels than low-grade papillary BlCa ($p = 0.007$), in tissue samples. The same was observed in urine samples from the validation set ($p = 0.0072$), a result which was extensive to VIM_{me} ($p = 0.0052$) (Supplementary Figure S1). No additional associations were disclosed between VIM_{me} and *miR663a_{me}* levels and other standard clinical variables, including patients' age and gender.

Follow-up data was available for 91 (out of 94) IPO Porto's BlCa patients that provided tissue samples. The median follow-up time was 66 months (range: 1–203 months). At the last follow-up timepoint, 30 patients were alive with no evidence of cancer, 12 patients were alive with disease, 29 had deceased due to BlCa and 23 died from other causes. Univariable and multivariable Cox regression analysis were performed, including the variables grade, invasion of muscular layer, gender and age. As expected, a poor outcome was depicted for patients with higher grade and muscle invasive BlCa ($p = 0.001$ and $p < 0.0001$, respectively) (Table 3). In the multivariate model for disease-specific survival, *miR663a_{me}* levels, higher grade and muscle invasion were independent predictors of outcome ($p = 0.04$, $p = 0.035$ and $p = 0.031$, respectively; Table 3). Moreover, after categorization into NMIBC vs. MIBC, tumours with higher *miR663a_{me}* levels implied a 3.7-fold increased risk of cancer-related death among patients with MIBC (95% CI: 1.32–10.25, $p = 0.013$; Supplementary Figure S2). Contrarily, no associations were found for *miR663a_{me}* or VIM_{me} levels concerning disease-free survival.

Table 3. Cox regression models assessing the potential of clinical and VIM_{me} and *miR663a_{me}* levels in the prediction of disease-specific survival for bladder carcinoma (BlCa) patients.

Disease-specific Survival	Variables	Hazard Ratio (HR)	95% CI for OR	<i>p</i>
Univariate	Invasion of muscular layer	6.15	2.76–13.72	0.0001
	Grade			
	PLG vs. PHG	15.59	2.03–119.94	0.008
	PLG vs. IHG	32.83	4.31–250.06	0.001
	Age	2.34	0.98–5.59	0.060
	Gender	1.02	0.39–2.70	0.970
	<i>miR663a</i> methylation \leq median	1.61	0.75–3.48	0.225
Multivariate	VIM methylation \leq median	1.07	0.50–2.28	0.861
	Invasion of muscular layer	3.54	1.12–11.19	0.031
	Grade			
	PLG vs. PHG	8.03	0.97–66.32	0.053
	PLG vs. IHG	11.89	1.18–119.37	0.035
	<i>miR663a</i> methylation \leq median	2.67	1.05–6.81	0.040
	VIM methylation \leq median	1.12	0.51–2.42	0.783

CI—confidence interval; OR—odds ratio; PLG—papillary low-grade; PHG—papillary high-grade; IHG—invasive high-grade.

4. Discussion

Bladder cancer is a major health concern worldwide, with an expected significant increase in incidence and mortality within the next two decades [1,2]. Early detection is critical for adequate management, aiming to reduce disease-specific mortality, as well as the economic burden imposed by BlCa treatment and follow-up. Because currently available diagnostic tools require invasive examination [13,14], development of non-invasive and less costly tests for early detection and monitoring are likely to have a significant impact in clinical practice. Although several molecular biomarkers, including epigenetic-based, have been developed for that end, discrimination of BlCa from other urinary tract malignancies and, more importantly, from benign conditions causing haematuria, including inflammatory diseases, remains a challenge. Indeed, most control samples used in biomarker discovery studies, including our own, mostly comprise normal/healthy donors, disregarding the fact that a biomarker-based test would be offered to an “at-risk” population, including patients experiencing suspicious symptoms. Therefore, based on two previously published studies by our research team [11,12], we tested whether a *miR663a_{me}* and VIM_{me} multiplex panel could accurately

discriminate BlCa from normal individuals and those afflicted with inflammatory conditions of the genitourinary tract.

Because both *miR663a_{me}* and *VIM_{me}* were previously assessed using two different “simplex” multi-gene biomarker panels, we firstly tested *miR663a_{me}* and *VIM_{me}* in multiplex in a consecutive series of primary BlCa tissue samples and normal urothelial mucosae to confirm those previous results. Indeed, employing a multiplex reaction allows for downscaling the initial tissue/body fluid sample requirements, but also the quantity of DNA required for each test [18]. Remarkably, as expected, the *miR663a_{me}*-*VIM_{me}* multiplex panel discriminated BlCa from NB tissues with high sensitivity and specificity (96.3% and 88.2%, respectively), confirming the previous observations for the two markers separately [11,12]. In urine samples from the testing set, although the performance of the multiplex panel was slightly inferior to that of tissues, 92.6% sensitivity and 90% NPV was reached. Indeed, it should be recalled that a relatively small number of cancer cells are exfoliated into urine, which are subsequently “diluted” among a larger population of normal-looking urothelial cells. Thus, the tumour DNA content in urine is actually minute [19] and sensitivity over 90% should be regarded as a very encouraging result. Furthermore, in the validation set, comprising a larger independent cohort, specificity of the *miR663a_{me}*-*VIM_{me}* multiplex panel increased to 86%, further increasing the potential usefulness of the test.

It should be emphasised, however, that the foremost aim of this study was to assess the multiplex panel ability to discriminate BlCa from IC, since this panel is envisaged to be tested in an “at-risk” population, including individuals complaining of haematuria, many of which will be found to harbour urinary tract inflammatory conditions. Although, in this setting, sensitivity and specificity were slightly reduced, NPV increased (86.8%), which is an important finding [20]. Indeed, it is expected that among tested individuals, most will not have a neoplastic condition and, thus, the higher the NPV, the larger the proportion of those subjects that will not be submitted to confirmatory, invasive, procedures, supporting the good performance of the test in discriminating patients negative for malignant condition. Importantly, an LR (+) of 2.86 and an LR (–) of 0.21 values were observed, indicating that a negative result decreases by 30% the probability of misdiagnosis [17].

Despite the fact that several studies suggest various genomic mutations and/or proteins’ expression deregulation as biomarkers for BlCa detection and prognostication [21], the search for novel epigenetic biomarkers, mostly DNA methylation-based, for BlCa detection has been attempted by several research teams, probably due to the stability of the markers and the possibility of high-throughput tests. Although some of those previous studies report an apparently superior performance to the panel reported herein, it should be recalled that in most cases the patients’ series were smaller, only healthy donors were included as controls or these were comprised of a mixed group of healthy donors and patients with diverse urological diseases, and/or did not use a multiplex approach, which might impact in sample availability, testing time length and cost [22–28]. Roperch et al. proposed a three gene multiplex methylation panel (*HS3ST2*, *SEPTIN9* and *SLIT2*) combined with *FGFR3* mutations assessment, age and smoking-status at time of diagnosis in a multivariate model, for diagnosis of NMIBC in urine samples, disclosing 97.6% sensitivity and 84.8% specificity, in a smaller control cohort [29]. Nonetheless, this strategy might be more difficult to implement in clinical practice, since it requires both mutation and methylation analyses, in which the multiplex is performed in two distinct gene duplex reactions. Similarly, Dahmcke et al. proposed a six gene methylation panel (*SALL3*, *ONECUT2*, *CCNA1*, *BCL2*, *EOMES* and *VIM*) combined with the mutational analysis of *TERT* and *FGFR3*, for early detection of BlCa, in urine samples, comparing BlCa patients and patients with gross haematuria [30]. Although this panel disclosed higher sensitivity (97%), specificity was similar (76.9%) [30], and, once again, our test uses a single technique in a single reaction, requiring less amount of sample, enabling shorter response time, reduced technical skills and lower cost.

Although urine cytology and UroVysion™ fluorescence in situ hybridization (FISH) assay are the two most commonly used urine-based tests in daily practice, they present important limitations. On one hand, UroVysion™ presents a not-negligible rate of false positive results; on the other hand,

urine cytology has limited accuracy, especially in low grade tumours detection [6,31,32]. Although no direct comparison can be done with UroVysion™, the 91.6% PPV obtained for the multiplex panel clearly demonstrates higher accuracy in identifying true positive BlCa cases. In the present study, urine cytology reached 41% sensitivity, which was easily surpassed by the 86% displayed by *miR663a_{me}-VIM_{me}* multiplex panel. Notwithstanding, urine cytology remains an easy-to-perform and informative test, as it allows pathologists to have the first look at exfoliated neoplastic cells in urine. Having that in mind, we propose an algorithm where a urine cytology and the *miR663a_{me}-VIM_{me}* multiplex panel could be combined as first-line diagnostic tests in patients with common urinary complaints, with the ultimate goal of reducing the number of unnecessary cystoscopies, which are invasive, uncomfortable and costly procedures (Figure 5).

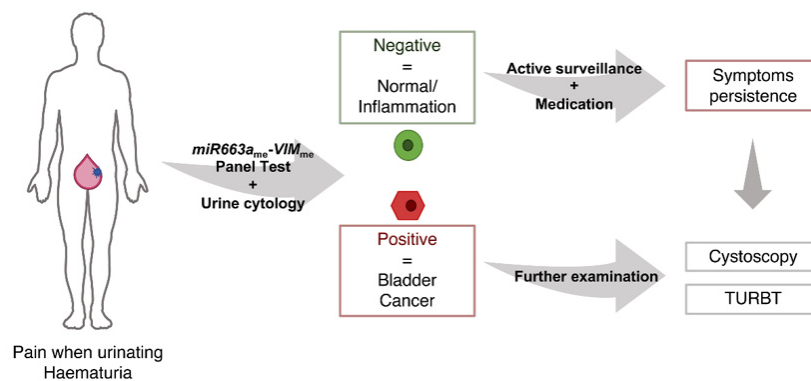


Figure 5. Proposed algorithm for the combination of urine cytology and *VIM_{me}-miR663a_{me}* panel as a first-line diagnostic tests in patients with common urinary complaints. (TURBT—Transurethral Resection of Bladder Tumour).

In this work, we further explored the prognostic ability of the gene methylation markers, aiming to strengthen its clinical potential. Interestingly, survival analysis revealed that high *miR663a_{me}* levels independently predicted poor disease-specific survival in BlCa patients, especially those with MIBC. Thus, the *miR663a_{me}-VIM_{me}* multiplex panel not only conveys diagnostic, but also prognostic information.

Taking into account the promising results obtained, unveiling the putative biological relevance of *miR663a* and *VIM* promoter methylation in bladder carcinogenesis may provide new important insights. *VIM* encodes for vimentin, an intermediate filament characteristic of cells with mesenchymal phenotype, not expressed in most normal epithelia (including urothelium), nor in most carcinomas [33]. *VIM* de-novo expression or overexpression has been reported in various epithelial cancers, including those of prostate [34], breast [35] and lung [36], associating with increased tumour growth and invasion. In these instances, vimentin expression has been associated with epithelial to mesenchymal transition (EMT), a biological process associated with tumour invasiveness [33]. Although *VIM* promoter methylation has been proposed as a detection and/or prognostic marker for other malignancies, biological functions are yet to be truly explored. Moreover, microRNAs have been extensively implicated in urological malignancies [37]. Interestingly, a dual role has already been described for *miR663a*, having a tumour suppressive activity in thyroid carcinoma [38] and glioblastoma [39], whereas an oncogenic function was reported in prostate cancer [40] and osteosarcoma [41]. Additionally, *miR663a*'s downregulation fostered cell proliferation by JunD overexpression in small-cell lung carcinoma [42], and *HMGA2* in hepatocellular carcinoma [43], while Transforming Growth Factor-1 (TGF-β1) [44] overexpression was linked with invasion in the tumour type. Nevertheless, it should be recalled that not all biomarkers require to have a relevant biological role in tumorigenesis.

Importantly, to assure accuracy and validity of the proposed methylation multiplex test, additional validation by others, with larger sets of samples from prospectively collected data (from both BlCa and inflammatory conditions) is warrant.

5. Conclusions

In summary, we demonstrated that a *miR663a_{me}*-*VIM_{me}* multiplex panel accurately identifies BlCa, allowing for precise identification of this common neoplasm in urine samples. Importantly, it also discriminates BlCa patients from those with urinary tract inflammatory conditions, although with inferior performance comparatively to healthy subjects. Thus, the implementation of this panel might assist clinicians in better stratifying patients for confirmatory, invasive examinations, ultimately improving the cost-effectiveness of BlCa diagnosis and management. Moreover, in the same analysis, *miR663a_{me}* analysis would identify patients at higher risk for cancer progression, further highlighting the promise of this panel for patient monitoring.

Supplementary Materials: The following are available online at <http://www.mdpi.com/2077-0383/9/2/605/s1>, Figure S1: Distribution of *miR663a_{me}* and *VIM_{me}* levels in bladder carcinoma tissue samples categorised by grade; Figure S2: Kaplan-Meier curves representing disease-specific survival according to *miR663a_{me}* status; Table S1: Sequences of the primers and probes used in the quantitative methylation-specific PCR experiments; Table S2: Performance of *VIM_{me}*, *miR663a_{me}* and *VIM_{me}-miR663a_{me}* panel for the detection of bladder cancer in Tissues and Testing Set.

Author Contributions: Conceptualization, S.M.-R., R.H. and C.J.; methodology, S.M.-R., A.B., J.T.-M., I.C., D.M., P.M. and J.O.; formal analysis, S.M.-R. and L.A.; writing—original draft preparation, S.M.-R.; review and editing, R.H., C.J. and A.L.-B.; supervision, R.H. and C.J. All authors have read and agreed to the published version of the manuscript.

Funding: This research was funded by the Research Center of Portuguese Institute of Porto (CI-IPOP-27-2016). S.M.-R. was supported by the FCT—Fundação para a Ciência e Tecnologia Grant (SFRH/BD/112673/2015).

Acknowledgments: The authors are grateful to the patients that volunteered to provide samples and to all the personnel of the Departments of Pathology (section of Cytopathology) and of Urology of Portuguese Oncology Institute of Porto that kindly collaborated in this study.

Conflicts of Interest: The authors declare no conflict of interest. The funders had no role in the design of the study; in the collection, analyses or interpretation of data; in the writing of the manuscript, or in the decision to publish the results.

References

1. Ferlay, J.; Ervik, M.; Lam, F.; Colombet, M.; Mery, L.; Piñeros, M.; Znaor, A.; Soerjomataram, I.; Bray, F. Global Cancer Observatory: Cancer Tomorrow. Available online: <https://gco.iarc.fr/tomorrow/home> (accessed on 26 October 2019).
2. Antoni, S.; Ferlay, J.; Soerjomataram, I.; Znaor, A.; Jemal, A.; Bray, F. Bladder Cancer Incidence and Mortality: A Global Overview and Recent Trends. *Eur. Urol.* **2017**, *71*, 96–108. [[CrossRef](#)]
3. Sanli, O.; Dobruch, J.; Knowles, M.A.; Burger, M.; Alemozaffar, M.; Nielsen, M.E.; Lotan, Y. Bladder cancer. *Nat. Rev. Dis. Primers* **2017**, *3*, 17022. [[CrossRef](#)]
4. International Agency for Cancer Research. *WHO Classification of Tumours of the Urinary System and Male Genital Organs*, 4th ed.; Moch, H., Ulbright, T., Humphrey, P., Reuter, V., Eds.; IARC: Lyon, France, 2016.
5. Kaufman, D.S.; Shipley, W.U.; Feldman, A.S. Bladder cancer. *Lancet (London, England)* **2009**, *374*, 239–249. [[CrossRef](#)]
6. Babjuk, M.; Burger, M.; Comperat, E.M.; Gontero, P.; Mostafid, A.H.; Palou, J.; van Rhijn, B.W.G.; Roupert, M.; Shariat, S.F.; Sylvester, R.; et al. European Association of Urology Guidelines on Non-muscle-invasive Bladder Cancer (TaT1 and Carcinoma In Situ)—2019 Update. *Eur. Urol.* **2019**, *76*, 639–657. [[CrossRef](#)]
7. Alfred Witjes, J.; Lebrecht, T.; Comperat, E.M.; Cowan, N.C.; De Santis, M.; Bruins, H.M.; Hernandez, V.; Espinos, E.L.; Dunn, J.; Rouanne, M.; et al. Updated 2016 EAU Guidelines on Muscle-invasive and Metastatic Bladder Cancer. *Eur. Urol.* **2017**, *71*, 462–475. [[CrossRef](#)]
8. Leal, J.; Luengo-Fernandez, R.; Sullivan, R.; Witjes, J.A. Economic Burden of Bladder Cancer Across the European Union. *Eur. Urol.* **2016**, *69*, 438–447. [[CrossRef](#)]
9. Esteller, M. Epigenetics in cancer. *N. Engl. J. Med.* **2008**, *358*, 1148–1159. [[CrossRef](#)] [[PubMed](#)]
10. Costa-Pinheiro, P.; Montezuma, D.; Henrique, R.; Jeronimo, C. Diagnostic and prognostic epigenetic biomarkers in cancer. *Epigenomics* **2015**, *7*, 1003–1015. [[CrossRef](#)] [[PubMed](#)]









11. Costa, V.L.; Henrique, R.; Danielsen, S.A.; Duarte-Pereira, S.; Eknaes, M.; Skotheim, R.I.; Rodrigues, A.; Magalhaes, J.S.; Oliveira, J.; Lothe, R.A.; et al. Three epigenetic biomarkers, GDF15, TMEFF2, and VIM, accurately predict bladder cancer from DNA-based analyses of urine samples. *Clin. Cancer Res.* **2010**, *16*, 5842–5851. [[CrossRef](#)] [[PubMed](#)]
12. Padrao, N.A.; Monteiro-Reis, S.; Torres-Ferreira, J.; Antunes, L.; Leca, L.; Montezuma, D.; Ramalho-Carvalho, J.; Dias, P.C.; Monteiro, P.; Oliveira, J.; et al. MicroRNA promoter methylation: A new tool for accurate detection of urothelial carcinoma. *Br. J. Cancer* **2017**, *116*, 634–639. [[CrossRef](#)]
13. Heller, M.T.; Tublin, M.E. In search of a consensus: Evaluation of the patient with hematuria in an era of cost containment. *Am. J. Roentgenol.* **2014**, *202*, 1179–1186. [[CrossRef](#)] [[PubMed](#)]
14. Grover, S.; Srivastava, A.; Lee, R.; Tewari, A.K.; Te, A.E. Role of inflammation in bladder function and interstitial cystitis. *Ther. Adv. Urol.* **2011**, *3*, 19–33. [[CrossRef](#)] [[PubMed](#)]
15. Humphrey, P.A.; Moch, H.; Cubilla, A.L.; Ulbright, T.M.; Reuter, V.E. The 2016 WHO Classification of Tumours of the Urinary System and Male Genital Organs-Part B: Prostate and Bladder Tumours. *Eur. Urol.* **2016**, *70*, 106–119. [[CrossRef](#)] [[PubMed](#)]
16. Pearson, H.; Stirling, D. DNA extraction from tissue. In *PCR Protocols*, 2nd ed.; Bartlett, J.M.S., Stirling, D., Eds.; Humana Press: Totowa, NJ, USA, 2003.
17. McGee, S. Simplifying likelihood ratios. *J. Gen. Intern. Med.* **2002**, *17*, 646–649. [[CrossRef](#)]
18. Guest, P.C. Multiplex Biomarker Approaches to Enable Point-of-Care Testing and Personalized Medicine. *Methods Mol. Biol.* **2017**, *1546*, 311–315. [[CrossRef](#)]
19. Larsen, L.K.; Lind, G.E.; Guldborg, P.; Dahl, C. DNA-Methylation-Based Detection of Urological Cancer in Urine: Overview of Biomarkers and Considerations on Biomarker Design, Source of DNA, and Detection Technologies. *Int. J. Mol. Sci.* **2019**, *20*, 2657. [[CrossRef](#)]
20. Anna K Füzéry, D.W.C. Cancer Biomarker Assays: Performance Standards. In *Biomarkers in Cancer Screening and Early Detection*, 1st ed.; Srivastava, S., Ed.; John Wiley & Sons: Hoboken, NJ, USA, 2017; pp. 267–276.
21. Tan, W.S.; Tan, W.P.; Tan, M.Y.; Khetrapal, P.; Dong, L.; de Winter, P.; Feber, A.; Kelly, J.D. Novel urinary biomarkers for the detection of bladder cancer: A systematic review. *Cancer Treat. Rev.* **2018**, *69*, 39–52. [[CrossRef](#)]
22. Chihara, Y.; Kanai, Y.; Fujimoto, H.; Sugano, K.; Kawashima, K.; Liang, G.; Jones, P.A.; Fujimoto, K.; Kuniyasu, H.; Hirao, Y. Diagnostic markers of urothelial cancer based on DNA methylation analysis. *BMC Cancer* **2013**, *13*, 275. [[CrossRef](#)]
23. Wang, Y.; Yu, Y.; Ye, R.; Zhang, D.; Li, Q.; An, D.; Fang, L.; Lin, Y.; Hou, Y.; Xu, A.; et al. An epigenetic biomarker combination of PCDH17 and POU4F2 detects bladder cancer accurately by methylation analyses of urine sediment DNA in Han Chinese. *Oncotarget* **2016**, *7*, 2754–2764. [[CrossRef](#)]
24. Yegin, Z.; Gunes, S.; Buyukalpelli, R. Hypermethylation of TWIST1 and NID2 in tumor tissues and voided urine in urinary bladder cancer patients. *DNA Cell Biol.* **2013**, *32*, 386–392. [[CrossRef](#)]
25. Renard, I.; Joniau, S.; van Cleynenbreugel, B.; Collette, C.; Naome, C.; Vlassenbroeck, I.; Nicolas, H.; de Leval, J.; Straub, J.; Van Criekinge, W.; et al. Identification and validation of the methylated TWIST1 and NID2 genes through real-time methylation-specific polymerase chain reaction assays for the noninvasive detection of primary bladder cancer in urine samples. *Eur. Urol.* **2010**, *58*, 96–104. [[CrossRef](#)] [[PubMed](#)]
26. Yu, J.; Zhu, T.; Wang, Z.; Zhang, H.; Qian, Z.; Xu, H.; Gao, B.; Wang, W.; Gu, L.; Meng, J.; et al. A novel set of DNA methylation markers in urine sediments for sensitive/specific detection of bladder cancer. *Clin. Cancer Res.* **2007**, *13*, 7296–7304. [[CrossRef](#)] [[PubMed](#)]
27. Sun, J.; Chen, Z.; Zhu, T.; Yu, J.; Ma, K.; Zhang, H.; He, Y.; Luo, X.; Zhu, J. Hypermethylated SFRP1, but none of other nine genes “informative” for western countries, is valuable for bladder cancer detection in Mainland China. *J. Cancer Res. Clin. Oncol.* **2009**, *135*, 1717–1727. [[CrossRef](#)]
28. Chan, M.W.; Chan, L.W.; Tang, N.L.; Tong, J.H.; Lo, K.W.; Lee, T.L.; Cheung, H.Y.; Wong, W.S.; Chan, P.S.; Lai, F.M.; et al. Hypermethylation of multiple genes in tumor tissues and voided urine in urinary bladder cancer patients. *Clin. Cancer Res.* **2002**, *8*, 464–470. [[PubMed](#)]
29. Roperch, J.P.; Grandchamp, B.; Desgrandchamps, F.; Mongiat-Artus, P.; Ravery, V.; Ouzaid, I.; Roupert, M.; Phe, V.; Ciofu, C.; Tubach, F.; et al. Promoter hypermethylation of HS3ST2, SEPTIN9 and SLIT2 combined with FGFR3 mutations as a sensitive/specific urinary assay for diagnosis and surveillance in patients with low or high-risk non-muscle-invasive bladder cancer. *BMC Cancer* **2016**, *16*, 704. [[CrossRef](#)]

30. Dahmcke, C.M.; Steven, K.E.; Larsen, L.K.; Poulsen, A.L.; Abdul-Al, A.; Dahl, C.; Guldborg, P. A Prospective Blinded Evaluation of Urine-DNA Testing for Detection of Urothelial Bladder Carcinoma in Patients with Gross Hematuria. *Eur. Urol.* **2016**, *70*, 916–919. [[CrossRef](#)]
31. Brimo, F.; Vollmer, R.T.; Case, B.; Aprikian, A.; Kassouf, W.; Auger, M. Accuracy of urine cytology and the significance of an atypical category. *Am. J. Clin. Pathol.* **2009**, *132*, 785–793. [[CrossRef](#)]
32. Lavery, H.J.; Zaharieva, B.; McFaddin, A.; Heerema, N.; Pohar, K.S. A prospective comparison of UroVysion FISH and urine cytology in bladder cancer detection. *BMC Cancer* **2017**, *17*, 247. [[CrossRef](#)]
33. Satelli, A.; Li, S. Vimentin in cancer and its potential as a molecular target for cancer therapy. *Cell Mol. Life Sci.* **2011**, *68*, 3033. [[CrossRef](#)]
34. Singh, S.; Sadacharan, S.; Su, S.; Belldegrun, A.; Persad, S.; Singh, G. Overexpression of vimentin: Role in the invasive phenotype in an androgen-independent model of prostate cancer. *Cancer Res.* **2003**, *63*, 2306–2311.
35. Kokkinos, M.I.; Wafai, R.; Wong, M.K.; Newgreen, D.F.; Thompson, E.W.; Waltham, M. Vimentin and Epithelial-Mesenchymal Transition in Human Breast Cancer—Observations in vitro and in vivo. *Cells Tissues Organs* **2007**, *185*, 191–203. [[CrossRef](#)] [[PubMed](#)]
36. Al-Saad, S.; Al-Shibli, K.; Donnem, T.; Persson, M.; Bremnes, R.M.; Busund, L.T. The prognostic impact of NF-kappaB p105, vimentin, E-cadherin and Par6 expression in epithelial and stromal compartment in non-small-cell lung cancer. *Br. J. Cancer* **2008**, *99*, 1476–1483. [[CrossRef](#)] [[PubMed](#)]
37. Jerónimo, C.; Henrique, R. Epigenetic biomarkers in urological tumors: A systematic review. *Cancer Lett.* **2014**, *342*, 264–274. [[CrossRef](#)] [[PubMed](#)]
38. Wang, Z.; Zhang, H.; Zhang, P.; Dong, W.; He, L. MicroRNA-663 suppresses cell invasion and migration by targeting transforming growth factor beta 1 in papillary thyroid carcinoma. *Tumour Biol.* **2015**, *37*, 7633–7644. [[CrossRef](#)]
39. Shi, Y.; Chen, C.; Yu, S.; Liu, Q.; Rao, J.; Zhang, H.R.; Xiao, H.L.; Fu, T.W.; Long, H.; He, Z.; et al. MiR-663 suppresses oncogenic function of CXCR4 in glioblastoma. *Clin. Cancer Res.* **2015**, *21*, 4004–4013. [[CrossRef](#)]
40. Jiao, L.; Deng, Z.; Xu, C.; Yu, Y.; Li, Y.; Yang, C.; Chen, J.; Liu, Z.; Huang, G.; Li, L.C.; et al. MiR-663 induces castration-resistant prostate cancer transformation and predicts clinical recurrence. *J. Cell Physiol.* **2014**, *229*, 834–844. [[CrossRef](#)]
41. Huang, C.; Sun, Y.; Ma, S.; Vadamotoo, A.S.; Wang, L.; Jin, C. Identification of circulating miR-663a as a potential biomarker for diagnosing osteosarcoma. *Pathol. Res. Pract.* **2019**, *215*, 152411. [[CrossRef](#)]
42. Zhang, Y.; Xu, X.; Zhang, M.; Wang, X.; Bai, X.; Li, H.; Kan, L.; Zhou, Y.; Niu, H.; He, P. MicroRNA-663a is downregulated in non-small cell lung cancer and inhibits proliferation and invasion by targeting JunD. *BMC Cancer* **2016**, *16*, 315. [[CrossRef](#)]
43. Huang, W.; Li, J.; Guo, X.; Zhao, Y.; Yuan, X. MiR-663a inhibits hepatocellular carcinoma cell proliferation and invasion by targeting HMGA2. *Biomed. Pharmacother.* **2016**, *81*, 431–438. [[CrossRef](#)]
44. Zhang, C.; Chen, B.; Jiao, A.; Li, F.; Sun, N.; Zhang, G.; Zhang, J. MiR-663a inhibits tumor growth and invasion by regulating TGF- β 1 in hepatocellular carcinoma. *BMC Cancer* **2018**, *18*, 1179. [[CrossRef](#)]



Article

Sirtuins' Deregulation in Bladder Cancer: SIRT7 Is Implicated in Tumor Progression through Epithelial to Mesenchymal Transition Promotion

Sara Monteiro-Reis ^{1,†}, Ana Lameirinhas ^{1,2,†}, Vera Miranda-Gonçalves ¹,
Diana Felizardo ^{1,3}, Paula C. Dias ^{1,3}, Jorge Oliveira ⁴, Inês Graça ¹, Céline S. Gonçalves ^{5,6},
Bruno M. Costa ^{5,6}, Rui Henrique ^{1,3,7} and Carmen Jerónimo ^{1,7,*}

¹ Cancer Biology and Epigenetics Group, IPO Porto Research Center (CI-IPOP), Portuguese Oncology Institute of Porto (IPO Porto), Rua Dr. António Bernardino de Almeida, 4200-072 Porto, Portugal; sara.raquel.reis@ipoporto.min-saude.pt (S.M.-R.); ana.lameirinhas@ipoporto.min-saude.pt (A.L.); vera.miranda.goncalves@ipoporto.min-saude.pt (V.M.-G.); dianafelizardo@gmail.com (D.F.); paula.dias@ipoporto.min-saude.pt (P.C.D.); maria.ines.graca@ipoporto.min-saude.pt (I.G.); henrique@ipoporto.min-saude.pt (R.H.)

² Master in Oncology, Institute of Biomedical Sciences Abel Salazar-University of Porto (ICBAS-UP), Rua de Jorge Viterbo Ferreira n.º 228, 4050-313 Porto, Portugal

³ Department of Pathology, Portuguese Oncology Institute of Porto, 4200-072 Porto, Portugal

⁴ Urologic Clinic, Portuguese Oncology Institute of Porto (IPO Porto), Rua Dr. António Bernardino de Almeida, 4200-072 Porto, Portugal; jorge.oliveira@ipoporto.min-saude.pt

⁵ Life and Health Sciences Research Institute (ICVS), School of Medicine, University of Minho, Campus de Gualtar, 4710-057 Braga, Portugal; celinegoncalves@med.uminho.pt (C.S.G.); bfmcosta@med.uminho.pt (B.M.C.)

⁶ ICVS/3B's-PT Government Associate Laboratory, Braga/Guimarães, University of Minho, Campus de Gualtar, 4710-057 Braga, Portugal

⁷ Department of Pathology and Molecular Immunology, Institute of Biomedical Sciences Abel Salazar-University of Porto (ICBAS-UP), Rua de Jorge Viterbo Ferreira n.º 228, 4050-313 Porto, Portugal

* Correspondence: carmenjeronimo@ipoporto.min-saude.pt; Tel.: +351-225084000

† These authors contributed equally to this work.

Received: 12 March 2020; Accepted: 23 April 2020; Published: 25 April 2020



Abstract: Sirtuins are emerging players in cancer biology and other age-related disorders, and their putative role in bladder cancer (BlCa) remains elusive. Further understanding of disease biology may allow for generation of more effective pathway-based biomarkers and targeted therapies. Herein, we aimed to illuminate the role of sirtuins' family in BlCa and evaluate their potential as disease biomarkers and therapeutic targets. SIRT1-7 transcripts and protein levels were evaluated in a series of primary BlCa and normal bladder mucosa tissues. SIRT7 knockdown was performed through lentiviral transduction in MGHU3, 5637 and J82 cells and its functional role was assessed. SIRT1, 2, 4 and 5 expression levels were significantly lower in BlCa, whereas SIRT6 and 7 were overexpressed, and these results were corroborated by TCGA cohort analysis. SIRT7 transcript levels were significantly decreased in muscle-invasive vs. papillary BlCa. In vitro studies showed that SIRT7 downregulation promoted cells migration and invasion. Accordingly, increased EMT markers expression and decreased E-Cadherin (CDH1) was observed in those BlCa cells. Moreover, increased EZH2 expression and H3K27^{me3} deposition in E-Cadherin promoter was found in sh-SIRT7 cells. We demonstrated that sirtuins are globally deregulated in BlCa, and specifically SIRT7 downregulation is implicated in EMT, fostering BlCa invasiveness through EZH2-CDH1 axis.

Keywords: bladder cancer; SIRT7; EMT

1. Introduction

Bladder cancer (BlCa) is the 9th most common cancer type worldwide, with an estimated 400,000 new cases and 160,000 deaths per year, in both genders [1]. Men are more susceptible and in more developed regions, BlCa represents has the 6th highest incidence among different cancers. BlCa may be categorized according to clinical, pathological, or molecular characteristics. Muscle-invasive bladder cancer (MIBC) which accounts for about 20% of all cases, represents the more aggressive form, being more likely to progress and metastasize, whereas non-muscle-invasive bladder cancer (NMIBC) is mostly characterized by multiple local recurrences, which, over time, also entail increased risk of invasion. Indeed, although most newly diagnosed patients present NMIBC (approximately 80%), there is variable risk of progression, with increased morbidity [2–4].

Sirtuins (SIRT) are a family of NAD⁺-dependent deacetylases highly conserved among all living organisms. Seven different SIRT (SIRT1–7) are described in mammals, also known as Class III histone deacetylases (HDACs), which differing among each other in substrate specificity and catalytic activity [5]. Within the cell, these enzymes participate in control of important biological processes, including cell division, differentiation, metabolism, genomic stability, survival, senescence and organismal lifespan [6]. In addition, SIRT expression is deregulated in many cancer types [7–9]. SIRT1 and SIRT3 may be up- or downregulated depending on the cancer type, acting either as oncogenes (e.g., colorectal or oral cancer) [10,11], or tumor suppressors (e.g., SIRT1 in bladder cancer, SIRT1 and SIRT3 in breast and prostate cancer) [12,13]. SIRT2 and SIRT4, on the other hand, are considered tumor suppressor, downregulated in glioma and hepatocellular carcinoma (SIRT2) [14,15], and bladder, gastric and lung cancer (SIRT4) [16], among others. Although little is known about the role of SIRT5 in neoplastic transformation, it is overexpressed in non-small-cell lung cancer (NSCLC) [17]. Concerning SIRT6, it is downregulated in several cancers, including hepatocellular carcinoma [18,19], but it is overexpressed in breast cancer and NSCLC [20,21]. Finally, an oncogenic function has been proposed for SIRT7 as it was found overexpressed in several epithelial cancers [22,23]. Moreover, SIRT7 is mostly localized in the nucleus and its deacetylase function needs to be disclosed, with only a few well characterized substrates reported [24,25]. SIRT7 deacetylase activity is related with histones, disclosing highly selective activity for lysine 18 of histone H3 (H3K18Ac), notwithstanding other protein targets involved in cell homeostasis and stress response [24]. SIRT7 is also involved in ribosomes biogenesis and other mechanisms of cell proliferation [26,27].

Although sirtuins have been characterized in various neoplasms, their putative role in BlCa development and progression remains elusive with only a few published studies to date [12,16,28]. Thus, we sought to comprehensively characterize SIRT expression in BlCa tissues, comparing with normal bladder mucosa, assessing their potential as prognostic biomarkers. Furthermore, the phenotypic impact of SIRT7 deregulation in BlCa cells was also evaluated.

2. Results

2.1. Sirtuins Transcript Levels Characterization in Bladder Urothelial Carcinoma

Transcript levels of all sirtuins (SIRT1–7) were evaluated in 94 BlCa samples (UCC) by RT-qPCR and compared with normal mucosa (controls). Statistically significant differences were disclosed for all sirtuins, except for *SIRT3* (MW $p = 0.0612$; Figure 1A). Reduced *SIRT1*, 2, 4 and 5 expression levels were depicted in BlCa (MW $p < 0.0001$ for all; Figure 1A), whereas *SIRT6* and *SIRT7* were overexpressed (MW $p < 0.0001$ for both; Figure 1B). In TCGA dataset, SIRTs expression in BlCa compared to paired NB samples disclosed similar results, with a significant decrease of *SIRT1* and *SIRT3* expression (MW $p < 0.0001$ and $p = 0.0422$, respectively; Figure S1A), and significant increase in *SIRT6* and *SIRT7* expression in BlCa tissues (MW $p < 0.0001$ for both; Figure S1B).

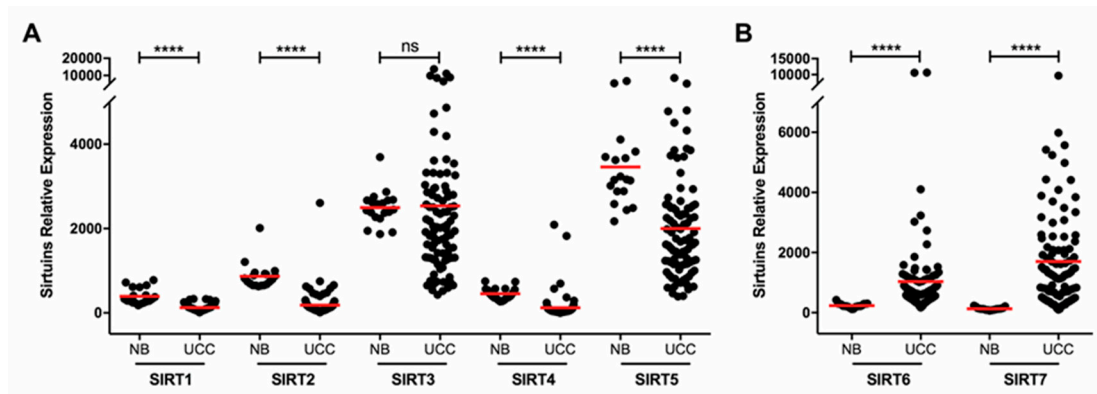


Figure 1. Sirtuin family transcript levels characterization in bladder urothelial carcinoma. Characterization of SIRT1, SIRT2, SIRT3, SIRT4 and SIRT5 (A), and SIRT6 and SIRT7 (B) in the bladder cancer and normal mucosae cohorts, by quantitative RT-PCR. **** $p < 0.0001$, ns—nonsignificant. UCC—urothelial cell carcinoma, NB—normal bladder mucosae.

2.2. SIRT7 Expression Is Decreased in Invasive and TCGA “Basal-Like” Urothelial Carcinoma

Characterization of SIRTs expression was then evaluated according to tumor subtype. Overall, lower transcript levels were observed in invasive high-grade carcinomas (IHG) comparing with papillary low-grade carcinomas (PLG) (Figure S2A), although statistical significance was only reached for SIRT7 (KW $p < 0.0001$; Figure 2A). Additionally, significantly decreased SIRT7 expression was also observed in IHG compared to papillary high-grade carcinomas (PHG) (Figure 2A). Contrarily, SIRT4 expression levels were significantly higher in IHG compared to PLG (KW $p = 0.0012$; Figure S2A). The same analysis was also performed in a TCGA bladder urothelial cancer cohort and a similar SIRTs expression profile was found, with IHG showing significantly increased SIRT4 expression levels comparing to PLG, whereas SIRT5 and SIRT6 expression levels were decreased (Figure S2B). Furthermore, in TCGA dataset, SIRT7 expression was significantly lower in IHG compared to PHG and PLG (KW $p < 0.0001$ for both; Figure 2B), although no significant differences were disclosed between PLG and PHG.

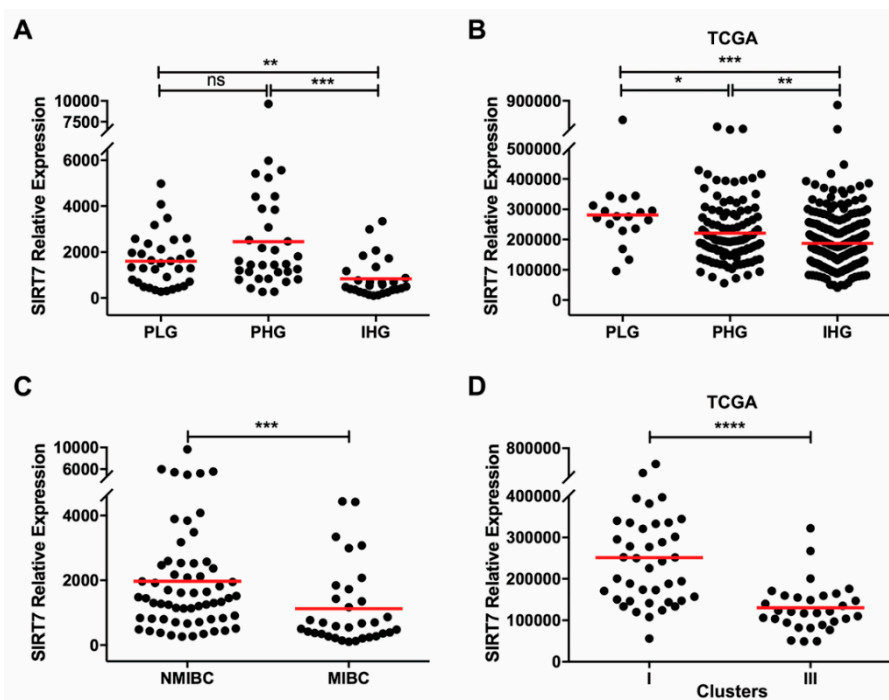


Figure 2. Cont.

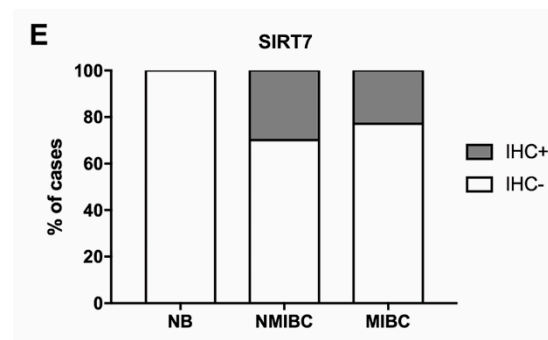


Figure 2. SIRT7 expression downregulation in invasive and TCGA “basal-like” urothelial tumors. Characterization of SIRT7 gene expression in the bladder cancer cohort (A) and TCGA cohort (B) categorized by clinical grade. Characterization of SIRT7 gene expression in the bladder cancer cohort categorized by non-muscle invasive and muscle invasive bladder cancer (C). SIRT7 gene expression according to TCGA molecular clusters analysis in the TCGA cohort (D). SIRT7 immunohistochemistry results for the normal and tumor tissue samples cohort, categorized by non-muscle invasive and muscle invasive bladder cancer, regarding the calculated immunoscore (E). * $p < 0.05$, ** $p < 0.01$, *** $p < 0.001$ and **** $p < 0.0001$. PLG—papillary low-grade, PHG—papillary high-grade, IHG—invasive high-grade, NMIBC—non-muscle invasive bladder cancer, MIBC—muscle invasive bladder cancer.

Concerning pathological stage, two categories were considered: pTa-1/NMIBC (tumors confined to the bladder mucosa), and pT2-4/MIBC (tumors that invade the bladder muscular layer or beyond). In MIBC, *SIRT4* expression levels were significantly higher (MW $p = 0.0009$) and *SIRT7* levels were significantly lower (MW $p = 0.0006$; Figure 2C) comparing with NMIBC. In TCGA cohort, no statistically significant differences were disclosed, since only two cases are classified as NMIBC. Furthermore, in both IPO Porto’s and TCGA cohorts, no association was found between SIRTs expression levels and patients’ gender or age at diagnosis.

Since alterations in *SIRT7* altered expression were concordant in both cohorts, we further assessed the prognostic value of *SIRT7* expression. Of the 94 patients enrolled, four were lost to follow-up. The median follow-up time of BICa patients was 72 months (range: 1–248 months). At the last follow-up time point, 44 patients were alive with no evidence of cancer, eight patients were alive with disease, 10 had died from other causes and 28 had deceased due to BICa. In IPO Porto’s cohort, high tumor grade and pathological stage, as well as more advanced age at diagnosis, were significantly associated with shorter overall survival in multivariable Cox-regression model ($p = 0.031$, $p = 0.037$ and $p = 0.030$, respectively). Although *SIRT7* expression levels did not associate with patients’ prognosis in IPO Porto’s cohort, in TCGA dataset, cases with lower *SIRT7* expression (percentile 25) disclosed shorter overall survival, although only in univariable analysis ($p = 0.028$). Moreover, sirtuins’ expression did not associate with disease-free survival, both considering the total cohort of patients and in patients without (NMIBC) or with (MIBC) invasive disease, separately.

Furthermore, TCGA clusters for molecular markers signatures in BICa were also carried out. These clusters categorize samples using various known molecular characteristics. Cluster I subset consists of tumors with “papillary-like” morphology and higher expression of epithelial markers like E-cadherin (ECAD), whereas cluster III is characterized by low ECAD expression and high cytokeratins expression, consistent with a “basal-like” phenotype [29]. *SIRT7* expression was significantly lower in “basal-like” phenotype (cluster III) than in “papillary-like” phenotype (cluster I) (MW $p < 0.0001$, Figure 2D).

Immunoexpression analysis showed that both normal urothelial and BICa cells expressed nuclear SIRT7 (Figure S3). Although no significant correlation was found between *SIRT7* mRNA and protein levels, higher staining intensity and/or percentage of positive cells was observed in BICa compared to normal urothelium (Figure 2E). Furthermore, a slight reduction of *SIRT7* expression in MIBC was depicted (Figure 2E), paralleling *SIRT7* transcript level results.

2.3. SIRT7 Expression in Bladder Cancer Cell Lines

SIRT7 nuclear protein levels were evaluated in five BlCa cell lines and one immortalized normal urothelial cell line (SV-HUC1), where MGHU3, J82 and 5637 cells displayed the highest SIRT7 protein levels (Figure 3A). The lowest levels were found in the more aggressive cell line, namely TCCSUP cell line derived from a Grade IV carcinoma, whereas MGHU3 derived from a Grade I carcinoma, 5637 from a Grade II carcinoma, and J82 cell line originated from a Grade III carcinoma.

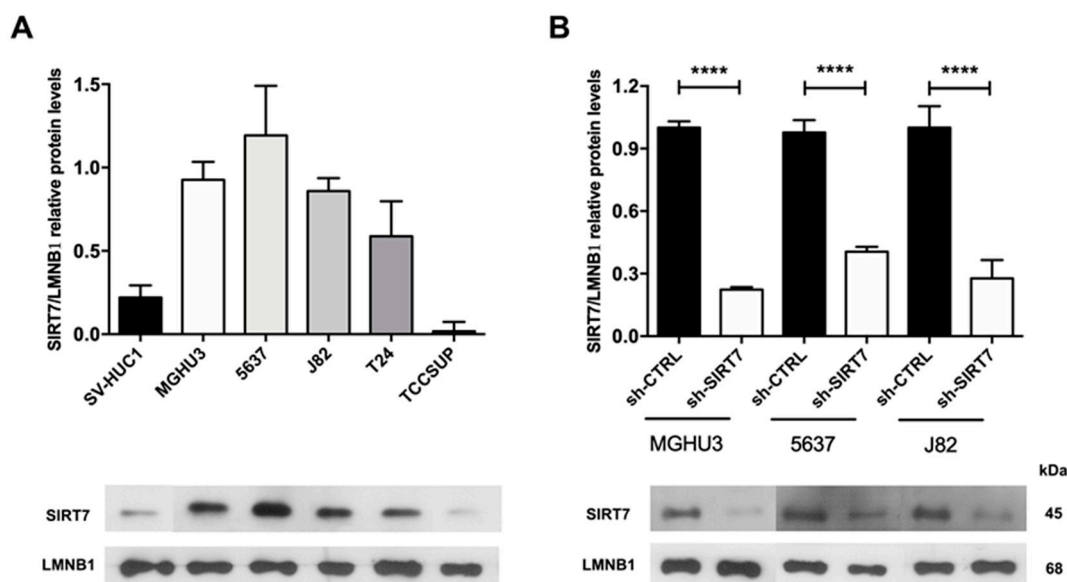


Figure 3. SIRT7 expression in bladder cancer cell lines. Expression of SIRT7 nuclear protein (A) in bladder cancer cell lines by Western blot; results are representative of three independent experiments with mean \pm SD. Confirmation of SIRT7 knockdown in MGHU3, 5637 and J82 cell lines at nuclear protein level (B) by Western blot; **** $p < 0.0001$, results are representative of three independent experiments with mean \pm SD.

Because these three cell lines disclosed the highest SIRT7 nuclear protein expression, they were chosen for lentiviral downregulation experiments. Before transfection, SIRT7 nuclear localization was confirmed by immunofluorescence for the three selected cell lines (Figure S4). Furthermore, after lentiviral transfection, a significant reduction was achieved for the three cell lines (MW $p < 0.0001$; Figure 3B), and reduced SIRT7 nuclear expression was confirmed by immunofluorescence in sh-SIRT7 cells compared to sh-scramble/CTRL cells.

2.4. SIRT7 Downregulation Promotes Invasiveness and EMT in Bladder Cancer Cells

Although no significant alterations in cell proliferation (Figure 4A) and apoptosis (Figure 4B) were found in sh-SIRT7 vs. sh-scramble/CTRL MGHU3 and J82 cells, 5637 sh-SIRT7 displayed a higher proliferation rate (especially at the 48 h time-point), and reduced apoptosis levels ($p < 0.001$ and $p < 0.01$, respectively). Moreover, a significant increase in cell migration was observed at all time points in MGHU3, 5637 and J82 sh-SIRT7 cells (Figure 4C), and the same was depicted for cell invasion (Figure 4D).

Moreover, sh-SIRT7 cells disclosed E-cadherin (or ECAD, an epithelial marker) decreased expression compared to wild type cell lines that expressed this protein (MGHU3 and 5637), whereas significantly increased N-cadherin (or NCAD, mesenchymal marker) protein levels were found in all tested cell lines. Moreover, these results were corroborated by immunofluorescence analysis for the same markers in the same cell lines (Figure S5). Furthermore, EMT transcription factors, SLUG and SNAIL, paralleled the same expression pattern as ECAD in the same cell lines (Figure 4E).

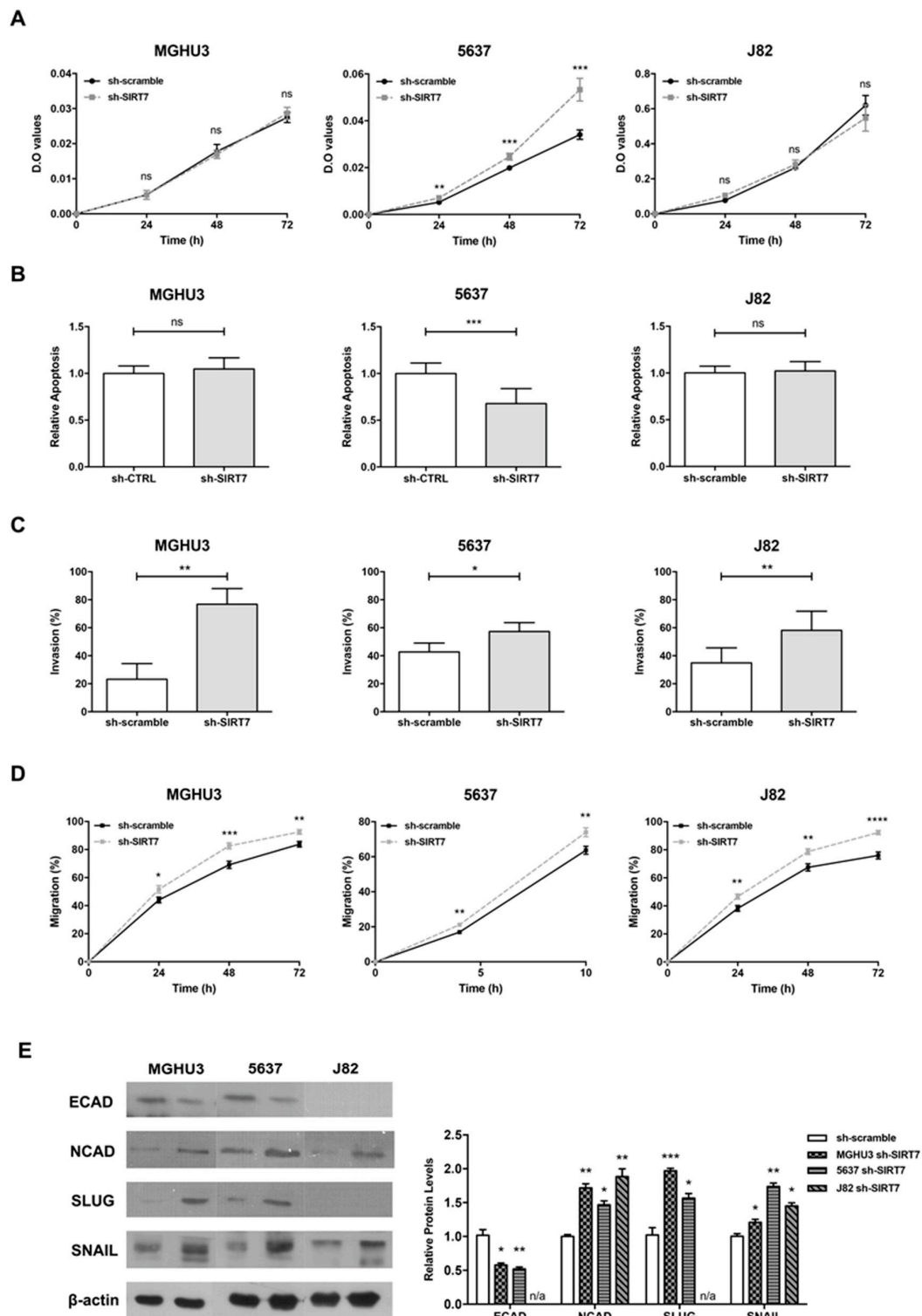


Figure 4. SIRT7 downregulation promotes invasiveness and EMT in bladder cancer cells. Effect of SIRT7 knockdown for MGHU3, 5637 and J82 cell lines at (A) cell viability by MTT assay, (B) apoptosis-cell death by APOPercentage assay, (C) cell invasion by BD Biocoat Matrigel Invasion Chambers and (D) cell migration by wound-healing assay; * $p < 0.05$, ** $p < 0.01$, *** $p < 0.001$ and **** $p < 0.001$; results are representative of three independent experiments with mean \pm SD, each of them in triplicates. Expression of epithelial and mesenchymal markers and EMT transcription factors (E) in MGHU3, 5637 and J82 SIRT7 knockdown by western blot; results are representative of three independent experiments with mean \pm SD.

2.5. SIRT7 Downregulation Associates with E-Cadherin Repression Mediated by Histone Methyltransferase EZH2

Because a global increase in both invasion and migration were found in sh-SIRT7 cell lines, with a concomitant decrease of the epithelial marker and key EMT player ECAD (*CDH1* gene), we further investigated the expression of *CDH1* in tissue samples from IPO Porto's cohort. Indeed, MIBC showed decreased *CDH1* transcript levels and *CDH2* upregulation (MW $p < 0.0001$ and $p = 0.0011$, respectively; Figure S6). Moreover, *SIRT7* and *CDH1* transcript levels positively correlated ($r = 0.58$, 95% CI 0.422 to 0.704, $p < 0.0001$) whereas *SIRT7* and *CDH2* transcript levels negatively correlated ($r = -0.22$, 95% CI -0.403 to -0.00187 , $p < 0.05$) in MIBC patients.

As *CDH1*, which is transcriptionally regulated by *EZH2* [a *SIRT7* substrate [30]], was found decreased in MIBC cases, and taking into account the previous results in *SIRT7* modulated cell lines (Figure 4), we decided to explore the interplay between *SIRT7*, *EZH2* and *CDH1/ECAD*. Indeed, *EZH2* transcript levels were significantly higher in BlCa tissues compared to NB samples (MW $p < 0.0001$, Figure 5A). Furthermore, MIBC depicted the highest *EZH2* transcript levels (MW $p = 0.0444$, Figure 5B), and an inverse expression pattern was depicted for *SIRT7* and *EZH2* transcripts in MIBC (Figure S7). Moreover, *EZH2* protein levels were significantly increased in sh-SIRT7 5637 cells (chosen because it showed differences in all phenotypic assays), compared to sh-CTRL cells (MW $p < 0.01$, Figure 5C).

Additionally, since *EZH2* represses several genes, including *CDH1*, through its histone methyltransferase activity, especially by histone 3 lysine 27 tri-methylation ($H3K27^{me3}$) deposition within the respective promoters, PLA, co-immunoprecipitation (co-IP) and ChIP assays were performed. Firstly, PLA assay showed that *EZH2* and *SIRT7* physically interact in sh-CTRL 5637 cells ($p < 0.0001$; Figure 5D), and that sh-SIRT7 cells showed more $H3K27^{me3}$ mark ($p < 0.001$; Figure 5D). Next, a co-IP with an acetylated-lysine antibody disclosed higher acetylated *EZH2* in sh-SIRT7 cells, comparatively to sh-CTRL cells (Figure 5E). Lastly, a ChIP assay was performed to assess the deposition of $H3K27^{me3}$ mark at *CDH1* promoter region in all transfected cell lines. As expected, increased $H3K27^{me3}$ was observed across the *CDH1* promoter in sh-SIRT7 cells, with a significant increase in both MGHU3 and J82 cells (2-way ANOVA $p = 0.01$; Figure 5F), suggesting that *CDH1* repression associated with *SIRT7* downregulation occurs through *EZH2* overexpression.

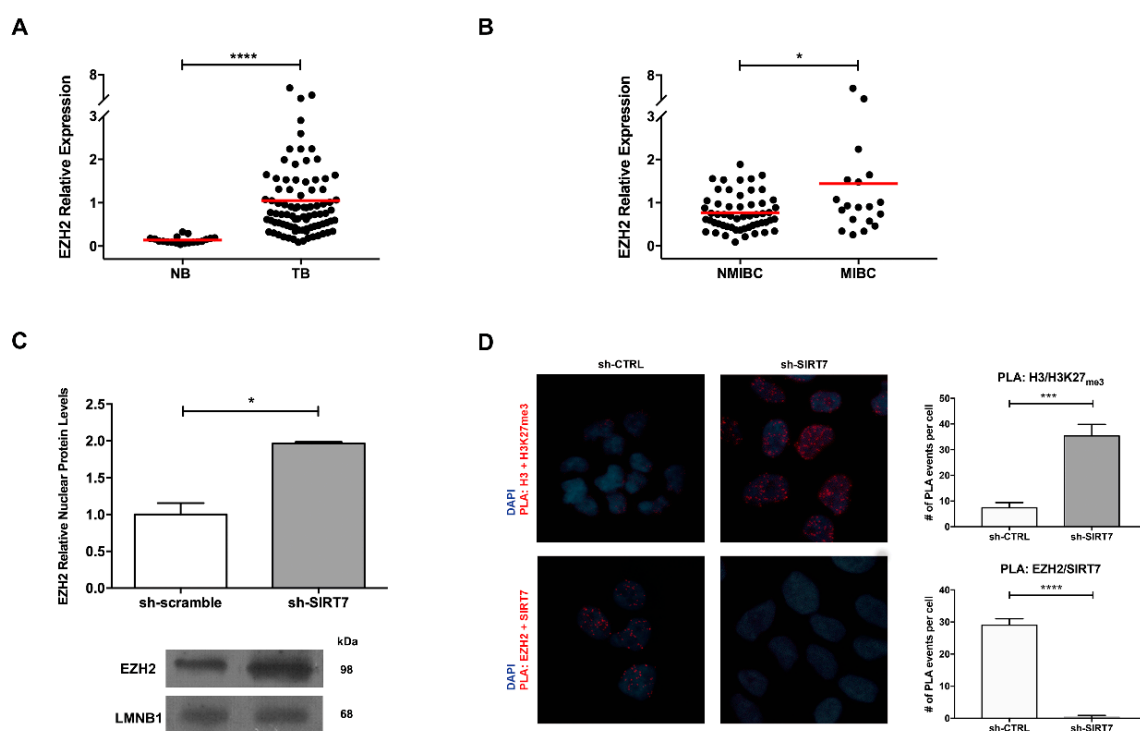


Figure 5. Cont.

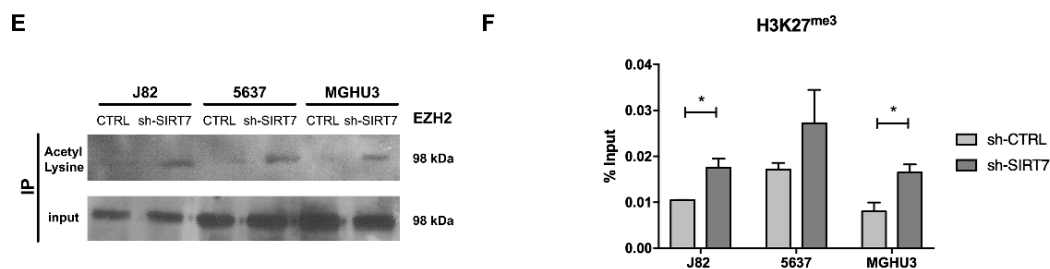


Figure 5. SIRT7 downregulation associates with E-Cadherin repression mediated by histone methyltransferase EZH2. Characterization of EZH2 gene expression in the bladder cancer and normal mucosae cohort (A), and in non-muscle invasive and muscle-invasive bladder cancer cases (B), by quantitative RT-qPCR. Characterization of EZH2 protein expression (C) in 5637 sh-CTRL and sh-SIRT7 cells, by western blot analysis. Proximity Ligation Assay for assessment of interaction of Histone 3 with Histone 3 lysine 27 tri-methylation (H3K27^{me3}) and EZH2 with SIRT7, in 5637 sh-scramble and sh-SIRT7 cells (100× magnification) (D). Western blot analysis for EZH2 protein, after co-immunoprecipitation assay with acetyl-lysine antibody in J82, 5637 and MGHU3 sh-scramble/CTRL and sh-SIRT7 cells (E). Chromatin immunoprecipitation results for H3K27me3 deposition across the CDH1 gene promoter, in MGHU3, 5637 and J82 sh-scramble/CTRL and sh-SIRT7 cells (F). * $p < 0.05$, *** $p < 0.001$ and **** $p < 0.0001$.

3. Discussion

Sirtuins, also known as Class III HDACs, are involved in many biological processes, including cell division, differentiation, metabolism, genomic stability, survival, senescence and organismal lifespan [6], and variable SIRT7 deregulated expression has been reported in many cancer types [7–9]. Remarkably, sirtuins may act either as oncogenes or tumor suppressor genes in different tumor models [12–16]. Thus, better understanding of the biological role of these unique enzymes in tumorigenesis might provide novel biomarkers for disease management as well as putative therapeutic targets.

Herein, we report, for the first time, a comprehensive evaluation of sirtuins (*SIRT1-7*) mRNA expression in a series of 94 BICa cases from a single institution and respective validation in TCGA dataset, comparing with normal bladder mucosa. Significant differences were depicted for all sirtuins, except for *SIRT3*, with *SIRT1*, 2, 4 and 5 downregulation and *SIRT6* and 7 overexpression. These findings were mostly validated in TCGA dataset, especially for *SIRT6* and *SIRT7*. Previous studies on BICa have mainly focused on *SIRT1* and *SIRT4* and were mostly based in publicly available datasets only [12,16], not providing a global picture of sirtuin deregulation in BICa. Interestingly, besides significant differences between BICa and urothelium, differential expression of some sirtuins was also disclosed between tumors with dissimilar clinical and biological behavior. Interestingly, although *SIRT7* was overexpressed in BICa, the more aggressive tumors (IHG) disclosed significantly lower expression levels compared to PLG and PHG, both in IPO Porto's and TCGA cohorts. Furthermore, in MIBC both *SIRT7* transcript and protein disclosed a significant reduction compared to NMIBC. Remarkably, previous reports on *SIRT7* in uterus, colon, kidney, ovary and prostate cancers revealed increased expression levels [22,24]. Nevertheless, in all those models, a strict oncogenic role was proposed for *SIRT7*, whereas our findings suggest that, at the least in bladder carcinogenesis, *SIRT7* may play a dual role, eventually context-dependent. Furthermore, although we did not find significant differences in *SIRT6* transcript levels between PHG and IHG tumors (either in our and TCGA cohort), nor between different stages of MIBC, Wu et al. reported that *SIRT6* protein levels declined significantly from T2 to T4 MIBC, which also suggests that the functional importance of sirtuins may change along cancer progression [28]. The observed decreased overall survival in BICa patients with lower *SIRT7* expression in TCGA cohort (eventually associated with higher grade and stage, as well as molecular BICa subtype) further suggests that decreased *SIRT7* impacts on neoplastic cell biology, promoting a more aggressive phenotype.

Taking in consideration *SIRT7* expression patterns in normal and neoplastic urothelium, we sought to characterize the effects of its deregulated expression at molecular level. Thus, after characterization of *SIRT7* transcript and protein expression levels in neoplastic and benign urothelial cell lines, three cell lines were chosen for further experiments as their profile more closely replicated that of a spectrum of BlCa tissues. Interestingly, *in vitro* phenotypic assays demonstrated that although *SIRT7* downregulation did not affect cell proliferation or apoptosis, with the exception of 5637 cell line, rather impairing cell motility, decreasing both cell migration and cell invasion capabilities in all modulated cell lines. These effects immediately suggested a putative association between *SIRT7* and EMT, a process that is key for tumor invasion and metastazation [31,32]. This hypothesis was confirmed as *SIRT7* knockdown significantly associated with decreased E-Cadherin expression and augmented expression of a mesenchymal marker (N-Cadherin), and EMT-inducing transcription factors (SLUG and SNAIL), in the modulated BlCa cells. Although only a few studies investigated the relationship between sirtuins and EMT [33], *SIRT7* depletion in PC3 prostate cancer cell line was shown to impair migration and invasiveness, reprogramming neoplastic cells towards epithelial gene expression [22]. Our results indicate the opposite trend in BlCa cells, which might be due to the pleiotropic effects of sirtuins and/or the dissimilar molecular profile of prostate and urothelial cancer cells [34].

Remarkably, we found that the mechanism by which *SIRT7* affects *CDH1* expression, and thus EMT, is probably linked to EZH2. EZH2 is a well-known member of the polycomb repressive complex 2 (PRC2), described as being involved in the transcription repression by catalyzing the repressive H3K27^{me3} mark at several gene promotes, including *CDH1* [35–37]. Previously, proteomic analyses demonstrated that among 250 candidate substrates, EZH2 was a *SIRT7* substrate [30,38]. In our study, sh-*SIRT7* cells showed increased total and acetylated EZH2 expression, followed by decreased ECAD protein. Concurrently, increased H3K27^{me3} deposition at *CDH1* promoter was also observed in the same cells. Thus, when *SIRT7* is downregulated, EZH2 activity might be enhanced by acetylation, contributing to *CDH1* transcription repression through H3K27^{me3} deposition in its promoter, as previously reported [30]. *CDH1* repression and concomitant EMT transcription factors' upregulation (e.g., SNAIL and SLUG), might then lead to a shift from epithelial to mesenchymal phenotype, allowing for increased cancer cell motility. Indeed, upregulation of these specific EMT transcription factors, due to diverse upstream signals and post-transcriptional mechanisms, also corroborates our hypothetic mechanism. Indeed, both SNAIL and SLUG were shown to cooperate with PRC2, and specifically with EZH2, towards controlling the expression of several genes, relevant for neural crest development, including *CDH1* [39,40]. Moreover, during EMT, Snail was proven to recruit EZH2 to specific genomic sites by the enrollment of the long non-coding RNA HOTAIR [41]. Thus, our results suggest that EMT transcription factors' upregulation in sh-*SIRT7* BlCa cells might be due to the phenotypic shift in invasion and migration and, at the molecular level, by recruitment of EZH2 to specific targets.

Thus far, only a limited number of upstream *SIRT7* transcription regulators, such as histone deacetylase 3 (HDAC3) and the X-box binding protein 1 (XBP1) molecules have been identified [42,43]. At post-transcriptional level, *SIRT7* was shown be negatively regulated by microRNAs, such as those from microRNA-125 family [44]. However, few reports deal with *SIRT7* regulation by post-translational modifications [45–47]. Hence, it would be important to further explore how regulation of *SIRT7* occurs in BlCa, and unveil how *SIRT7* expression shift occurs from non-invasive to invasive BlCa.

Moreover, although discovery of new prognostic biomarkers for BlCa is imperative for more effective disease management, the aim of our study was mostly to uncover how expression of all sirtuins was altered in BlCa, and to investigate whether they might be implicated in bladder carcinogenesis and/or disease progression and invasiveness. Indeed, we were able to demonstrate that for *SIRT7*. Nonetheless, the analyzed cohort was composed by patients diagnosed over a large time span (1991–2011) and the small number of events occurring in this cohort precluded a more robust and detailed statistical analysis.

Overall, our results suggest that increased *SIRT7* expression occurs during urothelium neoplastic transformation, which usually results in the formation of non-invasive, papillary neoplasms or flat

lesions like urothelial carcinoma in situ [48]. At this stage, it is likely that SIRT7 is involved in promoting cell growth and survival, which are key to neoplastic development, eventually through deacetylation of H3K18 [24]. Then, transition to an invasive phenotype might require SIRT7 downregulation, involving EZH2 upregulation and acetylation, among other mechanisms, which promote EMT. Although the mechanism of SIRT7 deregulation in BlCa remains elusive, it is tempting to speculate whether it might be due to epigenetic mechanisms, which allow for the suggested plasticity of SIRT7 gene expression during carcinogenesis and tumor progression.

4. Materials and Methods

4.1. Patients and Samples

Patients with primary bladder urothelial carcinoma (UCC), treated with transurethral resection (TUR) or radical cystectomy, between 1991 and 2011 at Portuguese Oncology Institute of Porto (IPO Porto), Portugal ($n = 94$). A set of 19 morphologically normal bladder mucosa (NB) tissue samples was obtained from BlCa-free individuals (prostate cancer patients submitted to radical prostatectomy) and served as controls. All specimens were fresh-frozen at $-80\text{ }^{\circ}\text{C}$ and subsequently cut in a cryostat for confirmation of representativity and nucleic acid extraction. From each specimen, fragments were collected, formalin-fixed, and paraffin embedded for routine histopathological examination, including grading and pathological staging, by a dedicated uropathologist [49]. Relevant clinical data was collected from clinical charts (Table 1). Patients and controls were enrolled after informed consent. This study was approved by the institutional review board (Comissão de Ética para a Saúde) of IPO Porto (CES103-14).

Table 1. Clinical and histopathological parameters of Bladder Cancer patients, and gender and age distribution of control set individuals.

Clinicopathological Features	Bladder UCC	Normal Bladder Mucosae
Patients, n	94	19
Gender, n (%)		
Males	78 (83)	19 (100)
Females	16 (17)	0
Median age, yrs (range)	69 (45–91)	63 (48–75)
Grade, n (%)		
Papillary, low-grade	33 (35)	n.a.
Papillary, high-grade	33 (35)	n.a.
Invasive, high-grade	28 (30)	n.a.
Pathological Stage, n (%)		
pTa/pT1 (NMIBC)	61 (65)	n.a.
pT2-4 (MIBC)	33 (35)	n.a.

(UCC—Urothelial Cell Carcinoma; yrs—years; NMIBC—non-muscle invasive bladder cancer; MIBC—muscle invasive bladder cancer).

4.2. Real-Time Quantitative PCR (RT-qPCR)

RNA was extracted from tissues and from MGHU3, 5637 and J82 sh-scramble and sh-SIRT7 cells using TRIzol[®] (Invitrogen, Carlsbad, CA, USA), according to manufacturer's instructions. For tissue RNA, cDNA synthesis was performed using the High Capacity cDNA Reverse Transcription Kit (Applied Biosystems[®], Foster City, CA, USA), according to manufacturer's instructions. Sirtuins transcript levels were quantified by RT-qPCR. Expression levels were evaluated using 4.5 μL of diluted cDNA, 5 μL of TaqMan[®] Universal PCR Master Mix No AmpErase[®] UNG (Applied

Biosystems®) and 0.5 µL of TaqMan® Gene Expression Assay, specific for each sirtuin and reference genes, as described in Table S1 (Applied Biosystems®). Each sample was run in triplicate and the RT-qPCR conditions were: 2 min at 50 °C, followed by enzyme activation for 10 min at 95 °C, and 45 cycles which included a denaturation stage at 95 °C for 15 s and an extending stage at 60 °C for 60 s. *HPRT* and *SDHA* were both used as reference genes for normalization. Relative expression of target genes tested in each sample was determined as: [Gene Expression Level = (Gene Mean Quantity/(*HPRT1* & *SDHA*) Mean Quantity) × 1000].

Concerning cell lines, 1000 ng of RNA were reverse transcribed using RevertAid RT kit (Thermo Fisher Scientific Inc., Waltham, MA, USA), according to manufacturer's instructions. For 100 ng of cDNA, *SIRT7* and *NCAD* transcript levels were quantified using TaqMan® Gene Expression Assay, as described above, in 396 well plates LightCycler480II (Roche, Basel, Switzerland). For *ECAD* and *EZH2* genes, transcription levels were also evaluated in J82 sh-scramble and sh-SIRT7 cells in 396 well plates LightCycler480II (Roche) using Xpert Fast SYBER Mastermix Blue (GRiSP Research Solutions, Porto, Portugal) with specific primers (S2). Transcript levels for studied genes were then evaluated using $\Delta\Delta C_t$ method, with *HPRT* and *BGUS* housekeeping genes as reference genes.

4.3. Immunohistochemistry

Immunohistochemistry was performed using the Novolink™ Max Polymer Detection System (Leica Biosystems, Wetzlar, Germany). Three-µm thick tissue sections from formalin-fixed and paraffin-embedded BlCa (corresponding to 88 of the 94 cases, for which there was archived tissue available) and controls ($n = 25$, consisting of normal urothelial mucosa collected from the urethra of nephrectomy specimens with renal cell tumors) were cut, deparaffinized and rehydrated. Antigen retrieval was accomplished by microwaving the specimens at 800 W for 20 min in 10 mM sodium citrate buffer, pH = 6. Endogenous peroxidase activity was blocked by incubating the sections in 0.6% hydrogen peroxide solution for 20 minutes. Primary monoclonal antibody for *SIRT7* (HPA053669, Sigma-Aldrich™, St. Louis, MO, USA) was used in 1:500 dilution, and incubated at room-temperature (RT) for one hour. Then, 3,3'-diaminobenzidine (Sigma-Aldrich™) was used as chromogen for visualization and slides were mounted with Entellan® (Merck-Millipore, Burlington, MA, USA). Normal testicular tissue, showing intense *SIRT7* immunoreactivity was used as positive control. *SIRT7* immunoexpression was evaluated by a dedicated uropathologist and cases were classified using a semi-quantitative scale for both staining intensity (0—no staining; 1—intensity lower than normal urothelium; 2—intensity equal to normal urothelium; 3—intensity higher than normal urothelium) and percentage of positive cells (0—< 10%; 1—10–33%; 2—33–67%; 3—> 67%), in each tumor. Staining intensity and percentage of positive cell results were then combined in a single score (Score S = staining intensity × percentage of positive cells) assigned to each tumor, and further stratified into low expression ($S < 4 = \text{IHC-}$) and high expression ($S \geq 4 = \text{IHC+}$) groups, which correspond to cases with less than 33% stained cells or staining intensity lower than normal urothelium, and cases with at least 33% stained cells with an intensity equal to or higher than normal urothelium.

4.4. TCGA Dataset Analysis in Bladder Urothelial Carcinoma Patients

The Cancer Genome Atlas (TCGA) dataset was interrogated for data on *SIRT1-7* expression and clinical information, when available, of 408 BlCa patients and 19 matched controls. All expression data from samples hybridized at the University of North Carolina, Lineberger Comprehensive Cancer Center, using Illumina HiSeq 2000 RNA Sequencing version 2 analysis, were downloaded from the GDC data portal (<https://portal.gdc.cancer.gov/>). Biospecimen Core Resources (BCRs) provided the clinical data of each patient. This data is available for download through the GDC data portal (<https://portal.gdc.cancer.gov/>) (Table 2).

Table 2. Clinical and histopathological parameters of bladder cancer patients, and gender and age distribution of control set individuals from TCGA cohort.

Clinicopathological Features	Bladder UCC	Matched Normal Bladder Mucosae
Patients, <i>n</i>	408	19
Gender, <i>n</i> (%)		
Males	301 (83)	10 (53)
Females	107 (17)	9 (47)
Median age, yrs (range)	69 (34–90)	71 (48–90)
Grade, <i>n</i> (%)		
Papillary, low-grade	18 (4)	n.a.
Papillary, high-grade	112 (28)	n.a.
Invasive, high-grade	278 (68)	n.a.
Pathological stage, <i>n</i> (%)		
pTa/pT1 (NMIBC)	2 (1)	n.a.
pT2-4 (MIBC)	406 (99)	n.a.

(UCC—Urothelial Cell Carcinoma; yrs—years; NMIBC—non-muscle invasive bladder cancer; MIBC—muscle invasive bladder cancer)

4.5. Cell Lines Culture

5637, J82, T24 and TCCSUP BICa cell lines and normal bladder cell line SV-HUC1 were selected for this study. All cell lines were purchased from ATCC and grown using recommended medium (Biochrom-Merck, Berlin, Germany) supplemented with 10% fetal bovine serum (FBS, Biochrom) and 1% penicillin/streptomycin (GIBCO, Invitrogen) at 37 °C and 5% CO₂. Mycoplasma test was regularly performed for all cell lines using TaKaRa PCR Mycoplasma Detection Set (Clontech Laboratories, Mountain View, CA, USA).

4.6. Lentiviral Transduction

SIRT7 knockdown was performed through lentiviral transduction in J82 cell line using GIPZTM Lentiviral shRNA particles (DharmaconTM, Lafayette, CO, USA), and in MGHU3 and 5637 cell lines using SMARTvectorTM Inducible Lentiviral shRNA particles (target sequence: 5'-CCCTGCGTGCTGGTGAAGA-3'). All sh-SIRT7 vectors included the green fluorescent protein (GFP). Briefly, cells were seeded in 12 well/plate at density of 4×10^4 cells/well and incubated during 24 h in humidified chamber at 37 °C and 5% CO₂. Then, culture medium was removed and 500 µL of completed medium with 8 µg/mL polybrene and lentiviral sh-SIRT7 particles with MOI 10 concentration were added. After 48 h, 1 µg/mL of puromycin dihydrochloride (Clontech Laboratories) was added to select stably transfected cells. For MGHU3 and 5637 cells, after puromycin selection, a treatment was performed with 100 ng/mL doxycycline in order to induce the Tet-On 3 G bipartite induction system. Additionally, J82, MGHU3 and 5637 control cells were generated using a non-target scramble shRNA under the same previously described conditions.

For clone selection, 10, 20 and 50 cells/well were seeded in 96 well plate after stable selection, and the isolated clones were grown until confluence for protein extraction, and subsequent western blot analysis for SIRT7 expression. Moreover, sh-SIRT7 cells were observed under the fluorescence microscope for GFP expression.

4.7. Protein Extraction

BICa cell lines, sh-scramble/CTRL and sh-SIRT7 cells were grown until 80% confluence and homogenized in Kinexus lysis buffer supplemented with proteases inhibitors cocktail. Then,

cells were sonicated for 5 cycles of 30 s ON and 30 s OFF (Bioruptor[®], Diagenode, Liège, Belgium). After centrifugation, the supernatant was collected, and total protein was quantified according to the Pierce BCA Protein Assay Kit (Thermo Fisher Scientific Inc.), according to the manufacture procedure.

For subcellular fractionation, Nuclear Extract kit (Active Motif, Carlsbad, CA, USA) was used. Briefly, bladder cancer cell lines, sh-scramble/CTRL and sh-SIRT7 cells were washed in 1 X PBS with phosphate inhibitors and scrapped. Subsequently, cells were suspended in hypotonic buffer and incubated on ice during 15 min. Additionally, a detergent was added, and samples were centrifuged at 14,000 rpm during 30 s at 4 °C. Supernatant (cytoplasmic fraction) was collected and stored at −80 °C until use. Then, cell pellets were resuspended and incubated in a complete lysis buffer solution (lysis buffer with proteases inhibitor cocktail and 10 mM DTT), following centrifugation and supernatant (nuclear fraction) collection and storage at −80 °C. Nuclear and cytoplasmic proteins were then quantified using the Pierce BCA Protein Assay Kit (Thermo Fisher Scientific Inc.), according to manufacture procedure.

4.8. Western Blot and Co-Immunoprecipitation

Aliquots of 30 µg total protein was separated in 10% polyacrylamide gel by SDS-PAGE and transferred onto an immunoblot PVDF membrane (Bio-Rad Laboratories, Hercules, CA, USA) in a 25 mM Tris-base/glycine buffer using a Trans-Blot Turbo Transfer system (Bio-Rad Laboratories). Membranes were blocked with 5% milk in TBS/0.1% Tween (TBS/T pH = 7.6) for 1 hour at RT. After incubation with primary antibodies for SIRT7 (1:350, HPA053669, Sigma-Aldrich) or EZH2 (1:500, NCL-L-EZH2, Leica Biosystems) for 1 h 30 min at RT, the membranes were washed in TBS/T and incubated with secondary antibody coupled with horseradish peroxidase for 1 h at RT. The bound was visualized by chemiluminescence (Clarity WB ECL substrate, Bio-Rad) and quantification was performed using band densitometry analysis from the ImageJ software (version 1.6.1, National Institutes of Health). β-Actin (1:10,000, A1978, Sigma-Aldrich) for total protein and cytoplasmic protein analysis, and Laminin B1 (1:1000, D4Q42, Cell Signaling Technologies, Danvers, MA, USA) for nuclear protein, were used as loading controls. For co-immunoprecipitation assays, 200 µg of total protein from cell lysates were incubated with anti-acetylated-lysine antibody (#9441, Cell Signaling Technology) and immunoprecipitated with Protein A/G magnetic beads (#16-663, Sigma-Aldrich) overnight at 4 °C. The final eluates were blotted with EZH2 primary antibody, as detailed above. Detailed information about western blot can be found at Figure S8.

4.9. Immunofluorescence (IF)

Wild-type MGHU3, 5637 and J82, sh-scramble/CTRL and/or sh-SIRT7 cells were seeded on cover slips at 20,000 cells/well, overnight. Briefly, cells were fixed in methanol during 10 min and then blocked with 5% bovine serum albumin (BSA) during 30 min. After overnight SIRT7 (1:500, HPA053669, Sigma-Aldrich), ECAD (1:150, #3195, Cell Signaling Technology) and/or NCAD (1:50, #13116, Cell Signaling Technology) incubation at RT, cells were incubated with secondary antibody anti-rabbit IgG-TRITC (1:500, T6778, Sigma-Aldrich) during 1 h at RT. Finally, after 1× PBS wash, cells were stained with 4',6-diamidino-2-phenylindole (DAPI) (AR1176, BOSTER Biological Technologies (Pleasanton, CA, USA) in mounting medium. Pictures were taken on a IX51 fluorescence microscope (Olympus, Tokyo, Japan) equipped with an Olympus XM10 digital camera using CellSens software.

4.10. Chromatin Immunoprecipitation (ChIP)

Chromatin immunoprecipitation (ChIP) analysis was performed in sh-scramble/CTRL and sh-SIRT7 cells. For the crosslink step, formaldehyde solution (Sigma) was added to adherent cells ($\sim 1 \times 10^7$) media at 1% final concentration, and after an 8 minutes' incubation at RT, reaction was immediately stopped by adding 1.5 mL of 2.5 M glycine and incubating for 5 min. Cells were then washed twice with ice-cold 1× PBS, scrapped, harvested and centrifuged at 4 °C.

Cell pellets were homogenized with cell lysis buffer (10 mM Tris-HCL pH7.5, 10 mM NaCl, 0.5% NP-40) and left on ice for 1 h30, with intermittent vortexing, and then centrifuged at 4 °C. At this point, pellets were re-suspended in nuclei lysis buffer (50 mM Tris-HCL pH = 7.5, 10 mM EDTA pH = 8, 1% SDS) and incubated for 15 min on ice, followed by adding of 2× volumes of IP dilution buffer (16.7 mM Tris-HCL pH7.5, 167 mM NaCl, 1.2 mM EDTA pH = 8, 0.01% SDS). Chromatin was solubilized and sheared to 200–400 bp fragments using an ultra-sonicator (Bioruptor[®], Diagenode) for 15 cycles of 30 s ON and 30 s OFF. Soluble chromatin was then centrifuged and stored at –80 °C until further use.

Before immunoprecipitation (IP), each 50 µL of chromatin was 1:10 diluted in dilution buffer (1.2 mM EDTA pH = 8, 16.7 mM Tris pH = 8, 167 mM NaCl, 1.1% Triton X-100, 0.01% SDS), and 5 µL of this solution was reserved in a new tube for the input control. After this, 20 µL of protein A+G magnetic beads (Millipore) were added to each IP sample, as well as ChIP-grade antibodies for Histone H3 (ab1791, Abcam, Cambridge, UK), tri-methylation of lysine 27 of histone H3 (H3K27me³, 07-449, Millipore), positive control (RNA polymerase II) and negative control (mouse IgG), at assay dependent concentration. IPs were incubated overnight at 4 °C with rotation. After incubation, magnetic beads were precipitated using 1.5 mL tubes magnet rack and washed with four different salt concentration buffers. At this point, elution buffer (50 mM Tris-HCL pH = 7.5, 10 mM EDTA pH = 8, 1% SDS) was added to all samples and input control, as well as 200 µg/mL of RNase A, following an incubation of 30 min at 37 °C. After this, samples were incubated with proteinase K for 2 h at 62 °C, followed by an incubation of 10 min at 95 °C, for cross-link reversion.

DNA was extracted from samples using the Qiaquick gel extraction kit (Qiagen, Hilden, Germany), according to manufacture procedures, and stored at –20 °C until further use. For qPCR, two pairs of primers for CDH1 promoter were designed, both for ~325 bp before TSS (F—5'-TAACCC ACCTAGACCCTAGCAA-3', R—5'-GCTGATTGGCTGAGGGTTCA-3') and for ~600 bp before TSS (F—5'-ACCTGTACTCCCAGCTACTAGA-3', R—5'-GATGGGGTCTCACTCTTTCACC-3'). RT-qPCR was performed as mentioned above, and the relative amount of promoter DNA was normalized using Input Percent method.

4.11. Proximity Ligation Assay (PLA)

Sh-scramble/CTRL and sh-SIRT7 cells, were seeded in 1 cm² coverslips and allowed to grow overnight. Then, cells were fixed in 4% formaldehyde (Sigma) for 10 min and permeabilized in 0.5% Triton X-100 (Sigma), for 5 min, at RT and gently stirred. PLA assay was performed using the commercial kit Duolink In Situ (OLINK Bioscience, Uppsala, Sweden), according to manufacturer's instructions. The antibodies used were Histone H3 (ab1791, Abcam, Cambridge, UK), tri-methylation of Lysine 27 of Histone H3 (H3K27me³, 07-449, Millipore), SIRT7 (HPA053669, Sigma-Aldrich) and EZH2 (NCL-L-EZH2, Leica Biosystems). After the procedure, cells were stained with 4',6-diamidino-2-phenylindole (DAPI) (AR1176, BOSTER Biological Technology, Pleasanton, CA, USA) in mounting medium. Pictures were taken on an Olympus IX51 fluorescence microscope equipped with an Olympus XM10 digital camera using CellSens software.

4.12. Cell Viability Assay

To assess the role of SIRT7 in cell growth, 3-(4,5-dimethylthiazol-2-yl)-2,5-diphenyltetrazolium (MTT) assay (Sigma-Aldrich) was performed. Briefly, sh-scramble/CTRL and sh-SIRT7 cells were seeded at 3000 cell/well density, overnight, in 96 well plate. Then, 5 µg/mL MTT solution in completed MEM medium was incubated during 1 h at 37 °C for 0 h, 24 h, 48 h and 72 h. Then, formazan crystals formed were dissolved in dimethyl sulfoxide (DMSO) and spectrophotometric measurement was done at 540 nm, using 655 nm as a reference absorbance (Fluostar Omega, BMG Labtech, Offenburg, Germany). The optical density (OD) obtained for 24 h, 48 h and 72 h was normalized for the 0 h time point. At least three independent experiments were performed.

4.13. Apoptosis Assay

Apoptosis was assessed using the APOPercentage™ kit (Biocolor Ltd., Belfast, Northern Ireland, UK). This assay uses a dye that is integrated by cells undergoing at early stage of apoptosis due to phosphatidylserine transmembrane movements, which results in APOPercentage dye incorporation by cells. Briefly, sh-scramble/CTRL and sh-SIRT7 cells were seeded in 24 well plate at density of 25,000 cell/well and incubated during 72 h in a humidified chamber at 37 °C and 5% CO₂. At this time point, cells were incubated with 300 µL/well of APOPercentage dye solution at ratio 1:20 respectively, during 20 min at 37 °C. Then, cells were washed with PBS1 X and detached from well plate with Tryple™ Express (GBICO) during 10 min at 37 °C. After that, APOPercentage Dye Release reagent was added and plate were vigorously agitated during 15 min, following colorimetric measurement at 550 nm with 620 nm reference filter (Fluostar Omega). The H₂O₂ was used as a positive control. The OD obtained for apoptosis assay was normalized for the OD obtained by viability assay at the same time point. At least three independent experiments were performed.

4.14. Wound Healing Assay

Cells were seeded in 6 well plate at a density of 7.5×10^5 cell/well and allowed reach confluence at 37 °C, 5% CO₂. Then, a “wound” was made by manual scratching with a 200 µL pipette tip and cells were gently washed with 1× PBS. The “wounded” areas were photographed in specific wound sites (two sites for each wound) at 40× magnification using an Olympus IX51 inverted microscope equipped with an Olympus XM10 Digital Camera System every 24 h until wound closure. The relative migration distance (5 measures by wound) was calculated with the following formula: relative migration distance (%) = $(A-B)/C \times 100$, where A is the width of cell wound at 0 h incubation, B is the width of cell wound after specific h of incubation, and C is the width mean of cell wound for 0 h of incubation. For relative migration distance, the results were analyzed using the beWound-Cell Migration Tool (Version 1.5) [50]. At least three independent experiments were performed.

4.15. Invasion Assay

Invasion capacity of sh-scramble/CTRL and sh-SIRT7 cells was evaluated using a 24 well BD Biocoat Matrigel Invasion Chambers (BD Biosciences, San Jose, CA, USA). After rehydration of BD Matrigel Chambers during 2 h with MEM medium at 37 °C, cells at a density of 25,000 cells/ insert were seeded and incubated during 24 h at 37 °C in 5% CO₂. Then, the non-invading cells were removed by with swab and invaded cells were fixed with methanol and staining with DAPI. Invaded cells were counted on an Olympus IX51 fluorescence microscope equipped with an Olympus XM10 digital camera using CellSens software. The % invasion normalized for total of amount cell seeded in BD Matrigel Chamber.

4.16. Statistical Analysis

All statistical analyses were performed using IBM® SPSS® Statistic software version 23 (IBM-SPSS Inc., Chicago, IL, USA) and graphs were built using GraphPad Prim 7.0 (GraphPad Software Inc., La Jolla, CA, USA). Significance level was set at $p < 0.05$, and Bonferroni’s correction was used when appropriate.

For both BiCa cohorts (IPO’s and TCGA), when applicable, Mann-Whitney U test (MW) was used to test for differences in sirtuins expression levels between NB and UCC tissue samples, pathological stages of cases divided in Ta-1 (NMIBC) and T2-4 (MIBC), and patients’ gender, and to assess differences in sh-scramble versus sh-SIRT7 conditions. Kruskal-Wallis test (KW) was performed to test for differences among UCC subtypes (papillary-low grade, papillary-high grade and invasive-high grade). Spearman’s rho was used to assess the correlation between SIRTs expression levels and age of the patients at diagnosis, and between SIRT7 and ECAD or NCAD expression levels. Associations

between clinical grade or pathological stage and immunoexpression results were assessed by chi-square or Fisher's exact test, and Somers'd directional measure was also computed.

Disease-specific and disease-free survival curves (Kaplan-Meier with log rank test) were computed for standard variables (tumor stage and grade) and for categorized SIRT7s transcript levels. Moreover, the same analyses were also performed separately for NMIBC and MIBC cases. A Cox-regression model comprising all significant variables (univariable and multivariable model) was computed to assess the relative contribution of each variable to the follow-up status.

5. Conclusions

In conclusion, this study provides a global view on sirtuin family expression deregulation in BlCa. Specifically, SIRT7 overexpression seems to play an important role in the first steps of urothelial carcinogenesis, whereas subsequent downregulation is associated with acquisition of an invasive and aggressive phenotype, through stimulation of EMT phenotype involving the SIRT7-EZH2-CDH1 axis. Although further studies are required to clarify the mechanism underlying SIRT7 deregulation in BlCa, it might constitute an attractive target for innovative therapeutic strategies.

Supplementary Materials: The following are available online at <http://www.mdpi.com/2072-6694/12/5/1066/s1>, Figure S1: Characterization of sirtuins' family in the TCGA bladder cancer cohort; Figure S2: Characterization of Sirtuin family gene expression in the bladder cancer cohort and TCGA cohort categorized by clinical grade; Figure S3: Representative images for SIRT7 immunohistochemical expression in normal urothelium and bladder urothelial carcinoma tissue sections; Figure S4: Representative images for SIRT7 immunofluorescent expression in MGHU3, 5637 and J82 bladder cancer cell lines; Figure S5: Representative images for E-Cadherin and N-Cadherin immunofluorescent expression in sh-CTRL and sh-SIRT7 MGHU3, 5637 and J82 bladder cancer cell lines; Figure S6: Characterization of *CDH1* and *CDH2* gene expression in bladder cancer and normal mucosae tissues, and in non-muscle invasive and muscle-invasive bladder cancer cases; Figure S7: Heat map showing *SIRT7* and *EZH2* expression in muscle invasive bladder cancer cases; Table S1: Reference of TaqMan® gene expression assays for studied genes; Table S2: Primer sequences used in RT-PCR for studied genes, Figure S8: Detailed information about western blot Figures 3, 4E and 5C,E.

Author Contributions: Conceptualization, R.H. and C.J.; methodology, S.M.-R., A.L., V.M.-G., D.F., P.C.D., J.O., I.G., C.S.G. and B.M.C.; formal analysis, S.M.-R., A.L. and C.J.; writing—original draft preparation, S.M.-R.; writing—review and editing, R.H. and C.J.; supervision, C.J.; project administration, R.H. and C.J.; funding acquisition, C.J. All authors have read and agreed to the published version of the manuscript.

Funding: This research was supported by the Research Center of the Portuguese Oncology Institute of Porto (CI-IPOP-FBGEBC-27 and PI 74-CI-IPOP-19-2016), by Fundação para a Ciência e Tecnologia (FCT) (PhD fellowships SFRH/BD/112673/2015 to S.M.-R and SFRH/BD/92786/2013 to C.S.G.; IF/00601/2012 to B.M.C.), and by Fundo Europeu de Desenvolvimento Regional (FEDER) (post-doctoral fellowships IPO/ESTIMANORTE-01-0145-FEDER-000027 to V.M.-G. and COMPETE/FEDER/FCT_CI-IPOP-BPD/UID/DTP/00776/2013 to I.G.).

Conflicts of Interest: The authors declare no conflict of interest. The funders had no role in the design of the study; in the collection, analyses, or interpretation of data; in the writing of the manuscript, or in the decision to publish the results.

References

1. Torre, L.A.; Bray, F.; Siegel, R.L.; Ferlay, J.; Lortet-Tieulent, J.; Jemal, A. Global cancer statistics, 2012. *CA Cancer J. Clin.* **2015**, *65*, 87–108. [[CrossRef](#)] [[PubMed](#)]
2. Sanli, O.; Dobruch, J.; Knowles, M.A.; Burger, M.; Alemozaffar, M.; Nielsen, M.E.; Lotan, Y. Bladder cancer. *Nat. Rev. Dis. Primers* **2017**, *3*, 17022. [[CrossRef](#)] [[PubMed](#)]
3. Babjuk, M.; Bohle, A.; Burger, M.; Capoun, O.; Cohen, D.; Comperat, E.M.; Hernandez, V.; Kaasinen, E.; Palou, J.; Roupert, M.; et al. EAU Guidelines on Non-Muscle-invasive Urothelial Carcinoma of the Bladder: Update 2016. *Eur. Urol.* **2017**, *71*, 447–461. [[CrossRef](#)] [[PubMed](#)]
4. Alfred Witjes, J.; Lebrecht, T.; Comperat, E.M.; Cowan, N.C.; De Santis, M.; Bruins, H.M.; Hernandez, V.; Espinos, E.L.; Dunn, J.; Rouanne, M.; et al. Updated 2016 EAU Guidelines on Muscle-invasive and Metastatic Bladder Cancer. *Eur. Urol.* **2017**, *71*, 462–475. [[CrossRef](#)] [[PubMed](#)]
5. Carafa, V.; Rotili, D.; Forgiione, M.; Cuomo, F.; Serretiello, E.; Hailu, G.S.; Jarho, E.; Lahtela-Kakkonen, M.; Mai, A.; Altucci, L. Sirtuin functions and modulation: From chemistry to the clinic. *Clin. Epigenetics* **2016**, *8*, 61. [[CrossRef](#)] [[PubMed](#)]

6. Vaquero, A. The conserved role of sirtuins in chromatin regulation. *Int. J. Dev. Biol.* **2009**, *53*, 303–322. [[CrossRef](#)]
7. Bosch-Presegue, L.; Vaquero, A. The dual role of sirtuins in cancer. *Genes Cancer* **2011**, *2*, 648–662. [[CrossRef](#)]
8. Martinez-Pastor, B.; Mostoslavsky, R. Sirtuins, metabolism, and cancer. *Front. Pharmacol.* **2012**, *3*, 22. [[CrossRef](#)]
9. Chalkiadaki, A.; Guarente, L. The multifaceted functions of sirtuins in cancer. *Nat. Rev. Cancer* **2015**, *15*, 608–624. [[CrossRef](#)]
10. Chen, X.; Sun, K.; Jiao, S.; Cai, N.; Zhao, X.; Zou, H.; Xie, Y.; Wang, Z.; Zhong, M.; Wei, L. High levels of SIRT1 expression enhance tumorigenesis and associate with a poor prognosis of colorectal carcinoma patients. *Sci. Rep.* **2014**, *4*, 7481. [[CrossRef](#)]
11. Alhazzazi, T.Y.; Kamarajan, P.; Joo, N.; Huang, J.Y.; Verdin, E.; D’Silva, N.J.; Kapila, Y.L. Sirtuin-3 (SIRT3), a novel potential therapeutic target for oral cancer. *Cancer* **2011**, *117*, 1670–1678. [[CrossRef](#)] [[PubMed](#)]
12. Wang, R.H.; Sengupta, K.; Li, C.; Kim, H.S.; Cao, L.; Xiao, C.; Kim, S.; Xu, X.; Zheng, Y.; Chilton, B.; et al. Impaired DNA damage response, genome instability, and tumorigenesis in SIRT1 mutant mice. *Cancer Cell* **2008**, *14*, 312–323. [[CrossRef](#)] [[PubMed](#)]
13. Kim, H.S.; Patel, K.; Muldoon-Jacobs, K.; Bisht, K.S.; Aykin-Burns, N.; Pennington, J.D.; van der Meer, R.; Nguyen, P.; Savage, J.; Owens, K.M.; et al. SIRT3 is a mitochondria-localized tumor suppressor required for maintenance of mitochondrial integrity and metabolism during stress. *Cancer Cell* **2010**, *17*, 41–52. [[CrossRef](#)] [[PubMed](#)]
14. Hiratsuka, M.; Inoue, T.; Toda, T.; Kimura, N.; Shirayoshi, Y.; Kamitani, H.; Watanabe, T.; Ohama, E.; Tahimic, C.G.; Kurimasa, A.; et al. Proteomics-based identification of differentially expressed genes in human gliomas: Down-regulation of SIRT2 gene. *Biochem. Biophys. Res. Commun.* **2003**, *309*, 558–566. [[CrossRef](#)]
15. Kim, H.S.; Vassilopoulos, A.; Wang, R.H.; Lahusen, T.; Xiao, Z.; Xu, X.; Li, C.; Veenstra, T.D.; Li, B.; Yu, H.; et al. SIRT2 maintains genome integrity and suppresses tumorigenesis through regulating APC/C activity. *Cancer Cell* **2011**, *20*, 487–499. [[CrossRef](#)]
16. Jeong, S.M.; Xiao, C.; Finley, L.W.; Lahusen, T.; Souza, A.L.; Pierce, K.; Li, Y.H.; Wang, X.; Laurent, G.; German, N.J.; et al. SIRT4 has tumor-suppressive activity and regulates the cellular metabolic response to DNA damage by inhibiting mitochondrial glutamine metabolism. *Cancer Cell* **2013**, *23*, 450–463. [[CrossRef](#)]
17. Lu, W.; Zuo, Y.; Feng, Y.; Zhang, M. SIRT5 facilitates cancer cell growth and drug resistance in non-small cell lung cancer. *Tumour Biol.* **2014**, *35*, 10699–10705. [[CrossRef](#)]
18. Sebastian, C.; Mostoslavsky, R. The role of mammalian sirtuins in cancer metabolism. *Semin. Cell Dev. Biol.* **2015**, *43*, 33–42. [[CrossRef](#)]
19. Marquardt, J.U.; Fischer, K.; Baus, K.; Kashyap, A.; Ma, S.; Krupp, M.; Linke, M.; Teufel, A.; Zechner, U.; Strand, D.; et al. Sirtuin-6-dependent genetic and epigenetic alterations are associated with poor clinical outcome in hepatocellular carcinoma patients. *Hepatology* **2013**, *58*, 1054–1064. [[CrossRef](#)]
20. Khongkow, M.; Olmos, Y.; Gong, C.; Gomes, A.R.; Monteiro, L.J.; Yague, E.; Cavaco, T.B.; Khongkow, P.; Man, E.P.; Laohasinnarong, S.; et al. SIRT6 modulates paclitaxel and epirubicin resistance and survival in breast cancer. *Carcinogenesis* **2013**, *34*, 1476–1486. [[CrossRef](#)]
21. Bai, L.; Lin, G.; Sun, L.; Liu, Y.; Huang, X.; Cao, C.; Guo, Y.; Xie, C. Upregulation of SIRT6 predicts poor prognosis and promotes metastasis of non-small cell lung cancer via the ERK1/2/MMP9 pathway. *Oncotarget* **2016**, *7*, 40377–40386. [[CrossRef](#)] [[PubMed](#)]
22. Malik, S.; Villanova, L.; Tanaka, S.; Aonuma, M.; Roy, N.; Berber, E.; Pollack, J.R.; Michishita-Kioi, E.; Chua, K.F. SIRT7 inactivation reverses metastatic phenotypes in epithelial and mesenchymal tumors. *Sci. Rep.* **2015**, *5*, 9841. [[CrossRef](#)] [[PubMed](#)]
23. Bartosch, C.; Monteiro-Reis, S.; Almeida-Rios, D.; Vieira, R.; Castro, A.; Moutinho, M.; Rodrigues, M.; Graca, I.; Lopes, J.M.; Jeronimo, C. Assessing sirtuin expression in endometrial carcinoma and non-neoplastic endometrium. *Oncotarget* **2016**, *7*, 1144–1154. [[CrossRef](#)] [[PubMed](#)]
24. Barber, M.F.; Michishita-Kioi, E.; Xi, Y.; Tasselli, L.; Kioi, M.; Moqtaderi, Z.; Tennen, R.I.; Paredes, S.; Young, N.L.; Chen, K.; et al. SIRT7 links H3K18 deacetylation to maintenance of oncogenic transformation. *Nature* **2012**, *487*, 114–118. [[CrossRef](#)] [[PubMed](#)]
25. Paredes, S.; Villanova, L.; Chua, K.F. Molecular pathways: Emerging roles of mammalian Sirtuin SIRT7 in cancer. *Clin. Cancer Res.* **2014**, *20*, 1741–1746. [[CrossRef](#)] [[PubMed](#)]

26. Ford, E.; Voit, R.; Liszt, G.; Magin, C.; Grummt, I.; Guarente, L. Mammalian Sir2 homolog SIRT7 is an activator of RNA polymerase I transcription. *Genes Dev.* **2006**, *20*, 1075–1080. [[CrossRef](#)] [[PubMed](#)]
27. Chen, S.; Seiler, J.; Santiago-Reichert, M.; Felbel, K.; Grummt, I.; Voit, R. Repression of RNA polymerase I upon stress is caused by inhibition of RNA-dependent deacetylation of PAF53 by SIRT7. *Mol. Cell* **2013**, *52*, 303–313. [[CrossRef](#)] [[PubMed](#)]
28. Wu, M.; Dickinson, S.L.; Wang, X.; Zhang, J. Expression and function of SIRT6 in muscle invasive urothelial carcinoma of the bladder. *Int. J. Clin. Exp. Pathol.* **2014**, *7*, 6504–6513.
29. Cancer Genome Atlas Research Network. Comprehensive molecular characterization of urothelial bladder carcinoma. *Nature* **2014**, *507*, 315–322. [[CrossRef](#)]
30. Zhang, C.; Zhai, Z.; Tang, M.; Cheng, Z.; Li, T.; Wang, H.; Zhu, W.G. Quantitative proteome-based systematic identification of SIRT7 substrates. *Proteomics* **2017**, *17*. [[CrossRef](#)]
31. Kalluri, R.; Weinberg, R.A. The basics of epithelial-mesenchymal transition. *J. Clin. Investig.* **2009**, *119*, 1420–1428. [[CrossRef](#)] [[PubMed](#)]
32. Nieto, M.A.; Huang, R.Y.; Jackson, R.A.; Thiery, J.P. EMT: 2016. *Cell* **2016**, *166*, 21–45. [[CrossRef](#)] [[PubMed](#)]
33. Palmirotta, R.; Cives, M.; Della-Morte, D.; Capuani, B.; Lauro, D.; Guadagni, F.; Silvestris, F. Sirtuins and Cancer: Role in the Epithelial-Mesenchymal Transition. *Oxidative Med. Cell. Longev.* **2016**, *2016*, 3031459. [[CrossRef](#)] [[PubMed](#)]
34. Robertson, A.G.; Kim, J.; Al-Ahmadie, H.; Bellmunt, J.; Guo, G.; Cherniack, A.D.; Hinoue, T.; Laird, P.W.; Hoadley, K.A.; Akbani, R.; et al. Comprehensive Molecular Characterization of Muscle-Invasive Bladder Cancer. *Cell* **2017**. [[CrossRef](#)] [[PubMed](#)]
35. Nichol, J.N.; Dupere-Richer, D.; Ezponda, T.; Licht, J.D.; Miller, W.H., Jr. H3K27 Methylation: A Focal Point of Epigenetic Dereglulation in Cancer. *Adv. Cancer Res.* **2016**, *131*, 59–95. [[CrossRef](#)]
36. Herranz, N.; Pasini, D.; Diaz, V.M.; Franci, C.; Gutierrez, A.; Dave, N.; Escriva, M.; Hernandez-Munoz, I.; Di Croce, L.; Helin, K.; et al. Polycomb complex 2 is required for E-cadherin repression by the Snail1 transcription factor. *Mol. Cell. Biol.* **2008**, *28*, 4772–4781. [[CrossRef](#)] [[PubMed](#)]
37. Cho, H.M.; Jeon, H.S.; Lee, S.Y.; Jeong, K.J.; Park, S.Y.; Lee, H.Y.; Lee, J.U.; Kim, J.H.; Kwon, S.J.; Choi, E.; et al. microRNA-101 inhibits lung cancer invasion through the regulation of enhancer of zeste homolog 2. *Exp. Ther. Med.* **2011**, *2*, 963–967. [[CrossRef](#)]
38. Gall Troselj, K.; Novak Kujundzic, R.; Ugarkovic, D. Polycomb repressive complex's evolutionary conserved function: The role of EZH2 status and cellular background. *Clin. Epigenetics* **2016**, *8*, 55. [[CrossRef](#)]
39. Stemmler, M.P.; Eccles, R.L.; Brabletz, S.; Brabletz, T. Non-redundant functions of EMT transcription factors. *Nat. Cell Biol.* **2019**, *21*, 102–112. [[CrossRef](#)]
40. Tien, C.L.; Jones, A.; Wang, H.; Gerigk, M.; Nozell, S.; Chang, C. Snail2/Slug cooperates with Polycomb repressive complex 2 (PRC2) to regulate neural crest development. *Development* **2015**, *142*, 722–731. [[CrossRef](#)]
41. Battistelli, C.; Cicchini, C.; Santangelo, L.; Tramontano, A.; Grassi, L.; Gonzalez, F.J.; de Nonno, V.; Grassi, G.; Amicone, L.; Tripodi, M. The Snail repressor recruits EZH2 to specific genomic sites through the enrollment of the lncRNA HOTAIR in epithelial-to-mesenchymal transition. *Oncogene* **2017**, *36*, 942–955. [[CrossRef](#)] [[PubMed](#)]
42. Liu, G.F.; Lu, J.Y.; Zhang, Y.J.; Zhang, L.X.; Lu, G.D.; Xie, Z.J.; Cheng, M.; Shen, Y.; Zhang, Y. C/EBPalpha negatively regulates SIRT7 expression via recruiting HDAC3 to the upstream-promoter of hepatocellular carcinoma cells. *Biochim. Biophys. Acta* **2016**, *1859*, 348–354. [[CrossRef](#)] [[PubMed](#)]
43. Shin, J.; He, M.; Liu, Y.; Paredes, S.; Villanova, L.; Brown, K.; Qiu, X.; Nabavi, N.; Mohrin, M.; Wojnoonski, K.; et al. SIRT7 represses Myc activity to suppress ER stress and prevent fatty liver disease. *Cell Rep.* **2013**, *5*, 654–665. [[CrossRef](#)] [[PubMed](#)]
44. Kim, J.K.; Noh, J.H.; Jung, K.H.; Eun, J.W.; Bae, H.J.; Kim, M.G.; Chang, Y.G.; Shen, Q.; Park, W.S.; Lee, J.Y.; et al. Sirtuin7 oncogenic potential in human hepatocellular carcinoma and its regulation by the tumor suppressors MiR-125a-5p and MiR-125b. *Hepatology* **2013**, *57*, 1055–1067. [[CrossRef](#)]
45. Grob, A.; Roussel, P.; Wright, J.E.; McStay, B.; Hernandez-Verdun, D.; Sirri, V. Involvement of SIRT7 in resumption of rDNA transcription at the exit from mitosis. *J. Cell Sci.* **2009**, *122*, 489–498. [[CrossRef](#)]
46. Sun, L.; Fan, G.; Shan, P.; Qiu, X.; Dong, S.; Liao, L.; Yu, C.; Wang, T.; Gu, X.; Li, Q.; et al. Regulation of energy homeostasis by the ubiquitin-independent REG γ proteasome. *Nat. Commun.* **2016**, *7*, 12497. [[CrossRef](#)]

47. Jiang, L.; Xiong, J.; Zhan, J.; Yuan, F.; Tang, M.; Zhang, C.; Cao, J.; Chen, Y.; Lu, X.; Li, Y.; et al. Ubiquitin-specific peptidase 7 (USP7)-mediated deubiquitination of the histone deacetylase SIRT7 regulates gluconeogenesis. *J. Biol. Chem.* **2017**, *292*, 13296–13311. [[CrossRef](#)]
48. Solomon, J.P.; Hansel, D.E. The Emerging Molecular Landscape of Urothelial Carcinoma. *Surg. Pathol. Clin.* **2016**, *9*, 391–404. [[CrossRef](#)]
49. Edge, S.B.; Compton, C.C. The American Joint Committee on Cancer: The 7th edition of the AJCC cancer staging manual and the future of TNM. *Ann. Surg. Oncol.* **2010**, *17*, 1471–1474. [[CrossRef](#)]
50. Moreira, A.H.J.; Queirós, S.; Vilaça, J.L. Biomedical Engineering Solutions Research Group, Life and Health Sciences Research Institute, University of Minho. Available online: <http://www.besurg.com/sites/default/files/beWoundApp.zip> (accessed on 21 April 2020).



© 2020 by the authors. Licensee MDPI, Basel, Switzerland. This article is an open access article distributed under the terms and conditions of the Creative Commons Attribution (CC BY) license (<http://creativecommons.org/licenses/by/4.0/>).

RESEARCH

Open Access



Practicability of clinical application of bladder cancer molecular classification and additional value of epithelial-to-mesenchymal transition: prognostic value of vimentin expression

João Lobo^{1,2,3}, Sara Monteiro-Reis^{1,3}, Catarina Guimarães-Teixeira¹, Paula Lopes^{1,2}, Isa Carneiro^{1,2}, Carmen Jerónimo^{1,3*}  and Rui Henrique^{1,2,3*}

Abstract

Background: Bladder cancer (BlCa) taxonomy has proved its impact in patient outcome and selection for targeted therapies, but such transcriptomic-based classification has not yet translated to routine practice. Moreover, epithelial-to-mesenchymal transition (EMT) has shown relevance in acquisition of more aggressive BlCa phenotype. We aimed to test the usefulness of the molecular classification, as defined by immunohistochemistry (a routinely performed and easy-to-implement technique), in a well-defined BlCa cohort of both non-muscle invasive (NMIBC) and muscle invasive (MIBC) disease. Also, we aimed to assess the additional prognostic value of the mesenchymal marker vimentin to the stratification strategy.

Methods: A total of 186 samples were available. Immunohistochemistry/RT-qPCR for luminal markers GATA3/FOXA1, basal markers KRT5/KRT6A and vimentin were performed.

Results: mRNA expression levels of the markers positively correlated with immunoexpression scores. We found substantial overlapping in immunoexpression of luminal and basal markers, evidencing tumor heterogeneity. In MIBC, basal tumors developed recurrence more frequently. NMIBC patients with higher vimentin immunoexpression endured poorer disease-free survival, and increased expression was observed from normal bladder-NMIBC-MIBC-metastases.

Conclusions: The classification has the potential to be implemented in routine, but further adjustments in practical scoring should be defined; focusing on additional markers, including those related to EMT, may further refine BlCa molecular taxonomy.

*Correspondence: carmenjeronimo@ipporto.min-saude.pt;
henrique@ipporto.min-saude.pt

†João Lobo, Sara Monteiro-Reis, Catarina Guimarães-Teixeira shared first authorship

‡Carmen Jerónimo, Rui Henrique joint senior authors

¹ Cancer Biology and Epigenetics Group IPO Porto Research Center (GEBC CI-IPOP), Portuguese Oncology Institute of Porto (IPO Porto) & Porto Comprehensive Cancer Center (PCCC), R. Dr. António Bernardino de Almeida, 4200-072 Porto, Portugal

Full list of author information is available at the end of the article



© The Author(s) 2020. This article is licensed under a Creative Commons Attribution 4.0 International License, which permits use, sharing, adaptation, distribution and reproduction in any medium or format, as long as you give appropriate credit to the original author(s) and the source, provide a link to the Creative Commons licence, and indicate if changes were made. The images or other third party material in this article are included in the article's Creative Commons licence, unless indicated otherwise in a credit line to the material. If material is not included in the article's Creative Commons licence and your intended use is not permitted by statutory regulation or exceeds the permitted use, you will need to obtain permission directly from the copyright holder. To view a copy of this licence, visit <http://creativecommons.org/licenses/by/4.0/>. The Creative Commons Public Domain Dedication waiver (<http://creativecommons.org/publicdomain/zero/1.0/>) applies to the data made available in this article, unless otherwise stated in a credit line to the data.

Keywords: Bladder cancer, Molecular classification, Pathology, Luminal, Basal, Vimentin, EMT

Background

Bladder cancer (BlCa) is one of the most incident cancers worldwide. It ranks ninth in prevalence, with a number of estimated new cases and cancer-related deaths of 549,393 and 199,922, respectively [1–3]. These figures are estimated to almost double by 2040 [1], representing an important toll on health services [4]. Most BlCa cases correspond to urothelial carcinoma, which is often divided into two major forms: 75–80% of all patients are diagnosed with non-muscle invasive BlCa (NMIBC), characterized by frequent recurrences and eventual progression to invasion; and the remaining 20–25% patients present with muscle-invasive BlCa (MIBC), which constitutes an aggressive, locally invading carcinoma, with propensity for metastization [5, 6]. On the therapeutic front, the clinical management of NMIBC and MIBC cases is very distinct, and it remained almost unchanged until the approval of immune checkpoint inhibitors in first-line or metastatic settings [7–9]. Nevertheless, a considerable percentage of BlCa patients do not benefit from current treatment options. Clinicians still have to deal with a high number of cases with recurrence and progression and, as a result, patients endure a long follow-up, making BlCa one of the costliest malignancies worldwide [4]. Hence, there is a need to improve risk stratification of these patients and to uncover biomarkers that may better select patients to the specific therapy that will give the higher benefit with less toxicity. In this line, an effort has been made to improve BlCa classification; various research teams have reported the importance of a molecular stratification of BlCa, and presented classifications based on different molecular traits, either for all urothelial carcinomas, or focusing on NMIBC and MIBC separately [10–20]. This molecular stratification is also useful for predicting responses to current treatment options, and provides insights for the development of new therapies [14, 21–24]. Although specific differences in classification emerge out of each research group analyses, they all share as an overlapping feature the existence of two major BlCa subtypes—basal/squamous and luminal—for MIBC cases [25]. Briefly, basal/squamous subtype is mainly composed of advanced stage tumors and metastatic disease, being enriched in inactivating mutations and deletions of *TP53* and *RBI*, whereas the luminal subtype is associated with papillary histopathological features, and enriched in fibroblast growth factor receptor 3 (*FGFR3*) mutations [26, 27]. An effort has been made to reach a single consensus classification and to generate a list of specific biomarkers (such as *FOXA1*, *GATA3*, *KRT5/6* and *KRT14*)

that can be effectively translated from wide screening genomic and transcriptomics analyses into the clinic for any BlCa setting (both MIBC or NMIBC) [13, 26]. However, to date, this has not been achieved. On the other hand, the role of epithelial-to-mesenchymal transition (EMT) in BlCa prognosis has been widely discussed [28]. It has been shown to be highly related to an aggressive tumor biology, culminating in poor clinical outcome both in NMIBC and MIBC, namely poorer survival, increased recurrences, propensity to metastasize, and inferior response to treatment [29–33].

Herein, we aimed to characterize the expression of a set of markers for defining both luminal and basal/squamous subtypes in a well characterized patient cohort of BlCa, looking for clinicopathological correlates and testing their potential for clinical application, both within MIBC and NMIBC cases. Moreover, we explored the value of adding the expression of a classic EMT marker, vimentin (*VIM*), to the risk stratification strategy. We have chosen *VIM* because among the EMT markers it is routinely performed in all Pathology departments and it has been consistently associated with BlCa prognosis, including in our previous *in silico* analysis [28].

Methods

Patients and samples

126 patients with primary BlCa (urothelial carcinoma) treated with transurethral resection (TUR) or radical cystectomy/cystoprostatectomy between 1991 and 2011 at the Portuguese Oncology Institute of Porto (IPO Porto) were retrospectively selected for the study. A set of 25 morphologically normal bladder mucosa tissue samples was obtained from BlCa-free individuals (prostate cancer patients submitted to radical prostatectomy with no bladder lesions) and served as controls. Additionally, a total of 35 metastases from BlCa were also included in the study. All specimens were formalin-fixed and paraffin-embedded for routine pathological examination by a dedicated uropathologist and used for immunohistochemistry studies. For some patients (see detailed numbers below) freshly collected tissue could be additionally obtained (a section matching the one embedded in paraffin). These were stored immediately at -80°C after surgical intervention and subsequently cut in a cryostat for confirmation of representativity. These freshly collected samples were specifically used for nucleic acid extraction (for mRNA expression analyses). Staging was performed using the American Joint Committee on Cancer (AJCC) 8th Edition manual [34]. Relevant clinical data was

collected from clinical charts, by an investigator blinded to other study findings. A summary of the study cohort is presented in Table 1.

Patients and controls were enrolled after informed consent. This study was approved by the institutional review board (Comissão de Ética para a Saúde) of IPO Porto (CES103-14).

Immunohistochemistry

In total, 186 samples were available for immunohistochemistry studies: the 126 primary BlCa specimens, plus the 25 normal bladder mucosae and 35 BlCa metastases. Immunohistochemistry methods are described in detail in Additional file 1: Table S1. Briefly, three micrometer-thick tissue sections from the formalin-fixed and paraffin-embedded samples were ordered, antigen retrieval was performed, and slides were incubated with the primary antibodies for FOXA1, GATA3, CK5/6 and VIM. Then, 3,3'-diaminobenzidine (Sigma-Aldrich™) was used as chromogen for visualization and slides were counterstained with hematoxylin. Appropriate tissue controls were used per run.

Immunoexpression patterns were evaluated by a dedicated uropathologist. Cases were classified using a semi-quantitative scale for both staining intensity (0—no staining; 1—low intensity, only barely discernible at 400× magnification; 2—moderate intensity, well appreciated at 400× magnification but faint at 100× magnification; 3—high intensity, strong and well appreciated at 40× magnification) and percentage of positive cells (0—<10%; 1—10–33%; 2—33–67%; 3—>67%), in each case. Results were then combined in a single continuous

score (Score S = staining intensity × percentage of positive cells) assigned to each tumor.

BlCa specimens were considered “basal-like” when at least focal positivity for CK5/6 was detected (independently of positivity for FOXA1 or GATA3), with the remaining samples (with complete absence of expression of CK5/6) being considered “luminal-like”, following the classification of Choi et al., centered on basal keratin expression for defining subtypes [22].

Real-time quantitative PCR (RT-qPCR)

As mentioned, mRNA expression analyses were performed on fresh frozen tissues, available for 108 of the patients included in the study (all were run for *VIM* expression, and 83 for *FOXA1*, *GATA3*, *KRT5* and *KRT6A*, due to sample limitation issues). RNA was extracted from tissues using TRIzol® (Invitrogen, Carlsbad, CA, USA), according to manufacturer's instructions. RNA quantification and purity were assessed in NanoDrop™ Lite Spectrophotometer (Cat. ND-LITE, Thermo Scientific™). cDNA synthesis was performed using the RevertAid™ RT Reverse Transcription Kit (Cat. K1691, Thermo Scientific™). The reaction was performed in MyCycler™ Thermal Cycler System (Cat. 1709703, Bio-Rad) using the following conditions: 5 min at 25 °C, 60 min at 42 °C and 5 min at 70 °C. *VIM* mRNA expression levels were evaluated using 4.5 µL of diluted cDNA, 5 µL of TaqMan® Universal PCR Master Mix No AmpErase® UNG (Applied Biosystems®) and 0.5 µL of TaqMan® Gene Expression Assay, specific for *VIM* gene—assay ID Hs00185584. For normalization purposes, two TaqMan® Gene Expression assays were used as internal controls: beta-glucuronidase—*GUSB*—assay ID Hs99999908, Applied biosystems®; and Hypoxanthine–guanine phosphoribosyltransferase—*HPRT1*—assay ID Hs01003267. RT-qPCR was run in 96-well plates, in an ABI 7500 Real Time PCR System (Thermo Fisher) in the following conditions: 2 min at 50 °C, followed by enzyme activation for 10 min at 95 °C, and 45 cycles which included a denaturation stage at 95 °C for 15 s and an extending stage at 60 °C for 60 s. Serial dilutions of cDNA obtained from Human Reference Total RNA (Cat. 750500, Agilent Technologies®) were used to compute standard curves for each plate. All experiments were run in triplicate and two negative controls were included in each plate. Relative expression of target genes tested in each sample was determined as: [Gene Expression Level = (Gene Mean Quantity / (*HPRT1* & *GUSB*) Mean Quantity) × 1000].

For *GATA3*, *FOXA1*, *KRT5* and *KRT6A* genes, transcript levels were also assessed using 2.5 µL of diluted cDNA, 0.25 µL of forward and reverse primers (Additional file 2: Table S2), 5 µL of Xpert Fast SYBER

Table 1 Clinicopathological features of the study cohort

Clinicopathological features of the immunohistochemistry cohort	Primary bladder cancer
Individuals, n	126
Gender, n (%)	
Male	101 (80.2)
Female	25 (19.8)
Median age, years (range)	71 (61–77)
Grade, n (%)	
Papillary, low-grade	28/126 (22.2)
Papillary, high-grade	20/126 (15.9)
Invasive, high-grade	78/126 (61.9)
Pathological Stage, n (%) ^a	
pTa/pT1 (NMIBC)	51/123 (41.5)
pT2-4 (MIBC)	72/123 (58.5)

NMIBC non-muscle invasive bladder cancer, MIBC muscle invasive bladder cancer

^a For 3 patients stage could not be ascertained as clinical data was missing/not available to the investigators

Mastermix Blue (GRiSP Research Solutions, Porto, Portugal) and 2 μL of bidistilled water. *GUSB* was used for normalization and plates were set as described above. The run followed the following conditions: 2 min at 95 °C, followed by 45 cycles of 5 s at 95 °C and 30 s at 60 °C, followed by the melt curve stage.

Statistical analysis

Data was tabulated using Microsoft Excel 2016 and analyzed and plotted using GraphPad Prism 6 and IBM Statistical Package for Social Sciences (SPSS v24). Percentages were calculated based on the number of cases with available data. Individual data points are plotted, together with median and interquartile range. Mann–Whitney and Kruskal–Wallis tests were used for comparing expression levels among samples, as necessary. p-values were adjusted for multiple comparisons using Dunn’s test. Chi square and Fisher exact test were used as necessary for establishing associations between categorical variables. Spearman correlation test was used to correlate continuous variables. Disease-specific survival (DSS) and disease-free survival (DFS) curves were plotted using Kaplan–Meier statistics, and Cox regression models with respective hazard ratios (HR) were computed, including multivariable analysis. Statistical significance was set at $p < 0.05$.

Results

Clinical outcome of “luminal-like” and “basal-like” BICa patients as determined by immunohistochemistry

There were no significant differences between the age distribution of patients with NMIBC and MIBC ($p = 0.951$). A total of 56/126 (44.4%) BICa specimens showed “basal-like” features (following the Choi et al. stratification strategy, based on CK5/6 expression [22]). This occurred more frequently in MIBC (34/72, 47.2%) compared to NMIBC (20/51, 39.2%). However, 51/56 (91.1%) of the cases showing CK5/6 immunoreexpression also exhibited immunoreexpression of at least one of the markers GATA3/FOXA1, evidencing that most tumors show evidence of staining for both kinds of markers, in scattered cells. Four tumors showed no immunoreexpression of either CK5/6, FOXA1 or GATA3 (three of those being MIBC) (Table 2). For the latter, we performed additional immunohistochemistry for neuroendocrine markers to look for the presence of the neuroendocrine-like molecular type of BICa [10]. Indeed, one of the cases showed clear-cut strong immunoreexpression of neuroendocrine markers synaptophysin, chromogranin and CD56 (Additional file 3: Fig. S1).

For MIBC, there was no significant association between the luminal/basal-like subtype (as defined by immunohistochemistry, described above) and the event

Table 2 Immunoreexpression of luminal and basal markers in the bladder cancer cohort

	GATA3 and FOXA1 –	GATA3 and/or FOXA1 +
WHOLE COHORT		
CK5/6 –	4 (3.1%)	66 (52.4%)
CK5/6 +	5 (4.0%)	51 (40.5%)
NMIBC		
CK5/6 –	1 (2.0%)	30 (58.8%)
CK5/6 +	1 (2.0%)	19 (37.2%)
MIBC		
CK5/6 –	3 (4.2%)	35 (48.6%)
CK5/6 +	4 (5.5%)	30 (41.7%)

MIBC muscle invasive bladder cancer, NMIBC non-muscle invasive bladder cancer

of metastization ($p = 0.933$). Within NMIBC, the “basal-like” cases disclosed disease recurrence in 8/20 cases (40.0%) and the “luminal-like” in a similar proportion of cases (13/31, 41.9%). However, considering MIBC, “basal-like” cancer developed recurrence in 11/34 cases (32.4%), whereas in “luminal-like” this occurred in a lower proportion of patients [only 5/38 cases (13.2%)].

Concerning survival analyses, the luminal/basal-like classification did not show significant impact on DSS or DFS, both for NMIBC or MIBC (NMIBC: $p = 0.762$ and $p = 0.625$; MIBC: $p = 0.346$, $p = 0.185$, respectively). Illustrative examples of immunoreexpression patterns for the several markers are depicted in Fig. 1.

Correlation between luminal/basal markers mRNA expression and protein expression

We then checked for reproducibility between protein and transcript levels of the markers under study. Importantly, we found a significant, positive (albeit moderate), correlation between transcript levels of *GATA3* and its protein expression as assessed by immunoreexpression score ($r = 0.36$, $p = 0.010$). However, the same was not found for *FOXA1* ($r = 0.10$, $p = 0.3460$). For basal markers *KRT5* and *KRT6A*, mRNA expression showed a significant positive, also moderate, correlation with the immunoreexpression score ($r = 0.49$, $p < 0.0001$; and $r = 0.68$, $p < 0.0001$). Tumor samples with absent immunoreexpression of *GATA3*, *FOXA1* and *CK5/6* showed significantly lower transcript levels of *GATA3*, *FOXA1* and *KRT5/KRT6A*, respectively ($p < 0.001$, $p = 0.0130$, $p < 0.0001$ and $p = 0.0278$) (Fig. 2).

Additional value of VIM expression in predicting clinical outcome

VIM transcript levels were significantly higher in MIBC compared to NMIBC ($p = 0.0001$, Fig. 3a). This was

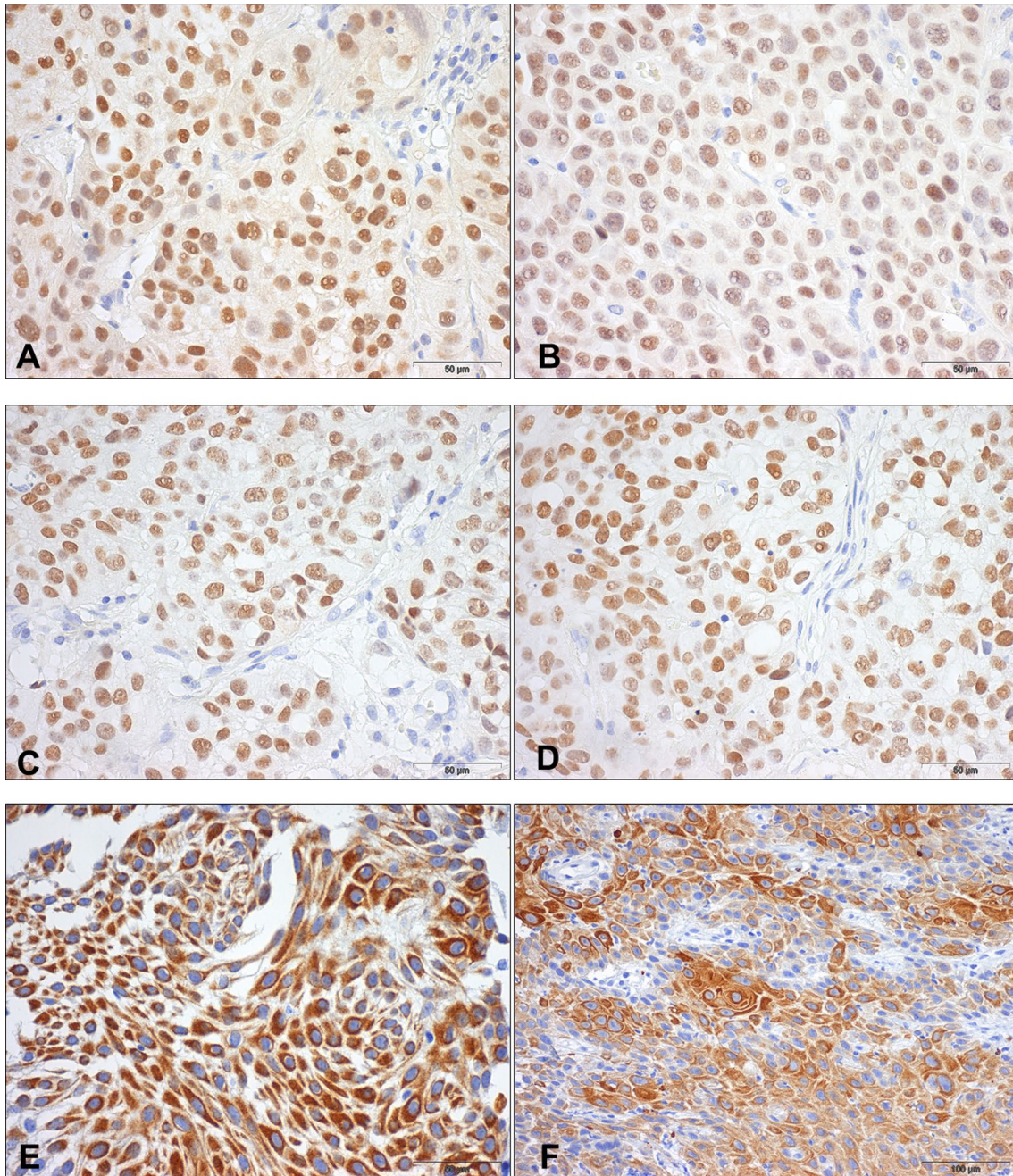
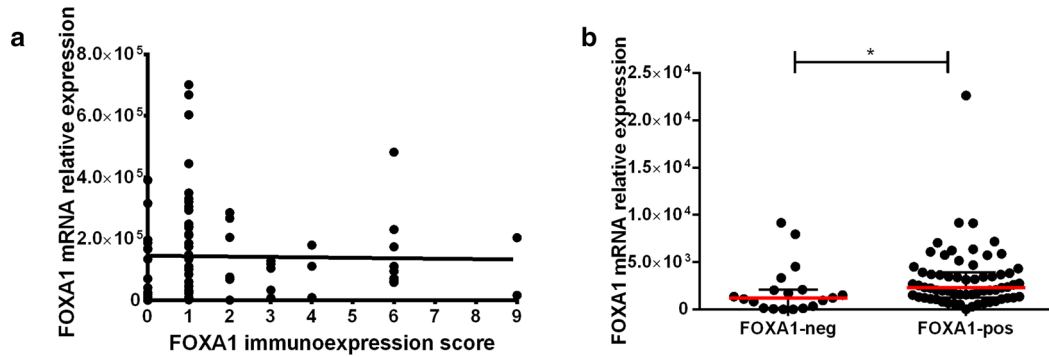


Fig. 1 Immunoreexpression of luminal and basal markers in the bladder cancer cohort. **a, b** FOXA1 strong and diffuse immunoreexpression in two bladder cancer specimens, one NMIBC (**a**) and one MIBC (**b**); **c, d**: GATA3 strong and diffuse immunoreexpression in two bladder cancer specimens, one NMIBC (**c**) and one MIBC (**d**); **e, f**: CK5/6 strong multifocal immunoreexpression in two bladder cancer specimens, one NMIBC (**e**) and one MIBC (**f**)

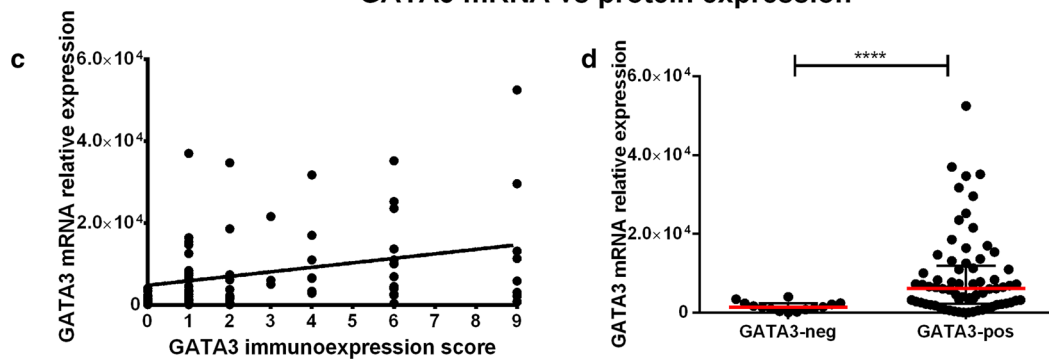
(See figure on next page.)

Fig. 2 Correlation between mRNA and protein expression of the several luminal and basal markers in the bladder cancer cohort (both MIBC and NMIBC included). FOXA1 (**a** and **b**), GATA3 (**c** and **d**), KRT5 (**e** and **f**) and KRT6A (**g** and **h**) analyses. mRNA expression levels are plotted as relative expression levels, normalized to GUSB. Red dash and bars represent median and interquartile range. The immunoreexpression score (intensity x percentage) is plotted in the xx-axis. The graphs include n = 83 matched samples (*p < 0.05; ****p < 0.0001)

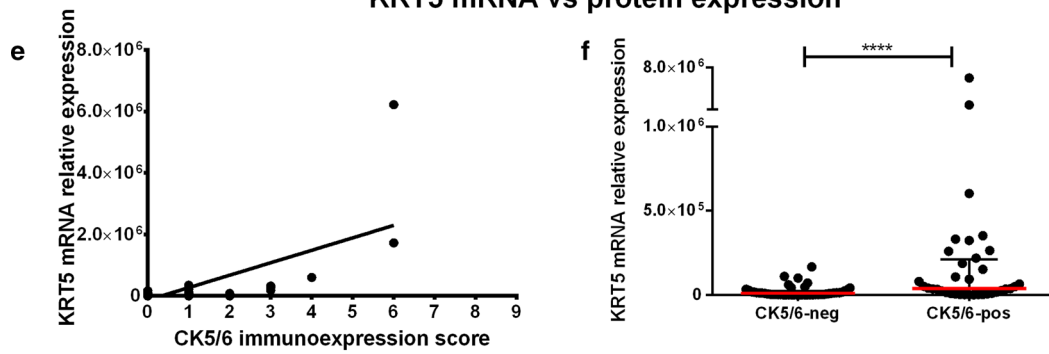
FOXA1 mRNA vs protein expression



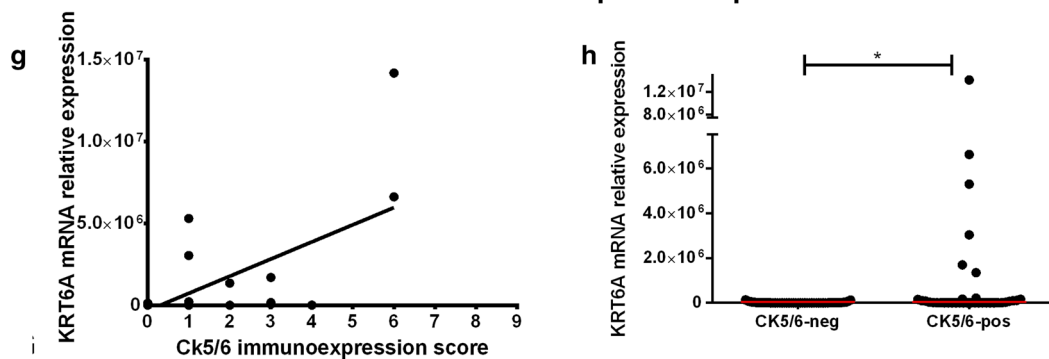
GATA3 mRNA vs protein expression

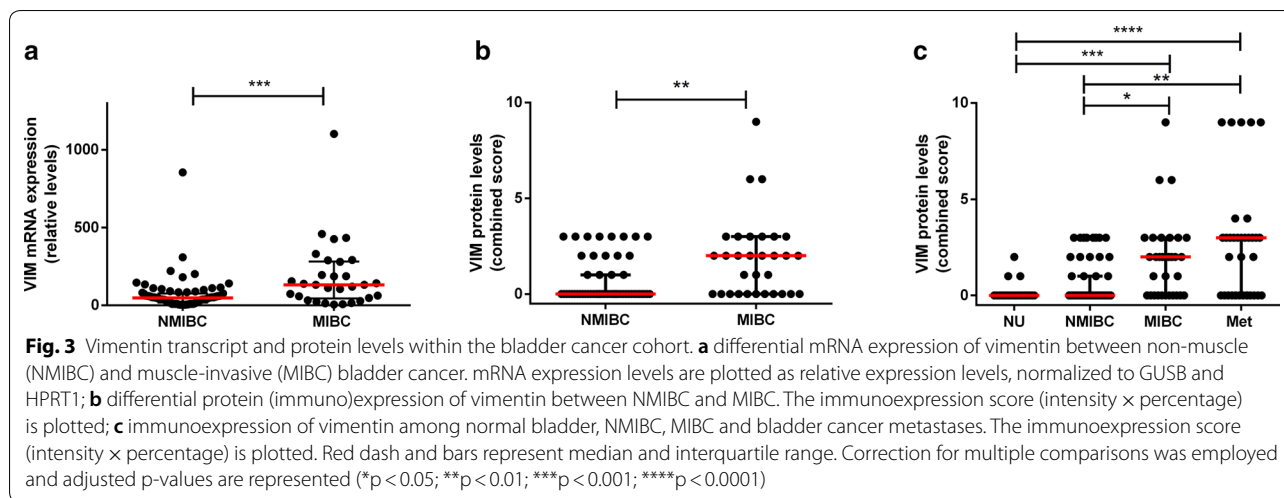


KRT5 mRNA vs protein expression



KRT6A mRNA vs protein expression





additionally validated at protein level by immunohistochemistry (p = 0.0013, Fig. 3b). Moreover, there was an overall progressive increase in immunoexpression scores for VIM, which were lower in normal urothelium and NMIBC, followed by MIBC, and attained the highest levels in BlCa metastases (p < 0.0001, Fig. 3c). Specifically, VIM immunoexpression scores were significantly higher in MIBC and metastases compared to normal urothelium and to NMIBC (after correction for multiple comparisons), however, differences between normal urothelium and NMIBC categories did not reach statistical significance (Fig. 3c).

VIM immunoexpression score did not have a significant impact on DSS and DFS for MIBC patients (p = 0.141 and p = 0.512, respectively). It also did not significantly influence DSS of NMIBC patients (p = 0.296). Importantly, however, NMIBC patients with VIM immunoexpression in tumor cells endured significantly worse DFS (p = 0.005, Fig. 4). DFS of NMIBC patients with VIM immunoexpression was significantly poorer (HR = 3.541, 95% confidence interval 1.402–8.943), and this was maintained after adjusting for patients’ age (HR = 3.678, 95% confidence interval 1.435–9.423) and tumor grade (HR = 3.223, 95% confidence interval 1.104–9.408). Illustrative examples of VIM immunoexpression patterns are depicted in Fig. 5.

Discussion

BlCa remains a clinically challenging disease, owing to heterogeneity in presentation, progression and distinct treatment strategies. On the one hand, NMIBC is the most frequent BlCa phenotype [35], and disease recurrence is very frequent. Substantial research efforts have been put towards uncovering non-invasive, liquid biopsy-based biomarkers for accurately diagnosing and

following-up these patients [36, 37]. One major gap in NMIBC relates to patient prognostication and risk stratification after resection, fundamental for establishing the most appropriate follow-up strategy. In this context, tissue biomarkers that predict relapse may be clinically useful, especially if easily and reproducibly assessed, by cost-effective methodologies [38]. On the other end of the spectrum, around 20–25% of patients present already with MIBC. This subtype has dismal prognosis and survival has remained overall unchanged in the last couple of decades. Recently, immunotherapy has proved useful in the metastatic setting, with several agents being approved and shown to be effective [39, 40]. However, again, there is a need for better biomarkers predictive of response to specific agents [41, 42], that can be determined in tissue samples upon radical cystectomy and also non-invasively, in liquid biopsy context.

Being such a heterogeneous disease, molecular classification of BlCa was introduced and gained popularity in the past years [10–20]. It is intended to meet these current needs, improving risk stratification of BlCa, and also aiding in identifying specific targets that can be druggable with specific agents. The several analyses concur in the fact that two major types of BlCa are molecularly defined, with important prognostication value: the “luminal” and the “basal” cancers. Such classification is achieved based on genomic and transcriptomic analyses, which point to differential expression of specific markers among tumors: the basal cytokeratins *KRT5/KRT6A* and *KRT14*, as hallmarks of basal BlCa, and the luminal markers *FOXA1* and *GATA3*, as hallmarks of luminal cancer. The value of the classification seems undoubtful; however, and despite multiple confirmations of this, such classification is still not being used in routine clinical practice. There is a lack of works attempting to validate it in the diagnostic setting

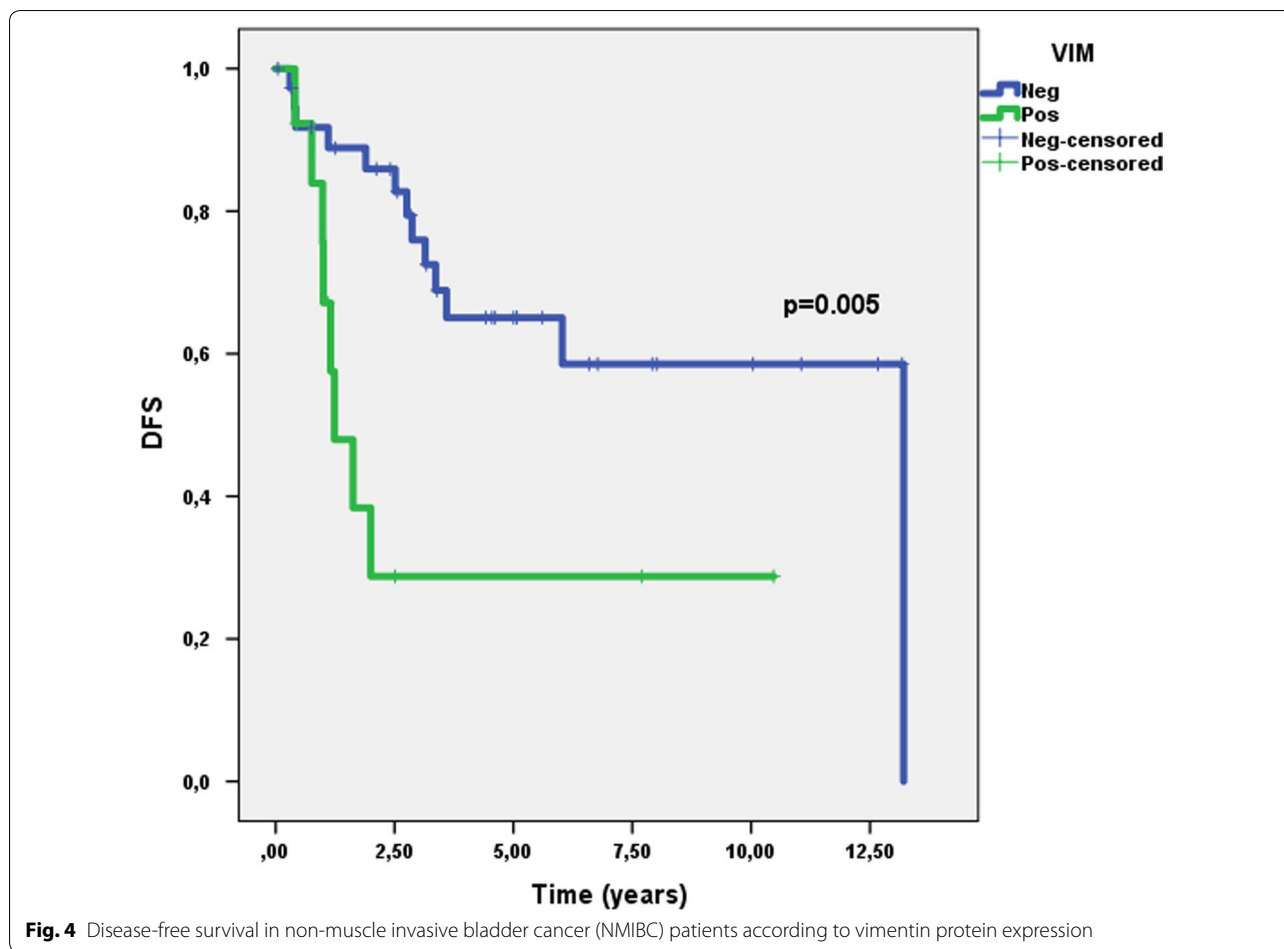


Fig. 4 Disease-free survival in non-muscle invasive bladder cancer (NMIBC) patients according to vimentin protein expression

using immunohistochemistry, with the ones available also finding difficulties in purely classifying the tumors into subtypes or retrieving the same prognostic value [18, 22]. The main aim of our work was to assess the protein expression of these markers and attempt to classify these tumors in a well-defined cohort of BlCa, representative of the diagnostic routine of a tertiary cancer center.

We have witnessed substantial overlapping in protein expression of luminal and basal markers within BlCa specimens, with 40.5% of our cohort showing protein expression of both types of markers. Such overlapping was maintained across both MIBC and NMIBC. We believe that this may be explained by intratumor heterogeneity and specific tumor cell clones within the tumor mass (also acknowledged by Kamoun et al. [10]), which are captured by immunohistochemistry technique, but may go unnoticed in wide transcriptomic analyses. Moreover, we provide data not only on expression patterns in MIBC, but also in NMIBC. The former depicted higher proportion of CK5/6 positive cases (47.2% versus 39.2%), but basal features could be already pinpointed in NMIBC, as well. Although in NMIBC this did not

dictate differences in recurrence, it might be due to small size of our cohort; on the same line, the proportion of recurrences in MIBC was higher in cases with CK5/6 expression (32.4% versus 13.2%), again with the lack of significant impact on DFS likely due to small number of cases tested (or simply because of other cohort selection issues, like for Choi et al. [22]). Additionally, the neuroendocrine-like subtype was recently added to the classification [10], and we identified one such case within the four tumors negative for both luminal and basal markers. We hypothesize that the remaining cases might also belong in this category, but they are still changing their program and progressing towards a more pronounced neuroendocrine phenotype. Overall, the classification proposed based on expression of these markers remains informative and has potential to be translated to practice if appropriate definitions and methodologies are set (i.e. accurate definitions of “luminal” and “basal” tumors at the protein level, as determined by immunohistochemistry should be established and validated, in order to maintain the clinical value). Prospective, multicenter studies with systematic evaluation of these markers by the same

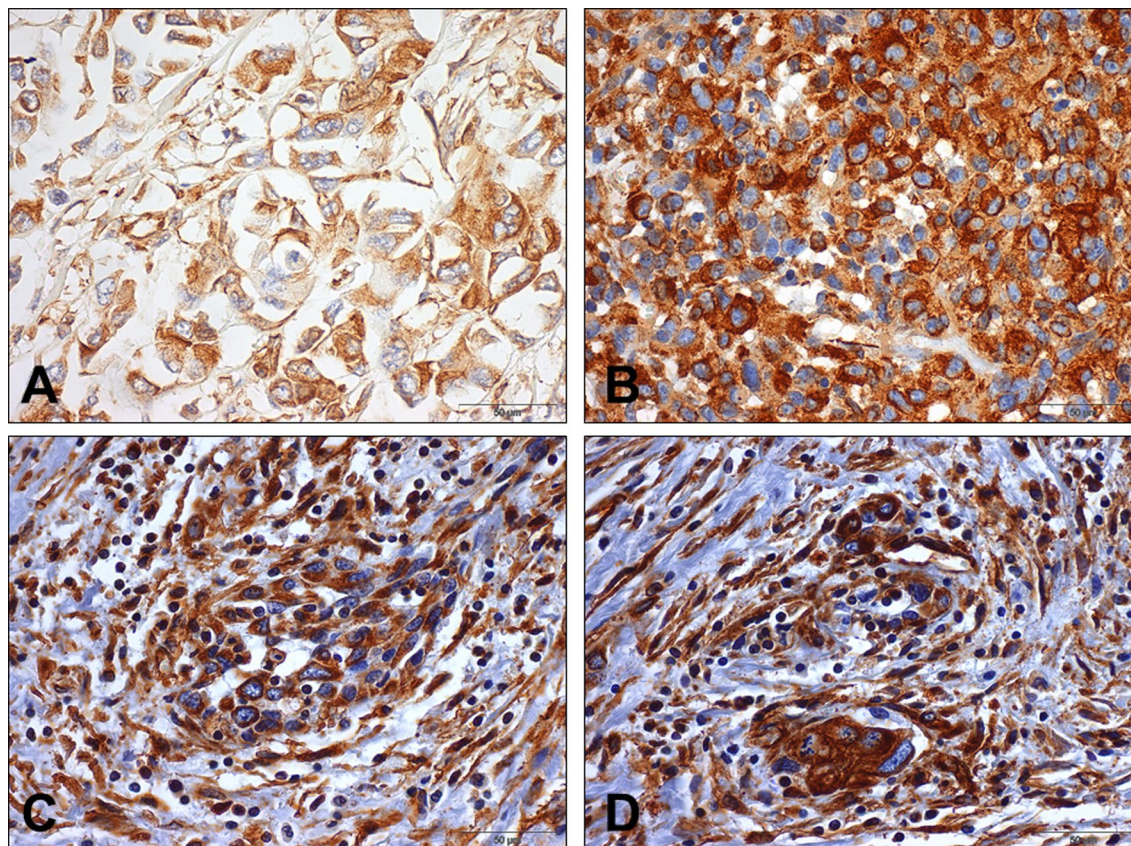


Fig. 5 Immunoeexpression of vimentin in the bladder cancer cohort. **a, b**: immunoeexpression of vimentin in primary bladder cancer specimens, one NMIBC (**a**) and one MIBC (**b**); **c** and **d**: immunoeexpression of vimentin in bladder cancer metastases

methodology and reporting system should be instrumental for achieving a consensus. We found significant positive correlations between mRNA expression levels of *GATA3*, *KRT5* and *KRT6A* and the matched immunoeexpression scoring for the same markers on the same samples (like in the work of Choi et al. [22]). This also substantiates the applicability of the classification. We hypothesize that the classification could also be extended to upper urothelial tract carcinomas, a work ongoing in our Group, with 15/57 tumors (26.3%) showing CK5/6 immunoeexpression (data not shown).

In another setting, the EMT signaling pathway and its players have been implicated in acquisition of a more aggressive cancer phenotype among various tumor models, demonstrated both *in vitro*, *in vivo* and validated in clinical studies with human specimens [43, 44]. The role of expression of epithelial markers such as E-cadherin, the phenomenon of cadherin switch and overexpression of mesenchymal markers (like Snail, Twist, ZEB1/2, Slug and VIM) has been shown across tumor models [45–48]. BlCa is no exception, with studies evidencing that mesenchymal features significantly associate with higher

propensity for disease recurrence, metastatic spread, tumor progression and worse prognosis, including poorer survival and treatment resistance [31, 33, 49–52]. In this work, we have assessed the role of the intermediate filament *VIM*, characteristic of cells with mesenchymal phenotype, not expressed in most normal epithelia (including urothelium), in predicting prognosis of BlCa patients. In accordance, we have shown that *VIM* mRNA and protein expression levels were significantly higher in MIBC compared to NMIBC, illustrating association with increased stage (Fig. 3a, b). The increase in *VIM* protein expression within increasingly aggressive samples (Fig. 3c) reflects the influence of EMT in acquisition of a more aggressive phenotype. Finally, translating this to patient outcome, patients with NMIBC disclosing higher *VIM* expression were shown to have shorter DFS (Fig. 4), even when adjusting (in multivariable analysis) for patient age and grade. Indeed, *VIM de-novo* expression or overexpression has been consistently reported in various epithelial cancers, including those of prostate, breast and lung, associating with increased tumor growth, invasion, poor prognosis, and ultimately, with EMT [53–55].

In BlCa, several reports suggest that VIM associates with higher grade and stage [32, 56, 57], and with propensity for recurrence and metastasis; however, vimentin immunohistochemistry is not routinely performed when assessing BlCa specimens. Also, VIM was shown to be expressed in 100% of the cases of sarcomatoid urothelial carcinoma (along with positivity for other mesenchymal markers such as Snail in a high proportion of cases), a particularly aggressive form of the disease, with dismal prognosis [58]. Our work goes further and indicates the clinical potential of VIM as a prognostic marker within luminal vs. basal-like BlCa cases, although larger studies, including both NMIBC and MIBC, are needed to confirm this hypothesis.

Limitations of this work include its retrospective nature, and the relatively low number of samples with complete clinical information available. Also, not all samples in which immunohistochemistry was performed had fresh-frozen material available for performing transcript analyses. Moreover, although immunohistochemistry may be subjected to inter-observer variability, it is a widespread technique, used in routine histopathology, allowing for evaluating morphology simultaneously and perceiving details related to tumor heterogeneity. Importantly, this work also extends the molecular classification to NMIBC, which should be further explored in the future.

Conclusions

In conclusion, we show that BlCa molecular classification has the potential to be effectively translated to the diagnostic routine, but effort must be made to consistently define the tumor categories acknowledged by transcriptomic studies using routine techniques, with the ultimate goal of maintaining the same clinically meaningful input. On the other hand, expression of EMT markers may be useful for predicting relapse and adjusting therapeutic strategy, like VIM in our work, in which it provided useful prognostic information and dictated survival outcome. Adjunctive markers to the molecular classification merit attention as they might further improve BlCa molecular taxonomy.

Supplementary information

Supplementary information accompanies this paper at <https://doi.org/10.1186/s12967-020-02475-w>.

Additional file 1: Table S1. Immunohistochemistry methods.

Additional file 2: Table S2. Primers sequences.

Additional file 3: Figure S1: Immunoeexpression of neuroendocrine markers in a bladder cancer specimen negative for CK5/6, FOXA1 and GATA3. A: CD56; B: Synaptophysin; C: Chromogranin.

Abbreviations

BlCa: Bladder cancer; NMIBC: non-muscle invasive bladder cancer; MIBC: Muscle invasive bladder cancer; FGFR3: Fibroblast growth factor receptor 3; EMT: Epithelial-to-mesenchymal transition; VIM: Vimentin; TUR: Transurethral resection; AJCC: American Joint Committee on Cancer; DSS: Disease-specific survival; DFS: Disease-free survival; HR: Hazard ratios.

Acknowledgements

Not applicable.

Authors' contributions

JL, SM-R and CG-T performed molecular analyses and wrote the manuscript. JL collected the clinical data and reviewed histological specimens. IC prepared the histological sections for immunohistochemistry. PL performed immunohistochemistry. JL assessed the immunohistochemistry. JL, SM-R and CG-T analyzed the data. CJ and RH supervised the work and revised the manuscript. All authors read and approved the final manuscript.

Funding

This research was funded by Research Center of Portuguese Institute of Porto (CI-IPOP-27-2016). JL and SM-R are recipients of fellowships from FCT - Fundação para a Ciência e Tecnologia (SFRH/BD/132751/2017 and SFRH/BD/112673/2015, respectively).

Availability of data and materials

The datasets used and/or analyzed during the current study are available from the corresponding author on reasonable request.

Ethics approval and consent to participate

This study was approved by the ethics committee of Portuguese Oncology Institute of Porto (Comissão de Ética para a Saúde-CES103-14). All procedures performed in studies involving human participants were in accordance with the ethical standards of the institutional and/or national research committee and with the 1964 Helsinki declaration and its later amendments or comparable ethical standards.

Consent for publication

Not applicable.

Competing interest

The authors declare that they have no competing interests.

Author details

¹ Cancer Biology and Epigenetics Group IPO Porto Research Center (GEBC CI-IPOP), Portuguese Oncology Institute of Porto (IPO Porto) & Porto Comprehensive Cancer Center (P.CCC), R. Dr. António Bernardino de Almeida, 4200-072 Porto, Portugal. ² Department of Pathology, Portuguese Oncology Institute of Porto (IPOP), R. Dr. António Bernardino de Almeida, 4200-072 Porto, Portugal. ³ Department of Pathology and Molecular Immunology, Institute of Biomedical Sciences Abel Salazar, University of Porto (ICBAS-UP), Rua Jorge Viterbo Ferreira 228, 4050-513 Porto, Portugal.

Received: 13 April 2020 Accepted: 30 July 2020

Published online: 05 August 2020

References

- Bray F, Ferlay J, Soerjomataram I, Siegel RL, Torre LA, Jemal A. Global cancer statistics 2018: GLOBOCAN estimates of incidence and mortality worldwide for 36 cancers in 185 countries. *CA Cancer J Clin*. 2018;68:394–424.
- Saginala K, Barsouk A, Aluru JS, Rawla P, Padala SA, Barsouk A. Epidemiology of Bladder Cancer. *Med Sci*. 2020;8:15.
- Antoni S, Ferlay J, Soerjomataram I, Znaor A, Jemal A, Bray F. Bladder cancer incidence and mortality: a global overview and recent trends. *Eur Urol*. 2017;71:96–108.
- Leal J, Luengo-Fernandez R, Sullivan R, Witjes JA. Economic burden of bladder cancer across the European Union. *Eur Urol*. 2016;69:438–47.
- Sanli O, Dobruch J, Knowles MA, Burger M, Alemezaffar M, Nielsen ME, Lotan Y. Bladder cancer. *Nat Rev Dis Primers*. 2017;3:17022.

6. Moch H, Ullbright T, Humphrey P, Reuter V. WHO Classification of Tumours of the Urinary System and Male Genital Organs (4th Edition). IARC: Lyon; 2016.
7. Rouanne M, Lorient Y, Lebret T, Soria JC. Novel therapeutic targets in advanced urothelial carcinoma. *Crit Rev Oncol Hematol*. 2016;98:106–15.
8. Powles T, Eder JP, Fine GD, Braiteh FS, Lorient Y, Cruz C, Bellmunt J, Burris HA, Petrylak DP, Teng SL, et al. MPDL3280A (anti-PD-L1) treatment leads to clinical activity in metastatic bladder cancer. *Nature*. 2014;515:558–62.
9. Davarpanah NN, Yuno A, Trepel JB, Apolo AB. Immunotherapy: a new treatment paradigm in bladder cancer. *Curr Opin Oncol*. 2017;29:184.
10. Kamoun A, de Reynies A, Allory Y, Sjadahl G, Robertson AG, Seiler R, Hoadley KA, Groeneveld CS, Al-Ahmadie H, Choi W, et al. A consensus molecular classification of muscle-invasive bladder cancer. *Eur Urol*. 2020;77:420–33.
11. Tan TZ, Rouanne M, Tan KT, Huang RY, Thiery JP. Molecular subtypes of urothelial bladder cancer: results from a meta-cohort analysis of 2411 tumors. *Eur Urol*. 2019;75:423–32.
12. Dyrskjot L. Molecular subtypes of bladder cancer: academic exercise or clinical relevance? *Eur Urol*. 2019;75:433–4.
13. Lerner SP, Robertson AG. Molecular subtypes of non-muscle invasive bladder cancer. *Cancer Cell*. 2016;30:1–3.
14. Blinova E, Roshchin D, Kogan E, Samishina E, Demura T, Deryabina O, Suslova I, Blinov D, Zhdanov P, Osmanov U, et al. Patient-derived non-muscular invasive bladder cancer Xenografts of main molecular subtypes of the tumor for Anti-Pd-1 treatment assessment. *Cells*. 2019;8:526.
15. Dyrskjot L, Thykjaer T, Kruhoffer M, Jensen JL, Marcussen N, Hamilton-Dutoit S, Wolf H, Orntoft TF. Identifying distinct classes of bladder carcinoma using microarrays. *Nat Genet*. 2003;33:90–6.
16. Blaveri E, Simko JP, Korkola JE, Brewer JL, Baehner F, Mehta K, Devries S, Koppie T, Pejavar S, Carroll P, Waldman FM. Bladder cancer outcome and subtype classification by gene expression. *Clin Cancer Res*. 2005;11:4044–55.
17. Lindgren D, Frigyesi A, Gudjonsson S, Sjadahl G, Hallden C, Chebil G, Veerla S, Ryden T, Mansson W, Liedberg F, Hoglund M. Combined gene expression and genomic profiling define two intrinsic molecular subtypes of urothelial carcinoma and gene signatures for molecular grading and outcome. *Cancer Res*. 2010;70:3463–72.
18. Sjadahl G, Lauss M, Lovgren K, Chebil G, Gudjonsson S, Veerla S, Patschan O, Aine M, Ferno M, Ringner M, et al. A molecular taxonomy for urothelial carcinoma. *Clin Cancer Res*. 2012;18:3377–86.
19. Marzouka NA, Eriksson P, Rovira C, Liedberg F, Sjadahl G, Hoglund M. A validation and extended description of the Lund taxonomy for urothelial carcinoma using the TCGA cohort. *Sci Rep*. 2018;8:3737.
20. Cancer Genome Atlas Research N. Comprehensive molecular characterization of urothelial bladder carcinoma. *Nature*. 2014;507:315–22.
21. Todenhofer T, Seiler R. Molecular subtypes and response to immunotherapy in bladder cancer patients. *Transl Androl Urol*. 2019;8:S293–5.
22. Choi W, Porten S, Kim S, Willis D, Plimack ER, Hoffman-Censits J, Roth B, Cheng T, Tran M, Lee IL, et al. Identification of distinct basal and luminal subtypes of muscle-invasive bladder cancer with different sensitivities to frontline chemotherapy. *Cancer Cell*. 2014;25:152–65.
23. Rosenberg JE, Hoffman-Censits J, Powles T, van der Heijden MS, Balar AV, Necchi A, Dawson N, O'Donnell PH, Balmanoukian A, Lorient Y, et al. Atezolizumab in patients with locally advanced and metastatic urothelial carcinoma who have progressed following treatment with platinum-based chemotherapy: a single-arm, multicentre, phase 2 trial. *Lancet*. 2016;387:1909–20.
24. Seiler R, Ashab HAD, Erho N, van Rhijn BWG, Winters B, Douglas J, van Kessel KE, Franssen van de Putte EE, Sommerlad M, Wang NQ, et al. Impact of molecular subtypes in muscle-invasive bladder cancer on predicting response and survival after neoadjuvant chemotherapy. *Eur Urol*. 2017;72:544–54.
25. Stone L. Bladder cancer: two molecular subtypes identified. *Nat Rev Urol*. 2016;13:566.
26. Robertson AG, Kim J, Al-Ahmadie H, Bellmunt J, Guo G, Cherniack AD, Hinoue T, Laird PW, Hoadley KA, Akbani R, et al. Comprehensive molecular characterization of muscle-invasive bladder cancer. *Cell*. 2018;174:1033.
27. McConkey DJ, Choi W. Molecular subtypes of bladder cancer. *Curr Oncol Rep*. 2018;20:77.
28. Monteiro-Reis S, Lobo J, Henrique R, Jeronimo C. Epigenetic mechanisms influencing epithelial to mesenchymal transition in bladder cancer. *Int J Mol Sci*. 2019;20:297.
29. Garg M, Singh R. Epithelial-to-mesenchymal transition: event and core associates in bladder cancer. *Front Biosci*. 2019;11:150–65.
30. Moussa RA, Khalil EZI, Ali AI. Prognostic role of epithelial-mesenchymal transition markers “E-Cadherin, beta-Catenin, ZEB1, ZEB2 and p63” in bladder carcinoma. *World J Oncol*. 2019;10:199–217.
31. McConkey DJ, Choi W, Marquis L, Martin F, Williams MB, Shah J, Svatek R, Das A, Adam L, Kamat A, et al. Role of epithelial-to-mesenchymal transition (EMT) in drug sensitivity and metastasis in bladder cancer. *Cancer Metastasis Rev*. 2009;28:335–44.
32. Singh R, Ansari JA, Maurya N, Mandhani A, Agrawal V, Garg M. Epithelial-To-mesenchymal transition and its correlation with clinicopathologic features in patients with urothelial carcinoma of the bladder. *Clin Genitourin Cancer*. 2017;15:e187–97.
33. Liu B, Miyake H, Nishikawa M, Fujisawa M. Expression profile of epithelial-mesenchymal transition markers in non-muscle-invasive urothelial carcinoma of the bladder: correlation with intravesical recurrence following transurethral resection. *Urol Oncol*. 2015;33(110):e111–8.
34. Amin MB: AJCC Cancer Staging Manual, 8th Edition. 2017.
35. Aldousari S, Kassouf W. Update on the management of non-muscle invasive bladder cancer. *Can Urol Assoc J*. 2010;4:56–64.
36. Monteiro-Reis S, Blanca A, Tedim-Moreira J, Carneiro I, Montezuma D, Monteiro P, Oliveira J, Antunes L, Henrique R, Lopez-Beltran A, Jeronimo C. A multiplex test assessing MiR663a and VIM in urine accurately discriminates bladder cancer from inflammatory conditions. *J Clin Med*. 2020;9:605.
37. Avogbe PH, Manel A, Vian E, Durand G, Forey N, Voegelé C, Zvereva M, Hosen MI, Meziani S, De Tilly B, et al. Urinary TERT promoter mutations as non-invasive biomarkers for the comprehensive detection of urothelial cancer. *EBioMedicine*. 2019;44:431–8.
38. Babjuk M, Bohle A, Burger M, Capoun O, Cohen D, Comperat EM, Hernandez V, Kaasinen E, Palou J, Roupert M, et al. EAU guidelines on non-muscle-invasive urothelial carcinoma of the bladder: update 2016. *Eur Urol*. 2017;71:447–61.
39. Farina MS, Lundgren KT, Bellmunt J. Immunotherapy in urothelial cancer: recent results and future perspectives. *Drugs*. 2017;77:1077–89.
40. Lobo J, Jeronimo C, Henrique R. Targeting the immune system and epigenetic landscape of urological tumors. *Int J Mol Sci*. 2020;21:829.
41. Lodewijk I, Duenas M, Rubio C, Munera-Maravilla E, Segovia C, Bernardini A, Teixeira A, Paramio JM, Suarez-Cabrera C. Liquid biopsy biomarkers in bladder cancer: a current need for patient diagnosis and monitoring. *Int J Mol Sci*. 2018;19:2514.
42. Yang Y, Miller CR, Lopez-Beltran A, Montironi R, Cheng M, Zhang S, Koch MO, Kaimakliotis HZ, Cheng L. Liquid biopsies in the management of bladder cancer: next-generation biomarkers for diagnosis, surveillance, and treatment-response prediction. *Crit Rev Oncol*. 2017;22:389–401.
43. Dongre A, Weinberg RA. New insights into the mechanisms of epithelial-mesenchymal transition and implications for cancer. *Nat Rev Mol Cell Biol*. 2019;20:69–84.
44. Kang Y, Massague J. Epithelial-mesenchymal transitions: twist in development and metastasis. *Cell*. 2004;118:277–9.
45. Ferreira C, Lobo J, Antunes L, Lopes P, Jeronimo C, Henrique R. Differential expression of E-cadherin and P-cadherin in pT3 prostate cancer: correlation with clinical and pathological features. *Virchows Arch*. 2018;473:443–52.
46. Lobo J, Petronilho S, Newell AH, Coach J, Harlow G, Cruz A, Lopes P, Antunes L, Bai I, Walker E, Henrique R. E-cadherin clone 36 nuclear staining dictates adverse disease outcome in lobular breast cancer patients. *Mod Pathol*. 2019;32:1574–86.
47. Piva F, Giulietti M, Santoni M, Occhipinti G, Scarpelli M, Lopez-Beltran A, Cheng L, Principato G, Montironi R. Epithelial to mesenchymal transition in renal cell carcinoma: implications for cancer therapy. *Mol Diagn Ther*. 2016;20:111–7.
48. Huang L, Wu RL, Xu AM. Epithelial-mesenchymal transition in gastric cancer. *Am J Transl Res*. 2015;7:2141–58.
49. Guo CC, Majewski T, Zhang L, Yao H, Bondaruk J, Wang Y, Zhang S, Wang Z, Lee JG, Lee S, et al. Dysregulation of EMT drives the progression to clinically aggressive sarcomatoid bladder cancer. *Cell Rep*. 2019;27(1781–1793):e1784.

50. Luo Y, Zhu YT, Ma LL, Pang SY, Wei LJ, Lei CY, He CW, Tan WL. Characteristics of bladder transitional cell carcinoma with E-cadherin and N-cadherin double-negative expression. *Oncol Lett.* 2016;12:530–6.
51. Bryan RT. Cell adhesion and urothelial bladder cancer: the role of cadherin switching and related phenomena. *Philos Trans R Soc Lond B Biol Sci.* 2015;370:20140042.
52. Zhao J, Dong D, Sun L, Zhang G, Sun L. Prognostic significance of the epithelial-to-mesenchymal transition markers e-cadherin, vimentin and twist in bladder cancer. *Int Braz J Urol.* 2014;40:179–89.
53. Singh S, Sadacharan S, Su S, Beldegrun A, Persad S, Singh G. Overexpression of vimentin: role in the invasive phenotype in an androgen-independent model of prostate cancer. *Cancer Res.* 2003;63:2306–11.
54. Kokkinos MI, Wafai R, Wong MK, Newgreen DF, Thompson EW, Waltham M. Vimentin and epithelial-mesenchymal transition in human breast cancer—observations in vitro and in vivo. *Cells Tissues Organs.* 2007;185:191–203.
55. Al-Saad S, Al-Shibli K, Donnem T, Persson M, Bremnes RM, Busund LT. The prognostic impact of NF-kappaB p105, vimentin, E-cadherin and Par6 expression in epithelial and stromal compartment in non-small-cell lung cancer. *Br J Cancer.* 2008;99:1476–83.
56. Baumgart E, Cohen MS, Silva Neto B, Jacobs MA, Wotkowicz C, Rieger-Christ KM, Biolo A, Zeheb R, Loda M, Libertino JA, Summerhayes IC. Identification and prognostic significance of an epithelial-mesenchymal transition expression profile in human bladder tumors. *Clin Cancer Res.* 2007;13:1685–94.
57. Paliwal P, Arora D, Mishra AK. Epithelial mesenchymal transition in urothelial carcinoma: twist in the tale. *Indian J Pathol Microbiol.* 2012;55:443–9.
58. Sanfrancesco J, McKenney JK, Leivo MZ, Gupta S, Elson P, Hansel DE. Sarcomatoid urothelial carcinoma of the bladder: analysis of 28 cases with emphasis on clinicopathologic features and markers of epithelial-to-mesenchymal transition. *Arch Pathol Lab Med.* 2016;140:543–51.

Publisher's Note

Springer Nature remains neutral with regard to jurisdictional claims in published maps and institutional affiliations.

Ready to submit your research? Choose BMC and benefit from:

- fast, convenient online submission
- thorough peer review by experienced researchers in your field
- rapid publication on acceptance
- support for research data, including large and complex data types
- gold Open Access which fosters wider collaboration and increased citations
- maximum visibility for your research: over 100M website views per year

At BMC, research is always in progress.

Learn more biomedcentral.com/submissions

